OXAZOLINE DIRECTED LITHIATION OF CALIX[4]ARENE AND FERROCENE

by

Simon Anthony Herbert

Submitted in partial fulfilment of the requirements for the degree

Doctor of Philosophy

at

Stellenbosch University

Department of Chemistry and Polymer Science

Faculty of Science

Supervisor: Dr. Gareth E. Arnott

December 2011

DECLARATION

By submitting this thesis electronically, I declare that the entirety of the work contained therein is my own, original work, that I am the sole author thereof (save to the extent explicitly otherwise stated), that reproduction and publication thereof by Stellenbosch University will not infringe any third party rights and that I have not previously in its entirety or in part submitted it for obtaining any qualification.

Date: .....

ABSTRACT

The use of chiral oxazoline directed lithiation provides a highly diastereoselective (up to >99% *de*) route to *meta* functionalised inherently chiral calixarenes. This methodology can be used on both the butylated and debutylated calixarene systems and is tolerant of a wide range of different electrophillic quenches allowing access to a structurally diverse range of inherently chiral *meta*-functionalised calixarenes. The oxazoline directing group can be removed via hydrolysis, generating a range of functionalised calixarene carboxylic acids in high *ee*. We also demonstrate that the use of derivative alkyllithiums such as cyclopentyl lithium can provide significantly enhanced diastereoselectivity over the conventional organolithiums such as *sec*-butyl lithium, when employed in ortholithiation reactions of this nature. The differences in diastereoselectivity associated with the different alkyllithiums can be tied, in certain cases, to the steric bulkiness associated with the individual reagents. In this regard we have found that the use of the so called Tolman angle or cone angle approach allows quantification of the relative steric bulk of the alkyllithium. We also detail that the oxazoline directing group provides a hitherto unknown ability to be diastereoselectively tuned through the choice of the ligand system in the ortholithiation reaction. In this regard the development of a series of diglyme based ligands have proved to provide a highly diastereoselective means of inverting the chirality from that which the use of the conventional TMEDA ligand is able to generate (up to –92% *de*). The use of diglyme ligands to invert the sense of chirality is also shown to occur on the ferrocenyloxazoline system and presents an apparently general and hitherto unknown facet of asymmetric oxazoline directed ortholithiation. This diglyme induced inversion has been shown to be controlled through a secondary nitrogen coordinated mechanism that is able to operate with chiral oxazolines.

OPSOMMING

Die gebruik van chirale oksasoliengerigte litiëring verskaf ’n hoogs diastereoselektiewe (tot en met >99% *do*) roete om *meta*gefunksionaliseerde, inherente chirale calixareen produkte te sintetiseer. Deur gebruik te maak van verskillende elektrofiele kan die metodologie toegepas word op beide gebutileerde en de-gebutileerde calixareen sisteme om ’n reeks uiteenlopende inherente chirale, *meta*-gefunksionaliseerde calixareen produkte te vorm. Die oksasolien groep kan daarna verwyder word deur hidroliese om ’n reeks gefunksionaliseerde calixareenkarboksielsure te vorm in baie hoë *eo*. Ons het ook gedemonstreer dat die gebruik van afgeleide alkiel-litiums, soos siklopentiel-litium, kan bydrae tot aansienlik verhoogde diastereoselektiwiteit as dit vergelyk word met meer algemene organolitiums soos *sek*-butiellitium, tydens ortolitiëring reaksies van hierdie natuur. Die verskille in diastereoselektiwiteit kan verbind word, in sekere gevalle, tot die steriese bonkigheid van die individuele reagense. Deur gebruik te maak van die sogenaamde Tolmanhoeke of die koniesehoek benadering is dit moontlik om die relatiewe steriese bonkighied van alkiellitiums te kwantifiseer. Daar was ook bepaal dat die oksasoliengroep die ongekende vermoë besit om die diastereoselektiwiteit van die produk te stem deur die keuse van verskillende ligand sisteme tydens die ortolitiëring reaksie. Daar was bepaal dat die chiralitiet van die produkte omgekeer kan word op ’n hoogs diastereoselektiewe manier, deur gebruik te maak van ’n reeks ontwikkelde diglymegebaseerde ligande, indien dit vergelyk word met die produkte wat deur die konvensionele TMEDA gegenereer was (tot en met –92% *do*). Die gebruik van diglyme ligande was ook getoets op ferroseenoksasolien sisteme en dit was bevind dat dieselfde omkering in chiraliteit ook plaasvind wat aanleiding kan gee tot 'n oënskynlik algemene en tot nou toe onbekende faset van asimmetriese oksasoliengerigte *orto*-litiëring. Dit is bepaal dat hierdie diglyme geïnduseerde omkering in chiraliteit beheer word deur middel van 'n sekondêre stikstofgekoördineerde meganisme, wat in staat is om saam te werk met chirale oksasoliene.

ACKNOWLEDGEMENTS

I would firstly like to acknowledge the contribution that my supervisor Dr Gareth Arnott has made to this work, both academically, as well as to me personally with his enthusiasm and support that he has always so freely given. I would also like to thank Prof Jonathan Clayden for hosting me at the University of Manchester, and for the excellent experience it has offered me. I am also indebted to Dr Catherine Esterhuizen for her patience and advice in all matters computational. My thanks goes out to all the members of the technical services who have facilitated this work, and in many cases for providing exceptional service. I would also like to thank the following organisations for financially supporting this work: Stellenbosch University, Ernst & Ethel Ericksen Trust, The HB Thom Foundation, The Harry Crossley Foundation, Sasol and lastly the Commonwealth Scholarship Commission. My sincere thanks to all the members of the Arnott and Clayden groups, who have provided excellent chemical companionship and advice as well as perhaps more importantly for their friendship! I am deeply indebted to Julien, Nicole, Tia and Dewald for all their editing skills and finesse with Word, and to my family and friends, great and small, especially to Tia, for all their love understanding and tolerance! My thanks to Dr Pawel Wisniewski who many years ago provided me with the push and support I needed, and lastly to Martin and Barbara for all your love, advice and wisdom.

PUBLICATIONS

Herbert, S. A., Arnott, G. E., “An Asymmetric Ortholithiation Approach to Inherently Chiral Calix[4]arenes” *Org. Lett.*, **2009**, 11 (21), pp 4986–4989.

Herbert, S.A., Arnott, G. E., “Synthesis of Inherently Chiral Calix[4]arenes: Stereocontrol through Ligand Choice” *Org Lett.*, **2010**, 12, (20), pp 4600-4603.

TABLE OF CONTENTS

CHAPTER 1 – General Introduction
1.1 Calixarenes and Inherent Chirality ... 1
1.1.1 History of Calixarenes ... 1
1.1.2 Synthesis of Calixarenes ... 2
1.1.3 Conformation of Calixarenes ... 3
1.1.4 Introduction of Chirality into Calixarenes ... 5
1.1.5 Inherent Chirality of Calixarenes ... 8
1.1.6 Classification of Inherent Chirality ... 10
1.1.7 Lower-rim Inherently-Chiral Calixarenes ... 11
1.1.8 Upper-rim Inherently-Chiral Calixarenes ... 13
1.2 Ferrocenes and Planar Chirality ... 17
1.2.1 History of Ferrocenes ... 17
1.2.2 Synthesis and Functionalisation of Ferrocenes ... 18
1.2.3 Chirality of Ferrocenes ... 18
1.2.4 Descriptors of Planar Chirality ... 19
1.2.5 Planar Chiral Ferrocene Ligands ... 20
1.3 Methods of Stereoselectively Imparting Chirality into Planar Systems ... 20
1.3.1 Chiral Lithium Bases ... 21
1.3.2 Chiral Directing Groups ... 21
1.4 Alkyllithiums and the Mechanism of Ortholithiation ... 23
1.4.1 Alkyllithiums in solution ... 23
1.4.2 Aggregation and Reactivity of Alkyllithiums ... 24
1.4.3 Classes of Directing Groups and the Mechanism of Ortholithiation ... 26
1.4.4 Synthesis of Alkyllithiums ... 28
1.4.5 Oxazoline Directed Ortholithiation ... 30
1.4.6 Configurational Stability of Organolithiums ... 32
1.4.7 Other Reactions of Lithiated Compounds ... 33
1.5 Proposed Project and Target Molecule ... 34
1.6 References ... 36
CHAPTER 2 – Synthesis of Isopropyl Oxazoline Calixarene ... 43
2.1 Retrosynthetic Analysis ... 43
2.2 Synthesis of Amine Calixarene 2.4 ... 44
2.3 Iodination of Calix[4]arene ... 48
2.4 Halogen Metal Exchange Reactions ... 50
2.5 Synthesis of Oxazoline Calixarene ... 60
2.6 Summary and Future Work ... 61
2.7 References ... 62

CHAPTER 3 – Ortholithiation Reactions 64
3.1 Ortholithiation of Model Compounds 64
3.2 Synthesis of Alkyllithiums 66
3.3 Ortholithiation of Oxazoline Calixarene 2.1 69
3.4 Determination of Diastereoselectivity of Ortholithiation 73
3.5 Optimization of Selectivity and Yield of Ortholithiation Reaction 75
3.5.1 Temperature and Solvent 76
3.5.2 TMEDA to Alkyllithium Ratio 77
3.5.3 Other Additives 77
3.5.4 Yield of sBuLi Reaction 78
3.5.5 Optimisation of Alkyllithium 78
3.5.6 Further Investigation of the THF Inversion in Diastereoselectivity 82
3.6 Conclusion and Future Work 83
3.7 References 84
CHAPTER 4 – Further Functionalisation and Removal of the Oxazoline 86
4.1 Further Functionalisation of Calixarene 86
4.2 Determination of Configuration of Major Diastereomer 94
4.3 Hydrolysis of the Oxazoline 95
4.4 Conclusion and Future Work 98
4.5 References 98
CHAPTER 5 – Ortholithiation of Non-Butylated Calixarene Oxazoline 100
5.1 Synthesis of a Non-Butylated Calixarene Oxazoline 100
5.2 Ortholithiation of Non-Butylated Calixarene 103
5.3 Optimisation of the Ortholithiation of Non-Butylated Oxazoline 105
5.3.1 Reaction Time and Concentration 105
5.3.2 Solvent 106
5.3.3 Alkyllithium Optimisation 108
5.3.4 Additive Optimisation 109
5.3.5 Thermal Stability of the Lithiated Intermediate 118
5.4 Determination of Configuration of Major Product 118
5.5 Conclusion and Future Work 119
5.6 References 120
CHAPTER 6 – Ortholithiation of *t*Bu-Oxazoline Calixarenes 121
6.1 Synthesis and Ortholithiation of *t*Bu-Oxazoline Debutylated Calixarene 121
6.1.1 Determination of the Configuration of the Major Diastereomer 123
6.2 Synthesis and Ortholithiation of *t*Bu-Oxazoline Butylated Calixarene 125
6.2.1 Determination of the Configuration of the Major Diastereomer 127
6.3 Conclusion and Future Work 128

6.4 References 128
CHAPTER 7 – Ortholithiation of Ferrocenyloxazolines 129
7.1 Synthesis of Isopropyl Ferrocenyloxazoline 129
7.2 Ortholithiation of Isopropyl-Ferrocenyloxazoline 130
7.2.1 Effect of Alkyllithium on Diglyme Induced Inversion in Diastereoselectivity. 131
7.2.2 Effect of Derivative Diglyme Structures 132
7.2.3 Effect of Temperature 135
7.2.4 Other Ligands 135
7.3 Mechanistic Study 137
7.3.1 Experiment Design 137
7.3.2 Size of the Substituent on the Oxazoline 139
7.3.3 Position of Substituent on the Oxazoline 141
7.3.4 Assignment of Configuration of Diastereomers 145
7.4 Conclusion and Future Work 149
7.5 References 150
CHAPTER 8 – Mechanistic Discussion and Conclusion 151
8.1 General Mechanism 151
8.2 TMEDA and the Effect of Solvent 154
8.2.1 Conformational Analysis of Oxazoline Calixarenes 157
8.3 Effect of Alkyllithiums 160
8.3.1 Tolman Angle 161
8.4 Structural Role of Oxazoline and the *t*-Butyl Groups on the Calixarene in the Ortholithiation Reaction 165
8.5 Diglyme 166
8.5.1 Rotation of Oxazoline Explored through Computational Methods 170
8.6 Conclusion 175
8.7 References 176
CHAPTER 9 – Experimental 178
9.1 General Practices 178
9.1.1 Solvents and Reagents 178
9.1.2 Temperature Control 178
9.1.3 Inert Conditions 178
9.1.4 Chromatography 178
9.1.5 Characterisation 179
9.2 Chapter 2 180
9.3 Chapter 3 191
9.4 Chapter 4 196
9.5 Chapter 5 209

9.6 Chapter 6 216
9.7 Chapter 7 221
9.8 Chiral Aminols 228
9.9 Model Compounds 230
9.10 Grignard and Lithium reagents. 233
9.11 Ligands 235
9.12 References 238
Appendix I – Structural Analysis of Calixarenes using ^{1}H NMR Spectroscopy 239
A1.1 Interpretation of ^{1}H NMR spectra 239
A1.2 References 243
Appendix II – Selected Computation Data 244
A2.1 DFT optimisations of calixarene conformations (rb3lyp/6-31+g(d,p)) 244
A2.2 Rotation of oxazoline (DFT rb3lyp/6-31) 262

And here I am, for all my lore,
The wretched fool I was before.
Called Master of Arts and Doctor to boot,
For ten years almost I confute
And up and down, wherever it goes
I drag my students by the nose –
And see that for all our Science and Art
We can know nothing. It burns my heart.

That I need not with work and woe
Go on to say what I do not know;
That I might see what secret force
Hides in the world and rules its course.
Envisage the creative blazes
Instead of rummaging in phrases

-- FAUST

(Johann Wolfgang von Goethe)

CHAPTER 1

General Introduction

1.1 Calixarenes and Inherent Chirality

1.1.1 History of Calixarenes

Calixarenes have been the subject of widespread interest since the late 1970s[1] due to their unique properties imparted by their bowl shape. They have been employed in a number of different fields which include; their use as chiral ligands for metal mediated asymmetric catalysis,[2] as enzymatic mimics,[3] supports in separation science,[4] in solid–phase gas storage[5] and in the separation of gaseous mixtures.[6] This diverse range of applications has been attributed to their "chameleon–like chemical nature".[7]

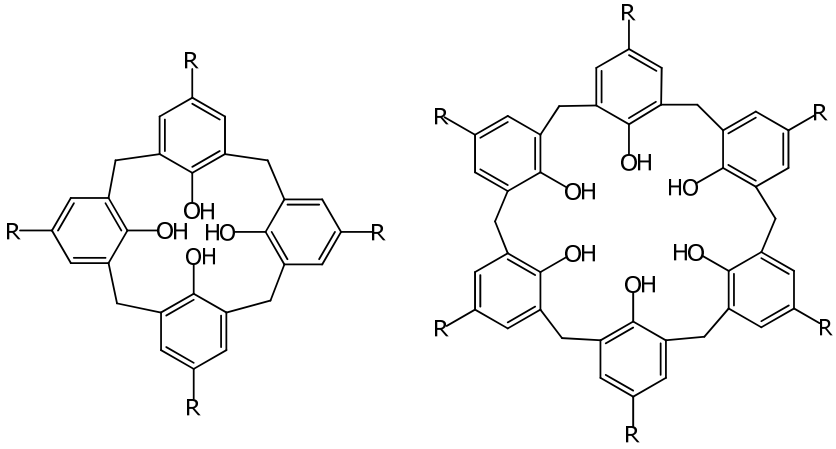

Figure 1.1: Calix[4]arene and calix[6]arene.

The beginnings of calixarene synthesis date back as far as 1872 when Adolf von Baeyer produced a hard brittle substance from his reaction between phenol and formaldehyde.[8] In the early part of the 20th century popularisation of these condensation products occurred with the introduction of the commercially successful Bakelite.[9] Its favourable non–conductive and heat resistant properties lead to its incorporation into a myriad of household and industrial products. Inspired by the commercial success of the Bakelite product, increased industrial and academic interest in these substances was generated and research into these condensation products has continued unabated until the present day, although perhaps the goals have shifted.

1.1.2 Synthesis of Calixarenes

The first true synthesis of calixarenes as we know them, came from work in the 1940s and 1950s by Zinke.[10,11] Zinke recognised that the complexity of condensation products between phenol and formaldehyde arose mainly due to the numerous cross–linking options afforded by the possibility of di–*ortho* and *para* linkage of the phenolic units. In an effort to simplify the complexity of these materials, he used *p*–alkylated phenols which limited possible cross–linking to the two *ortho* positions, the result of which was the calixarene as we know it. Zinke was also able to correctly recognise the cyclic nature of the products of his reactions, however it was not until the advent of modern analytical techniques that the structures could be definitively elucidated.[12–17] The seminal work by Gutsche and co–workers in the 1970s and 1980s propelled the family of calixarene molecules into the forefront of scientific interest in supramolecules,[18–21] and it is perhaps fitting that Gutsche also coined the name calixarene from, as he saw it, the similarity of the molecule to the Greek 'calyx' vase.[22]

As already mentioned, calixarenes are produced from the base–catalysed dehydration of *p*–alkylated phenols and formaldehyde. As calixarenes can have a large number of different ring sizes [4,5,6,7,8,9,10,12], it was important that a degree of control over the formation of a particular ring size was obtained before they could really be studied.[21] The processes through which formation of the different calixarenes occur are of a complex nature and there is still some disagreement surrounding the exact mechanism through which cyclisation occurs.[1] It does however appear that the initial step is the formation of hydroxymethyl phenol units (**1.1** – Scheme 1.1) due to the condensation of formaldehyde with phenol. The resulting hydroxymethyl phenol unit then combines with a second molecule of phenol forming a biarylmethyl oligomer **1.2**, which in turn can combine with other units to form other linear oligomers from which ultimately the calixarene product is assembled. The exact process through which these linear units combine to form the cyclic calixarene products is still the subject of some debate, and it has been suggested that the formation of the linear units might be under equilibrium themselves.[1] For instance the formation of calix[4]arene could progress through a single four–membered oligomer cyclising, two two–membered units combining, or four one–membered units, through a hydrogen–bonded template to form the ring product.[1] Calix[4]arene has also shown to be formed by fragmentation of calix[8]arene.[1] The formation of a particular ring size is known to be dependent on the temperature of the reaction, the concentration and nature of the base, and the solvent.[1]

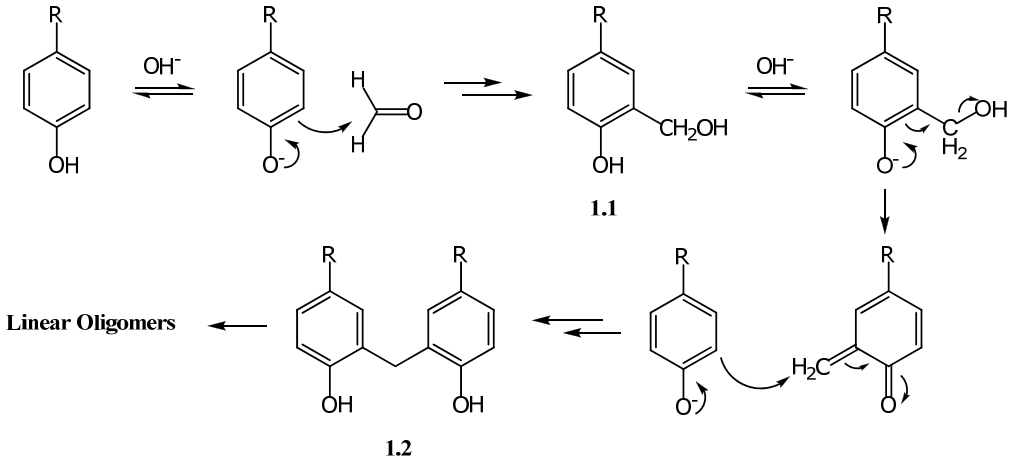

Scheme 1.1: Formation of linear oligomers.[1]

1.1.3 Conformation of Calixarenes

Calixarenes as cyclic molecules can adopt a large number of different conformations,[20] however this discussion will be limited only to those of calix[4]arene. In the solid state calix[4]arene has been shown to exist in the cone conformation.[1] This structure is attained through the formation of an intramolecular octameric hydrogen bonded ring between the phenolic groups which force the molecule into the cone conformation.[15,20,23] This interaction is so strong that the cone conformation is formed in the solid state regardless of the nature of the alkyl groups *para* to the phenolic positions.[1] It is also this strong interaction which has allowed calixarenes to be exploited as solid phase gas sorbtion and separation devices, as pores can be created by removal of guest molecules with retention of the cone conformation through this substantial interaction.[5,6]

With the advent of NMR techniques the dynamics of calixarenes in solution could be studied, revealing their extensive mobility and dynamic nature.[13,14] It was found that inversion of the calix[4]arene in solution occurs very rapidly even at room temperature, rather like the inversion of cyclohexane.[14,20] Thus analogously, the substituents on the methylene bridges of the calixarenes undergo inversion from an equatorial position to an axial position (Scheme 1.2), and vice versa.[1,14,24–26]

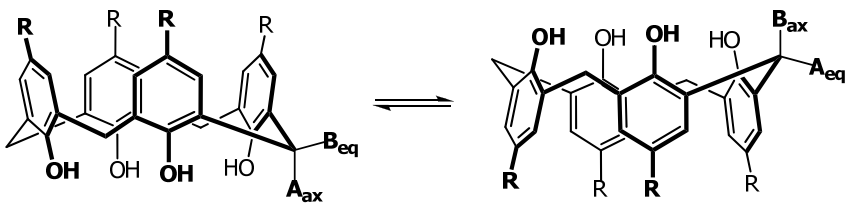

Scheme 1.2: Inversion of calix[4]arene in solution.

A means of preventing calixarenes from inverting in solution has been to functionalise the phenolic positions with bulky groups, which inhibit through–the–annulus rotation of the phenolic positions and hence inversion of the molecule.[1,21] Commonly this is accomplished by either esterification or etherification of the phenolic positions,[1,21] however other strategies have also been employed.[27] If the octameric hydrogen–bonded ring is disrupted through functionalisation of the molecule, a whole new range of conformations of the calixarene can be attained and its behaviour becomes somewhat less predictable. Without the strong hydrogen bonds directing the conformation, the steric bulk of the substituents on the molecule appears to play a more important role in determining the conformation of the molecule. Functionalised calixarenes can occupy the cone, partial cone, 1,2–alternate and 1,3–alternate conformations (Figure 1.2).[20]

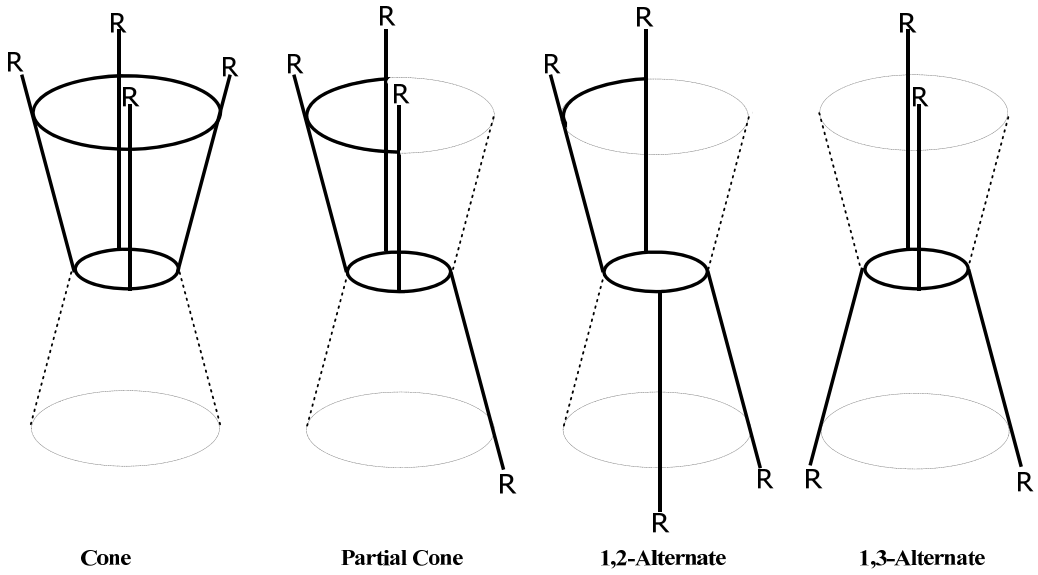

Figure 1.2: Conformations of calix[4]arene.

The cone conformation can be further divided into a true cone and the pinch cone/boat,[25] which is adopted in the solid state due to interruption of the hydrogen–bonded pattern in the phenolic positions. The pinch cone is no longer perfectly cylindrical, but rests with two aromatic rings lying at an outwards angle with the two adjacent rings positioned inwards (Figure 1.3).

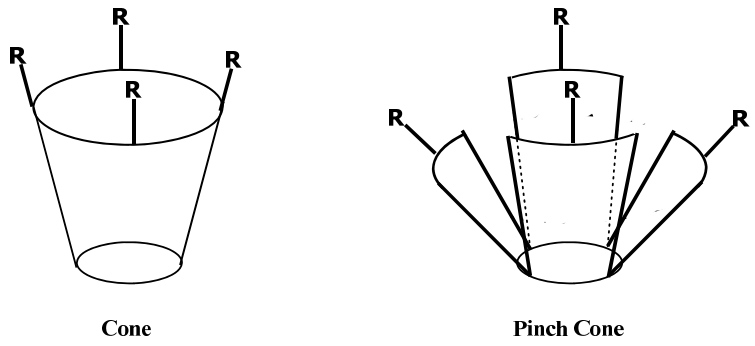

Figure 1.3: Cone and Pinch Cone conformations.

The calixarene molecule can be divided into three distinct regions, namely the upper– rim, the lower –rim and the methylene bridges, as shown in Figure 1.4. Synthetic modification to the calixarene can thus be classified according to the region modified, for example upper–rim (endo) functionalised molecules,[28,29] lower–rim (exo),[30,31] and those functionalised on the methylene bridges.[32,33]

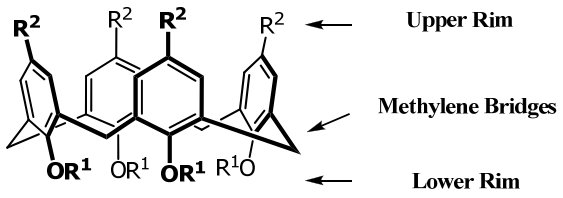

Figure 1.4: Different regions of the calixarene.

1.1.4 Introduction of Chirality into Calixarenes

Numerous functionalisation techniques have been applied on calixarenes,[1] however a fascinating aspect of the functionalisation of calixarenes is the possibility of creating chirality in the molecule. Chirality can either be introduced by the attachment of a chiral moiety to the molecule,[1] or as a consequence of the asymmetric functionalisation of the calixarene.[1,34,35] The latter is more synthetically complex, however it presents an interesting challenge, as the asymmetric product does not involve conventional sp^3 chirality but is a consequence of non–superposable three–dimensional spatial character.[36]

Chirality associated with form rather than with a point or central chirality can be classified into a number of different subgroups depending of the molecule being described. These descriptors include; planar chirality as is found in ferrocenes,[37,38] axial chirality such as in BINAP compounds (Figure 1.5),[39] supramolecular chirality where molecules assemble in such a manner as to induce

chirality to the structure,[36,40] helical chirality such as in DNA and proteins[41] and inherent chirality as is found in calixarenes.[1]

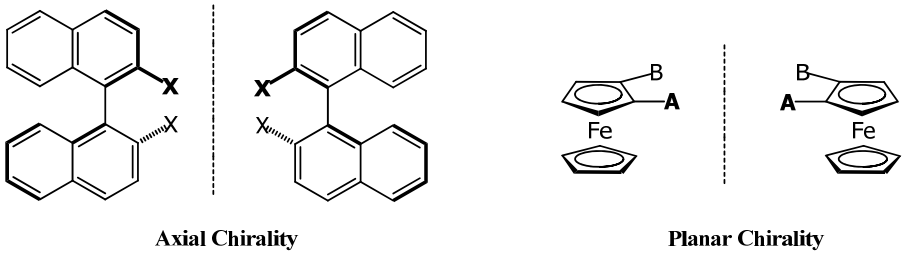

Figure 1.5: Common forms of non–sp^3 chirality.

A convenient means of classifying functionalised calixarene molecules was proposed by Shinkai *et al.*[42,43] Using this classification system, a calixarene synthesised from four identical oligomer units, can be denoted as a AAAA (C_4) structure, as illustrated in Figure 1.6. Functionalisation at any of the regions discussed (upper/lower rim, or methylene bridges), results in the symmetry of the molecule changing. If a single different functional group is present in the molecule (described as AAAB) the symmetry is reduced to C_v. If two different functional groups are present either an ABAB (C_{2v}) or AABB (C_v) type results. The introduction of three (ABCA or AABC) or four different groups (ABCD) creates the possibility of inherent–chirality in the molecules, as both the ABCA and ABCD structures are non–superposable and therefore chiral. Perhaps somewhat unexpectedly ABAC structures are achiral, as rotation by 180 degrees renders the ACAB motif (its mirror image).

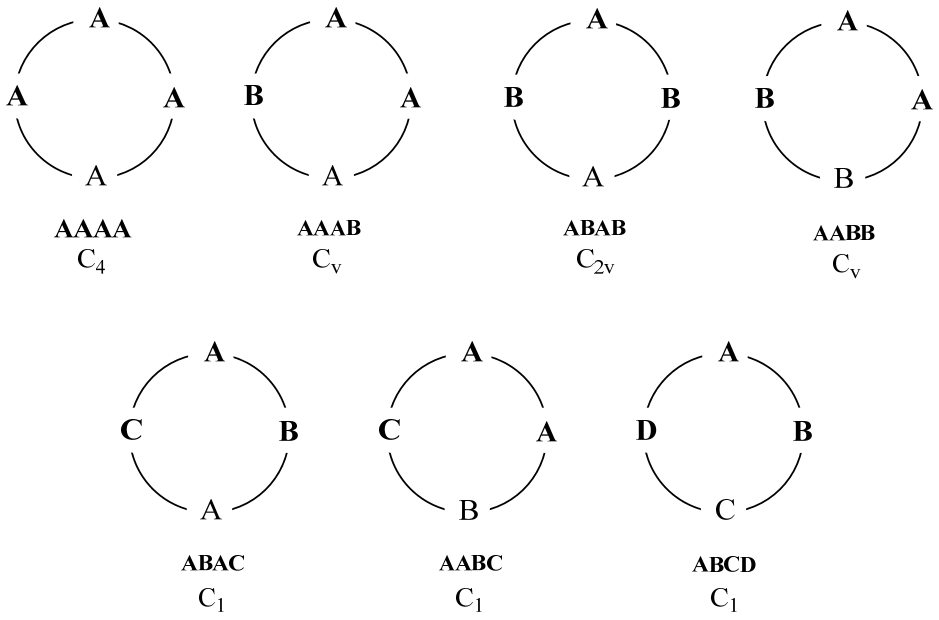

Figure 1.6: Systematic classification system for calixarenes.[43]

Functionalisation of the upper rim, lower rim or the methylene bridges of the calixarene can induce asymmetry, as can combinations of the aforementioned regions, creating the possibility for a large number of different forms of inherently chiral calixarenes. A few examples (by no means comprehensive) of different inherently chiral calixarenes are shown below in Figure 1.7.

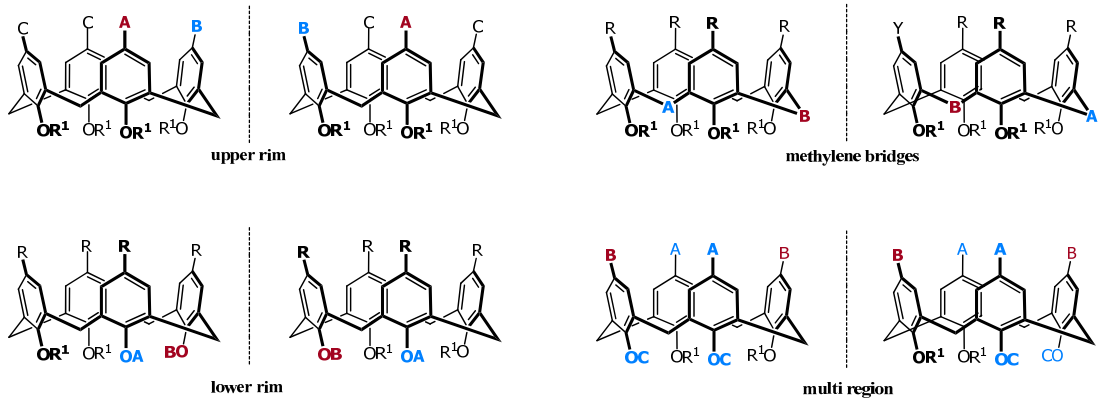

Figure 1.7: Inherent chirality in calix[4]arene.

Upper rim inherent chirality can also be introduced by functionalising a ring (or multiple rings) at one of the *meta* positions, as shown in Figure 1.8. In following Shinkai's general approach to classification we will refer to this type of structural motif as AAAA*, or AAAB* type (with the * denoting the meta–functionalised position).

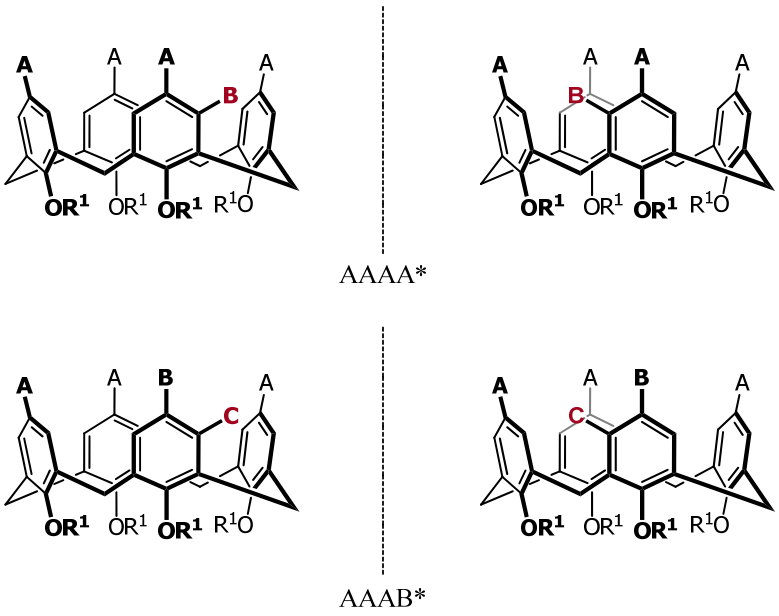

Figure 1.8: *Meta*–functionalised inherently chiral calixarenes.

A subtlety of inherently chiral calixarenes arises due to the molecule's ability to rapidly interconvert between two cone conformations in solution. Just as interconversion between the

axial and equatorial protons occurs on the methylene bridges in solution due to through the annulus rotation (Scheme 1.2), so does the sense of chirality associated with the upper and lower rim of functionalised motifs (Scheme 1.3). For example, an AABC motif will be in equilibrium with its AACB enantiomer in solution at room temperature through this inversion process. For this reason if "permanent" inherent–chirality is to be created, it is necessary by synthetic means to prevent the molecule from inverting in solution thereby eliminating the interconversion between the two enantiomeric forms (Scheme 1.3).[1]

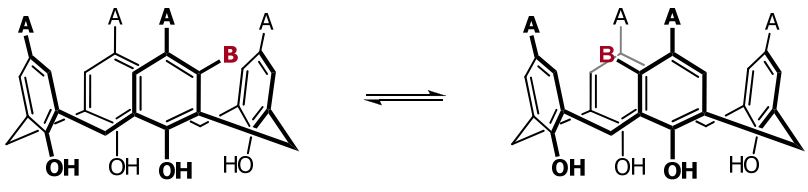

Scheme 1.3: Interconversion of unlocked inherently chiral calix[4]arene in solution.

The first chiral calixarene was synthesised in 1979 by Gutsche *et al.* by lower–rim esterification with the chiral camphorsulfonyl group.[44] This form of chirality is however not unique to the calixarene structure and does not exploit the spatial character of the calixarene molecule. There are numerous examples of the introduction of similar chiral moieties onto the upper–rim of the molecule,[45–47] as well as a review by Sirit *et al.* encompassing the use of chiral moieties in calixarenes.[48]

1.1.5 Inherent Chirality of Calixarenes

The first introduction of inherent chirality into a calixarene was also accomplished by Gutsche *et al.*[49] Using a painstaking stepwise approach, reduced–symmetry calixarene **1.4** was synthesised, which was in turn acetylated using Friedel–Craft conditions, and selectively oxidised to afford the inherently chiral compound **1.5** (Scheme 1.4). It was perhaps Böhmer and co–workers who first approached the systematic synthesis of an inherently chiral molecule,[34] when they obtained an AABC type calixarene by a stepwise synthesis from three different phenolic units (**1.6** –Scheme 1.5). However, the propensity of these molecules to invert in solution rendered them of limited value. Addressing this, Böhmer *et al.* used 1,3 alkylation (distal) of the phenolic positions of a C_2 symmetric calixarene **1.7** to immobilise the calixarene in solution, producing the first conformationally stable inherently chiral calix[4]arene **1.8**.[50]

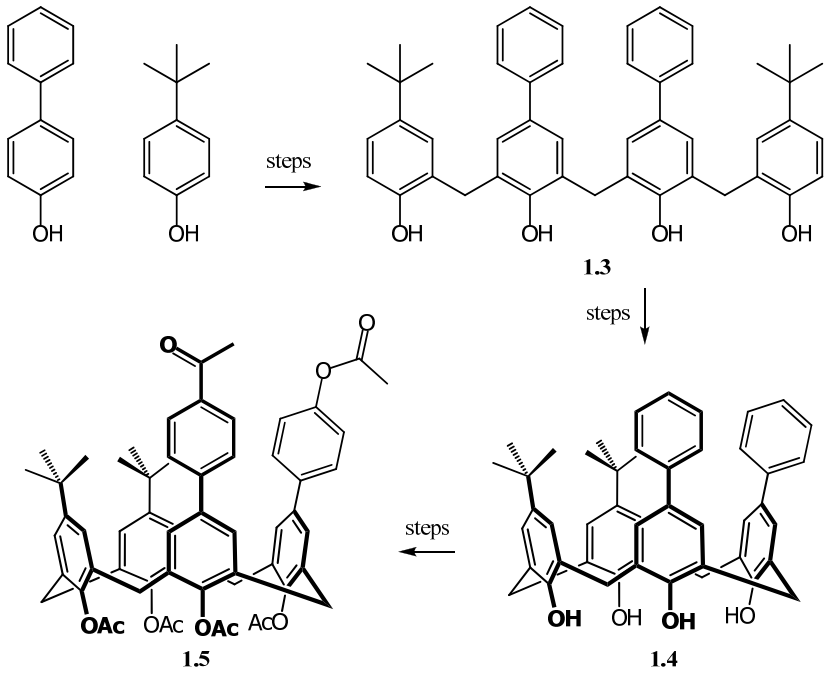

Scheme 1.4: Synthesis of first inherently chiral calixarene by Gutche and co–workers.[49]

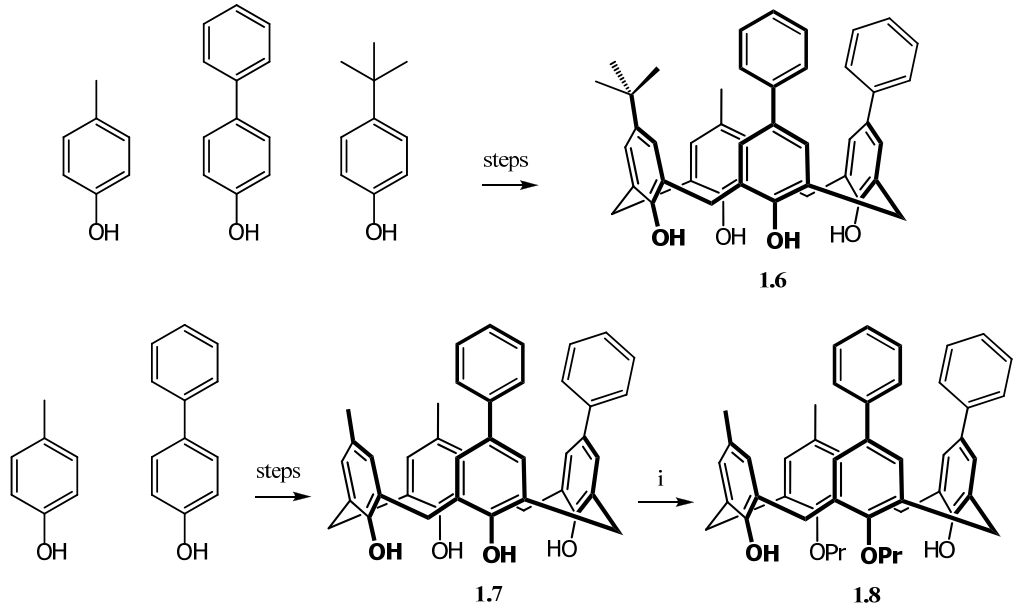

Scheme 1.5: Synthesis of inherently chiral calixarenes by Böhmer.[34,50] Conditions: i)*i*PrI, K_2CO_3.

This report was closely followed by a publication by Shinkai *et al.*, who produced inherently chiral *meta*–methylated calixarene **1.10** as well as demonstrating that it is possible to separate the antipodes using chiral HPLC.[51] Again, a stepwise procedure was utilised to produce the *meta*–methylated calixarene **1.9**, which in turn was globally propylated yielding the conformationally stable chiral calixarene **1.10**. The authors were also able to separate the two enantiomers using

chiral HPLC, and obtained oppositely symmetrical CD spectra for both antipodes, providing definitive proof of their chiral natures.

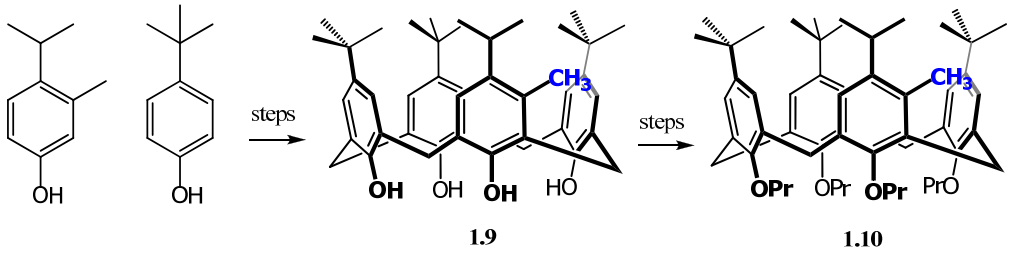

Scheme 1.6: Synthesis of inherently chiral calixarene **1.10** by Shinkai.[51]

As observed from the aforementioned reports, a reliance on stepwise procedures to produce inherently chiral calixarenes characterised these early reports, somewhat limiting the synthesis of inherently chiral molecules. Using an analogous approach it is also possible to produce – inherently chiral calixarenes from one of the lower symmetry conformers (such as the partial cone or 1,2 alternate conformations).[43]

A number of selective functionalisation techniques were developed in the early 1990's which greatly aided the development of inherently chiral calixarene synthesis,[1] by providing a means of de–symmetrising the calixarene without requiring a stepwise approach to the reduced symmetry calixarene starting material. Generally selective functionalisation of calixarenes is accessed through initial functionalisation of the lower rim, which fortunately can be mono, di (proximally or distally) or tri functionalised with a surprising degree of control.[1] Selective esterification[1,30,52] and etherification[1,28 31] of the lower rim is commonly used to create differences in the electronic properties of the rings, which can in turn be exploited to selectively functionalise the upper rim.[28] Using this approach it is possible to selectively halogenate,[1,53,54] nitrate,[29,55] arylate,[1] alkylate[1,56] and remove *t*–butyl group(s) by reverse Friedel–Crafts alkylation,[30,57] on the upper rim of the calixarene.

1.1.6 Classification of Inherent Chirality

A convenient means of describing chirality associated with curvature has been proposed by Schiaffino *et al.*,[58] which has been widely used in the chemical literature of inherently chiral calixarenes.[59–61] This approach centres on first assigning priority to the different methylene bridges using the sequence rules,[62] and then observing either a cyclic clockwise (*cR*), or cyclic counter clockwise (*cS*) rotation from the perspective of an observer situated on the lowest priority methylene bridge facing into the bowl (the two options are sketched in Figure 1.9).

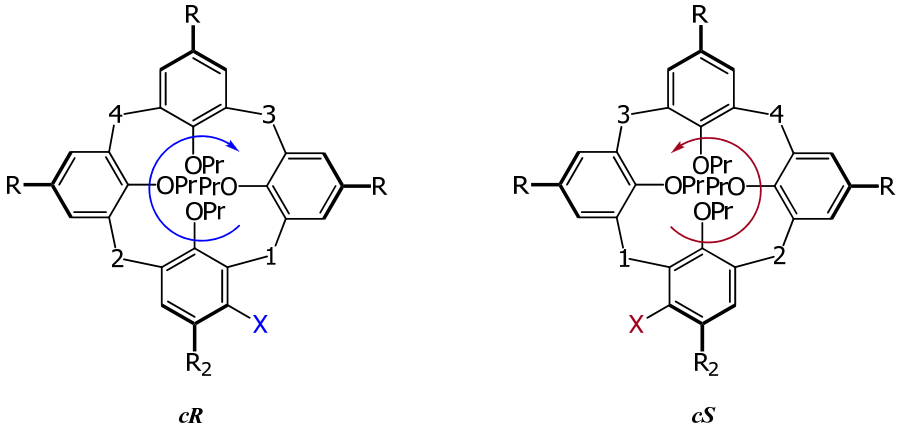

Figure 1.9: Schiaffino's description of inherent chirality on *meta*–functionalised calixarenes.[58]

A brief overview of the inherently chiral calixarene literature will follow, with a distinction being made between the lower rim, upper rim and multi–region inherently chiral molecules.

1.1.7 Lower –rim Inherently chiral Calixarenes

Following on from the initial reports of upper rim functionalised inherently chiral calixarenes,[63,64] Shinkai *et al.* also induced inherent chirality through asymmetric functionalisation of the lower rim.[65] Mono *O*–alkylation with 2–chloromethylpyridine (Pic), followed by *O*–dipropylation and separation of the proximally propylated product from the distally propylated product generated a racemic mixture of chiral calixarenes of the AABC form which could be separated by chiral HPLC (**1.11** – Figure 1.10). Ferguson *et al.* were able to selectively proximally di–Pic alkylate the lower rim, which could then be further functionalised with a range of alkylating agents also yielding AABC structures (**1.12)**.[66] The first ABCD motif was obtained a number of years later by Shu *et al*. (**1.13),** again using a sequential alkylation strategy.[67] The lower rim has also been used to create inherently chiral calixarene crown[n] ethers through bridging of the phenolic positions with ether linkages, which were subsequently resolved using chiral HPLC techniques (**1.14**).[68–70]

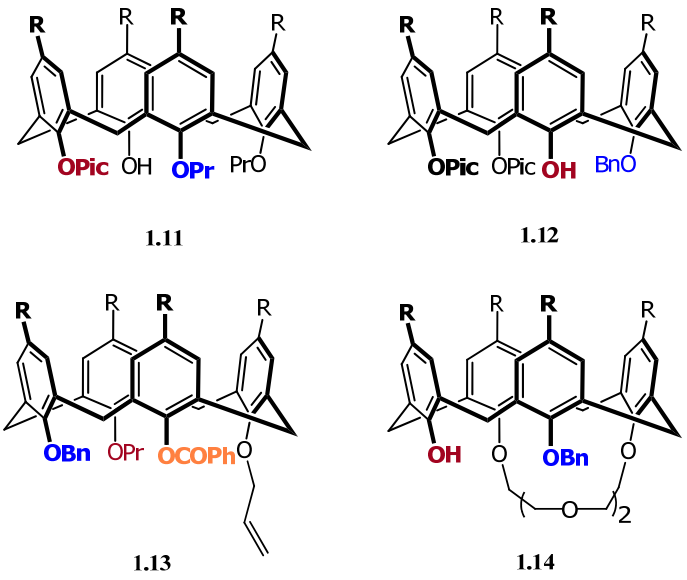

1.11 **1.12** **1.13** **1.14**

Figure 1.10: Lower rim inherently chiral calixarenes. Note: **1.11**,[71] **1.12**,[66] **1.13**,[67] **1.14**.[70], R = *t*Bu.

Separation of lower rim calixarene enantiomers has been accomplished by preparative chiral HPLC,[64,70,72] however this does not represent a highly practical approach to procuring large quantities of material. A means of overcoming this has been the use of chiral derivatisation reagents, which through coupling with the inherently chiral compound produces diastereomers, which can be used to aid their chromatographic separation. Matt *et al.* used both cholesteryl chloroformate and a chiral amide ((*R*)–$BrCH_2C(O)NHCHMePh$) for the derivatisation of, and purification of, their chiral phosphine oxide calixarenes, which induced partial chromatographic separation of the diastereomers.[73] Chiral camphorsulfonyl derivatisation of lower–rim functionalized inherently chiral calixarenes has been used to create as well as purify inherently chiral calixarenes,[74] as has chiral BINOL derivatisation.[75] Currently for lower rim functionalized calixarenes the use of chiral auxiliary moieties for the separation of the antipodes represents the most efficient means of obtaining optically pure lower rim inherently chiral calixarenes. The only report where a small diastereoselectivity has been reported (15% de), has been in the esterification of the lower–rim with camphorsulfonyl chloride by Kalchenko *et al.*,[74] with the selectivity appearing to stem from the kinetic preference for the formation of a particular diastereomer.

A number of these lower–rim functionalized molecules have also been evaluated as asymmetric ligands in metal–catalysed transformations with limited success.[73,76] From these reports it appears that although a degree of selectivity in the reactions has been observed, inherently chiral molecules of this nature fail to induce any significant selectivity into the coordination of the substrate with the lower–rim metal–calixarene complex, thereby failing to impart noteworthy control into the transformation.

1.1.8 Upper –rim Inherently Chiral Calixarenes

Functionalisation of the upper–rim of the calixarene presents a greater number of possibilities than lower–rim functionalisation does, due to the three upper rim positions available on each ring. The upper–rim can be functionalized as an AABC or ABCD type motif (similar to lower–rim functionalisation patterns), or the individual rings can be *meta* functionalised also creating chirality (AAAA*).

An early example of *meta*–functionalisation of a single aryl ring to provide an inherently chiral calixarene was reported by Verboom *et al.* in 1995 (**1.15** – Figure 1.11).[77] The authors used the directing effect of the *p*–acetamide–functionalized calixarene to selectively introduce a nitro or bromo group to the *meta* position on the upper–rim of a single ring. Swager *et al.*[78] utilized a step–wise approach similar to that used by Shinkai *et al.*[65] to construct inherently chiral calixarenes from four 4–bromo–3–methylphenol units (**1.16**) which is a A*A*A*A*–type. In a subsequent publication, Swager *et al.* conformationally locked this compound through tetracoordination of the calixarene's four phenolic oxygens to tungsten forming a η^4 calixareneWCl_2 complex.[27] Replacement of the two chlorine ligands with (1*S*, 2*S*)–trans–1,2–cyclohexanediol allowed the diastereomers to be separated by silica gel chromatography without dissociation of the metallo calix complex **1.17**. This represented the first resolution of an optically active metallo calixarene.

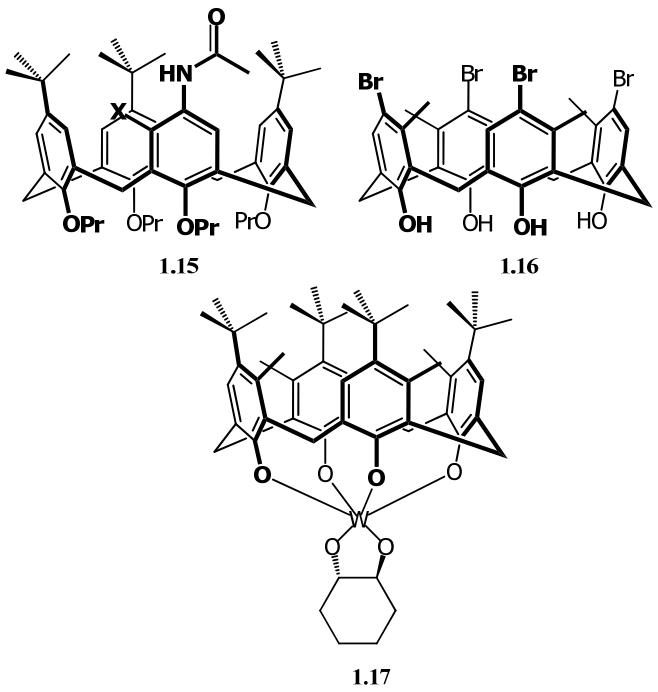

Figure 1.11: Upper–rim inherently chiral calix[4]arenes. Note: **1.15**,[77] **1.16**,[78] **1.17**,[27] X = Br/NO_2.

A further example of upper rim inherent–chirality was presented by Shinkai *et al.*, by functionalisation of the upper rim with two naphthalene rings presenting an AABB type structure (**1.18** – Scheme 1.7).[79] Notably, by controlling the nature of the base used in the ring closure reaction, preference for either the achiral AABB motif (**1.18**) or the inherently chiral ABAB (**1.19**) could be gained. Resolution of the racemic ABAB structure could be performed by preparative chiral HPLC chromatography.

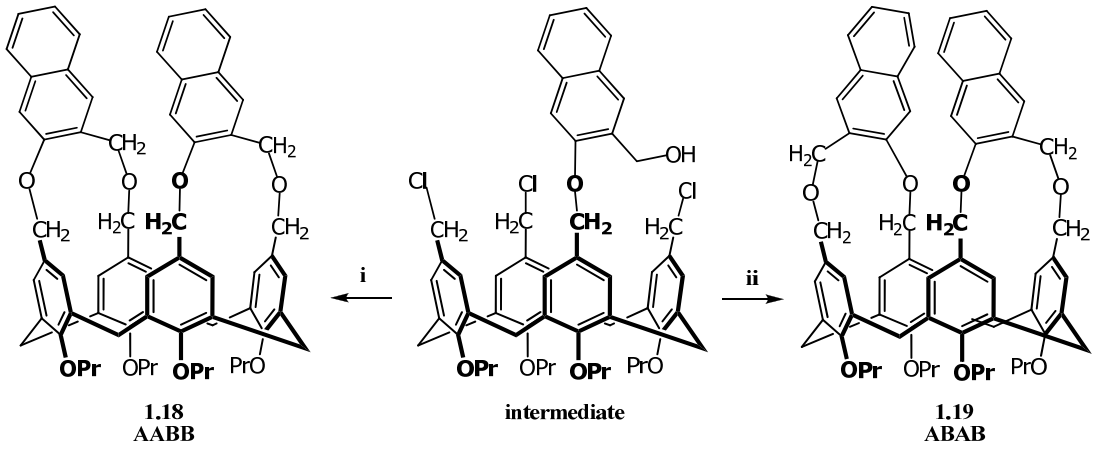

Scheme 1.7: Upper–rim naphthalene–based inherent chirality.[79] Note that an intermediate structure has been shown for clarity. Reagents and conditions: i) NaH, DMF, 3–hydroxymethyl–2–naphthol (HMN) (6 eq) ii) Na_2CO_3, Acetone, HMN (4 eq).

A number of other structural motifs have been synthesised recently (Figure 1.12), with particular attention being paid to the method through which separation of the enantiomers is achieved. The Huang group have developed a number of different chiral derivatisation– techniques for obtaining optically pure compounds.[59,80,81] In 2005 they prepared a chiral calix quinoline (**1.20** – Figure 1.12) which could be separated into its diastereomers by silica gel chromatography after esterification with *S*–BINOL.[80] They also used a modification of the procedure developed by Verboom *et al.*[77] (**1.21** – Figure 1.11) for the *meta* bromination or nitration of a single ring, by replacing the *p*–acetamide directing group with an L–Boc–proline group, which serves both as a directing group as well a chiral auxiliary to aid separation of the resulting diastereomers.[59] Huang *et al.* also utilised a non–enzymatic resolution[82,83] of the racemic *meta*–nitro amino calixarene **1.21** in Figure 1.12, by acylation of the amine with L–Boc–proline.[84] In the DCC and DMAP induced coupling of the amine calixarene and L–Boc proline, the coupling proved to exhibit the kinetically preferential formation of a specific diastereomer which allowed subsequent chromatographic separation of the enantiomers (20% yield 96% *ee*).

Shimizu *et al.* have focused on the synthesis of upper–rim AABC (**1.22** – Figure 1.12)[61,85] and ABCD (**1.23** – Figure 1.12)[86] type inherently chiral structures. The AABC structures were synthesised from a proximal dibromo precursor, by sequential lithium halogen exchange reactions,[61,85] with separation of the antipodes using chiral derivatisation with BINOL,[61] or chiral mandelic acid,[85] which preferentially forms a non–covalently bonded complex with one of the enantiomers. Using a similar sequential bromination, lithium halogen exchange strategy Shimizu *et al.* recently synthesised the first ABCD type upper rim structure,[86] with chiral derivatisation by esterification with camphorsulfonyl chloride, which again allows chromatographic separation of the diastereomers by preparative HPLC.

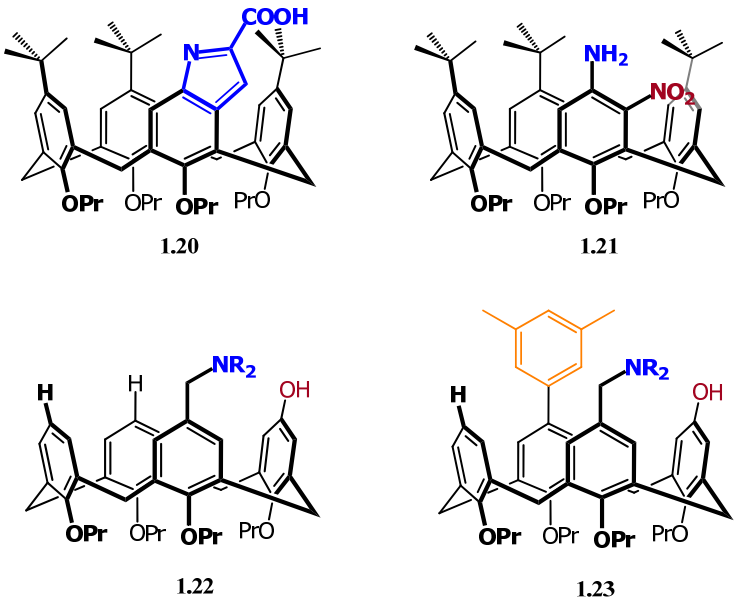

Figure 1.12: Recent upper rim inherently chiral calixarenes: **1.20**,[80] **1.21**,[59] **1.22**,[85] **1.23**.[86]

A number of potential applications of these molecules have been examined in the literature, including purification of racemic chiral acids by selective complexation[85] and their use as chiral ligands in enantioselective reactions.[60,81,86] Thus far, only moderate enantioselectivity has been obtained, however in this regard only a limited number of structural motifs have been explored.

As can be seen from this brief literature review, a great deal of emphasis has been placed on the method of resolving the enantiomers once inherent –chirality has been introduced into the calixarene structure. Indeed, without a resolution procedure, the potential uses of these molecules are likely to be of limited value. To the best of our knowledge, no stereoselective synthetic method for controlling the functionalisation of calix[4]arenes exists in the chemical literature. This indicated that the development of an asymmetric approach towards obtaining inherently chiral calixarenes could provide a worthy undertaking as well as a means of circumventing the need for resolution–based approaches for obtaining these molecules.

In discussing possible approaches towards the development of stereoselective methodology we wondered if it would be possible to draw inspiration from the methods used to produce planar chiral ferrocenes. At a first glance perhaps calixarenes and ferrocenes appear very different both in terms of structure as well as bonding, however similarities between them do exist in that both systems can be functionalised in an asymmetric fashion to produce chiral molecules. In the following section a brief overview of ferrocenes is given, with particular attention being paid towards the methods used for stereoselective functionalisation.

1.2 Ferrocenes and Planar Chirality

1.2.1 History of Ferrocenes

Since the discovery of ferrocene in the 1950's it has become one of the most studied organometallic compounds,[37,38] with widespread application in asymmetric catalysis,[87–89] medicinal chemistry[90] and the petrochemical industry.[91] The discovery of ferrocene dates back to 1951 when two independent publications reported the synthesis of a new organo–iron compound. Kealy and Pauson described that the addition of cyclopentadienylmagnesium bromide to iron dichloride produced an orange, crystalline solid with the composition of $C_{10}H_{10}Fe$ which they classified as dicyclopentadienyliron.[92] Miller *et al.* reported that in their efforts towards investigating the catalytic properties of organoiron compounds, the reaction of dicyclopentadiene and Fe_2O_3 at high temperature also produced dicyclopentadienyliron.[93] Perhaps the most striking property of this new organoiron compound was its remarkable stability, a feature often uncommon in organometallic compounds. These early reports incorrectly proposed a $Fe(\eta^1\text{–}C_5H_5)_2$ motif (**1.24 –** Figure 1.13) for the new organoiron compound, in part because the true π bonding structure of ferrocene was unknown in the chemical literature at this time. Kealy and Pauson did however correctly associate the remarkable stability of this new compound with the presence of an aromatised resonance structure (**1.25** – Figure 1.13),[92] even if they failed to identify its true motif.

There was immediate interest in the chemical community in this new compound and both Wilkinson *et al.*[94] and Fischer and Pfab[95] independently started working on the new compound, culminating in the correct elucidation of the true sandwich motif of ferrocene $Fe(\eta^5\text{–}C_5H_5)_2$ (**1.26** – Figure 1.13).[94,95] At the time this structure caused great debate and interest, as it contained a new form of bonding interaction that had not been observed in organometallic chemistry.[96] Further support for the suggested structure came in the form of early X–ray crystallography measurements which also suggested the staggered symmetric sandwich structure Fischer and Wilkinson had proposed.[97] The term ferrocene was coined by Whiting and co–workers and gradually was incorporated into the chemical literature.[98,99]

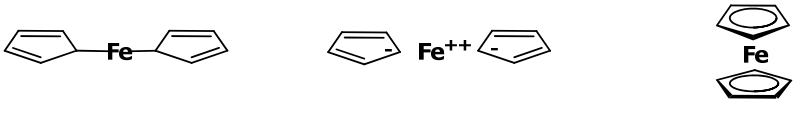

1.24 **1.25** **1.26**

Figure 1.13: Proposed structures of ferrocene. **1.24**,[92,93] **1.25**,[92] **1.26**.[94,95]

1.2.2 Synthesis and Functionalisation of Ferrocenes

A number of different routes have been employed to synthesise ferrocene, commonly however ferrocene is synthesised by transmetallation of sodium cyclopentadienide with ferrous chloride,[100] or using potassium hydroxide, freshly cracked cyclopentadiene and ferrous chloride.[101]

Turning to the functionalisation of ferrocene, soon after its discovery in 1952, Woodward and co–workers demonstrated its underlying electron rich aromatic character by showing that it could be diacetylated using Friedel–Crafts conditions in the presence of aluminium trichloride.[98] Following this initial report, a number of other publications quickly appeared describing methodology allowing functionalisation of the Cp rings.[102–105] Importantly, in the late fifties, it was also found that functionalisation could be achieved by lithiation of ferrocene with a suitable alkyllithium, followed by quenching with a range of electrophiles.[106–108]

1.2.3 Chirality of Ferrocenes

An important class of functionalized ferrocenes occurs where asymmetry is incorporated into the substituent creating central chirality in the molecule. A large variety of different chiral ferrocenes have been synthesized and separated into their antipodes using numerous methods, including resolution techniques, asymmetric synthesis and generation from the chiral pool.[37] However, as is the case of functionalized calixarenes, substituted ferrocenes can also contain a secondary characteristic of chirality in that, if two or more substituents are present, chirality associated with form can also be present in the structure. In the case of 1,2–substituted ferrocenes, this is known as planar chirality, however helical chirality can also be imparted by functionalisation of the second Cp ring.[37,38] The first example of a non–central chiral ferrocene that possessed an optical rotation appeared in a report by Thomson in 1959, when he presented a resolved ferrocenylcyclohexanone (**1.27** – Figure 1.14).[109] Following this report, Westman *et al.* prepared a chiral 3,1´–dimethyl–ferrocenylcarboxylic acid (**1.28** – Figure 1.14),[110] which also detailed resolution techniques for procuring both enantiomers. The two enantiomers proved to possess opposite optical rotations, proving their mirror image natures. This form of chirality was further elaborated by the work of Schlögl who proposed that these non–centrally chiral, non–superimposable structures were all examples of planar chirality.[111–113]

1.27 **1.28**

Figure 1.14: Early examples of planar chirality in ferrocenes. **1.27**[109] and **1.28**.[110]

1.2.4 Descriptors of Planar Chirality

A number of different conventions have been used to describe the sense of planar chirality in substituted ferrocenes.[37] Nevertheless, two descriptors have been most widely used. Schlögl proposed a simple system in which the observer regards the most substituted ring from above, following which the priorities of the substituents on that ring are assigned using Cahn – Ingold – Prelog rules and a left handed or right handed rotation can be described (assigned as *R* or *S* or $_pR$ or $_pS$) as shown in **A** of Figure 1.15.[111] However Cahn, Ingold and Prelog later proposed that planar chirality can be reduced to central chirality by presuming all atoms on the Cp ring are bound to iron forming a distorted tetrahedral carbon. Assignment of the highest priority substituent on the ring then gives the sense of chirality leading to a S_p or R_p (or *S* or *R*) descriptor (**B** in Figure 1.15).[114] Perplexingly, both naming systems tend to give the opposite descriptor, creating the very real possibility for confusion, especially in cases where the description system is not clearly indicated.

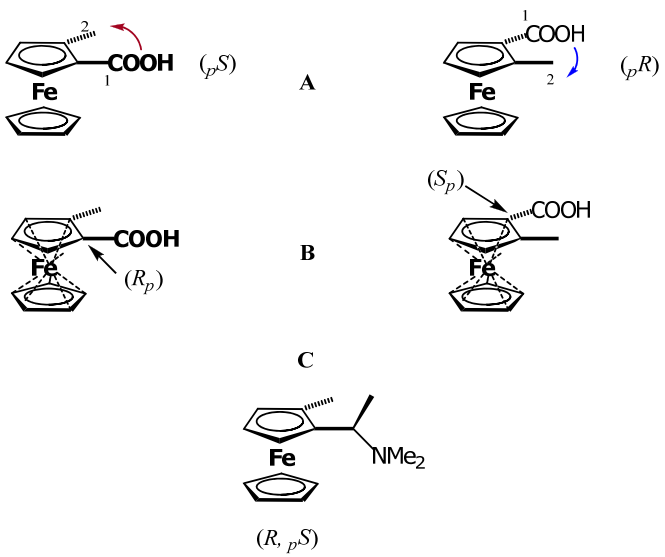

Figure 1.15: Descriptions of planar chirality. A – Schlögl,[111] B – Cahn – Ingold – Prelog.[114]

Lastly, in systems where central and planar chirality both exist, generally the descriptor of central chirality precedes the descriptor of planar chirality (**C** in Figure 1.15), however a number of publications have not followed this convention.[37]

1.2.5 Planar Chiral Ferrocene Ligands

In the field of asymmetric catalysis the use of chiral ferrocenyl ligands that possess planar chirality is widespread.[87,89] The exact role of planar chirality in inducing asymmetry into ligand–mediated catalysis has been the subject of some debate, and certainly in some cases the overwhelming controlling factor can be the presence of central chirality in the ligand.[88] In any event a large number of highly successful 1,2–substituted ferrocenes have found use in asymmetric catalysis.[87] A few selected examples of successful ferrocenyl ligands displaying planar chirality are shown below in Figure 1.16.

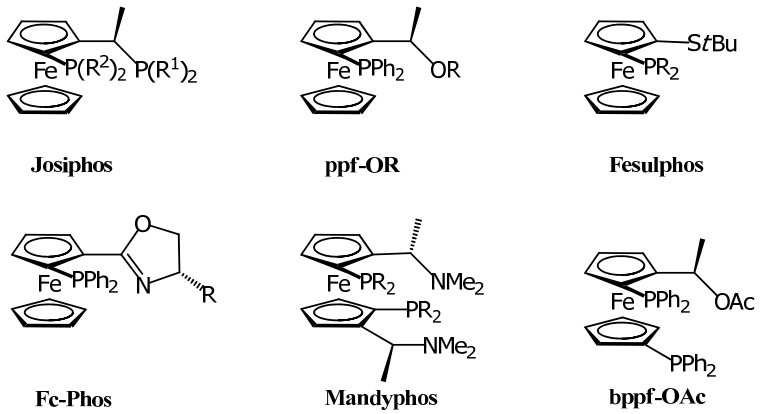

Figure 1.16: Selected ferrocenyl ligands displaying planar chirality.[87]

As the ability of ferrocenyl ligands to mediate metal induced asymmetric catalysis started to emerge, the demand for planar chiral ferrocenes grew, with efforts towards controlling the planar stereochemistry of functionalisation becoming increasingly important. The development of asymmetric methodology on the ferrocenyl system is detailed in the following section.

1.3 Methods of Stereoselectively Imparting Chirality into Planar Systems

In all of the examples of planar–chiral ferrocenyl ligands mentioned earlier, asymmetric methodology has been used to control their sense of planar chirality.[87,89] This has largely eliminated the need for the use of preparative HPLC or chiral derivatisation techniques to separate the antipodes, which have often been time consuming and/or low yielding.

In this regard, a widely exploited feature has been the ability of metallocenes to undergo lithiation. The use of chiral directing groups and chiral lithium bases have proved to exhibit good selectivity in the ortholithiation of planar systems such as ferrocenes[89] and chromium arenes.[115] In these systems the stereoselectivity of the reaction appears to be primarily generated by a facial

difference between the metal–coordinated face and the "free" uncomplexed face. The use of chiral lithium bases[116–118] or chiral directing groups[119–123] expresses the influence of chirality in the transition state by inducing stereo/diastereoselectivity into the formation of the planar chiral lithiated product due to the different facial environments. The introduction of a suitable electrophile into the reaction mixture reacts with the nucleophilic lithiated intermediate, allowing functionalisation with a wide range of groups.[124,125]

1.3.1 Chiral Lithium Bases

Chiral lithium bases were first used for the enantioselective functionalisation of ferrocenes in 1969 by Nozaki *et al.* using *s*BuLi and (−)–sparteine on an isopropyl functionalised ferrocene, albeit with poor selectivity stemming from the poor directing ability of the isopropyl moity.[116] The approach proved to be ahead of the then understanding of directed lithiation, and hence the idea of a chiral lithium base enantioselectively deprotonating ferrocene could only be brought to full fruition a number of years later. Sniekcus and co–workers exploited the chiral nature of *s*BuLi–sparteine complex for the efficient enantioselective (96% *ee*) functionalisation of amide functionalised ferrocenes (**1.29** – Scheme 1.8).[117] Similarly but with more modest selectivity Uemura *et al.* used chiral BINAP–coordinated alkyllithiums.[126] The use of a chiral lithium amide base with ferrocenes (**1.30** – Scheme 1.8) has also proved selective, albeit with a fairly modest *ee*.[118]

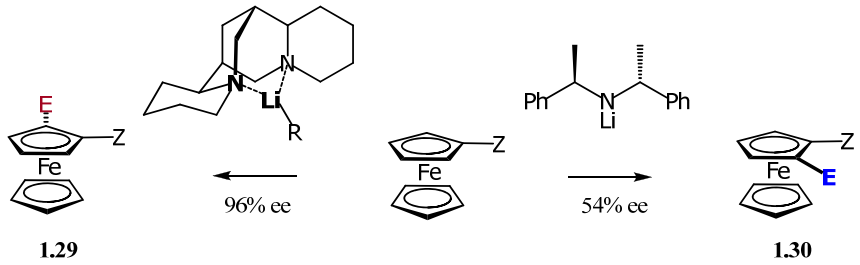

Scheme 1.8: Use of chiral lithium bases for enantioselective functionalisation of ferrocene. **1.29**, Z = $C(O)NiPr_2$[117] or Z = CH_2NR_2[126] **1.30**, Z = $P(O)Ph_2$.[118]

1.3.2 Chiral Directing Groups

Nozaki and co–workers also pioneered the use of chiral directing groups for the diastereoselective functionalisation of ferrocene using chiral amine **1.31** as shown in Scheme 1.9.[116] The selectivity of this approach was improved by Ugi *et al.* by moving the chiral centre closer towards the cyclopentyl ring which imparted greater control over the lithiation (**1.32**).[119,120] Replacement of the methyl group in Ugi's chiral amine with the more bulky isopropyl group[127] increases the selectivity of the reaction to above 99:1.

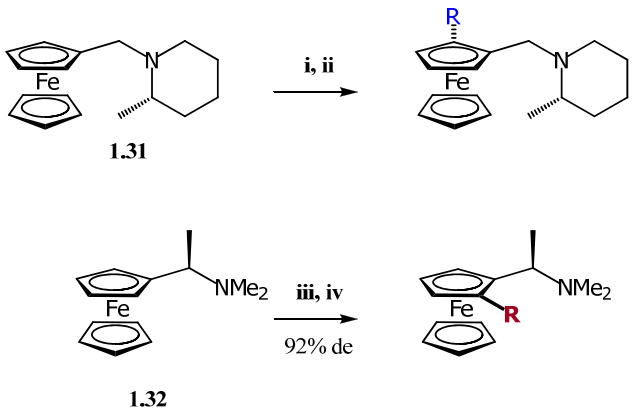

Scheme 1.9: Stereoselective functionalisation of ferrocene. **1.31**,[116] **1.32**.[119] Reagents and conditions: i) *n*BuLi, Et_2O–hexane, RT, ii) E^+, iii) *n*BuLi, Et_2O–hexane reflux, iv) E^+ 92% *de*.

The discovery in the 1980's of new, more versatile directing groups (particularly with respect to removal and metallation directing ability) led to their introduction in asymmetric functionalisation of ferrocenes. The use of chiral acetals (**1.33**),[122] sulphoxide (**1.34**),[128] oxazolines (**1.35**),[121,129,130] hydrazones (**1.36**)[131–133] and other amines (**1.37**)[134] have all been implemented in ferrocene functionalisation with a high degree of diastereoselective control. A number of these approaches have also been successfully implemented with chromium arenes.[135–137]

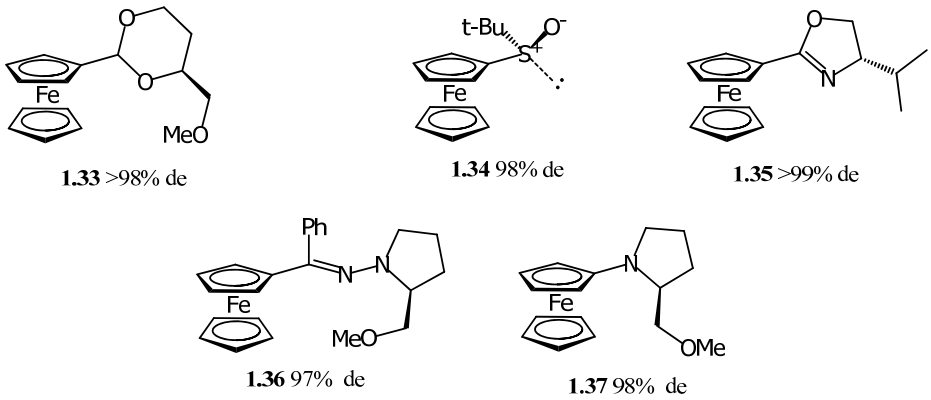

Figure 1.17: Examples of chiral diastereoselective ortholithiation directing groups employed on ferrocenes. **1.33**,[122] **1.34**,[128] **1.35**,[121,129,130] **1.36**,[131–133] **1.37**.[134]

As observed a number of different asymmetric approaches exist for the synthesis of planar–chiral ferrocenes utilising organolithium chemistry. In the following section, a discussion surrounding the properties of alkyllithiums and the mechanism of ortholithiation will be addressed, in an effort to highlight the means through which stereocontrol over the functionalisation of planar systems is achieved using organolithium chemistry.

1.4 Alkyllithiums and the Mechanism of Ortholithiation

The mechanism through which ortholithiation occurs is known to be complex, and to varying degrees probably relies on simplistic descriptions of highly complex mechanisms.[124,138] However the exquisite control ortholithiation approaches offer in terms of regioselectivity and stereocontrol in pro–chiral systems provides ample motivation for grappling with complexity in an effort to better appreciate and understand the factors behind these remarkable reactions. This brief discussion will begin with reviewing the general behaviour of alkyllithiums in solution.

1.4.1 Alkyllithiums in solution

Alkyllithiums are known to be essentially ionic compounds, displaying strong polarisation of the carbon lithium bond,[139] typically resulting in the aggregation of the alkyllithiums to stabilise this electron deficiency.[124,140] It is possible to make certain generalisations regarding aggregation states: the less sterically hindered the alkyllithium, the more prone it will be to aggregation.[124] For example; primary alkyllithiums (non–branched) exist as hexamers in hydrocarbon solutions, whereas secondary and tertiary alkyllithiums exist as tetramers.[124] The addition of coordinating (electron donating) or Lewis basic solvents/ligands to this mixture results in a change in the speciation of the alkyllithiums as an alternative source of electron density is available to the alkyllithiums and breakdown of the stabilising aggregates can occur.[124] Table 1.1 (taken in part from Clayden's *Organolithiums: Selectivity for synthesis*)[124] displays the general aggregation trends of a number of alkyllithiums in hydrocarbons and coordinating ethereal solvents: diethyl ether and tetrahydrofuran.

Table 1.1: Aggregation of alkyllithiums in solution.[124]

Hexameric	Tetrameric	Dimeric	Monomeric
Hydrocarbon Solution			
EtLi	*i*PrLi	$PhCH_2Li$	–
*n*BuLi	*s*BuLi		
MeLi	*t*BuLi		
In Et_2O or THF			
–	EtLi	*i*PrLi	$PhCH_2Li$
	*n*BuLi[1]	*s*BuLi	*t*BuLi
	MeLi	*t*BuLi[3]	
	*s*BuLi[2]	PhLi	

Notes: 1) *n*BuLi is present as a tetramer in Et_2O[141] and as a temperature dependent mixture of dimer and tetramer in THF.[142] 2) *s*BuLi remains a tetramer when only coordinated to TMEDA in hydrocarbons but is present as a dimer in THF or Et_2O.[124] 3) *t*BuLi displays a temperature dependent speciation between dimer and monomer in THF but exists predominantly as a dimer in Et_2O.[143]

1.4.2 Aggregation and Reactivity of Alkyllithiums

Intuitively, one would expect that the reactivity of a highly aggregated alkyllithium would be different to that of a lower aggregated form. For this particular reason, reactions involving alkyllithiums are often performed in ethereal solvents, and/or contain Lewis basic additives in hydrocarbon solutions, as the kinetic reactivity of a highly aggregated alkyllithium can be considerably worse than its pK_a value would suggest.[124] As observed in Table 1.1, the Lewis basic characteristics of ethereal solvents can be clearly seen in the general shift towards a lower aggregate form for all the alkyllithiums displayed. Deaggregating solvents/additives are not limited to the ethers, however, due to the extremely basic nature of alkyllithiums in solution, their Lewis basicity should be balanced by a strong resistance to attack/degradation by the alkyllithium.[124] The choice of solvent and reaction temperature should take into consideration the stability of the alkyllithium in that particular system, as all ethers and most additives are known to decompose in the presence of alkyllithium reagents.[144] A number of common additives used in alkyllithium chemistry, in decreasing order of activating effect[124] are HMPA, PMDTA, (−)–sparteine, DMPU, TMEDA, THF, TBME and Et_2O (Figure 1.18). The use of metal oxides as complexing agents has been shown to significantly increase the basicity of alkyllithiums, hence

mixtures of potassium *tertiary* butoxide and alkyllithiums have also been used, affording highly basic reagents (for example Schlossers base or LiCKOR).[124,145]

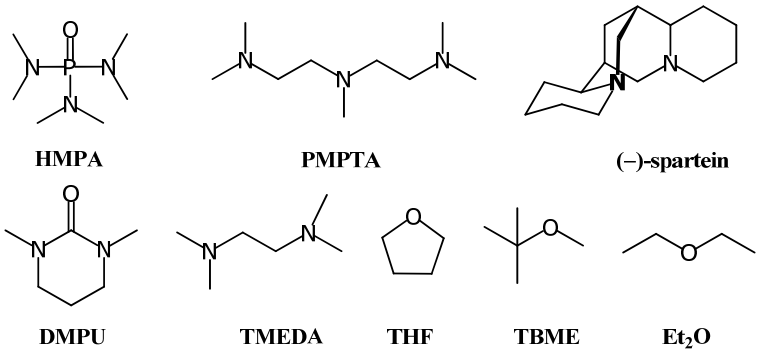

Figure 1.18: Common additives in alkyllithium chemistry.

The use of Lewis basic solvents/additives is known to increase the reactivity of the alkyllithium in solution, and it has been shown that the reactivity of an alkyllithium is strongly dependent on its speciation.[124,146,147] It is nonetheless, not possible to categorically state that the lower the aggregation state of the alkyllithium is the more reactive it will be.[148] This is certainly true in some circumstances, however other factors can play an important, but not always visible role, in the reaction.[124,149] Ligation that serves to stabilise the lower energy ground state of the alkyllithium complex will only effectively reduce the reactivity of the alkyllithium, as will strong ligation of a lower aggregation form of the alkyllithium.[148] Thus a successful ligand should effectively raise the energy of the ground state, possessing some coordination ability for the transition state, while being labile enough to allow the substrate access to the alkyllithium.[148] The stabilisation of the lithiated product by the solvent/ligand could also play a decisive role in determining the course of a reaction and ultimately determine the "reactivity" of alkyllithium.[124]

Due to the pyrophoric nature of many alkyllithium reagents, the study of their aggregation state is not experimentally simple. They have been studied using NMR techniques, by freezing point measurements, theoretical calculations, and in the solid state using x–ray diffraction.[140,150] Their speciation in solution is often temperature dependent, and known to change with the presence of impurities (such as lithium oxides which result from their reaction with oxygen).[146] From this brief overview of alkyllithiums in solution, it should be apparent that their behaviour cannot be straightforwardly explained, and due to this complexity, determination of the exact mechanisms through which lithiation reactions occur poses a considerable challenge.[148]

1.4.3 Classes of Directing Groups and the Mechanism of Ortholithiation

If one considers the pK_a of butane which is approximately 50,[151] and the pK_a of benzene which is approximately 43,[151] there is enough of a difference to assume that *n*BuLi should be able to deprotonate benzene based purely on thermodynamics. However, owing to the highly aggregated form of the alkyllithium in hydrocarbon solvents this reaction, in a practical sense, fails to occur without the addition of an additive. The tertiary alkyl group *t*BuH (derived from protonation of *t*BuLi) has a pK_a of 71[152] hence it should allow access to a wide range of lithiated aromatic systems, however, for the deprotonation to have any regioselective utility on functionalised systems, there either has to be a marked difference in pK_a of the different positions on the aromatic ring, or some other form of directing effect must be in operation. Fortunately, the electron deficient nature of alkyllithiums provides a handle through which regioselectivity can be controlled as the placement of a Lewis basic group on the arene can induce complexation between the substrate and the alkyllithium and consequently exposes the ortho protons to lithiation. There is however, often a subtle interplay between the relative acidity of aromatic protons and the proximity to a Lewis basic directing group as illustrated by the lithiation of *p*–methoxy–*N*,*N*–dimethylaniline **1.38** (Scheme 1.10).[153] The most acidic protons are *meta* to the amine or *ortho* to the methoxy group due to its inductive effect[154] and greater electronegativity.[155] When TMEDA is present in the solution, the Lewis acidic character of the alkyllithium is seemingly reduced, with predominant lithiation *ortho* to the methoxy group (**1.39**). Contrastingly, when only *n*BuLi is present, it coordinates with the Lewis basic amine, resulting in the most kinetically favourable lithiation occurring *ortho* to the amine (**1.40**), as opposed to thermodynamic lithiation *ortho* to the methoxy.

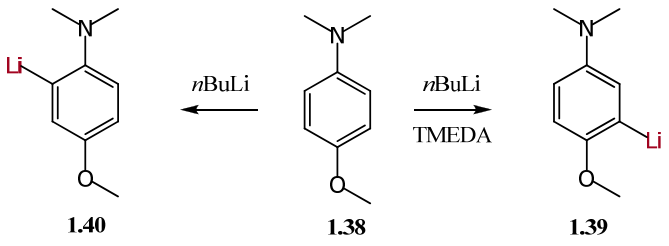

1.40 **1.38** **1.39**

Scheme 1.10: Lithiation of *p*–methoxy–*N*–*N*–dimethylbenzylamine.

A wide range of groups are known to direct ortholithiation and have been thoroughly discussed in Clayden *Organolithiums: Selectivity for Synthesis*,[124] as well as comprehensive reviews by Snickers[125] and Gschwend and Rodriguez.[154] Drawing on this excellent literature, ortholithiation directors can be broadly divided into the *N* and *N*+*O* class,[125] the *S*+*O* class,[156] the *O* class[123,135] and halogen directors.[124,149] A few selected examples of commonly used directing groups are

shown below in Figure 1.19.[124] Directing groups possess differing abilities to direct ortholithiation,[125] which is perhaps most evident in the range of temperatures required to perform lithiation. Strongly directing groups such as the *O*–carbamates, amides, sulphoxides, sulphones and sulphonamide easily facilitate ortholithiation at −78 ºC, where as ethers, anilines and remote amines are generally lithiated between −20 ºC and room temperature.

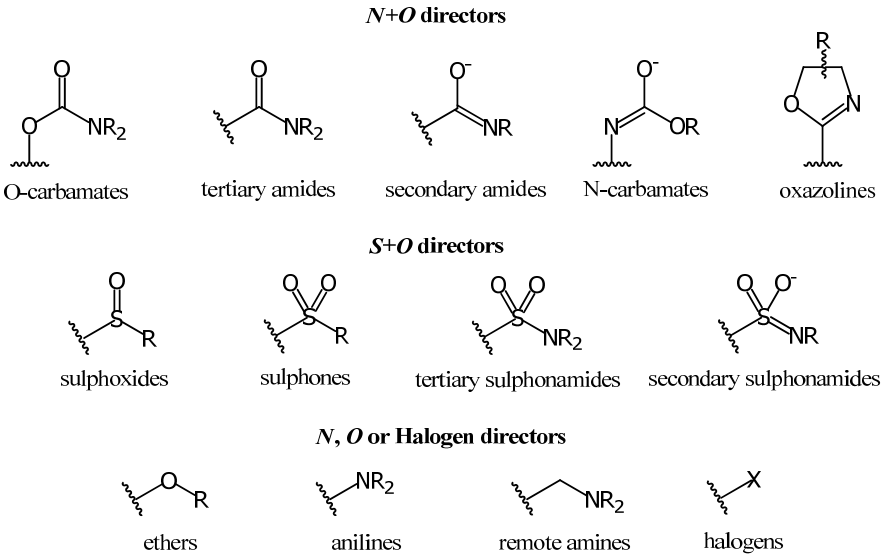

Figure 1.19: Common ortholithiation directing groups.[124]

The ability of a directing group to direct lithiation at low temperatures stems from its capability to acidify the ortho protons as well as providing a strong Lewis basic site to coordinate the alkyllithium. The combination of these two features in a good directing group must be balanced by a strong resistance to nucleophilic addition/degradation by the alkyllithium which is often accomplished by creating steric constraints around the electrophilic centre of the directing group.[124,125] The acidifying effect of a number of common directing groups has been established by Fraser *et al.*,[157] as has the influence of acidity in determining the regioselectivity of metallation in a review by Schlosser.[145,158]

The exact mechanism through which ortholithiation occurs is the subject of much discussion,[138,159] however a number of general comments regarding the mechanism can be made.[124] The directing group acts as a point of coordination for the alkyllithium and allows the formation of a complex between the substrate and the alkyllithium.[154] Directing groups could also possibly temporarily reduce the aggregation state of the alkyllithium.[154] It appears that this complexation is reversible,[160] however this point of coordination allows for the rate determining abstraction of a proton from the position *ortho* to the directing group and formation of the lithiated intermediate.[154,160] Stabilization of the lithiated intermediate by coordination to the directing

group,[125,154] seemingly also occurs, and is supported by observations that generally only a mono ortholithiated species forms even when excess alkyllithium is utilised.[161,162] Further evidence of a coordinated intermediate comes from the greater exothermic energy values for the quench of *p*–lithiated vs *O*–lithiated compounds.[163]

Ortholithiation has been studied computationally by a number of groups.[138,159,164,165] The results appear to confirm that pre–complexation of the alkyllithium with the directing group occurs, however there are a number of plausible mechanisms through which lithiation can occur, mainly due to different aggregation/complexation states of the alkyllithium. Collum *et al.* recently investigated the ortholithiation of aryl oxazolines using *n*BuLi and TMEDA, revealing some interesting mechanistic details.[138] As with previous reports regarding ortholithiation, the authors were forced to include a number of different forms of the alkyllithium TMEDA complexes (monomer, dimer, and triple ion see Figure 1.20), the energetics of which could not be directly numerically compared. They did find however that different forms of the alkyllithium complex behaved significantly differently with respect to *O* versus *N* coordination in the oxazoline system. Triple ion based calculations suggested generally minor energetic differences between both *O* or *N* coordination, whereas the monomer–based transitions had a marked preference for N coordination. Experimentally, it appears as if an *N*–coordinated mechanism occurs in cases with high selectivity.[166] Collum also observed that a large influence is exerted by the size and position of the substituents on the oxazolinyl ring on the preference between *O* versus *N* coordination. Therefore computationally it is not easy to predict mechanistically how the reaction proceeds, as both the steric effects of the substrate as well as the speciation of the alkyllithium complex appear to have far reaching implications for the course of the reaction.

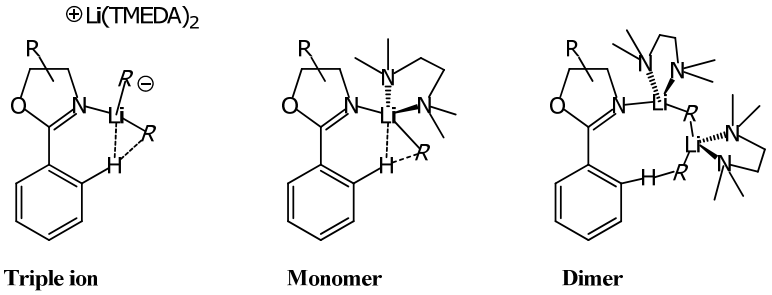

Figure 1.20: Transition states for the ortholithiation of an aryl oxazoline using RLi and TMEDA.[138]

1.4.4 Synthesis of Alkyllithiums

Alkyllithium reagents can be synthesised in a number of different ways (Scheme 1.11).[167] They can be made as the product of exchange reactions (permutational interconversion) with alkyl

halides (generally iodides or bromides) and alkyllithiums, usually using *t*BuLi.[167,168] This approach is generally limited to the preparation of primary short–lived specialist reagents due to the need for ethereal solvents during synthesis, thereby limiting their usefulness as their storage becomes problematic due to decomposition of the solvent.[124,144] They can also be synthesised by proton abstraction from hydrocarbons (ortholithiation falls under this wide class of reactions), using a pre–existing alkyllithium.[167,169]

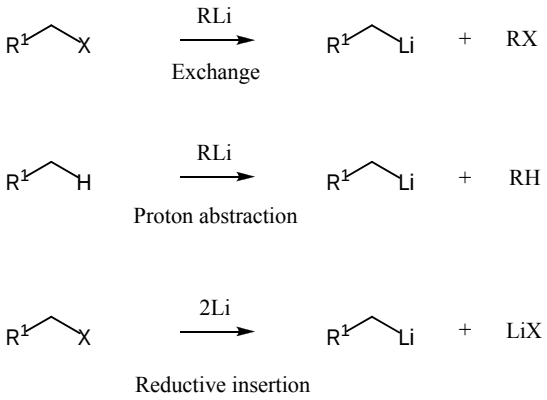

Scheme 1.11: Synthesis of organolithiums.

The most common route, employed for the synthesis of most commercial organolithium reagents, is the synthesis of alkyllithiums from alkyl halides and lithium metal by reductive insertion into the carbon halogen bond using two equivalents of lithium metal.[167,170–172] *The Chemistry of Organolithium Compounds* provides an excellent overview of the established methodology for the synthesis of a wide range of alkyllithium compounds by reductive insertion.[167] When synthesising alkyllithium reagents by this approach a number of factors must be carefully considered. Proton abstraction and elimination from unreacted alkyl halide starting material by the alkyllithium must be carefully controlled. For this precise reason alkyl chlorides are typically preferred, as they are most resistant to attack by the newly formed alkyllithium,[124] which fortunately is also complemented by the lower solubility of lithium chloride in ethereal solvents and hydrocarbons.[124] The rate of reaction relative to the rate of addition of the alkyl halide is therefore crucial in preventing undue exposure of the alkyl halide starting material to the newly formed organolithium compound.[173] Furthermore the stability of the alkyllithium in the solvent should also be considered, as decomposition of ethereal solvents in the presence of alkyllithiums is well known[124,144] (hence the use of ethereal solvents are often limited to low temperatures). Perplexingly though, the synthesis of alkyllithium reagents are often more readily accomplished in ethereal solvents or with addition of small quantities of ethereal additives in alkane solvents.[170,174] It has also been established that the presence of a sodium impurity (typically 1 – 2%)[175] in the lithium is preferable, if not a prerequisite, in the synthesis of alkyllithiums.[176]

The mechanism of formation of alkyllithiums proceeds by a single electron transfer to the σ* orbital of the C–X bond, promoting bond cleavage and the formation of the alkyl radical which is subsequently trapped by another lithium radical forming the alkyllithium.[124] Due to the stability of the intermediate alkyl radicals, the rate of formation of alkyllithiums follows the following order 3º>2º>1º, making it theoretically easier to form tertiary reagents. Practically however the basicity of the formed alkyllithium creates a greater chance of reacting with the starting alkyl halide.

1.4.5 Oxazoline Directed Ortholithiation

The incorporation of chiral oxazolines in asymmetric reactions can, to a large extent, be ascribed to the pioneering work of A.I. Meyers, who over the course of nearly twenty years demonstrated the remarkable ability of this heterocycle to both regioselectively and asymmetrically direct lithiations.[177] The use of chiral oxazolines for the diastereoselective functionalisation of ferrocene dates back to 1995 when simultaneous reports by Richards,[129] Uemera[130] and Sammakia[121] appeared detailing a new route to generating control over incorporation of planar chirality into the ferrocene structure. The selectivity of the reaction was determined to be highly sensitive to the choice of solvent, the alkyllithium and the addition of TMEDA,[178] with optimal results being obtained when the ferrocene was metallated using *n*BuLi or *s*BuLi in hexane in conjunction with the additive TMEDA. As already mentioned, oxazolines contain two possible heteroatoms (O or N) through which coordination of the alkyllithium can occur. Collum *et al.* indicated that theoretically it is difficult to determine which heteroatom will facilitate coordination and subsequent lithiation.[138,159] With ferrocenes, at any rate, an *N* coordinating mechanism appears to have been confirmed by the synthesis of a conformationally fixed ferrocenyloxazoline (**1.40** – Scheme 1.12) by Sammakia *et al.*[166] Lithiation of this compound produced a single diastereomer, thereby appearing to confirm a nitrogen–coordinating mechanism. The azaphilicity of alkyllithiums has been observed by a number of authors,[179–181] and seems to be supported by a study into the polarisation ($^{\delta+}$O–C=N$^{\delta-}$) of the imino moiety.[182] However the possibility of competing *O*–and *N*–directed lithiation also occurring has been expressed by a number of authors, which does create some doubt with respect to a purely nitrogen coordinated mechanism.[121,178,183]

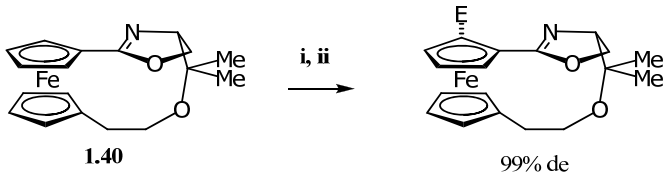

Scheme 1.12: Restricted conformation for conformation of *N*–directed pathway for ortholithiation.[166] Reagents and conditions: i) *s*BuLi, THF, ii) E^+.

Presuming nitrogen coordination during lithiation, the transition state of the oxazoline has been described. The R–group (alpha to the nitrogen) adopts a downwards direction towards the metal centre, allowing the lithium reagent to approach unhindered from above (Figure 1.21).[121,129,130] This is in contrast to the transition state involved in Ugi's amine[119] and Kagan's[128] chiral sulphoxide which sees the R groups pointing away from the metal centre during metallation seemingly trying to limit the thermodynamic penalty associated with this interaction (Figure 1.21). The same transition state is inferred from the configuration of the major diastereomer when Ugi's amine was employed on chromium arenes.[149,184] The same transition state has been postulated for chromium arenes oxazoline directed lithiation.[185] This conformation is almost certainly not the ground state for the ferrocenyloxazoline,[149] and hence the selectivity of the mechanism does not arise from the thermodynamically favoured conformation of the ferrocenyloxazoline, but is dictated through the interaction between the alkyllithium complex and the chiral environment of the oxazoline alkyl group. In contrast to the sulphoxide and amine results, the chiral centre of the oxazoline is further removed from the Cp ring and the iron centre, possibly reducing the thermodynamic penalty the oxazoline has to endure by adopting this conformation.[129] By comparing these dichotomous transition states, it is possible to imagine that there are two competing aspects potentially at play: one is the dynamics of the conformational interaction of the directing group and the metal centre, and the other is the interaction between the metal centre and the approaching alkyllithium, in conjunction with its coordination to the directing group. In an asymmetric ortholithiation reaction, one would want either one of these effects to dominate the transition state, but not competition between them.

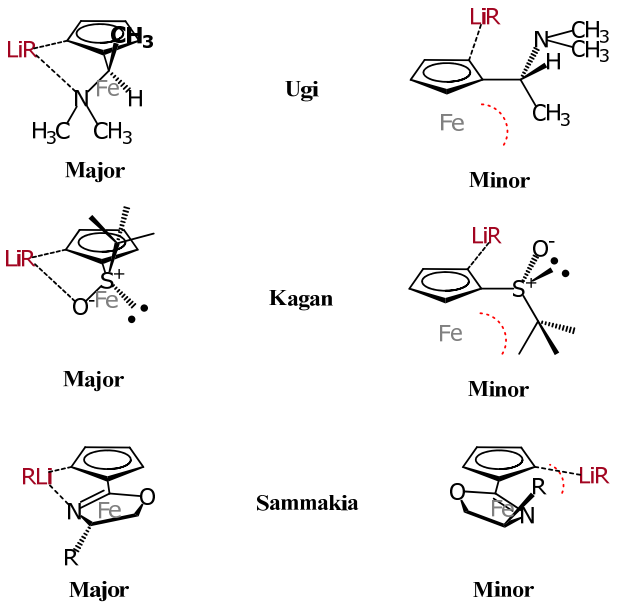

Figure 1.21: Transition states for ortholithiation of ferrocene. Ugi *et al.*,[119] Kagan *et al.*,[128] Sammakia *et al.*[166]

1.4.6 Configurational Stability of Organolithiums

Although often taken for granted, the configurational stability of the lithiated intermediate is important if diastereoselectivity is to be generated and maintained. The configurational instabilities of alkyllithiums are well documented, particularly with respect to their synthesis from chiral secondary and tertiary alkyl starting materials.[124] The stability of aryllithiums are less explicitly documented in the chemical literature, however stabilisation of the product of lithiation reactions is an important consideration, especially when regio/stereoselective synthesis is required. This concept is well illustrated with a rather surprising example from Meyers *et al.*[169] The authors observed that the use of ethoxyvinylithium in conjunction with HMPA resulted in lithiation *para* to the oxazoline of *m*–methoxy oxazoline **1.40** rather than the anticipated ortholithiation product (Scheme 1.13). If the reactions were performed at low temperatures and then allowed to warm to 0 ºC, complete conversion of the *para*–lithiated product **1.41** to the *ortho* lithiated product **1.42** was observed. Thus the coordinating effect of the strongly directing oxazoline group appeared to allow conversion of the kinetic product to the thermodynamically more stable product. This example also illustrates that significant stabilisation can be achieved through coordination of the aryllithium to the oxazoline directing group, which would appear to indicate that the aryllithium ortho to the oxazoline directing group should be thermodynamically stable. Clearly however this work by Meyers indicates that aryllithiums are not necessary stable, and intermolecular lithium transfer may occur,[169,186] although the occurrence of regioselective thermodynamic and kinetic aromatic lithiation products has rarely been seen.[169,187]

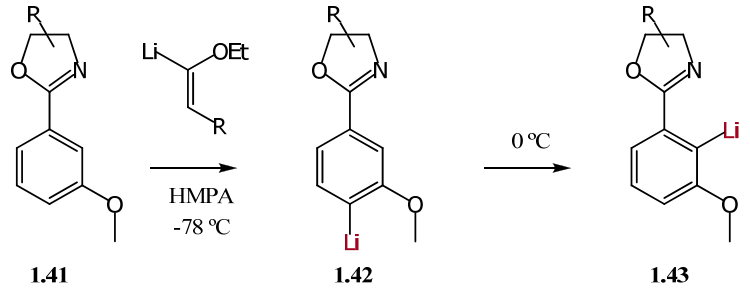

Scheme 1.13: Thermodynamic rearrangement of lithiated product.

Returning to experiments performed on ferrocenes, Kagan *et al.* claim that the diastereoselectivity observed for the ortholithiation of their chiral ferrocene acetal is under kinetic control.[122,123] This statement is supported by a decrease in selectivity when lithiation was performed at increased temperatures. However, no decrease in diastereoselectivity was reported when the lithiated intermediate was warmed to room temperature, indicating the thermodynamic stability of the lithiated intermediate.

1.4.7 Other Reactions of Lithiated Compounds

A number other reactions associated with *ortho* directing groups are also known. The formation of benzynes from ortho lithiated products has been well established.[188,189] Elimination of LiCl from the ortholithiated product **1.44** results in the formation of the benzyne intermediate **1.45**, which is then selectively alkylated alpha to the oxazoline by addition of an alkyllithium (**1.46** – Scheme 1.14), due to the coordination of the alkyllithium complex with the oxazoline directing group.[124]

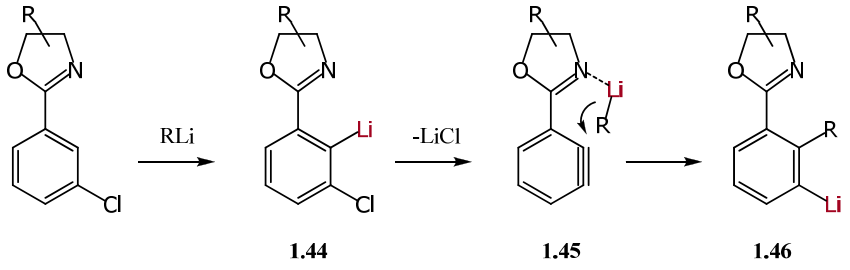

Scheme 1.14: Benzyne formation and regioselective alkylation.[189]

Another possible reaction that can occur on aryl oxazolines is 1,2 addition of the alkyllithium to the arene,[177] causing dearomatisation.[124,190] In work by Meyers *et al.*[177] on chiral naphthyl oxazolines (**1.47** – Scheme 1.15), formation of the expected ortholithiation product failed to occur and instead addition of the alkyl group from the secondary alkyllithium to the aromatic system was observed (**1.48** – Scheme 1.15). The intermediate product could be quenched

diastereoselectively (*anti* addition) with various electrophiles, leading to the formation of the 1,2 addition products (**1.49** – Scheme 1.15).

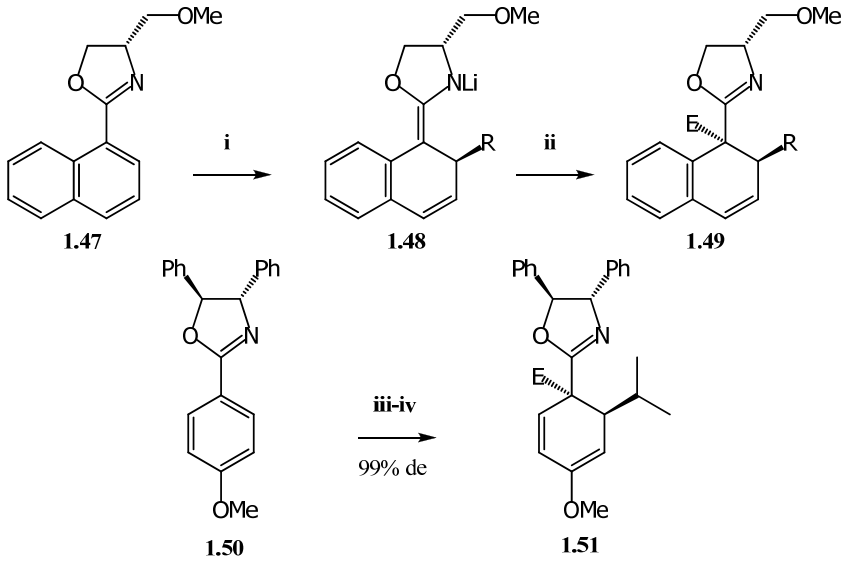

Scheme 1.15: Dearomatisation reactions. Reagents and conditions: i) RLi, THF, ii) E^+,iii) *i*PrLi, DMPU, THF, iv) MeI > 99% de.

In an extension of this initial work to simple aromatic systems, Clayden *et al.* utilised chiral diphenyl aryl oxazolines **1.50** to induce diastereoselectivity into the dearomatisation reaction on a simple arene *en route* to the synthesis of carbosugars (**1.51** – Scheme 1.15).[190] It was determined that the presence of a DMPU complex with secondary alkyllithiums was critical to the preference of the reaction to form the dearomatised product. It should be noted that other groups have also induced diastereoselectivity into this reaction by utilising stoichiometric complexation to metals.[191]

1.5 Proposed Project and Target Molecule

As briefly discussed, the lack of stereoselective functionalisation methodology for obtaining inherently chiral calixarenes appeared to suggest that a need existed for an investigation into an asymmetric approach. Inherently chiral calixarenes can be subdivided into a number of different categories depending on the region of the molecule that is functionalised, namely the upper rim, lower rim or multi–region. Owing to the structural diversities of these molecules the development of a general asymmetric approach towards inherently chiral molecules would be extremely challenging, hence we decided to focus on developing asymmetric access towards a single motif. In addressing our choice as to which structure of inherent chirality we wanted to access, we found

inspiration in 1,2–disubstituted ferrocenes which have found celebrated use as asymmetric ligands in multiple metal catalysed transformations (**1.52** – Figure 1.22).[38,87] In terms of exploring this structure with calixarenes, upper rim *meta*–functionalised examples (**1.53** – Figure 1.22) have not been well explored as ligands in asymmetric reactions, hence we decided to target an asymmetric approach towards this class of inherently chiral calixarene.

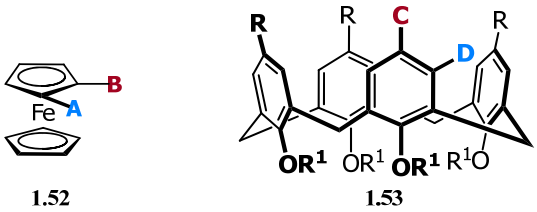

1.52 **1.53**

Figure 1.22: 1,2–Disubstituted ferrocene and 1,2 *meta*–functionalised calixarene.

In terms of addressing how asymmetry would be imparted during functionalisation, an approach that has proved successful in ferrocenes is the use of chiral ortholithiation directing groups. In choosing an ortholithiation director group we required a chemically robust and easily synthetically accessible functionality, that also possessed the qualities inherent to powerful directing groups. These criteria appeared to be met by chiral oxazolines,[177] which can be easily obtained from amino acid sources,[192] are known to be robust,[193] are powerful ortholithiation directors,[125,177] and have been shown to provide a highly selective route to planar chiral ferrocenes.[178] A further possible benefit to the use of an oxazoline directing group is the large number of asymmetric ligands that contain this functionality as basic coordinating groups.[194]

The calixarene system afforded us a number of choices, namely: which calix[n]arene should be used, what protection strategy should be employed for the phenolic positions and should the methodology be attempted on a butylated or debutylated system (Figure 1.23)? As calix[4]arene is the most studied calixarene,[1] it appeared that the development of asymmetric methodology on this system would be of the greatest potential interest for the chemical community. A number of protection strategies have been employed in calixarenes,[1] however esters[30] or ethers are most commonly used.[31] Being unsure of the stability of the ester functionality to alkyllithiums it appeared that alkylation of the phenolic positions was preferable. We also decided to first attempt the reaction with retention of the *t*–butyl groups on the upper rim of the calixarene. We thought that possible steric interactions between the oxazoline and the *t*–butyl groups could result in the oxazoline adopting a preferential conformation that could lead to diastereoselectivity when lithiated. There are a number of different oxazolines that have been employed for pro–chiral lithiations,[177] however the isopropyl oxazoline appeared to be a simple and relatively inexpensive

option, which had also yielded impressively high diastereoselectivity in the hands of other researchers.[178]

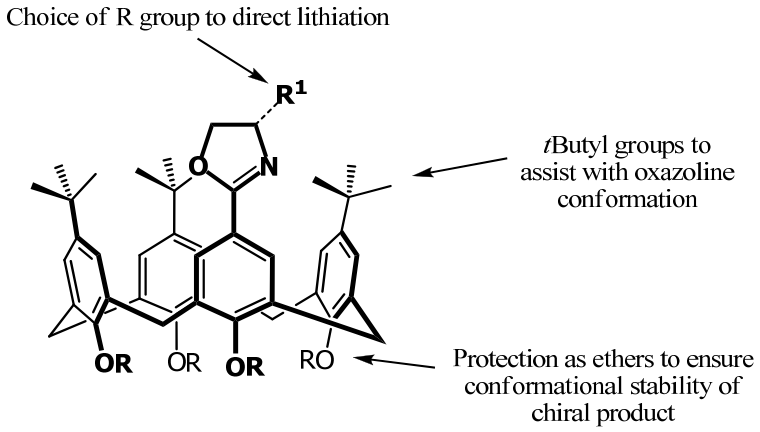

Figure 1.23: Target oxazoline calixarene.

The initial undertaking would be to obtain the oxazoline functionalised calixarene, followed by its attempted ortholithiation and functionalisation, and determination of the diastereoselectivity afforded by this methodology. Having ascertained if this proposed approach enabled a degree of selectivity to be obtained, the removal of the oxazoline group would be attempted in order to illustrate that this methodology allows for further functionalisation of the calixarene. Having performed these preliminary undertakings, further optimisation of the directing group would be attempted, as well as investigating the mechanism/effects surrounding the reaction.

1.6 References

(1) Gutsche, D. C. *Calixarenes: an introduction* 2ed.; RSC Publishing: Cambridge, 2008.

(2) Wieser, C.; Dieleman, C. B.; Matt, D. *Coord. Chem. Rev.* **1997**, *165*, 93.

(3) Agrawal, Y. K.; Bhatt, H. *Bioinorg. Chem. Appl.* **2004**, *2*, 237.

(4) Ludwig, R. *Microchim. Acta.* **2005**, *152*, 1.

(5) Atwood, J. L.; Barbour, L. J.; Jerga, A. *Science* **2002**, *296*, 2367.

(6) Atwood, J. L.; Barbour, L. J.; Jerga, A. *Angew. Chem. Int. Ed.* **2004**, *43*, 2948.

(7) Van Dienst, E.; Bakker, W. I. I.; Engbersen, J. F. J.; Verboom, W.; Reinhoudt, D. N. *Pure Appl. Chem.* **1993**, *65*, 387.

(8) Baeyer, A. v. *A. Ber* **1872**, *5*, 1094.

(9) Baekeland, L. H. *J. Ind. Eng. Chem.* **1913**, *4*, 737.

(10) Zinke, A.; Ott, R.; Garrana, F. H. *Monatsh. Chem.* **1958**, *89*, 135.

(11) Zinke, A.; Ziegler, E. *Fette Seifen* **1950**, *52*, 588.

(12) Cornforth, J. W.; D'Arcy Hart, P.; Nicholls, G. A.; Rees, R. J. W.; Stock, J. A. *Br. J. Pharmacol. Chem.* **1955**, *10*, 73.

(13) Gueniffe. H; Kammerer, H.; Klesper, E. *Makromol. Chem.* **1972**, *162*, 199.

(14) Kammerer, H.; Happel, G.; Caesar, F. *Makromol. Chem.* **1972**, *162*, 179.

(15) Andreetti, G. D.; Ungaro, R.; Pochini, A. *J. Chem. Soc., Chem. Commun.* **1979**, 1005.

(16) Andreetti, G. D.; Ungaro, R.; Pochini, A. *J. Chem. Soc., Chem. Commun.* **1981**, 533.

(17) Coruzzi, M.; Andreetti, G. D.; Bocchi, V.; Pochini, A.; Ungaro, R. *J. Chem. Soc., Perkin Trans. 2* **1982**, 1133.

(18) Gutsche, C. D.; Iqbal, M.; Stewart, D. *J. Org. Chem* **1986**, *51*, 742.

(19) Gutsche, C. D.; Pagoria, P. F. *J. Org. Chem.* **1985**, *50*, 5795.

(20) Gutsche, C. D.; Bauer, L. J. *Journal of the American Chemical Society* **1985**, *107*, 6052.

(21) Gutsche, C. D. *Accounts of Chemical Research* **1983**, *16*, 161.

(22) Gutsche, C. D.; Dhawan, B.; No, K. H.; Muthukrishnan, R. *J. Am. Chem. Soc.* **1981**, *103*, 3782.

(23) Andreetti, G. D.; Pochini, A.; Ungaro, R. *J. Chem. Soc., Perkin Trans. 2* **1983**, 1773.

(24) Simaan, S.; Biali, S. E. *J. Phys. Org. Chem.* **2004**, *17*, 752.

(25) Dahan, E.; Biali, S. E. *J. Org. Chem.* **1991**, *56*, 7269.

(26) Grootenhuis, P. D. J.; Kollman, P. A.; Groenen, L. C.; Reinhoudt, D. N.; Van Hummel, G. J.; Ugozzoli, F.; Andreetti, G. D. *J. Am. Chem. Soc.* **1990**, *112*, 4165.

(27) Xu, B.; Carroll, P. J.; Swager, T. M. *Angew. Chem. Int. Ed.* **1996**, *35*, 2094.

(28) Van Loon, J. D.; Arduini, A.; Coppi, L.; Verboom, W.; Pochini, A.; Ungaro, R.; Harkema, S.; Reinhoudt, D. N. *J. Org. Chem.* **1990**, *55*, 5639.

(29) Verboom, W.; Durie, A.; Egberink, R. J. M.; Asfari, Z.; Reinhoudt, D. N. *J. Org. Chem.* **1992**, *57*, 1313.

(30) See, K. A.; Fronczek, F. R.; Watson, W. H.; Kashyap, R. P.; Gutsche, C. D. *J. Org. Chem.* **1991**, *56*, 7256.

(31) Iwamoto, K.; Araki, K.; Shinkai, S. *J. Org. Chem.* **1991**, *56*, 4955.

(32) Scully, P. A.; Hamilton, T. M.; Bennett, J. L. *Org. Lett.* **2001**, *3*, 2741.

(33) Gormar, G.; Seiffarth, K.; Schulz, M.; Zimmermann, J.; Flamig, G. *Macromol. Chem. Phys.* **1990**, *191*, 81.

(34) Bohmer, V.; Merkel, L.; Kunz, U. *J. Chem. Soc., Chem. Commun.* **1987**, 896.

(35) Zheng, Y.–S.; Luo, J. *J. Inclusion Phenom. Macrocyclic Chem.*, **2011**, 35.

(36) Szumna, A. *Chem. Soc. Rev.*, **2010**, *39*, 4274.

(37) Togni, A.; Hayashi, T. *Ferrocenes: Homogeneous Catalysis, Organic Synthesis, Materials Science*; Wiley–VCH, 1995.

(38) Stepnicka, P.; Editor *Ferrocenes: Ligands, Materials and Biomolecules*; John Wiley & Sons Ltd., 2008.

(39) Berthod, M.; Mignani, G.; Woodward, G.; Lemaire, M. *Chem. Rev.* **2005**, *105*, 1801.

(40) Mateos–Timoneda, M. A.; Crego–Calama, M.; Reinhoudt, D. N. *Chem. Soc. Rev.* **2004**, *33*, 363.

(41) Sola, J.; Helliwell, M.; Clayden, J. *J. Am. Chem. Soc.*, **2010**, *132*, 4548.

(42) Iwamoto, K.; Shimizu, H.; Araki, K.; Shinkai, S. *J. Am. Chem. Soc.* **1993**, *115*, 12228.

(43) Iwamoto, K.; Shimizu, H.; Araki, K.; Shinkai, S. *J. Am. Chem. Soc.* **1993**, *115*, 3997.

(44) Muthukrishnan, R.; Gutsche, C. D. *J. Org. Chem.* **1979**, *44*, 3962.

(45) Soi, A.; Pfeiffer, J.; Jauch, J.; Schurig, V. *Tet. Asymm.* **1999**, *10*, 177.

(46) Sansone, F.; Barboso, S.; Casnati, A.; Fabbi, M.; Pochini, A.; Ugozzoli, F.; Ungaro, R. *Eur. J. Org. Chem.* **1998**, 897.

(47) Yanagihara, R.; Tominaga, M.; Aoyama, Y. *J. Org. Chem.* **2002**, *59*, 6865.

(48) Sirit, A.; Yilmaz, M. *Turk. J. Chem.* **2009**, *33*, 159.

(49) Kwang, H. N.; Gutsche, C. D. *J. Org. Chem.* **1982**, *47*, 2713.

(50) Bohmer, V.; Wolff, A.; Vogt, W. *J. Chem. Soc., Chem. Commun.* **1990**, 968.

(51) Shinkai, S.; Arimura, T.; Kawabata, H.; Murakami, H.; Araki, K.; Iwamoto, K.; Matsuda, T. *Journal of the Chemical Society–Chemical Communications* **1990**, 1734.

(52) Shu, C.–M.; Liu, W.–C.; Ku, M.–C.; Tang, F.–S.; Yeh, M.–L.; Lin, L.–G. *J. Org. Chem.* **2002**, *59*, 3730.

(53) Linnane, P.; James, T. D.; Shinkai, S. *J. Chem. Soc., Chem. Commun.* **1995**, 1997.

(54) Timmerman, P.; Verboom, W.; Reinhoudt, D. N.; Arduini, A.; Grandi, S.; Sicuri, A. R.; Pochini, A.; Ungaro, R. *Synthesis–Stuttgart* **1994**, 185.

(55) Beer, P. D.; Cooper, J. B. *Chem. Commun.* **1998**, 129.

(56) Zheng, Y. S.; Huang, Z. T. *Synth. Commun.* **1997**, *27*, 1237.

(57) Vanloon, J. D.; Arduini, A.; Verboom, W.; Ungaro, R.; Vanhummel, G. J.; Harkema, S.; Reinhoudt, D. N. *Tetrahedron Lett.* **1989**, *30*, 2681.

(58) Dalla Cort, A.; Mandolini, L.; Pasquini, C.; Schiaffino, L. *N. J. Chem.* **2004**, *28*, 1198.

(59) Xu, Z.–X.; Zhang, C.; Zheng, Q.–Y.; Chen, C.–F.; Huang, Z.–T. *Org. Lett.* **2007**, *9*, 4447.

(60) Shirakawa, S.; Shimizu, S. *Eur. J. Org. Chem.* **2009**, 1916.

(61) Shirakawa, S.; Tanaka, Y.; Kobari, T.; Shimizu, S. *New J. Chem. FIELD Full Journal Title:New Journal of Chemistry* **2008**, *32*, 1835.

(62) IUPAC *J. Org. Chem.* **1968**, *35*, 2849.

(63) Shinkai, S.; Arimura, T.; Satoh, H.; Manabe, O. *J. Chem. Soc., Chem. Commun.* **1987**, 1495.

(64) Shinkai, S.; Arimura, T.; Kawabata, H.; Murakami, H.; Araki, K.; Iwamoto, K.; Matsuda, T. *J. Chem. Soc., Chem. Commun.* **1990**, 1734.

(65) Iwamoto, K.; Yanagi, A.; Arimura, T.; Matsuda, T.; Shinkai, S. *Chem. Lett.* **1990**, 1901.

(66) Ferguson, G.; Gallagher, J. F.; Giunta, L.; Neri, P.; Pappalardo, S.; Parisi, M. *J. Org. Chem.* **1994**, *59*, 42.

(67) Shu, C.–M.; Chung, W.–S.; Wu, S.–H.; Ho, Z.–C.; Lin, L.–G. *J. Org. Chem.* **1999**, *64*, 2673.

(68) Lhotak, P.; Dudic, M.; Stibor, I.; Petrickova, H.; Sykora, J.; Hodacova, J. *Chem. Commun.* **2001**, 731.

(69) Okada, Y.; Mizutani, M.; Ishii, F.; Nishimura, J. *Tetraherdon Lett.* **1997**, *38*, 9013.

(70) Arnaud–Neu, F.; Caccamese, S.; Fuangswasdi, S.; Pappalardo, S.; Parisi, M. F.; Petringa, A.; Principato, G. *J. Org. Chem.* **1997**, *62*, 8041.

(71) Matt, D.; Loeber, C.; Vicens, J.; Asfari, Z. *J. Chem. Soc., Chem. Commun.* **1993**, 604.

(72) Jin, T.; Jin, T.; Monde, K. *Chem. Commun.* **1998**, 1357.

(73) Dieleman, C.; Steyer, S.; Jeunesse, C.; Matt, D. *J. Chem. Soc., Dalton Trans.* **2001**, 2508.

(74) Yakovenko, A. V.; Boyko, V. I.; Danylyuk, O.; Suwinska, K.; Lipkowski, J.; Kalchenko, V. I. *Org. Lett.* **2007**, *9*, 1183.

(75) Luo, J.; Zheng, Q.–Y.; Chen, C.–F.; Huang, Z.–T. *Chem. Eur. J.* **2005**, *11*, 5917.

(76) Jeunesse, C.; Dieleman, C.; Steyer, S.; Matt, D. *J. Chem. Soc., Dalton Trans.* **2001**, 881.

(77) Verboom, W.; Bodewes, P. J.; van Essen, G.; Timmerman, P.; van Hummel, G. J.; Harkema, S.; Reinhoudt, D. N. *Tetrahedron.* **1995**, *51*, 499.

(78) Fu, D.–K.; Xu, B.; Swager, T. M. *J. Org. Chem.* **1996**, *61*, 802.

(79) Ikeda, A.; Yoshimura, M.; Lhotak, P.; Shinkai, S. *J. Chem. Soc., Perkin Trans. 1* **1996**, 1945.

(80) Miao, R.; Zheng, Q.–Y.; Chen, C.–F.; Huang, Z.–T. *J. Org. Chem.* **2005**, *70*, 7662.

(81) Xu, Z.–X.; Li, G.–K.; Chen, C.–F.; Huang, Z.–T. *Tetrahedron.* **2008**, *64*, 8668.

(82) Vedejs, E.; Jure, M. *Angew. Chem. Int. Ed.* **2005**, *44*, 3974.

(83) Bellemin–Laponnaz, S.; Tweddell, J.; Ruble, J. C.; Breitling, F. M.; Fu, G. C. *Chem. Commun.* **2000**, 1009.

(84) Xu, Z.–X.; Zhang, C.; Yang, Y.; Chen, C.–F.; Huang, Z.–T. *Org. Lett.* **2008**, *10*, 477.

(85) Shirakawa, S.; Moriyama, A.; Shimizu, S. *Eur. J. Org. Chem.* **2008**, 5957.

(86) Shirakawa, S.; Kimura, T.; Murata, S.–i.; Shimizu, S. *J. Org. Chem.* **2009**, *74*, 1288.

(87) Gómez Arrayás, R.; Adrio, J.; Carretero, J. C. *Angew. Chem. Int. Ed.* **2006**, *45*, 7674.

(88) Dai, L.–X.; Tu, T.; You, S.–L.; Deng, W.–P.; Hou, X.–L. *Acc. Chem. Res.* **2003**, *36*, 659.

(89) Atkinson, R. C. J.; Gibson, V. C.; Long, N. J. *Chem. Soc. Rev.* **2004**, *33*, 313.

(90) Fouda, M. F. R.; Abd–Elzaher, M. M.; Abdelsamaia, R. A.; Labib, A. A. *Appl. Organomet. Chem.* **2007**, *21*, 613.

(91) Herrmann, W. A.; *Ferrocene as a gasoline and fuel additive*. Wiley–VCH Verlag GmbH: 2002; Vol. 1, p 586.

(92) Kealy, T. J.; Pauson, P. L. *Nature* **1951**, *168*, 1039.

(93) Miller, S. A.; Tebboth, J. A.; Tremaine, J. F. *J. Chem. Soc.* **1952**, 632.

(94) Wilkinson, G.; Rosenblum, M.; Whiting, M. C.; Woodward, R. B. *J. Am. Chem. Soc.* **1952**, *74*, 2125.

(95) Fischer, E. O.; Pfab, W. *Z. Naturforsch.(B)* **1952**, *7*, 377.

(96) Laszlo, P.; Hoffmann, R. *Angew. Chem. Int. Ed.* **2000**, *39*, 123.

(97) Eiland, P. F.; Pepinsky, R. *J. Am. Chem. Soc.* **1952**, *74*, 4971.

(98) Woodward, R. B.; Rosenblum, M.; Whiting, M. C. *J. Am. Chem. Soc.* **1952**, *74*, 3458.

(99) Page, J. A.; Wilkinson, G. *J. Am. Chem. Soc.* **1952**, *74*, 6149.

(100) Wilkinson, G. *Org. Synth.* **1956**, *36*, 31.

(101) Jolly, W. L. *The Synthesis and Characterization of Inorganic Compounds*; Prentice–Hall Inc, 1970.

(102) Arimoto, F. S.; Haven, A. C. *J. Am. Chem. Soc.* **1955**, *77*, 6295.

(103) Weinmayr, V. *J. Am. Chem. Soc.* **1955**, *77*, 3012.

(104) Rausch, M. D.; Fischer, E. O.; Grubert, H. *J. Am. Chem. Soc.* **1960**, *82*, 76.

(105) Lindsay, J. K.; Hauser, C. R. *J. Org. Chem.* **1957**, *22*, 355.

(106) Rausch, M.; Vogel, M.; Rosenberg, H. *J. Org. Chem.* **1957**, *22*, 900.

(107) Weliky, N.; Gould, E. S. *J. Am. Chem. Soc.* **1957**, *79*, 2742.

(108) Mayo, D. W.; Shaw, P. D.; Rausch, M. *Chem. Ind.* **1957**, 1388.

(109) Thomson, J. B. *Tetrahedron Lett.* **1959**, 26.

(110) Westman, L.; Rinehart, K. L. *Acta Chem. Scand.* **1962**, *16*, 1199.

(111) Schloegl, K. *Top. Stereochem.* **1967**, *1*, 39.

(112) Schloegl, K. *Fortschr. Chem. Forsch.* **1966**, *6*, 479.

(113) Falk, H.; Schloegl, K.; Steyrer, W. *Monatsh. Chem.* **1966**, *97*, 1029.

(114) Cahn, R. S.; Ingold, C.; Prelog, V. *Angew. Chem. Int. Ed.* **1966**, *5*, 385.

(115) Rosillo, M.; Dominguez, G.; Perez–Castells, J. *Chem. Soc. Rev.* **2007**, *36*, 1589.

(116) Aratani, T.; Gonda, T.; Nozaki, H. *Tetrahedron Lett.* **1969**, 5453.

(117) Tsukazaki, M.; Tinkl, M.; Roglans, A.; Chapell, B. J.; Taylor, N. J.; Snieckus, V. *J. Am. Chem. Soc.* **1996**, *118*, 685.

(118) Price, D.; Simpkins, N. S. *Tetrahedron Lett.* **1995**, *36*, 6135.

(119) Marquarding, D.; Klusacek, H.; Gokel, G.; Hoffmann, P.; Ugi, I. *J. Am. Chem. Soc.* **1970**, *92*, 5389.

(120) Marquard.D; Klusacek, H.; Gokel, G.; Hoffmann, P.; Ugi, I. *Angew. Chem. Int. Ed* **1970**, *9*, 371.

(121) Sammakia, T.; Latham, H. A.; Schaad, D. R. *J. Org. Chem.* **1995**, *60*, 10.

(122) Riant, O.; Samuel, O.; Kagan, H. B. *J. Am. Chem. Soc.* **1993**, *115*, 5835.

(123) Riant, O.; Samuel, O.; Flessner, T.; Taudien, S.; Kagan, H. B. *J. Org. Chem.* **1997**, *62*, 6733.

(124) Clayden, J. *Organolithiums: Selectivity for Synthesis*; Pergamon: London, 2002; Vol. 23.

(125) Snieckus, V. *Chem. Rev.* **1990**, *90*, 879.

(126) Nishibayashi, Y.; Arikawa, Y.; Ohe, K.; Uemura, S. *J. Org. Chem.* **1996**, *61*, 1172.

(127) Deus, N.; Robles, D.; Herrmann, R. *J. Organomet. Chem.* **1990**, *386*, 253.

(128) Rebiere, F.; Riant, O.; Ricard, L.; Kagan, H. B. *Angew. Chem. Int. Ed.* **1993**, *32*, 568.

(129) Richards, C. J.; Damalidis, T.; Hibbs, D. E.; Hursthouse, M. B. *Synlett* **1995**, 74.

(130) Nishibayashi, Y.; Uemura, S. *Synlett* **1995**, 79.

(131) Enders, D.; Peters, R.; Lochtman, R.; Raabe, G.; Runsink, J.; Bats, J. W. *Eur. J. Org. Chem.* **2000**, 3399.

(132) Enders, D.; Peters, R.; Lochtman, R.; Raabe, G. *Angew. Chem. Int. Ed.* **1999**, *38*, 2421.

(133) Enders, D.; Peters, R.; Lochtman, R.; Runsink, J. *Synlett* **1997**, 1462.

(134) Ganter, C.; Wagner, T. *Chem. Ber.* **1995**, *128*, 1157.

(135) Kondo, Y.; Green, J. R.; Ho, J. *J. Org. Chem.* **1991**, *56*, 7199.

(136) Aube, J.; Heppert, J. A.; Milligan, M. L.; Smith, M. J.; Zenk, P. *J. Org. Chem.* **1992**, *57*, 3563.

(137) Uemura, M.; Daimon, A.; Hayashi, Y. *J. Chem. Soc., Chem. Commun.* **1995**, 1943.

(138) Chadwick, S. T.; Ramirez, A.; Gupta, L.; Collum, D. B. *J. Am. Chem. Soc.* **2007**, *129*, 2259.

(139) Weiss, E. *Angew. Chem. Int. Ed.* **1993**, *32*, 1501.

(140) Stey, T.; Stalke, D. In *The Chemistry of Organolithium Compounds*; Rappoport, Z., Marek, I., Eds.; John Wiley & Sons: 2004, p 47.

(141) West, P.; Waack, R. *J. Am. Chem. Soc.* **1967**, *89*, 4395.

(142) McGarrity, J. F.; Ogle, C. A. *J. Am. Chem. Soc.* **1985**, *107*, 1805.

(143) Hoffmann, R. W.; Kemper, B. *Tetrahedron Lett.* **1981**, *22*, 5263.

(144) Stanetty, P.; Mihovilovic, M. D. *J. Org. Chem.* **1997**, *62*, 1514.

(145) Schlosser, M. *Angew. Chem. Int. Ed.* **2005**, *44*, 376.

(146) McGarrity, J. F.; Ogle, C. A.; Brich, Z.; Loosli, H. R. *J. Am. Chem. Soc.* **1985**, *107*, 1810.

(147) Bailey, W. F.; Luderer, M. R.; Jordan, K. P. *J. Org. Chem.* **2006**, *71*, 2825.

(148) Collum, D. B. *Acc. Chem. Res.* **1992**, *25*, 448.

(149) Clayden, J. In *The Chemistry of Organolithium Compounds*; Rappoport, Z., Marek, I., Eds.; John Wiley & Sons: 2004, p 495.

(150) Jemmis, E.; Gopakuma, G. In *The Chemistry of Organolithium Compounds*; Rappoport, Z., Marek, I., Eds.; John Wiley & Sons: 2004, p 1.

(151) Clayden, J.; Greeves, N.; Warren, S.; Wothers, P. *Organic Chemistry*; Oxford University Press, 2000.

(152) Anslyn, E.; Dougherty, D. *Modern Physical Organic Chemistry*; 3rd ed.; University Science: New York, 2006.

(153) Slocum, D. W.; Jennings, C. A. *J. Org. Chem.* **1976**, *41*, 3653.

(154) Gschwend, H. W.; Rodriguez, H. R. *Heteroatom–facilitated lithiations*, 1979; Vol. 26.

(155) Slocum, D. W.; Jennings, C. A. *J. Org. Chem.* **1976**, *41*, 3653.

(156) Iwao, M.; Iihama, T.; Mahalanabis, K. K.; Perrier, H.; Snieckus, V. *J. Org. Chem.* **1989**, *54*, 24.

(157) Fraser, R. R.; Bresse, M.; Mansour, T. S. *J. Am. Chem. Soc.* **1983**, *105*, 7790.

(158) Schlosser, M. *Angew. Chem. Int. Ed.* **1998**, *37*, 1497.

(159) Chadwick, S. T.; Rennels, R. A.; Rutherford, J. L.; Collum, D. B. *J. Am. Chem. Soc.* **2000**, *122*, 8640.

(160) Anderson, D. R.; Faibish, N. C.; Beak, P. *J. Am. Chem. Soc.* **1999**, *121*, 7553.

(161) Jones, F. N.; Zinn, M. F.; Hauser, C. R. *J. Org. Chem.* **1963**, *28*, 663.

(162) Jones, F. N.; Vaulx, R. L.; Hauser, C. R. *J. Org. Chem.* **1963**, *28*, 3461.

(163) Klumpp, G. W.; Sinnige, M. J. *Tetrahedron Lett.* **1986**, *27*, 2247.

(164) Saa, J. M.; Deya, P. M.; Suner, G. A.; Frontera, A. *J. Am. Chem. Soc.* **1992**, *114*, 9093.

(165) José , M. S. *Helv. Chim. Acta* **2002**, *85*, 814.

(166) Sammakia, T.; Latham, H. A. *J. Org. Chem.* **1996**, *61*, 1629.

(167) Leroux, F.; Schlosser, M.; Zohar, E.; Marek, I. In *The Chemistry of Organolithium Compounds*; Rappoport, Z., Marek, I., Eds.; John Wiley & Sons: 2004, p 435.

(168) Negishi, E.; Swanson, D. R.; Rousset, C. J. *J. Org. Chem.* **1990**, *55*, 5406.

(169) Shimano, M.; Meyers, A. I. *J. Am. Chem. Soc.* **1994**, *116*, 10815.

(170) Ziegler, K.; Colonius, H. *Justus Liebigs Ann. Chem.* **1930**, *479*, 135.

(171) Bartlett, P. D.; Swain, C. G.; Woodward, R. B. *J. Am. Chem. Soc.* **1941**, *63*, 3229.

(172) Gilman, H.; Bebb, R. L. *J. Am. Chem. Soc.* **1939**, *61*, 109.

(173) Bryce–Smith, D.; Turner, E. E. *J. Chem. Soc.* **1953**, 861.

(174) Morrison, R. C.; Hall, R. W.; Schwindeman, J. A.; Kamienski, C. W.; Engel, J. F.; Patent, U. S., Ed.; (FMC Corp., USA). US, 1994; Vol. U S 5,211,888.

(175) Smith, W. N. *J. Organomet. Chem.* **1974**, *82*, 1.

(176) Kamienski, C. W.; Esmay, D. L. *J. Org. Chem.* **1960**, *25*, 1807.

(177) Meyers, A. I. *J. Org. Chem.* **2005**, *70*, 6137.

(178) Sammakia, T.; Latham, H. A. *J. Org. Chem.* **1995**, *60*, 6002.

(179) Remenar, J. F.; Collum, D. B. *J. Am. Chem. Soc.* **1997**, *119*, 5573.

(180) Lucht, B. L.; Collum, D. B. *J. Am. Chem. Soc.* **1996**, *118*, 2217.

(181) Remenar, J. F.; Collum, D. B. *J. Am. Chem. Soc.* **1998**, *120*, 4081.

(182) Durig, J. R.; Riethmil.S; Li, Y. S. *J. Chem. Phys.* **1974**, *61*, 253.

(183) Meyers, A. I.; Gabel, R.; Mihelich, E. D. *J. Org. Chem.* **1978**, *43*, 1372.

(184) Blagg, J.; Davies, S. G.; Goodfellow, C. L.; Sutton, K. H. *J. Chem. Soc., Perkin Trans. 1* **1987**, 1805.

(185) Kundig, E. P.; Ripa, A.; Bernardinelli, G. *Angew. Chem. Int. Ed.* **1992**, *31*, 1071.

(186) Ziegler, F. E.; Fowler, K. W. *J. Org. Chem.* **2002**, *41*, 1564.

(187) Barner, B. A.; Meyers, A. I. *J. Am. Chem. Soc.* **2002**, *106*, 1865.

(188) Pansegrau, P. D.; Rieker, W. F.; Meyers, A. I. *J. Am. Chem. Soc.* **1988**, *110*, 7178.

(189) Meyers, A. I.; Pansegrau, P. D. *Tetrahedron Lett.* **1983**, *24*, 4935.

(190) Clayden, J.; Parris, S.; Cabedo, N.; Payne, A. H. *Angew. Chem. Int. Ed.* **2008**, *47*, 5060.

(191) Pape, A. R.; Kaliappan, K. P.; Kundig, E. P. *Chem. Rev.* **2000**, *100*, 2917.

(192) McKennon, M. J.; Meyers, A. I.; Drauz, K.; Schwarm, M. *J. Org. Chem.* **1993**, *58*, 3568.

(193) Greene, T. W.; Wuts, P. G. M. *Protective Groups in Organic Synthesis. 2nd Ed*, 1991.

(194) Hargaden, G. C.; Guiry, P. J. *Chem. Rev.* **2009**, *109*, 2505.

CHAPTER 2

Synthesis of Isopropyl Oxazoline Calixarene

2.1 Retrosynthetic Analysis

Our initial target was the synthesis of a mono–functionalised calixarene containing a suitable chiral oxazoline through which lithiation could be directed.[1] A number of existing strategies have been employed for the upper rim functionalisation of calix[4]arenes,[2,3] however for our intended purpose a selective mono–functionalisation strategy would be required for the introduction of a single directing group onto the *para* position of the upper rim while preserving the other *t*–butyl groups on the molecule. There are a number of existing methodologies that fit this criterion,[3] however, owing to the stability of the propyl protection strategy employed for a mono–nitration procedure,[4] this approach appeared to suit our purposes. When employing an alkylation strategy, generally propylation of the phenolic positions is used, as this is the smallest alkyl group permissible to retain conformational control on the calixarene molecule.[5]

A retrosynthetic analysis of the target oxazoline calixarene **2.1** was undertaken as shown in Scheme 2.1. Oxazoline calixarene **2.1** was disconnected through a functional group interconversion (FGI) to the carboxylic acid **2.2**. Carboxylic acid **2.2** could be obtained by carboxylation of an aryl metal intermediate (lithium or magnesium) which in turn could be generated from a halide precursor **2.3**. The halide could be disconnected through a Sandmeyer–type transformation to the known amine **2.4**,[6] which could be synthesised using the mono–nitration procedure previously discussed.[4] Having decided on an approach, the synthesis of the effective starting material, amine **2.4**, is discussed in the following section.

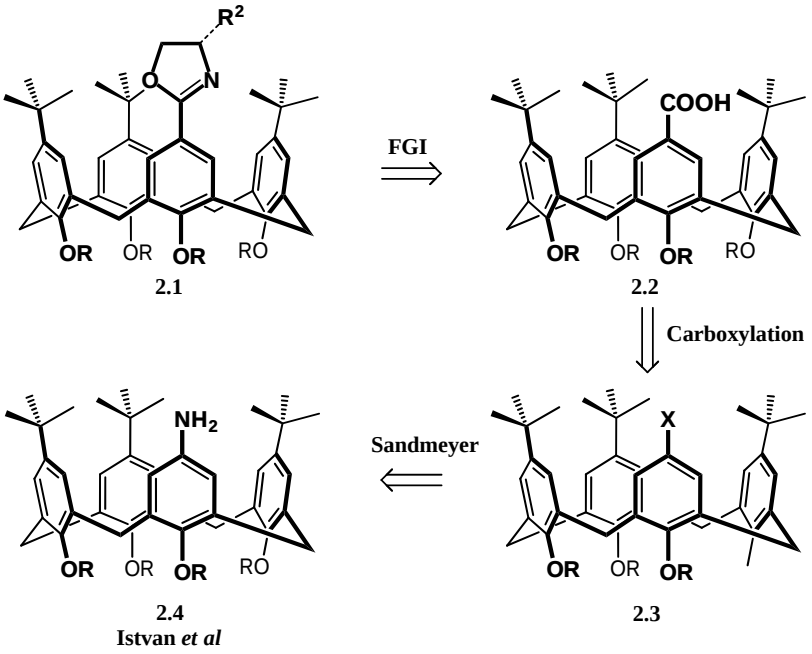

Scheme 2.1: Retrosynthetic analysis of oxazoline **2.1** target molecule.

2.2 Synthesis of Amine Calixarene 2.4

A widely employed method developed by Gutsche *et al.* was chosen for the synthesis of calix[4]arene **2.5**, using a base–catalysed condensation between formaldehyde and 4–*t*–butylphenol as shown in Scheme 2.2.[7] Purification of the calixarene is easily accomplished by crystallisation from toluene, affording a toluene–calixarene co–crystal in high purity.

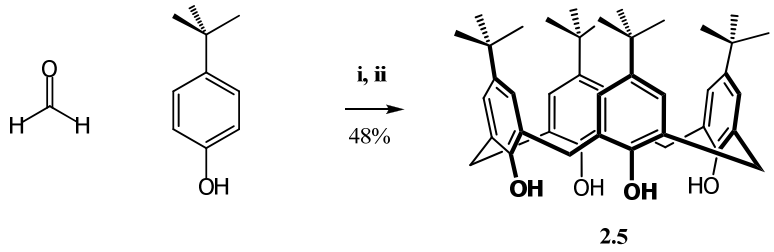

Scheme 2.2: Synthesis of calix[4]arene 2.5. Reagents and conditions: i) NaOH (0.045 eq), ii) Ph_2O, Δ, 4 h

The ^{1}H NMR spectra of calix[4]arene has been well studied in the literature,[3,8,9] however a few aspects of the spectrum are worth highlighting for the reader unfamiliar with the molecule. The simplicity of the ^{1}H NMR spectrum of calixarene **2.5** reveals the symmetrical nature (C_4) of the perfect cone conformation that the calixarene adopts (Figure 2.1). A room temperature spectrum of calixarene **2.5** displays poorly defined signals for the methylene bridges. On cooling the sample to 0 ºC, two well defined signals are observed, with the temperature dependence of these

signals being attributed to the inversion of the molecule in solution.[3,8,10-12] Ungaro *et al.* identified the upfield signals as belonging to the equatorial protons on the methylene bridge (H_e),[13] with the downfield signals being attributed to the axial protons (H_a). Inspection of the methylene bridging signals also allows the conformation (cone, pinch cone, partial cone etc.) to be determined.[14]

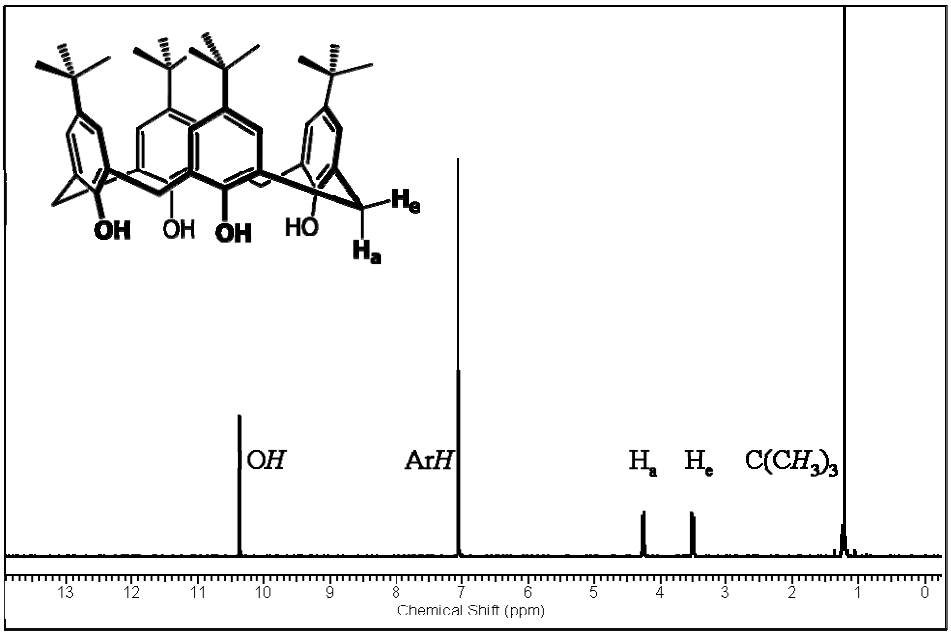

Figure 2.1: ^{1}H spectrum of calix[4]arene **2.5** at 0 ºC with solvent signals removed for clarity.

Triprotection (Scheme 2.3) of the phenolic groups was performed according to a procedure developed by Shinkai *et al.* using a mixture of barium oxide and barium hydroxide octahydrate with an excess of propyl iodide.[5] The surprising choice of base was developed by trial and error in other work by the same authors;[15] reasons for its success appear to stem from the presence of templating counter ions, or the lack thereof.[5] In other experiments performed in our research group using either BaO or $Ba(OH)_2$, poor yields of the desired product were recorded – hence the combination of the oxide and hydroxide appear to be a prerequisite for successfully obtaining the desired cone conformation product in high yield. Tripropoxy calixarene **2.6** is easily crystallised from a EtOH/DCM mixture, enabling large scale reactions to be readily performed.

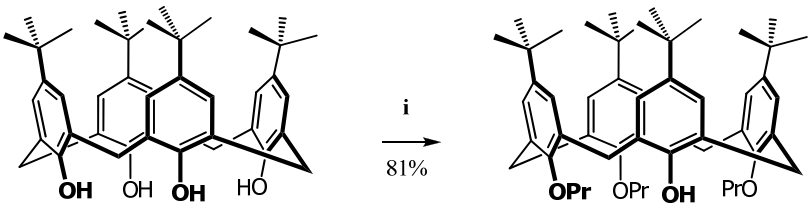

2.5 **2.6**

Scheme 2.3: Selective trialkylation of phenolic groups. Reagents and conditions: i) DMF, BaO (3.3 eq), $Ba(OH)_2 \cdot 8H_2O$ (5.8 eq), PrI (28 eq), rt, 2h.

The ^{1}H NMR spectrum of the calixarene **2.6** revealed the loss in symmetry in the product (C_4 to C_V) due to the tri–alkylation of the phenolic positions, as well as indicating that the molecule now prefers to sit in a pinch cone or boat conformation. The change to the pinch cone is presumably due to the loss of stabilisation achieved by the octameric hydrogen bonding system which was present between the four phenolic positions responsible for the true cone of **2.5**.[11] There was also a considerable shift in the position of the phenolic proton from 10.35 ppm in the parent calixarene **2.5** to 5.58 ppm in **2.6**, which is again indicative of the weakening of the hydrogen bond system.[11,16]

Having tri–propoxy calixarene **2.6** in hand, the means of controlling the selective mono–nitration of the calixarene was created.[4] The greater activating effect of the single phenolic group promotes the selective replacement of the *para t*–butyl group by a nitro group as shown in Scheme 2.4.[4] Nitration presumably progresses through the nitronium ion intermediate through an *ipso*–nitration type mechanism.[17] The reaction proceeds extremely rapidly, and is thus somewhat difficult to control. Despite the slight unpredictability of the reaction, the synthesis of highly crystalline nitro calixarene **2.7** in consistently good yields was achieved.

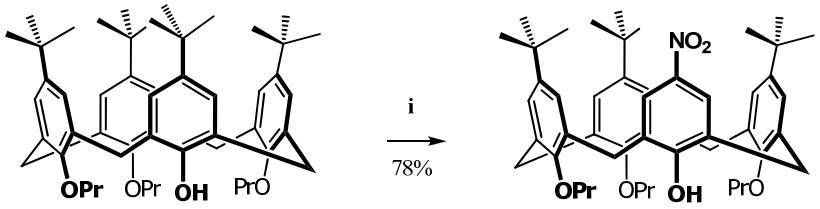

2.6 **2.7**

Scheme 2.4: Mono–nitration of triprotected calixarene. Reagents and conditions: i) conc HNO_3 (7.2 eq), DCM, AcOH, 0 ºC to rt, 12 m.

Unsurprisingly inspection of the ^{1}H NMR spectrum of **2.7** indicates the presence of a pinch cone conformation. In addition by inspection of the *t*–butyl groups signals, it can be determined that the functionalised nitro ring and its opposite counterpart lie outwards, presumably due to the

smaller steric bulk of the phenolic group on the nitro–group functionalised ring (for a more thorough explanation see Appendix I).

Alkylation of the final phenolic moiety was achieved in good yields using sodium carbonate and a large excess of propyl iodide in refluxing acetonitrile (Scheme 2.5). However, approximately 48 hours were required before the presence of starting material **2.7** could no longer be detected in the reaction mixture.

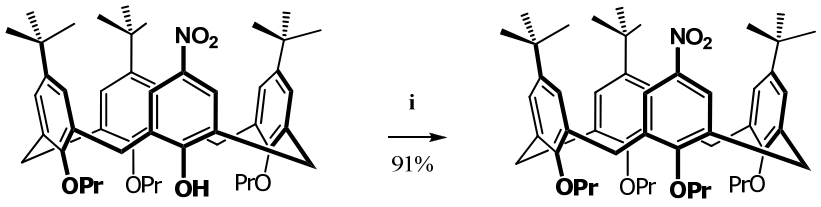

2.7 **2.8**

Scheme 2.5: Alkylation of the fourth phenolic group. Reagents and conditions i) Na_2CO_3 (3 eq), PrI (18 eq), MeCN, Δ, 48 h.

Interpretation of the ^{1}H NMR spectrum of calixarene **2.8** indicated that a change in conformation of the molecule had occurred, with the functionalised nitro ring and its opposite counterpart now lying inwards. Presumably, this change is due to the increase in steric interaction between the newly alkylated phenolic position and the other propyl groups, and the relatively small nature of the nitro group relative to the *t*–butyl groups.

Due to the long reaction and excess of propyl iodide required to alkylate the fourth position, the possibility of a microwave assisted synthesis appeared attractive. A reaction was performed at 200 ºC in DMF using potassium carbonate and propyl iodide (Scheme 2.6). Inspection of a TLC of the reaction appeared to indicated that the correct product had been formed, which represented a considerable reduction in time (48 hours to 4 minutes), and the required amount of propyl iodide (18 to 3 equivalents). However, inspection of the ^{1}H NMR spectrum of the product **2.9** revealed this product to be in the partial cone conformation. Reactions with potassium carbonate gave higher proportions of the partial cone conformer (as deduced by inspection of the ^{1}H NMR spectra of the mixture), while reactions using sodium carbonate appeared to have greater proportions of the desired pinch cone conformer. The mixture of conformations obtained in these reactions led to the abandonment of this approach. It should not be discounted that further optimisation of conditions could allow this microwave–assisted alkylation to be performed with control over the conformation of the product.

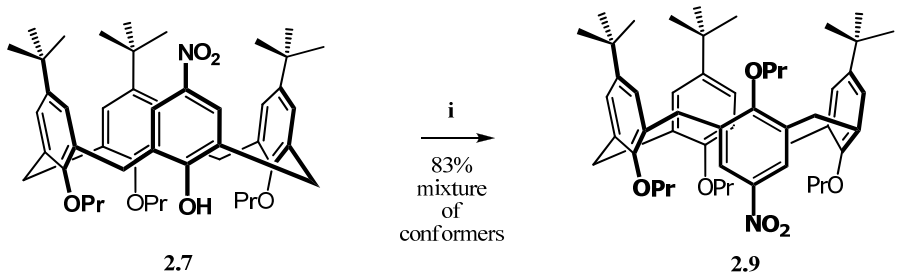

2.7 **2.9**

Scheme 2.6: Microwave assisted alkylation of fourth phenolic group. Reagents and conditions: i) K_2CO_3 (3 eq), PrI (3 eq), DMF, 200 ºC, 4 minutes.

Having successfully synthesised nitro calixarene **2.8**, the reduction of the nitro group to the amine was achieved in consistently high yields under hydrogen transfer conditions with palladium on carbon and hydrazine hydrate (Scheme 2.7), yielding amino calixarene **2.4**.[6] Purification of the amine was readily achieved by crystallisation from dichloromethane and ethanol, yielding a DCM co–crystal. From the ^{1}H NMR spectrum of **2.4** it was possible to determine that the molecule adopted a similar conformation to that of nitro calixarene **2.8**, with the amine group and the opposite ring facing inwards and the two adjacent rings leaning outwards.

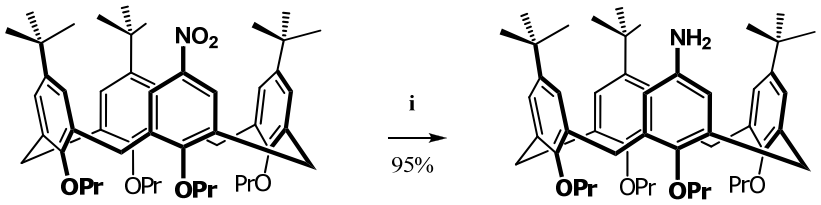

2.8 **2.4**

Scheme 2.7: Synthesis of amino calixarene **2.4** Reagents and conditions: i) Pd/C (0.1 eq), H_2NNH_2 (2.6 eq), EtOH, Δ, 1.5 h.

2.3 Iodination of Calix[4]arene

Thus far, the sequence of reactions performed to synthesise amino calixarene **2.4** had been reported in the chemical literature. A wide choice of reaction conditions for conversion of amino calixarene **2.4** to the desired halogenated calixarene existed.[18,19] This broad range of reactions covers the replacement of aromatic amines by either bromide, chloride, iodide or cyano groups via a diazonium salt intermediate generally using cuprous salts.[20,21] Recently, Knochel *et al.* reported a one pot protocol for the iodination of aryl amines using *p*–toluenesulfonic acid, potassium iodide and sodium nitrite,[22] which appeared to be an attractive option due to its relatively simple experimental procedure. The implementation of this methodology proved to be highly effective in

the formation of the crystalline iodo calixarene **2.10** as shown in Scheme 2.8. ^{1}H NMR spectroscopy indicated that **2.10** adopted the same conformation as its amine precursor.

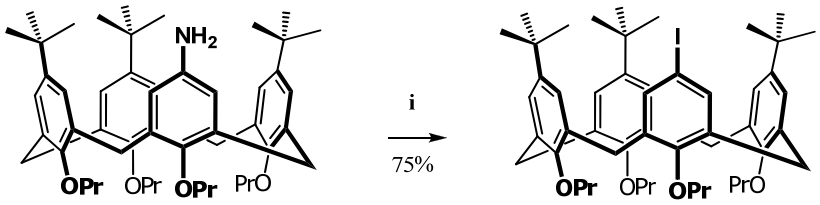

2.4 **2.10**

Scheme 2.8: Preparation of iodo calixarene **2.10**. Reagents and conditions: i) TsOH (3 eq), MeCN, $NaNO_2$ (2.5 eq), KI (3 eq), rt, 1.5 h.

Iodo calixarene **2.10** also proved to be highly crystalline, and could be easily purified by crystallisation from ethanol and dichloromethane. A number of crystalline forms of **2.10** appeared to form. However, when rapidly crystallised from a ethanol–dichloromethane mixture consistent formation of a dichloromethane co–crystal occurred (DCM:**2.10**; 0.5:1). Somewhat surprisingly, the persistence of a by–product in crystallised and column purified material was observed. This was later identified to be protonated calixarene **2.11** (Figure 2.2). The persistence of protonated product in crystallised iodo **2.10** seems to indicate a in–discriminate incorporation of the protonated compound **2.11** into the crystal lattice. This hypothesis is seemingly also supported by the repeated failure of attempts to crystallise pure **2.11** without the presence of iodo **2.10**. Formation of **2.11** could be associated with degradation of the diazonium salt intermediate, prior to displacement with nucleophilic iodine. Identification of protonated **2.11** was hampered by the compound displaying a large singlet for the three protons on the un–butylated ring instead of the expected triplet and doublet coupling patterns. Reasons for this coupling pattern are unknown, but confirmation of the structures of protonated calixarene **2.11** was confirmed by HR–MS and ^{13}C NMR spectroscopy.

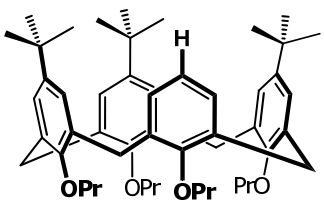

2.11

Figure 2.2: Protonated by–product **2.11** from iodination reaction.

2.4 Halogen Metal Exchange Reactions

Having procured iodo calixarene **2.10**, the introduction of the carboxy group was attempted using a lithium iodine exchange reaction with *n*BuLi, followed by quenching with solid carbon dioxide. These efforts did indeed yield the desired product acid **2.2**, but consistently low yields were obtained (Scheme 2.9). Inspection of the crude reaction mixtures by TLC indicated the presence of what appeared to be large amounts of unreacted starting material; this proved to be the protonated calixarene **2.11**. It was anticipated that this high yielding by–product was a result of the addition of a proton to the lithiated intermediated.

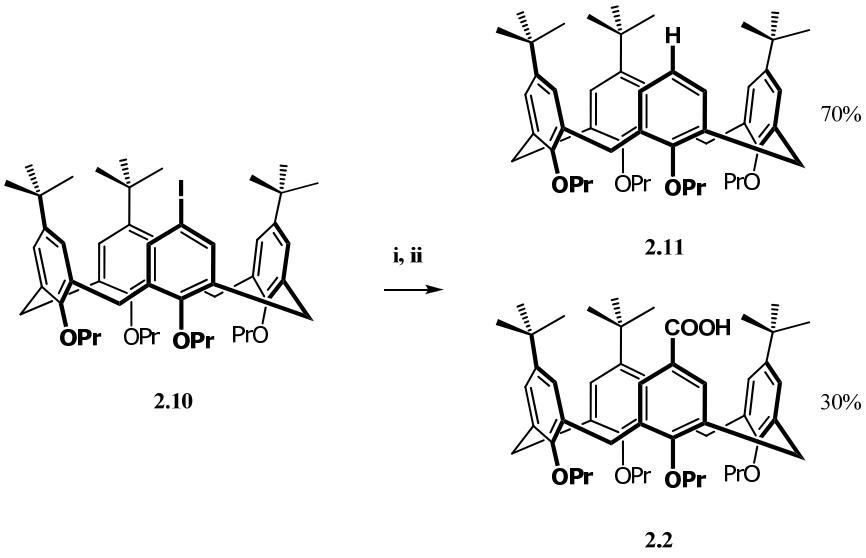

Scheme 2.9: Synthesis of carboxylic acid calixarene via lithium iodine exchange. Reagents and conditions: i) *n*BuLi (1.1 eq), THF, –78 ºC, 15 m ii) CO_2 (s).

The difficulty in tracking the source of protons apparently causing the low yields in the lithium iodine exchange reaction was complicated by the use of CO_2 as an electrophile, as its delivery as a dry reagent to a reaction mixture is fraught with experimental difficulty. A further potential problem when using CO_2 is the possibility of an unreacted organometallic compounds reacting with the carboxylate salt intermediate, thereby forming ketone by–products.[23] In order to prevent this occurring, the introduction of CO_2 into the reaction should be rapid and involve the use of excess equivalents of CO_2. For these reasons the lithiated compound was usually poured rapidly into a beaker of solid CO_2, which had been freshly generated from a dry gaseous source. Despite these precautions, repeated attempts to increase the yield of the exchange reaction proved fruitless.

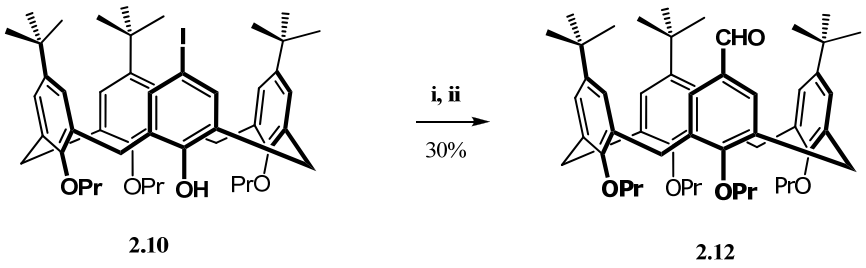

2.10 **2.12**

Scheme 2.10: Preparation of formyl calixarene through lithium iodine exchange. Reagents and conditions: i) *n*BuLi (2 eq), THF,–78 ºC, 6 m ii) DMF (2.6 eq).

Dimethyl formamide was chosen as an electrophile as the resulting formyl functionality could be potentially oxidised to the target acid, providing a secondary synthetic route for obtaining the target oxazoline calixarene **2.2**. However, the yields of formyl calixarene **2.12** were similar to those of carboxy calixarene **2.2** (Scheme 2.10). This suggested that the by–product formation was due to an internal source of protons rather than an external source relating to the use of CO_2. Surprisingly the poor yields continued even after prolonged heating of iodo calixarene **2.10** under high vacuum.

The propensity for calixarenes to form inclusion compounds is well known,[3,24,25] and had been observed with the formation of DCM calixarene co–crystals with amino **2.4** and iodo **2.10** (as identified by ^{1}H NMR spectroscopy and thermal gravimetric analysis). Prolonged drying of these co–crystals at room temperature (under 1mm Hg) failed to eliminate the persistence of the included DCM molecule, and we found that drying at 90 ºC under vacuum was required to remove the DCM guest molecules. The potential for complexation of water through hydrogen bonding within the four alkylated phenolic positions coupled with the higher boiling point of water could present a considerable challenge in removing trapped water molecules from the structure. This theory seemed to be substantiated by the appearance of very broad water signals in the ^{1}H NMR spectra of a number of compounds, possibly indicating varying shielding effects.

From these results, it appeared that insufficient drying of the compounds could be the primary reason for the low yields in many of the earlier exchange reactions. Inspection of the literature yielded a number of techniques that have been used to liberate trapped protic solvents from large bowl shaped molecules.[26,27] Sherburn *et al.*,[27] utilised a solvating – de–solvating technique with freshly distilled dry aprotic solvents under inert conditions before attempting exchange reactions. Another technique that has been used has been to stir sodium hydride with the solvated halogenated starting material before the addition of the alkyllithium to the solution.[28,29] The incorporation of both of these techniques into the pre–drying of calixarene **2.10,** before the addition of *n*BuLi, only led to a minor improvement in yield to 45%.

Another option for the optimisation of lithium–halogen exchange reactions involves the use of different alkyllithiums.[1] *t*BuLi is particularly useful in exchange reactions when two equivalents of the reagent are used,[1] as the second equivalent reacts non–reversibly with the *t*–butyl–halide (**C** – Scheme 2.11) product of the initial exchange reaction, making the exchange reaction irreversible (**D** and **E** – Scheme 2.11).

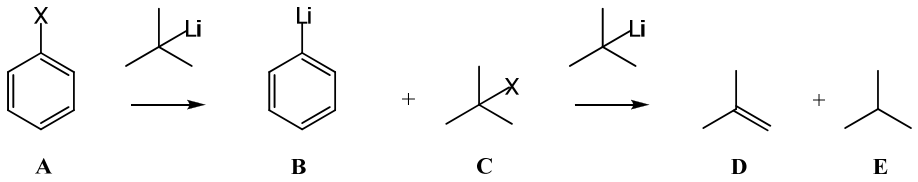

Scheme 2.11: Secondary reaction of *t*BuLi with tertiary alkyl halide formed from exchange reaction.

The use of *t*BuLi in the exchange reaction on iodo calixarene **2.10** was tested with no increase in the yield of the acid **2.2**. The reaction proved to exhibit the formation of a second by–product **2.13** (associated with the addition of a *t*–butyl group from the alkyllithium). The ^{1}H NMR spectrum indicated that the molecule was highly symmetric in nature with the presence of four *t*–butyl groups (as a pair of singlets due to the symmetry of the molecule in the pinch cone conformation).

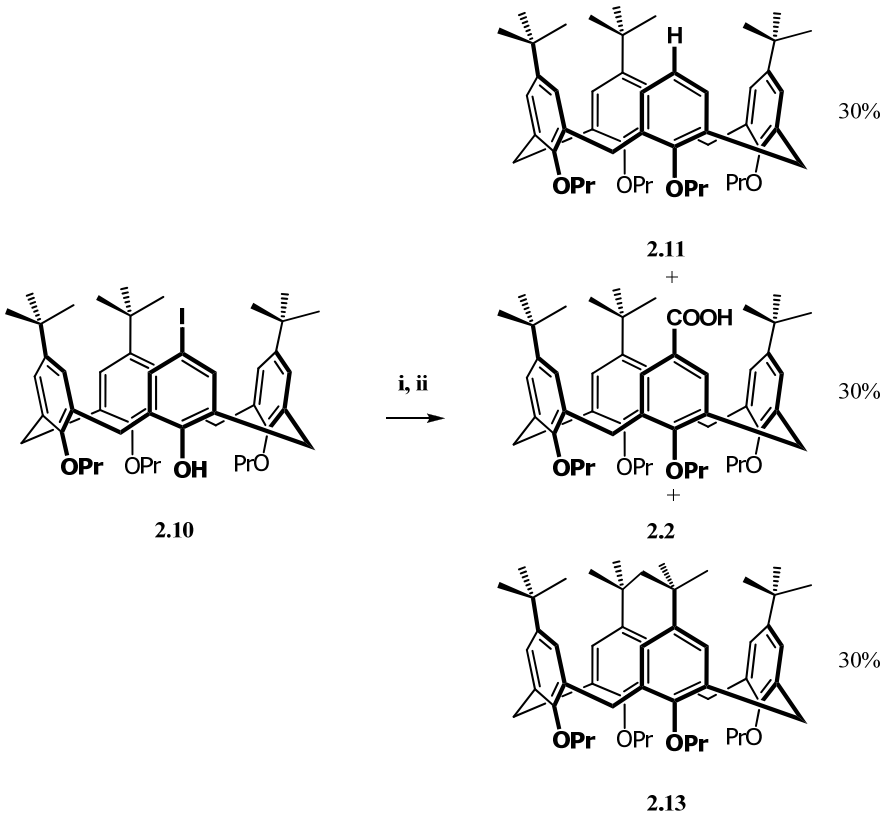

Scheme 2.12: Lithium iodine exchange reaction using *t*BuLi. Reagents and conditions: i) NaH, *t*BuLi (2.5 eq), THF, –78 °C, 15 minutes, ii) CO_2.

This coupling product was somewhat unexpected, nonetheless other authors have observed the formation of coupling products in high temperature lithium halogen exchange reactions.[30,31] Recently, Bailey *et al.* observed the formation (less than 1%) of coupling products in the exchange reaction of an aryl bromide compound (Scheme 2.13).[30] Mechanistically, they attributed the formation of these products to the ortholithiation of the bromo compound (**B** – Scheme 2.13), rather than the anticipated exchange reaction, followed by elimination of lithium bromide,[1,32,33] which led to the formation of the benzyne intermediate (**C** – Scheme 2.13). This benzyne reacts without regioselectivity with alkyl or aryllithium compounds in the reaction mixture, forming a range of coupling products (**D** – Scheme 2.13).

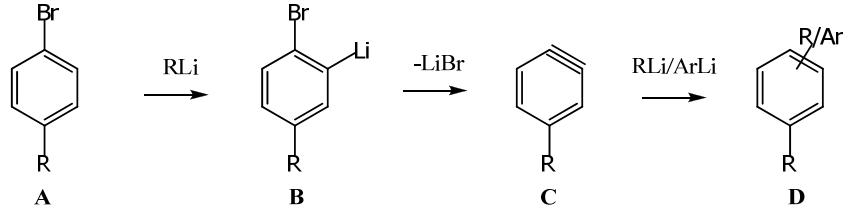

Scheme 2.13: Coupling product formation as postulated by Bailey *et al.*[30]

Negishi *et al.* also observed that specifically the use of THF in room temperature exchange reactions, promoted the formation of coupling products with primary alkyllithium reagents in appreciable yields.[31] They suggested that the formation of these coupling products arose from an initial exchange reaction, followed by a reaction between the aryllithium and the alkyl halide. Negishi and co–workers failed to observe the formation of coupling products when secondary and tertiary lithium reagents were used, presumably due to the poor electrophilicity of the corresponding alkyl halides, however good yields with primary alkyllithiums occurred with no observable loss of regiospecificity. These results do not point towards a benzyne intermediate, but appear similar to products attainable through a Wurtz type coupling.[34]

The formation of **2.13** poses some very interesting questions, as this represents a rapid low temperature coupling reaction between a tertiary alkyllithium reagent and an aryl iodide, almost certainly not involving an ortholithiation route. These results require further investigation, as does evaluating the role that sodium hydride plays in this unexpected reaction.

In order to improve the yield of the exchange reaction on the calixarene, we wondered if instead of utilising the highly reactive lithium organometallic intermediate to form the carboxylate, the milder aryl magnesate could be used instead. Formation of aryl magnesiates can be achieved either by direct oxidative insertion of magnesium metal into the aryl halogen bond using the classical Grignard approach;[23] by transmetallation of an aryl organometallic species with a suitable magnesium salt/magnesium metal;[35] or by magnesium halogen exchange reaction with a preformed alkyl Grignard (Scheme 2.14).[36-38]

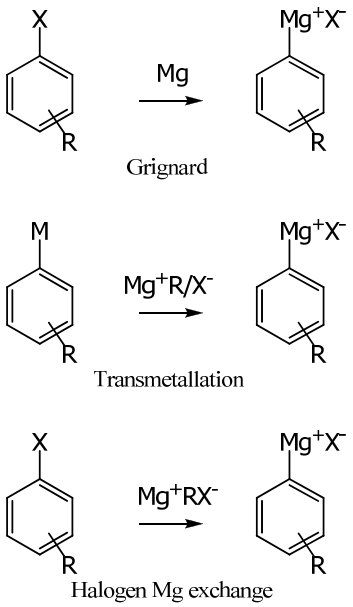

Scheme 2.14: Formation of arylmagnesiates.

While all approaches ultimately yield the same product (albeit with differences in the counter ions), magnesium–halogen exchange has recently gained popularity in the chemical literature due to its ability to tolerate sensitive functional groups within the molecule that could not be attained by direct magnesiation.[36] To a large degree this popularity can be attributed to findings by the Knochel group who have demonstrated that the presence of lithium salts (particularly LiCl) greatly enhance the rate of the exchange reaction between brominated and iodinated aryl species and Grignard reagents.[39] This rate enhancement has been attributed to the extra negative charge formed at the magnesium centre by the formation of the Grignard reagent–lithium salt complex, as well as breaking up the polymeric aggregates of the Grignard reagents into more reactive complexes.[40] Magnesium halogen exchange reactions are conveniently performed using *i*PrMg·LiCl$_2$, and the scope of magnesium halogen exchange reactions have been thoroughly explored in the chemical literature.[36,37,39-41] While our system did not possess sensitive functional groups, it appeared to be an attractive option due to its widespread incorporation and success in the chemical literature since its introduction.[36,37,39-41]

The synthesis of the Grignard reagent required a number of attempts due to the poor quality of the magnesium at our disposal. We found that stirring the magnesium overnight under nitrogen assisted the removal of the oxidised outer layer and allowed the reaction to initiate,[23] (Scheme 2.15) as witnessed by the change in colour of the solution and the evolution of heat. Owing to the availability of 2–chlorobutane, initial reactions involved the preparation of *s*BuMg·LiCl$_2$ (**2.14**) rather than the standard *i*PrMg·LiCl$_2$.

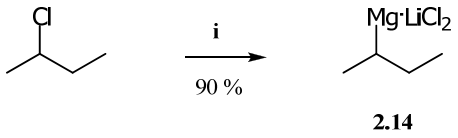

2.14

Scheme 2.15: Preparation of *s*BuMg·LiCl$_2$. Reagents and conditions: i) Mg (1.7 eq), LiCl$_2$ (1 eq), THF, rt, 24 h.

A colourimetric titration based method utilising 2,2′–bipyridine and an acidic alcohol was used to determine the concentration of the active Grignard reagent.[23] It was found that magnesium iodine exchange occurred within two hours at room temperature in THF on the calixarene, and quenching with solid CO_2 yielded the desired acid **2.2** with an immediate improvement in yield (Scheme 2.16). Both *s*BuMg·LiCl$_2$ (**2.14**) and *i*PrMg·LiCl$_2$ (**2.15**) produced similar results, however the use of the isopropyl reagent was preferable as its acid product (unreacted Grignard reagent reacting with the carbon dioxide electrophile) could be more easily extracted into water in the workup procedure. It was generally necessary to purify the carboxylic acid product **2.2** by

column chromatography, as the lower yields and the greater by product formation were not conducive to purification by crystallisation.

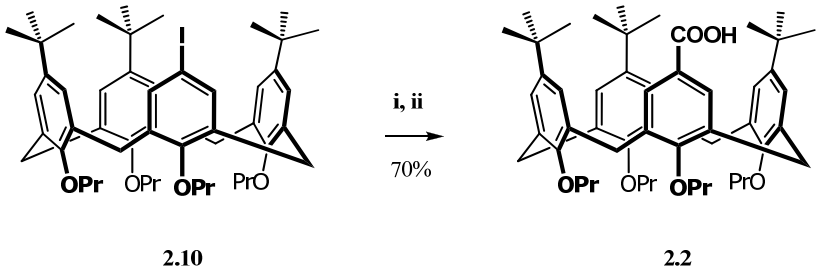

2.10 **2.2**

Scheme 2.16: Synthesis of carboxylic acid **2.2** via iodine magnesium exchange. Reagents and conditions: i) *i*PrMg·LiCl$_2$ (4 eq), THF, rt, 2 h, ii) CO_2 (exs).

An examination of the ^{1}H NMR spectrum of the acid **2.2** reveals that the molecule again lies in the same conformation as iodo calixarene **2.10** (refer to Appendix I). A further aspect of the ^{1}H NMR spectra of this family of functionalized calixarene molecules that has as yet not been discussed is the signals attributed to the O*C*H$_2$ groups of the propoxy ethers. As seen in Figure 2.3 a typical pattern is visible through a wide range of these molecules.

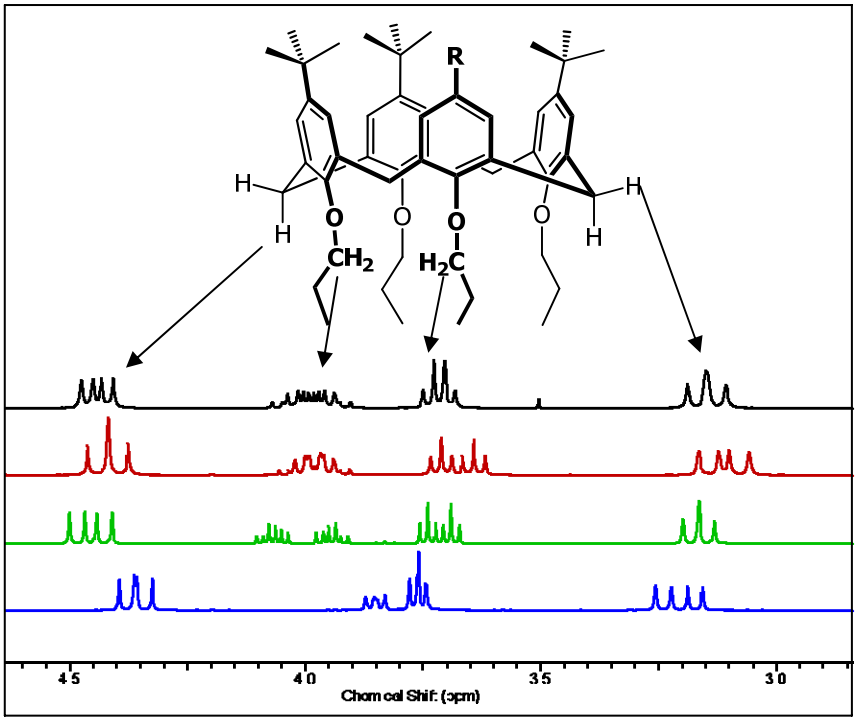

Figure 2.3: Splitting patterns of O*C*H$_2$ propyl signals. Key: tri–protected calixarene **2.6** bottom (blue), nitro calixarene **2.7** bottom middle (green), bromo calixarene **2.16** top middle (red), acid calixarene **2.2** top (black).

The OCH_2 propoxy signals are found around approximately 4 ppm, between the axial and equatorial methylene bridge signals (4.5 ppm and 3.2 ppm respectively). The upfield OCH_2 signal is visible as two triplets (sometimes with coalescence) whereas the downfield group displays significantly more complex coupling patterns. This complex downfield signal can be assigned to the outward lying rings (which for compounds, **2.7**, **2.16**, and **2.2** are the two non–functionalised rings). If one of these protons is replaced, an sp^3 chiral centre is created as well as inherent chirality, hence the complexity of these signals can be attributed to their diastereotopic nature as shown in Figure 2.4. This is not the case for the OCH_2 on the functionalised ring as these protons are enantiotopic, which accounts for their less complex triplet coupling pattern.

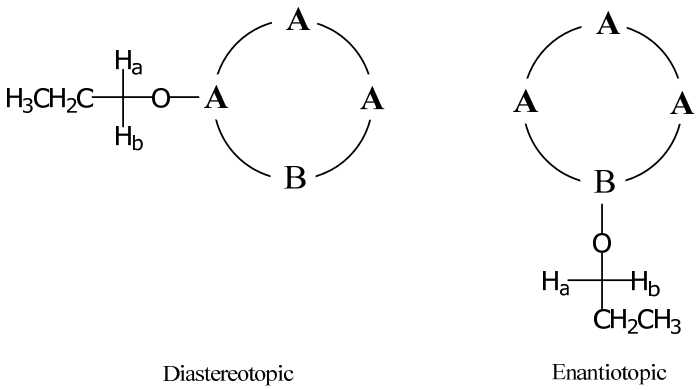

Figure 2.4: Diastereotopic propoxy OCH_2 protons on a functionalised calixarene.

Due to the large number of experiments that were performed optimising exchange conditions, a reasonable quantity of protonated calixarene **2.11** was available. The possibility of recycling material by bromination was very attractive, since a second exchange reaction would yield acid **2.2**. Bromination of **2.11** using *N*–bromosuccinimide in methyl ethyl ketone was performed producing **2.16** quantitatively (Scheme 2.17).[42-44]

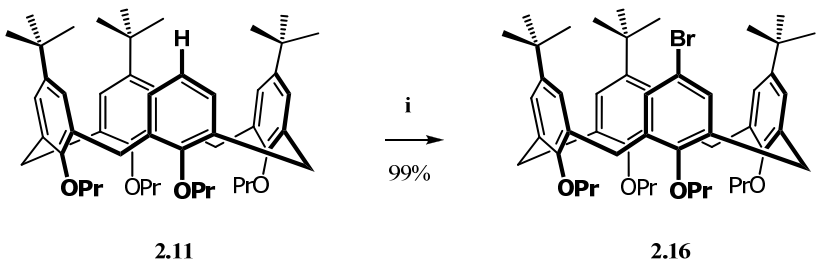

2.11 **2.16**

Scheme 2.17: Bromination of protonated by product **2.11**. i) NBS (1.1 eq), MEK, rt, 18 h.

Having observed that the conversion of iodo calixarene **2.10** to acid **2.2** using magnesium iodine exchange produced better results than the iodine lithium exchange reaction, a magnesium bromine exchange reaction was attempted on bromo calixarene **2.16**. The exchange reaction between *i*PrMg·$LiCl_2$ **2.15** and bromo **2.16** failed to produce any magnesiated product after 90 minutes at room temperature, and only starting material was recovered. This was unexpected as there was literature precedent for bromine–magnesium exchanges using *i*PrMg·$LiCl_2$ **2.15** reaction with bromo arenes.[40] It is nonetheless known that the magnesium bromine exchange reaction is slower than magnesium iodine exchange, in addition, the rate shows strong dependency on the electron–withdrawing/donating ability of other functional groups in the molecule.[39] The bromine–magnesium exchange reaction was not investigated further; pleasingly however, lithium–bromine exchange on bromo **2.16** with *n*BuLi produced yields consistently above 80% for conversion to carboxylic acid **2.2** when quenched with CO_2 (Scheme 2.18).

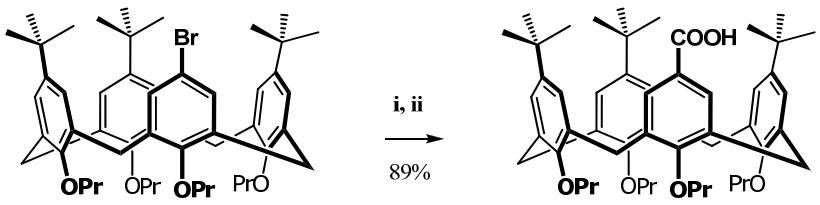

2.16 **2.2**

Scheme 2.18: Preparation of acid calixarene **2.2** from bromo calixarene **2.16**. Reagents and conditions: i) NaH (0.2 eq), *n*BuLi (2.5 eq), THF, –78 °C, 15 m ii) CO_2.(s).

Examination of the chemical literature provides a few plausible explanations when trying to rationalise the differences between the different halogenated calixarenes when subjected to lithium–halogen exchange conditions. The exact mechanisms by which this reaction occurs are not yet fully understood and seem likely to occur through at least two different pathways, one of a radical nature and the other involving the formation of an intermediate "ate" complex between the alkyllithium and the aryl or alkyl halide.[1,34] Thus differences in yield could simply be due to different reaction pathways, and the stabilities of the intermediaries. Lithium–halogen exchange reactions are kinetically controlled and thus an equilibrium between the alkyllithium, the alkyl or aryl halide and the lithiated product of the reaction is established.[45] The rate of reactivity of aryl halides increases in the order ArF<ArCl<ArBr<ArI,[45] and is so rapid with aryl iodides that it has been shown to occur possibly even before deprotonation of hydroxyl groups in the same reaction mixture.[46,47] Considering the potential for the presence of water in the molecule, another explanation for the disparity between bromo calixarene **2.16** and iodo calixarene **2.10** could also be due to the difference in rates of the two exchange reactions. Given the literature evidence for

exchange reactions with aryl iodides occurring at similar rates to the deprotonation of hydroxyl groups, it is possible that the exchange on the iodo calixarene **2.10** simply occurs before the alkyllithium can react with any residual protic solvents, especially if the protic compounds are encased within the molecule. Once the exchange has occurred, the lithiated calixarene could potentially be quenched by the slow release/decomplexation of residual protic compounds in a non–reversible reaction, which leads to the formation of protonated by product **2.11**. It is possible that the slower rate of the bromine–lithium exchange reaction allows for reaction between residual proton sources before formation of the lithiated calixarene intermediate. However, the strict drying conditions employed for both compounds suggest that trapped protic solvents are perhaps not the true cause of the differences between the yields. We also considered the possibility that competitive E2 elimination reaction was occurring between the alkyl halide generated in the exchange reaction (*n*BuI or *n*BuBr) and the aryl lithium intermediate, resulting in the formation of **2.11**, with the alkyl iodide being more prone to elimination than the alkyl bromide. However a number of factors count against this argument. Firstly, more than two equivalents of the alkyllithium were used, making it more likely that if elimination were occurring, the more basic unreacted *n*BuLi would be quenched preferentially to the lithiated calixarene. Secondly, alkylation of aryl lithium compounds with alkyl iodides in appreciably yields have been recorded in the chemical literature,[48-50] which would not be the case if competitive E2 reactions with alkyl iodides with aryl lithium compounds was an appreciable problem.

While at this stage, we cannot provide a solid explanation for the observed difference in reactivity between iodo **2.10** and bromo **2.16**, perhaps a combination of the aforementioned factors could account for the variation in yield, or possibly, some as yet undiscovered aspect of the halogen–lithium exchange mechanism.

Owing to the high yield of the carboxylation reaction on bromo calixarene **2.16**, the possibility of using a debutylation reaction to gain access to protonated calixarene **2.11** in order to simplify the reaction sequence used to obtain the acid **2.2** was investigated. Debutylation on calixarenes is usually accomplished using aluminium trichloride with toluene or phenol through a reverse Friedel–Crafts type reaction. The difficulty lies in the selective removal of a *single t*–butyl group from a triprotected compound in a procedure analogous to the nitration reaction to produce **2.7**. This reaction has been successfully performed by other researchers on the tri–ester protected calixarenes,[51] however no examples exist of selective debutylation with propoxy protecting groups. An attempt at implementing the literature conditions used to selectively debutylate a tri–ester protect calixarene (using aluminium trichloride and toluene) on tripropoxy calixarene **2.6**,[51] resulted in the formation of a distal dipropyl tetra debutylated calixarene **2.17** (Scheme 2.19). The

distal nature of **2.17** was deduced by the symmetrical nature of its ^{1}H NMR spectrum. Other researchers have investigated the use of aluminium trichloride for the removal of propoxy groups on calixarenes;[52] however they observed a lack of regiocontrol in these reactions. This result indicates that the number of equivalents of aluminium trichloride was almost certainly excessive, and the reaction temperature could perhaps also be reduced, however no further effort was made to selectively remove a single *t*–butyl group, due to concerns regarding the electronic suitability of **2.6** to this reaction.

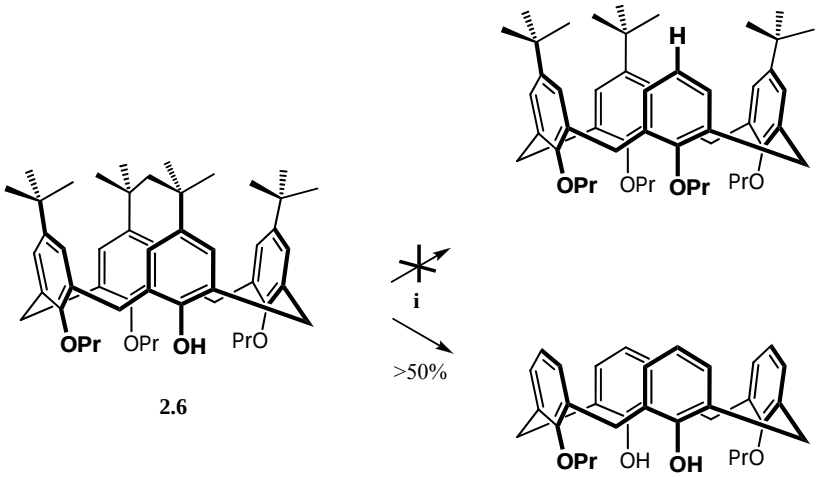

2.6 **2.17**

Scheme 2.19: Attempted mono–debutylation of tripropyl calixarene. Reagents and conditions: i) $PhCH_3$, $AlCl_3$ (27 eq), rt, 2 h.

2.5 Synthesis of Oxazoline Calixarene

Having secured an effective synthetic pathway for calixarene acid **2.2**, the synthesis of the target calixarene oxazoline was attempted. A range of different oxazolines have been used in the literature,[53] however, the availability of L–valine, from which a chiral aminol starting material can easily be derived,[54] appeared an attractive option. L–valine was reduced using sodium borohydride and iodine to L–valinol **2.18** using a procedure developed by Meyers *et al.* (Scheme 2.20).[54] It was noted that the quality of sodium borohydride used is vital if good yields are to be obtained.

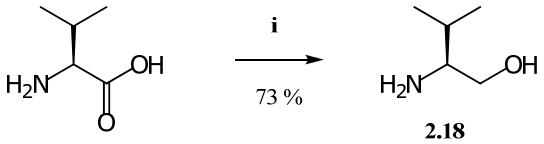

2.18

Scheme 2.20: Synthesis of L–valinol from L–valine. i) $NaBH_4$ (2.4 eq), THF, I_2 (1.02 eq), Δ, 18 h, 20% KOH rt, 5 h.

Activation of acid calixarene **2.2** was accomplished by reaction with thionyl chloride to yield the corresponding acid chloride. A solution of the unpurified acyl chloride suspended in dichloromethane was then slowly added to a mixture of L–valinol and triethylamine in DCM at 0 ºC resulting in the chemoselective formation of the amide **2.19** (Scheme 2.21).

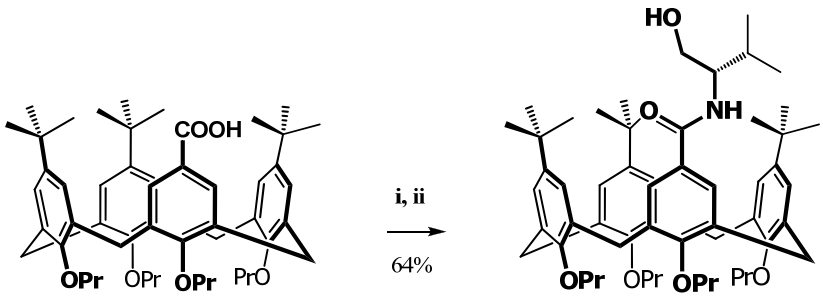

2.2 **2.19**

Scheme 2.21: Preparation of L–valinol amide **2.19**. Reagents and conditions: i) $SOCl_2$ (36 eq), Δ, 3 h ii) L–valinol (1.5 eq), Et_3N (3 eq), DCM, 0 ºC to rt, 24 h.

The dehydration of amide **2.19** was induced by reaction with *p*–toluene sulfonyl chloride, triethylamine and DMAP in dichloromethane (Scheme 2.22).[55] The oxazoline **2.1** was successfully synthesised, however, purification by silica gel column chromatography was hampered by the similar R_f values of the oxazoline and unreacted toluene sulphonyl chloride. Examination of the ^1H NMR spectrum of the oxazoline calixarene **2.1** revealed the oxazoline–functionalised ring and its opposite counterpart sitting upright with the two adjacent rings leaning outwards.

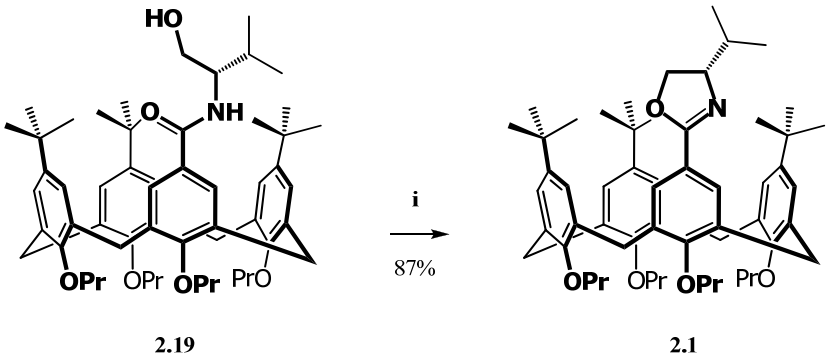

2.19 **2.1**

Scheme 2.22: Dehydration of amide 2.19 to form oxazoline 2.1. Reagents and conditions: i) *p*–toluene sulfonyl chloride (1.3 eq), triethylamine (3 eq), DMAP (cat), DCM, rt, 18 h.

Fortuitously, an investigation into the major by product from the synthesis of amide **2.19** revealed the concomitant formation of the oxazoline **2.1**. It appeared that the oxazoline could be forming due to the reaction of amide **2.19** with residual thionyl chloride causing ring closure. Indeed, a literature search revealed the existence of established methodology for the use of thionyl chloride in the formation of oxazolines from amides.[56,57] Using this approach it was possible to produce the oxazoline **2.1** in high yields from the acid **2.2** without the need for intermediate purification of the amide **2.19** (Scheme 2.23).

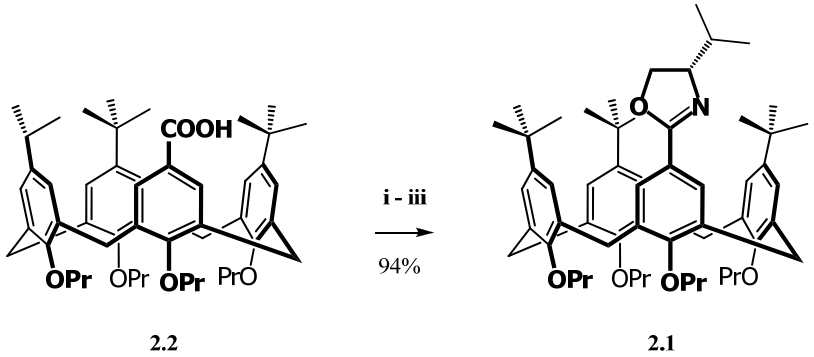

2.2 **2.1**

Scheme 2.23: Revised synthesis of oxazoline. Reagents and conditions: i) $SOCl_2$ (exs) Δ, 3 h ii) Et_3N, L–valinol (1.7 eq), DCM, 0 ºC, rt, 24 h iii) $SOCl_2$ (14 eq), DCM, rt, 18 h.

2.6 Summary and Future Work

With the oxazoline calixarene **2.1** in hand, the focus of the study was turned towards establishing conditions that would allow its *meta* functionalisation through ortholithiation. Due to the plethora of conditions employed in the literature for ortholithiation,[1,58,59] we anticipated that considerable optimisation of the reaction conditions would be required. Having established these conditions, an investigation into the diastereoselectivity of the reaction would then be undertaken. The results of these studies are presented in Chapter 3 below.

2.7 References

(1) Clayden, J. *Organolithiums: Selectivity for Synthesis*; Pergamon: London, 2002; Vol. 23.

(2) Van Loon, J. D.; Arduini, A.; Coppi, L.; Verboom, W.; Pochini, A.; Ungaro, R.; Harkema, S.; Reinhoudt, D. N. *J. Org. Chem.* **1990**, *55*, 5639.

(3) Gutsche, D. C. *Calixarenes: an introduction* 2ed.; RSC Publishing: Cambridge, 2008.

(4) Verboom, W.; Durie, A.; Egberink, R. J. M.; Asfari, Z.; Reinhoudt, D. N. *J. Org. Chem.* **1992**, *57*, 1313.

(5) Iwamoto, K.; Araki, K.; Shinkai, S. *J. Org. Chem.* **1991**, *56*, 4955.

(6) Bitter, I.; Gruen, A.; Toth, G.; Szollosy, A.; Horvath, G.; Agai, B.; Toke, L. *Tetrahedron* **1996**, *52*, 639.

(7) Gutsche, C. D.; Iqbal, M. *Org. Synth.* **1990**, *68*, 234.

(8) Kammerer, H.; Happel, G.; Caesar, F. *Makromol. Chem.* **1972**, *162*, 179.

(9) Gueniffe.H; Kammerer, H.; Klesper, E. *Makromol. Chem.* **1972**, *162*, 199.

(10) Simaan, S.; Biali, S. E. *J. Phys. Org. Chem.* **2004**, *17*, 752.

(11) Dahan, E.; Biali, S. E. *J. Org. Chem.* **1991**, *56*, 7269.

(12) Grootenhuis, P. D. J.; Kollman, P. A.; Groenen, L. C.; Reinhoudt, D. N.; Van Hummel, G. J.; Ugozzoli, F.; Andreetti, G. D. *J. Am. Chem. Soc.* **1990**, *112*, 4165.

(13) Arduini, A.; Pochini, A.; Reverberi, S.; Ungaro, R. *J. Chem. Soc., Chem. Commun.* **1984**, 981.

(14) Gutsche, C. D.; Bauer, L. J. *J. Am. Chem. Soc.* **1985**, *107*, 6052.

(15) Shinkai, S.; Arimura, T.; Kawabata, H.; Murakami, H.; Araki, K.; Iwamoto, K.; Matsuda, T. *J. Chem. Soc., Chem. Commun.* **1990**, 1734.

(16) Wolff, A.; Boehmer, V.; Vogt, W.; Ugozzoli, F.; Andreetti, G. D. *J. Org. Chem.* **2002**, *55*, 5665.

(17) Clayden, J.; Greeves, N.; Warren, S.; Wothers, P. *Organic Chemistry*; Oxford University Press, 2000.

(18) Sandmeyer, T. *Ber.*, *17*, 2650.

(19) Sandmeyer, T. *Ber.*, *17*, 1633.

(20) Doyle, M. P.; Siegfried, B.; Dellaria, J. F. *J. Org. Chem.* **1977**, *42*, 2426.

(21) Hodgson, H. H. *Chem. Rev.* **1947**, *40*, 251.

(22) Krasnokutskaya, E. A.; Semenischeva, N. I.; Filimonov, V. D.; Knochel, P. *Synthesis-Stuttgart* **2007**, 81.

(23) Vogel, A. I.; Furniss, B. S.; Hannaford, A. J.; Rogers, V.; Smith, P. W. G.; Tatchell, A. R. *Vogel's Textbook of Practical Organic Chemistry*, 1978.

(24) Andreetti, G. D.; Pochini, A.; Ungaro, R. *J. Chem. Soc., Perkin Trans. 2* **1983**, 1773.

(25) Coruzzi, M.; Andreetti, G. D.; Bocchi, V.; Pochini, A.; Ungaro, R. *J. Chem. Soc., Perkin Trans. 2* **1982**, 1133.

(26) Dueno, E. E.; Bisht, K. S. *Tetrahedron* **2004**, *60*, 10859.

(27) Barrett, E. S.; Irwin, J. L.; Turner, P.; Sherburn, M. S. *J. Org. Chem.* **2001**, *66*, 8227.

(28) Miller, A. K.; Byun, D. H.; Beaudry, C. M.; Trauner, D. *Proc. Natl. Acad. Sci. U. S. A.* **2004**, *101*, 12019.

(29) Meyers, A. I.; Willemsen, J. J. *Tetrahedron* **1998**, *54*, 10493.

(30) Bailey, W. F.; Luderer, M. R.; Jordan, K. P. *J. Org. Chem.* **2006**, *71*, 2825.

(31) Merrill, R. E.; Negishi, E. *J. Org. Chem.* **1974**, *39*, 3452.

(32) Pansegrau, P. D.; Rieker, W. F.; Meyers, A. I. *J. Am. Chem. Soc.* **1988**, *110*, 7178.

(33) Meyers, A. I.; Pansegrau, P. D. *Tetrahedron Lett.* **1983**, *24*, 4935.

(34) Bailey, W. F.; Patricia, J. J. *J. Organomet. Chem.* **1988**, *352*, 1.

(35) *Synthesis of Organometallic Compounds A Practical Guide*; Komiya, S., Ed.; John Wiley & Sons: New York, 1997.

(36) Knochel, P.; Dohle, W.; Gommermann, N.; Kneisel, F. F.; Kopp, F.; Korn, T.; Sapountzis, I.; Vu, V. A. *Angew. Chem. Int. Ed.* **2003**, *42*, 4302.

(37) Boymond, L.; Rottlander, M.; Cahiez, G.; Knochel, P. *Angew. Chem. Int. Ed.* **1998**, *37*, 1701.

(38) Villieras, J. *Bull. Soc. Chim. Fr.* **1967**, 1520.

(39) Krasovskiy, A.; Straub, B. F.; Knochel, P. *Angew. Chem. Int. Ed.* **2006**, *45*, 159.

(40) Krasovskiy, A.; Knochel, P. *Angew. Chem. Int. Ed.* **2004**, *43*, 3333.

(41) Varchi, G.; Kofink, C.; Lindsay, D. M.; Ricci, A.; Knochel, P. *Chem. Commun.* **2003**, 396.

(42) Gutsche, C. D.; Pagoria, P. F. *J. Org. Chem.* **1985**, *50*, 5795.

(43) Xu, Z.-X.; Zhang, C.; Zheng, Q.-Y.; Chen, C.-F.; Huang, Z.-T. *Org. Lett.* **2007**, *9*, 4447.

(44) Verboom, W.; Bodewes, P. J.; van Essen, G.; Timmerman, P.; van Hummel, G. J.; Harkema, S.; Reinhoudt, D. N. *Tet.* **1995**, *51*, 499.

(45) Gilman, H.; Jones, R. G. *J. Am. Chem. Soc.* **2002**, *63*, 1439.

(46) Bailey, W. F.; Patricia, J. J.; Nurmi, T. T.; Wang, W. *Tetrahedron Lett.* **1986**, *27*, 1861.

(47) Taylor, R. *Tetrahedron Lett.* **1975**, 435.

(48) Sharp, J. T.; Skinner, C. E. D. *Tetrahedron Lett.* **1986**, *27*, 869.

(49) Tolbert, L. M.; Khanna, R. K.; Popp, A. E.; Gelbaum, L.; Bottomley, L. A. *J. Am. Chem. Soc.* **1990**, *112*, 2373.

(50) Clayden, J.; Fletcher, S. P.; McDouall, J. J. W.; Rowbottom, S. J. M. *J. Am. Chem. Soc.* **2009**, *131*, 5331.

(51) Dospil, G.; Schatz, J. *Tetrahedron Lett.* **2001**, *42*, 7837.

(52) Matvieiev, Y. I.; Boyko, V. I.; Podoprigorina, A. A.; Kalchenko, V. I. *J. Inclusion Phenom. Macrocyclic Chem.* **2008**, *61*, 89.

(53) Meyers, A. I. *J. Org. Chem.* **2005**, *70*, 6137.

(54) McKennon, M. J.; Meyers, A. I.; Drauz, K.; Schwarm, M. *J. Org. Chem.* **1993**, *58*, 3568.

(55) Sammakia, T.; Latham, H. A. *J. Org. Chem.* **1996**, *61*, 1629.

(56) Meyers, A. I.; Gabel, R.; Mihelich, E. D. *J. Org. Chem.* **1978**, *43*, 1372.

(57) Reuman, M.; Meyers, A. I. *Tetrahedron* **1985**, *41*, 837.

(58) Snieckus, V. *Chem. Rev.* **1990**, *90*, 879.

(59) Gschwend, H. W.; Rodriguez, H. R. *Heteroatom-facilitated lithiations*, 1979; Vol. 26.

CHAPTER 3

Ortholithiation Reactions

3.1 Ortholithiation of Model Compounds

Having successfully synthesised oxazoline calixarene **2.1**, we wanted to determine if it could be asymmetrically ortholithiated. It should be mentioned that a number of possible concerns regarding the feasibility of our approach existed, including steric constraints preventing lithiation, and the possibility of lateral lithiation of the benzylic methylene bridges which has been reported to occur on the calixarene.[1]

In order to gain a better understanding of the conditions we were likely to need for the ortholithiation of oxazoline **2.1**, we initially undertook a series of reactions on a suitable model compound. The commercially available 4–iodo–phenol was transformed in good yield in three easily accomplished steps to model oxazoline **3.3**. We hoped that the use of the para–propoxy oxazoline model **3.3** would emulate the electronic structure of oxazoline calixarene **2.1** (Scheme 3.1).

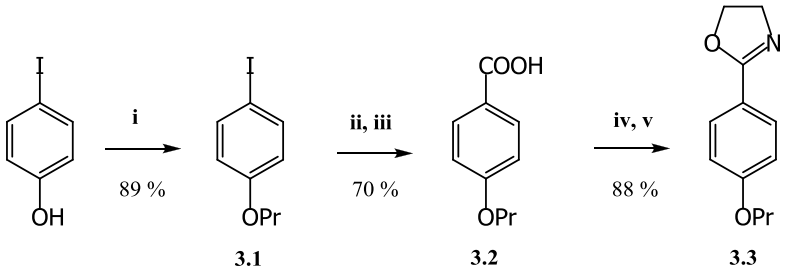

Scheme 3.1: Synthesis of model ethyl oxazoline propyl phenol **3.3**. Reagents and conditions: i) K_2CO_3 (2 eq), DMF, *n*PrI (3.8 eq), ii) *s*BuMg.$LiCl_2$ (2 eq), rt, 2 h, iii) CO_2 (exs), iv) $SOCl_2$ (exs), rt, 16 h, v) ethanolamine (2 eq), Et_3N (3 eq), DCM, rt, 24 h, vi) $SOCl_2$ (exs), DCM, rt, 12 h.

There are numerous conditions that have been reported in the literature for oxazoline–directed ortholithiation; among these there are a surprising degree of variation in conditions.[2-4] In cases where diastereoselective lithiation is performed, particular detail has been given to the choice of solvent, alkyllithium and additive.[3,5,6]

Following a literature procedure for a structurally related compound,[7] ortholithiation of oxazoline **3.3** using *n*BuLi in diethyl ether at 0 ºC was attempted, followed by quenching after 4 hours with

iodomethane. Surprisingly, only starting material was recovered and no observable formation of an ortholithiated product was detected. Increasing the number of equivalents of *n*BuLi resulted in the disappearance of the starting material, however, we again failed to detect the desired *ortho* functionalised product. It is known that oxazoline can undergo addition reactions, both to the aryl system as well as potentially also to the 'imine' carbon centre.[3] Beak and co–workers observed the formation of addition products in reactions using *t*BuLi with aryl oxazolines,[8] with addition of *t*–butyl groups into the aryl system.

Owing to the failures of the primary alkyllithium reagent *n*BuLi, we decided to investigate the use of a secondary alkyllithium as there is substantial literature precedent for their use with aryl oxazolines at lower temperatures.[2,6,9,10] The procurement of commercial secondary and tertiary reagents was investigated, however long shipping times led us to consider synthesising them in house. The synthesis of the alkyllithiums used in this study are presented in the following section.

Using *s*BuLi, the ortholithiation of oxazoline model **3.3** at 0 ºC was attempted, pleasingly furnishing the anticipated *ortho* methylated product **3.4**, albeit in moderate yield (~ 40%). A second product **3.5**, associated with the addition of an *s*–butyl group (from the alkyllithium) was also isolated. In contrast to the findings of Beak *et al*,[8] the addition of the alkyllithium to the aryl ring did not occur, but instead suggested nucleophilic addition of the alkyllithium at the imidate centre of the oxazoline. After hydrolysis during workup of the *N*,*O* acetal intermediate this resulted in the formation of ketone **3.5** (Scheme 3.2).

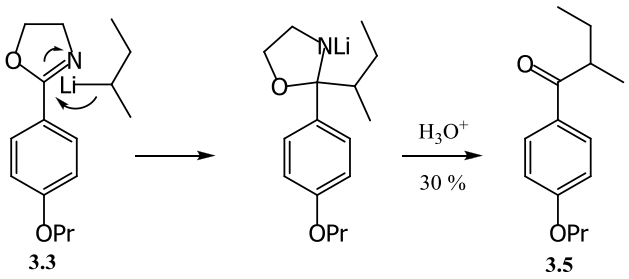

Scheme 3.2: Formation of addition product ketone **3.5**. Reagents and conditions: *s*BuLi (1.2 eq), Et_2O, 0 ºC, 4 h.

Owing to the formation of addition product **3.5**, we decided to attempt ortholithiation at a lower temperature. Inspection of the literature on a structurally related compounds revealed that ortholithiation could be achieved in 30 minutes using *i*PrLi in THF at −78 ºC.[9] Implementation of these conditions furnished the *ortho*–methylated product **3.4** in a good yield of 90% (Scheme 3.3). We also produced formyl product **3.6** using stringently dried DMF as the electrophile, although

the formyl product was found not to be stable under the conditions required for silca gel column chromatography.

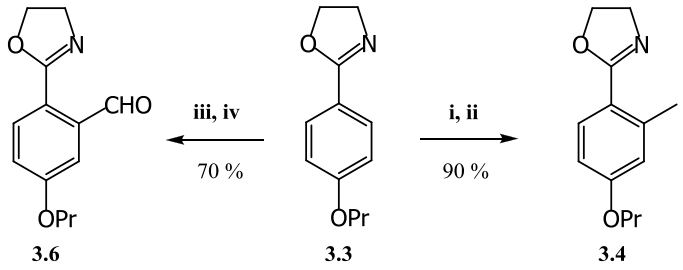

3.6 **3.3** **3.4**

Scheme 3.3: Ortholithation of model compound **3.3**. Reagents and conditions: i) *s*BuLi (1.2 eq), THF, −78 ºC, 35 m. ii) MeI (6.8 eq), iii) *s*BuLi (1.6 eq), THF, −78 ºC, 35 m, iv) DMF (8 eq).

3.2 Synthesis of Alkyllithiums

The synthesis of alkyllithium reagents requires exacting experimental technique, as both lithium metal and the alkyllithium products are highly flammable, and can spontaneously combust upon exposure to air. The quality of the lithium is also important for the successful synthesis of these reagents, in particular the quality of the metal at the surface. The presence of a sodium impurity in the lithium has been observed to be vital in aiding the formation of alkyllithiums.[11] It has been shown that for the formation of certain alkyllithiums, 5 to 30 mol % of sodium in the reactor greatly improves the yield of the alkyllithium, particularly the very capricious 2–ethylhexyllithium.[12]

Exposure of lithium to oxygen and moisture during handling quickly results in the formation of an oxide layer on the surface of the metal. This outer layer of oxide greatly retards the formation of alkyllithiums, and it was found that the preparation of alkyllithiums using poor quality lithium results in poor conversion. One means of overcoming this problem is by preparing lithium sand: which is prepared by melting metallic lithium (>180 ºC) in sodium dried mineral oil, followed by rapidly stirring the mixture until fine particles of lithium have formed. After the dispersion has formed, the mixture is cooled, solidifying into finely divided lithium particles.[13,14] Another technique that is useful for preparing the surface of the lithium is to briefly expose the lithium metal (under strict inert conditions) to dry *i*PrOH.[15] This should be done in the absence of other solvents, otherwise rapid oxidation can occur, making it difficult to control. After careful removal of the remaining *i*PrOH, the resulting grey lithium–isopropoxide encrusted lithium is suspended in dry pentane and sonicated. Sonication breaks off the isopropoxide crust, which can then be removed by cannula or syringe leaving the lithium with a bright metallic lustre.[15] It has also been

reported that the addition of small quantities of ethers to the alkane solvent can improve the conversion of alkyl halides to the desired alkyllithium,[16] even if theoretically the quantity of ether added eventually consumes an equimolar quantity of alkyllithium. Activation of the lithium metal before addition of the alkyl halide is also generally performed, by stirring with a small quantity of an active alkyllithium[16] or lithium hydride which seems to aid the initiation of the reaction.[17] Another approach that proved to be successful was placing the reaction vessel in a sonicator during the reaction, which removes the coating that forms around the lithium during the reaction and in certain instances led to a higher yield of the alkyllithium than conventional approaches allowed.

Ideally, the use of finely powdered lithium is preferable for the synthesis of alkyllithiums due to its high surface area, however its highly activated nature can cause spontaneous combustion on contact with oxygen, therefore its use is experimentally challenging. A particularly challenging part of the synthesis of alkyllithiums is the quenching of the unreacted lithium after the reaction is complete. The synthesis of alkyllithium reagents must be performed under argon, and specifically not under nitrogen as red/brown particles of lithium nitride form upon exposure of the metal to nitrogen.[18]

In high yielding reactions we observed that upon addition of the alky halide a rapid purple discolouration of the lithium surface was evident. If this discolouration failed to occur, lower yields generally resulted. This is presumably due to elimination reactions occurring instead of the intended oxidative insertion. Using the discussed general principles and procedures MeLi,[18] *s*BuLi,[19] *i*PrLi, *c*HexLi, *c*PentLi and *t*BuLi[11] were synthesized, with standardization by colourimetric titration (Table 3.1).[20] Yields for these reagents typically were in the order of 50 – 65%, except for the synthesis of *t*BuLi and MeLi which were synthesised with yields of greater than 80%.

Table 3.1: Synthesis of alkyllithiums.

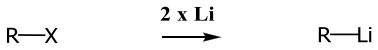

Entry	R	X	Lithium (eq)	Conditions	Addition /ml.h^{-1}	% Yield
1	Me	I	Sand (7)	Et_2O, rt	7.5	88
2	*s*Bu	Cl	Ingots (3)	Pentane, Δ	8.5	62
3	*s*Bu	Cl	iPrOH cleaned ingots (3)	Pentane, Δ, sonication	5	86
4	*i*Pr	Cl	Ingots (3)	Pentane, Δ	7	65
5	*i*Pr	Cl	*i*PrOH cleaned ingots (3)	Pentane, Δ, sonication	8	40
6	*c*Hex	Br	Ingots (3)	Pentane, Δ	4	5
7	*c*Hex	Cl	*i*PrOH cleaned ingots (4)	Et_2O, –12 °C,	8	30
8	*c*Pent	Cl	Sand (6)	Pentane, Δ	4	55
9	*t*Bu	Cl	Powder (15)	THF (0.05 eq), Pentane, Δ	13	80
10	*t*Bu	Cl	Sand (14)	THF (0.05 eq), Pentane, Δ	13	2

Owing to the low basicity of MeLi, it can be synthesised in diethyl ether (Entry 1 –

Table 3.1), which undoubtedly greatly aids in its formation. We found that performing the synthesis of *s*BuLi in the sonicator led to a significant improvement in the yield (Entry 2 – Table 3.1). The synthesis of *c*HexLi[21] proved to be highly problematic, with consistently low yielding reactions occurring (Entry 6 – Table 3.1). Reasons for this could possibly be attributed to the greater susceptibility of the starting alkyl chloride to undergo elimination reactions. Generally this reagent is synthesised in diethyl ether at low temperatures,[22] or by lithium halogen exchange.[23] Indeed when we used Et_2O as the solvent the yield was improved, although the conversion was still relatively low compared to the other secondary reagents (Entry 7 – Table 3.1). The synthesis of tertiary reagents is known to occur more rapidly than secondary reagents,[3,22] which coupled to the high quality of the lithium dispersion used in the reaction could account for the high yield recorded for *t*BuLi (Entry 9 – Table 3.1). Attempts at synthesising *t*BuLi from lithium ingots failed (Entry 10 – Table 3.1).

3.3 Ortholithiation of Oxazoline Calixarene 2.1

Returning to the ortholithiation of calixarene oxazoline **2.1**: application of the conditions developed for the model compound, (THF, 1.6 eq *s*BuLi, –78 ºC, 40 minutes) failed to give any

noticeable sign of an ortholithiated product, pleasingly though, no evidence of benzylic lithiation of the methylene bridges was observed.[1] Taking cognisance of the thermal stability of secondary alkyllithiums in ethereal solvents,[24] we attempted to increase the reaction temperature (Et_2O, 3 eq *s*BuLi, −45 ºC, 4 hours) again with no observable product formation.

There is widespread literature precedent for the use various additives in ortholithiation reactions,[2,3] thus TMEDA (2 eq) was added to a *s*BuLi diethyl ether reaction at −45 ºC, with quenching after 4.5 hours with DMF. The appearance of a number of new compounds was observed on TLC, which could be isolated by column chromatography, however, no sign of the anticipated formyl peak in the ^{1}H NMR spectra of these compounds (or the crude mixture) was observed. Owing to the experience of decomposition of the formyl product **3.6**, it appeared likely that decomposition of the product had occurred during purification.

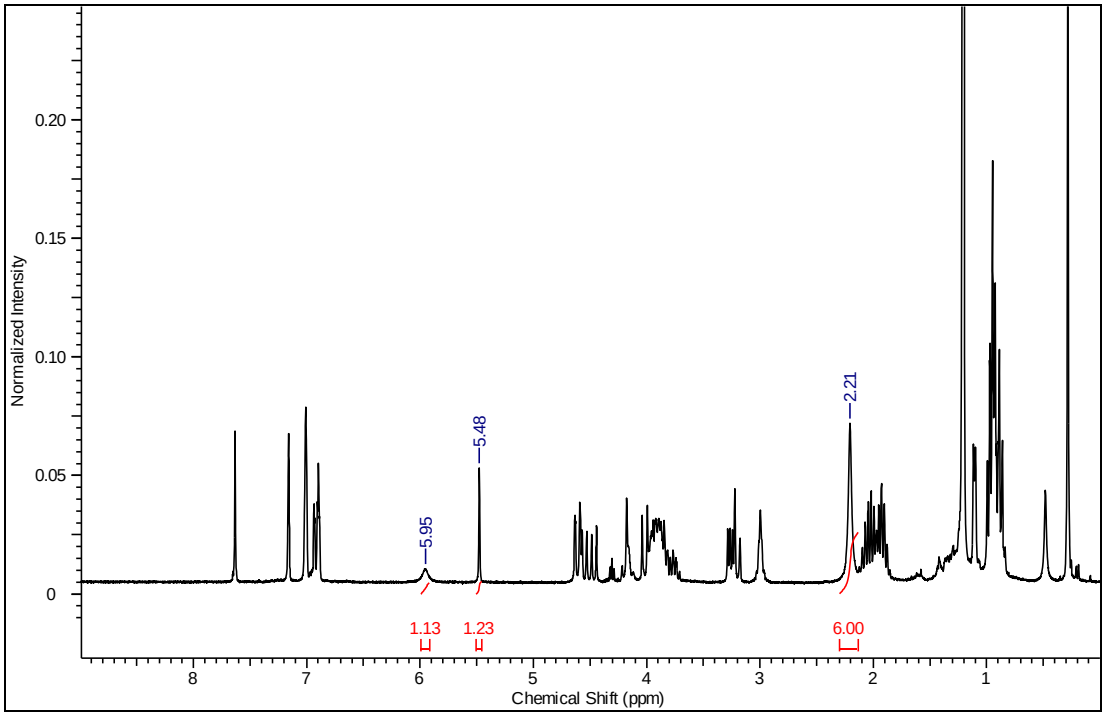

Figure 3.1: ^{1}H NMR spectrum of ortholithiation product **3.7** (50 °C Benzene–d_6).

Inspection of the isolated compounds revealed the formation of certain products associated with the addition of the alkyllithium to the oxazoline (approximately 10%), as well a compound possessing only seven aromatic protons (as evidenced by ^{1}H NMR spectroscopy) strongly indicating that ortholithiation had occurred (Figure 3.1). In trying to elucidate the structure of this molecule, a number of features of the ^{1}H NMR spectrum were used to gain insight into what appears to be attached to the molecule. All signals from the oxazoline functionality were present, however there are additional signals at 5.95, 5.48 and a broad singlet at 2.21 ppm. The expected

reaction of DMF with an aryllithium sees the cleavage of the *C—N* bond upon workup with the formation of the formyl product as shown in Scheme 3.4. The extra signals observed in the ^{1}H NMR spectrum seem to indicate the presence of additional atoms in the structure that cannot be explained by a simple rearrangement of the formyl product. If the intermediate product from the reaction of DMF with the lithiated intermediate is depicted, the obvious mechanism through which rearrangement could occur would be addition of the oxy anion to the imidate centre of the oxazoline (Option 2 in Scheme 3.4).

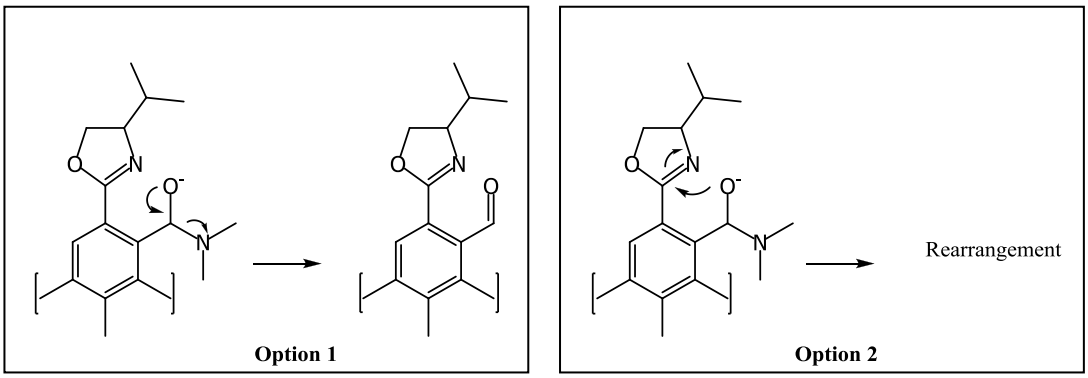

Scheme 3.4: Possible mechanistic pathways for decomposition of initial product of DMF reaction.

Examination of the ^{1}H NMR spectrum of the product (Figure 3.1) suggested that the singlet at 5.33 ppm could be assigned to an isolated methine, with the broad singlet at 2.42 ppm being attributed to the *N,N* dimethyl peaks. In a review of the literature regarding rearrangement of ortho substituted oxazolines, a number of potential structures were identified.[7,25,26] Interestingly, *ortho* substituted oxazolines have been used as starting materials for producing lactones (the ortholithiation is generally followed by acid hydrolysis).[25,26] The most likely structure we identified was similar to a structure reported by Meyers and co–workers,[27] whose approach was later used by Schow *et al.* (as shown in Scheme 3.5).[7]

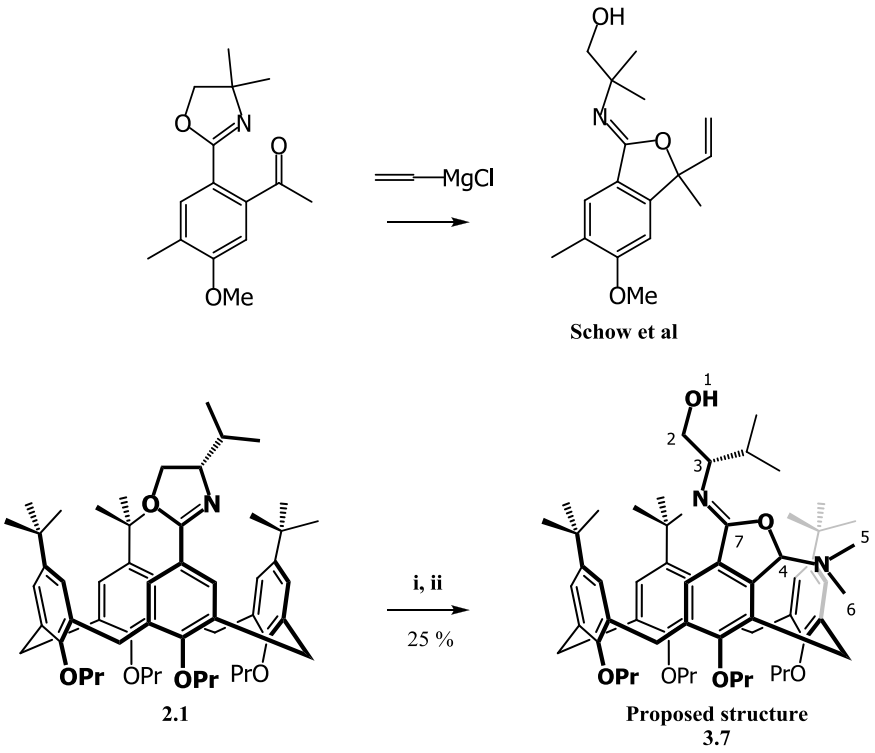

Scheme 3.5: Literature structure of rearrangement of oxazoline and proposed structure of DMF product 3.7. Reagents and Conditions: i) *s*BuLi (5 eq), TMEDA (4 eq), Et_2O, −40 ºC, 4 h (ii) DMF (exs), −40 ºC to rt, NH_4Cl.

Extensive 2D NMR analysis (GCOSY, GHMBC, GHMQC, NOESY obtained at 50 ºC owing to the better resolution of the broad singlet at 2.42 ppm) offered strong support for proposed structure **3.7** through the indication of a weak coupling of the hydroxyl peak (atom 1) at 5.64 ppm to the chiral chain (atom 2). Interpretation of the 2D results were hampered by the lack of coupling through the imine C=N bond, however GHMBC indicates coupling of atom 4 to atom 7, which when viewed in conjunction with the lack of coupling from atoms 2 and 3 to the aryl ring, appear to confirm the proposed ring structure. An IR spectrum of the compound is rather ambiguous, as the signal at 1668 cm^{-1} could be due to an amide C=O stretch or that of a C=N stretch. Repeated attempts at crystallisation of **3.7** failed to produce diffraction quality crystals. A mass spectrum of the compound was obtained, which initially appeared to indicate the formation of the formyl product as evidenced by the large peak at 900.61 (which corresponds to a M+H signal for the formyl product). However, closer inspection revealed a minor peak at 945.6, which corresponds to the M+ peak of the rearranged product **3.7**. Coupled HR–MSMS analysis of the 945.6 peak, returned fragmentation to the 900.61 peak, confirming that the 945.6 peak is indeed that of the M+ fragment of rearranged structure **3.7**. Attempted hydrolysis of **3.7** in a 2M HCl–acetone mixture failed, and only starting material was recovered after stirring overnight.

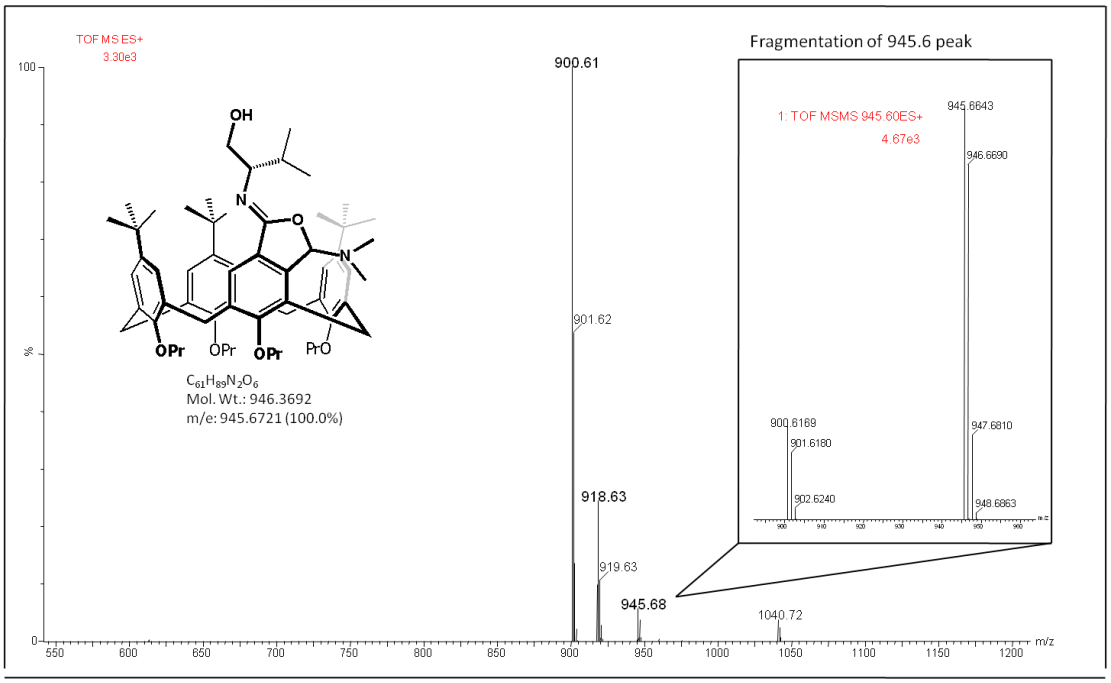

Figure 3.2: Mass spectrum of DMF rearranged product **3.7**. Note: The MSMS fragmentation pattern of peak 945.6 is shown, indicating fragmentation to 900.6. Similar fragmentation of the water adduct 918.6 to 900.6 was observed. The m/e calculated mass is based on the M+H value.

To further investigate this rearrangement, the reaction was repeated and the crude reaction mixture analysed by ^{1}H NMR spectroscopy. The spectrum revealed the presence of the same product, indicating that the rearrangement occurred before exposure of the compound to the mildly acidic silica gel used in the purification process. The presence of the *N*,*N*–dimethyl amine functionality in **3.7** (from *N*,*N*–dimethyl formaldehyde) also indicates that the formation of **3.7** is probably not associated with the rearrangement of a formyl product, but rather forms from a secondary reaction of the unhydrolysed *N*,*O*–acetal intermediate with the oxazoline imidate centre (Scheme 3.4). To test if the rearrangement was due to instability of the intermediate, the reaction was repeated, however the temperature was held at −45 ºC for 1 hour after the addition of the DMF. This was followed by the addition of aqueous ammonium chloride solution at −45 ºC. Only starting material was recovered from this reaction, indicating that higher temperatures were required for reaction of DMF with the lithiated calixarene intermediate. Having observed the sensitivity of the formylated model compound **3.6** to the mildly acidic conditions of the silica gel, the reaction was repeated[i] and quenched with deionised water instead of ammonium chloride (reaction conditions iii and iv — Scheme 3.6). A crude ^{1}H NMR spectroscopic analysis of the mixture indicated the presence of a formylated product (**3.8** – Scheme 3.6) and a minor amount of the rearranged product **3.7**. This result indicated that the intermediate (Scheme 3.4) can be

[i] (using a different alkyllithium and conditions)

induced to form rearranged product **3.7** by protonation of the nitrogen in the oxazoline (through the acidic ammonium chloride solution used during workup) activating the imidate centre and inducing nucleophilic addition and cyclisation (reaction conditions i and ii – Scheme 3.6). Purification of **3.8** was not attempted due to its expected instability.

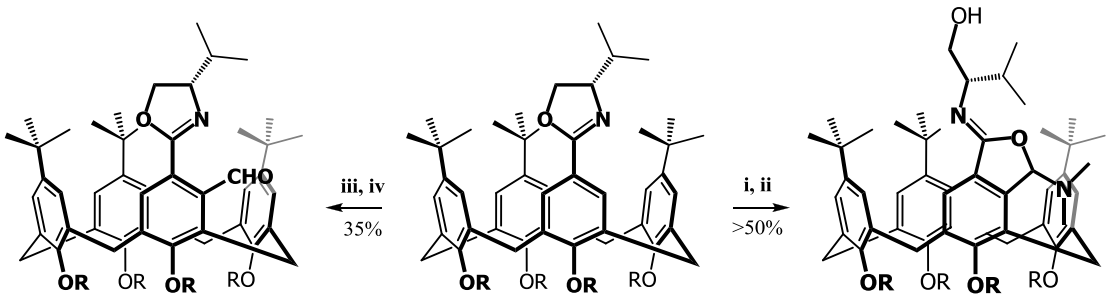

3.8 **2.1** **3.7**

Scheme 3.6: Ortholithiation products using DMF as an electrophile. Reagents and Conditions: i) *i*PrLi (3 eq), TMEDA (6 eq), Et_2O, −45 ºC, 5 h (ii) DMF (10 eq), aq NH_4Cl, iii) *c*PentLi (5 eq), TMEDA (10 eq), Et_2O, −78 ºC, 24 h, iv) DMF (5 eq), H_2O.

As observed on the model compound, the use of DMF can represent an experimental challenge, often produced low yields. Under the same experimental conditions the use of iodomethane (**3.9** – Scheme 3.7) resulted in a yield of greater than 80% being recorded, as determined from the ^1H NMR spectrum of the mixture. Unfortunately, this reaction was complicated by our inability to separate the product from the starting material by chromatographic means.

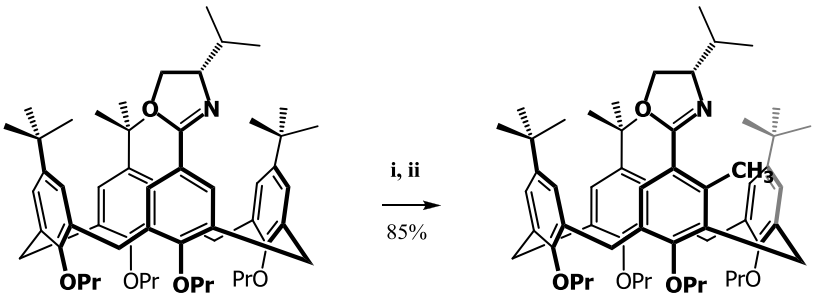

2.1 **3.9**

Scheme 3.7: Methylation of oxazoline **2.1**. Reagents and Conditions: i) *s*BuLi (3 eq), TMEDA (6 eq), Et_2O, −45 ºC, 4 h (ii) MeI (exs), −45 ºC to rt, NH_4Cl.

3.4 Determination of Diastereoselectivity of Ortholithiation

Having demonstrated that oxazoline–directed ortholithiation presented a viable method for the *meta* functionalisation of the calixarene, an investigation into the diastereoselectivity of this

reaction could be pursued. Inspection of the crude reaction mixtures of rearranged product **3.7** and methylated compound **3.9** revealed what appeared to be the presence of major and minor diastereomers in the reaction mixture. However, from these spectra we were unable to identify the diastereomers unambiguously.

A large number of methods have been employed for the determination of the diastereoselectivity, including HPLC, GC and NMR techniques, however the use of NMR spectroscopy was an alluring option since, provided the signals for the separate diastereomers can be identified, no further method development would be required. Considering the large number of signals present in the proton spectrum of oxazoline **2.1**, the use of another spin–active element, such as phosphorus or fluorine appeared attractive[28,29] to simplify quantification of the diastereomeric ratio. In a review of the literature surrounding the use of electrophilic fluorine reagents a number of possible options came to light.[30,31] Molecular fluorine is the most basic source of electrophilic fluorine available,[32] however its use experimentally challenging owing to its high reactivity and toxicity, making its incorporation into standard laboratories impractical. As a result other electrophilic sources of fluorine have been developed including Selectfluor,[32,33] *N*–fluoro–o–benzenedisulfonimide (NFOBS)[33] and *N*–fluorobenzenesulphonimide (NFSI),[34] as shown in Figure 3.3

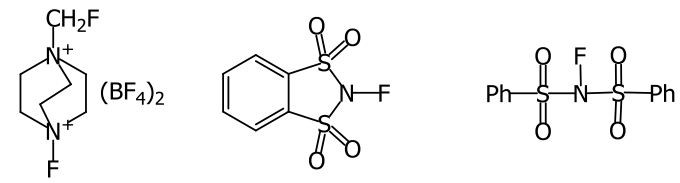

Selectfluor NFOBS NFSI

Figure 3.3: Electrophillic sources of fluorine

The use of the commercially available reagent Selectfluor was attempted first, however apparently owing to its low solubility in ethereal solvents no evidence of fluorination of ortholithiated calixarene **2.1** was observed. Following this NFSI was tested, as it is known to be soluble in ethereal solvents and has been applied in organolithium reactions[35] successful fluorination of **2.1** in 60% yield was observed (Scheme 3.8), yielding major **3.10** and minor **3.11** diastereomers (determination of the configuration of these diastereomers will be discussed in the following chapter).

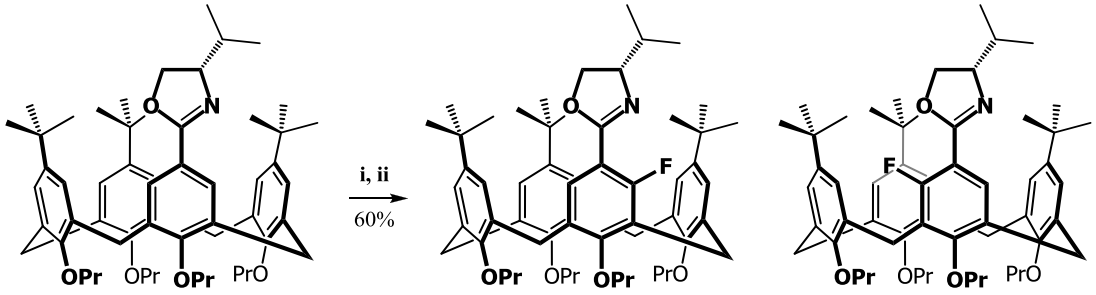

2.1 **3.10** **3.11**

Scheme 3.8: Fluorination of oxazoline calixarene **2.1**. Reagents and conditions: *s*BuLi (2.5 eq), TMEDA (6 eq), Et_2O, −44 ºC, 4 h, ii) NFSI (6 eq), −44 ºC to rt.

Inspection of the ^{19}F NMR spectrum provided a clear indication as to the selectivity of the reaction; two separate signals were visible at −113.29 ppm (major) and −114.25 ppm (minor) respectively (Figure 3.4). Integration of the signals provided a means of quantifying the selectivity between the two diastereomers.[29]

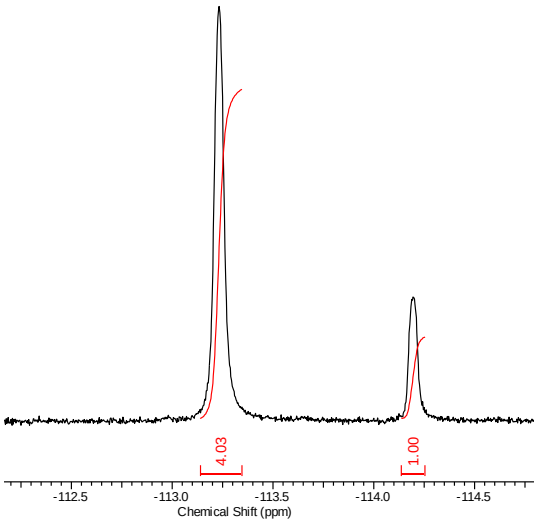

Figure 3.4: ^{19}F spectrum of fluorinated products **3.10** (major) and **3.11** (minor).

Validation of the ^{19}F NMR ratio came from inspection of the ^{1}H NMR spectrum, with the same ratio being observed in a number of separate regions of the spectrum.

3.5 Optimization of Selectivity and Yield of Ortholithiation Reaction

As noted from the results obtained by Sammakia *et al.*, there are a number of parameters that have been shown to affect the selectivity of ortholithiation reactions using chiral oxazolines,[5,6] including the solvent, additive, temperature and alkyllithium.[3] Having already observed that

without TMEDA ortholithiation failed to occur to any significant degree in diethyl ether, we expected that a number of these factors could play an important role in both the rate of the reaction and on the selectivity.

3.5.1 Temperature and Solvent

A step–wise reduction in reaction temperature was performed while monitoring of yield and the selectivity of the reaction (Table 3.2). Pleasingly, a reduction in temperature increased the diastereoselectivity of the reaction, as well as reducing by –product formation associated with addition of the alkyllithium. Rather surprisingly, we found the ortholithiation reaction could be successfully performed at −78 ºC, as the use of oxazolines on non–activated systems has been reported as being limited to −45 ºC.[2]

Table 3.2: Effect of temperature on yield and *dr* in the ortholithiation of oxazoline **2.1**.

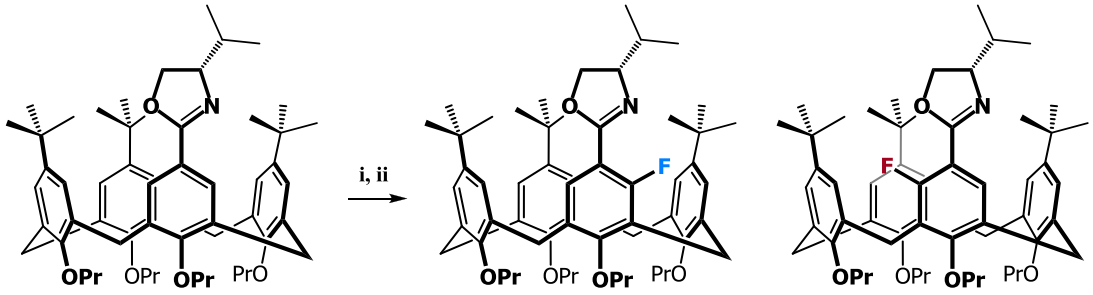

2.1 **3.10** **3.11**

Entry	Alkyllithium	Temp /ºC	% Yield	Ratio **3.10**:**3.11**
1	*s*BuLi	–45	77	5.3:1
2	*s*BuLi	–65	75	5.7:1
3	*s*BuLi	–78	39	7.2:1

Reagents and conditions: i) *s*BuLi (2.5 eq), Et_2O, TMEDA (6 eq), 4 h. ii) NFSI (3.4 eq). Yield determined by ^1H NMR, *dr* determined by ^{19}F NMR.

Having determined the optimal temperature for lithiation, the effect of different solvents on the lithiation was investigated. A range of ethereal solvents were tested along with the non–coordinating pentane (Table 3.3). The use of other ethereal solvents (iPr_2O and TBME) resulted in decreased selectivity when compared to diethyl ether. Reactions performed in THF caused a notable decrease in selectivity, on the other hand with an increased yield when compared to the results in that of diethyl ether. The use of pentane appeared to retard both the yield of the reaction and the selectivity of the reaction. This was rather surprising as work by Sammakia *et al.*,[5] displayed the greatest selectivity (>99% *dr*) when reactions were performed in pentane–TMEDA

mixtures on the oxazoline–directed ortholithiation of ferrocene. This result could perhaps also be related to the lower solubility of NSFI with the alkane solvent system and not a true indication of the extent or selectivity of ortholithiation in this reaction. Further investigation was not carried out.

Table 3.3: Effect of solvent on yield and *dr*.

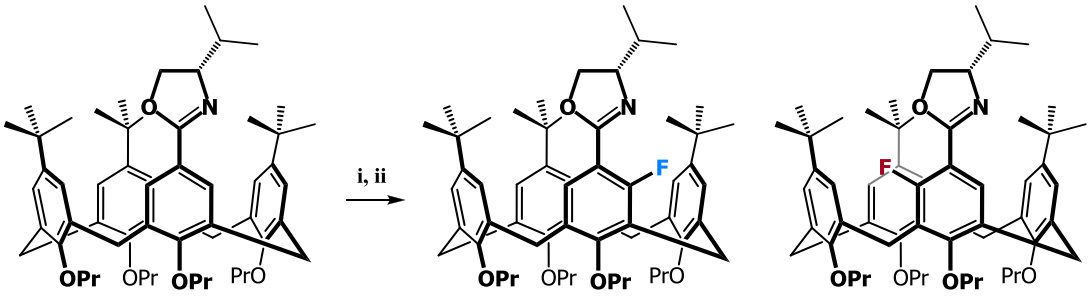

2.1 **3.10** **3.11**

Entry	Alkyllithium	Solvent	% Yield	Ratio **3.10**:**3.11**
1	*s*BuLi	Pentane	8	2.2:1
2	*s*BuLi	Toluene	78	5.5:1
3	*s*BuLi	THF	55	1.8:1
4	*s*BuLi	TBME	78	3.3:1
5	*s*BuLi	*i*Pr_2O	35	7.3:1
6	*s*BuLi	Et_2O	39	7.3:1

Reagents and conditions: i) *s*BuLi (2.5 eq), Et_2O, TMEDA (6 eq), 4 h. ii) NFSI (3.4 eq). Yield determined by ^{1}H NMR, *dr* determined by ^{19}F NMR.

3.5.2 TMEDA to Alkyllithium Ratio

Having observed the effect of the solvent on the diastereoselectivity of the reaction, it appeared to indicate that the ratio of TMEDA to that of the alkyllithium could also influence the selectivity of the reaction. A step–wise investigation into the effect of the ratio of alkyllithium to TMEDA was initiated at −78 ºC, with minor differences being observed when the RLi:TMEDA ratio was varied between 1:1.5 and 1:4. Hence a ratio of 1:2 was used.

3.5.3 Other Additives

Having observed how important the presence of TMEDA was in increasing the selectivity of the reaction, we screened a range of other known additives to see what their effects would be. Hexamethylphosphoramide (HMPA), *N*,*N*′–dimethylpropylideneurea (DMPU) and (−)–sparteine

were all tested in diethyl ether, without any observable sign of ortholithiation occurring. No visible sign of dearomatisation products could be detected when DMPU was used, which has been shown to be promoted by its use as an addative.[9] Triethylamine and trimethylamine were also tested without any observable product formation.

3.5.4 Yield of sBuLi Reaction

To improve the yield of the ortholithiation reaction at −78 ºC, the reaction time was extended (Table 3.4), and a small improvement in conversion noted. Observing how ineffectual pentane was at facilitating ortholithiation/fluorination, we noted that the alkyllithiums were stored in alkane solvents, possibly negatively affecting the reaction. We therefore removed the alkane solvents from the alkyllithium prior to initiation of the reaction. This added to the complexity of the experimental protocol, but pleasingly, increased the yield without affecting the selectivity of the transformation. We also chose to increase the number of equivalents of the alkyllithium, which furnished fluoro **3.10** in good yield.

Table 3.4: Optimisation of *s*BuLi reaction yield.

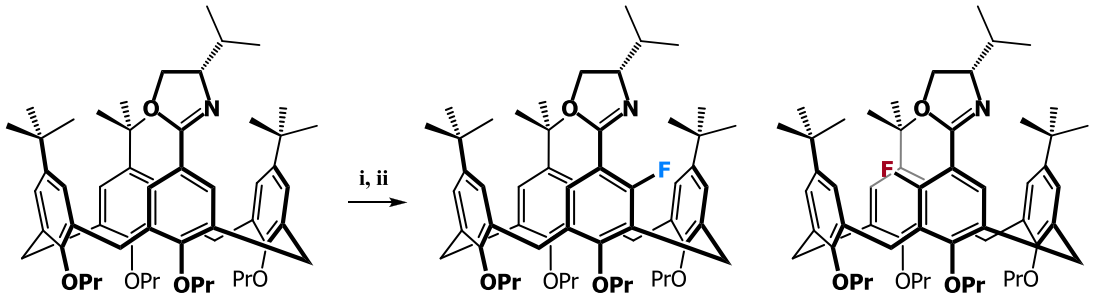

2.1 **3.10** **3.11**

Entry	Alkyllithium	Time /h	Reaction Conditions	% Yield	Ratio **3.10**:**3.11**
1	*s*BuLi (3)	4.5	Standard	39	7.5:1
2	*s*BuLi (3)	8	Standard	59	7.7:1
3	*s*BuLi (3)	4.5	Removal of pentane	66	7.5:1
4	*s*BuLi (6)	4.5	Removal of pentane	73	7.2:1

Reagents and conditions: Reagents and conditions: i) As per table. ii) NFSI (1.7 eq to *s*BuLi) –78 ºC, NSFI (3.4 eq), –78 ºC to rt, 12 h, Yield determined by ^{1}H NMR, *dr* determined by ^{19}F NMR.

3.5.5 Optimisation of Alkyllithium

Having observed the different diastereoselectivities generated in the ferrocenyloxazolines when different alkyllithiums were used by Sammakia *et al.*,[36] we were interested in observing what

effect changing the alkyllithium would have on the ortholithiation of the calixarene system. Initially, we had investigated the use of the primary reagent *n*BuLi, but failed to observe ortholithiation of oxazoline **2.1**. Supposing the insufficient basicity of the primary reagent to affect ortholithiation, we turned to the tertiary reagent *t*BuLi. Attempts at ortholithiation at −78 ºC failed to produce any significant formation (>5%) of fluorinated compounds **3.10** and **3.11**. An increase in reaction temperature above −65 ºC resulted in significant quantities of addition products forming, without ortholithiation occurring.

The formation of the addition product was only detected in reactions performed in diethyl ether with added TMEDA at temperatures above –78 ºC, while attempts at using *t*BuLi in THF resulted in recovery of the starting material. The elucidation of the exact structure of the addition product was hampered by the highly complex ^{1}H NMR spectrum which appeared to show the presence of diastereomers, possibly rotamers/conformers, as well as a mixture of products. The ^{13}C NMR spectrum of the addition product indicated a weak signal at 205.1 ppm, which suggested that the molecule contained a ketone functionality, however the presence of the chiral amino chain was also visible. We deduced therefore that the addition product contained an inseparable mixture of a *t*–butyl ketone **3.12** and an *N,O* acetal addition product **3.13** (Scheme 3.9), which was confirmed by HR–MS. We supposed that addition of the *t*–butyl anion to the imidate centre occurred, resulting in formation of *N,O* acetal **3.13** which was partially hydrolysed to ketone **3.12** during work up. Although of little use, ^{1}H NMR spectroscopy indicated that formation of the *N,O* acetal **3.13** occurred with a *dr* of approximately 71% between the two diastereomers occurred, the configuration of which were not determined. Hydrolysis of the mixture of **3.13** and **3.12** in aqueous acidic acetone lead exclusively to the ketone **3.12** in quantitative yield.

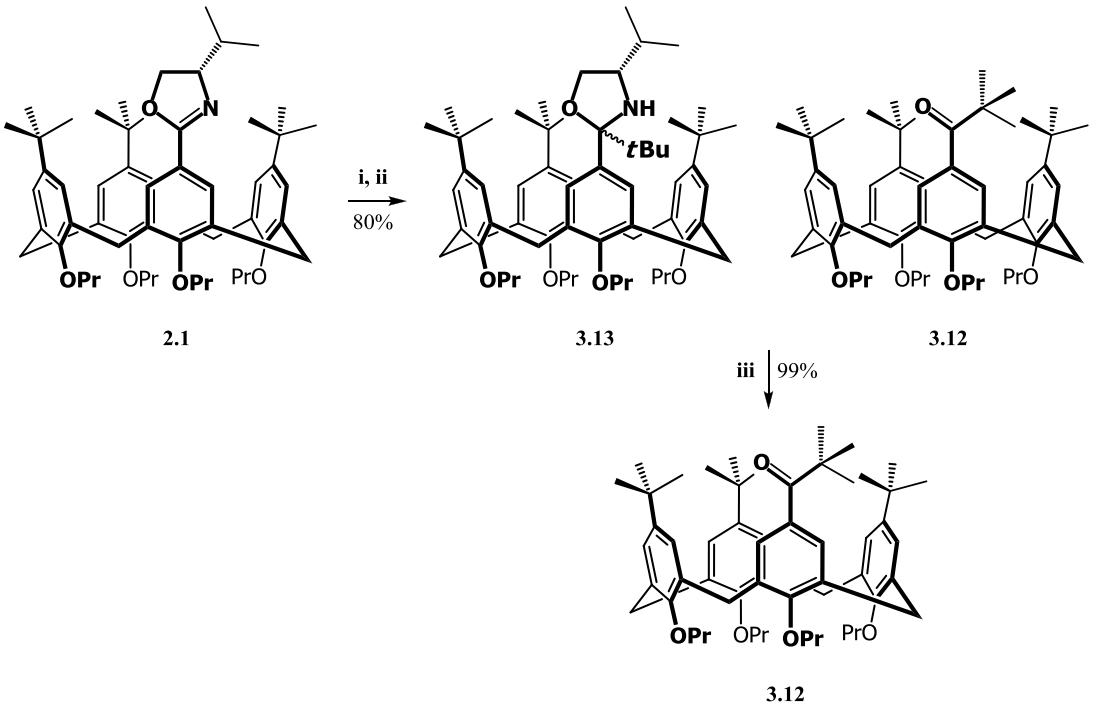

2.1 **3.13** **3.12** **3.12**

Scheme 3.9: Formation of *t*BuLi addition products **3.12** and **3.13**. Reagents and conditions: i) *t*BuLi (4 eq), Et_2O, TMEDA (12 eq), −45 ºC, 1.5 h, iii) H_2O, iii) 2M HCl in acetone, rt, 18 h.

Continuing our investigation into the effect of the alkyllithium, we wondered if other secondary alkyllithiums would further improve the selectivity of the lithiation. Owing to the necessity of having to synthesise our own alkyllithiums, we were in the fortunate position of being able to access a range of uncommon reagents. *i*PrLi was synthesised and, pleasingly, increased the selectivity considerably more than *s*BuLi (16:1 compared to 7.5:1 **3.10**:**3.11**) as shown in Table 3.5, albeit with a reduced yield.

Intrigued by this result, we realised that there are numerous other secondary alkyllithiums that could be synthesised, and many possible reagents that have not been evaluated in this regard. We chose to examine the cyclic reagents, cyclopentyl lithium (*c*PentLi) and cyclohexyl lithium (*c*HexLi), to observe the effect a cyclic structure would have on the selectivity. As already mentioned the synthesis of *c*HexLi proved challenging. After a number of attempts, sufficient quantities of reagent were obtained, allowing its evaluation in the ortholithiation of oxazoline **2.1**. The use of this reagent also returned increased selectivity, but with poor conversion. Observing the effectiveness of the cyclic reagent we undertook the synthesis of *c*PentLi, which when implemented in the ortholithiation of **2.1,** led to a significant improvement of the selectivity (26.5:1 **3.10**:**3.11**) far surpassing the selectivities achieved with the other reagents attempted up to that point (Table 3.5).

Table 3.5: Effect of alkyllithium on yield and *dr* in the ortholithiation of oxazoline **2.1**.

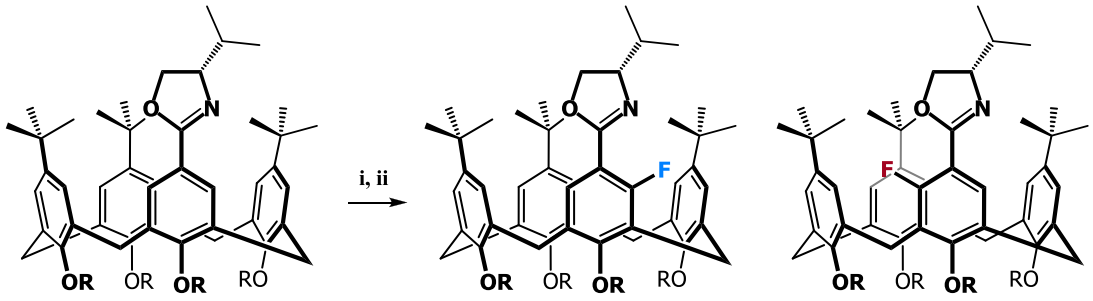

2.1 **3.10** **3.11**

Entry	Alkyllithium	% Yield	Ratio **3.10**:**3.11**
1[a]	*n*BuLi	0	–
2[a]	*t*BuLi	5	1.4:1
3[b]	*s*BuLi	39	7.5:1
4[a]	*i*PrLi	5	16:1
5[c]	*c*HexLi	17	11:1
6[a]	*c*PentLi	36	26.5:1

Reagents and conditions: Et_2O, TMEDA (2 eq to RLi), –78 °C, NFSI (1.7 eq to RLi), [a]RLi (6 eq), [b]RLi (3 eq), [c]RLi (4 eq). Yield determined by ^1H NMR, *dr* determined by ^{19}F NMR.

In order to optimise the yield of the *c*PentLi–induced ortholithiation, which proved to be significantly slower than the *s*BuLi reaction, it was necessary to remove the pentane prior to the reaction in addition to extending the reaction time to 24 hours (Table 3.6). This furnished reaction yields of above 70% without loss of diastereoselectivity. The concentration of the reaction is also an important consideration in determining the extent of ortholithiation and subsequent conversion to **3.10** and **3.11**. It was determined that a concentration of approximately 0.15 M of the calixarene **2.1** in the solvent system should be used for optimal yield.

Table 3.6: Optimisation of *c*PentLi ortholithiation.

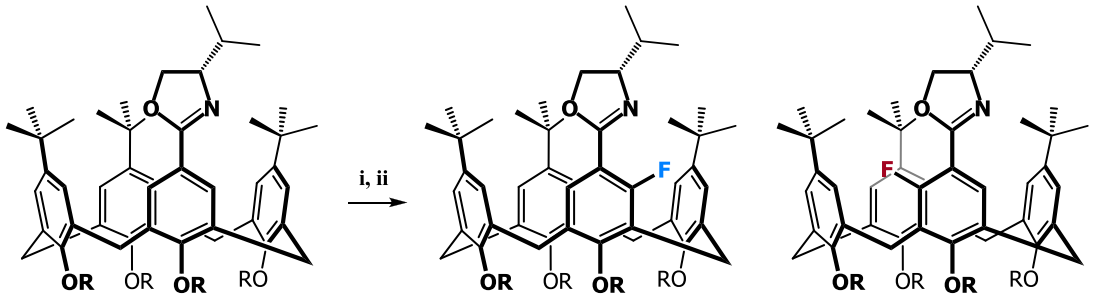

2.1 **3.10** **3.11**

Entry	Alkyllithium	Time /h	% Yield	Ratio **3.10**:**3.11**
1	*c*PentLi (3)	6	36	25.5:1
2	*c*PentLi (3)	13	59	25.2:1
3	*c*PentLi (3)	18	64	29.5:1
4	*c*PentLi (6)	24	74	25.5:1

Reagents and conditions: i) *c*PentLi, Et_2O, TMEDA (2 eq to RLi). –78 °C, ii) NFSI (3.4 eq), –78 °C to rt, 12 h, Yield determined by ^{1}H NMR, *dr* determined by ^{19}F NMR.

As *c*PentLi was synthesized from bromo and chloro alkyl halides, the effects of LiCl and LiBr on the selectivity of the reaction required consideration. The presence of lithium salts in other organolithium–based reactions has been shown to significantly influence the stereoselectivity and regioselectivity, specifically when using lithium amides.[37-40] In order to ascertain whether the presence of residual lithium salts could be inducing differences in the selectivity, we doped independent reaction mixtures with both of the salts. This failed to affect the selectivity, and when used in excess, considerably retarded the reaction yield. Following the same protocol, the presence of lithium hydride in the reaction mixture (which can be formed as a by –product from the degradation of the alkyllithium reagents in solution),[22] was also determined to be in–consequential.

3.5.6 Further Investigation of the THF Inversion in Diastereoselectivity

The difference in selectivity induced by the use of THF in the ortholithiation of oxazoline **2.1** was so pronounced that we considered the possibility that a purely THF–mediated ortholithiation was competing with the TMEDA coordinated lithiation. This was confirmed by performing a reaction in THF in the absence of TMEDA, which surprisingly revealed a small reversal in selectivity (Table 3.7). In an effort to see if this trend occurred for other alkyllithiums, a number of other

reagents were tested. *t*BuLi and *c*PentLi failed to ortholithiate the calixarene in THF, however the use of *i*PrLi resulted in a moderate increase in the reversal of selectivity.

Table 3.7: THF mediated ortholithiation

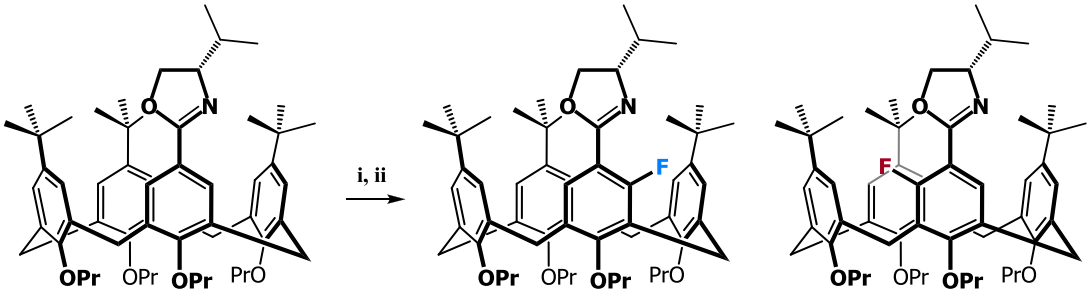

2.1 **2.10** **2.11**

Entry	Alkyllithium	Solvent	Additive	% Yield	Ratio **3.10**:**3.11**
1[a]	*s*BuLi	THF	TMEDA	55	1.8:1
2[a]	*i*PrLi	THF	TMEDA	44	4.5:1
3[a]	*s*BuLi	THF	–	49	1:1.7
4[b]	*i*PrLi	THF	–	12	1:2.4
5[a]	*t*BuLi	THF	–	0	–
6[a]	*c*PentLi	THF	–	0	–

Reagents and conditions: i) [a]RLi (4 eq), Et_2O, [b]RLi (3 eq) TMEDA (6 eq), −78 °C, 4 h, ii) NFSI (3.4 eq). Yield determined by ^{1}H NMR, *dr* determined by ^{19}F NMR.

3.6 Conclusion and Future Work

In conclusion we have demonstrated an asymmetric approach to the synthesis of inherently chiral calixarenes using chiral oxazoline–directed ortholithiation. It was found that the selectivity of the reaction was sensitive to solvent, temperature, the nature of additive, and the choice of alkyllithium. In order to prove the generality and applicability of this reaction for the diastereoselective synthesis of *meta*–substituted inherently–chiral calixarenes, functionalisation with a range of electrophiles needed to be performed. In addition, the removal of the chiral oxazoline from the calixarene would further demonstrate the scope of this methodology. This is the subject of the following chapter.

3.7 References

(1) Scully, P. A.; Hamilton, T. M.; Bennett, J. L. *Org. Lett.* **2001**, *3*, 2741.

(2) Snieckus, V. *Chem. Rev.* **1990**, *90*, 879.

(3) Clayden, J. *Organolithiums: Selectivity for Synthesis*; Pergamon: London, 2002; Vol. 23.

(4) Gschwend, H. W.; Rodriguez, H. R. *Heteroatom-facilitated lithiations*, 1979; Vol. 26.

(5) Sammakia, T.; Latham, H. A. *J. Org. Chem.* **1995**, *60*, 6002.

(6) Sammakia, T.; Latham, H. A.; Schaad, D. R. *J. Org. Chem.* **1995**, *60*, 10.

(7) Schow, S. R.; Bloom, J. D.; Thompson, A. S.; Winzenberg, K. N.; Smith, A. B. *J. Am. Chem. Soc.* **1986**, *108*, 2662.

(8) Beak, P.; Kerrick, S. T.; Gallagher, D. J. *J. Am. Chem. Soc.* **1993**, *115*, 10628.

(9) Clayden, J.; Parris, S.; Cabedo, N.; Payne, A. H. *Angew. Chem. Int. Ed.* **2008**, *47*, 5060.

(10) Reuman, M.; Meyers, A. I. *Tetrahedron* **1985**, *41*, 837.

(11) Kamienski, C. W.; Esmay, D. L. *J. Org. Chem.* **1960**, *25*, 1807.

(12) Morrison, R. C.; Dover, B. T.; Kamienski, C. W.; Patent, U., Ed.; Fmc Corp (Fmcc): US, 1993; Vol. US P 5211887.

(13) Bartlett, P. D.; Swain, C. G.; Woodward, R. B. *J. Am. Chem. Soc.* **1941**, *63*, 3229.

(14) Belzner, J.; Bunz, U.; Semmler, K.; Szeimies, G.; Opitz, K.; Schluter, A. D. *Chem. Ber.* **1989**, *122*, 397.

(15) Fraenkel, G.; Henrichs, M.; Hewitt, J. M.; Su, B. M.; Geckle, M. J. *J. Am. Chem. Soc.* **1980**, *102*, 3345.

(16) Morrison, R. C.; Hall, R. W.; Schwindeman, J. A.; Kamienski, C. W.; Engel, J. F.; App., E. P., Ed.; Fmc Corp (Fmcc): Eur. Pat. App., 1993; Vol. EP 92-202236 A1 19930203, .

(17) Weiss, W.; Dolling, E.; Schneider, B. 2003, p 16 pp.

(18) Lusch, M. J.; Phillips, W. V.; Sieloff, R. F.; Nomura, G. S.; House, H. O. *Org. Synth.* **1984**, *62*, 101.

(19) Bryce-Smith, D.; Turner, E. E. *J. Chem. Soc.* **1953**, 861.

(20) Winkle, M. R.; Lansinger, J. M.; Ronald, R. C. *J. Chem. Soc., Chem. Commun.* **1980**, 87.

(21) Johnson, O. H.; Nebergall, W. H. *J. Am. Chem. Soc.* **1949**, *71*, 1720.

(22) Leroux, F.; Schlosser, M.; Zohar, E.; Marek, I. In *The Chemistry of Organolithium Compounds*; Rappoport, Z., Marek, I., Eds.; John Wiley & Sons: 2004, p 435.

(23) Vrancken, E.; Alexakis, A.; Mangeney, P. *Eur. J. Org. Chem.* **2005**, 1354.

(24) Stanetty, P.; Mihovilovic, M. D. *J. Org. Chem.* **1997**, *62*, 1514.

(25) Morrow, G. W.; Swenton, J. S.; Filppi, J. A.; Wolgemuth, R. L. *J. Org. Chem.* **1987**, *52*, 716.

(26) Napoletano, M.; Norcini, G.; Pellacini, F.; Marchini, F.; Morazzoni, G.; Fattori, R.; Ferlenga, P.; Pradella, L. *Bioorg. Med. Chem.* **2002**, *12*, 5.

(27) Meyers, A. I.; Hanagan, M. A.; Trefonas, L. M.; Baker, R. J. *Tetrahedron* **1983**, *39*, 1991.

(28) Hana, N. *Chirality* **2001**, *13*, 731.

(29) Parker, D. *Chem. Rev.* **1991**, *91*, 1441.

(30) Taylor, S. D.; Kotoris, C. C.; Hum, G. *Tetrahedron* **1999**, *55*, 12431.

(31) Lal, G. S.; Pez, G. P.; Syvret, R. G. *Chem. Rev.* **1996**, *96*, 1737.

(32) Nyffeler, P. T.; Duron, S. G.; Burkart, M. D.; Vincent, S. P.; Wong, C. H. *Angew. Chem. Int. Ed.* **2005**, *44*, 192.

(33) Davis, F. A.; Han, W.; Murphy, C. K. *J. Org. Chem.* **1995**, *60*, 4730.

(34) Differding, E.; Duthaler, R. O.; Krieger, A.; Ruegg, G. M.; Schmit, C. *Synlett* **1991**, 395.

(35) Nie, J. Y.; Kirk, K. L. *J. Fluorine Chem.* **1995**, *74*, 297.

(36) Sammakia, T.; Latham, H. A. *J. Org. Chem.* **1996**, *61*, 1629.

(37) Hoepker, A. C.; Gupta, L.; Ma, Y.; Faggin, M. F.; Collum, D. B. *J. Am. Chem. Soc.*, *133*, 7135.

(38) Ma, Y.; Hoepker, A. C.; Gupta, L.; Faggin, M. F.; Collum, D. B. *J. Am. Chem. Soc.*, *132*, 15610.

(39) Tetlow, D. J.; Hennecke, U.; Raftery, J.; Waring, M. J.; Clarke, D. S.; Clayden, J. *Org. Lett.*, *12*, 5442.

(40) Lee, J.; Choi, W. B.; Lynch, J. E.; Volante, R. P.; Reider, P. J. *Tetrahedron Lett.* **1998**, *39*, 3679.

CHAPTER 4

Further Functionalisation and Removal of the Oxazoline

4.1 Further Functionalisation of Calixarene

To expand the chiral oxazoline–directed asymmetric functionalisation of the calixarene, it was desirable to prove that this methodology could be used to produce both enantiomers of the *meta*–functionalised calixarene through inverting the sense of central chirality of the oxazoline. We anticipated that this should be possible because of the results obtained using chiral ortholithiation directing groups on ferrocenes, which had shown inversion of the sense of planar chirality created in the reaction with inversion of the central chirality of the directing group.[1,2] In this regard, the enantiomer **4.1** of oxazoline **2.1**, was synthesised from the D–valine–derived (*R*)–valinol. The synthesis of the D–valine–derived oxazoline **4.1** was accomplished in good yield, using the same methodology used to synthesise **2.1** (Scheme 4.1).

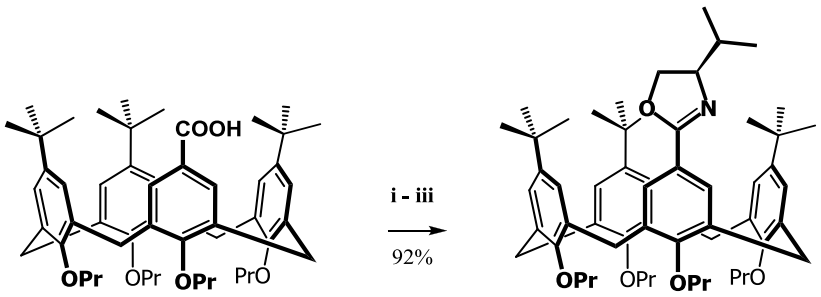

2.2 **4.1**

Scheme 4.1: Synthesis of (*R*)–oxazoline. Reagents and conditions: i) $SOCl_2$ (exs), Δ, 3 h, ii) Et_3N (3.6 eq), D–valinol (1.2 eq), DCM, 0 ºC, rt, 24 h iii) $SOCl_2$ (6.9 eq), DCM, rt, 18 h.

Oxazoline **4.1** was ortholithiated with *c*PentLi and TMEDA, yielding fluorinated diastereomers **4.2** and **4.3** (Scheme 4.2), with the selectivity and yield of the reaction being comparable to the results achieved with the ortholithiation of **2.1**. Importantly, the diastereomerically enriched mixture proved to possess the opposite optical rotation to that of fluoro–diastereomers **3.10** and **3.11**.

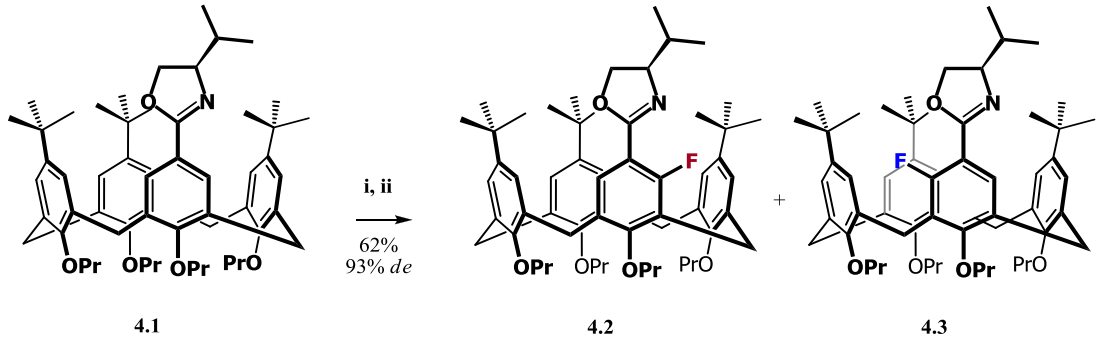

4.1 **4.2** **4.3**

Scheme 4.2: Synthesis of fluoro–diastereomers. Reagents and conditions: i) *c*PentLi (5 eq), TMEDA (10 eq), Et_2O, −78 ºC, 24 h, ii) NFSI (9 eq), *de* determined by ^{19}F NMR.

As already demonstrated, the calixarene can be successfully formylated **3.8**,[1] methylated **3.9** and fluorinated **3.10** in good yields, however, the general application of this reaction needed to be proved with a range of other electrophiles. A wide range of electrophiles have been employed in the chemical literature for functionalisation of ortholithiated compounds.[3] Due to the propensity of oxazolines to undergo rearrangement as observed with DMF product **3.7**, we were cautious with our choice of electrophile. A further consideration was that, for simplicity, the use of prochiral electrophiles was undesirable, nonetheless the ability of the chiral environment (oxazoline and inherently chiral calixarene) to impart control onto secondary sp^3 chirality presents an interesting prospect. Bearing these factors in mind, five other electrophiles were tested, with the results shown in Table 4.1.

[1] As mentioned in Chapter 3, complications via rearrangement in the formylation reaction (**9a**) were observed.

Table 4.1: Functionalisation of oxazoline **2.1**.

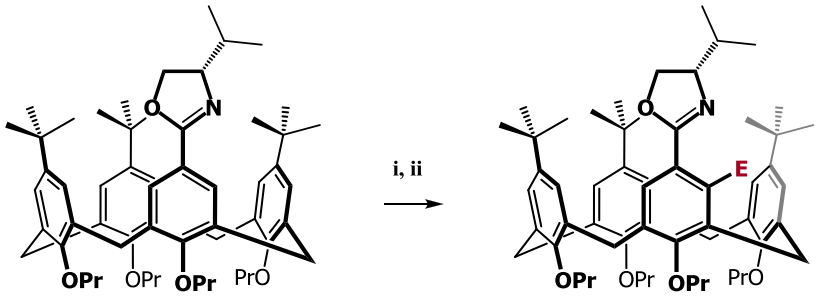

SH2X **SH4D - SH4H**

Entry	Product	E^+	Conditions	E	Isolated Yield
1	**4.4**	TMSCl	14.5 h, 3.2 eq *c*PentLi	TMS	62[a]
2	**4.5**	PPh_2Cl	24 h, 5 eq *c*PentLi	$POPh_2$	70[b]
3	**4.6**	EtOC(O)Cl	18 h, 3.1 eq *c*PentLi	COOEt	73[a]
4	**4.7**	Me_2S_2	24 h, 6 eq *c*PentLi	SMe	73[b]
5	**4.8**	$BrCH_2CH_2Br$	24 h, 5 eq *c*PentLi	Br	72[a]

Reagents and conditions: i) As per table with addition of TMEDA (2 eq to alkyllithium), Et2O, TMEDA (2 eq to RLi) ii) E+. Notes: [a]Product isolated with greater than 92% *dr* as determined by ^{1}H NMR. [b]Product isolated as single diastereomer by ^{1}H or ^{31}P NMR.

The use of trimethylsilyl chloride (TMSCl) as an electrophile proved somewhat capricious, even after careful purification of the reagent (Entry 1 – Table 4.1).[4] Silylated product **4.4** was identified by ^{1}H and ^{13}C NMR spectroscopy, however, analysis by HRMS (ESI+) revealed no presence of the M^+ peak. Instead the water adduct [M+H_2O–TMS] was observed, presumably due to the lability of the TMS group in the ionisation conditions used in the instrument. A further complication that arose from the silylation reaction was the formation of a di–TMS product **4.9** with *N*–silylation of the oxazoline also occurring (Scheme 4.3) as evidenced from ^{1}H and ^{13}C NMR spectra. Analysis of **4.9** by HRMS revealed the loss of a single TMS group from the compound which now appeared as the mono–TMS functionalised molecule [M+H –TMS], again perhaps being indicative of the lability of the TMS group under these ionisation conditions. Careful control of the number of equivalents of TMSCl, and a reduction in the time allowed for the lithiated calixarene to react with the TMSCl electrophile, returned acceptable yields of mono–TMS compound **4.4** were returned.

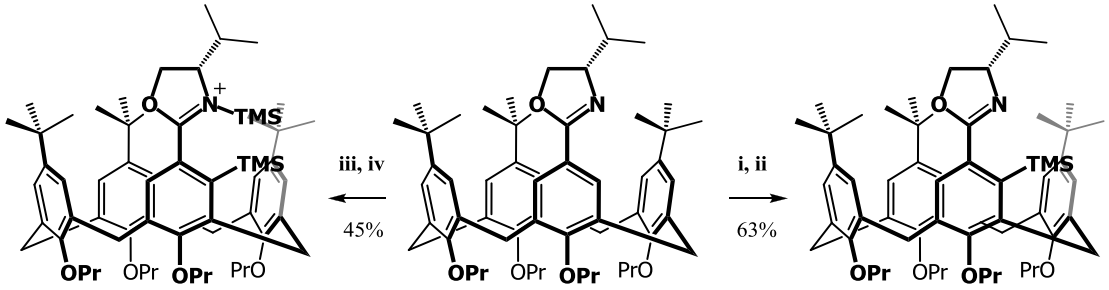

4.9 **2.1** **4.4**

Scheme 4.3: Formation of TMS oxazoline and by–product. Reagents and conditions: i) *c*PentLi (3.2 eq), TMEDA (6.4 eq), Et_2O, −78 ºC, 14.5 h, ii) TMSCl (9 eq), −78 ºC to rt, 6 h, iii) *c*PentLi (6 eq), TMEDA (12 eq), Et_2O, −78 ºC, 30 h, iv) TMSCl (13 eq), −78 ºC to rt, 12 h.

Ortholithiation of oxazoline **2.1** followed by reaction with diphenylphosphine chloride resulted in rapid oxidation of the diphenyl phosphine calixarene product to the crystalline phosphine oxide **4.5** (Entry 2 – Table 4.1). No trace of the diphenylphosphine product was detected in ^{31}P NMR spectra of the crude reaction mixture, even after carefully controlling the reaction conditions and limiting the exposure of the reaction to oxygen. The instability of the product appears to be in contrast to some other upper rim phosphine calixarene compounds, which are reportedly relatively stable.[5] However, for the purposes of our study, obtaining the highly crystalline and stable phosphine oxide was sufficient and, in fact, proved beneficial, as crystallisation of this compound from DCM and ethanol resulted in a diastereomerically pure product (as evidenced by the ^{1}H and ^{31}P NMR spectra of the product).

The synthesis of ethyl ester **4.6**, through reaction with freshly distilled ethyl chloroformate provided a means of adding a single carbon unit to the calixarene in a respectable yield (Entry 3 – Table 4.1). Quenching with dimethyl disulfide successfully yielded the methyl thioether **4.7** in reproducibly good yields (Entry 4 – Table 4.1). It also proved to be possible to separate the diastereomers of the thioether product by silica gel column chromatography, thereby providing access to an enantiomerically pure, inherently chiral, calixarene. Finally, it was shown that quenching with 1,2 dibromoethane allowed access to bromo calixarene (**4.8**) in good yield (Entry 5 – Table 4.1).

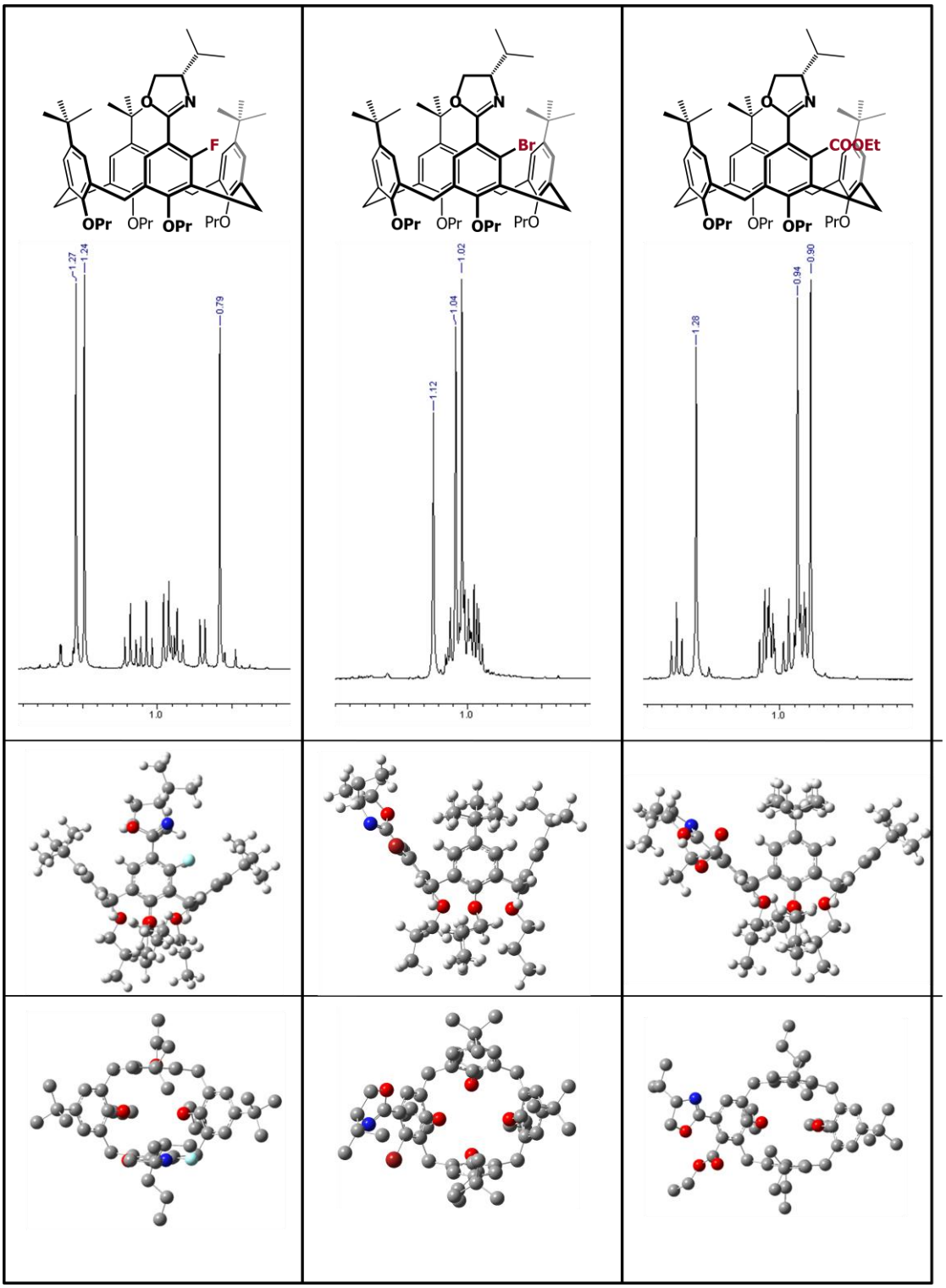

Figure 4.1: ^{1}H NMR and optimised structures of functionalised calixarenes **3.10** (DFT rbly3lp 6–31G), **4.8** (SE PM3), **4.6** (DFT rbly3lp 6–31G).

Three different conformations (computationally optimised[6] structures are presented in Figure 4.1) of functionalised calixarene can be detected through inspection of the ^{1}H spectra (see Appendix I for interpretation of spectra): one with the functionalised aryl ring lying inwards: an intermediate class with the molecule adopting a conformation resembling a true cone; and lastly one with the

non–functionalised distal rings lying outwards. Determination of the conformations that the molecules adopt is made possible by inspection of the shifts of the signals in the ^{1}H NMR spectra associated with the *t*–butyl on the molecule (Figure 4.1). For instance, fluoro calixarene **3.10** lies with the functionalised ring inwards, which is expressed by the distal *t*–butyl group to the functionalised ring experiencing anisotropic shielding from the two proximal rings, and the signal consequently appearing at an upfield position relative to the other two *t*–butyl signals. Conversely, ester **4.6** adopts the opposite conformation, which is evidenced from the shielded nature of the two *t*–butyl proximal signals to the functionalised ring. The true cone of bromo **4.8** can be conferred through the tight grouping of the *t*–butyl signals as shown in Figure 4.1.

Table 4.2: Conformation of functionalized molecules.

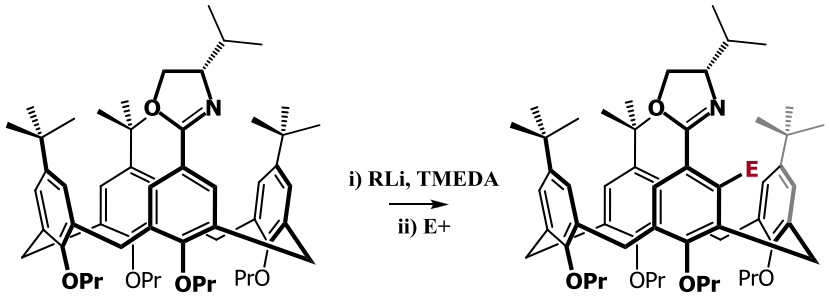

SH2X

Entry	Product	E	Conformation of molecule.
1	**3.8**	CHO	Pinch cone conformation with functionalised ring inwards
	4.4	TMS	
	3.10	F	
	3.9	Me	
2	**3.7**	DMF rearranged	Cone conformation with functionalised ring slightly outwards but narrow separation of *t*–butyl groups.
	4.7	SMe	
	4.8	Br	
3	**4.5**	$POPh_2$	Pinch cone conformation with functionalised ring outwards
	4.6	CO_2Et	
	4.9	2 x TMS	

From Table 4.2 it would appear that the smaller functional groups (CHO, CH_3, F) allow the functionalised ring to lean forwards medium–sized groups (SMe, Br) impart a true cone, and the large groups ($POPh_2$, COOEt) force an outward leaning conformation. It would appear that the conformation that the molecule adopts is to a large degree a reflection of the steric bulk of the substituent on the upper rim. Subtleties exist within this series, however, with the relatively bulky

TMS–functionalised calixarene **4.4** choosing to adopt the inward conformation, perhaps being indicative that solvent effects also playing a role in determining the conformation of the molecule. Certainly, the propensity of calixarenes to host molecules within their cavities has been well established in the chemical literature.[7-11]

In an effort to further our understanding of the manner in which the conformation of the molecule is changed through functionalisation, a number of the functionalised calixarenes were modelled computationally.[6] Our approach centred on taking both the inward and outward orientated conformations of a few representative functionalised calixarenes (fluoro **3.10**, bromo **4.8**, and ethyl ester **4.6**), and performing DFT (6–31G) optimisations (Figure 4.2). Calculations suggest that the fluoro calixarene would prefer to adopt the upright position in the pinch cone, whereas ethyl ester **4.6** more significantly prefers an outward leaning position. In these cases, theoretical data fits with empirical results, suggesting that steric effects play a large role in determining the conformation. However, the experimentally inferred true cone structure of bromo **4.8** was not detected in DFT optimisations, with only pinch cones being located as global minima, indicating that the molecule would strongly prefer an outward conformation. This result is possibly due to the gas phase nature of the calculations failing to account for subtle solvent interactions, again possibly hinting at the role of the solvent in determining conformation. Interestingly, optimisation using semi–empirical (SE) calculation using a PM3 basic set converge to a true cone conformation for bromo **4.8**. Further modelling with comparison to ^{1}H NMR solution structures, would certainly help in understanding the gap between theory and experimental data.

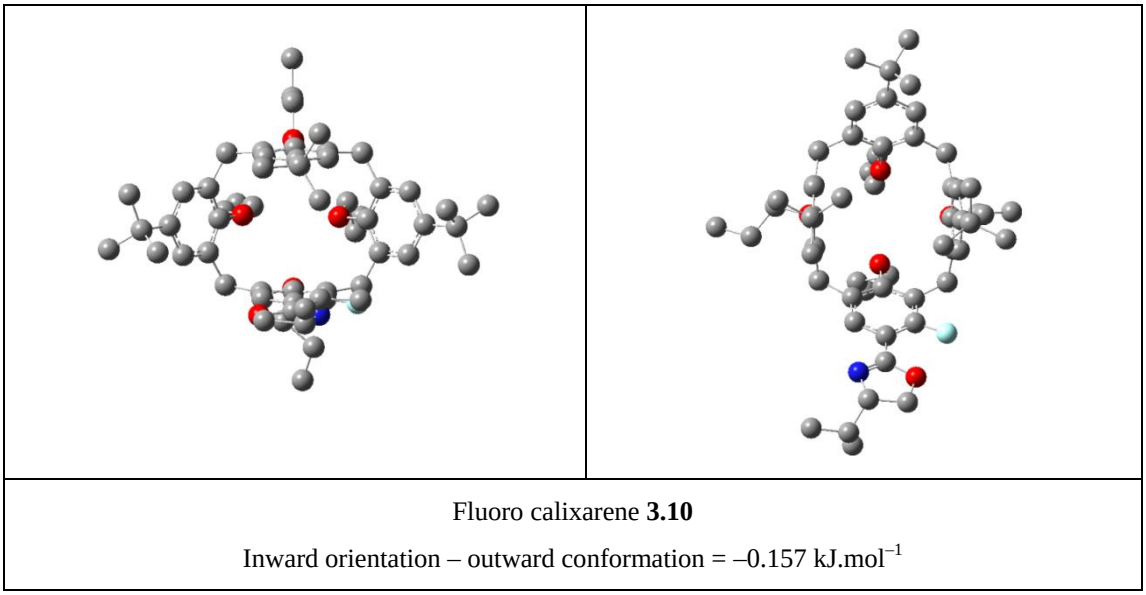

Fluoro calixarene **3.10**

Inward orientation – outward conformation = –0.157 kJ.mol^{-1}

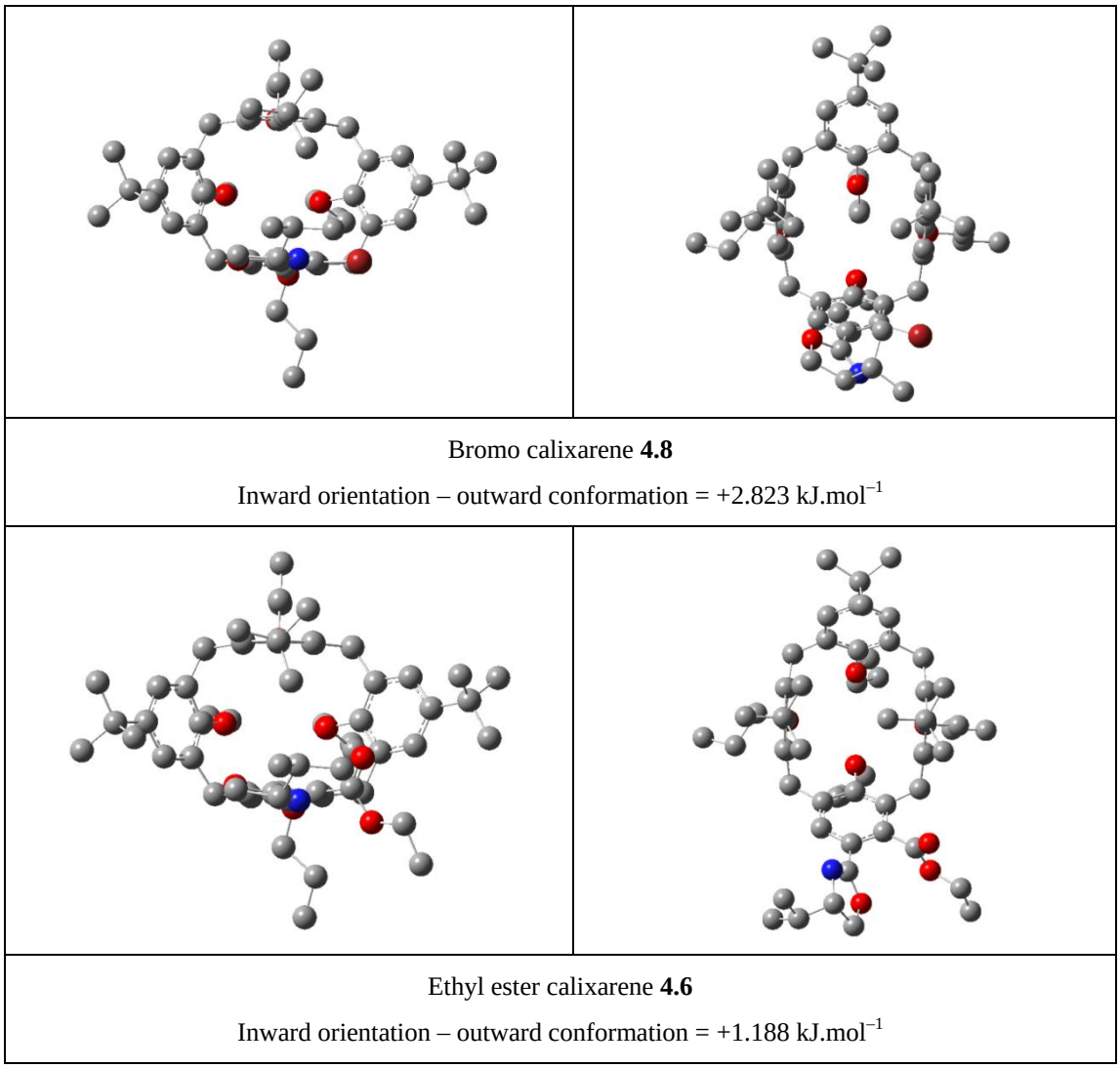

Figure 4.2: DFT (6–31G) optimised conformations of functionalised calixarenes.

Returning to the functionalisation of the calixarene, it should be mentioned that the use of a number of other electrophiles was also attempted, with disappointing yields or complex product formation. Acetone and acetic anhydride failed to produce obvious signs of ortholithiated product, and other authors have also observed low yields with their use on lithiated compounds, presumably due to competing enolisation reactions.[12,13] Trimethyl borate was also tested and did appear to successfully functionalize the calixarene, however, the appearance of multiple fluorescent products on attempted silica gel column purification seemed to indicate that some form of rearrangement had occurred, therefore further experimentation was not attempted. Solid CO_2 was also tested, again with apparent rearrangement of the oxazoline ring, further illustrating the propensity of the oxazoline to rearrange.[14,15]

4.2 Determination of Configuration of Major Diastereomer

The primary question that needed to be addressed regarding the functionalisation of the calixarene was the configuration of the major diastereomer. The easiest means of answering this question was to obtain a single–crystal structure of one of the ortholithiation products, and then using the known chirality (*S*) of the oxazoline directing group assign a configuration to the major diastereomer.

In this regard, a number of attempts were made to crystallise different *meta*–functionalised products of the ortholithiation reaction. These efforts were frustrated by the continued formation of microcrystalline materials not suitable for single crystal diffraction. Compared to other calixarene compounds, crystallisation of calixarenes with the isopropyl oxazoline moiety proved to be much more difficult. After a number of attempts, slow crystallisation of the diphenyl phosphine oxide calixarene (**4.5**) from a DCM–EtOH mixture yielded diffraction–quality crystals, the structure of which was elucidated by single crystal X–ray diffraction (Figure 4.3).

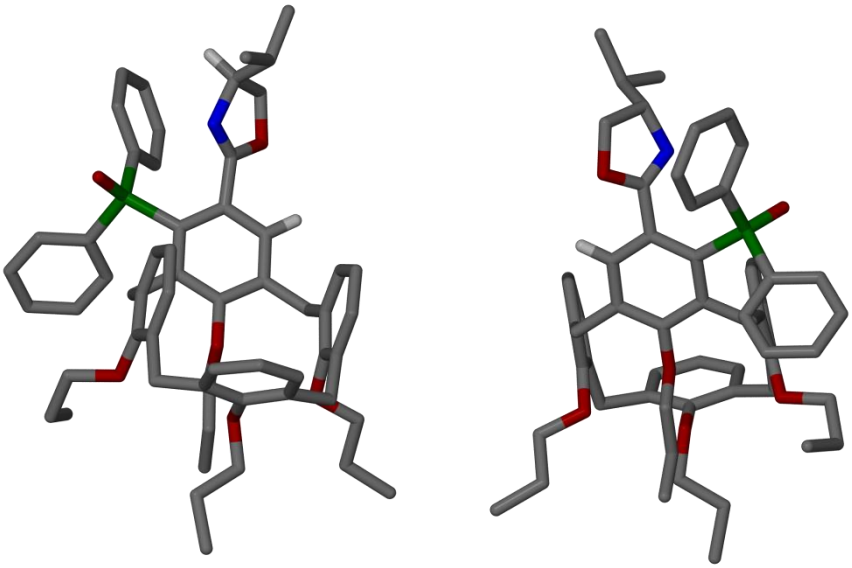

Figure 4.3: Capped–stick presentation of **4.5** as elucidated from single–crystal structure. For clarity all *t*–butyl groups, and hydrogen atoms (baring the hydrogen *ortho* to the oxazoline) have been removed as well as the solvents used for crystallisation (dichloromethane and ethanol). Colours: carbon grey, nitrogen blue, phosphorous green and oxygen red.

Using the description of chirality associated with curvature as proposed by Schiaffino *et al.*,[16] it was possible to determine that the major diastereomer was in a (*cR*) configuration. From a methodological perspective this was important information: in addition it provides the foundation for a mechanistic discussion regarding the ortholithiation reaction.

4.3 Hydrolysis of the Oxazoline

There are a large number of procedures that can be used to hydrolyse oxazolines,[15,17-20] which maybe an indication that their removal is not always simple or easily accomplished. It is also a testament to the stability of the oxazoline functionality, which has prompted its use as protecting groups for acids.[21] The conventional approach involves either an acid– or base–catalysed hydrolysis in alcoholic or aqueous media.[17] A second, widely used, approach involves *N*–methylation of the oxazoline,[22] which then allows reduction to an aldehyde using sodium borohydride[23] or hydrolysis to the corresponding acid.[24]

Observing the success of the *N*–methylation approach in the literature,[24] we decided to attempt this approach to activate the oxazoline to hydrolysis. Methylation of fluoro oxazoline **3.10** with methyl iodide was performed in quantitative yield, followed by attempted base–catalysed hydrolysis in an aqueous THF solution (Scheme 4.4). After 5 days at reflux a significant amount of the methylated starting material was still observed in the mixture, with only 10% of fluoro acid **4.10** being recovered (Scheme 4.4). In an effort to see if the yield of the hydrolysis reaction could be improved, the reaction was repeated under microwave conditions at 180 ºC for 1 hour in a basic methanol and water mixture, with similar results. Increasing the microwave assisted reaction time to 3.5 hours returned a small improvement in conversion, although the reaction remained sluggish even when using the high boiling *n*BuOH and extended reaction times (Scheme 4.4).

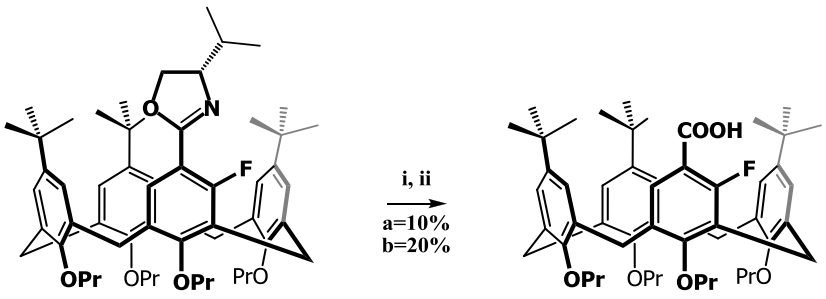

3.10 **4.10**

Scheme 4.4: Hydrolysis of fluoro oxazoline **3.10**. Reagents and conditions: a: i) MeI (exs), rt, 18 h ii) 3M NaOH, THF, Δ, 5 d, b: i) MeI (exs), rt, 18 h, ii) Microwave assisted synthesis, *n*BuOH, 3M NaOH, 195 ºC, 5 h.

As the base–catalysed method appeared unsuitable for hydrolysis of the oxazoline, the use of a different approach was investigated.[15] The procedure involved a two step process: initial hydrolysis of the oxazoline to the amide using a glacial acetic acid/water mixture, followed by

base–catalysed hydrolysis of the amide to the acid. It had been observed in previous attempts that reactions performed in basic aqueous alcoholic solutions showed little presence of the amide, but suffered from low conversion of the oxazoline to the amide. The use of the aqueous acid successfully hydrolysed the oxazoline to the amide, but displayed sluggish conversion of the amide to the acid. The second step of basic hydrolysis appeared to rapidly convert the amide to the acid. Hydrolysis of fluoro oxazoline **4.2** using this method successfully furnished the fluoro acid **4.10** in a vastly improved yield of 78%. Application of this method in the hydrolysis of the other functionalised calixarene oxazolines is shown below in Table 4.3, generally proceeding in good yield.

Table 4.3: Hydrolysis of functionalised oxazolines.

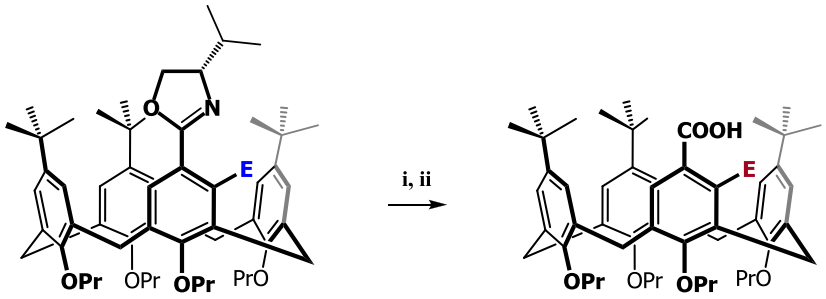

Entry	Starting Material (E)	Conditions i)	Conditions ii)	Product (E)	% Yield
1	**3.10** (F)	170 ºC, 1 h	140 ºC, 1 h	**4.10** (F)	78
2	**4.2** (F)	170 ºC, 1.25 h	150 ºC, 2 h	**4.11** (F)	88
3	**4.4** (TMS)	170 ºC, 1 h	150 ºC, 2 h	**4.12** (TMS)	0
4	**4.5** ($POPH_2$)	170 ºC, 1.5 h	150 ºC, 2 h	**4.13** ($POPh_2$)	99
5	**4.6** (COOEt)	170 ºC, 4 h	150 ºC, 2 h	**4.14** (COOH)	72
6	**4.7** (SMe)	170 ºC, 1 h	140 ºC, 0.5 h	**4.15** (SMe)	41
7	**4.8** (Br)	170 ºC, 1 h	120 ºC, 1 h	**4.16** (Br)	72

Reagents and conditions: i) 20 % aqueous acetic acid ii) 4 M NaOH, EtOH.

It proved necessary to slightly modify the reaction time and temperature for the different functionalised calixarenes, to optimise conversion to the corresponding *meta*–functionalised calixarene acids (Table 4.3). With the exception of TMS functionalised **4.4** and thioether **4.7**, the reaction could be optimised to produce good yields of the desired carboxylic acids. Exposure of TMS functionalised oxazoline **4.4** to hydrolysis conditions resulted in the formation of multiple products. This was not altogether surprising given that the removal of TMS groups under basic conditions has been reported in the chemical literature.[25] It was noted that slow conversion of

thioether **4.7** to the intermediate amide occurred, however increased reaction time merely led to the increased formation of by products, resulting in the poor yield of thioether acid **4.15**. Conversely phosphorus oxide **4.5** could be quantitatively converted to the highly crystalline acid **4.13**. The ethyl ester **4.6** underwent concomitant hydrolysis of the ester functionality, resulting in a di–acid **4.14**. This di–acid exhibited unique solubility and conformational characteristics (insoluble in MeCN, DMSO, EtOH, acetone and partially soluble in DCM, $CHCl_3$), and repeated efforts to obtain an acceptable ^{1}H NMR spectrum failed ($CDCl_3$, d_6–acetone, d_6–benzene, d_6–DMSO) possibly due to slow conformational interconversion of the molecule in these solvents, as evidenced from the broad and poorly defined signals. High temperature ^{1}H NMR spectroscopy failed to improve the resolution of these regions. Only the use of d_4–acetic acid afforded a sharp ^{1}H NMR spectrum and confirmed its identity. The success of d_4–acetic acid suggests the presence of hydrogen bonding inter/intramolecular interactions in the calixarene, which results in the molecule interconverting between different conformational forms/dimers/aggregates, creating the poorly defined ^{1}H spectra. The introduction of the strongly hydrogen bonding acetic acid disrupts these interactions, resulting in greater uniformity in the conformational distribution and the well defined ^{1}H NMR spectra. Closer examination of the reaction mixtures of the hydrolysis of the ethyl ester also revealed the presence of mono–acid **2.2**, indicating that *meta*–decarboxylation occurred during the harsh conditions necessary for hydrolysis. The regioselectivity of this reaction is apparently governed by the greater activation of the position *para* to the propoxy group, destabilising the transition state at this position and inducing the preference for the *meta*–decarboxylated product. It was found that trituration or crystallisation from an acetonitrile/water mixture greatly aided purification of the *meta*–functionalised carboxylic acids.

A brief conformational analysis of these compounds reveals some interesting results. The removal of the oxazoline group reduces the steric bulk of the functionalised ring and, consequently, a greater number of the molecules lie in a cone or pinched cone conformation with the functionalised ring lying inwards (Entries 1 and 2 – Table 4.4). Only the phosphine oxide acid **4.13** lies with the functionalised ring facing outwards (Entries 3 – Table 4.4).

Table 4.4: Conformation of hydrolysed products.

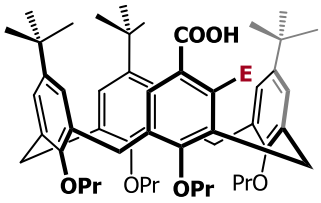

Entry	Product (E)	Conformation
1	**4.14 (**COOH**)** **4.16** (Br)	Cone (close separation of t–butyl groups)
2	**4.15** (SMe) **4.10** (F)	Pinch cone with functionalised group facing inwards
3	**4.13** ($POPh_2$)	Pinch cone with functional group facing outwards

The optical rotation of these molecules varied wildly, from the minor rotation for the fluoro acid **4.10**, to a fairly strong rotation of +92º for the phosphine oxide (**4.13**). The fact that these molecules are optically active, confirms their inherent chirality and provides proof of the enantiomerically enriched nature of the mixtures, as a result of the diastereoselectivity imparted during their synthesis. A general observation regarding the optical activity of these molecules is that the larger the *meta*–substituent on the calixarene, the greater the optical activity.

4.4 Conclusion and Future Work

In this chapter, the generality of the methodology has been developed by demonstrating that the ortholithiation allows functionalisation with a range of electrophiles. It was also shown that the oxazoline–directing moiety can be removed by hydrolysis, allowing access to a range of *meta*–functionalised carboxy calixarenes. In the following section the synthesis of a debutylated calixarene oxazoline and its use will probe the effect that the *t*–butyl groups of the calixarene have on the diastereoselectivity and rate of the reaction is described.

4.5 References

(1) Sammakia, T.; Latham, H. A.; Schaad, D. R. *J. Org. Chem.* **1995**, *60*, 10.

(2) Riant, O.; Samuel, O.; Flessner, T.; Taudien, S.; Kagan, H. B. *J. Org. Chem.* **1997**, *62*, 6733.

(3) Snieckus, V. *Chem. Rev.* **1990**, *90*, 879.

(4) Perrin, D. D.; Armarego, W. L. F. *Purification of Laboratory Chemicals. 3rd Ed*, 1988.

(5) Bagatin, I. A.; Matt, D.; Thonnessen, H.; Jones, P. G. *Inorg. Chem.* **1999**, *38*, 1585.

(6) Frisch, M. J.; Trucks, G. W.; Schlegel, H. B.; Scuseria, G. E.; Robb, M. A.; Cheeseman, J. R.; Scalmani, G.; Barone, V.; Mennucci, B.; Petersson, G. A.; Nakatsuji, H.; Caricato, M.; Li, X.; Hratchian, H. P.; Izmaylov, A. F.; Bloino, J.; Zheng, G.; Sonnenberg, J. L.; Hada, M.; Ehara, M.; Toyota, K.; Fukuda, R.; Hasegawa, J.; Ishida, M.; Nakajima, T.; Honda, Y.; Kitao, O.; Nakai, H.; Vreven, T.; Montgomery, J., J. A. ; Peralta, J. E.; Ogliaro, F.; Bearpark, M.; Heyd, J. J.; Brothers, E.; Kudin, K. N.; Staroverov, V. N.; Kobayashi, R.; Normand, J.; Raghavachari, K.; Rendell, A.; Burant, J. C.; Iyengar, S. S.; Tomasi, J.; Cossi, M.; Rega, N.; Millam, N. J.; Klene, M.; Knox, J. E.; Cross, J. B.; Bakken, V.; Adamo, C.; Jaramillo, J.; Gomperts, R.; Stratmann, R. E.; Yazyev, O.; Austin, A. J.; Cammi, R.; Pomelli, C.; Ochterski, J. W.; Martin, R. L.; Morokuma, K.; Zakrzewski, V. G.; Voth, G. A.; Salvador, P.; Dannenberg, J. J.; Dapprich, S.; Daniels, A. D.; Farkas, Ö.; Foresman, J. B.; Ortiz, J. V.; Cioslowski, J.; Fox, D. J.; Gaussian 09 Revision A.1 ed. Wallingford CT, 2009.

(7) O'Malley, S.; Alhashimy, N.; O'Mahony, J.; Kieran, A.; Pryce, M.; Nolan, K. *Tetrahedron Lett.* **2007**, *48*, 681.

(8) Alessandro, C.; Francesco, S.; Andrea, S.; Luca, P.; Marco, M.; Nelsi, Z.; Franco, U.; Rocco, U. *Eur. J. Org. Chem.* **2003**, *2003*, 1475.

(9) Iwamoto, K.; Yanagi, A.; Arimura, T.; Matsuda, T.; Shinkai, S. *Chem. Lett.* **1990**, 1901.

(10) Atwood, J. L.; Barbour, L. J.; Jerga, A. *Science* **2002**, *296*, 2367.

(11) Atwood, J. L.; Barbour, L. J.; Jerga, A. *Angew. Chem. Int. Ed.* **2004**, *43*, 2948.

(12) Schow, S. R.; Bloom, J. D.; Thompson, A. S.; Winzenberg, K. N.; Smith, A. B. *J. Am. Chem. Soc.* **1986**, *108*, 2662.

(13) Smith, A. B.; Schow, S. R.; Bloom, J. D.; Thompson, A. S.; Winzenberg, K. N. *J. Am. Chem. Soc.* **1982**, *104*, 4015.

(14) Morrow, G. W.; Swenton, J. S.; Filppi, J. A.; Wolgemuth, R. L. *J. Org. Chem.* **1987**, *52*, 716.

(15) Napoletano, M.; Norcini, G.; Pellacini, F.; Marchini, F.; Morazzoni, G.; Fattori, R.; Ferlenga, P.; Pradella, L. *Bioorg. Med. Chem.* **2002**, *12*, 5.

(16) Dalla Cort, A.; Mandolini, L.; Pasquini, C.; Schiaffino, L. *N. J. Chem.* **2004**, *28*, 1198.

(17) Reuman, M.; Meyers, A. I. *Tetrahedron* **1985**, *41*, 837.

(18) Tan, Q. T.; Li, H. Y.; Wen, J. W.; Jiang, C.; Wang, X.; You, T. P. *Synth. Commun.* **2005**, *35*, 2289.

(19) Oi, S.; Aizawa, E.; Ogino, Y.; Inoue, Y. *J. Org. Chem.* **2005**, *70*, 3113.

(20) Levin, J. I.; Weinreb, S. M. *Tetrahedron Lett.* **1982**, *23*, 2347.

(21) Greene, T. W.; Wuts, P. G. M. *Protective Groups in Organic Synthesis. 2nd Ed*, 1991.

(22) Barner, B. A.; Meyers, A. I. *J. Am. Chem. Soc.* **2002**, *106*, 1865.

(23) Nordin, I. C. *J. Heterocycl. Chem.* **1966**, *3*, 531.

(24) Laursen, B.; Denieul, M. P.; Skrydstrup, T. *Tetrahedron* **2002**, *58*, 2231.

(25) Ganter, C.; Wagner, T. *Chem. Ber.* **1995**, *128*, 1157.

CHAPTER 5

Ortholithiation of Non–Butylated Calixarene Oxazoline

5.1 Synthesis of a Non–Butylated Calixarene Oxazoline

In seeking to answer the question of what role the *t*–butyl groups on the calixarene played in the ortholithiation reaction, the synthesis of the non–butylated calixarene oxazoline was designed. When performing a retro–synthetic analysis of the target oxazoline **5.1**, the initial disconnection would be to a mono–acid **5.2** (Scheme 5.1). This in turn could be obtained using a carboxylation reaction from a halogenated precursor **5.3**, following a similar analysis to that used to produce oxazoline **2.1**. Inspection of the chemical literature revealed established methodology to produce a mono–bromo calixarene,[1] from the parent *t*–butyl calixarene **2.5**.

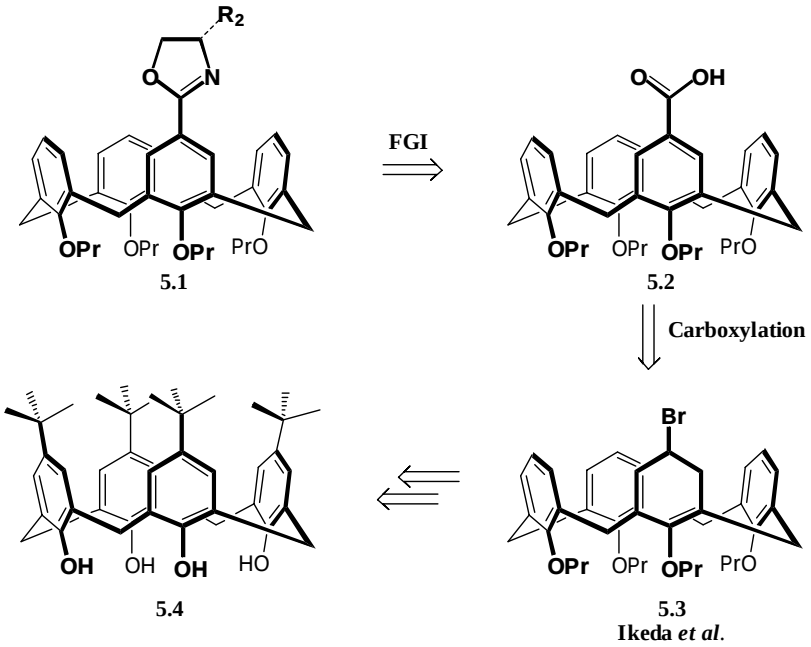

Scheme 5.1: Retrosynthetic analysis of non–butylated calixarene oxazoline.

Following this proposed sequence, the synthesis of mono–bromo calixarene **5.3** was undertaken following established literature procedures (Scheme 5.2). Firstly, global debutylation of the parent *t*–butyl calixarene **2.5** using the Lewis acid $AlCl_3$ and phenol in a reverse Friedel Crafts reaction was undertaken, yielding debutylated calixarene **5.4** in appreciable yield.[2] Purification could be achieved using trituration from diethyl ether, making it possible to perform the reaction

on a large scale (up to 20 g). Conversion of debutylated calixarene **5.4** to the tetrapropylated product **5.5** was accomplished using NaH and propyl iodide.[3] Again, it was possible to perform large scale reactions, as trituration (2M HCl) followed by crystallisation (methanol) afforded **5.5** in high purity. Mono–bromination was accomplished using NBS, affording bromo calixarene **5.3**,[1] along with trace quantities of a di–bromo compound, which could be separated using silica gel chromatography. Nevertheless it was usually possible to obtain sufficiently pure bromo calixarene **5.3** simply by crystallisation from a DCM–methanol mixture.

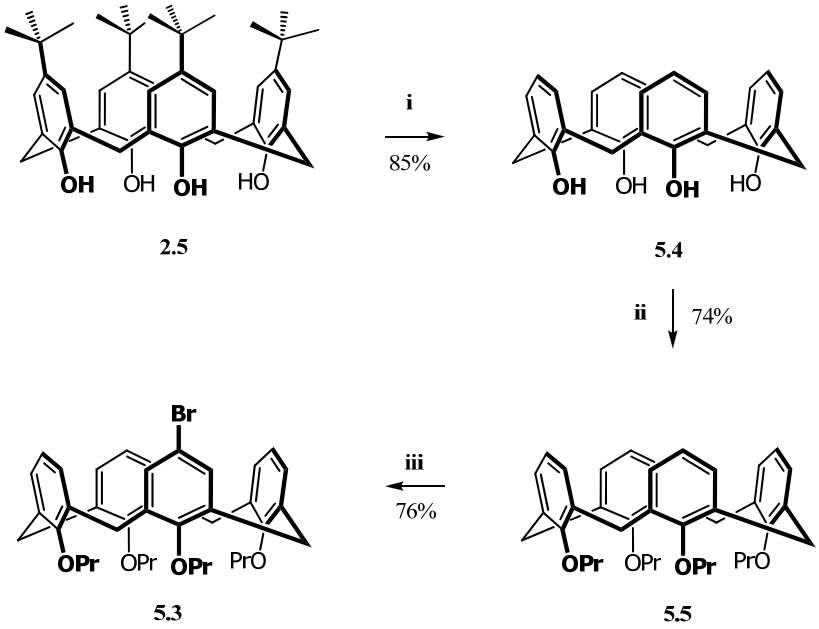

Scheme 5.2: Synthesis of mono–bromo debutylated calixarene. Reagents and conditions: i) $AlCl_3$ (eq 4.8), phenol (1.2 eq), toluene, 0 ºC to rt, 3 h ii) NaH (17 eq), *n*PrI (10 eq), DMF, 0 to rt, 12 h, iii) NBS (1.1 eq), MEK, rt, 18 h.

Fastidious drying of bromo calixarene **5.3** under vacuum, followed by lithium bromine exchange and quenching with solid CO_2 afforded the desired acid **5.2** in good yield (Scheme 5.3). Attempts at using magnesium–bromine exchange failed to occur in a room temperature reaction.

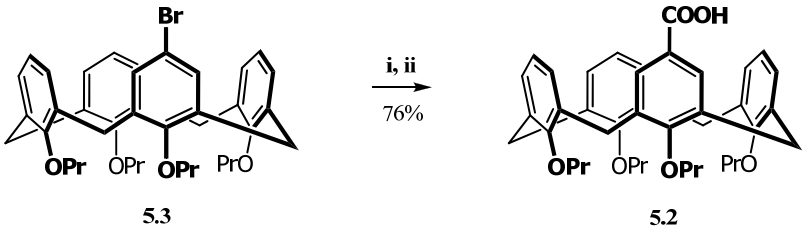

Scheme 5.3: Synthesis of mono acid debutylated calixarene **5.2**. Reagents and conditions: i) *n*BuLi (2 eq), NaH (0.2 eq), THF, −78 ºC, 30 m, ii) CO_2 (s)

Synthesis of the debutylated oxazoline **5.1** was attempted using the established methodology used for synthesis of oxazoline **2.1**, by conversion to the acid chloride using thionyl chloride, coupling with L–valinol to yield the amide intermediate which was cyclised *in situ* using thionyl chloride.[i] Disappointingly, a lower than anticipated yield was recorded for the conversion to the oxazoline from the acid (54%), in contrast to the excellent yields obtained for the synthesis of the *t*–butyl calixarene oxazoline **2.1** (Scheme 5.4).

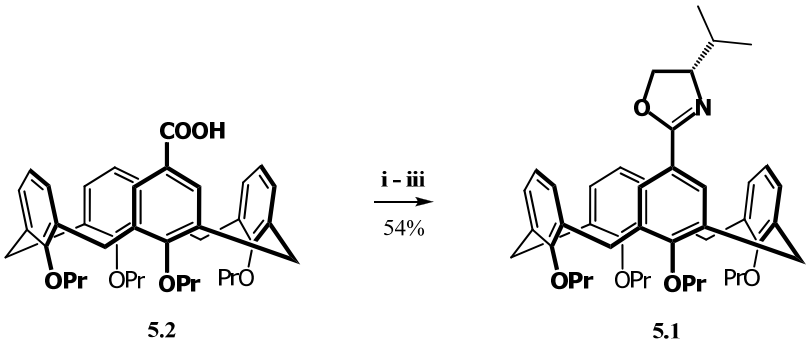

5.2 5.1

Scheme 5.4: Synthesis of debutylated oxazoline **5.1**. Reagents and conditions: i) $SOCl_2$ (exs) ii) Et_3N (3 eq), L–valinol (1.3 eq), DCM, 0 ºC, rt, 24 h iii) $SOCl_2$ (7 eq), DCM, rt, 24 h.

Perplexingly, despite the repetition of the reaction, similarly yields were obtained. Initially it was feared that decomposition of the acid calixarene **5.2** was occurring during the generation of the acid chloride using the rather harsh thionyl chloride, however, isolation of the amide intermediate revealed near quantitative conversion. Applying the standard ring closure conditions (thionyl chloride) to the amide resulted in retention of appreciable quantities of what appeared to be starting material as well as the formation of additional by –products. Isolation of these materials proved to be capricious, due to apparent instability. However, it appeared that at least one of the products was associated with a chloride intermediate, which, by its isolation, suggested sluggish cyclisation to form the oxazoline. The reasons for the difference in reactivity between the butylated and debutylated calixarene amides are unknown, so it was decided to attempt different ring closure conditions in an effort to improve the yield of the reaction.

The use of *p*–toluenesulfonyl chloride[4] was attempted, however the presence of starting material was still observed either after a number of days of stirring at room temperature. No benefit was obtained by heating the reaction mixture or by the application of microwave irradiation. The addition of DMAP and pyridine also failed to improve the reaction yield. Fortunately in the end the use of mesyl chloride resulted in the rapid and significantly cleaner formation of the desired oxazoline **2.1** (Scheme 5.5).

i First synthesised by C. Wolter, G. Arnott

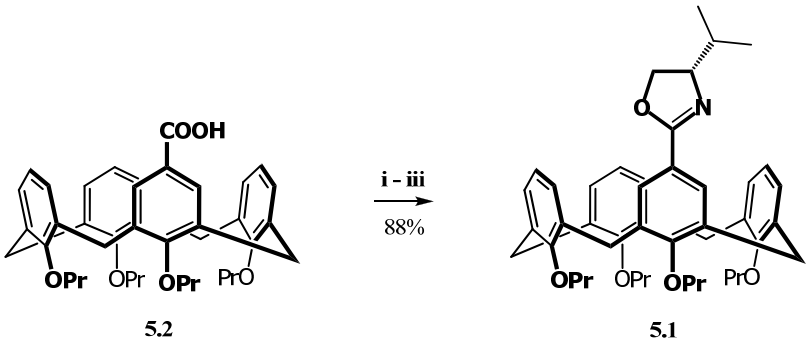

5.2 **5.1**

Scheme 5.5: Mesylation route to oxazoline **5.1**. i) Oxalyl choride (6 eq) ii) Et_3N (3 eq), L–valinol (1.3 eq), DCM, 0 ºC, rt, 24 h iii) MsCl (6 eq), DCM, rt, 24 h.

The greater reactivity of mesyl chloride over tosyl chloride can also be explained by two distinctly different mechanistic pathways, with mesylation proceeding *via* a sulfene intermediate which is formed *in situ* by proton abstraction from mesyl chloride by the base present in the solution (Scheme 5.6).[5] This is in contrast to the S_N2 mechanism undergone during tosylation with tosyl chloride.[6] Unsurprisingly, in the light of the mechanism of mesylation, reaction of mesyl chloride with the calixarene amide in the absence of triethylamine failed to yield any sign of oxazoline formation.

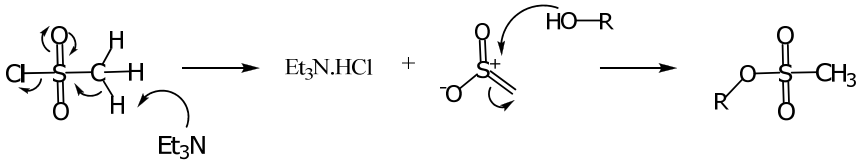

Scheme 5.6: Mechanism of formation of methanol sulfonyl esters.

5.2 Ortholithiation of Non–Butylated Calixarene

Having oxazoline **5.1** in hand, we were eager to investigate the diastereoselectivity of the ortholithiation reaction. An initial test reaction quenched with NFSI, revealed only starting material according to TLC. However the ^1H and ^{19}F NMR spectra of the crude sample revealed the presence of an ortholithiated product (approximately 75%), suggesting that the fluorinated product **5.6** and the starting oxazoline possessed the same R_f value. Attempts at using different solvent systems to induce separation of the product from the starting material failed. Closer inspection of the ^{19}F NMR spectrum of the fluorinated product **5.6** displayed a large doublet, and a number of aromatic ^{19}F signals of similar chemical shift. The appearance of these additional signals made identification of the diastereomers uncertain, and we thought that coalescence of the two diastereomers could also possibly be occurring. In an effort to resolve the signals, high

temperature NMR spectroscopy was performed, and perplexingly the number of minor signals in the ^{19}F NMR spectra of the sample increased. Cooling of the sample revealed the persistence of these new signals, indicating sample instability or possible side reactions occurring. It is possible that fluorination of the other ring systems with unreacted NFSI could be occurring.

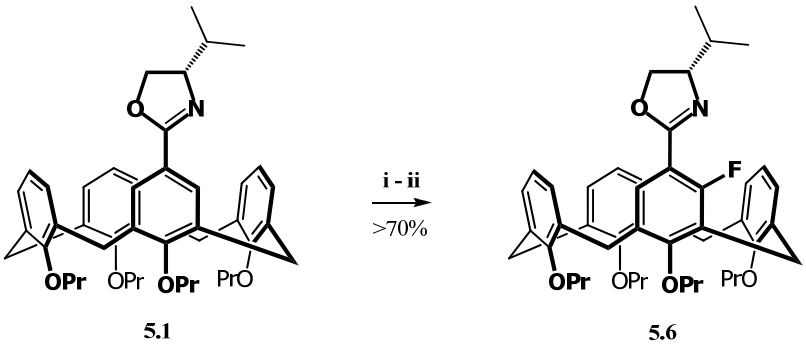

5.1 **5.6**

Scheme 5.7: Ortholithiation of oxazoline **5.1**. Reagents and conditions: 18a i) *c*PentLi/*i*PrLi (5 eq), TMEDA (10 eq), Et_2O, −78 ºC, 24 h, ii) NFSI (8.5 eq), −78 ºC to rt, 12 h.

Owing to the uncertainty associated with the fluorinated product **5.6**, the use of another electrophile was investigated. We had observed that dimethyl disulphide had returned high yields when used in other alkyllithium reactions, including the ortholithiation of oxazoline **2.1**. Ortholithiation of oxazoline **5.1** with subsequent quenching with dimethyl disulphide yielded thioether **5.7**. Again, purification was complicated due to the identical R_f values of the product and starting material, regardless of the choice of solvent. Fortunately, the reaction proved to proceed in high yield (typically above 85%), leaving only trace quantities of starting material. Inspection of the aromatic region of the ^1H spectrum of **5.7** revealed the presence of two non–coalescent singlets, which could be identified as a major diastereomer (**5.7**) and a minor diastereomer (**5.8**) (Figure 5.1). Careful integration of these two signals, allowed the ratio of the diastereomers **5.7** and **5.8** to be calculated.

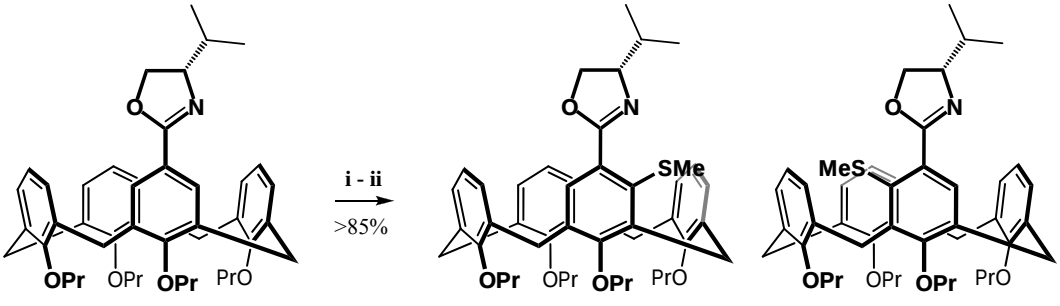

5.1 **5.7** **5.8**

Scheme 5.8: Synthesis of thioether oxazolines **5.7** and **5.8**. Reagents and conditions: i) *c*PentLi (5 eq), TMEDA (10 eq), Et_2O, −78 ºC, 4.5 h, ii) Me_2S_2 (10 eq), −78 ºC to rt, 12 h.

Deconvolution using Spinworks software of the ^{1}H NMR aromatic signals of diastereomers **5.7** and **5.8** was performed to increase our ability to accurately determine the ratio between the two signals, using the inbuilt simulation function (Figure 5.1).[7]

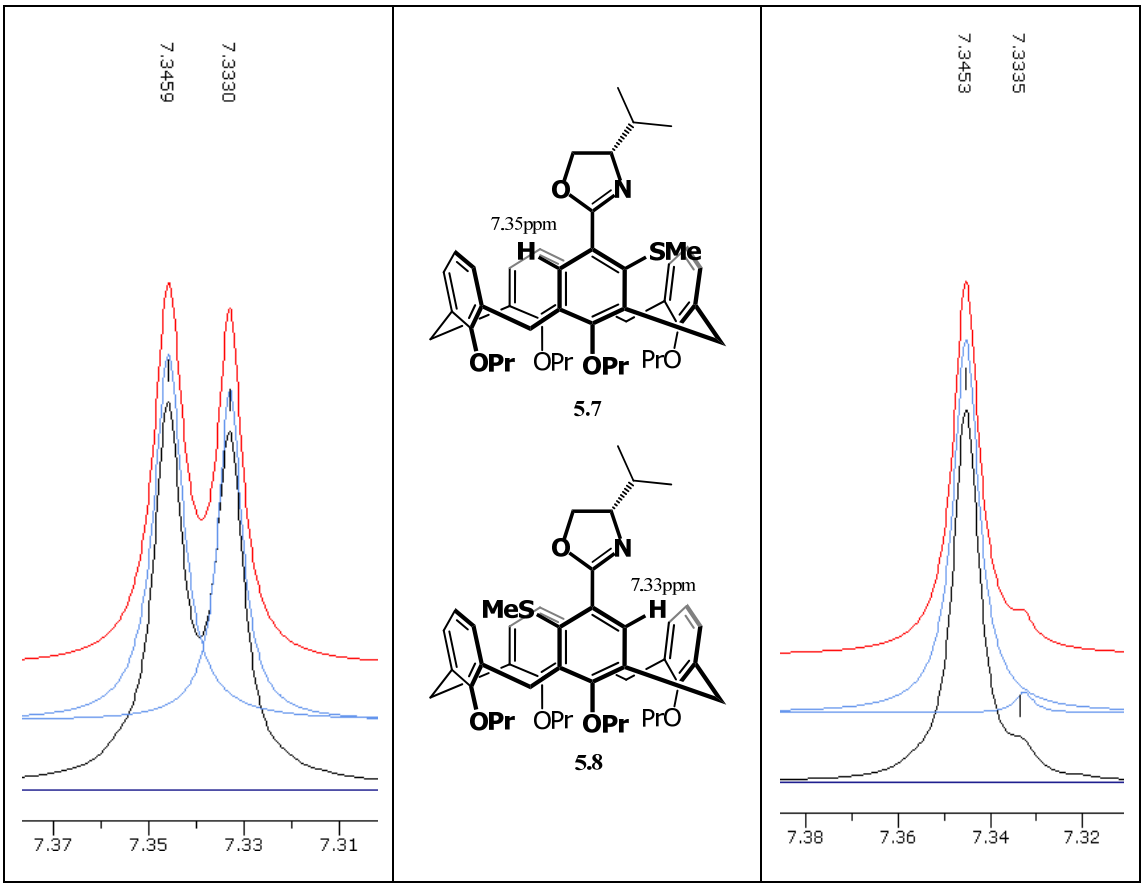

Figure 5.1: ^{1}H NMR spectrum and simulated spectra of thioether **5.7** and **5.8**. Shift of **5.7** (7.35 ppm), **5.8** (7.33 ppm). ^{1}H experimental spectra in black, simulations in blue (individual) and red (sum of individual).

5.3 Optimisation of the Ortholithiation of Non–Butylated Oxazoline

As shown with calixarene **2.1**, a number of parameters can influence the diastereoselectivity and yield of the ortholithiation reaction. These parameters include: the reaction time, concentration, the choice of solvent, alkyllithium, additive, and the temperature of the reaction. Having synthesised oxazoline **5.1**, an investigation into some of these factors was undertaken to build up an understanding of the reactivity of **5.1**. Our initial goal was to gain a qualitative understanding of the rate of the reaction as evidenced by the reaction time and concentration.

5.3.1 Reaction Time and Concentration

We initially applied the same reaction conditions as used for oxazoline **2.1**, (18 hours at −78 ºC), which returned a good yield. We found however that the reaction time could be decreased to 5

hours with generally excellent yields being obtained (it is possible to reduce this further depending on the choice of alkyllithium). We also observed that the reaction could be performed at a lower concentration (0.05 M) for oxazoline **5.1** compared to the higher concentrations required for ortholithiation of isopropyl oxazoline **2.1** (0.15 M) without reducing the yield.

As the reaction rate appeared to be significantly faster without the presence of the *t*–butyl groups of the calixarene, their influence on the diastereoselectivity of the reaction could now be determined. In order to investigate this we independently probed the different parameters shown to influence the diastereoselectivity of the ortholithiation of oxazoline **2.1**.

5.3.2 Solvent

Firstly, an investigation into the effect of solvent on the diastereoselectivity of the reaction was initiated. Previously we had observed that the reaction performed best in diethyl ether, with the presence of TMEDA being a requirement for good diastereoselectivity. Initially we investigated if the reaction would occur without the presence of TMEDA in a number of ethereal solvents. In contrast to the *t*–butyl calixarene oxazoline **2.1**, we found that high yields of the ortholithiated product occurred in all of the common ethereal solvents (Table 5.1 entries 1 – 4); unsurprisingly pentane and toluene gave poor yields (Table 5.1 entries 5 and 6). The diastereoselectivity of these reactions was, however, particularly poor especially for the more strongly coordinating solvents THF and TBME.[8]

Table 5.1: Effect of solvent on ortholithiation of oxazoline **5.1**.

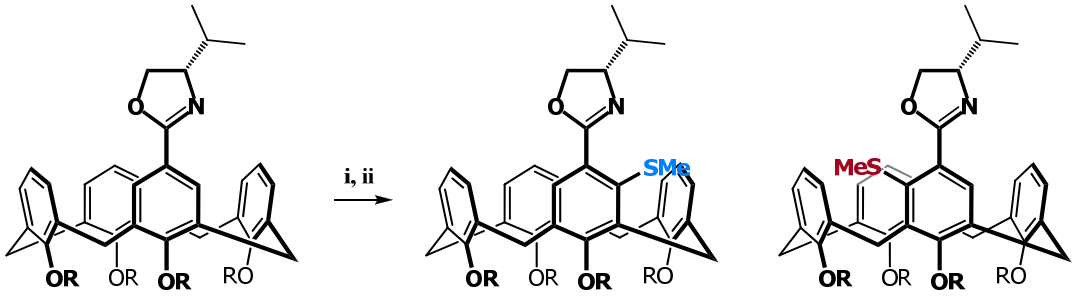

5.1 **5.7** **5.8**

Entry	Solvent[a]	Additive[b]	% Yield	Ratio **5.7**:**5.8**
1	Et_2O		92	1.5:1
2	THF		>95	1.2:1
3	*t*BuOMe		>95	1.2:1
4	*i*Pr_2O		55	1.6:1
5	Pentane		0	–
6	Toluene		0	–
7	Et_2O	TMEDA	>95	14:1
8	THF	TMEDA	93	3.2:1
9	*t*BuOMe	TMEDA	>95	13:1
10	*i*Pr_2O	TMEDA	>95	16:1
11	Pentane	TMEDA	>95	19:1
12	Toluene	TMEDA	93	8:1

Reagents and conditions: i) [a]sBuLi (5 eq) [b]TMEDA (10 eq), −78 °C, 5 h. ii) Me_2S_2 (10 eq), −78 °C to rt, 12 h. Yield determined by ^{1}H NMR, *dr* determined by ^{1}H NMR.

The introduction of TMEDA to the reaction mixture resulted in a significant improvement in the diastereoselectivity of the reaction for the ethereal solvents, notably for the less strongly coordinative solvents Et_2O and *i*Pr_2O. The use of a pentane–TMEDA combination produced the greatest diastereoselectivity without negatively affecting the yield. This was in stark contrast to the results obtained for oxazoline **2.1**. The reasons for the difference between toluene and pentane (entries 11 and 12) are unknown, with significantly less control being exhibited in toluene. The presence of Li–Π interactions is well established in the chemical literature,[9,10] perhaps indicating the toluene does not remain altogether uninvolved in the reaction pathway.

5.3.3 Alkyllithium Optimisation

Next, an examination of the role of the alkyllithium in the ortholithiation of **5.1** was undertaken. We started by testing a number of different alkyllithiums in THF without the presence of TMEDA, in an attempt to investigate if the reversal effect that we noted for ortholithiation of oxazoline **2.1** occurred on the debutylated system. In contrast to our expectations, we observed that the primary reagent *n*BuLi successfully ortholithiated oxazoline **5.1**, albeit in poor yield. Unlike oxazoline **2.1**, no inversion in selectivity when using THF was observed, with poor diastereocontrol being exhibited for every alkyllithium tested (Table 5.2 entries 1 – 3). A range of alkyllithiums were then tested in pentane with the addition of TMEDA (Table 5.2 entries 4 – 9). The use of *n*BuLi produced a moderate yield, perhaps being indicative of the reduced basicity of the primary reagent, nonetheless there was substantial diastereoselectivity of 43:1. Having observed the high selectivity generated by the use of the primary reagent, we also tested MeLi; no ortholithiation could be observed, presumably because MeLi is known to be strongly aggregating and generally less reactive.[8] A similar trend was observed as with oxazoline **2.1**, in that *i*PrLi and *c*PentLi gave increased selectivities over *s*BuLi, however in contrast to oxazoline **2.1** almost no difference was observed between the two alkyllithiums. The use of the tertiary reagent *t*BuLi resulted in good conversion to the desired product, but moderate selectivity was recorded.

Table 5.2: Effect of alkyllithium on ortholithiation of oxazoline **5.1**.

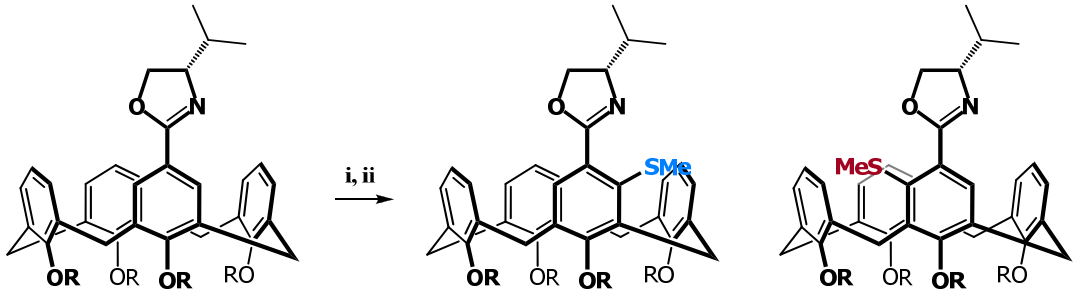

5.1 **5.7** **5.8**

Entry	Alkyllithium[a]	Solvent	Additive[b]	% Yield	Ratio **5.7**:**5.8**
1	*n*BuLi	THF		4	1.4:1
2	*s*BuLi	THF		>95	1.1:1
3	*c*PentLi	THF		37	1.3:1
4	*n*BuLi	Pentane	TMEDA	47	43:1
5	MeLi	Pentane	TMEDA	0	–
6	*s*BuLi	Pentane	TMEDA	>95	19:1
7	*i*PrLi	Pentane	TMEDA	>95	33:1
8	*c*PentLi	Pentane	TMEDA	>95	33:1
9	*t*BuLi	Pentane	TMEDA	95	6:1

Reagents and conditions: i) [a]RLi (5 eq) [b]TMEDA (10 eq), –78 °C, 5 h. ii) Me_2S_2 (10 eq), –78 °C to rt, 12 h. Yield determined by ^{1}H NMR, *dr* determined by ^{1}H NMR.

5.3.4 Additive Optimisation

There are numerous additives that can and have been used in ortholithiation reactions.[8] A question we have had from the beginning of this study is why the use of TMEDA has generally returned such good selectivities whereas the use of other solvents and additives either failed to allow ortholithiation to occur, or did so with significantly reduced selectivity? In an effort to explore this, we examined the effect of different additives on the ortholithiation of oxazoline **5.1** as the ease with which it could be lithiated made it useful for exploring the structural effects of different ligands. For clarity we have separated the different additives into nitrogen donors (Figure 5.2) and oxygen donors (Figure 5.3).

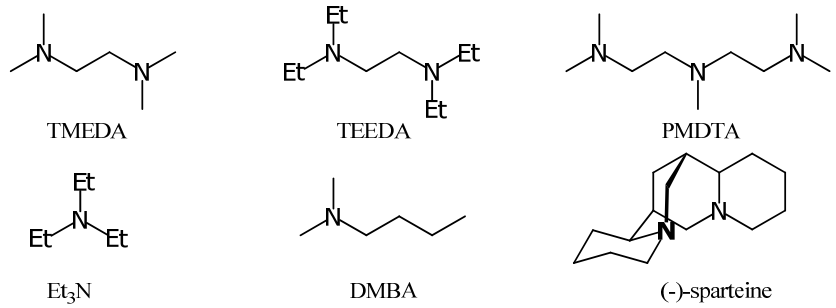

Figure 5.2: Nitrogen additives used in ortholithiation reactions.

We first investigated what effect increasing the bulk of TMEDA to tetraethyl ethylene diamine (TEEDA) would have on the reaction (Entry 2 – Table 5.3), observing a large decrease in diastereoselectivity (19:1 to 2:1). The use of the tri–dentate pentamethyl diethylene triamine (PMDTA) in pentane (Entry 3 – Table 5.3) failed to allow ortholithiation to occur, however, we suspected that this could be due to the poor solubility characteristics of PMDTA in pentane. To overcome the solubility problem, a reaction was performed with PMDTA in THF, which did facilitate ortholithiation but with poor selectivity (1.3:1). The monodentate ligand triethyl amine facilitated ortholithiation, with similar selectivities obtained to the bulky bidentate TEEDA. In an effort to match the dimethylated nature of TMEDA in a monodentate ligand, *N*,*N*–dimethylbutylamine (DMBA) was synthesised and tested, returning moderate product formation, although in significantly reduced selectivity (2:1). These collective results suggest that the high diastereoselectivities associated with the use of TMEDA are as a result of its bidentate character, and its relatively sterically unhindered dimethylated structure.

We also tested the bidentate chiral nitrogen ligand (−)–sparteine, which is known to be a powerful coordinator as well as potentially providing increased diastereomeric selectivities.[8,11] No product of a lithiation reaction could be detected, and presuming a mis–match between the chiral environments of the oxazoline and (−)–sparteine we synthesised the opposite enantiomer of oxazoline calixarene **5.1** using D–valinol, returning oxazoline **5.9** in moderate yield (Scheme 5.9).

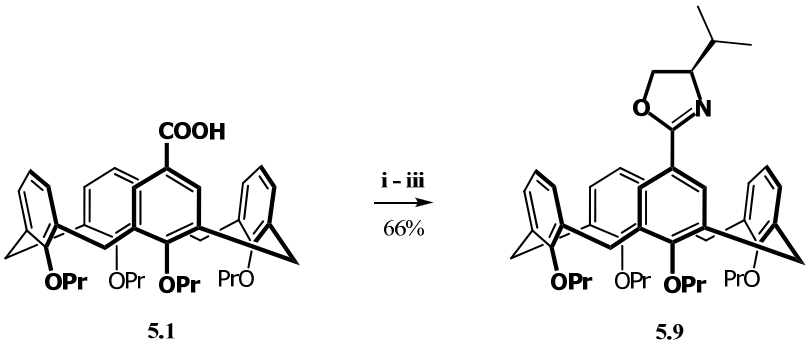

5.1 **5.9**

Scheme 5.9: Synthesis of oxazoline enantiomer **5.9**. i) Oxalyl choride (11 eq) ii) Et_3N (3 eq), D–valinol (1.4 eq), DCM, 0 ºC, rt, 24 h iii) MsCl (6 eq), DCM, rt, 24 h.

Attempted ortholithiation of **5.9** with (−)–sparteine also failed to induce ortholithiation, possibly indicating incompatible steric environments between the calixarene and the alkyllithium complex.

Table 5.3: Effect of *N*–donor ligands of on the ortholithiation of oxazoline **5.1**.

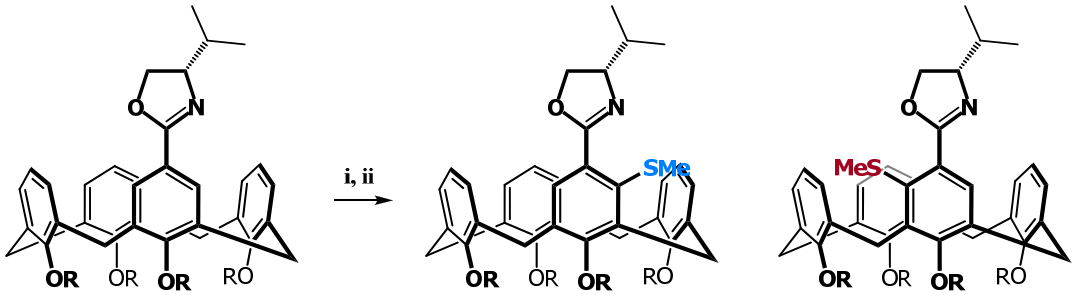

5.1 **5.7** **5.8**

Entry	Solvent[a]	Additive[b]	Yield	Ratio **5.7**:**5.8**
1	Pentane	TMEDA	>95	19:1
2	Pentane	TEEDA	80	2:1
3	Pentane	PMDTA	0	–
4	THF	PMDTA	85	1.3:1
5	Pentane	Et_3N	20	2:1
6	Pentane	DMBA	60	2:1
7	Pentane	(–)–Sparteine	0	–
8[c]	Pentane	(–)–Sparteine	0	–

Reagents and conditions: i) [a]sBuLi (5 eq), 5 h, −78 ºC [b]Additive (10 eq) ii) Me_2S_2 (10 eq). [c]Orthlithiation performed on enantiomer **5.9**. Yield determined by ^{1}H NMR, *dr* determined by ^{1}H NMR.

Next, oxygen–based donors (Figure 5.3) were investigated (Table 5.4). Obviously ethereal solvents fit this descriptor, hence they could be included in this investigation.

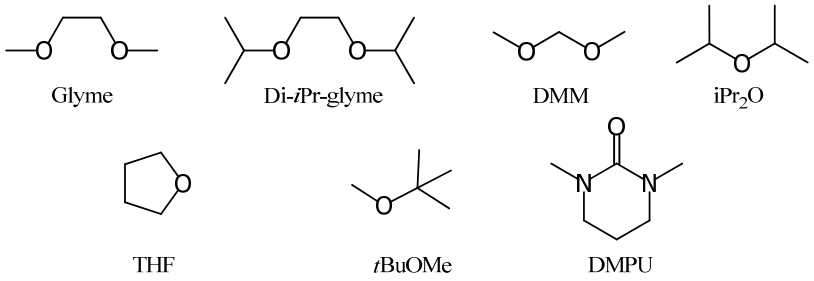

Figure 5.3: Oxygen based ligands.

We attempted to use an O donor structural analogue of TMEDA, glyme (Entry 1 – Table 5.4). Structurally, the trigonal pyramidal geometry of a nitrogen ligand cannot be matched by an oxygen based analogue. Surprisingly, we observed that the use of this ligand resulted in a moderate inversion in selectivity, albeit with only 45 % conversion. Glyme is known to have a limited half life with secondary alkyllithiums, hence we rationalised that this could be negatively effecting the reaction yield.[12] The inversion in selectivity generated by the use of the bidentate oxygen ligand was certainly unanticipated and warranted further investigation. We synthesised the more bulky di–isopropyl ethyl ether **5.10** (di–*i*Pr–glyme) in an attempt to determine whether increasing the bulk of this reagent could improve the inversion of selectivity. The use of this ligand returned a racemic mixture of antipodes **5.7** and **5.8** in moderate yield (Entry 2 – Table 5.4). The use of dimethoxy methane (DMM) also returned a racemic mixture, however literature evidence indicated that this ligand appears to act in a mono–dentate capacity with alkyllithiums.[13] As already observed, mono–dentate ligands iPr$_2$O, THF and *t*BuOMe (Entries 4 to 6 – Table 5.4) all failed to produce significant control over the diastereoselectivity of the reaction, either producing racemic mixtures or slightly favouring the formation of thioether **5.7**.

Table 5.4: Effect of *O*–donor ligands on the ortholithiation of oxazoline **5.1**.

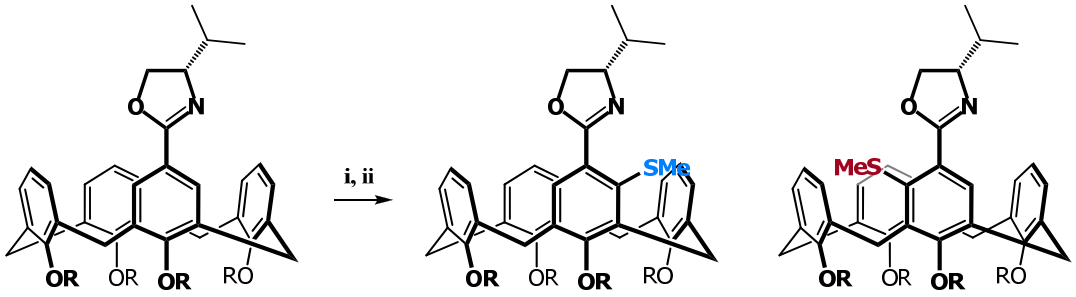

5.1 **5.7** **5.8**

Entry	Solvent[a]	Additive[b]	% Yield	Ratio **5.7**:**5.8**
1	Pentane	Glyme	45	1:1.6
2	Pentane	Di–*i*Pr–glyme	66	1:1
3	Pentane	DMM	50	1:1
4	iPr_2O	iPr_2O	55	1.6:1
5	THF	THF	>95	1.1:1
6	Pentane	*t*BuOMe	95	1:1
7	Pentane	DMPU	5	1:1

Reagents and conditions: i) [a]sBuLi (5 eq), −78 ºC, 5 h, [b]Additive (10 eq) ii) Me_2S_2 (10 eq). Yield determined by ^{1}H NMR, *dr* determined by ^{1}H NMR.

The use of the strongly coordinating DMPU failed to produce notable conversion to the ortholithiation product, without exhibiting significant diastereocontrol (Entry 7 – Table 5.4), however, we noted what appeared to be the formation of a dearomatised product, with incorporation of the alkyllithium and the electrophile.[14] The exact stereochemistry of the dearomatised product **5.11** was not determined, and only a single diastereomer was isolated. It was observed that the compound decomposed slowly in the NMR tube, apparently with elimination of the thioether and rearomatisation. This reaction was not optimised, and further elucidation of the structure of this product is also required.

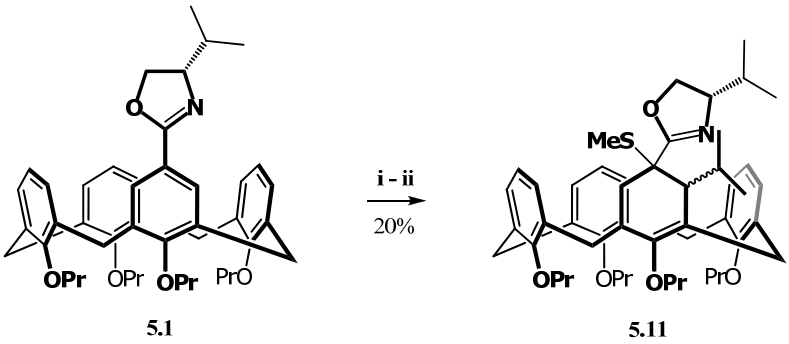

5.1 **5.11**

Figure 5.4: Proposed structure of dearomatised product **5.11**. Reagents and conditions: i) *i*PrLi (5 eq), DMPU (10 eq), THF, −78 ºC, 5 h ii) Me_2S_2 (10 eq).

Returning to the ortholithiation using oxygen coordinative ligands, the application of the strongly coordinating mono–dentate ligand HMPA also produced the inversion of selectivity that first caught our attention with the use of glyme (Entry 1 – Table 5.5). Observing that the inversion appeared to be related to strongly coordinating oxygen–donor ligands, we attempted ortholithiation using the tridentate diglyme as a ligand, resulting in the high yield of the ortholithiated product with appreciable inversion in selectivity (Entry 2 – Table 5.5). We also tested a number of crown ethers, which returned low yields without noteworthy selectivity being observed.

Table 5.5: Effect of *O*–donor ligands on oxazoline **5.1** continued.

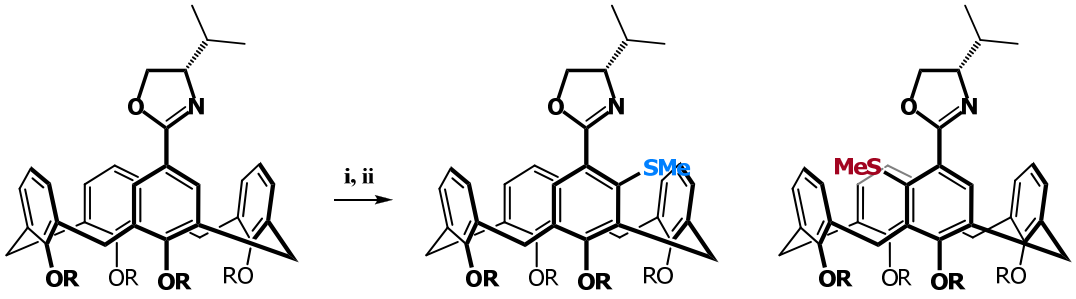

5.1 **5.7** **5.8**

Entry	Solvent[a]	Additive[b]	% Yield	Ratio **5.7**:**5.8**
1	Pentane	HMPA	58	1:1.7
2	Pentane	Diglyme	>95	1:4.2
3	Pentane	18–crown–6	0	–
4	Pentane	15–crown–5	15	1.1:1

Reagents and conditions: i) [a]sBuLi (5 eq), –78 ºC, 5 h, [b]Additive (10 eq) ii) Me_2S_2 (10 eq), –78 ºC to rt, 12 h. Yield determined by ^{1}H NMR, *dr* determined by ^{1}H NMR.

Taking note of the large influence of the choice of alkyllithium in determining the diastereoselectivity in the TMEDA–mediated ortholithiation, we attempted to optimise the HMPA and diglyme–based inversion by screening a number of alkyllithiums (Table 5.6). We found with both diglyme and HMPA that the best choice of alkyllithium to induce the inversion in selectivity was *s*BuLi. This was in contrast to the results obtained with TMEDA, where generally poorer selectivities were recorded for *s*BuLi compared to *i*PrLi and *c*PentLi.

Table 5.6: Effect of alkyllithium on HMPA and diglyme mediated ortholithiation of oxazoline **5.1**.

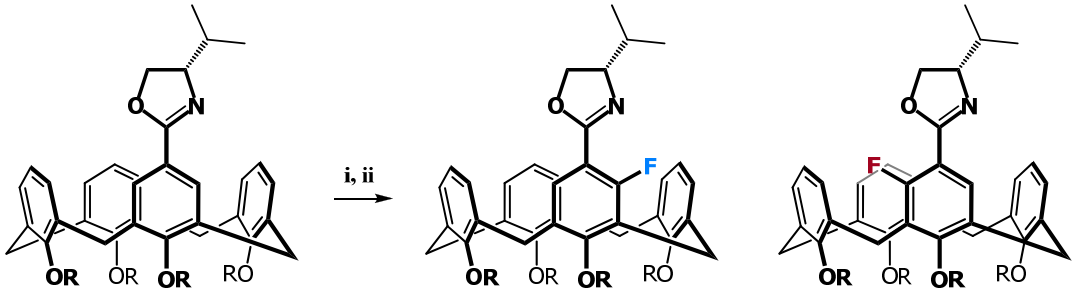

5.1 **5.7** **5.8**

Entry	Alkyllithium[a]	Additive[b]	% Yield	Ratio **5.7**:**5.8**
1	*n*BuLi	HMPA	3	1.2:1
2	*s*BuLi	HMPA	58	1:1.7
3	*i*PrLi	HMPA	42	1:1.5
4	*t*BuLi	HMPA	75	1.6:1
7	*s*BuLi	Diglyme	95	1:4.2
5	*i*Pr	Diglyme	24	1:1.5
6	*t*BuLi	Diglyme	25	1:1.3

Reagents and conditions: i) [a]Alkyllithium (5 eq), –78 ºC, 5 h, [b]Additive (10 eq) ii) Me_2S_2 (10 eq), −78 ºC to rt, 12 h. Yield determined by ^{1}H NMR, *dr* determined by ^{1}H NMR.

Having observed that different alkyllithiums induced variations in the switch in selectivity, we wondered what effect derivatisation of the diglyme ligand structure would have. We tested this hypothesis by using the commercially available diethylene gycol diethyl ether (di–Et–diglyme), observing a moderate improvement in the inversion (1:4.5 compared to 1:4.2). To extend this trend we wondered whether the incorporation of more bulky alkyl groups would further improve the selectivity of the reaction (Figure 5.5). The next obvious extension of the ligand series would be to test the di–isopropyl diethylene glycol ligand **5.12** (di–*i*Pr–diglyme) to observe if the

reversal in selectivity could be further extended. As this reagent is not commercially available, a synthetic approach to it was required.

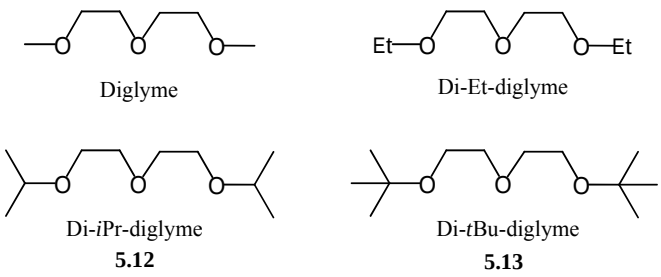

Figure 5.5: Diglyme ligands.

The synthesis of the diglyme derivative ligands was accomplished by firstly ditosylating diethylene glycol using tosyl chloride. We found that the ditosylation reaction proceeded rapidly upon the addition of DMAP to the mixture, affording the ditosylated product **5.14** in high yield. Key to this approach was the development of a simple purification procedure, as large amounts of the ditosyl material was required for the synthesis of the ligands. We found that after workup, dissolving the crude solid in hot toluene, followed by the addition of a minor amount of petroleum ether, resulted in the selective crystallisation of the ditosyl product, allowing large quantities of product to be produced in a single reaction (up to 40 g).

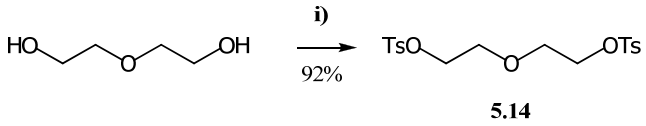

Scheme 5.10: Synthesis of ditosyl diglyme **5.14**. Reagents and conditions: TsCl (2.2 eq), Et_3N (3 eq), DMAP (cat), DCM, 0 °C to rt, 24 h.

Refluxing the di—tosylated compound in isopropanol in an effort to generate di–*i*Pr–diglyme proceeded extremely sluggishly and, even after four days of reflux, significant proportions of starting material remained. Using the Williamson ether synthesis approach, refluxing sodium isopropoxide (generated *in situ* from sodium metal and isopropanol) returned di–*i*Pr–diglyme **5.12** in good yield.

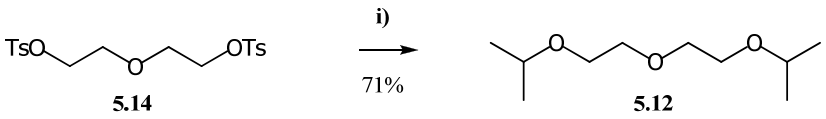

Scheme 5.11: Synthesis of di–iPr–diglyme. Reagents and conditions: *i*PrOH (exs), Na (5.6 eq), THF, Δ, 24 h.

Implementation of the di–*i*Pr–diglyme ligand **5.12** resulted in a noteworthy improvement in the inversion in diastereoselectivity (1:6.4), with retention of the high yields that had characterised these reactions so far (Entry 3 – Table 5.7). Observing the success of the di–isopropyl ligand, we wondered how the more bulky di–*t*–butyl diethyl glycol **5.13** (di–*t*Bu–diglyme) ligand would perform with its increased steric bulk.

The synthesis of the di–*t*Bu–diglyme ligand **5.13** was achieved using the same method. Yields of the desired product were however considerably lower, with significant proportions of a lower boiling by–product being isolated. Characterisation revealed that a competitive elimination reaction was occurring, forming mono–*t*–butyl vinyl ether **5.15**. Presumably formation of di–vinyl ether also occurs, but its low boiling point (28 °C) frustrates detection.

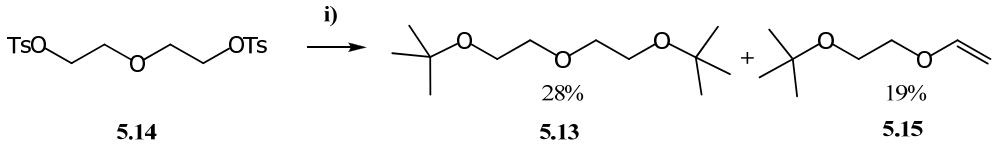

Scheme 5.12: Synthesis of di–*t*Bu–diglyme **5.13**. Reagents and conditions: *t*BuOH (exs), Na (5.7 eq), THF, Δ, 24 h.

In an effort to limit the formation of **5.15**, a number of different conditions were screened. Changing the solvent to the low boiling diethyl ether or the high boiling toluene returned similar yields of product **5.13**, without appearing to significantly influence the formation of by– product **5.15**. It appeared that the greater steric bulk and basicity of the tertiary butoxide anion, compared to the secondary alkoxide, caused increased elimination of the tosyl group (to form alkene **5.15**) limiting the desired S_N2 reaction. The use of the less basic lithium *t*–butoxide failed to improve the overall yield of the reaction.

Implementation of di–*t*Bu–diglyme ligand **5.13** in the ortholithiation reaction (Entry 4 – Table 5.7) provided a significant enhancement in the inversion in diastereocontrol (1:12) in excellent yield. This result indicated that for appreciable inversion, the steric bulk of the alkyl groups on the end of the chain, coupled to the tri–dentate nature of the ligand, is a requirement.

Table 5.7: Effect of derivatisation of diglyme ligands on the ortholithiation reaction.

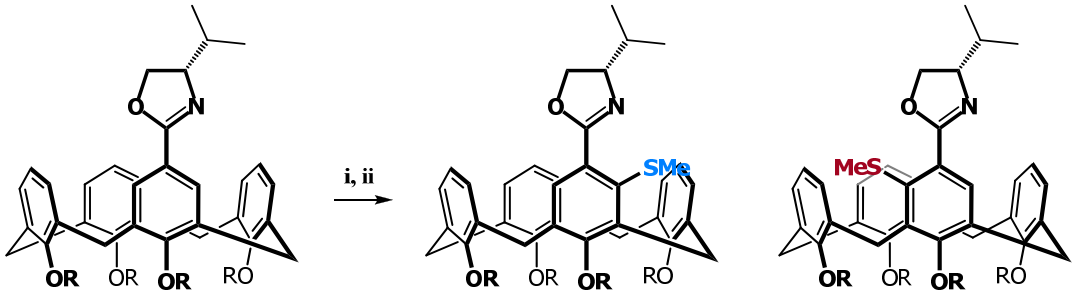

5.1 **5.7** **5.8**

Entry	Alkyllithium[a]	Additive[b]	% Yield	Ratio **5.7**:5.8
1	*s*BuLi	Diglyme	95	1:4.2
2	*s*BuLi	Di–Et–diglyme	95	1:4.5
3	*s*BuLi	Di–*i*Pr–diglyme	88	1:6.4
4	*s*BuLi	Di–*t*Bu–diglyme	95	1:12

Reagents and conditions: i) [a]Alkyllithium (5 eq), –78 ºC, 5 h, [b]Additive (10 eq) ii) Me_2S_2 (10 eq), –78 ºC to rt, 12 h. Yield determined by ^{1}H NMR, *dr* determined by ^{1}H NMR.

5.3.5 Thermal Stability of the Lithiated Intermediate

In seeking to determine the mechanism in which the diastereoselectivity was generated in the ortholithiation reaction, we wanted to rule out the possibility that the enhanced thermodynamic stability of one of the diastereomers was driving the process. We investigated this by ortholithiating **5.1** with 1.2 equivalents of *s*BuLi in pentane with TMEDA with the reaction being held at –78 ºC for ten hours to ensure complete conversion to the lithiated intermediate, followed by quenching with dimethyl disulphide. A second reaction with identical conditions was held at –78 ºC for seven hours, after which it was warmed to 0 ºC for three hours. Both reactions returned identical selectivities, indicating that the lithiated intermediate appeared to be thermodynamically stable under the reaction conditions, proving that the diastereoselectivity is not due to a thermodynamic preference for a single diastereomer.

5.4 Determination of Configuration of Major Product

Lastly, we needed to confirm the stereochemistry of the ortholithiated product. Having achieved success with crystallisation of phosphine oxide functionalised calixarene **4.5**, we employed the same approach to determine the configuration of the diastereomers. We performed an ortholithiation using TMEDA, followed by quenching with diphenylphosphine chloride, with *in*

situ oxidation yielded the crystalline phosphine–oxide **5.16**. After a number of attempts, slow evaporation of a DCM–ethanol mixture yielded single crystals of the phosphine oxide **5.16**. Elucidation, by single crystal X–ray diffraction, indicated the major diastereomer produced using TMEDA was in the *cR* configuration, consistent with the major diastereomer obtained by ortholithiation of *t*–butyl calixarene oxazoline **2.1**.

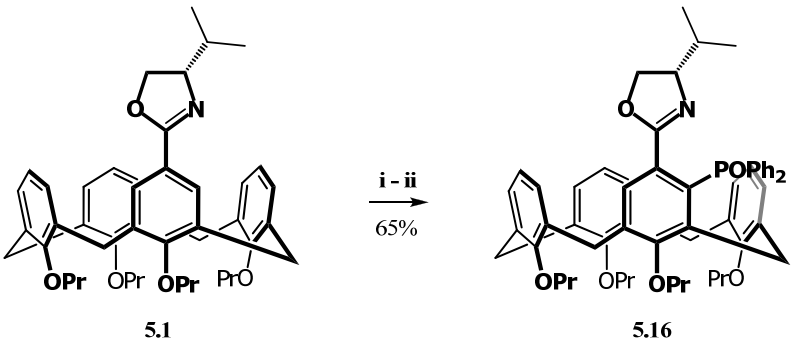

Figure 5.6: Synthesis of phosphine oxide **5.16**. Reagents and conditions: i) *i*PrLi (5 eq), TMEDA (10 eq), Pentane, −78 ºC, 5 h ii) Ph_2PCl (10 eq), −78 ºC to rt, 12 h.

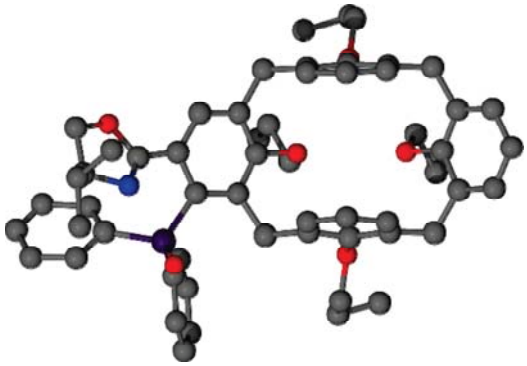

Figure 5.7: Crystal structure of phosphine oxide **5.16** viewed from above. Note hydrogen atoms removed for clarity.

5.5 Conclusion and Future Work

In this chapter we have demonstrated that the *t*–butyl groups on the calixarene are not a requirement for inducing diastereomeric selectivity into the ortholithiation reaction, and high selectivities (up to 43:1) can be obtained using TMEDA ligated ortholithiation. It has also been shown, in a qualitative fashion, that the rate of the reaction was considerable faster with the presence of the *t*–butyl groups on the structure. Furthermore, it has been determined that the diastereomeric selectivity is strongly related to the ligand/solvent used in the reaction, and can, in fact, be inverted by the use of HMPA and to a greater extent diglyme–mediated ortholithiation (1:12). The use of diglyme ligands in asymmetric organolithium transformations has, to the best

of our knowledge, not been explored in the chemical literature and in this regard the ability of these ligands (specifically di–*t*Bu–diglyme) to switch the diastereomeric selectivity is an important finding. This remarkable inversion generated by the diglyme structure could have important implications in other areas of asymmetric organolithium chemistry.

In the following chapter we continue to probe the oxazoline–directed ortholithiation of the calixarene system to observe if higher selectivities can be obtained by increasing the steric bulk of the substituent on the oxazoline.

5.6 References

(1) Ikeda, A.; Yoshimura, M.; Lhotak, P.; Shinkai, S. *J. Chem. Soc., Perkin Trans. 1* **1996**, 1945.

(2) Gutsche, C. D.; Pagoria, P. F. *J. Org. Chem.* **1985**, *50*, 5795.

(3) Iwamoto, K.; Araki, K.; Shinkai, S. *J. Org. Chem.* **1991**, *56*, 4955.

(4) Sammakia, T.; Latham, H. A. *J. Org. Chem.* **1996**, *61*, 1629.

(5) Clayden, J.; Greeves, N.; Warren, S.; Wothers, P. *Organic Chemistry*; Oxford University Press Oxford, 2000.

(6) Gordon, I. M.; Maskill, H.; Ruasse, M. F. *Chem. Soc. Rev.* **1989**, *18*, 123.

(7) Marat, K.; SpinWorks 3.1.7 ed.; University of Manitoba: 2010.

(8) Clayden, J. *Organolithiums: Selectivity for Synthesis*; Pergamon: London, 2002.

(9) Stey, T.; Stalke, D. In *The Chemistry of Organolithium Compounds*; Rappoport, Z., Marek, I., Eds.; John Wiley & Sons, New York: 2004, p 47.

(10) Jemmis, E.; Gopakuma, G. In *The Chemistry of Organolithium Compounds*; Rappoport, Z., Marek, I., Eds.; John Wiley & Sons, New York: 2004, p 1.

(11) Laufer, R. S.; Veith, U.; Taylor, N. J.; Snieckus, V. *Org. Lett.* **2000**, *2*, 629.

(12) Fitt, J. J.; Gschwend, H. W. *J. Org. Chem.* **1984**, *49*, 209.

(13) Bergander, K.; He, R. X.; Chandrakumar, N.; Eppers, O.; Gunther, H. *Tetrahedron* **1994**, *50*, 5861.

(14) Clayden, J.; Parris, S.; Cabedo, N.; Payne, A. H. *Angew. Chem. Int. Ed.* **2008**, *47*, 5060.

CHAPTER 6

Ortholithiation of *t*Bu–Oxazoline Calixarenes

6.1 Synthesis and Ortholithiation of *t*Bu–Oxazoline Debutylated Calixarene

Thus far, all ortholithiation performed on the calixarene system had utilised an isopropyl oxazoline as the directing group, however a number of other functionalised oxazolines have been used in asymmetric lithiations in the liaterature.[1–5] While numerous possibilities exist for exploring the role of the substitution pattern on the oxazoline, we were interested in observing what effect increasing the steric bulk from the isopropyl group to the *t*–butyl group would have, especially in the light of the excellent diastereomeric control that Sammakia and co-workers had demonstrated when using the *t*–butyl ferrocenyloxazoline.[4,6] As we had developed synthetic access to both de–butylated and butylated calixarene oxazolines, we began our investigation on the more easily lithiated de–butylated calixarene system, to test the diastereocontrol afforded by the larger directing group.

Coupling of L–*tert*–leucinol with carboxylic acid **5.2** followed by ring closure using the established methodology yielded *t*–butyl oxazoline **6.1** in good yield.

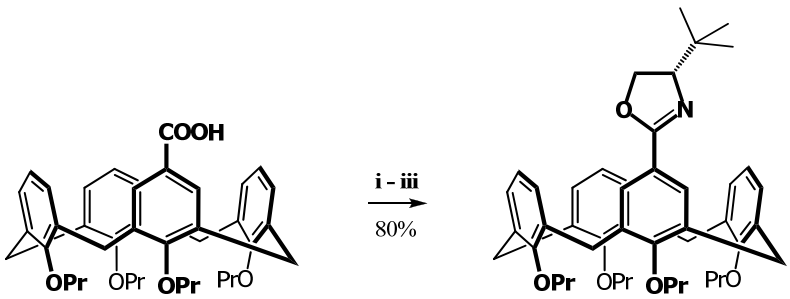

5.2 **6.1**

Scheme 6.1: Synthesis of *t*Bu–oxazoline debutylated calixarene **6.1**. Reagents and conditions: i) Oxalyl chloride (3 eq), DCM, rt, 3 h, ii) L–*tert*–leucinol (1.2 eq), Et_3N (6 eq), DCM, 0 °C to rt, 15 h, iii) MsCl (3 eq), DCM, rt, 3 h.

We initially tested a range of alkyllithiums in conjunction with the additive TMEDA (Table 6.1). We were surprised to note that the diastereoselectivity generated by the use of different alkyllithiums did not follow the same trend as we had observed in the isopropyl oxazoline system, in that *s*BuLi gave the best selectivity for thioether **6.2** (120:1), whereas *n*BuLi (9:1) returned considerably reduced control. The use of the tertiary reagent *t*BuLi, unexpectantly displayed a

reversal in diastereoselectivity, returning a strong preference for the formation of thioether **6.3** (1:11), in a moderate yield (Entries 5 – 7 Table 6.1). In an effort to improve the yield of this reaction, the reaction time was extended to twelve hours but it was found that only a marginal improvement in yield was obtained. In the case of reactions performed in pentane, the formation of coloured precipitates were observed, possibly indicating that an alkyllithium complex was precipitating out of solution, perhaps accounting for the low conversion. To overcome this, diethyl ether was used in addition to extending the reaction time to twenty hours, this returned an improved yield of 75% without reducing the inversion in diastereoselectivity.

Table 6.1: Ortholithiation of *t*Bu Oxazoline **6.1**.

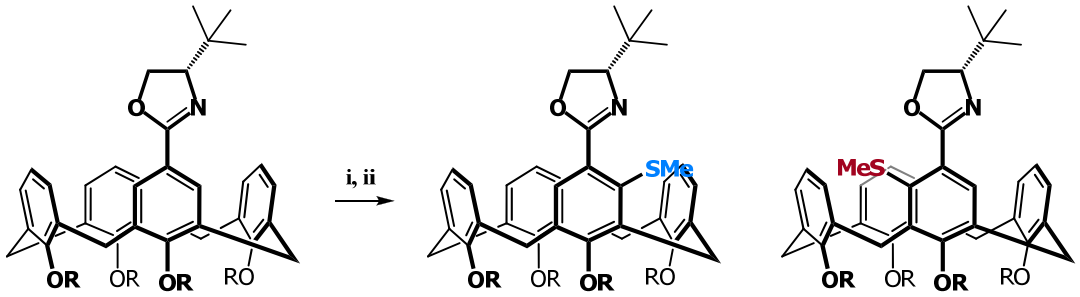

6.1 **6.2** **6.3**

Entry	Solvent[a]	Alkyllithium[b]	Additive[c]	Time	% Yield	Ratio **6.2**:**6.3**
1	Pentane	*n*BuLi	TMEDA	5	3	9:1
2	Pentane	*i*PrLi	TMEDA	5	67	115:1
3	Pentane	*c*PentLi	TMEDA	5	67	57:1
4	Pentane	*s*BuLi	TMEDA	5	95	120:1
5	Pentane	*t*BuLi	TMEDA	5	34	1:11
6	Pentane	*t*BuLi	TMEDA	12	54	1:11
7	Et_2O	*t*BuLi	TMEDA	20	75	1:11
8	THF	*i*PrLi	–	5	62	1.5:1
9	THF	*s*BuLi	–	5	88	1.3:1
10	THF	*t*BuLi	–	5	0	–
12	Et_2O	*s*BuLi	–	5	88	1.2:1

Reagents and conditions: [a]−78 ºC, 5 h,, [b]Alkyllithium (5 eq) [c]TMEDA (10 eq) ii) Me_2S_2 (10 eq). −78 ºC to rt, 12 h, Yield determined by ^{1}H NMR, *dr* determined by ^{1}H NMR.

The use of THF as a solvent without the additive TMEDA returned negligible diastereocontrol (Entries 8 – 12 Table 6.1), similar to the results obtained for ortholithiation of isopropyl oxazoline

5.1, with a minor preference being observed for thioether **6.2**. The use of diethyl ether returned similar poor selectivity.

In a brief exploration into the effect of additives capable of inverting the selectivity with isopropyl oxazoline **5.1**, the use of HMPA, diglyme and di–*t*Bu–diglyme were investigated as ligands in the ortholithiation of *t*–butyl oxazoline **6.1** (Table 6.2). It was observed that while a preference for the formally minor diastereomer **6.3** was obtained, the ability to control the inversion in selectivity appeared to be reduced in relation to the ortholithiation of isopropyl oxazoline **5.1**. Notably, the diglyme:*s*BuLi combination returned an almost racemic mixture of thioethers **6.2** and **6.3**. To gain a more rounded understanding of the effectiveness of these ligands, further experimentation with different alkyllithiums was required.

Table 6.2: Ortholithiation of *t*–butyl oxazoline **6.1** using different additives.

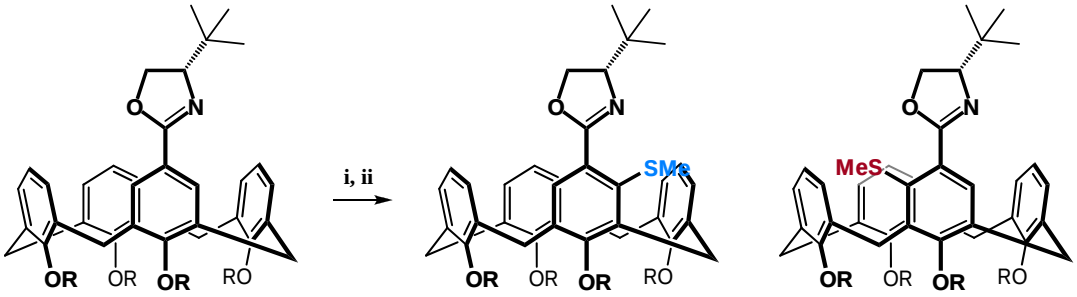

6.1 **6.2** **6.3**

Entry	Solvent[a]	Alkyllithium[b]	Additive[c]	% Yield	Ratio **6.2**:**6.3**
1	Pentane	*s*BuLi	HMPA	30	1:2.2
2	Pentane	*s*BuLi	Diglyme	38	1.1:1
3	Pentane	*t*BuLi	Diglyme	17	1:5.4
4	Pentane	*s*BuLi	di–*t*Bu–diglyme	33	1:3.4

Reagents and conditions: [a]5 h, −78 ºC, [b]Alkyllithium (5 eq), [c]Additive (10 eq), ii) Me_2S_2 (10 eq). −78 ºC to rt, Yield determined by ^{1}H NMR, *dr* determined by ^{1}H NMR.

6.1.1 *Determination of the Configuration of the Major Diastereomer*

In order to prove the configuration of the major diastereomer **6.2**, we chose to remove the directing group and compare the optical rotation of the chiral acid product to the optical rotation of a similarly functionalised acid of known configuration. Rather than simply hydrolysing **6.2**, we chose to demonstrate the versatility of the ortholithiation method by producing a bromo functionalised molecule **6.4**, with subsequent hydrolysis of the bromo product to produce an inherently chiral bromo acid. Bromo calixarene **6.4** was produced in good yield by quenching the

lithiated intermediate with dibromoethane (Scheme 6.2). Hydrolysis of bromo calixarene **6.4** was performed according to our standard conditions, yielding bromo acid **6.5** (Scheme 6.2). We observed that the rate of hydrolysis of the amide intermediate appeared to be significantly improved by the use of lithium hydroxide as opposed to the standard sodium hydroxide.

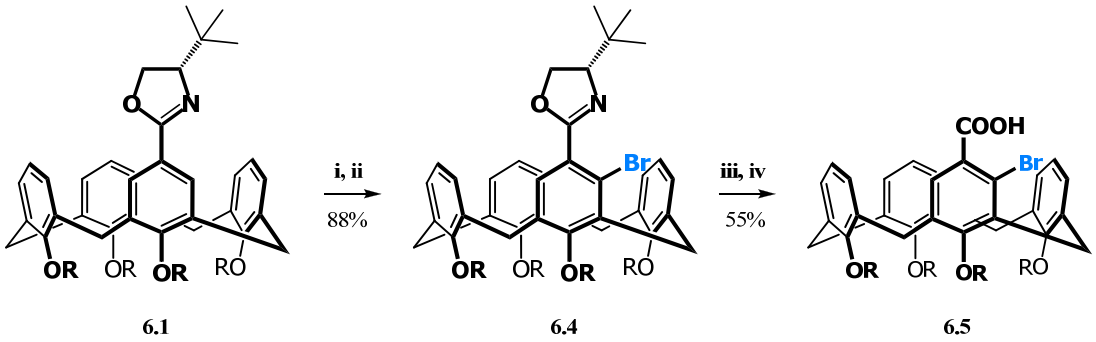

6.1 **6.4** **6.5**

Scheme 6.2: Synthesis of bromo acid **6.5**. Reagents and conditions: i) *s*BuLi (5 eq), TMEDA (10 eq), pentane –78 °C, 5 h, ii) dibromoethane (exs), –78 °C to rt, 12 h, iii) AcOH, H_2O, 170°C, 1 h, iv) EtOH, H_2O LiOH, 150 °C, 1 h.

Using an analogous approach, isopropyl oxazoline **5.1** was functionalised using dibromoethane in good yield, producing bromo oxazoline **6.6,** which after hydrolysis of the oxazoline yielded bromo acid **6.7** (Scheme 6.3). Measurement of the optical rotation of acids **6.5** (–10.8°) and **6.7** (–11.2°) confirmed their identical stereochemistry.

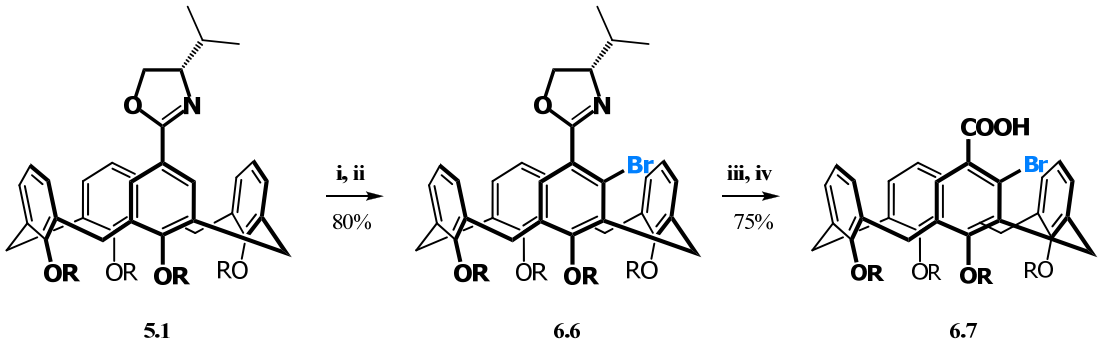

5.1 **6.6** **6.7**

Scheme 6.3: Synthesis of bromo acid **6.7**. Reagents and conditions: i) *s*BuLi (5 eq), TMEDA (10 eq), pentane –78 °C, 5 h, ii) dibromoethane (exs), –78 °C to rt, 12 h, iii) AcOH, H_2O, 170°C, 1 h, iv) EtOH, H_2O LiOH, 150°C, 1 h.

Having demonstrated the success of the *t*–butyl oxazoline at diastereomerically controlling ortholithiation on the debutylated calixarene, we wondered if its use in the butylated calixarene system would also impart greater control over the lithiation.

6.2 Synthesis and Ortholithiation of *t*Bu–Oxazoline Butylated Calixarene

Using the same method for the synthesis of isopropyl oxazoline **2.1**, *t*–butyl oxazoline **6.8** was generated in good yield from acid **2.2** (Scheme 6.4).

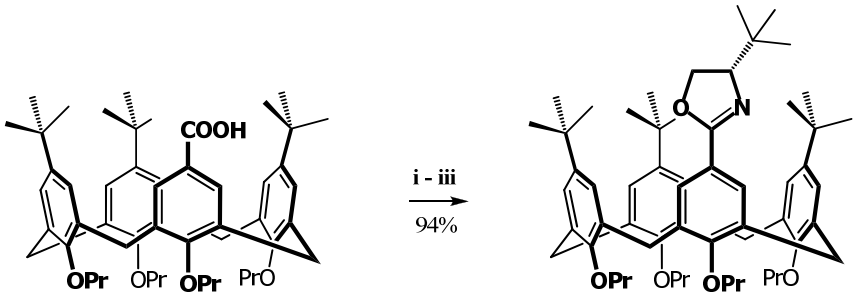

2.2 **6.8**

Scheme 6.4: Synthesis of *t*Bu–oxazoline debutylated calixarene **6.8**. Reagents and conditions: i) Thionyl chloride (exs), Δ, 3 h, ii) L–*tert*–leucinol (1.2 eq), Et_3N (3.6 eq), 0 °C to rt, 18 h, iii) thionyl chloride (16 eq), DCM, 18 h.

Turning to the ortholithiation of **6.8**, we found that the reaction proceeded extremely sluggishly. This was somewhat expected, as the ortholithiation of the butylated isopropyl oxazoline **2.1**, relative to the debutylated calixarene systems, also occurred significantly more slowly. To increase the yield, reactions were performed at high concentration and with removal of the alkyl solvent from the lithium reagent before the reaction. An HPLC–based method for quantification of the diastereomers and the starting material was developed in order to more accurately determine the yield and diastereoselectivity. Initially, we tested a number of different solvents with the TMEDA ligand (Entries 1 – 4 Table 6.3), observing that the best yield and control were obtained when using diethyl ether. Testing a range of alkyllithiums in diethyl ether with TMEDA returned almost perfect diastereocontrol for the formation of thioether **6.9,** perhaps unsurprisingly, in moderate to poor yield even with extended reaction times (Entries 5 – 8, Table 6.3). In most instances, the reaction was so selective that it was not possible to detect the minor diastereomer. Similar to the ortholithiation of debutylated *t*–butyl oxazoline **6.1**, it was observed that *t*BuLi generated an inversion in diastereoselectivity, with the reaction now preferentially generating thioether **6.10**. By increasing the reaction time to forty–eight hours, the yield of the *s*BuLi:TMEDA reaction was improved (80%), with the improved yield allowing quantification of the diastereoselectivity (>500:1). Extending the reaction time of the *t*BuLi:TMEDA reaction, also returned an improved yield (50%) however with reduced diastereoselectivity. Increased formation of products associated with the addition of the alkyllithium reagent into the molecule (~10%) was also detected for the extended *t*BuLi:TMEDA reaction.

Table 6.3: Ortholithiation of *t*Bu Oxazoline **6.8**.

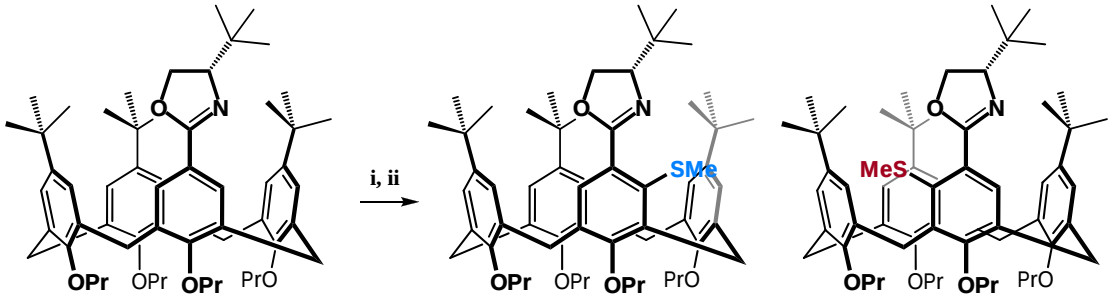

6.8 **6.9** **6.10**

Entry	Solvent	Alkyllithium[a]	Additive[b]	Time /h	% Yield	Ratio **6.9**:**6.10**
1	Et_2O	*s*BuLi	TMEDA	24	57	>200:1
2	THF	*s*BuLi	TMEDA	24	8	12.2:1
3	Toluene	*s*BuLi	TMEDA	24	10	5.5:1
4	Pentane	*s*BuLi	TMEDA	24	45	199:1
5	Et_2O	*n*BuLi	TMEDA	24	2	>200:1
6	Et_2O	*i*PrLi	TMEDA	24	25	>200:1
7	Et_2O	*c*PentLi	TMEDA	24	27	>200:1
8	Et_2O	*t*BuLi	TMEDA	24	6	1:6.9
9	Et_2O	*s*BuLi	TMEDA	48	81	635:1
10	Et_2O	*t*BuLi	TMEDA	48	50	1:3.1
11	THF	*i*PrLi	–	24	7	5:1
12	THF	*s*BuLi	–	24	29	2.7:1
13	THF	*t*BuLi	–	24	5	>100:1
14	Et_2O	*s*BuLi	di–*t*Bu–diglyme	24	12	1:3.7

Reagents and conditions: [a]Alkyllithium (5 eq), −78 ºC, [b]TMEDA (10 eq) ii) Me_2S_2 (10 eq), −78 ºC to rt 12 h, Yield and *dr* determined by HPLC.

Reactions performed solely in THF resulted in an erosion of selectivity compared to the TMEDA ligated reaction (Entries 8 – 10 Table 6.3), however, the selectivity of the reaction was significantly more controlled than had been observed with the other calixarene oxazolines tested thus far. The combination of *t*BuLi:THF produced a strong preference for thioether **6.9** in contrast to the results obtained using TMEDA with this alkyllithium. The use of the additive di–*t*Bu–diglyme induced a moderate inversion in selectivity, again with reduced control compared to

isopropyl oxazoline **5.1**. Due to the preliminary nature of this study, further experimentation with alkyllithiums and ligands is required to fully illustrate the potential and behaviour of this system.

To complete the study of the *t*–butyl oxazoline directing group, the determination of the configuration of thioethers **6.9** and **6.10** was required, which is discussed in the following section.

6.2.1 *Determination of the Configuration of the Major Diastereomer*

To determine the configuration of the diastereomers produced from the ortholithiation reaction, we chose to install the *t*–butyl oxazoline on a methyl thioether carboxylic acid **4.15** of known configuration produced from the ortholithiation of butylated isopropyl oxazoline **2.1**. This method had a second objective, in that owing to the high selectivity and low yield of the ortholithiation reaction on butylated *t*–butyl oxazoline **6.8,** we wanted to ensure that both thioether diastereomers **6.9** and **6.10** were correctly identified in the HPLC trace. Due to this secondary objective, a highly enantiomerically enriched starting material of **4.15** was not used, as the presence of both a major and minor diastereomer in the product was required.

Conversion of methyl thioether carboxylic acid **4.15** to *t*–butyl oxazoline thioether **6.4** was performed using our standard coupling methodology. Comparison of the ^{1}H NMR spectra with the retention times of the peaks on a HPLC trace confirmed the configuration of inherent chirality of thioether diastereomers **6.9** and **6.10**. We noted that diastereoselectivity could occur during the formation of **6.11** due to preferential coupling between the chiral aminol and a single enantiomer of acid **4.15**. Efforts were made to limit this problem by the use of a large excess of L–*tert*–leucinol. A slight reduction in the ratio between the diastereomers was observed. This is likely to be the result of small differences in the polarity of diastereomeric mixture **6.11** resulting in the loss of one diastereomer during column chromatography.

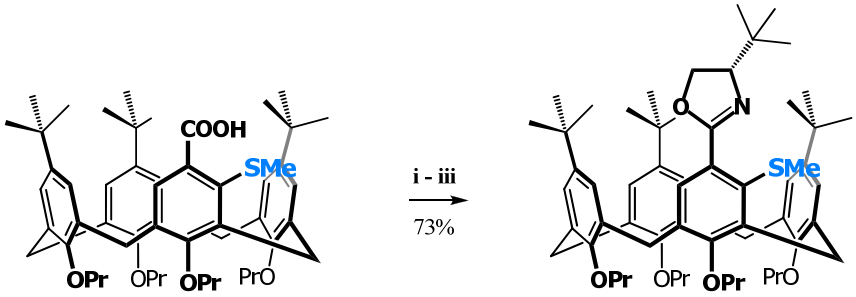

4.15 **6.11**

Scheme 6.5: Synthesis of thioether **6.11** from thioether acid **4.15**. Reagents and conditions: i) Oxalyl chloride (exs), DCM, rt, 4 h, ii) Et_3N (exs), L–*tert*–leucinol (exs), DCM, 12 h, iii) mesyl chloride (exs), 3 h, rt.

6.3 Conclusion and Future Work

In this chapter we have demonstrated that the use of the *t*–butyl oxazoline directing group produces remarkable diastereocontrol over the functionalisation of both butylated (>500:1) and debutylated (120:1) calixarenes. It has been observed that the diastereocontrol can be significantly influenced by the choice of the alkyllithium, with the use of *t*BuLi producing a notable inversion in diastereoselective control. The use of di–*t*Bu–diglyme was observed to promote a reversal in diastereoselectivity for both *t*–butyl oxazolines, but in reduced fashion compared to isopropyl oxazoline **5.1**. We acknowledge that further optimisation of conditions on these two systems should be performed, however this preliminary study certainly indicates the powerful controlling influence provided by the *t*–butyl oxazoline. In the following chapter we return to the diglyme–induced inversion, by exploring when the powerful ability of the ligands to switch the selectivity to the synthesis of the formally minor diastereomer could be exploited in the ortholithiation of ferrocenyloxazolines.

6.4 References

(1) Meyers, A. I. *J. Org. Chem.* **2005**, *70*, 6137.

(2) Manoury, E.; Fossey, J. S.; Ait–Haddou, H.; Daran, J. C.; Balavoine, G. G. A. *Organometallics.* **2000**, *19*, 3736.

(3) Clayden, J.; Clayton, J.; Harvey, R. A.; Karlubikova, O. *Synlett* **2009**, 2836.

(4) Sammakia, T.; Latham, H. A.; Schaad, D. R. *J. Org. Chem.* **1995**, *60*, 10.

(5) Clayden, J.; Parris, S.; Cabedo, N.; Payne, A. H. *Angew. Chem. Int. Ed.* **2008**, *47*, 5060.

(6) Sammakia, T.; Latham, H. A. *J. Org. Chem.* **1995**, *60*, 6002.

CHAPTER 7

Ortholithiation of Ferrocenyloxazolines

7.1 Synthesis of Isopropyl Ferrocenyloxazoline

On observing the success of diglyme for inducing an inversion in diastereoselectivity in the calixarene system, we wondered if other prochiral oxazoline–directed lithiations would display a similar trend. In this regard we targeted isopropyl ferrocenyloxazoline[1-3] which can be highly diastereoselectivly functionalised when using the TMEDA ligand.[4] Due to the widespread employment of planar chiral ferrocenyl ligands in asymmetric catalysis,[5-7] the prospect of being able to generate both diastereomers from the same chiral starting material adds significant value to the development of diastereo–tuneable methodology.

A number of synthetic methods exist for the synthesis of ferrocenyloxazoline in the chemical literature.[8] Nevertheless as a result of our success with coupling chiral aminols with acyl chlorides followed by ring closure, we chose a similar approach for the ferrocene system.[2,3] In adopting this strategy, the first compound that we needed to synthesise was a ferrocenyl carboxylic acid.

A number of different approaches have been used to synthesise carboxylic acid ferrocenes, for example oxidation of Friedel–Crafts products;[9,10] or mono–lithiation followed by quenching with carbon dioxide.[11] Using the latter process, carboxy ferrocene **7.1** was synthesised in good yield using superbase conditions (*t*BuOK and *t*BuLi) followed by quenching with gaseous CO_2 (Scheme 7.1).[11] The water–soluble nature of the carboxy anion makes the reaction very scalable, as purification of the acid product can be readily accomplished by extraction into a basic solution, which upon acidification selectively yields the desired mono–acid by precipitation.

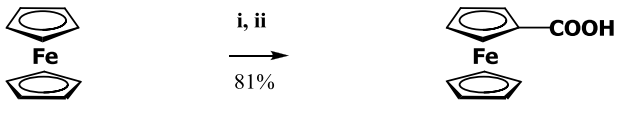

7.1

Scheme 7.1: Synthesis of ferrocenylcaroboxylic acid **7.1**. Reagents and conditions: i) *t*BuLi (2 eq), *t*BuOK (0.1 eq), THF, –78 °C, 1 h, ii) CO_2 (g, exs), –78 °C to rt 1 h.

Having acid **7.1** in hand, the corresponding acid chloride was synthesised *in situ* using oxalyl chloride, which when reacted with L–valinol, cleanly produced the chiral amide in high yield. A surprising variety of conditions have been used to cyclise amides to oxazolines on the ferrocene system,[8] often using tosyl chloride.[3,4] Owing to our observation that mesyl chloride provided a highly effective means of forming oxazolines in the calixarene system, we decided to attempt cyclisation using mesyl chloride on the ferrocene amide. Pleasingly, reaction of mesyl chloride rapidly afforded the desired isopropyl ferrocenyloxazoline **7.2** in excellent yield (Scheme 7.2).

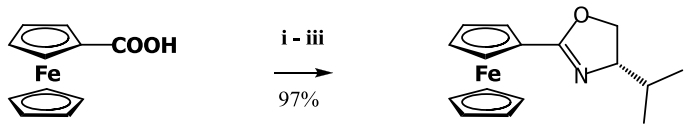

7.1 **7.2**

Scheme 7.2: Synthesis of isopropyl ferrocenyloxazoline. Reagents and conditions: i) Oxalyl chloride (3 eq), DCM, rt, 2 h, ii) L–valinol (1.2 eq), Et_3N, DCM, 0 °C to rt, 12 h, iii) Mesyl chloride (3 eq), Et_3N (3 eq), DCM, rt, 2 h.

The basic nature of oxazoline **7.2** was observed during workup, where it was found to be readily partitioned into acidic aqueous phases from Et_2O solutions. This feature is also evident during column chromatography, with the need for basification of the acidic silica to prevent protonation (visible through the formation of a deep red colour) of the oxazoline. The water miscibility of these compounds can be used advantageously to separate functionalised ferrocenyloxazolines from unwanted impurities through judicious use of acidic or basic conditions.

7.2 Ortholithiation of Isopropyl–Ferrocenyloxazoline

Having the desired ferrocenyloxazoline **7.2**, we investigated its ortholithiation using TMEDA and diglyme as ligands. Initially, we repeated the conditions used by Sammakia *et al.*,[4] in order to compare the diastereoselectivity generated by the different alkyllithiums against those using the diglyme ligand. Similar selectivities to those reported by Sammakia and co–workers (when using the three standard alkyllithiums in THF) were recorded when quenching with dimethyl disulphide (Entries 1 to 3 – Table 7.2), yielding a moderate diastereoselectivity for the formation of thioether **7.3** over minor diastereomer **7.4**.

Table 7.1: Ortholithiation of *i*Pr–oxazoline **7.2** using common additives and diglyme.

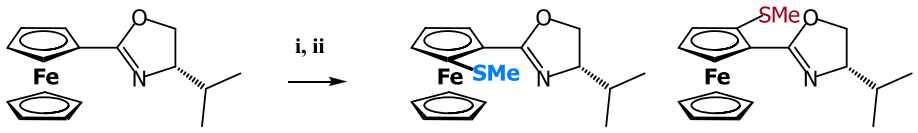

7.2 **7.3** **7.4**

Entry	Solvent	Alkyllithium[a]	Additive[b]	Yield	Ratio **7.3**: **7.4**
1[c]	THF	*n*BuLi		30	2.3:1
2[c]	THF	*s*BuLi		82	5:1
3[c]	THF	*t*BuLi		53	7:1
4[d]	Pentane	*n*BuLi	TMEDA	58	170:1

Reagents and conditions: i) [a]Alkyllithium (1.5 eq) [b]Additive (2 eq), –78 °C, 2 h. ii) Me_2S_2 (10 eq) –78 °C to rt, 12 h, [c]Yield and *dr* determined by ^{1}H NMR, [d]Yield and *dr* by HPLC.

Ortholithiation with the addition of the TMEDA ligand returned almost perfect diastereoselective control for formation of thioether **7.3**. To accurately quantify the yield and the diastereoselectivity of the reaction, we developed an HPLC–based method for quantification of the three compounds (oxazoline **7.2** and diastereomers **7.3** and **7.4**), as coalescence in the ^{1}H NMR spectrum created difficulties in obtaining accurate data from the reaction. Having successfully repeated the ortholithiation and functionalisation of the ferrocenyloxazoline system, we began investigating the reaction using diglyme as a ligand.

7.2.1 Effect of Alkyllithium on Diglyme Induced Inversion in Diastereoselectivity

Sammakia *et al.*[4] had found that the greatest diastereoselectivity was returned when reactions were performed in pentane. We attempted to emulate these conditions using the diglyme ligand, but repeated attempts returned poor conversion to the ortho–functionalised product. By substituting pentane for toluene we did, however, observe that this allowed the reaction to proceed in generally excellent yield. We tested a range of different alkyllithiums with diglyme, observing that the primary reagents (*n*BuLi and EtLi) proved to give the greatest inversion in selectivity, in contrast to the results obtained on the calixarenes where *s*BuLi provided the greatest control (Entry 1 – Table 7.2).

Table 7.2: Ortholithiation of isopropyl–oxazoline **7.2** using diglyme.

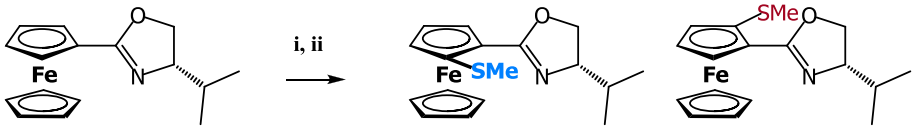

7.2 **7.3** **7.4**

Entry	Solvent	Alkyllithium[a]	Additive[b]	% Yield	Ratio **7.3**:**7.4**
1	Toluene	*n*BuLi	Diglyme	98	1:1.4
2	Toluene	*s*BuLi	Diglyme	96	2.7:1
3	Toluene	*t*BuLi	Diglyme	78	15:1
4	Toluene	MeLi	Diglyme	0	0
5	Toluene	EtLi	Diglyme	54	1:1.2
6	Toluene	PhLi	Diglyme	0	0

Reagents and conditions: i) [a]Alkyllithium (1.5 eq), [b]Additive (2 eq), –78 °C, 2 h. ii) MeSSMe (10 eq) –78 °C to rt, 12 h, Yield and *dr* by HPLC.

The inversion appeared less evident than with the calixarene system, therefore we were eager to test the more bulky diglyme derivatives that had proved to provide enhanced inversion on the calixarene system.

7.2.2 Effect of Derivative Diglyme Structures

The use of the commercially available dibutyl diglyme (di–*n*Bu–diglyme) improved the inversion from that recorded with diglyme from 1:1.4 to 1:1.9 (Entry 2– Table 7.3). Interested in expanding the sequence of diglyme ligands, we wondered how a diphenyl diglyme **7.5** (di–Ph–diglyme) ligand would perform. In order to test this, the synthesis of the crystalline di–Ph–diglyme was accomplished in good yield from the di–tosyl–diglyme precursor (Scheme 7.3).

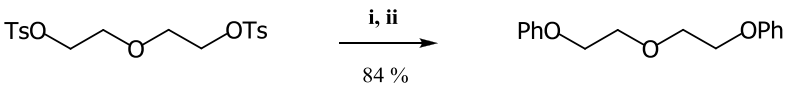

Scheme 7.3: Synthesis of di–phenyl diglyme **7.5**. Reagents and conditions: i) Phenol (3.7 eq), NaH (3.7 eq), DMF, rt, 1 h, ii) ditosyl diglyme (1 eq), rt, 48 h.

Employing di–Ph–diglyme **7.5** in the ortholithiation of **7.2**, returned poor conversion with negligible preference (1:1.1) for the formation of thioether **7.4** (Entry 3 – Table 7.3). Returning to di–*i*Pr–diglyme, which had exhibited respectable diastereocontrol in the calixarene system, significantly improved the preference for the formation of **7.4** over **7.3** to 1:3.8 (Entry 2 – Table

7.3). Finally ortholithiation ligated by di–*t*Bu–diglyme further improved the diastereomeric preference for **7.4** to 1:5.6, representing a considerable inversion in selectivity when compared to TMEDA. Observing the significance of the bulk of the alkyl group on the diglyme ligand in improved the selectivity, we wondered whether it would be possible to further increase the steric bulk of the terminal alkyl substituents. We reasoned that alkylation of the diglyme structure with 3–ethyl–3–pentanol would yield a di–triethyl diglyme ligand **7.6** (di–triEt–diglyme) which should be more bulky than the di–*t*Bu–diglyme ligand. Employing a dimesyl diglyme precursor, di–triEt–diglyme was synthesised in low yield (Scheme 7.4).

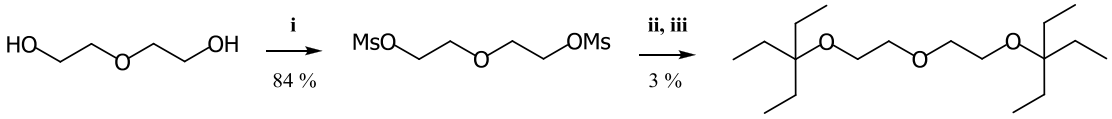

Scheme 7.4: Synthesis of di–triethyl diglyme **7.6**. Reagents and conditions: i) MsCl (2.5 eq), Et_3N (3.2 eq), DCM, 0 °C to rt, 18 h, ii) 3–ethyl–3–pentanol (2.3 eq), NaH (2.3 eq), Δ, 1.5 h, iii) dimesyl diglyme Δ, 18 h.

Unfortunately, the use of di–triEt–diglyme in the reaction failed to improve the diastereoselectivity of the reaction as hoped, instead returning a small preference for the formation of **7.3** (Entry 6 – Table 7.3). The low yield of the reaction coupled with the poor diastereocontrol could indicate that there is a maximum steric bulk of the ligand:alkyllithium complex in relation to the oxazoline directing group. It is also possible that the very bulky alkyl chains prevent coordination of the tridentate diglyme structure with the alkyllithium in the necessary conformation required for the inversion mechanism to occur.

We observed that by protonating the ferrocenyloxazoline products using 3M HCl it was possible to selectively extract the functionalised ferrocenyloxazolines from diethyl ether into the acidic aqueous layer. The diglyme ligands display a strong affinity for the organic phase, making it possible to recover a significant portion of the ligand after a reaction, which can then be reused after purification by distillation.

Table 7.3: Optimisation of diglyme ligand for ortholithiation of *i*Pr–oxazoline **7.2**.

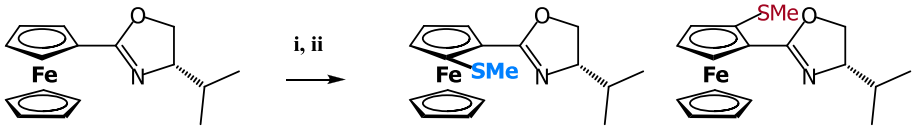

7.2 **7.3** **7.4**

Entry	Solvent	Alkyllithium[a]	Additive[b]	% Yield[c]	Ratio **7.3**:**7.4**
1	Toluene	*n*BuLi	Diglyme	98	1:1.4
2	Toluene	*n*BuLi	Di–nBu–diglyme	56	1:1.9
3	Toluene	*n*BuLi	Di–Ph–diglyme	9	1:1.1
4	Toluene	*n*BuLi	Di–iPr–diglyme	88	1:3.8
5	Toluene	*n*BuLi	Di–tBu–diglyme	85	1:5.6
6	Toluene	*n*BuLi	Di–triEt–diglyme	18	1.7:1

Reagents and conditions: i) [a]Alkyllithium (1.5 eq) [b]Additive (2 eq), –78 °C, 2 h, ii) Me_2S_2 (10 eq), –78 °C to rt, 12 h. [c]Yield determined by HPLC, *dr* determined by HPLC.

In an attempt to improve the diastereoselectivity of the inversion, an investigation into the ratio between the alkyllithium and di–*t*Bu–diglyme was undertaken. It was determined that lower concentrations of the diglyme ligand resulted in a decrease in the diastereoselectivity, as shown in Table 7.4. For optimal control it was determined that greater than 2.5 equivalents of the ligand should be used in relation to the alkyllithium.

Table 7.4: Optimisation of ligand to alkyllithium ratio for ortholithiation of *i*Pr–oxazoline **7.2**.

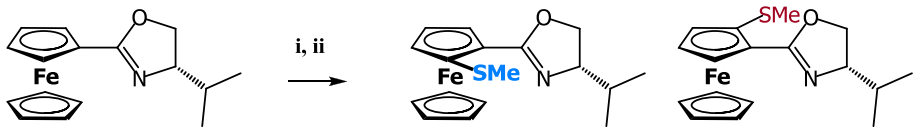

7.2 **7.3** **7.4**

Entry	Additive	Alkyllithium[a]	RLi:Additive[b]	% Yield[c]	Ratio **7.3**:**7.4**
1	Di–*t*Bu–diglyme	*n*BuLi	1:0.75	76	1:4.8
2	Di–*t*Bu–diglyme	*n*BuLi	1:1.3	85	1:5.6
3	Di–*t*Bu–diglyme	*n*BuLi	1:2	95	1:5.6
4	Di–*t*Bu–diglyme	*n*BuLi	1:2.5	70	1:6.1
5	Di–*t*Bu–diglyme	*n*BuLi	1:3	85	1:6.1

Reagents and conditions: 1) [a]Alkyllithium (2eq) [b]Additive as per table, –78 °C, 2 h, ii) Me_2S_2 (10 eq), –78 °C to rt, 12 h, [c]Yield determined by HPLC, *dr* determined by HPLC.

7.2.3 Effect of Temperature

By decreasing the reaction temperature to −86ºC it is possible to further improve the selectivity of the reaction, for both the diglyme and the di–*t*–butyl ligands (Table 7.5). Efforts to further lower the reaction temperature proved unsuccessful.

Table 7.5: Optimisation of temperature for ortholithiation of isopropyl oxazoline **7.2** with diglyme ligands.

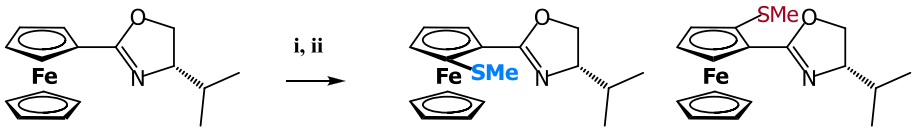

7.2 **7.3** **7.4**

Entry	Additive	Alkyllithium[a]	Temperature /°C	% Yield[c]	Ratio **7.3**:**7.4**
1	Diglyme	*n*BuLi	−78	98	1:1.4
2	Diglyme	*n*BuLi	−86	97	1:1.9
3	Di–*t*Bu–diglyme	*n*BuLi	−78	70	1:6.1
4	Di–*t*Bu–diglyme	*n*BuLi	−86	90	1:7.1

Reagents and conditions: 1) [a]Alkyllithium (2 eq) [b]Additive (5 eq), –78 °C, 2 h, ii) Me_2S_2 (10 eq), –78 °C to rt, 12 h, [c]Yield determined by HPLC, *dr* determined by HPLC.

7.2.4 Other Ligands

To probe the manner in which the inversion of selectivity is generated, a number of other ligands were examined to determine whether similar inversions were possible with other ligand structures (Figure 7.1).

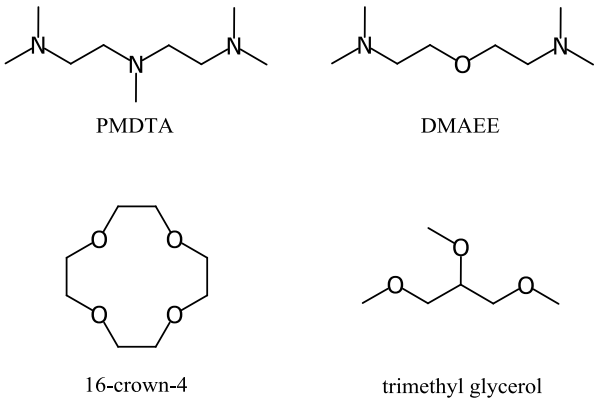

Figure 7.1: Ligands used in ortholithiation reactions.

As had already observed on the calixarene system, the inversion appeared to be related to multi–dentate ligands, hence this criterion dictated the choice of ligands that we tested. The tri–dentate nitrogen donor *N,N,N,N,N*–pentamethyldiethylenetriamine (PMDTA) resulted in a strong preference for the formation of **7.3** (25:1), similar to the bi–dentate TMEDA ligand (Entry 1 – Table 7.6). We entertained the idea that the central nitrogen atom in the PMDTA structure could be preventing the inversion mechanism occurring, hence we wondered if replacement with an oxygen atom would significantly influence this. The commercially available 2– –(dimethylamino)ethyl ether (DMAEE) resulted in considerable erosion of the high selectivity observed for PMDTA (25:1 to 2.4:1), however, a preference for the formation of **7.3** (Entry 2 – Table 7.6) was still observed. In light of this result, it would appear that the central atom in the structure does play an important role in chelating the organolithium, nevertheless the nature of and the steric bulk surrounding the terminal heteroatoms are the decisive factors in determining the diastereoselectivity.

We also investigated a structural isomer of diglyme, trimethoxy glycerol. The synthesis of trimethoxy glycerol was accomplished in a two step reaction from epichlorohydrin following a literature procedure.[12] Employing trimethoxy glycerol in the ortholithiation reaction also returned a preference for **7.3** (5.4:1) albeit in low yield (Entry 3 – Table 7.6), although it is uncertain if this structure is able to function in a tri–dentate capacity. The tetra–dentate 16–crown–4 returned a strong preference for the formation of **7.3** (22:1), also in a relatively low yielding reaction (Entry 4 – Table 7.6). 16—Crown–4 almost certainly strongly complexes the lithium cation,[13] however as previously seen from the use of di–triEt–diglyme (Entry 6 – Table 7.3), the reaction seems to exhibit a maximum steric tolerance of the alkyllithium ligand complex. We were very interested in accessing 12–crown–3, but attempts at synthesising it failed to produce sufficient quantities for it to be tested as a ligand in the reaction.

Table 7.6: Evaluation of other ligands for the ortholithiation of *i*Pr–oxazoline **7.2**.

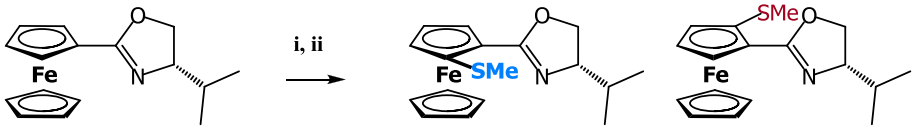

7.2 **7.3** **7.4**

Entry	Alkyllithium[a]	Additive	% Yield[c]	Ratio **7.3**:**7.4**
1	*n*BuLi	PMDTA	96	25:1
2	*n*BuLi	DMAEE	95	2.4:1
3	*n*BuLi	Trimethoxy glycerol	34	5.4:1
4	*n*BuLi	16–crown–4	30	22:1

Reagents and conditions: i) [a]Alkyllithium (2 eq) [b]Additive (5 eq), –78 °C, 2 h, ii) Me_2S_2 (10 eq), –78 °C to rt, 12 h, [c]Yield determined by HPLC, *dr* determined by HPLC.

From these collective results it again appears that the reversal in diastereoselectivity is associated with a tri–dentate oxygen based ligand of a particular structural motif. Interestingly the reversal is seemingly confined to oxygen based ligands as PMDTA and the mixed tridentate nitrogen oxygen ligand failed to produce any significant reversal.

Having proved that the diglyme–mediated reversal in diastereoselectivity with oxazoline–directed lithiation is not simply a facet of the calixarene system but also occurs on ferrocenyloxazolines, we turned our efforts towards trying to understand the mechanism of the reaction.

7.3 Mechanistic Study

7.3.1 Experiment Design

The first step towards elucidating the mechanism through which the reversal occurs would be to determine which heteroatom in the oxazoline coordinates the alkyllithium during lithiation. Sammakia and co–workers have presented compelling evidence that preferential coordination of the nitrogen in the oxazoline to the alkyllithium complex occurs during ortholithiation on the ferrocenyloxazoline system.[14] The key to this important result lay in the ortholithiation of a conformationally restrained ferrocenyloxazoline **1.40**, which when ortholithiated returned a single diastereomer (Scheme 7.5), proving coordination to the nitrogen had occurred during ortholithiation.

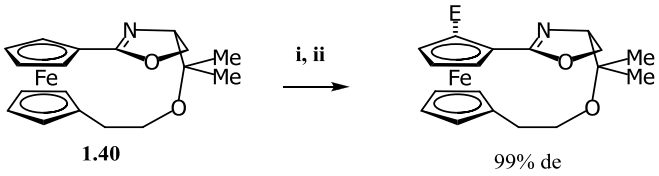

Scheme 7.5: Ortholithiation of conformationally constrained ferrocenyloxazoline. Reagents and conditions: i) *s*BuLi, THF, –78 °C, 2 h, ii) E^+.

Owing to the diglyme–induced inversion in selectivity, we questioned the possibility that a switch between nitrogen and an oxygen coordinative mechanism could be inducing the inversion in diastereoselectivity. One means of answering this question would be to repeat Sammakia's approach and ortholithiate **1.40** with an alkyllithium in the presence of diglyme. The synthesis of the constrained ferrocenyloxazoline **1.40** involves a low yielding multistep approach, which makes obtaining practical quantities of the compound tedious and time consuming. In addition, the effect of the heteroatom containing linker between the oxazoline and the lower Cp ring cannot be presumed to remain entirely innocent in the sequence of events leading to an ortholithiation. It could potentially influence the reaction through the steric bulk imposed by the linking chain, or through the presence of a coordinative oxygen heteroatom in the linker. Ortholithiation of **1.40** also presents an 'unnatural' situation in which lithiation is directed only from a *planar* conformation of the oxazoline to the Cp ring. This is certainly not the case in 'normal' ferrocenyloxazolines, in which the oxazoline is freely able to rotate between conformations, giving ample opportunity for complexation of a heteroatom in the oxazoline with the alkyllithium complex to occur in an *out of plane* conformation of the oxazoline relative to the Cp ring. For this reason we decided to adopt a different tactic in addressing this question.

If the use of diglyme ligands was initiating a switch between oxygen and nitrogen coordination (**A** in Scheme 7.6), it should be possible to influence the equilibrium of this reaction, and therefore the diastereoselectivity, by varying the substitution pattern on the oxazoline ring. A shift towards enhanced *O* coordination should occur if the size of the substituent in the proximity of the nitrogen atom is increased, conversely, it should decrease if reduced in size (**B** in Scheme 7.6). Similarly by moving the chiral substituent closer to the oxygen atom, the diastereocontrol should be increased in an oxygen coordinative mechanism (**C** in Scheme 7.6). We reasoned that by taking a multidimensional approach it should be possible to gain an understanding of how the substitution pattern of the oxazoline influences the inversion in diastereoselectivity and therefore determine which heteroatom was facilitating coordination of the alkyllithium:ligand complex both with TMEDA and diglyme.

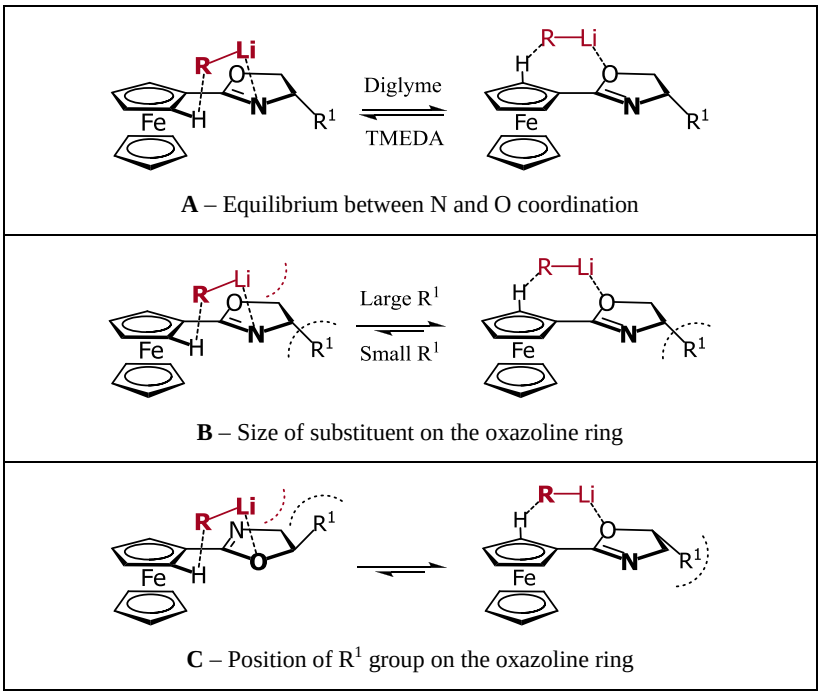

Scheme 7.6: *N* vs *O* coordination of the alkyllithium to the oxazoline. RLi represents a simplified alkyllithium:ligand complex of unknown nature.[14,15]

7.3.2 Size of the Substituent on the Oxazoline

Initially we decided to explore the effect of increasing the size of the substituent on the oxazoline would have on the diglyme–mediated reversal in selectivity. An obviously larger substituent would be the *t*–butyl group, hence we targeted the synthesis and ortholithiation of the *t*Bu–ferrocenyloxazoline **7.7**.[3,4] The synthesis of *t*Bu–ferrocenyloxazoline **7.7** was accomplished in excellent yield from acid **7.1**, in a procedure analogous to that used to synthesise oxazoline **7.2** (Scheme 7.7).

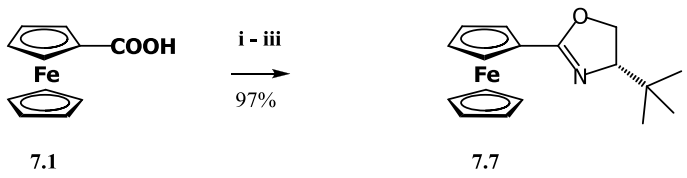

Scheme 7.7: Synthesis of *t*Bu–ferrocenyloxazoline **7.7**. Reagents and conditions: i) Oxalyl chloride (3 eq), DCM, rt, 3 h, ii) L–*tert*–leucinol (1.2 eq), Et_3N, DCM, 0 °C to rt 12 h, iii) Mesyl chloride (3 eq), Et_3N (3 eq), DCM, rt, 4 h.

We subjected oxazoline **7.7** to ortholithiation using a range of conditions and ligands, and found that the high selectivity generated with TMEDA is significantly eroded (81:1 compared to 5.1:1), but not reversed when using diglyme ligands (Table 7.7). While this arguably represents a significant shift in diastereocontrol, it is clear that increasing the steric bulk of the substituent on the oxazoline leads to large reduction in the diglyme–generated inversion compared to the results

obtained for the ortholithiation of isopropyl ferrocenyloxazoline **7.2** (1:1.4). This occurs even when using the di–*t*Bu–diglyme ligand which had proved so successful in inverting the diastereoselectivity on isopropyl ferrocenyloxazoline **7.2** (1:7.1 compared to 1.3:1).

Table 7.7: Ortholithiation of *t*Bu–ferrocenyloxazoline.

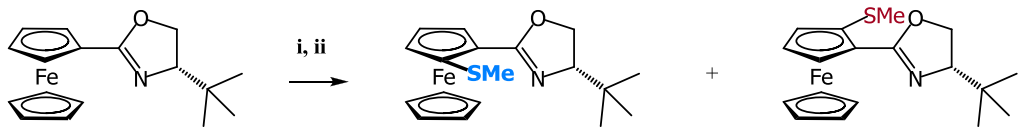

7.7 **7.8** **7.9**

Entry	Solvent	Alkyllithium[a]	Additive[b]	% Yield	Ratio **7.8**:**7.9**
1[c]	THF	*n*BuLi	–	87	6.9:1
2[c]	Toluene	*n*BuLi	TMEDA	95	81:1
3[d]	Toluene	*n*BuLi	Diglyme	90	5.1:1
4[d]	Toluene	*s*BuLi	Diglyme	30	20:1
5[d]	Toluene	*t*BuLi	Diglyme	92	12:1
6[c]	Toluene	*n*BuLi	Di–*t*Bu–diglyme	26	1.3:1
7[c]	Toluene	*s*BuLi	Di–*t*Bu–diglyme	23	8.0:1

Reagents and conditions: i) [a]Alkyllithium (2 eq), [b]Additive (5 eq), –78 °C, 2 h, ii) Me_2S_2 (10 eq), –78 °C to rt, 12 h, [c]Yield and *dr* determined by HPLC, [d]Yield determined by ^{1}H NMR, *dr* determined by ^{1}H NMR.

Observing that increasing the size of the substituent did not favour the inversion, we wondered what effect of reducing the size of the alkyl group on the oxazoline would have. With this in mind, we targeted the synthesis and ortholithiation of the methyl ferrocenyloxazoline **7.10**,[1] which using the standard methodology was accomplished in good yield (Scheme 7.8).

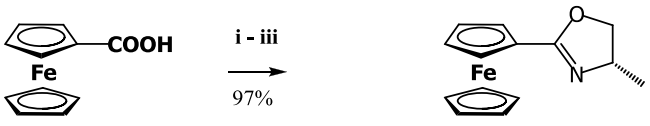

7.1 **7.10**

Scheme 7.8: Synthesis of Me–ferrocenyloxazoline **7.10**. Reagents and conditions: i) Oxalyl chloride (3 eq), DCM, rt, 3 h, ii) (*S*)–(+)–2–amino–1–propanol (1.1 eq), Et_3N, DCM, 0 °C to rt, 12 h, iii) Mesyl chloride (3 eq), Et_3N (3 eq), DCM, rt, 2 h.

The use of THF and *n*BuLi induced a minor preference for diastereomer **7.12**, which strongly reverted to **7.11** when TMEDA was used as a ligand both with *n*BuLi and more so with *s*BuLi. Di–*t*Bu–diglyme resulted in a strong preference for the formation of **7.12** (Entry 4 – Table 7.8) most significantly with *n*BuLi, following a similar trend to that observed with the other

ferrocenyloxazolines. Clearly less bulky substituents alpha to nitrogen on the oxazoline ring favour the reversal in diastereoselectivity.

Table 7.8: Ortholithiation of Me–ferrocenyloxazoline.

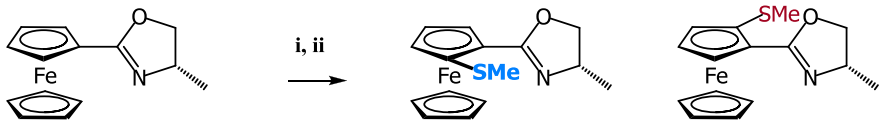

7.10 **7.11** **7.12**

Entry	Solvent	Alkyllithium[a]	Additive	% Yield[c]	Ratio **7.11**:**7.12**
1	THF	*n*BuLi		98	1:1.6
2	Toluene	*n*BuLi	TMEDA	93	38:1
3	Toluene	*s*BuLi	TMEDA	89	51:1
4	Toluene	*n*BuLi	Di–*t*Bu–diglyme	94	1:6.1
5	Toluene	*s*BuLi	Di–*t*Bu–diglyme	88	1:2.4

Reagents and conditions: i) [a]Alkyllithium (2 eq), [b]Additive (5 eq), –78 °C, 2 h, ii) MeSSMe (10 eq), –78 °C to rt, 12 h, [c]Yield determined by HPLC, *dr* determined by HPLC.

Turning to the position of the controlling stereocentre on the oxazoline ring, the effect of moving the stereocentre away from the proximity of the nitrogen to the oxygen centre was investigated.

7.3.3 Position of Substituent on the Oxazoline

It was anticipated that removing the chiral centre's stereochemical information away from the nitrogen should limit the diastereoselectivity for a nitrogen–coordinative mechanism, while potentially increasing the diastereoselectivity for an oxygen coordinated reaction. Due to the commercial availability of (*S*)–(+)–1–amino–2–propanol, and having observed that the use of the Me–ferrocenyloxazoline allowed the inversion to occur, we decided to synthesise and ortholithiate the β–Me–ferrocenyloxazoline.

Using the standard conditions, β–Me–ferrocenyloxazoline **7.13** was formed in high yield from acid **7.1** and (*S*)–(+)–1–amino–2–propanol (Scheme 7.9). Oxazoline **7.13** appeared to be sensitive to degradation, hence it was purified prior to use.

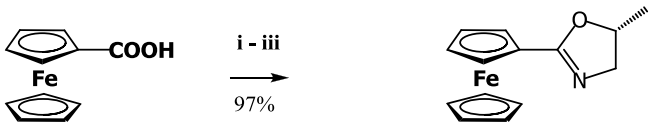

7.1 **7.13**

Scheme 7.9: Synthesis of β–Me–ferrocenyloxazoline **7.13**. Reagents and conditions: i) Oxalyl chloride (3 eq), DCM, rt, 4 h, ii) (*S*)–(+)–1–amino–2–propanol (1.1 eq), Et_3N, DCM, 0 °C to rt, 12 h, iii) Mesyl chloride (3 eq), Et_3N (3 eq), DCM, rt, 4 h.

We noted that during the synthesis of the oxazoline, ring closure of the short lived mesyl intermediate would occur with inversion of stereochemistry due to the S_N2 reaction occurring at this position. While this reaction should be stereospecific, the possibility of epimerisation at the centre could not be entirely dismissed. Other authors have used similar strategies for the synthesis of oxazolines with substituents at the oxygen stereocentre, without any observable loss of stereochemical information, which led us to believe that epimerisation should not be a problem.[16-18]

Ortholithiation of β–Me–ferrocenyloxazoline was performed using three conditions, THF, TMEDA and di–*t*Bu–diglyme with *n*BuLi as a means of probing its general reactivity (Table 7.9). We found that almost no diastereocontrol was afforded by any of the three conditions. Owing to the poor diastereoselectivity, the assignment of the configuration of the 'major' diastereomer produced in the TMEDA ligated reaction was not possible.

Table 7.9: Ortholithiation of β–Me–ferrocenyloxazoline.

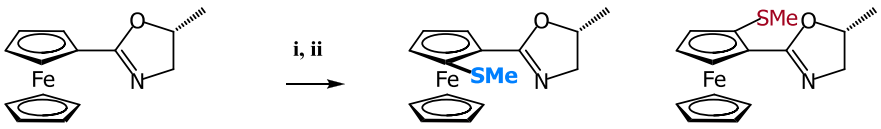

7.13 **7.14**

Entry	Solvent	Alkyllithium[a]	Additive	% Yield[c]	Ratio
1	THF	*n*BuLi		78	1:1.1
2	Toluene	*n*BuLi	TMEDA	83	1:1.2
3	Toluene	*n*BuLi	Di–*t*Bu–diglyme	51	1:1

Reagents and conditions: i) [a]Alkyllithium (2 eq), [b]Additive (5 eq), –78 °C, 2 h, ii) Me_2S_2 (10 eq), –78 °C to rt, 12 h,[c]Yield determined by HPLC, *dr* determined by HPLC.

In rationalising these results, it is clear that the diastereoselectivity is dependent on the chiral environment surrounding the nitrogen atom. While this result does suggest that a nitrogen coordinative mechanism operates both for TMEDA and diglyme, it cannot be used as conclusive

proof that an oxygen coordinative mechanism does not occur. By moving the substituent on the oxazoline away from the proximity of the nitrogen atom, the equilibrium between these two mechanisms could simply have shifted away from the oxygen coordinative reaction, due to a lowering of the steric hindrance surrounding the nitrogen atom and the increase in steric hindrance surrounding the oxygen atom. To further probe this question, we wanted to ascertain what the nature of the directing effect in the presence of two chiral centres on the oxazoline ring.

We targeted the synthesis of a *trans*–diphenyl substituted oxazoline to ascertain the effect of having two chiral centres directing lithiation with the diglyme mediated reaction. The synthesis of the *trans*–diphenyl oxazoline **7.15** was accomplished using the standard methodology from ferrocenylacid **7.1** and (*S*,*R*)–1,2–diphenyl–2–aminoethanol.

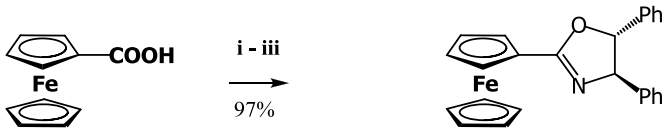

7.1 **7.15**

Scheme 7.10: Synthesis of *trans*–diphenyl ferrocenyloxazoline **7.15**. Reagents and conditions: i) Oxalyl chloride (3 eq), DCM, rt, 3 h, ii) (*S*,*R*)–1,2–diphenyl–2–aminoethanol (1.1 eq), Et_3N, DCM, 0 °C to rt, 18 h, iii) Mesyl chloride (3 eq), Et_3N (3 eq), DCM, rt, 2 h.

The ortholithiation of *trans*–diphenyl ferrocenyloxazoline **7.15**, using the three general conditions, THF, TMEDA and di–*t*Bu–diglyme with *n*BuLi was performed as shown in Table 7.10. Conventionally, the transition state of oxazoline–directed ortholithiation of metal arenes has been described as occurring with the substituent on the oxazoline facing downwards towards the metal centre, allowing the alkyllithium complex to approach unhindered from above.[1-3,19] The *trans* nature of the substituents on diphenyl ferrocenyloxazoline **7.15** imply that if a similar transition state is adopted for both the nitrogen– and oxygen–coordinated mechanisms, lithiation should preferentially occur on the same side of the ring for both diglyme and TMEDA. The use of THF produced a moderate diastereoselectivity for the formation of **7.16**, which was dramatically improved by the addition of TMEDA and inverted with di–*t*Bu–diglyme.

Table 7.10: Ortholithiation of *trans*–diphenyl–ferrocenyloxazoline.

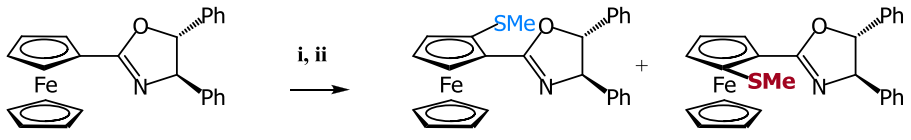

7.15 **7.16** **7.17**

Entry	Solvent	Alkyllithium[a]	Additive	% Yield[c]	Ratio **7.16**:**7.17**
1	THF	*n*BuLi		98	4.4:1
2	Toluene	*n*BuLi	TMEDA	97	75:1
3	Toluene	*n*BuLi	Di–*t*Bu–diglyme	96	1:3.8

Reagents and conditions: i) [a]Alkyllithium (2 eq) [b]Additive (5 eq), –78 °C, 2 h, ii) Me_2S_2 (10 eq), –78 °C to rt, 12 h, [c]Yield determined by HPLC, *dr* determined by HPLC.

In rationalising these results, it is interesting to observe that even with the *trans* nature of the substituents on the oxazoline, the diglyme–induced inversion still occurs, seemingly pointing towards only a nitrogen–coordinated mechanism. We reasoned that if the sense of central chirality alpha to the oxygen on the oxazoline ring was inverted, we could observe if the oxygen played a role in the ortholithiation reaction. If the reaction proceeded with the same diglyme–induced inversion, it would become apparent that irrespective of the ligand choice the reaction proceeded through a nitrogen coordinative mechanism only.

Inversion the chirality at the oxygen centre on a *trans*–diphenyl oxazoline yields a *cis*–diphenyl compound. A number of commercial sources of chiral aminols exist that can be exploited in this regard, eliminating the need for the diastereoselective synthesis of the starting material.[20] The synthesis of *cis*–diphenyl–ferrocenyloxazoline **7.18** was accomplished in moderate yield from acid **7.1** and the commercially available (*S*,*S*)–1,2–diphenyl–2–aminoethanol (Scheme 7.11). It should be noted that the configuration of chiral centres in (*R*,*R*)–*trans*–diphenyl oxazoline **7.15** and (*S*,*R*)–*cis*–diphenyl oxazoline **7.18** actually presents an inversion at the nitrogen stereocenter, nonetheless, the intended effect of this experiment remains valid. *Cis*–diphenyl ferrocenyloxazoline **7.18** appeared to be prone to decomposition, unlike the majority of the ferrocenyloxazolines used in this study, which could, in part, explain its moderate yield.

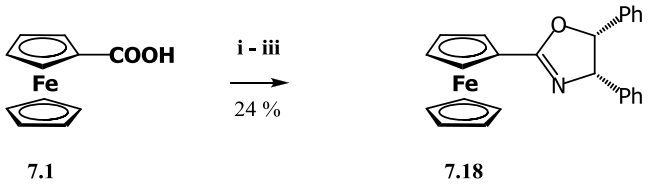

7.1 **7.18**

Scheme 7.11: Synthesis of cis–diPh–ferrocenyloxazoline **7.18**. Reagents and conditions: i) Oxalyl chloride (4 eq), DCM, rt, 4 h, ii) (*S,S*)–1,2–diphenyl–2–aminoethanol (1.1 eq), Et_3N, DCM, 0 °C to rt, iii) Mesyl chloride (3 eq), Et_3N (3 eq), DCM, rt, 4h.

Ortholithiation of **7.18** with the three standard conditions presented similar results to the *trans*–diPh–ferrocenyloxazoline **7.15**, again with di–*t*Bu–diglyme inducing an inversion in diastereoselectivity. (Table 7.11).

Table 7.11: Ortholithiation of *cis*–diphenyl–ferrocenyloxazoline.

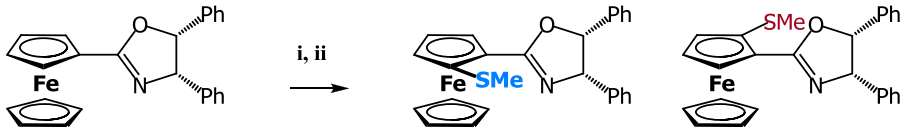

7.18 **7.19** **7.20**

Entry	Solvent	Alkyllithium[a]	Additive	% Yield[c]	Ratio **7.19**:**7.20**
1	THF	*n*BuLi		56	5.7:1
2	Toluene	*n*BuLi	TMEDA	94	41:1
3	Toluene	*n*BuLi	Di–*t*Bu–diglyme	91	1:3.5

Reagents and conditions: i) [a]Alkyllithium (2 eq) [b]Additive (5 eq), –78 °C, 2 h, ii) MeSSMe (10 eq), –78 °C to rt, 12 h, [c]Yield determined by HPLC, *dr* determined by HPLC.

Due to the diglyme–induced inversion still operating with the *cis*–diphenyl oxazoline **7.18**, it is possible to conclude that the coordinating heteroatom in the ortholithiation reaction must be nitrogen, with negligible influence from the oxygen heteroatom during ortholithiation. A mechanistic proposal for the diglyme inversion is presented in the following chapter.

7.3.4 Assignment of Configuration of Diastereomers

In this text so far, little mention has been made of the manner in which the configuration of the diastereomers produced from the ortholithiation reaction was determined. As a number of these compounds have already been reported and characterised in the chemical literature, our task at assigning the configuration became considerably easier. However, certain compounds have not been reported and a means of determining the configuration of the ortholithiated products was required.

One means of determining the configurations of the products would be to crystallise them, and use X–ray crystallography to elucidate their structures. However crystallisations can be laborious and certainly reliant on 'cooperation' by the compounds themselves in forming suitable crystals. In an attempt to circumvent these problems we wondered if it would be possible to use circular dichroism (CD) to elucidate the configuration of the compounds.[21] For this approach to be successful, the CD spectra associated with the configuration of planar chirality would need to dominate over the CD spectra associated with the central chirality of the oxazoline.

Upon inspection of the chemical literature we found that 1,2–disubstituted planar chiral ferrocenes can possess characteristic absorption bands representative of the configuration of planar chirality.[22] The strength of these bands has been found to be dependent on the strength of the polarisation of the substituent on the ferrocene, with the more strongly polarised systems giving rise to stronger so–called Cotton effects allowing the configuration of the planar chirality of the ferrocene to be determined.[22] In order to test the suitability of this method for determination of the sense of planar chirality, we initially collected the CD spectra (Graph 7.1) of a number of unsubstituted ferrocenyloxazolines (Figure 7.2). The spectra revealed limited absorption bands above 300 nm, while strong rotation is observed below 300 nm. Seemingly, the handedness of chiral centre adjacent to the nitrogen dominates the CD spectra of these unsubstituted compounds, as the *R* configuration of **7.15** presents an inverted absorbance below 300 nm compared to all the other *S* configured oxazolines tested.

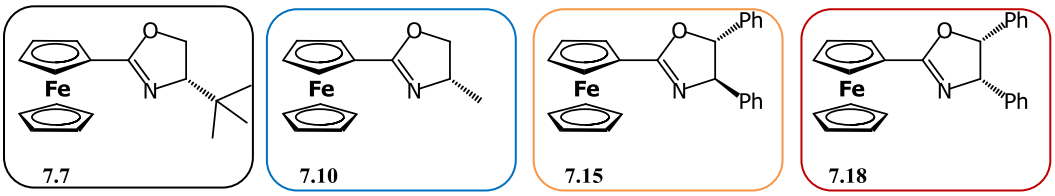

Figure 7.2: Ferrocenyl oxazolines used in CD spectra.

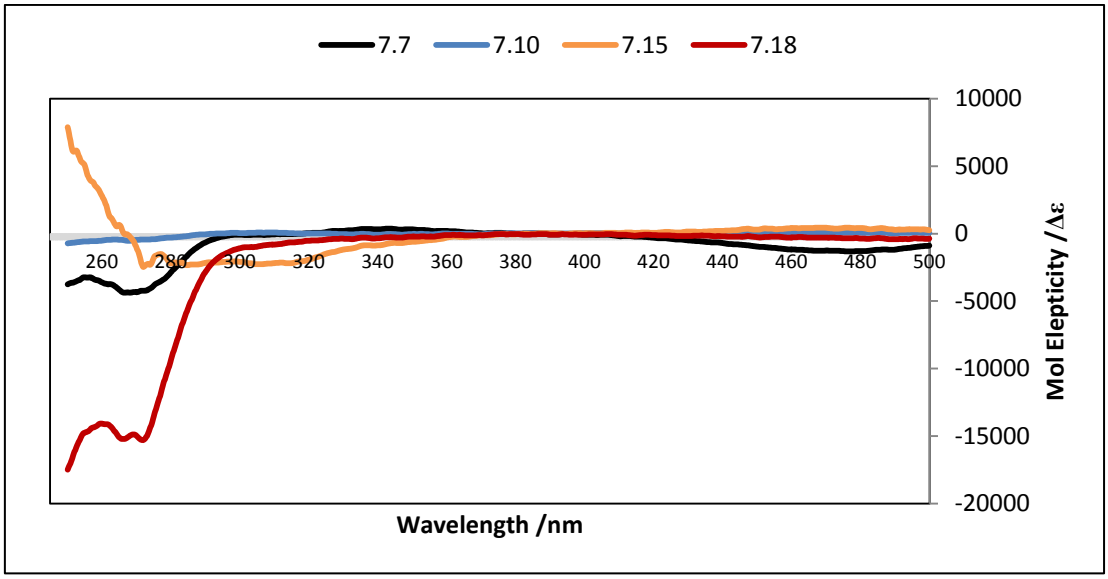

Graph 7.1: CD spectra of unsubstituted ferrocenyloxazolines

From the chemical literature it is possible to establish what the major diastereomer should be for the ortholithiation of the following oxazolines: isopropyl ferrocenyloxazoline **7.2**,[1,3] *t*–butyl ferrocenyloxazoline **7.7**,[3] methyl ferrocenyloxazoline **7.10**,[1] and the *trans*–diphenyl ferrocenyloxazoline **7.15**.[23] As the use of the diglyme ligands allowed in some cases the synthesis of both configurations of planar chirality we present the CD spectra for a series of planar chiral ferrocenyloxazoline thioethers where the sense of planar chirality is known (Figure 7.3).

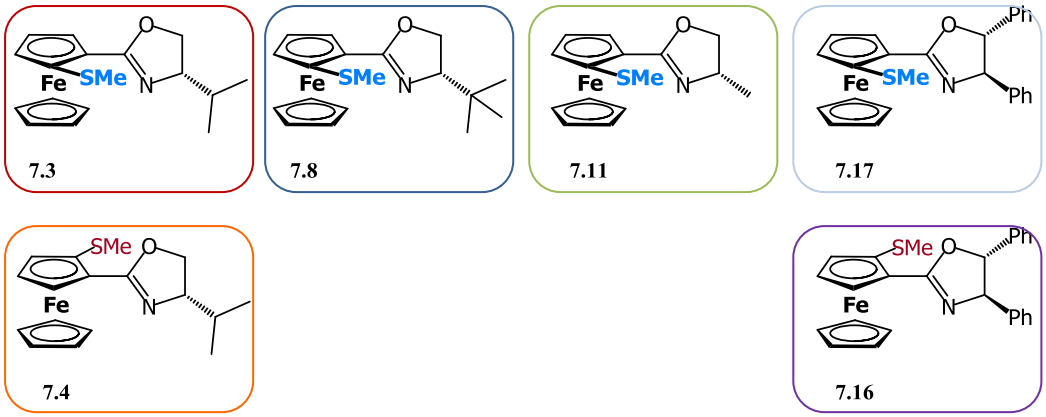

Figure 7.3: Selected planar chiral thioether ferrocenyloxazolines

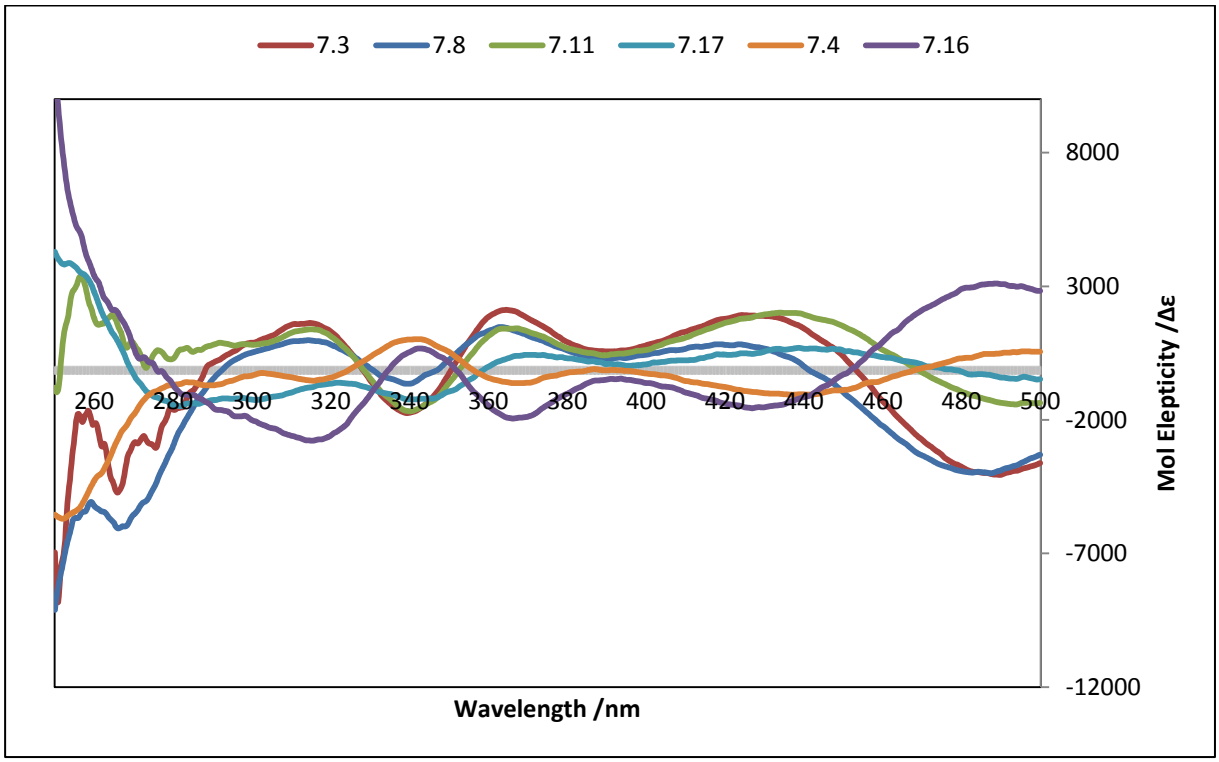

Graph 7.2: Standard CD spectra of known planar chirality.

From the CD spectra of these thioether–substituted ferrocenyloxazolines it is possible to ascertain which sense of planar chirality is present in the molecule (Graph 7.2). There are certainly minor discrepancies between the position and intensities of the bands, but a similar pattern arises which is clearly dependent on the configuration of planar chirality. It is also clear that the configuration of planar chirality imparted during ortholithiation is dependent on the handedness of central chirality adjacent to the nitrogen atom, with an (*S*) chiral centre giving rise to ($_p$*R*) planar chirality using TMEDA and ($_p$*S*) using the diglyme ligands.[24]

As the configuration of planar chirality in the *cis*–diphenyl ferrocenyl oxazoline was unconfirmed in the chemical literature we reasoned that by comparing the CD spectra of the two diastereomers **7.19** and **7.20** to the standard curves it should be possible to ascertain the handedness of the planar chirality (Graph 7.3).

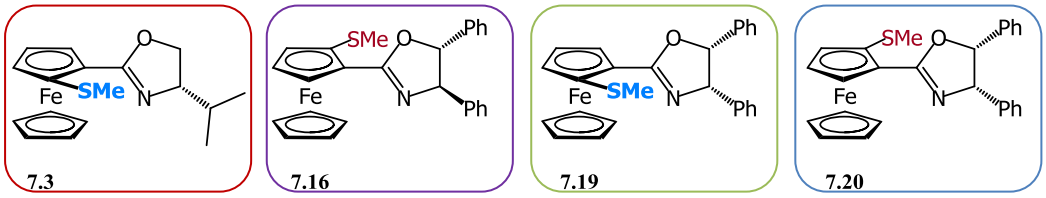

Figure 7.4: Substituted ferrocenyloxazoline for characterisation of planar chirality.

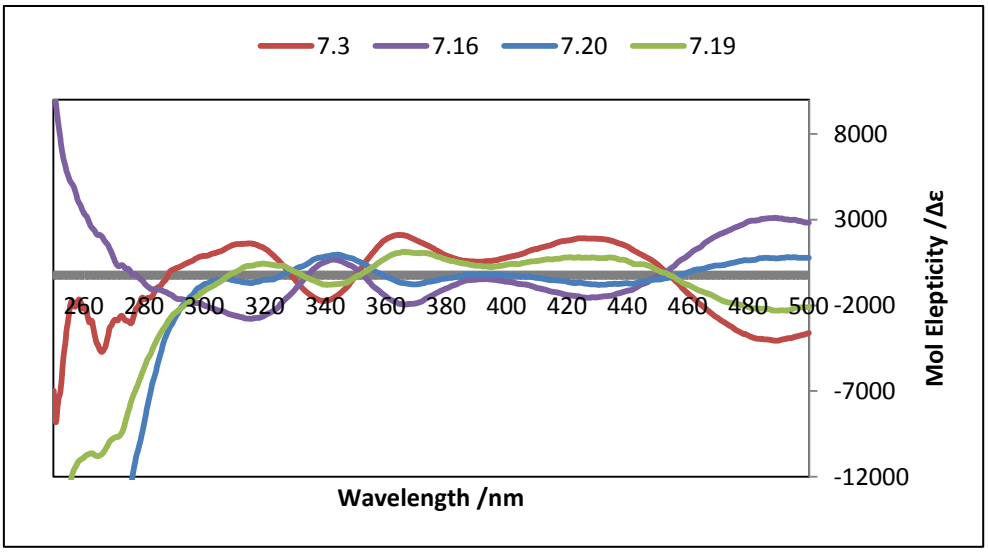

Graph 7.3: Determination of planar chirality via CD.

By comparing spectra of compounds of known planar chirality to the two unknown diastereomers it was possible to ascertain the sense of planar chirality of both diastereomers (Graph 7.3). Unsurprisingly it was found that the induction of asymmetry in the ortholithiation reaction is dictated by the central chirality adjacent to the nitrogen atom in the oxazoline ring.

7.4 Conclusion and Future Work

In this chapter we have demonstrated that the diglyme–induced inversion occurs not only in the calixarene system but also occurs in the ortholithiation of ferrocenyloxazolines with a maximum ratio of 1:7.1. By investigating the ortholithiation of differently substituted ferrocenyloxazolines we can conclude that the inversion in diastereoselectivity is generated through coordination to the nitrogen heteroatom in the oxazoline ring, and no evidence for a switch between coordination to the nitrogen and oxygen heteroatoms was found. In the following chapter a mechanistic

discussion relating to the results obtained both for the calixarene and ferrocene systems is addressed.

7.5 References

(1) Nishibayashi, Y.; Uemura, S. *Synlett* **1995**, 79.

(2) Richards, C. J.; Damalidis, T.; Hibbs, D. E.; Hursthouse, M. B. *Synlett* **1995**, 74.

(3) Sammakia, T.; Latham, H. A.; Schaad, D. R. *J. Org. Chem.* **1995**, *60*, 10.

(4) Sammakia, T.; Latham, H. A. *J. Org. Chem.* **1995**, *60*, 6002.

(5) Dai, L.-X.; Tu, T.; You, S.-L.; Deng, W.-P.; Hou, X.-L. *Acc. Chem. Res.* **2003**, *36*, 659.

(6) Gómez Arrayás, R.; Adrio, J.; Carretero, J. C. *Angew. Chem. Int. Ed.* **2006**, *45*, 7674.

(7) Stepnicka, P.; Editor *Ferrocenes: Ligands, Materials and Biomolecules*; John Wiley & Sons Ltd., 2008.

(8) Sutcliffe, O. B.; Bryce, M. R. *Tetrahedron: Asymmetry* **2003**, *14*, 2297.

(9) Batsanov, A. S.; Herault, D.; Howard, J. A. K.; Patrick, L. G. F.; Probert, M. R.; Whiting, A. *Organometallics.* **2007**, *26*, 2414.

(10) Federman, N. A.; Miller, J.; Faria, d. A. V.; Fujimoto, S. Y.; Afonso, M. M. D. F.; Archanjo, F. C.; Darin, V. A.; Andrade, e. S. M. L.; Borges, A. D. L.; Del, P. G. *Z. Anorg. Allg. Chem.* **2002**, *628*, 209.

(11) Witte, P.; Lal, T. K.; Waymouth, R. M. *Organometallics.* **1999**, *18*, 4147.

(12) Garcia, J. I.; Garcia-Marin, H.; Mayoral, J. A.; Perez, P. *Green. Chem.* **2010**, *12*, 426.

(13) Kitazawa, S.; Kimura, K.; Yano, H.; Shono, T. *J. Am. Chem. Soc.* **1984**, *106*, 6978.

(14) Sammakia, T.; Latham, H. A. *J. Org. Chem.* **1996**, *61*, 1629.

(15) Chadwick, S. T.; Ramirez, A.; Gupta, L.; Collum, D. B. *J. Am. Chem. Soc.* **2007**, *129*, 2259.

(16) Liu, H.; Xu, J.; Du, D.-M. *Org. Lett.* **2007**, *9*, 4725.

(17) Clayden, J.; Parris, S.; Cabedo, N.; Payne, A. H. *Angew. Chem. Int. Ed.* **2008**, *47*, 5060.

(18) Clayden, J.; Clayton, J.; Harvey, R. A.; Karlubikova, O. *Synlett* **2009**, 2836.

(19) Kundig, E. P.; Ripa, A.; Bernardinelli, G. *Angew. Chem. Int. Ed.* **1992**, *31*, 1071.

(20) Lupattelli, P.; Bonini, C.; Caruso, L.; Gambacorta, A. *J. Org. Chem.* **2003**, *68*, 3360.

(21) Ziegler, M.; von Zelewsky, A. *Coord. Chem. Rev.* **1998**, *177*, 257.

(22) Janowska, I.; Zakrzewski, J. *Tetrahedron Asymm.* **2003**, *14*, 3271.

(23) Nishibayashi, Y.; Segawa, K.; Arikawa, Y.; Ohe, K.; Hidai, M.; Uemura, S. *J. Organomet. Chem.* **1997**, *545-546*, 381.

(24) Schloegl, K. *Top. Stereochem.* **1967**, *1*, 39.

CHAPTER 8

Mechanistic Discussion and Conclusion

8.1 General Mechanism

Any mechanistic discussion surrounding oxazoline directed–lithiation must surely take note that the mechanism has thus far evaded explicit characterisation in the chemical literature, even for describing non–asymmetric transformations.[1-3] At the heart of this problem is that understanding the speciation of the alkyllithium during the transition state is very difficult to determine empirically, which, when added to the uncertainty of having two potentially coordinative heteroatoms in the oxazoline structure creates a serious challenge to the investigator.[1] Experimentally, it is evident that the oxazoline can provide beautiful control over asymmetric ortholithiations,[4] which provides un–controvertible evidence that, given the right environment, the ortholithiation occurs in a very precise fashion irrespective of the mire of questions and confounding variables we as chemists have had to ask to describe its operation. Hopefully however, with the lithiation of four separate calixarene oxazolines, in addition to a number of different ferrocenyloxazolines, we can pool these collective results and observations and distil out the key features accounting for the diastereoselective control.

In asymmetric ortholithiation reactions on ferrocenes and chromium arenes directed by chiral auxiliaries, two contrasting generalised transition states dependent on the nature of the directing group have been proposed in the chemical literature. The first approach centres on utilising the most energetically favourable conformation of the chiral directing group to induce controlled coordination of the alkyllithium, which induces asymmetric lithiation (Figure 8.1).[5] This transition state model is, however, seemingly under kinetic control, in that the directing group seeks to minimise the interaction with the metal centre.[5] This has been shown to occur on both ferrocenes with the Ugi amine **1.32**,[6,7] as well as with chiral sulphoxides,[8,9] and on chromium arenes with sulphoxides[10] and amines.[11] In accounting for the diastereoselectivity generated using chiral oxazolines, however, a second seemingly contradictory model has been proposed, in which substituent of the directing group now faces towards the metal centre during lithiation (Figure 8.1), almost certainly not adopting the most thermodynamically stable conformation.[3,12] In this second case, diastereocontrol is proposed to be created by the alkyllithium complex seeking to coordinate the directing group by approaching it from the least hindered arene face (i.e. away from the metal centre), with diastereoselectivity resulting from the alkyllithium complex seeking

to minimise interaction with the chiral substituent on the directing group. It is this second model that has reportedly characterised oxazoline–directed lithiation of ferrocenes[13-15] as well as chromium arenes.[16]

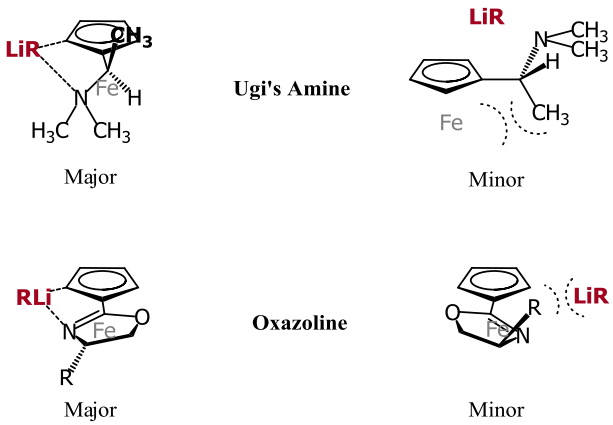

Figure 8.1: Transition states of Ugi's Amine **1.32** and ferrocenyloxazoline. Note: LiR represents an undefined alkyllithium complex. Note: A simplified ferrocene structure has been displayed.

In beginning our lithiation of isopropyl oxazoline **2.1** on the butylated calixarene system, we were unsure which general mechanism would create control. Would the interaction of the oxazoline with the *t*–butyl groups of the calixarene control the lithiation through a similar process observed with Ugi's amine, or conversely would an analogous transition state to the other ferrocenyloxazolines be observed? For the 'normal' coordinated transition state the stereochemistry of diphenyl phosphine **4.5** implied that control over the lithiation appeared to be generated by unfavourable interaction between the alkyllithium complex and the isopropyl group of the oxazoline, similar to the transition state proposed for the ferrocenyloxazolines. Therefore the key controlling feature in imparting asymmetry to this transformation is the ability of the alkyllithium complex to preferentially discriminate between coordination from inside and outside the calixarene bowl with the oxazoline (Figure 8.2), through unfavourable steric interactions. As mentioned this is analogous to the ortholithiation of ferrocenes and chromium arenes, where unfavourable steric, and possibly electronic interactions, disfavour approach of the alkyllithium from the metal–coordinated face of the arene. Our proposed transition state using this model is shown in Figure 8.2, and to a large extent relies on the evidence presented for coordination of the nitrogen in the oxazoline to the alkyllithium complex by Sammakia *et al*.[17]

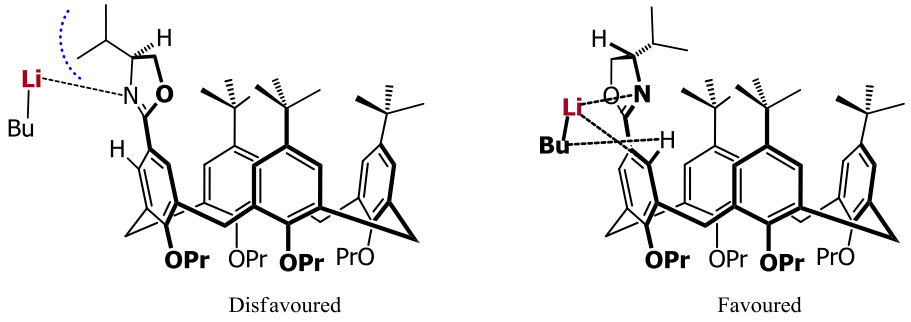

Figure 8.2: Proposed model for ortholithiation of isopropyl oxazoline **2.1**. Note: LiBu represents an alkyllithium complex of an unspecified nature.

A similar situation is observed for the ortholithiation of the debutylated isopropyl oxazoline **5.1** and *t*–butyl oxazolines calixarenes **6.1** and **6.8**, where the same negative interaction between the substituent on the oxazoline coupled with the alkyllithium preferentially seeking coordination from outside the calixarene bowl seemingly dictates selectivity. For all the ferrocenyloxazolines tested, the same conformation of transition state is inferred through the configuration of the functionalised products. By invoking a mechanistic description like this, the diastereoselectivity of the ortholithiation reactions appears to be under kinetic control in accordance with a commonly made claim regarding prochiral ortholithiations.[3,5,12,18] Certainly no sign of a thermodynamic rearrangement of the lithiated intermediate of isopropyl oxazoline **5.1** was observed, even when warming the lithiated intermediates to zero degrees. Similarly, although not systematically performed on all the calixarene oxazolines at our disposal, performing reactions at higher temperatures reduced the diastereoselectivity of the transformation, again indicating that control is achieved through kinetic processes.

While this general description of the mechanism could apply to reactions where good 'anticipated' diastereoselectivity is exhibited, perhaps the most prominent general feature of all the ortholithiation reactions is the extent with which the choice of solvent, alkyllithium and ligand influence the diastereoselectivity of the transformation. This is most evident when comparing the use of the TMEDA and diglyme ligands, which give considerable complementarity in diastereoselectivity. The degree to which these ligands can affect the selectivity of the reaction provides ample illustration that the general simplified models presented for explaining the diastereoselectivity of oxazoline–directed ortholithiation fail to properly account for the importance of the nature of the alkyllithium complex in the determining the selectivity of the transformation.[1]

Due to the interrelated nature of the parameters in the reaction, it is somewhat difficult to isolate their individual contributions. However, the following sections detail our efforts towards

elucidating the effect of the ligand and solvent system, alkyllithium, the contribution of the substituent on the oxazoline and the influence of the *t*–butyl groups on the calixarene structure in determining the course of the reaction. Our discussion begins with the contribution of the TMEDA ligand.

8.2 TMEDA and the Effect of Solvent

In the ortholithiation of isopropyl oxazoline **2.1**, we found very early in our study that the presence of TMEDA was a requirement for obtaining both good yields as well as control over the diastereoselectivity. From reviewing the ortholithiation of ferrocenyloxazolines, it is apparent that this feature is not unique to the calixarene system and significant improvements in diastereoselectivity with the presence of the TMEDA ligand must point towards a general feature of oxazoline–directed lithiation.[14,19] In the computational analysis of TMEDA mediated ortholithiations, Saá presented evidence that the rate enhancements that can be associated with the use of TMEDA as a ligand can to a large degree be attributed to the ability of the ligand to control the speciation of the alkyllithium in solution, with this then controlling the observed rate of the reaction.[2] It would not be unreasonable to suggest that the enhanced diastereocontrol obtained with the TMEDA–ligated mechanism could also be due to greater control over the speciation of the alkyllithium in solution. Collum and co–workers have suggested understanding the aggregation and solvation states of alkyllithiums in ortholithiation as being the key issue that needs to be addressed in order to understand ortholithiation reactions.[1,2]

In solution the TMEDA:*n*BuLi complex is known to exist as a dimer in hydrocarbons,[20,21] whereas in THF it exists as a temperature–dependent mixture of tetramers and dimers (simplified examples of different aggregate forms of alkyllithium are shown in Figure 8.3).[22,23] The determination of the speciation of *s*BuLi is made more complex by the chiral nature of the reagent, however taking *i*PrLi as a proxy, this reagent exists as a dimer in ether,[24] a symmetrical dimer when ligated by TMEDA,[25,26] and as a monomer when coordinated to the more bulky bidentate ligand tetraethylethylenediamine (TEEDA).[25] Determination of the speciation of alkyllithiums in solution is not simple, hence comprehensive data detailing the effects of solvent and ligands does not exist for many of even the relatively commonly used reagents, making discussions surrounding aggregation state in the mechanism all the more difficult.

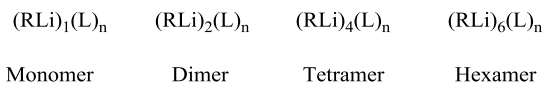

Figure 8.3: Different aggregates of alkyllithium complexes. Note: L_n is defined as a non–specified ligand/s.

In the investigation into where the diastereocontrol of the TMEDA–ligated ortholithiation stems from, it was evident that the bidentate nature of the ligand was important (Table 8.1). This was gleaned from comparing the diastereoselectivity of a TMEDA:*s*BuLi reaction with *N*,*N*–dimethylbutylamine (DMBA) and triethyl amine–ligated *s*BuLi reactions, which returned significantly reduced diastereocontrol.

Table 8.1: Investigation into the operation of the TMEDA ligand in the ortholithiation.

Entry	Solvent[a]	Additive	% Yield	Ratio **5.7**:**5.8**
1	Pentane	TMEDA	>95	19:1
2	Pentane	Et_3N	20	2:1
3	Pentane	DMBA	60	2:1
4	Pentane	TEEDA	80	2:1

It is, however, not simply the bidentate nature of the ligand that is important, but perhaps, surprisingly, also the relatively unhindered nature of the tetramethyl functionalisation that also generates that control. Increasing the steric bulk at the terminal positions of the bidentate tetraethylethylenediamine[20] (TEEDA) greatly reduces the diastereoselectivity, but again it is not possible to ascertain if the speciation of the TMEDA– and TEEDA–complexed alkyllithiums are comparable. There are reports of monomeric *i*PrLi:TEEDA structures in solution,[25] which contrast with the likely dimeric nature of the *s*BuLi:TMEDA complex. In the light of these experiments, and the large decreases in diastereocontrol evidenced with deviation from the TMEDA structure, it should perhaps be regarded as fortunate that such an effective ligand was found without the need for further structural refinement. The widespread use of TMEDA in alkyllithium based reactions is perhaps an indication of its effectiveness as a ligand, however the vast majority of these transformations are not asymmetric, in contrast to the diastereotopic lithiations performed on the calixarene oxazolines and ferrocenyloxazolines, where the true structural implications of the ligand are recognisable through changes in the diastereoselectivity.

From the chemical literature the true complexity of marrying the speciation of alkyllithium complexes with rate enhancements and or diastereoselectivities is apparent, with the large and variable competition between the solvent and ligand for complexation with the alkyllithium

making this a very difficult operation.[20,27] Indeed, even *i*PrLi:(–)–sparteine has been shown to exist as a mixed solvated dimer in diethyl ether,[28] illustrating the potential for structural complexity of alkyllithiums in solution. As a number of different solvent systems have been used in conjunction with the TMEDA ligand in this study, it is not possible to ascertain if a certain TMEDA:alkyllithium complex is responsible for the high diastereoselectivities exhibited by this ligand.

The possibility of competition between the ligands TMEDA and THF has been fairly well established in the literature,[27] and was certainly observed to occur in the ortholithiation of isopropyl oxazoline **2.1**. A large decrease in diastereomeric selectivity was observed when reactions were performed in a mixture of TMEDA and THF (Table 8.2), compared to the less strongly coordinating solvent diethyl ether.[3] By observing the small inversion displayed for the purely THF coordinated reaction, it appears sensible to tie the poor selectivity of the THF:TMEDA ligand system to competition between both ligands for control of the alkyllithium, with the different complexes producing different diastereoselectivities. This is a feature of all the reactions performed in THF, where the use of a THF:TMEDA mixture generated reduced diastereoselectivities compared to less strongly coordinating solvents such as pentane and diethyl ether (Table 8.2).

By inspecting the figures for the diastereoselectivities in Table 8.2, it is apparent that no reaction utilising THF as a solvent, particularly in the absence of TMEDA, occurs with significant diastereoselectivity. Reactions performed in a mixture of THF and TMEDA occurred with greater diastereoselectivity, however one can make a general observation regarding the use of ethereal solvents is that without the presence of TMEDA the reaction fails to occur with appreciable control. In the chemical literature THF is known to be a powerful coordinator of alkyllithiums,[3] hence it has been shown to be incompatible with asymmetric reactions involving the chiral (–)–sparteine ligand due to competitive effects.[24] One feature of the ortholithiation of isopropyl oxazoline **2.1** using THF as the solvent that was not anticipated was the reversal in diastereoselectivity that characterised this reaction. In trying to rationalise the source of this reversal we wondered if this could be due to the oxazoline experiencing an energetic penalty in adopting the necessary inward conformation for lithiation to occur through the ‘normal’ kinetic mechanism. In the literature of ferrocenyloxazolines, the use of THF has not promoted a reversal in diastereoselectivity, and generally proceeds with mild preference for the production of the same diastereomer produced from a TMEDA–ligated reaction.[4,14,29]

Table 8.2: Evidence of competition between THF and TMEDA.

Entry	Compound	Alkyllithium	Solvent	Additive	% Yield	Ratio
1	**2.1** *i*Pr *t*BC	*s*BuLi	THF	TMEDA	55	1.8:1
2	**2.1** *i*Pr *t*BC	*i*PrLi	THF	TMEDA	44	4.5:1
3	**2.1** *i*Pr *t*BC	*s*BuLi	THF	–	49	1:1.7
4	**2.1** *i*Pr *t*BC	*i*PrLi	THF	–	12	1:2.4
5	**5.1** *i*Pr HC	*s*BuLi	THF		>95	1.1:1
6	**5.1** *i*Pr HC	*c*PentLi	THF		37	1.3:1
7	**5.1** *i*Pr HC	*s*BuLi	THF	TMEDA	93	3.2:1
8	**6.1** *t*Bu HC	*i*PrLi	THF		62	1.5:1
9	**6.1** *t*Bu HC	*s*BuLi	THF		88	1.3:1
10	**6.8** *t*Bu *t*BC	*s*BuLi	THF	TMEDA	8	12.2:1
11	**6.8** *t*Bu *t*BC	*i*PrLi	THF		7	5:1
12	**6.8** *t*Bu *t*BC	*s*BuLi	THF		29	2.7:1
13	**7.2** *i*Pr Fc	*n*BuLi	THF		30	2.3:1
14	**7.2** *i*Pr Fc	*s*BuLi	THF		82	5:1
15	**7.2** *i*Pr Fc	*t*BuLi	THF		53	7:1

8.2.1 Conformational Analysis of Oxazoline Calixarenes

To investigate the conformations of the calixarene oxazoline system we embarked on a computational analysis of the various calixarene oxazolines used in this study. From ^{1}H NMR spectroscopy we ascertained that for isopropyl oxazoline **2.1** and *t*–butyl oxazoline **6.8** the molecule adopted a pinch cone with the oxazoline functionalised rings and their distal counterparts sitting upright and the two proximal rings leaning backwards. Using this information, DFT calculations (rb3lyp/6–31+g(d,p)) were used to optimise the inward and outward orientations of the four oxazoline calixarenes, allowing an energetic difference between the two conformations of the oxazoline to be calculated (Table 8.3).[30] Attempts at using solvent inclusion techniques (PCM, SCARF) failed, seemingly due of the size of the molecules themselves.[31] We observed that for all the molecules, a preference for the outward orientation of the substituent on the oxazoline occurred, with the presence of the *t*–butyl groups on the calixarene significantly increasing the preference for the outward conformation.

Table 8.3: Computational analysis of conformations of oxazoline calixarenes.

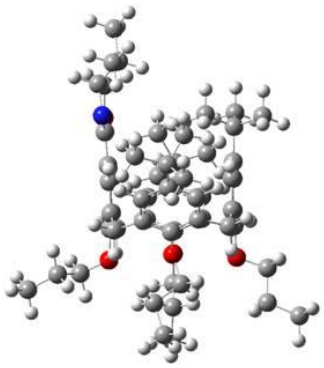 Isopropyl oxazoline **2.1** inward conformation Energy: –1688019.1288419 kcal.mol^{-1} ΔE: 0.303 kcal.mol^{-1}	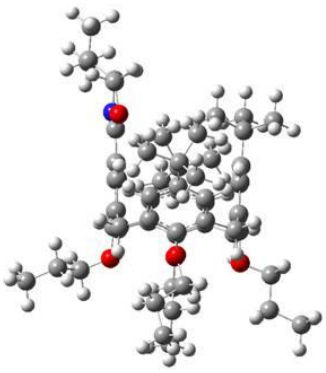 Isopropyl oxazoline **2.1** outward conformation Energy: –1688019.4320545 kcal.mol^{-1}
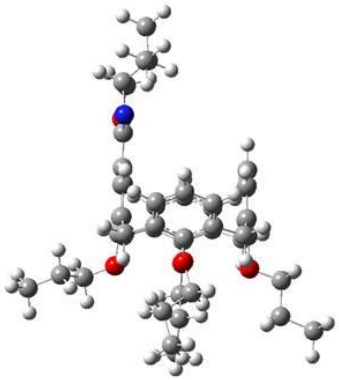 Isopropyl oxazoline **5.1** inward conformation Energy: –1391958.3959277 kcal.mol^{-1} ΔE: 0.027 kcal.mol^{-1}	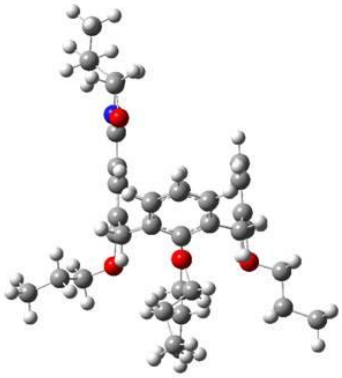 Isopropyl oxazoline **5.1** outward conformation Energy: –1391958.4230989 kcal.mol^{-1}
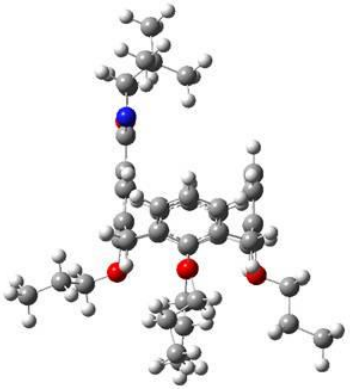 *t*–Butyl oxazoline **6.1** inward conformation Energy: –1416629.5134332 kcal.mol^{-1} ΔE: 0.028 kcal.mol^{-1}	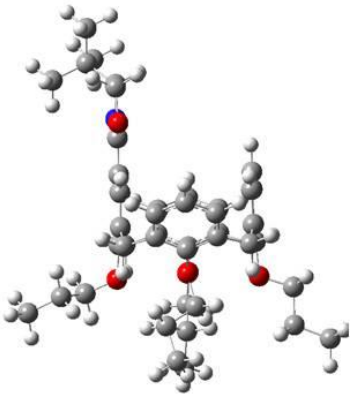 *t*–Butyl oxazoline **6.1** outward conformation Energy: –1416629.5414202 kcal.mol^{-1}

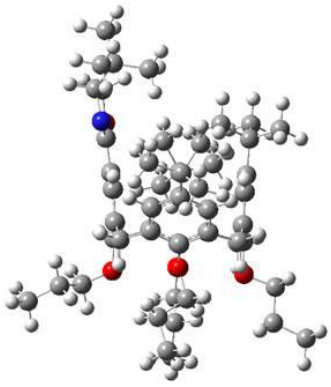	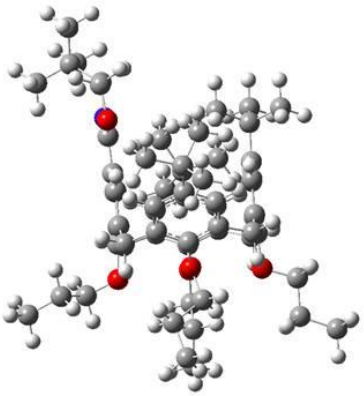
t–Butyl oxazoline **6.8** inward conformation Energy: –1712689.7257029 kcal.mol^{-1} ΔE: 0.824 kcal.mol^{-1}	*t*–Butyl oxazoline **6.8** outward conformation Energy: –1712690.5497483 kcal.mol^{-1}

For the debutylated calixarene oxazoline **5.1** and **6.1** this is relatively minor; substituting the difference in energy into the Boltzmann distribution equation (Equation 8.1) equates to 52 out of 100 molecules occupying the outward conformation at –78 °C. A greater difference in the distribution is noted for isopropyl oxazoline **2.1**, theoretically predicting 69 out of 100 molecules adopting the outward facing conformation, with *t*–butyl oxazoline **6.8** being yet more pronounced with a distribution of 89 out of 100 molecules being in the outward conformation at –78 °C.

$$\frac{N1}{N2} = g2/g1.\exp\left(\frac{-\Delta\epsilon}{kT}\right)$$

Equation 8.1: Boltzmann distribution equation. N1 and N2 represent two states, g1 and g2 is the degeneracy, Δε is the energy difference (expressed in J.mol^{-1}) k is the ideal gas constant (8.314 J.mol^{-1}.K^{-1}and T is temperature (expressed in Kelvin).

While the effects of solvent are not accounted for in these calculations, certainly the calculations suggest that a bias in the distribution between the two conformations exists for oxazoline **2.1**. Returning to the THF–mediated reversal, in the light of the computational analysis of isopropyl oxazoline **2.1**, it would appear possible that the reversal in selectivity observed could be the result of a conformationally driven reaction mechanism. Using the Gibbs free energy equation (Equation 8.2), a selectivity of 1:2.4 equates to an energy difference of approximately 0.33 kcal.mol^{-1} between the two pathways. This is remarkably similar to the theoretical calculation for the difference of energy between the two conformations of isopropyl oxazoline **2.1**.

$$\Delta\Delta G = -RTln\left(\frac{\mathbf{2.10}}{\mathbf{2.11}}\right)$$

Equation 8.2: Gibbs free energy equation.

Logically speaking if the reversal is entirely conformationally driven, the THF–ligated lithiation of *t*–butyl oxazoline **6.8** should display the greatest reversal in diastereoselectivity when lithiated with THF, as it possesses the greatest theoretical preference for the outward conformation of the oxazoline. This is, however, not the case, with a mild diastereoselective preference being exhibited on this system for the formation of the 'normal' diastereomer. Nevertheless this result does not altogether discount the conformationally controlled explanation of the result observed in THF for isopropyl oxazoline **2.1**. Although it appears that there could well be a large bias between the two conformations in favour of the outward orientation of the oxazoline, it also has a larger substituent on the oxazoline which potentially imparts greater steric control, thereby reducing the possibility of lithiation of the thermodynamic ground state. Indeed, significantly enhanced control over the TMEDA–ligated mechanism is also observed in this system (as evidenced from the diastereoselectivity) supporting the idea that greater control is imparted by the *t*–butyl group on the oxazoline. The THF–coordinated lithiation of the debutylated calixarene oxazolines **5.1** and **6.1** occurs with negligible diastereoselectivity, which fits with the thermodynamically controlled hypothesis, as there is no theoretical observation of any significant shift away from equity between the two conformations.

8.3 Effect of Alkyllithiums

A general feature of all the asymmetric ortholithiation reactions we performed on the calixarene oxazolines and the ferrocenyloxazolines was the difference in diastereoselectivity generated by the use of the different alkyllithiums. This effect has been well documented in the chemical literature.[4,5,29] However, due to our synthesis of alkyllithium reagents in house, we gained access to a number of 'unusual' alkyllithiums that have not been common used in asymmetric reactions of this nature. Most notable was the use of *c*PentLi, which was, by a factor of two, more selective than the next most selective alkyllithium when used to ortholithiate isopropyl oxazoline **2.1**. We questioned where these differences arose from, especially in the light of apparent trends in the diastereoselectivities with respect to the choice of alkyllithium. With the ferrocenyloxazolines Sammakia and co–workers have ascribed the differences associated with the choice of alkyllithiums as being due to the steric interaction between the alkyllithium complex and the oxazoline structures,[4,17] as well as associating competing oxygen coordinated pathways or non–coordinative deprotonation occurring should the 'limits of steric crowding' be reached. While these arguments appear reasonable, we were unsure of how the exact steric bulk of the different alkyllithiums actually compared to each other. Despite the large numbers of transformations

associated with alkyllithiums in the literature, no means of simply quantifying the steric bulk of different alkyllithiums appeared to exist.

To produce a simple description of the steric bulk of different alkyllithiums we wondered if the so called Tolman angle[32,33] or cone angle[34] approach which has found widespread use in describing the steric bulk of phosphine ligands could be applied here. This simple approach involves calculating the effective angle cut out for all the substituents on the atom acting as a donor (i.e. the phosphine) to the metal centre, summing these contributions and taking two thirds the value which is then used as an approximation for the steric contribution for the ligand.[35]

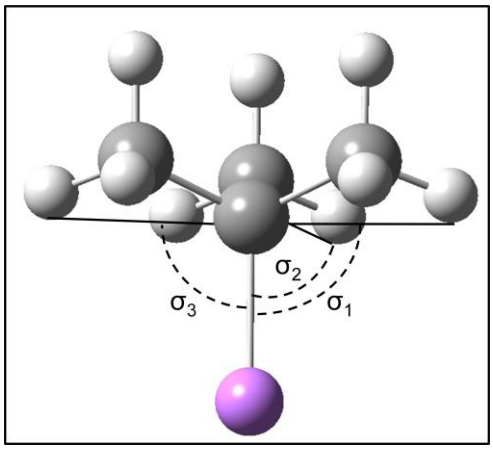

Figure 8. 4: Tolman angle calculation for *t*BuLi. Note: Tolman angle= $2/3\times(\sigma_1+\sigma_2+\sigma_3)$

8.3.1 Tolman Angle

One prerequisite for obtaining a Tolman angle is to have a suitable model for the ligand that one is trying to quantify. Originally this was done by building space filled CPK models of phosphine ligands then physically performing a measurement on a purpose built apparatus.[32] While this approach did succeed in proving that steric effects dominated in the phosphine ligands that Tolman was evaluating, this involves a time consuming and potentially inaccurate process. Other groups have used crystallographic data from which very accurate cone angles can be calculated. The use of the Cambridge Crystallographic Data Base provides in some instances increased accuracy due to multiple solid state structures of particular ligands allowing for a statistical approach.[34,35] While this represents an ideal case, the lack of solid state structures for many of the alkyllithiums used in our study renders this method of limited value, creating the need for a theoretical investigation into the optimisation of different alkyllithiums. This was performed using DFT (b3lyp/6–31+g(d,p)) calculations, allowing access to a wide range of theoretically optimised structures (Table 8.4).

In calculating the Tolman angles we used the van der Waals radii for the outermost atoms of the three substituents connected to the central carbon atom attached to the lithium centre, and then scribed out the angle between the substituent, the lithium centre, and the central carbon atom for each of the groups attached to this central carbon atom. The individual angles were summed and two thirds of the total taken as the calculated Tolman angle ('Li–centered angle'). We also calculated an angle associated with the central carbon atom using the same process ('C–centered angle'), due to both the lithium and the central carbon atom being intimately involved in abstracting a proton during ortholithiation. By comparing these two angles, it is clear that they are interrelated.

Table 8.4: Calculated Tolman angles and bond lengths of alkyllithiums (DFT b3lyp/6–31+g(d,p))

	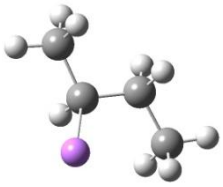	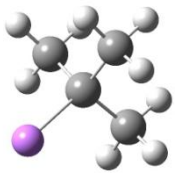
*n*BuLi Li–centered angle: 20.4 C–centered angle: 60.8 C–Li bond distance: 2.001 Å	*s*BuLi Li–centered angle: 52.8 C–centered angle: 92.2 C–Li bond distance: 2.026 Å	*t*BuLi Li–centered angle: 55.9 C–centered angle: 89.1 C–Li bond distance: 2.034 Å
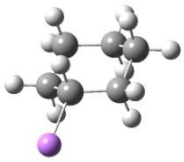	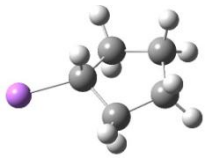	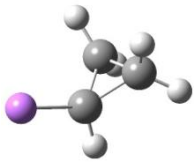
*c*HexLi Li–centered angle: 39.1 Li–centered angle: 75.1 C–Li bond distance: 2.019 Å	*c*PentLi Li–centered angle: 38.7 Li–centered angle: 74.7 C–Li bond distance: 2.006 Å	*c*PropLi Li–centered angle: 34.1 Li–centered angle: 59.2 C–Li bond distance: 1.960 Å
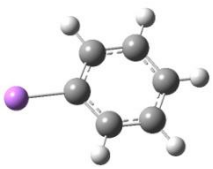	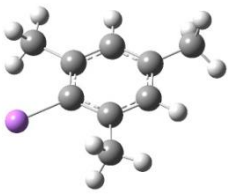	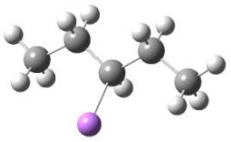
PhLi Li–centered angle: 35.1 C–centered angle: 59.6 C–Li bond distance: 1.970 Å	Mesityl–Li Li–centered angle: 64.5 C–centered angle: 86.0 C–Li bond distance: 1.979 Å	3–pentyl–Li Li–centered angle: 67.9 C–centered angle: 110.1 C–Li bond distance: 2.030 Å

A certain artefact of this method of calculation is that the fixed conformation of the optimised structure cannot account for the possibility of flexibility within the molecule, hence a mean average for the steric quantification of the compound is not calculated but rather relies heavily on the integrity of the optimised structure as a reflection of the mean distribution. In certain instances such as for *s*BuLi, relative to *i*PrLi a far greater steric environment is detected due to the 'extra' carbon atom in the chain creating a large steric barrier around the lithium atom. This is reflected in the rather large Tolman angle calculated for *s*BuLi particularly for the C–centered angle. In solution it is unlikely *s*BuLi will remain entirely in the optimised conformation, with the 'extra' carbon being able to freely rotate. This approach also fails to account for the speciation of the alkyllithium in solution, which is likely to have a large impact on determining its 'relative' steric bulk. However, while potential shortfalls exist in this method, adding further parameters to the system could simply serve to complicate matters further, especially in the light of all the unknown factors involving alkyllithium chemistry, most notably the speciation of the reagent during ortholithiation.

During the computational optimisations, we observed an interesting trend associated with the length of the lithium carbon bond, which follows known trends associated with the basicity of the alkyllithium reagents themselves. We also included in our calculations a number of other potential alkyllithiums which could have interesting properties associated with the steric features of the molecule. These include 3–lithium pentane, which is likely to be extremely bulky and the highly strained cyclopropyl lithium (*c*PropLi) which is likely due to its 'tied–back' structure to be a good representative of an unhindered alkyllithium.

Comparing the Tolman angles we calculated for both the Li–centred angle and the C–centred angle a strong linear relationship appears to exist between the diastereoselectivity of the ortholithiation of isopropyl oxazolines **2.1** and **5.1** (Table 8.5). An inverse relationship is observed between the steric bulk of the reagents and the selectivity of *t*–butyl oxazoline **6.1** relative to the isopropyl oxazolines. A notable outlier exists with the *t*BuLi reversal observed in this series, which if following only a steric trend should produce the greatest diastereoselectivity for the ortholithiation of *t*–butyl oxazoline **6.1**. However, it does seem reasonable that if a maximum steric crowding is reached, the reaction could proceed through a different mechanism, with entirely different diastereoselectivity resulting.

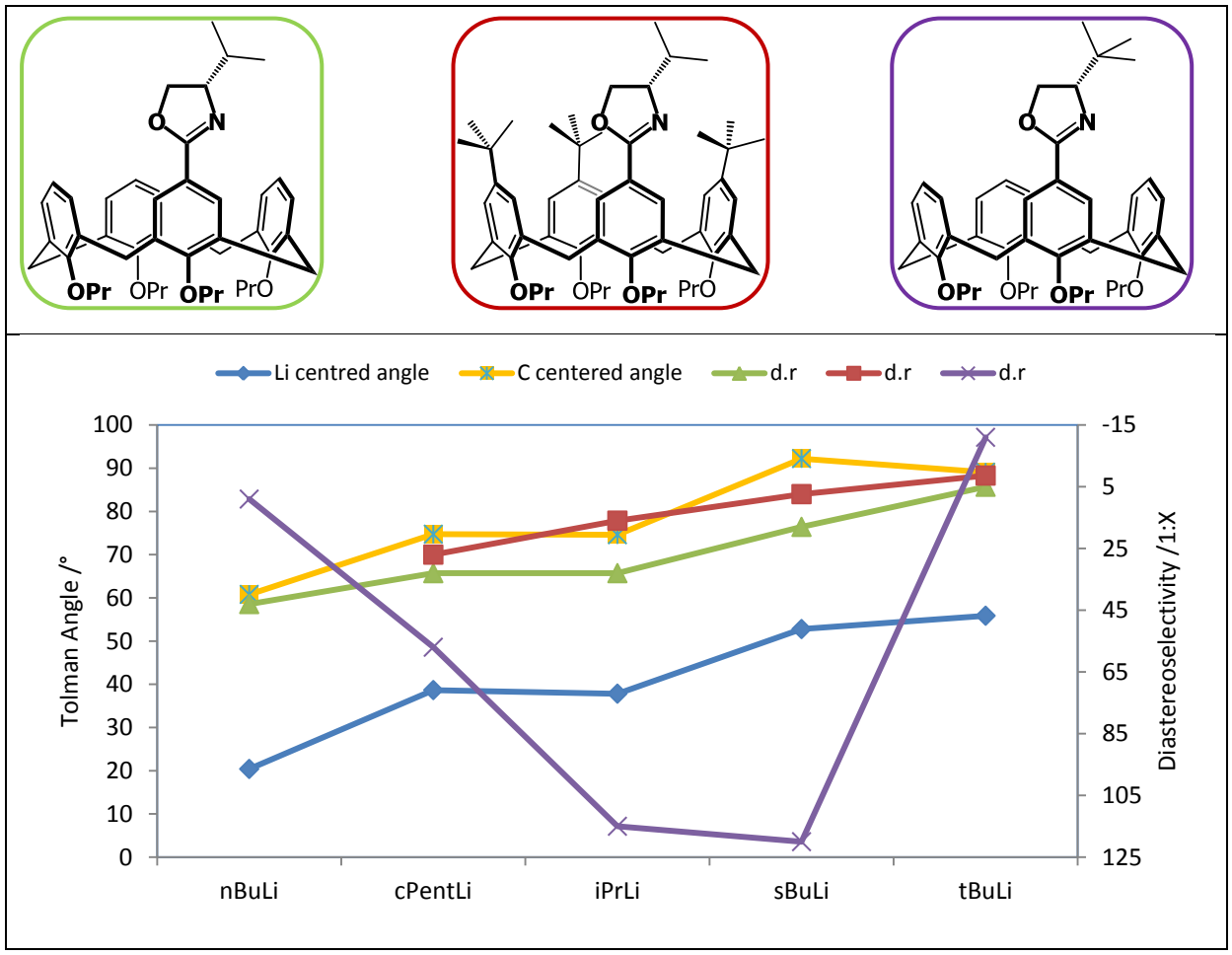

Table 8.5: Tolman angles plotted against *dr* values for lithiation of oxazoline calixarenes. Notes: Dual Y axis used, with the Tolman angle being read of the left hand axis, with *dr* (in the form 1:X, where X signifies the major diastereomer) being represented on the right hand axis.

While the Tolman angle approach appears to explain to a large degree that the different diastereoselectivities associated with the different alkyllithiums stem from steric affects, a number of subtleties in the series exist. Firstly *c*PentLi and *i*PrLi are predicted to have very similar steric environments. This is observed in the ortholithiation of debutylated calixarene isopropyl oxazoline **5.1** where both reagents impart the same diastereoselectivity to the reaction. However, the ortholithiation of isopropyl oxazoline **2.1** presents a different picture, with *c*PentLi (27:1) being more diastereoselective by a factor of nearly two compared to *i*PrLi (16:1). Furthermore, a large decrease in selectivity associated with the use of *c*PentLi (57:1) compared to *i*PrLi (115:1) is observed for the ortholithiation of *t*–butyl oxazoline **6.1,** which is also not predicted by the Tolman angle.

From these results it would again appear that more subtle features of the alkyllithium complex can also contribute to the diastereoselectivity of the reaction. It is altogether feasible that factors such as the 'length' of the reagent could also impact on the transition state for different substrates

causing differences observed in the diastereoselectivity of the reaction not based simply on the steric bulk associated around the lithium atom. While this simple approach cannot determine why certain steric environments are preferable, definite trends associated with the 'bulk' of the alkyllithiums in these reactions are observed. The key to understanding these factors could well lie in understanding the speciation of the alkyllithium during the lithiation, and it is quite likely that different aggregate forms of the reagents could have markedly different diastereoselectivities. Certainly, the use of different ligands in conjunction with the different alkyllithiums present very different diastereoselectivities. However, the steric fit of an alkyllithium within the confines of the operation of a particular complex appear to determine the observed diastereoselectivity of the transformation.

8.4 Structural Role of Oxazoline and the *t*–Butyl Groups on the Calixarene in the Ortholithiation Reaction

One of the early objectives of our study regarding the ortholithiation of the calixarene was what part the *t*–butyl groups on the calixarene played in controlling the diastereoselectivity of the reaction. It is not altogether impossible that the *t*–butyl groups aid the discrimination between the outside of the calixarene and the inside, increasing the facial preference of the alkyllithium complex for coordination with the oxazoline. However, comparison of the diastereoselectivities generated from the TMEDA–ligated ortholithiation of butylated isopropyl oxazoline **2.1** and debutylated isopropyl oxazoline **5.1** indicates that no significant role is played by the *t*–butyl groups in controlling the diastereoselectivity of the reaction (Figure 8.5). Certainly the relative rates of the two reactions (up to 30 hours for isopropyl oxazoline **2.1** compared to 5 hours for debutylated oxazoline **5.1**) illustrate that if anything the *t*–butyl groups on the calixarene serve to retard the rate of the reaction. This is supported by the computational data for energetic penalty experienced by oxazoline **2.1** when it adopts the inward conformation of the oxazoline required to undergo lithiation.

However, a subtlety of this relationship becomes evident when one notes the difference in diastereoselectivities between t–butyl oxazolines **6.1** and **6.8**. While both can be lithiated with great control, lithiation of butylated calixarene oxazoline **6.8** is achieved in such high diastereoselectivity by a range of different alkyllithiums that typically the minor diastereomer is simply not observed. This is in contrast to debutylated calixarene oxazoline **6.1** which shows a strong dependency of the diastereoselectivity on the nature of the alkyllithium complex. A drastic difference in the yields and relative rates of these two systems is indisputable, which could arise

from the thermodynamic penalty required to adopt the correct conformation for lithiation as well as the *t*–butyl groups on the calixarene serving to 'tighten up' the transition state in this instance.

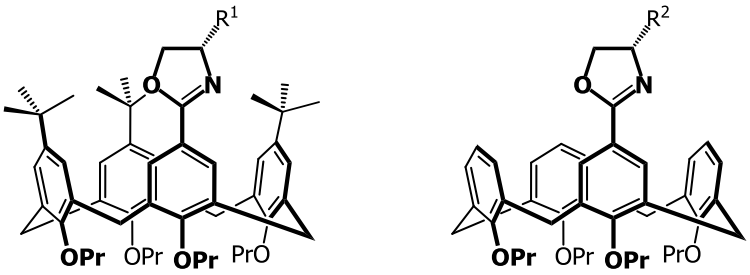

R^1 = *i*Pr **2.1**
R^1 = *t*Bu **6.8**

R^2 = *i*Pr **5.1**
R^2 = *t*Bu **6.1**

Figure 8.5: Calixarene oxazolines.

The role of the substituent on the oxazoline in the ortholithiation reaction is perhaps slightly more obvious. Increasing the steric bulk of the substituent from the isopropyl to the *t*–butyl significantly increases the control exhibited in the TMEDA ligated reaction. The opposite is true for the diglyme induced inversion; with all the calixarenes and ferrocenes tested, a decrease in inversion is recorded.

8.5 Diglyme

Turning to the diglyme induced inversion in selectivity, our efforts to understand how this inversion was generated focused first on determining through which heteroatom coordination to the alkyllithium occurred. If the stereochemistry of the product of the diglyme reaction is explained using the model presented by Sammakia,[14] Richards[13] and Uemura[15] for the asymmetric ortholithiation of ferrocenyloxazolines, it is difficult to envisage how the non–kinetically favourable transition state is induced with the use of bulky diglyme:alkyllithium complex. These two classical conformations are shown in Figure 8.6 where the kinetically favourable transition state **A** outcompetes the kinetically unfavourable transition state **B**.

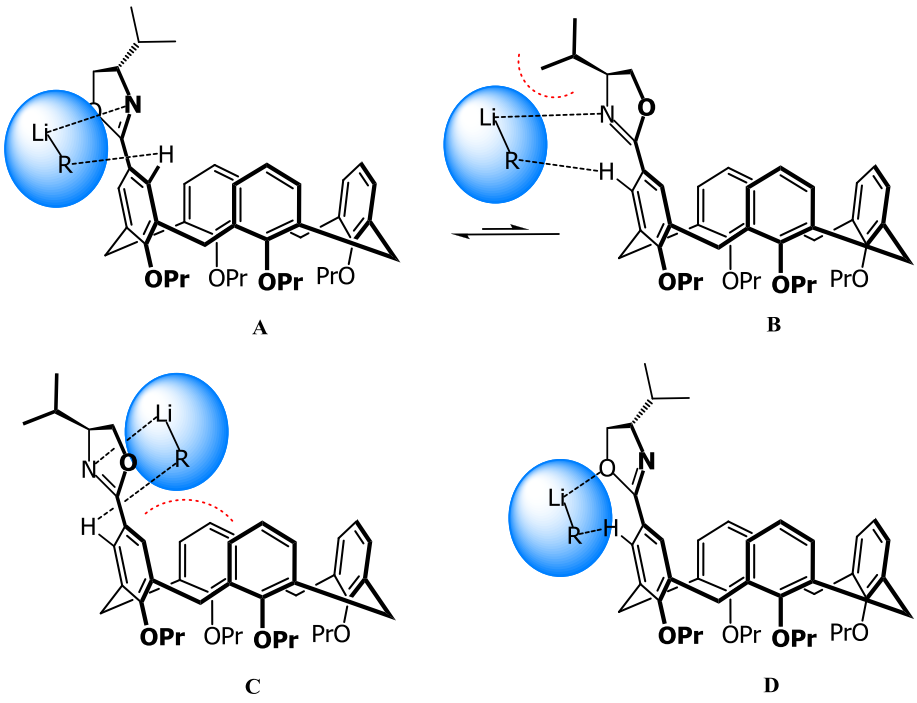

Figure 8.6: Transition states for ortholithiation reaction. Notes: Blue sphere represents an unknown alkyllithium complex. **A**: Approach of alkyllithium complex from outside the bowl with coordination to the nitrogen. **B**: Approach of alkyllithium from outside the bowl with steric clash with isopropyl group on oxazoline. **C**. Approach of alkyllithium from inside the bowl with steric clash with calixarene structure. **D**. Approach of alkyllithium from outside the bowl with coordination to oxygen.

We felt it would be unreasonable to expect that the alkyllithium complex could be induced to coordinate to the oxazoline from within the calixarene bowl, or from the iron coordinated face of the Cp ring to use the analogous transition state in the ferrocenyloxazoline system (C in Figure 8.6). As none of the three aforementioned transition states (**A**, **B** or **C**) appeared feasible in explaining the diglyme inversion, we wondered if possibly a competitive oxygen–coordinated pathway could be occurring (**C** in Figure 8.6). If the complex also approaches coordination with the oxazoline from outside the calixarene bowl and away from the bulk of the isopropyl group, could this possibly explain the stereochemistry of the diglyme inversion product?

A number of other authors have alluded to the possibility of oxygen–coordinated ortholithiation of oxazolines occuring.[4,36,37] This has been semi–supported by computational data, which have indicated that the energetic difference between *O*– and *N*–directed lithiation could be quite small (at least for certain species of alkyllithium TMEDA complexes),[1] however no definitive proof of an oxygen–coordinated mechanism has ever been presented. Since no significant effect was observed on the diglyme inversion by inverting the sense of chirality at the oxygen chiral centre in the *trans* and *cis* diphenyl ferrocenyloxazolines, the proposed oxygen coordinated mechanism was ruled out (the results of which are presented in Chapter 7). From these results it was determined

that a nitrogen–coordinated mechanism occurred for both the TMEDA and diglyme ligated mechanisms. Similarly THF (and by implication all the other ethers) must also coordinate through the same pathway, which is supported by the THF ligated ortholithiation of Sammakia's conformationally constrained ferrocenyloxazoline **1.40**. The aforementioned mechanistic argument (presented in Figure 8.6) still holds valid though, in that it appears impossible that the steric impositions of the iron/calixarene bowl and the substituent on the oxazoline are suddenly overcome, especially in the light of the fact that the most effective ligand at promoting the reversal was di–*t*–butyl–diglyme, which at face value is a very bulky tridentate oxygen ligand.

Table 8.6: Investigation into diglyme induced inversion.

Entry	Compound	Alkyllithium	Additive	% Yield	Ratio
1	**5.1** *i*Pr HC	*s*BuLi	Glyme	45	1:1.6
2	**5.1** *i*Pr HC	*s*BuLi	Di–*i*Pr–glyme	66	1:1
3	**5.1** *i*Pr HC	*s*BuLi	Diglyme	95	1:4.2
4	**5.1** *i*Pr HC	*i*PrLi	Diglyme	24	1:1.5
5	**5.1** *i*Pr HC	*t*BuLi	Diglyme	25	1:1.3
6	**5.1** *i*Pr HC	*s*BuLi	Diglyme	95	1:4.2
7	**5.1** *i*Pr HC	*s*BuLi	Di–Et–diglyme	95	1:4.5
8	**5.1** *i*Pr HC	*s*BuLi	Di–*i*Pr–diglyme	88	1:6.4
9	**5.1** *i*Pr HC	*s*BuLi	Di–*t*Bu–diglyme	95	1:12
10	**6.1** *t*Bu HC	*s*BuLi	Diglyme	38	1.1:1
11	**6.1** *t*Bu HC	*t*BuLi	Diglyme	17	1:5.4
12	**6.1** *t*Bu HC	*s*BuLi	di–*t*Bu–diglyme	33	1:3.4
13	**6.8** *t*Bu *t*BC	*s*BuLi	di–*t*Bu–diglyme	12	1:3.7
14	**7.2** *i*Pr Fc	*n*BuLi	Diglyme	98	1:1.4
15	**7.2** *i*Pr Fc	*n*BuLi	Di–*i*Pr–diglyme	88	1:3.8
16	**7.2** *i*Pr Fc	*n*BuLi	Di–*t*Bu–diglyme	85	1:5.6
17	**7.2** *i*Pr Fc	*n*BuLi	Di–triEt–diglyme	18	1.7:1
18	**2.1** *i*Pr tBC	*s*BuLi	Di–*t*Bu–diglyme	60	1:25

In briefly summarising the features that are required from the ligand for the inversion to occur, we found that they were specifically associated with strongly coordinative oxygen ligands, such as

HMPA, or contained multiple oxygen donors. The use of the bidentate glyme induced a moderate inversion, which was significantly improved by the addition of the third oxygen donor (i.e. diglyme). It is very specific to the diglyme structure, and structural isomers such as dimethoxy glycerol failed to impart any reasonable diastereocontrol, as did any of the crown ethers or the multidentate nitrogen ligands (see Table 8.6). Perhaps most importantly, we found that by increasing the bulk of the alkyl substituents at the terminal positions, the inversion was significantly enhanced. This enhancement was a consistent feature in all the calixarene oxazolines and ferrocenyloxazolines that we tested in this study. We observed in the calixarene oxazoline system that *s*BuLi appeared to be the most suitable reagent to induce the inversion. This was contrasted by the ferrocenyloxazoline series where it appeared that *n*BuLi was the most suitable for inverting the reaction. Using a steric argument, it would appear that optimisation based on the steric bulk of the alkyllithium within the confines of the operation of a specific complex induces the inversion. From this, one is prompted to assume that both diglyme complexes (for *n*BuLi and *s*BuLi) appear to be structurally very similar, almost certainly of the same aggregation state during ortholithiation.

The use of diglyme in organolithium transformations is not completely unprecedented, and recently a number of groups have achieved a certain amount of success in obtaining solid state structures of organolithium complexes with the ligand.[38,39] In all of these structures, diglyme is tri–coordinated to the organolithium species, certainly presenting a reasonable sterically hindered complex in which the ligand wraps itself around the lithium cation. In both of these reports the authors have also utilised the tridentate nitrogen donor PMDTA, which adopts a very similar coordination motif with the organolithium to the diglyme structures. The highly similar nature of the solid state structures of the diglyme and PMDTA alkyllithium complexes in the literature indicate that it might not simply be the nature of the structure of the complex that induces the inversion in selectivity, but is also intrinsically associated with the nature of the donor atoms in the ligand. Indeed a specific note appears in the publication by Wheatly *et al.* regarding the increased separation of the lithium carbanion ion pair in the case of PMDTA compared to diglyme (3.8 Å compared to 2.5 Å), which they attribute to its increased power as a Lewis base.[38] It would appear in the light of our results that the diglyme derivatives, specifically di–*t*Bu–diglyme, also act in a tridentate fashion. Speculatively one would say that increasing the steric bulk at the terminal positions must increase the steric bulk of the resulting alkyllithium complex, however an alternative viewpoint would be that the bulky *t*–butyl groups simply modify the shape of the complex. The argument would then be that the increase in reversal is not simply a consequence of steric bulk but rather of the diglyme:alkyllithium complex adopting a more favourable

conformation for the inversion. One could speculate, in the light of the solid state structures for the diglyme complexes, specifically again in relation to the contrast with the PMDTA structure, that the bulkiness is perhaps the more dominant factor.

After eliminating the possibility of an oxygen coordinative mechanism being responsible for the inversion in diastereoselectivity with diglyme, we wondered if the alkyllithium was coordinating to the oxazoline during the rotation of the oxazoline, when it briefly adopts an out of plane angle relative to the arene. Previously, we had observed that computationally the oxazolines certainly preferred an in–plane conformation relative to the arene, presumably through the stabilisation offered through overlap of the *p*–orbitals in the arene. To gain a better understanding of this process we attempted to calculate the values associated with the energetic profile of the rotation of the oxazoline between the global minima of the inward and outward conformations.

8.5.1 Rotation of Oxazoline Explored through Computational Methods

We approached the calculation by defining a dihedral angle associated with the oxazoline relative to the arene and performing systematic rotation of the dihedral angle, and then allowing optimisation of the rest of the structure to occur.[30] We found it was necessary not to use the 'z–matrix' method for the scan, but rather the 'modredundant' command which uses an *x*,*y*,*z* coordinate system. Use of the *z*–matrix method failed to return optimised structures, resulting in the calculation ceasing after a number of a set number of iterations regardless of the choice of basic set. The reasons for this are unknown, but could be related to the relatively large number of atoms in the calixarene structure. We also observed that due to the large size of the calixarene molecules, it was necessary to start the calculation from an optimised structure. Failure to do this often resulted in non–physical energies being calculated due to large scale deformation of the molecule and bond lengths and angles. This was overcome by inserting the coordinates of the crystal structure obtained for diphenyl phosphine calixarene **4.5** as the starting point for the calculations, which, due to its relatively low energy nature, could then be subjected to further calculation.

We started our optimisations on the *t*–butyl calixarene (the results for isopropyl oxazoline **2.1** are shown, however similar results were obtained for the *t*–butyl oxazoline **6.8**) system, but it was observed that it appeared that the molecule was deforming during the optimisation, resulting in a non–consistent optimisation, with rotation through 360° not yielding the same energy as the starting material (Graph 8. 1). Attempts at using the same starting geometry for each separate optimisation failed to improve the situation, resulting in highly variable energies. These results suggested that the rotation of the oxazoline resulted in deformation throughout the molecule,

which due to the large number of atoms and hence degrees of freedom in the calculation, leads to optimised structures that are not consistent with the global minima. Due to the computationally expensive nature of these calculations, DFT methods were not attempted on these molecules.

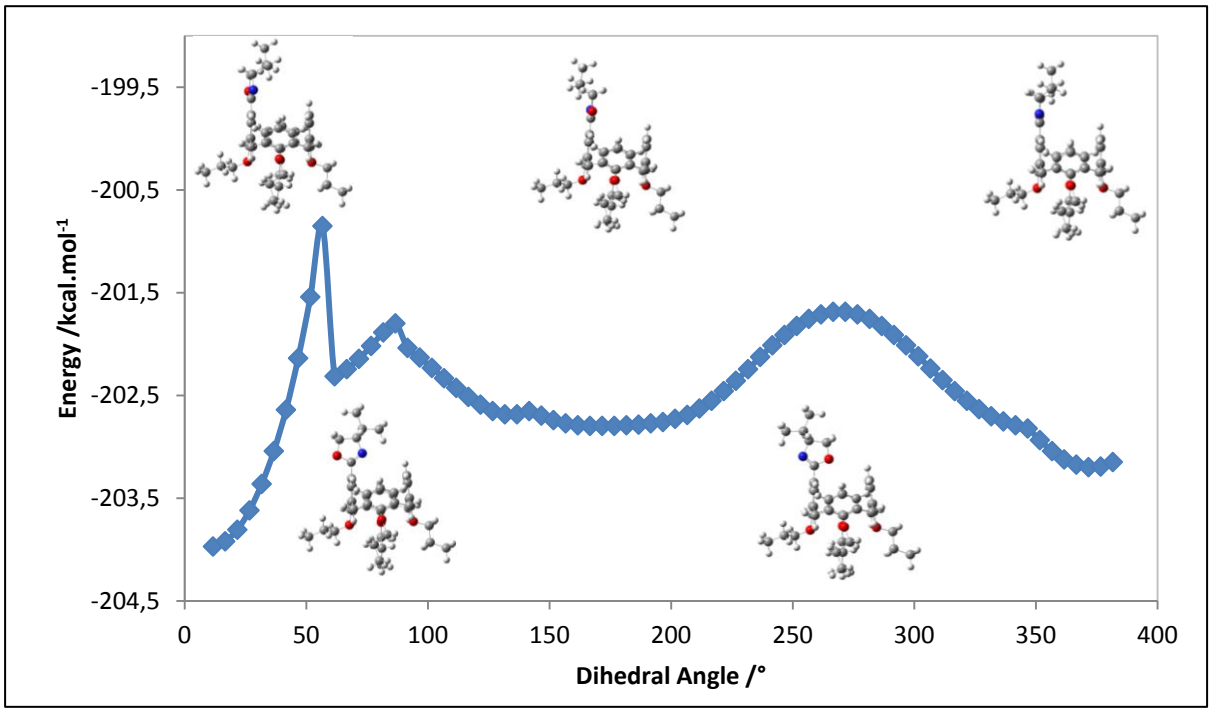

Graph 8. 1: SE (rpm3) rotation of oxazoline dihedral angle of *t*–butyl calixarene isopropyl oxazoline **2.1**. Notes: Difference between energy maxima and energy minima = 3.2 kcal.mol^{-1}

Pleasingly, removal of the *t*–butyl groups from the calixarene structures significantly improved our ability to perform a scan on the rotation of the oxazoline. Rotation of isopropyl oxazoline **5.1** with SE (rpm3) using the modredundant command generated what appeared to be reasonable data for the rotational barrier of the oxazoline. Repeating this calculation using DFT (rb3lyp/6–31) calculations (which are known to produce more realistic energies) returned a minimum energy barrier for rotation of the oxazoline of 7.9 kcal.mol^{-1}. The calculation beautifully illustrates the energetic penalty that the structure undergoes by removing the possibility of conjugation with the arene. It would be interesting to explore this structure through variable temperature NMR studies to observe if this value could be compared to an empirically generated value for the rotation of the oxazoline.

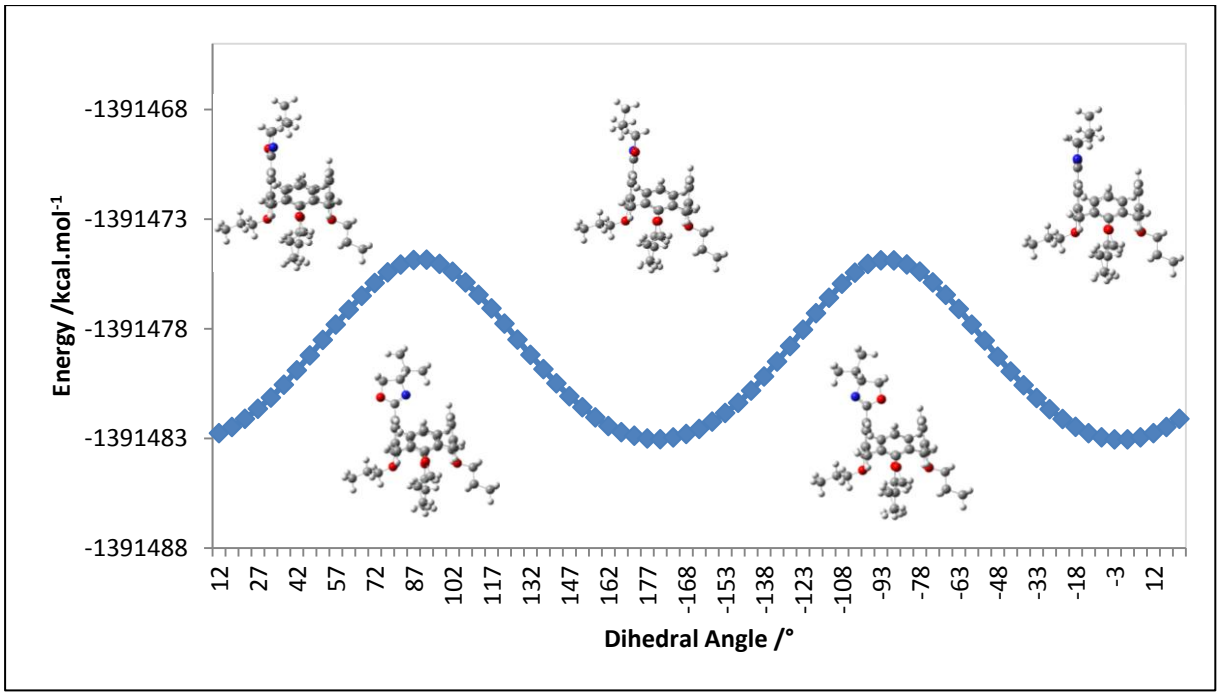

Graph 8.2: DFT (rb3lyp/6–31) rotation of isopropyl oxazoline calixarene **5.1**. Notes: Greatest energy barrier for rotation between energy minima =8.16 kcal.mol^{-1}, lowest barrier 7.91 kcal.mol^{-1}

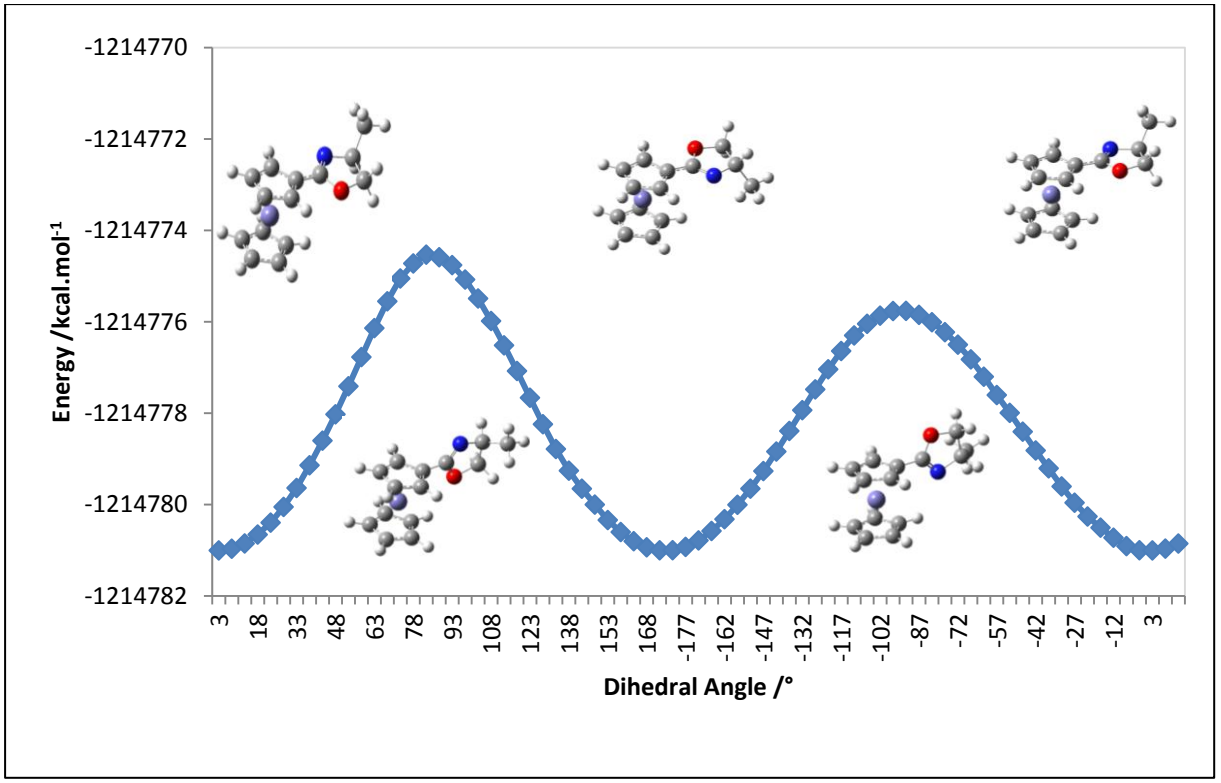

Graph 8.3: DFT (rb3lyp/6–31) rotation of Me ferrocenyloxazoline **7.8**. Notes: Greatest energy barrier for rotation between energy minima =6.47 kcal.mol^{-1}, lowest barrier 5.24 kcal.mol^{-1}

We observed a similar energetic profile for a scan performed on methyl ferrocenyloxazoline **7.8**, with the calculation suggesting a slightly smaller energy barrier (5.24 kcal.mol^{-1}) compared to the calixarene system (Graph 8.3).

From the solid state structures of diglyme–complexed alkyllithiums and lithium cations, it is evident that these ligands tend to wrap themselves around the lithium cation,[38,39] not dissimilar to structures obtained using PMDTA.[26] It is interesting that increasing the bulk of the diglyme ligand increases the reversal in diastereoselectivity. This could be associated with either the bulkier structure being able to preferentially lithiate via the reversal mechanism or perhaps simply by further limiting the operation of the 'normal' mechanism. Certainly, if THF and the other ethers, all solvents that fail to impart any notable diastereoselectivity to the reaction, are able to lithiate using both mechanisms (as deduced through the lack of diastereoselectivity), it would appear that the inversion induced by diglyme is a consequence of inhibiting the 'normal' pathway. Again if this is simply a structure–induced inversion, then PMDTA should also allow the reversal to occur, this is certainly not the case, as good selectivity in the favour of the 'normal' diastereomer results from the use of PMDTA. Returning to the empirical observation that PMDTA is a better Lewis base than diglyme,[38] it is likely that the increased lability of the oxygen based ligand is a secondary requirement for controlling the inversion in selectivity. The inverse of this argument is what perhaps generates the good characteristics of TMEDA as a ligand in the 'normal' reaction pathway. In the absence of other competitive ligands, TMEDA almost certainly acts in a bidentate fashion when complexing the alkyllithium, providing a relatively stable complex,[20] which perhaps displays a resilience to releasing the alkyllithium, forcing the 'normal' mechanism to occur. One factor is certain, and that is that the control in the mechanism is imparted by the substituent on the oxazoline, specifically in the proximity of the nitrogen atom.

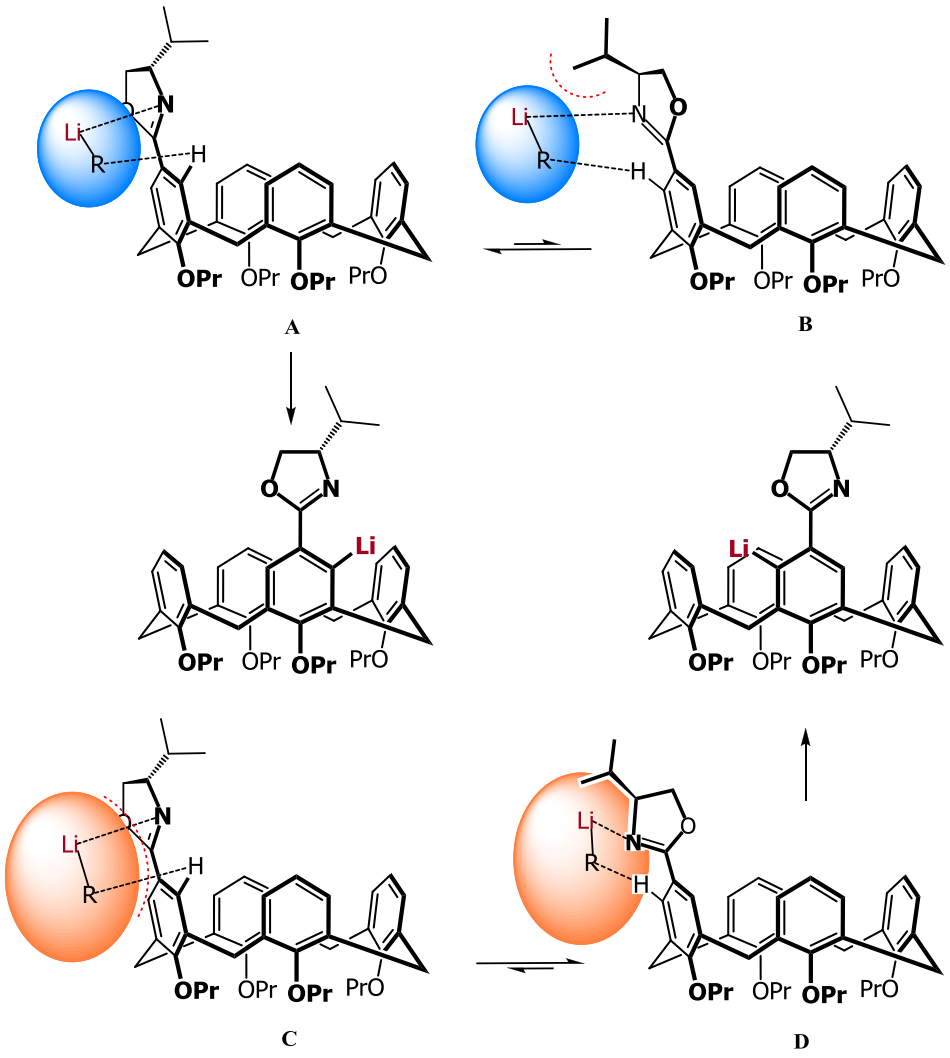

Figure 8.7: Possible TMEDA and Diglyme transition states. Note the blue sphere represents an alkyllithium TMEDA complex, with the orange sphere representing an alkyllithium diglyme complex.

In our computational studies on the oxazoline calixarene systems we observed that the oxazoline prefers the in–plane conformation relative to the arene, but that rotation is certainly possible at –78 °C. It appeared reasonable to suggest that if indeed the 'normal' mechanism occurred through ortholithiation of transition state **A**, perhaps the complex structure is such that it cannot approach coordination of the oxazoline in its normal in–plane energy minima (**C** in Figure 8.7). If an out–of–plane oxazoline conformation is responsible for coordinating the alkyllithium (**D** in Figure 8.7), explaining the stereochemistry of the subsequent lithiation product becomes challenging, in the light of the fact that increasing the size of the substituent on the oxazoline disfavours the reversal mechanism. However, the sterics factors associated with this intermediate complex could dictate that deprotonation of the 'normal' product is disfavoured, and rotation and lithiation of the other ortho position is simply more kinetically favourable from this intermediate complex. The last question would be, is the *t*BuLi inversion observed with *t*–butyl oxazoline **6.1** and **6.8** related

to the diglyme inversion? Is it a similar transition state occurring that leads to both inversions? Unfortunately, we cannot answer these questions at this time, however if this study has proved anything, it is that the current understanding fails to appreciate how chiral oxazolines are actually able to impart diastereoselectivity. Simply put, the speciation of the alkyllithium is clearly the most important consideration in this regard.

That there is such a large difference between the bidentate nitrogen donor TMEDA and the tridentate oxygen donor diglyme illustrates the subtleties associated with the mechanism of oxazoline–directed lithiation. If one takes into consideration the typically poor selectivity obtained for ortholithiations performed in ethereal solvents for oxazolines, in this study as well as in the chemical literature, it is perhaps indicative that oxygen donor ligands allow a number of mechanisms to occur. The ultimate question is what governs the TMEDA ligand having such high specificity for one pathway and diglyme for the other. Could it be associated with different aggregate forms of the alkyllithium, perhaps a dimer for TMEDA and a monomer for diglyme and the aggregates themselves having different affinities for each pathway? Perhaps the difference stems from the lability of the donor atoms in conjunction with a particular conformation or wrapping up of the alkyllithium in the ligand? These hypotheses must be tested in the future as they may help to refine this system, however the beautiful and ultimately highly surprising complementary effects offered by these two ligand systems introduce a hitherto unknown versatility into oxazoline directed ortholithiation. Perhaps more exciting is that the prospect of testing the diglyme ligands on other asymmetric organolithium transformations which represents an exciting goal for future work.

8.6 Conclusion

Over the course of this work we have demonstrated that chiral oxazolines can be used to provide a highly asymmetric route to *meta* functionalised inherently chiral calixarenes. This methodology can be used on both the butylated and debutylated calixarene systems, which with subsequent hydrolysis of the oxazoline directing group allows access to a range of functionalised calixarene carboxylic acids in high enantiomeric excess. We have also demonstrated, through the course of this work, that the use of derivative alkyllithium structures can provide significant increases in diastereoselectivity, and certainly calls for this to be investigated further in other asymmetric organolithium transformations. We have also demonstrated that the differences associated with the use of different alkyllithiums can to a large extent be ascribed to steric differences, with the implementation of the Tolman angle approach proving to provide a means of quantifying the

steric bulk of alkyllithiums. Our findings have also demonstrated that the oxazoline directing group provides a hitherto unknown ability to be diastereoselectively tuned through the choice of the ligand system. In this regard the development of a series of diglyme–based ligands have proved to provide a highly selective means of inverting the sense of chirality from that which the use of the TMEDA ligand is able to generate. We have also demonstrated that the diglyme induced inversion also occurs on the ferrocenyloxazoline, demonstrating that this a general and hitherto unknown facet of asymmetric oxazoline–directed ortholithiation.

The control imparted by chiral oxazolines does not rely on the strong arm tactics employed for directing groups like Ugi's amine **1.32**, which is generally lithiated at room temperature, but is of a rather sensitive and complex nature and relies heavily on the supporting environment provided by the ligands associated with the alkyllithium. However, this almost tentative nature, has suggested over the course of this work almost unprecedented diastereoselective versatility, and hopefully with further nurturing can be developed yet further.

8.7 References

(1) Chadwick, S. T.; Ramirez, A.; Gupta, L.; Collum, D. B. *J. Am. Chem. Soc.* **2007**, *129*, 2259.

(2) Saa, J. M. *Helv. Chim. Acta.* **2002**, *85*, 814.

(3) Clayden, J. *Organolithiums: Selectivity for Synthesis*; Pergamon: London, 2002; Vol. 23.

(4) Sammakia, T.; Latham, H. A. *J. Org. Chem.* **1995**, *60*, 6002.

(5) Clayden, J. In *Topics in Organometallic Chemistry*; Hodgson, D., Ed.; Springer Berlin / Heidelberg: 2003; Vol. 5, p 251.

(6) Marquarding, D.; Klusacek, H.; Gokel, G.; Hoffmann, P.; Ugi, I. *Angew. Chem. Int. Ed.* **1970**, *9*, 371.

(7) Marquarding, D.; Klusacek, H.; Gokel, G.; Hoffmann, P.; Ugi, I. *J. Am. Chem. Soc.* **1970**, *92*, 5389.

(8) Rebiere, F.; Riant, O.; Ricard, L.; Kagan, H. B. *Angew. Chem. Int. Ed.* **1993**, *32*, 568.

(9) Lagneau, N. M.; Chen, Y.; Robben, P. M.; Sin, H. S.; Takasu, K.; Chen, J. S.; Robinson, P. D.; Hua, D. H. *Tetrahedron* **1998**, *54*, 7301.

(10) Davies, S. G.; Loveridge, T.; Fatima, M.; Teixeira, C. C.; Clough, J. M. *J. Chem. Soc., Perkin Trans. 1* **1999**, 3405.

(11) Blagg, J.; Davies, S. G.; Goodfellow, C. L.; Sutton, K. H. *J. Chem. Soc., Perkin Trans. 1* **1987**, 1805.

(12) Clayden, J. In *The Chemistry of Organolithium Compounds*; Rappoport, Z., Marek, I., Eds.; John Wiley & Sons: 2004, p 495.

(13) Richards, C. J.; Damalidis, T.; Hibbs, D. E.; Hursthouse, M. B. *Synlett* **1995**, 74.

(14) Sammakia, T.; Latham, H. A.; Schaad, D. R. *J. Org. Chem.* **1995**, *60*, 10.

(15) Nishibayashi, Y.; Uemura, S. *Synlett* **1995**, 79.

(16) Kundig, E. P.; Ripa, A.; Bernardinelli, G. *Angew. Chem. Int. Ed.* **1992**, *31*, 1071.

(17) Sammakia, T.; Latham, H. A. *J. Org. Chem.* **1996**, *61*, 1629.

(18) Riant, O.; Samuel, O.; Kagan, H. B. *J. Am. Chem. Soc.* **1993**, *115*, 5835.

(19) Richards, C. J.; Mulvaney, A. W. *Tet. Asymm.* **1996**, *7*, 1419.

(20) Hoffmann, D.; Collum, D. B. *J. Am. Chem. Soc.* **1998**, *120*, 5810.

(21) Waldmuller, D.; Kotsatos, B. J.; Nichols, M. A.; Williard, P. G. *J. Am. Chem. Soc.* **1997**, *119*, 5479.

(22) West, P.; Waack, R. *J. Am. Chem. Soc.* **1967**, *89*, 4395.

(23) McGarrity, J. F.; Ogle, C. A. *J. Am. Chem. Soc.* **1985**, *107*, 1805.

(24) Carbone, G.; O'Brien, P.; Hilmersson, G. *J. Am. Chem. Soc.* **2010**, *132*, 15445.

(25) Strohmann, C.; Gessner, V. H.; Damme, A. *Chem. Commun.* **2008**, 3381.

(26) Gessner, V. H.; Daschlein, C.; Strohmann, C. *Chem. Eur. J.* **2009**, *15*, 3320.

(27) Collum, D. B. *Acc. Chem. Res.* **1992**, *25*, 448.

(28) Gallagher, D. J.; Kerrick, S. T.; Beak, P. *J. Am. Chem. Soc.* **1992**, *114*, 5872.

(29) Sutcliffe, O. B.; Bryce, M. R. *Tetrahedron: Asymmetry* **2003**, *14*, 2297.

(30) Frisch, M. J.; Trucks, G. W.; Schlegel, H. B.; Scuseria, G. E.; Robb, M. A.; Cheeseman, J. R.; Scalmani, G.; Barone, V.; Mennucci, B.; Petersson, G. A.; Nakatsuji, H.; Caricato, M.; Li, X.; Hratchian, H. P.; Izmaylov, A. F.; Bloino, J.; Zheng, G.; Sonnenberg, J. L.; Hada, M.; Ehara, M.; Toyota, K.; Fukuda, R.; Hasegawa, J.; Ishida, M.; Nakajima, T.; Honda, Y.; Kitao, O.; Nakai, H.; Vreven, T.; Montgomery, J., J. A. ; Peralta, J. E.; Ogliaro, F.; Bearpark, M.; Heyd, J. J.; Brothers, E.; Kudin, K. N.; Staroverov, V. N.; Kobayashi, R.; Normand, J.; Raghavachari, K.; Rendell, A.; Burant, J. C.; Iyengar, S. S.; Tomasi, J.; Cossi, M.; Rega, N.; Millam, N. J.; Klene, M.; Knox, J. E.; Cross, J. B.; Bakken, V.; Adamo, C.; Jaramillo, J.; Gomperts, R.; Stratmann, R. E.; Yazyev, O.; Austin, A. J.; Cammi, R.; Pomelli, C.; Ochterski, J. W.; Martin, R. L.; Morokuma, K.; Zakrzewski, V. G.; Voth, G. A.; Salvador, P.; Dannenberg, J. J.; Dapprich, S.; Daniels, A. D.; Farkas, Ö.; Foresman, J. B.; Ortiz, J. V.; Cioslowski, J.; Fox, D. J.; Gaussian 09 Revision A.1 ed. Wallingford CT, 2009.

(31) Suwattanamala, A.; Magalhães, A. L.; Gomes, J. A. N. F. *Chem. Phys.* **2005**, *310*, 109.

(32) Tolman, C. A. *J. Am. Chem. Soc.* **1970**, *92*, 2956.

(33) Tolman, C. A. *Chem. Rev.* **1977**, *77*, 313.

(34) Niksch, T.; Görls, H.; Weigand, W. *Eur. J. Inorg. Chem.* **2010**, 95.

(35) Muller, T. E.; Mingos, D. M. P. *Trans. Met. Chem.* **1995**, *20*, 533.

(36) Meyers, A. I.; Slade, J. *J. Org. Chem.* **1980**, *45*, 2785.

(37) Collum, D. B. *Acc. Chem. Res.* **1993**, *26*, 227.

(38) Campbell Smith, A.; Donnard, M.; Haywood, J.; McPartlin, M.; Vincent, M. A.; Hillier, I. H.; Clayden, J.; Wheatley, A. E. H. *Chem. Eur. J.* **2011**, *17*, 8078.

(39) Michel, R.; Herbst-Irmer, R.; Stalke, D. *Organometallics.* **2011**, *30*, 4379.

CHAPTER 9

Experimental

9.1 General Practices

9.1.1 Solvents and Reagents

Chemicals used in these experiments were purchased from Merck or Aldrich. Tetrahydrofuran, diethyl ether, toluene and pentane were distilled under nitrogen from sodium wire/sand using benzophenone as an indicator, alternatively they were dried for at least two days in a sealed Schlenk flask with 20% molecular sieves.[1] Solvent was also collected under inert conditions from a Innovative Technologies PureSolve PS-MP-5 solvent purification system. Dichloromethane was distilled under nitrogen from calcium hydride. Other reagents requiring purification were purified according to standard procedures.[2]

9.1.2 Temperature Control

Low temperature reactions were performed in a Dewar containing dry ice in acetone (–78 °C), or a slurry of ethanol, sodium chloride and ice (-20°C). Reactions requiring precise, extended low temperature control, were performed in a Dewar regulated with a Thermo Scientific Haake EK90 Immersion Cooler. Microwave reactions were performed in a Biotage Initiator microwave reactor.

9.1.3 Inert Conditions

Glassware was dried for at least an hour at 120 ºC, thereafter it was placed under vacuum of <0.5 mm Hg and cyclically flushed with nitrogen/argon and evacuated until it had reached RT. Standard Schlenk techniques were employed when necessary. All reactions were performed under a positive pressure of 2.8 kPa of 5.0 grade nitrogen or argon (Air Products).

9.1.4 Chromatography

All column chromatography was performed on Merck silica gel 60 (particle size 0.040-0.063 mm) using one of, or combinations of, petroleum ether, diethyl ether, ethyl acetate, toluene, dichloromethane, ethanol and methanol as a solvent. Thin layer chromatography (TLC) was carried out on aluminium backed Merck silica gel 60 F_{254} plates. Visualisation was performed

with a UV lamp; using iodine on silica; or by spraying with a Cerium Ammonium Molybdate (CAM) or ninhydrin (NIN) solution followed by heating.

9.1.5 Characterisation

All ^{1}H, ^{13}C, ^{19}F and ^{31}P nuclear magnetic resonance spectra were obtained using a 300 MHz Varian VNMRS (75 MHz for ^{13}C), 400 MHz Varian Unity Inova (100 MHz for ^{13}C), 600 MHz Varian Unity Inova (150 MHz for ^{13}C), Bruker Ultrashield 300, 400 or 500 MHz spectrometers, with deuterated solvents. Chemical shifts (δ) were recorded using the residual solvent peak or external reference. All chemical shifts are reported in ppm and all spectra were obtained at 25 °C unless otherwise reported. Data was processed using ACD/SpecManager product version 10.08 or Spinworks product version 3.1.7.[3] Deconvolution was performed with Spinworks product version 10.08 using the built in deconvolution processing features. For the purposes of ^{19}F experiments software baseline correction was required for the accurate integration of peak areas. Different relaxation times were investigated without effect on relative peak areas of two diastereomers.

Melting points were obtained using a Gallenkamp Melting Point Apparatus or a Kofler microscope melting point machine and are uncorrected. Infrared spectra were obtained using a Nexus Thermo-Nicolet FT-IR instrument using thin film (NaCl plate), or using the ATR attachment or using a ATi Perkin Elmer Spectrum RX1 FTIR spectrometer using thin film (NaCl). High resolution mass spectrometry was performed by CAF (Central Analytical Facility) at Stellenbosch University using a Waters API Q-TOF Ultima spectrometer, and at the University of Manchester on a Thermo Finnigan MAT 95XP mass. Routine mass spectroscopy was done using a Waters API Quattro Micro spectrometer at Stellenbosch University or at the University of Manchester using a Micromass Platform II. Optical rotations were recorded using a Bellingham + Stanley ADP 220 Polarimeter using a 1 dm cell or using Perkin-Elmer 241 Polarimeter using a cell with a pathlength of 0.25 dm.

9.2 Chapter 2

5,11,17,23-tetra-*tert*-butyl-calix[4]arene – (2.5)[4]

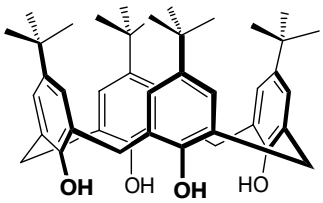

p-tert-Butyl phenol (66.0 g, 444 mmol), sodium hydroxide pellets (0.9 g, 20 mmol), 37% formaldehyde solution (41.5 ml, 554 mmol, 1.3 eq) and H_2O (2 ml) were added to a 2 L three-necked round-bottom flask. The flask was equipped with a mechanical stirrer and the contents stirred at RT until dissolution of the solids occurred, after which it was heated for approximately two hours at 110 ºC until the formation of a yellow highly viscous substance occurred, thereafter stirring was discontinued and was the flask was cooled to RT. Diphenylether (600 ml) was added and the mixture was stirred until dissolution of the solids occurred. Thereafter the flask was heated to 115 ºC under a steady stream of nitrogen (to remove residual water). The temperature was then raised to 160 ºC for 15 minutes, thereafter it was brought to reflux where it was maintained for 3 hours under nitrogen. The flask was cooled to RT and ethyl acetate (1 L) was added, thereafter it was stirred at RT for a further 30 minutes and left to stand for a further 30 minutes. The precipitate was filtered, washed with successive portions of ethyl acetate (2 x 100 ml), acetic acid (2 x 100 ml), and acetone (2 x 100 ml). The precipitate was re-dissolved in boiling toluene (1 l) and the volume of the solution reduced (750 ml) following which the solution was left to cool to RT with rapid formation of the white crystals occurring. The crystalline product was dried under vacuum at RT to afford a calixarene–toluene complex (**2.5**) (39.6 g, 53.4 mmol, 48%). Mp 338 °C (Toluene); R_f = 0.58 (DCM/PET, 50/50); ^{1}H NMR (300 MHz, CHLOROFORM-*d*, 0 ºC) δ ppm 1.22 (s, 36 H, C(CH_3)$_3$), 3.44 – 3.58 (m, 4 H, ArCH_2Ar), 4.18 – 4.36 (m, 4 H, ArCH_2Ar), 7.06 (s, 8 H, Ar*H*), 10.35 (s, 4 H, ArO*H*).

5,11,17,23-tetra-*tert*-butyl-26,27,28-tripropoxycalix[4]arene – (2.6)[5]

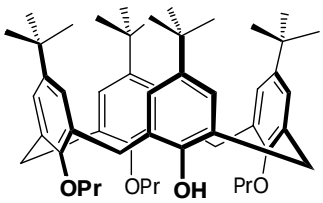

Calixarene **2.5** (12.2 g, 16.3 mmol), barium hydroxide octahydrate ($Ba(OH)_2{\cdot}8H_2O$), 20.8 g, 54 mmol, 3.3 eq), barium oxide (17.6 g, 94.5 mmol, 5.8 eq) and freshly distilled dimethyl formamide (230 ml) were added to a round-bottom flask (500 ml). The mixture was stirred at RT for 15 minutes, thereafter propyl iodide (55 ml, 459 mmol, 28 eq) was slowly added and stirring was continued for a further 2 hours under nitrogen. 1M HCl (200 ml) was added to the reaction followed by extraction with ethyl acetate (2 x 250 ml). The organic layers were combined, washed with H_2O (3 x 100 ml) followed by drying over $MgSO_4$ and the solvent removed under reduced pressure. Purification was achieved by crystallization from dichloromethane (20 ml) and ethanol (60 ml) affording pale yellow crystals (10.2 g, 13.2 mmol,

81%). Mp 190°C (EtOH/DCM); R_f = 0.65 (DCM:PET, 50:50); ^{1}H NMR (400 MHz, CHLOROFORM-*d*) δ ppm 0.83 (s, 18 H, C(C*H*$_3$)$_3$), 0.96 (t, *J*=7.6 Hz, 3 H, CH$_2$C*H*$_3$), 1.10 (t, *J*=7.4 Hz, 6 H, 2 x CH$_2$C*H*$_3$), 1.33 (s, 9 H, C(C*H*$_3$)$_3$), 1.35 (s, 9 H, C(C*H*$_3$)$_3$), 1.81 – 2.03 (m, 4 H, 2 x CH$_2$C*H*$_2$CH$_3$), 2.27 – 2.41 (m, 2 H, CH$_2$C*H*$_2$CH$_3$), 3.17 (d, *J*=12.6 Hz, 2 H, ArC*H*$_2$Ar), 3.24 (d, *J*=13.1 Hz, 2 H, ArC*H*$_2$Ar), 3.73 – 3.79 (m, 4 H, OC*H*$_2$CH$_2$), 3.82 – 3.89 (m, 2 H, OC*H*$_2$CH$_2$), 4.34 (d, *J*=13.1 Hz, 2 H, ArC*H*$_2$Ar), 4.38 (d, *J*=12.6 Hz, 2 H, ArC*H*$_2$Ar), 5.58 (s, 1 H, C$_{Ar}$O*H*), 6.50 – 6.55 (m, 4 H, Ar*H*), 7.06 (s, 2 H, Ar*H*), 7.14 (s, 2 H, Ar*H*); ^{13}C NMR (101 MHz, CHLOROFORM-*d*) δ ppm 9.62 (CH$_2$*C*H$_3$), 10.79 (2 x CH$_2$*C*H$_3$), 22.45 (CH$_2$*C*H$_2$CH$_3$), 23.40 (2 x CH$_2$*C*H$_2$CH$_3$), 31.06 (2 x C(*C*H$_3$)$_3$), 31.09 (Ar*C*H$_2$Ar), 31.36 (Ar*C*H$_2$Ar), 31.69 (C(*C*H$_3$)$_3$), 31.76 (C(*C*H$_3$)$_3$), 33.63 (2 x *C*(CH$_3$)$_3$), 33.82 (*C*(CH$_3$)$_3$), 34.11 (*C*(CH$_3$)$_3$), 76.28 (O*C*H$_2$CH$_2$), 77.81 (2 x O*C*H$_2$CH$_2$), 124.65 (*C*$_{Ar}$H), 124.75 (*C*$_{Ar}$H), 124.96 (*C*$_{Ar}$H), 125.57 (*C*$_{Ar}$H), 129.50 (*C*$_{Ar}$CH$_2$), 131.83 (*C*$_{Ar}$CH$_2$), 132.23 (*C*$_{Ar}$CH$_2$), 136.01 (*C*$_{Ar}$CH$_2$), 141.40 (*C*C(CH$_3$)$_3$), 144.97 (2 x *C*C(CH$_3$)$_3$), 145.48 (*C*C(CH$_3$)$_3$), 150.67 (2 x *C*$_{Ar}$OCH$_2$), 151.70 (*C*$_{Ar}$OCH$_2$), 153.94 (*C*$_{Ar}$OH).

11,17,23-tri-*tert*-butyl-5-nitro-26,27,28-tripropoxycalix[4]arene – (2.7)[6]

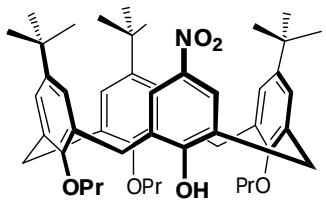

Tripropoxy calixarene **2.6** (4.5 g, 5.8 mmol), dichloromethane (50 ml) and acetic acid (29 ml) were added to a round-bottom flask (250 ml). The solution was cooled to 0 ºC and stirred for 5 minutes after which, 65 % nitric acid (2.9 ml, 42 mmol, 7.2 eq) was slowly added. The solution was allowed to warm to RT, and the progress of the reaction closely followed via TLC. The reaction was quenched after approximately 11 minutes by the addition of H_2O (50 ml). The organic and aqueous phases were separated, and the aqueous phase extracted with a further portion of dichloromethane (50 ml). The organic layers were combined, washed with H_2O (2 x 50 ml), saturated sodium bicarbonate solution (2 x 50 ml); finally a second solution of H_2O (50 ml). The organic layers were dried over $MgSO_4$ and the solvent removed under reduced pressure. The residual material was then taken up in dichloromethane (approximately 20 ml) and absolute ethanol (50 ml) and purification achieved via slow crystallisation yielding light yellow crystals of nitro calixarene **2.7** (3.5 g, 4.5 mmol, 78%). Mp 181°C (EtOH/DCM); R_f = 0.33 (EtOAc:PET, 3:97); ^{1}H NMR (400 MHz, CHLOROFORM-*d*) δ ppm 0.84 (s, 18 H, C(C*H*$_3$)$_3$), 0.96 (t, *J*=7.5 Hz, 3 H, CH$_2$C*H*$_3$), 1.11 (t, *J*=7.4 Hz, 6 H, 2 x CH$_2$C*H*$_3$), 1.36 (s, 9 H, C(C*H*$_3$)$_3$), 1.83 – 2.04 (m, 4 H, 2 x CH$_2$C*H*$_2$CH$_3$), 2.23 – 2.34 (m, 2 H, CH$_2$C*H*$_2$CH$_3$), 3.21 (d, *J*=12.7 Hz, 2 H, ArC*H*$_2$Ar), 3.41 (d, *J*=13.9 Hz, 2 H, ArC*H*$_2$Ar), 3.71 – 3.88 (m, 6 H, OC*H*$_2$CH$_2$), 4.29 – 4.38 (m, 4 H, ArC*H2*Ar), 6.47 (d, *J*=2.5 Hz, 2 H, Ar*H*), 6.61 (d, *J*=2.3 Hz, 2 H, Ar*H*), 7.17 (s, 2 H, Ar*H*), 7.24 (s, 1 H, C$_{Ar}$O*H*), 8.07 (s, 2 H, Ar*H*); ^{13}C NMR (101 MHz, CHLOROFORM-*d*) δ ppm 9.54 (CH$_2$*C*H$_3$), 10.71 (2 x CH$_2$*C*H$_3$), 22.54 (CH$_2$*C*H$_2$CH$_3$), 23.36 (2 x CH$_2$*C*H$_2$CH$_3$), 31.04 (Ar*C*H$_2$Ar), 31.09

($C(CH_3)_3$), 31.31 ($ArCH_2Ar$), 31.67 ($C(CH_3)_3$), 33.74 (2 x $C(CH_3)_3$), 34.15 ($C(CH_3)_3$), 76.14 (OCH_2CH_2), 78.00 (2 x OCH_2CH_2), 124.27 ($C_{Ar}H$), 124.36 ($C_{Ar}H$), 125.65 ($C_{Ar}H$), 125.67 ($C_{Ar}H$), 129.75 ($C_{Ar}CH_2$), 129.78 ($C_{Ar}CH_2$), 132.62 ($C_{Ar}CH_2$), 135.76 ($C_{Ar}CH_2$), 139.25 ($C_{Ar}NO_2$), 145.78 (2 x $CC(CH_3)_3$), 145.81 ($CC(CH_3)_3$), 151.69 (2 x $C_{Ar}OCH_2$), 153.75 ($C_{Ar}OCH_2$), 159.99 ($C_{Ar}OH$).

11,17,23-tri-*tert*-butyl-5-nitro-25,26,27,28-tetrapropoxycalix[4]arene – (2.8)

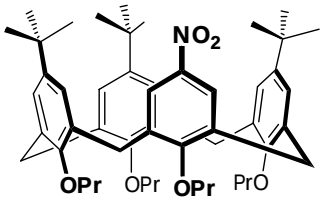

Nitro calixarene **2.7** (6.4 g, 8.4 mmol), sodium carbonate (1.8 g, 17 mmol, 2 eq) and acetonitrile (64 ml) were added to a round-bottom flask (150 ml). The mixture was brought to reflux under nitrogen and after 30 minutes propyl iodide (15 ml, 154 mmol, 18.3 eq) was added to the solution. The solution was refluxed for 48 hours after which it was cooled to RT and H_2O (100 ml) was added along with ethyl acetate (250 ml). The layers were separated, the aqueous layer extracted with a further portion of ethyl acetate (50 ml), the organic layers combined, washed with 1M HCl (100 ml), brine (50 ml) and dried over $MgSO_4$ and the solvent removed under reduced pressure. The product was purified by slow crystallisation from dichloromethane (20 ml) and ethanol (60 ml) affording white crystals (6.13 g, 7.6 mmol, 91%) Mp 218 °C (EtOH/DCM); R_f = 0.54 (EtOAc:PET, 7:93); ^{1}H NMR (400 MHz, CHLOROFORM-*d*) δ ppm 0.65 (s, 9 H, $C(CH_3)_3$), 0.94 (t, *J*=7.5 Hz, 6 H, CH_2CH_3), 1.08 – 1.14 (m, 6 H, CH_2CH_3), 1.39 (s, 18 H, $C(CH_3)_3$), 1.85 – 1.97 (m, 4 H, $CH_2CH_2CH_3$), 1.97 – 2.13 (m, 4 H, $CH_2CH_2CH_3$), 3.12 – 3.21 (m, 4 H, $ArCH_2Ar$), 3.69 (t, *J*=6.8 Hz, 2 H), 3.74 (t, *J*=6.9 Hz, 2 H, OCH_2CH_2), 3.91 – 3.98 (m, 2 H, OCH_2CH_2), 4.03 – 4.11 (m, 2 H, OCH_2CH_2), 4.43 (d, *J*=13.1 Hz, 2 H, $ArCH_2Ar$), 4.48 (d, *J*=12.9 Hz, 2 H, $ArCH_2Ar$), 6.23 (s, 2 H, Ar*H*), 7.14 (d, *J*=2.5 Hz, 2 H, Ar*H*), 7.17 (d, *J*=2.5 Hz, 2 H, Ar*H*), 7.28 (s, 2 H, Ar*H*); ^{13}C NMR (101 MHz, CHLOROFORM-*d*) δ ppm 9.82 (2 x CH_2CH_3), 10.62 (CH_2CH_3), 10.84 (CH_2CH_3), 23.05 (2 x $CH_2CH_2CH_3$), 23.40 ($CH_2CH_2CH_3$), 23.57 ($CH_2CH_2CH_3$), 30.68 ($C(CH_3)_3$), 31.06 ($ArCH_2Ar$), 31.14 ($ArCH_2Ar$), 31.68 (2 x $C(CH_3)_3$), 33.12 ($C(CH_3)_3$), 34.15 ($C(CH_3)_3$), 76.52 (2 x OCH_2CH_2), 77.13 (OCH_2CH_2), 77.67 (OCH_2CH_2), 123.07 ($C_{Ar}H$), 124.43 ($C_{Ar}H$), 125.13 ($C_{Ar}H$), 126.66 ($C_{Ar}H$), 131.86 ($C_{Ar}CH_2$), 134.16 ($C_{Ar}CH_2$), 135.15 ($C_{Ar}CH_2$), 136.23 ($C_{Ar}CH_2$), 142.52 ($C_{Ar}NO_2$), 144.37 ($CC(CH_3)_3$), 145.34 (2 x $CC(CH_3)_3$), 152.64 ($C_{Ar}OCH_2$), 154.72 (2 x $C_{Ar}OCH_2$), 160.65 ($C_{Ar}OCH_2$).

Partial cone 11,17,23-tri-*tert*-butyl-5-nitro-25,26,27,28-tetrapropoxycalix[4]arene – (2.9)

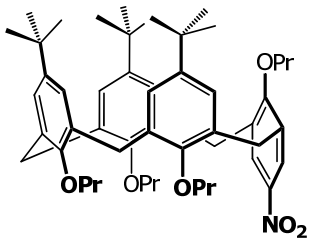

A mixture of **2.7** (1.1g, 1.4 mmol) and potassium carbonate (K_2CO_3, 0.58 g, 4.2 mmol, 3 eq) were added to a microwave vessel (5 ml). To this dimethylformamide (2.5 ml) and propyl iodide (0.41 ml, 4.2 mmol, 3 eq) were added and the flask crimped. The flask was subjected to 45 s of pre-stirring at RT, after which it was heated to 170 ºC for 4 minutes. The material was taken up in dichloromethane (2 x 50 ml) followed by washing with 1M HCl (50 ml). The organic layers were dried over $MgSO_4$ and the solvent removed under reduced pressure. The partial cone product was crystallized from dichloromethane (3 ml) and ethanol (20 ml) yielding pale yellow crystals (0.93 g, 1.15 mmol, 83%). R_f = 0.54 (EtOAc:PET, 7:93); 1H NMR (300 MHz, CHLOROFORM-*d*) δ ppm 0.66 (t, *J*=7.6 Hz, 3 H, CH_2CH_3) 1.03 (m, 18 H, $C(CH_3)_3$), 1.04 – 1.10 (m, 9 H, CH_2CH_3), 1.35 (s, 9 H, $C(CH_3)_3$), 1.82 – 2.05 (m, 8 H, $CH_2CH_2CH_3$), 3.04 (d, *J*=12.7 Hz, 2 H, $ArCH_2Ar$), 3.31 – 3.39 (m, 2 H, OCH_2CH_2), 3.46 – 3.56 (m, 2 H, OCH_2CH_2), 3.60 – 3.66 (m, 2 H, $ArCH_2Ar$, 2 x OCH_2CH_2), 3.73 – 3.86 (m, 6 H, $ArCH_2Ar$), 4.02 (d, *J*=12.7 Hz, 2 H, $ArCH_2Ar$), 6.58 (d, *J*=2.3 Hz, 2 H, Ar*H*), 6.82 (d, *J*=2.6 Hz, 2 H, Ar*H*), 7.11 (s, 2 H, Ar*H*), 8.23 (s, 2 H, Ar*H*).

11,17,23-tri-*tert*-butyl-5-amino-25,26,27,28-tetrapropoxycalix[4]arene – (2.4)[7]

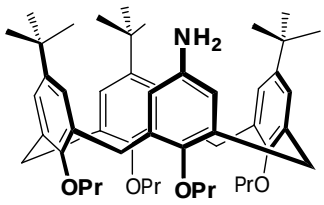

A round bottom flask (150 ml) was charged with ethanol (80 ml), tetrapropoxy nitro calixarene **2.8** (6.13 g, 7.6 mmol) and 10 % palladium on carbon (0.8 g, 0.76 mmol, 0.1 eq) sequentially. The mixture was brought to reflux and hydrazine hydrate (1 ml, 20 mmol, 2.6 eq) was slowly added. Reflux was maintained for 2 hours after which it was cooled to RT and filtered through Celite, which was subsequently washed with additional DCM (30 ml). Rapid formation of white micro-crystals occurred from the standing solution affording a **DCM.2.4** co-crystal. Further purification of the product was not requited and the product was dried under high vacuum at RT (5.7 g, 7.2 mmol, 95%). The DCM can be removed by heating under vacuum, or by simply dissolving the crystals in a suitable solvent followed by removal of the solvent under reduced pressure. Mp 191°C (EtOH/DCM); R_f = 0.46 (EtOAc:PET, 5:95); ^{1}H NMR (400 MHz, CHLOROFORM-d) δ ppm 0.80 (s, 9 H, $C(CH_3)_3$), 0.92 (t, *J*=7.5 Hz, 6 H, CH_2CH_3), 1.04 – 1.13 (m, 6 H, CH_2CH_3), 1.35 (s, 18 H, 2 x $C(CH_3)_3$), 1.83 – 1.97 (m, 4 H, $CH_2CH_2CH_3$), 2.00 – 2.11 (m, 4 H, $CH_2CH_2CH_3$), 3.02 (d, *J*=12.7 Hz, 2 H, $ArCH_2Ar$), 3.13 (d, *J*=12.9 Hz, 2 H, $ArCH_2Ar$), 3.60 (t, *J*=7.1 Hz, 2 H, OCH_2CH_2), 3.72 (t, *J*=6.9 Hz, 2 H, OCH_2CH_2), 3.92 – 4.03 (m, 4 H, OCH_2CH_2), 4.38 (d, *J*=12.7 Hz, 2 H, $ArCH_2Ar$), 4.46 (d, *J*=12.9 Hz, 2 H, $ArCH_2Ar$), 5.71 (s, 2 H, Ar*H*), 6.29 (s, 2 H, Ar*H*), 7.02 (d, *J*=2.5 Hz, 2 H, Ar*H*), 7.10 (d, *J*=2.5 Hz, 2 H, Ar*H*); ^{13}C NMR

(101 MHz, CHLOROFORM-*d*) δ ppm 9.86 (2 x CH_2CH_3), 10.76 (CH_2CH_3), 10.82 (CH_2CH_3), 23.02 (2 x $CH_2CH_2CH_3$), 23.40 ($CH_2CH_2CH_3$), 23.56 ($CH_2CH_2CH_3$), 30.97 ($C(CH_3)_3$), 31.09 ($ArCH_2Ar$), 31.20 ($ArCH_2Ar$), 31.73 (2 x $C(CH_3)_3$), 33.46 ($C(CH_3)_3$), 34.03 (2 x $C(CH_3)_3$), 76.49 (2 x OCH_2CH_2), 77.04 (OCH_2CH_2), 77.31 (OCH_2CH_2), 114.76 ($C_{Ar}H$), 124.48 ($C_{Ar}H$), 125.21 ($C_{Ar}H$), 125.70 ($C_{Ar}H$), 132.27 ($C_{Ar}CH_2$), 133.86 ($C_{Ar}CH_2$), 135.33 ($C_{Ar}CH_2$), 135.92 ($C_{Ar}CH_2$), 139.68 ($CArNH_2$), 143.67 ($C_{Ar}C(CH_3)_3$), 144.27 ($C_{Ar}C(CH_3)_3$), 148.65 ($C_{Ar}O$), 152.95 ($C_{Ar}O$), 155.02 (2 x $C_{Ar}O$).

11,17,23-tri-*tert*-butyl-5-iodo-25,26,27,28-tetrapropoxycalix[4]arene – (2.10)[8]

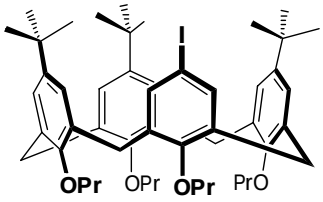

A mixture of amino calixarene **2.4** (4.0 g, 5.08 mmol) and *p*-toluene sulphonic acid (3 g, 15.3 mmol, 3.1 eq) were dissolved in acetonitrile (20 ml) in a round-bottom flask (100 ml). The solution was stirred at RT for 15 minutes after which it was cooled to approximately 10 ºC and sodium nitrite ($NaNO_2$, 0.70 g, 10.16 mmol, 2 eq) and potassium iodide (2.1 g, 12.7 mmol, 2.5 eq) dissolved in H_2O (3 ml) were cautiously added with rapid stirring over 5 minutes. The brown solution was then slowly warmed to RT and stirred for 1 hour. H_2O (50 ml) was added to the flask and its contents extracted with dichloromethane (2 × 80 ml). The organic layers were combined and washed with 10 % sodium thiosulphate solution (10 ml) followed by a saturated sodium bicarbonate solution (100ml). The organic layer was dried over $MgSO_4$ and the solvent removed under reduced pressure. The product **2.10** was crystallized from a 10 % dichloromethane ethanol solution yielding fine white crystals (3.6 g, 4.02 mmol, 79 %). Mp 196 °C (EtOH/DCM); R_f = 0.76 (PET, 100); IR (ATR): 2956 (m, –C–H stretch), 1470 (s, C=C stretch), 1202 (m, C–O stretch), 1012 (m, C–O stretch), 869 (m, C–H oop bend); ^{1}H NMR (400 MHz, CHLOROFORM-*d*) δ ppm 0.88 (s, 9 H, $C(CH_3)_3$), 0.94 (t, *J*=7.5 Hz, 6 H, CH_2CH_3), 1.04 – 1.13 (m, 6 H, CH_2CH_3), 1.34 (s, 18 H, $C(CH_3)_3$), 1.85 – 1.98 (m, 4 H, $CH_2CH_2CH_3$), 1.99 – 2.13 (m, 4 H, $CH_2CH_2CH_3$), 3.07 (d, *J*=12.6 Hz, 2 H, $ArCH_2Ar$), 3.15 (d, *J*=12.9 Hz, 2 H, $ArCH_2Ar$), 3.66 (t, *J*=7.1 Hz, 2 H, OCH_2CH_2), 3.72 (t, *J*=6.9 Hz, 2 H, OCH_2CH_2), 3.90 – 4.03 (m, 4 H, OCH_2CH_2), 4.37 (d, *J*=12.6 Hz, 2 H, $ArCH_2Ar$), 4.44 (d, *J*=12.9 Hz, 2 H, $ArCH_2Ar$), 5.30 – 5.32 (m, 2 H, Ar*H*), 6.37 (s, 2 H, Ar*H*), 6.73 (s, 2 H, Ar*H*), 7.00 (d, *J*=2.3 Hz, 2 H, Ar*H*), 7.11 (d, *J*=2.3 Hz, 2 H, Ar*H*); ^{13}C NMR (101 MHz, CHLOROFORM-*d*) δ ppm 9.88 (2 × CH_2CH_3), 10.61 (CH_2CH_3), 10.78 (CH_2CH_3), 23.05 (2 × $CH_2CH_2CH_3$), 23.33 ($CH_2CH_2CH_3$), 23.55 ($CH_2CH_2CH_3$), 30.70 (2 × $ArCH_2Ar$), 31.14 (2 × $ArCH_2Ar$), 31.44 ($C(CH_3)_3$), 31.66 (2 × $C(CH_3)_3$), 33.66 ($C(CH_3)_3$), 34.07 (2 × $C(CH_3)_3$), 76.54 (OCH_2CH_2), 77.13 (OCH_2CH_2), 77.31 (OCH_2CH_2), 77.49 (OCH_2CH_2), 85.70 (C*C*I), 124.58 (2 × $C_{Ar}H$), 125.00 (2 × $C_{Ar}H$), 126.08 (2 × $C_{Ar}H$), 132.09 (2 × $C_{Ar}CH_2$), 134.37 (2 × $C_{Ar}CH_2$), 135.85 (2 × $C_{Ar}CH_2$), 136.35 (2 × $C_{Ar}CH_2$), 136.41

(2 × C_{Ar}H), 144.27 ($CC(CH_3)_3$), 144.79 (2 × $CC(CH_3)_3$), 152.78 (C_{Ar}OPr), 154.70 (2 × $CCOCH_2$), 155.26 (C_{Ar}OPr); MS (ES+): *m/z* (%) = 904.5 (100) $[M+H_2O]^+$; HRMS–TOF MS ES+: *m/z* $[M+H_2O]^+$ calcd for $C_{52}H_{73}IO_5$: 904.4503; found: 904.4512.

11,17,23-tri-*tert*-butyl-25,26,27,28-tetrapropoxycalix[4]arene – (2.11)

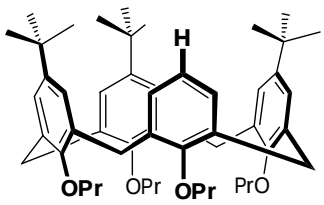

R_f = 0.76 (PET, 100); ^{1}H NMR (300 MHz, CHLOROFORM-*d*): δ ppm 0.80 (s, 9H, $C(CH_3)_3$), 0.92 (t, *J*=7.48 Hz, 6H, CH_2CH_3), 1.11 (m, 6H, CH_2CH_3), 1.37 (s, 18H, $C(CH_3)_3$), 1.91 (m, 4H, $CH_2CH_2CH_3$), 2.05 (m, 4H, $CH_2CH_2CH_3$), 3.12 (m, 4H, ArCH_2Ar), 3.69 (m, 4H, OCH_2CH_2), 4.00 (m, 4H, OCH_2CH_2), 4.40 – 4.48 (m, 4 H, ArCH_2Ar), 6.21 (s, 2H, Ar*H*), 6.25 (s, 3H, Ar*H*), 7.07 (d, *J*=2.49 Hz, 2H, Ar*H*), 7.11 (d, *J*=2.49 Hz, 2H, Ar*H*); ^{13}C NMR (CHLOROFORM-*d*, 101 MHz): δ ppm 9.85 (2 x CH_2CH_3), 10.79 (CH_2CH_3), 10.85 (CH_2CH_3), 23.06 (2 x $CH_2CH_2CH_3$), 23.49 ($CH_2CH_2CH_3$), 23.57 ($CH_2CH_2CH_3$), 31.06 (ArCH_2Ar), 31.22 ($C(CH_3)_3$), 31.74 (C(CH_3)3, ArCH2Ar), 33.45 ($C(CH_3)_3$), 34.05 (2 x $C(CH_3)_3$), 76.46 (2 x OCH_2CH_2), 76.97 (OCH_2CH_2), 77.12 (OCH_2CH_2), 122.32 (C_{Ar}H), 124.38 (C_{Ar}H), 125.35 (C_{Ar}H), 125.84 (C_{Ar}H), 127.18 (C_{Ar}H), 132.05 ($C_{Ar}CH_2$), 133.34 ($C_{Ar}CH_2$), 135.53 ($C_{Ar}CH_2$), 136.03 ($C_{Ar}CH_2$), 143.75 ($C_{Ar}C(CH_3)_3$), 144.33 (2 x $C_{Ar}C(CH_3)_3$), 152.84 ($C_{Ar}OCH_2$), 155.03 ($C_{Ar}OCH_2$), 155.14 (2 x $C_{Ar}OCH_2$); MS (ESI+): *m/z* (%) = 783 (100) $[M+]^+$; HRMS–Positive: *m/z* $[760.543]^+$ calcd for $C_{52}H_{72}O_4Na$: 786.553; found: 783.476.

11,17,23-tri-*tert*-butyl-5-carboxy-25,26,27,28-tetrapropoxycalix[4]arene – (2.2)

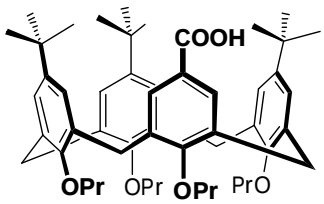

Iodo calixarene **2.10** (4.1 g, 4.6 mmol) was added to an oven dried Schlenk flask and placed under a vacuum of less than 0.5 mmHg with heating to 90 ºC for 5 hours. The crystals were solvated with dry THF (3 ml) and the solvent carefully removed under reduced pressure, after which the flask was again heated to 90 ºC under high vacuum for 1 hour. This process was repeated to ensure all traces of H_2O were removed. The flask was then cooled to 0 ºC and ***i*PrMg·LiCl$_2$** in THF (20 ml, 18.5 mmol, 4 eq) was slowly added under a positive pressure of nitrogen. The flask was then allowed to warm to RT and stirred for 1.5 hours. The solution was poured onto freshly condensed powdered CO_2 (350 ml) and the mixture allowed to warm to RT. Its contents were then taken up in DCM (200 ml) and washed with successive portions of 1 M HCl (50 ml), H_2O (2 × 100 ml) and saturated sodium bicarbonate solution (50 ml). The solvent was then removed under reduced pressure, and the product purified by silica gel chromatography yielding a white solid (2.22 g, 2.76 mmol, 60 %). Mp 287°C (EtOH/DCM); R_f = 0.21 (EtOAc:PET, 10:90); IR (film) cm^{-1}: 1962 (s, CH), 1688 (s, C=O), 1481 (m, C=C); ^{1}H NMR (300

MHz, CHLOROFORM-*d*) δ ppm 0.69 (s, 9 H, C(C*H*$_3$)$_3$), 0.94 (t, *J*=7.5 Hz, 6 H, CH$_2$C*H*$_3$), 1.06 – 1.14 (m, 6 H, CH$_2$C*H*$_3$), 1.36 (s, 18 H, C(C*H*$_3$)$_3$), 1.85 – 1.98 (m, 4 H, CH$_2$C*H*$_2$CH$_3$), 2.00 – 2.11 (m, 4 H, CH$_2$C*H*$_2$CH$_3$), 3.09 – 3.20 (m, 4 H, ArC*H*$_2$Ar), 3.67 – 3.76 (m, 4 H, OC*H*$_2$CH$_2$), 3.90 – 4.08 (m, 4 H, OC*H*$_2$CH$_2$), 4.42 (d, *J*=7.5 Hz, 2 H, ArC*H*$_2$Ar), 4.46 (d, *J*=7.5 Hz, 2 H, ArC*H*$_2$Ar), 6.26 (s, 2 H, C*H*), 7.11 (br. s, 4 H, C*H*), 7.18 (s, 2 H, C*H*), 10.55 – 11.70 (br. s, COO*H*); ^{13}C NMR (75 MHz, CHLOROFORM-*d*) δ ppm 9.89 (2 × CH$_2$*C*H$_3$), 10.64 (CH$_2$*C*H$_3$), 10.81 (CH$_2$*C*H$_3$), 23.08 (2 × CH$_2$*C*H$_2$CH$_3$), 23.41 (CH$_2$*C*H$_2$CH$_3$), 23.57 (CH$_2$*C*H$_2$CH$_3$), 30.87 (C(*C*H$_3$)$_3$), 31.14 (2 × ArCH$_2$Ar), 31.67 (2 × C(*C*H$_3$)$_3$, 2 × ArCH$_2$Ar), 33.23 (*C*(CH$_3$)$_3$), 34.10 (*C*(CH$_3$)$_3$, *C*(CH$_3$)$_3$), 76.50 (OCH$_2$CH$_2$), 76.58 (OCH$_2$CH$_2$), 77.32 (OCH$_2$CH$_2$), 77.43 (OCH$_2$CH$_2$), 123.03 (2 × *C*$_{Ar}$H), 124.47 (*C*COOH), 125.35 (2 × *C*$_{Ar}$H), 126.14 (2 × *C*$_{Ar}$H), 129.96 (2 × *C*$_{Ar}$H), 132.05 (2 × *C*$_{Ar}$CH$_2$), 133.96 (2 × *C*$_{Ar}$CH$_2$), 134.63 (2 × *C*$_{Ar}$CH$_2$), 135.85 (2 × *C*$_{Ar}$CH$_2$), 144.30 (*C*C(CH$_3$)$_3$), 144.89 (*C*C(CH$_3$)$_3$, *C*C(CH$_3$)$_3$), 152.70 (*C*$_{Ar}$OPr), 154.70 (2 × C*C*OCH$_2$), 159.99 (*C*$_{Ar}$OPr), 171.33 (C*C*OOH); MS (ES+): *m/z* (%) = 822.6 (100) [M+H$_2$O]$^+$; HRMS–TOF MS ES+: *m/z* [M+H$_2$O]$^+$ calcd for C$_{53}$H$_{74}$O$_7$: 822.5435; found: 822.5431.

Slightly better yields have been obtained with ***s*BuMg·LiCl$_2$** (60 – 65%).

11,17,23-tri-*tert*-butyl-5-benzaldehyde-25,26,27,28-tetrapropoxycalix[4]arene – (2.12)

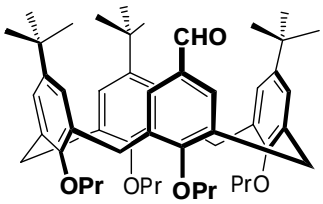

Iodo calixarene **2.10** (150 mg, 0.169 mmol) was placed in an oven dried 2 necked 25 ml flask along with THF (4 ml), thereafter the flask was cooled to –78 ºC Freshly titrated *n*BuLi (0.23 ml, 0.339 mmol, 2 eq) was slowly added to the flask. After 5 minutes DMF (0.1 ml, 1.3 mmol, 7.7 eq) was added to the flask and it was slowly warmed to RT over half an hour. The contents of the flask were then taken up with dichloromethane (50 ml) washed with 1M HCl (50 ml) and the aqueous layer extracted with a further portion of dichloromethane (50 ml). The organic layers were combined, dried over MgSO$_4$, the solvent removed under reduced pressure and the product was purified by column chromatography using EtOAc and PET (1:99 to 10:90), yielding formyl calixarene **2.12** (40 mg, 0.051 mmol, 30 %) as a white solid. R_f = 0.57 (EtOAc:PET, 10:90); ^{1}H NMR (CHLOROFORM-d, 400 MHz): δ ppm 0.69 (s, 9H, C(C*H*$_3$)$_3$), 0.94 (t, *J*=7.51 Hz, 6H, CH$_2$C*H*$_3$), 1.06 – 1.14 (m, 6H, CH$_2$C*H*$_3$), 1.35 (s, 18H, C(C*H*$_3$)$_3$), 1.86 – 1.97 (m, 4H, CH$_2$C*H*$_2$CH$_3$), 1.97 – 2.13 (m, 4H, CH$_2$C*H*$_2$CH$_3$), 3.13 (d, *J*=12.87 Hz, 2H, ArC*H*$_2$Ar), 3.19 (d, *J*=13.06 Hz, 2H, ArC*H*$_2$Ar), 3.70 (t, *J*=6.92 Hz, 2H, OC*H*$_2$CH$_2$), 3.75 (t, *J*=7.02 Hz, 2H, OC*H*$_2$CH$_2$), 3.91 – 3.99 (m, 2H, OC*H*$_2$CH$_2$), 4.00 – 4.08 (m, 2H, OC*H*$_2$CH$_2$), 4.43 (d, *J*=12.87 Hz, 2H, ArC*H*$_2$Ar), 4.48 (d, *J*=12.87 Hz, 2H, ArC*H*$_2$Ar), 6.24 (s, 2H, Ar*H*), 6.93 (s, 2H, Ar*H*), 7.09 – 7.13 (m, 4H, Ar*H*), 9.35 (s, 1H, C*H*O); ^{13}C NMR (151 MHz, CHLOROFORM-

d) δ ppm 9.88 (2 x CH_2CH_3), 10.62 (CH_2CH_3), 10.81 (CH_2CH_3), 23.07 (2 x $CH_2CH_2CH_3$), 23.42 ($CH_2CH_2CH_3$), 23.56 ($CH_2CH_2CH_3$), 30.94 ($ArCH_2Ar$), 31.03 ($C(CH_3)_3$), 31.17 ($ArCH_2Ar$), 31.68 (2 x $C(CH_3)_3$), 33.49 ($C(CH_3)_3$), 34.10 (2 x $C(CH_3)_3$), 76.54 (2 x OCH_2CH_2), 77.08 (OCH_2CH_2), 77.42 (OCH_2CH_2), 124.43 ($C_{Ar}H$), 125.17 ($C_{Ar}H$), 126.28 ($C_{Ar}H$), 129.55 ($C_{Ar}H$), 130.94 ($C_{Ar}CHO$), 132.10 ($C_{Ar}CH_2$), 134.50 ($C_{Ar}CH_2$), 134.82 ($C_{Ar}CH_2$), 135.96 ($C_{Ar}CH_2$), 144.13 ($C_{Ar}C(CH_3)_3$), 144.94 (2 x $C_{Ar}C(CH_3)_3$), 152.79 ($C_{Ar}O$), 154.73 (2 x $C_{Ar}O$), 160.82 ($C_{Ar}O$), 191.33 (*C*HO); MS (ESI+): m/z (%) = 806.6 (100) $[M+H_2O]^+$; HRMS–ES+: m/z [M+Na]+ calcd for $C_{53}H_{72}O_5Na$: 811.5277; found: 811.5306.

5,11,17,23-tetra-*tert*-butyl-25,26,27,28-tetrapropoxycalix[4]arene – (2.13)

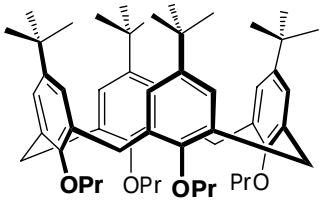

Iodo calixarene **2.10** (1.10 g, 1.24 mmol) was added to an oven dried Schlenk flask and cycled through repeated solvation with dry THF, followed by drying under vacuum of less than 0.5 mm Hg. A small amount of NaH (~50 mg) and dry THF (20 ml) were added to the flask and it was stirred at RT for 1 hour. The mixture was cooled to –78 ºC, and a *t*BuLi (1 ml, 2.5 mmol, 2.5 eq) was slowly added. The solution was stirred for 15 minutes, after which it was poured onto freshly condensed powdered CO_2 (350 ml) and allowed to warm to RT. Its contents were then taken up in DCM (200 ml) and washed with successive portions of 1 M HCl (50 ml), H_2O (2 × 100 ml) and saturated sodium bicarbonate solution (50 ml), the organic layers combined and dried over $MgSO_4$. The solvent was removed under reduced pressure, and the products purified by silica gel chromatography yielding a white solid **2.13** (390 mg, 0.47 mmol, 37 %). R_f = 0.76 (PET, 100); MS (ESI+): *m/z* (%) = 817.6 (100) $[M+H]^+$; HRMS–Positive: *m/z* $[M+H]^+$ calcd for $C_{56}H_{81}O_4$: 817.6135; found: 817.6115.

11,17,23-tri-*tert*-butyl-5-bromo-25,26,27,28-tetrapropoxycalix[4]arene – (2.16)

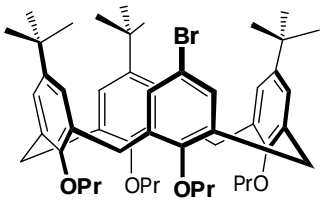

Protonated calixarene **2.11** (1.81 g, 2.38 mmol) and *N*-bromosuccinimide (0.51 g, 2.85 mmol) were taken up in freshly distilled methyl ethyl ketone (40 ml) and added to a round bottom flask (100 ml). The flask was wrapped in aluminium foil and gently warmed, and stirred overnight under an atmosphere of nitrogen. The solvent was removed under reduced pressure and the product was purified by silica gel chromatography using a 1% ethyl acetate petroleum ether solution. Further purification was achieved by crystallization from a 10% dichloromethane ethanol solution which yielded bromo calixarene **2.16** (quantitative yield.) Mp 195°C (EtOH/DCM); R_f = 0.76 (PET, 100); ^{1}H NMR (CHLROFORM-*d*, 300MHz): δ ppm 0.84 (s, 9H, $C(CH_3)_3$), 0.93 (t, *J*=7.56 Hz, 6H, CH_2CH_3), 1.07 (t, *J*=7.41 Hz, 3H, CH_2CH_3), 1.12 (t,

J=7.48 Hz, 3H, CH_2CH_3), 1.35 (s, 18H, $C(CH_3)_3$), 1.89 (m, 4H, $CH_2CH_2CH_3$), 2.06 (m, 4H, $CH_2CH_2CH_3$), 3.08 (d, *J*=12.91 Hz, 2H, $ArCH_2Ar$), 3.14 (d, *J*=12.91 Hz, 2H, $ArCH_2Ar$), 3.64 (t, *J*=7.04 Hz, 2H, OCH_2CH_2), 3.71 (t, *J*=6.90 Hz, 2H, OCH_2CH_2), 3.98 (m, 4H, OCH_2CH_2), 4.42 (m, 4H, $ArCH_2Ar$), 6.31 (s, 2H, Ar*H*), 6.48 (s, 2H, Ar*H*), 7.02 (d, *J*=2.35 Hz, 2H, Ar*H*), 7.13 (d, *J*=2.35 Hz, 2H, Ar*H*); ^{13}C NMR (75 MHz, CHLOROFORM-*d*) δ ppm 9.85 (2 x $CH_2CH_2CH_3$), 10.66 ($CH_2CH_2CH_3$), 10.82 ($CH_2CH_2CH_3$), 23.03 (2 x $CH_2CH_2CH_3$), 23.35 ($CH_2CH_2CH_3$), 23.57 ($CH_2CH_2CH_3$), 30.92 ($ArCH_2Ar$), 31.16 ($ArCH_2Ar$, $C(CH_3)_3$), 31.69 (2 x $C(CH_3)_3$), 33.54 ($C(CH_3)_3$), 34.08 (2 x $C(CH_3)_3$), 76.52 (OCH_2), 76.57 (OCH_2), 77.12 (OCH_2), 114.48 ($C_{Ar}Br$), 124.54 ($C_{Ar}H$), 125.03 ($C_{Ar}H$), 126.18 ($C_{Ar}H$), 130.21 ($C_{Ar}H$), 131.97 ($C_{Ar}CH_2$), 134.50 ($C_{Ar}CH_2$), 135.79 ($C_{Ar}CH_2$), 136.02 ($C_{Ar}CH_2$), 144.29 ($C_{Ar}C(CH_3)_3$), 144.80 (2 x $C_{Ar}C(CH_3)_3$), 152.74 ($C_{Ar}OCH_2$), 154.34 ($C_{Ar}OCH_2$), 154.82 (2 x $C_{Ar}OCH_2$); MS (ESI+): m/z (%) = 856 (100) $[M+NH_4]^+$; HRMS–Positive: *m/z* $[M+H]^+$ calcd for $C_{52}H_{75}NO_4Br$: 856.4874; found: 856.4863.

25 ,27-dipropoxycalix[4]arene – (2.17)

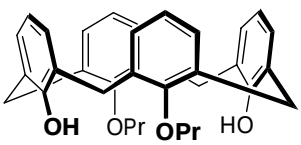

A three necked, oven dried flask under argon was charged with tripropyl calixarene **2.6** (1.10 g, 1.42 mmol), aluminum trichloride (5.16 g, 38.4 mmol, 27 eq) and dry toluene (100 ml). The mixture was stirred at RT for 4 hours, after which 1 M HCl (50 ml) was slowly added. The mixture was stirred at RT for a further 12 hours, after which the organic contents of the flask were extracted into EtOAc (3 x 50 ml), dried over $MgSO_4$ and the solvent removed under reduced pressure. Purification of the mixture was accomplished by column chromatography (PET:EtOAc 99:1 to 95:5). Rapid crystallisation was accomplished from an EtOH:DCM mixture, affording an opaque crystalline product. R_f = 0.47 (EtOAc:PET, 5:95); ^{1}H NMR (400 MHz, CHLOROFORM-*d*) δ ppm 1.34 (t, *J*=7.4 Hz, 6 H, CH_2CH_3), 2.05 – 2.15 (m, 4 H, $CH_2CH_2CH_3$), 3.40 (d, *J*=12.9 Hz, 4 H, $ArCH_2Ar$), 4.00 (t, *J*=6.2 Hz, 4 H, OCH_2CH_2), 4.35 (d, *J*=12.9 Hz, 4 H, $ArCH_2Ar$), 6.67 (t, *J*=7.4 Hz, 2 H, Ar*H*), 6.76 (t, *J*=7.6 Hz, 3 H, Ar*H*), 6.94 (d, *J*=7.6 Hz, 4 H, Ar*H*), 7.08 (d, *J*=7.4 Hz, 4 H, Ar*H*), 8.33 (s, 2 H, ArO*H*): ^{13}C NMR (101 MHz, CHLOROFORM-*d*) δ ppm 10.91 (2 x CH_2CH_3), 23.49 (2 x $CH_2CH_2CH_3$), 31.42 (4 x $ArCH_2Ar$), 78.30 (2 x OCH_2CH_3), 118.92 ($C_{Ar}H$), 125.26 ($C_{Ar}H$), 128.13 ($C_{Ar}CH_2$), 128.38 ($C_{Ar}H$), 128.88 ($C_{Ar}H$), 133.47 ($C_{Ar}CH_2$), 151.86 (2 x $C_{Ar}O$), 153.34 (2 x $C_{Ar}O$).

11,17,23-tri-*tert*-butyl-5-((*S*)-1-hydroxyl-3-methylbutyl)- 25,26,27,28-tetrapropoxycalix[4]areneamide – (2.19)

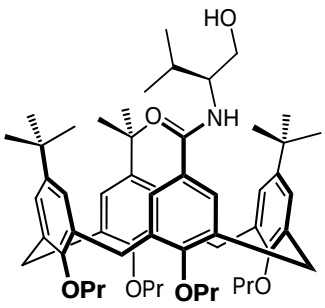

Carboxy calixarene **2.2** (0.82 g, 1.02 mmol) was added to a round-bottom flask (50 ml) fitted with a reflux condenser under an atmosphere of nitrogen. Freshly distilled thionyl chloride (5 mL, 69 mmol, 68 eq) was added, the flask stirred for 10 minutes at RT, after which it was brought to reflux for 1.75 hours. The solvent was then removed under reduced pressure, after which the flask was placed under high vacuum for half an hour. The contents of the flask were then taken up dry dichloromethane (10 ml) and slowly added at 0 ºC to a stirred mixture of L-valinol (133 mg, 1.32 mmol), triethyl amine (0.3 mL, 2.2 mmol, 1.1 eq) in dry DCM (5 ml) under nitrogen. The mixture was warmed to RT and left to stir overnight, after which a further portion of dichloromethane (50 ml) was added to the flask along with saturated sodium bicarbonate solution (20 ml). The layers were separated and the aqueous layer extracted with dichloromethane (5 x 40 ml), the organic layers combined, dried over $MgSO_4$, and the solvent removed under reduced pressure. Purification was achieved by silica gel chromatography using a gradient elution of PET and EtOAc (1:99 to 50:50) to yield amide calixarene **2.19** (0.81 g, 0.91 mmol, 89 %) Rf = 0.26 (EtOAc:PET, 25:75); ^{1}H NMR (CHLOROFORM-*d*, 400MHz): δ ppm 0.72 (s, 9H, C(C*H*$_3$)$_3$), 0.91 – 0.97 (m, 12H, CH$_2$C*H*$_3$, CH(C*H*$_3$)$_2$), 1.09 – 1.13 (m, 6H, CH$_2$C*H*$_3$), 1.33 (s, 9H, C(C*H*$_3$)$_3$), 1.34 (s, 9H, C(C*H*$_3$)$_3$), 1.85 – 1.97 (m, 5H, CH$_2$C*H*$_2$CH$_3$, C*H*(CH$_3$)$_2$), 1.99 – 2.14 (m, 4H, CH$_2$C*H*$_2$CH$_3$), 3.13 (d, *J*=9.24 Hz, 2H, ArC*H*$_2$Ar), 3.17 (d, *J*=9.10 Hz, 2H, ArC*H*$_2$Ar), 3.58 – 3.74 (m, 7H, OC*H*$_2$CH$_2$, OC*H*$_2$CHN, OCH$_2$C*H*N), 3.92 – 4.06 (m, 4H, OC*H*$_2$CH$_2$), 4.43 (d, *J*=8.95 Hz, 2H, ArC*H*$_2$Ar), 4.48 (d, *J*=8.80 Hz, 2H, ArC*H*$_2$Ar), 5.8 (d, *J*=7.04 Hz, 1H, N*H*), 6.27 (s, 2H, Ar*H*), 6.93 (d, *J*=2.35 Hz, 1H, Ar*H*), 6.97 (d, *J*=2.35 Hz, 1H, Ar*H*), 7.07 – 7.11 (m, 4H, Ar*H*); ^{13}C NMR (75 MHz, CHLOROFORM-*d*) δ ppm 9.86 (CH$_2$*C*H$_3$), 9.88 (CH$_2$*C*H$_3$), 10.61 (CH$_2$*C*H$_3$), 10.79 (CH$_2$*C*H$_3$), 18.84 (CH(*C*H$_3$)$_2$), 19.52 (CH(*C*H$_3$)$_2$), 23.05 (CH$_2$*C*H$_2$CH$_3$), 23.07 (CH$_2$*C*H$_2$CH$_3$), 23.35 (CH$_2$*C*H$_2$CH$_3$), 23.54 (CH$_2$*C*H$_2$CH$_3$), 29.24 (*C*H(CH$_3$)$_2$), 31.01 (Ar*C*H$_2$Ar), 31.08 (C(*C*H$_3$)$_3$), 31.15 (Ar*C*H$_2$Ar), 31.17 (Ar*C*H$_2$Ar), 31.71 (C(*C*H$_3$)$_3$), 33.37 (*C*(CH$_3$)$_3$), 34.05 (*C*(CH$_3$)$_3$), 34.07 (*C*(CH$_3$)$_3$), 57.72 (CH$_2$*C*HN), 64.57 (CH*C*H$_2$OH), 76.52 (O*C*H$_2$CH$_2$), 76.57 (O*C*H$_2$CH$_2$), 77.08 (O*C*H$_2$CH$_2$), 77.43 (O*C*H$_2$CH$_2$), 124.45 (*C*$_{Ar}$H), 124.60 (*C*$_{Ar}$H), 124.93 (*C*$_{Ar}$H), 125.01 (*C*$_{Ar}$H), 126.15 (*C*$_{Ar}$H), 126.18 (*C*$_{Ar}$H), 126.35 (*C*$_{Ar}$H), 126.63 (*C*$_{Ar}$H), 127.24 (*C*$_{Ar}$CNO), 132.08 (*C*$_{Ar}$CH$_2$), 132.14 (*C*$_{Ar}$CH$_2$), 134.08 (*C*$_{Ar}$CH$_2$), 134.48 (*C*$_{Ar}$CH$_2$), 134.53 (*C*$_{Ar}$CH$_2$), 135.89 (*C*$_{Ar}$CH$_2$), 135.94 (*C*$_{Ar}$CH$_2$), 144.00 (*C*$_{Ar}$C(CH$_3$)$_3$), 144.82 (*C*$_{Ar}$C(CH$_3$)$_3$), 144.85 (*C*$_{Ar}$C(CH$_3$)$_3$), 152.78 (*C*$_{Ar}$O), 154.75 (*C*$_{Ar}$O), 158.46 (*C*$_{Ar}$O), 167.61 (C$_{Ar}$*C*ON).

11,17,23-tri-*tert*-butyl-5-((*S*)-4-isopropyl-4,5-dihydrooxazol-2-yl)- 25,26,27,28-tetrapropoxycalix[4]arene – (2.1)

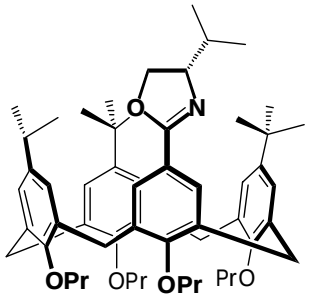

Carboxyl calixarene **2.2** (1.59 g, 1.92 mmol) and freshly distilled thionyl chloride (5 ml, 69 mmol, 36 eq) were added to a 2 necked round-bottom flask (50 ml) fitted with a reflux condenser. The solution was stirred under argon for 10 minutes at RT, thereafter it was brought to reflux for 1.75 hours. The remaining thionyl chloride was removed under reduced pressure, while maintaining inert conditions, affording an orange solid. The solid was dissolved in dry DCM (10 ml) and the solvent again removed under reduced pressure, followed by high vacuum drying (to remove residual traces of thionyl chloride). The contents of the flask were then taken up in dry dichloromethane (15 ml) and slowly added to a mixture of L-valinol (290 mg, 2.9 mmol, 1.5 eq), triethyl amine (1.2 ml, 9 mmol, 4.7 eq) in dry DCM (10 ml) at 0 ºC under a positive pressure of argon. The solution was then allowed to warm to RT and left to stir overnight. The contents of the flask were taken up in additional DCM (50 ml) and washed with sodium bicarbonate solution (20 ml). The aqueous layer was extracted with DCM (3 × 100 ml), the organic layers combined, dried over $MgSO_4$ and the solvent removed under reduced pressure yielding a light orange solid. The solid was dried under high vacuum following which it was taken up in dry DCM (15 ml) and transferred to a dry reaction vessel (25 ml) under argon. Thionyl chloride (2 ml, 28 mmol, 14 eq) was added to the flask and it was stirred for 12 hours at RT. Water was cautiously added to the vessel until frothing ceased, following which sodium bicarbonate solution (30 ml) and additional DCM (50 ml) was added to the flask. Upon separation of the layers the aqueous phase was extracted with DCM (3 × 100 ml), the organic layers combined, dried over $MgSO_4$ and the solvent removed under reduced pressure. Purification was achieved by silica gel chromatography (EtOAc:PET 1:99 to 20:80) yielding a white solid (1.62 g, 1.86 mmol, 94 % yield). Mp 178 °C (EtOH); $[\alpha]_D^{18.3}$ = – 17.0° (*c* 0.010, DCM); R_f = 0.70 (EtOAc:PET, 10:90); IR (film): 2960 (s, CH), 1652 (s, C=N), 1481 cm^{-1} (s, C=C); ^{1}H NMR (400MHz, CHLOROFORM-*d*): δ ppm 0.75 (s, 9H, C(C*H*$_3$)$_3$), 0.83 (d, *J*=6.64 Hz, 3H, CH(C*H*$_3$)$_2$), 0.91 – 1.00 (m, 9H, CH$_2$C*H*$_3$, CH(C*H*$_3$)$_2$), 1.07 (t, *J*=6.84 Hz, 3H, CH$_2$C*H*$_3$), 1.04 – 1.13 (t, *J*=6.93 Hz, 3H, CH$_2$C*H*$_3$), 1.33 (s, 9H, C(C*H*$_3$)$_3$), 1.33 (s, 9H, C(C*H*$_3$)$_3$), 1.62 (m, 1H, C*H*(CH$_3$)$_2$), 1.85 – 1.98 (m, 4H, CH$_2$C*H*$_2$CH$_3$), 1.99 – 2.13 (m, 4H, CH$_2$C*H*$_2$CH$_3$), 3.09 – 3.20 (m, 4H, ArC*H*$_2$Ar), 3.67 – 3.83 (m, 6H, OC*H*$_2$CH$_2$, OC*H*$_2$CHN, OCH$_2$C*H*N), 4.18 (m, 1H, OC*H*$_2$CHN), 4.43 (m, 4H, ArC*H*$_2$Ar), 6.3 (d, *J*=1.76 Hz, 2H, Ar*H*), 7.04 (d, *J*=1.95 Hz, 1H, Ar*H*), 7.07 (m, 3H, Ar*H*), 7.12 (d, *J*=2.93 Hz, 2H, Ar*H*); ^{13}C NMR (75 MHz, CHLOROFORM-*d*) δ ppm 9.91 (CH$_2$*C*H$_3$), 9.92 (CH$_2$*C*H$_3$), 10.63 (CH$_2$*C*H$_3$), 10.77 (CH$_2$*C*H$_3$), 18.54 (CH(*C*H$_3$)$_2$), 19.39 (CH(*C*H$_3$)$_2$), 23.06 (CH$_2$*C*H$_2$CH$_3$), 23.12 (CH$_2$*C*H$_2$CH$_3$), 23.36 (CH$_2$*C*H$_2$CH$_3$), 23.54

($CH_2CH_2CH_3$), 30.77 (ArCH_2Ar), 30.87 (ArCH_2Ar), 30.93 (C(CH_3)$_3$), 31.08 (ArCH_2Ar), 31.13 (ArCH_2Ar), 31.64 (2 × C(CH_3)$_3$), 33.23 (2 × C(CH_3)$_2$), 33.34 (C(CH_3)$_2$), 34.05 (CH(CH_3)$_2$), 70.09 (OCH_2CHN), 72.80 (OCH$_2$$CH$N), 76.51 (O$CH_2CH_2$), 76.58(O$CH_2CH_2$), 77.00 (O$CH_2CH_2$),77.21 (O$CH_2CH_2$), 121.57 ($C$CNO), 124.32 ($C_{Ar}$H), 124.79 ($C_{Ar}$H), 125.40 ($C_{Ar}$H), 125.45 ($C_{Ar}$H), 125.80 ($C_{Ar}$H), 125.86 ($C_{Ar}$H), 127.64 ($C_{Ar}CH_2$), 128.00 ($C_{Ar}CH_2$), 132.13 ($C_{Ar}$H), 132.31 ($C_{Ar}$H), 133.55 ($C_{Ar}CH_2$), 133.66 ($C_{Ar}CH_2$), 134.71 ($C_{Ar}CH_2$), 134.83 ($C_{Ar}CH_2$), 135.59 ($C_{Ar}CH_2$), 135.69 ($C_{Ar}CH_2$), 143.84 ($C$C($CH_3$)$_3$), 144.63 ($C$C($CH_3$)$_3$), 144.71 ($C$C($CH_3$)$_3$), 152.82 ($C_{Ar}$OPr), 154.69 (C$COCH_2$, C$COCH_2$), 157.95 ($C_{Ar}$OPr), 163.19 (C$C$NO); MS (ES+): *m/z* (%) = 872.6 (100) $[M+H]^+$; HRMS–TOF MS ES+: *m/z* $[M+H]^+$ calcd for $C_{58}H_{82}NO_5$: 872.6193; found: 872.6118.

9.3 Chapter 3

(*cR*)-11,17,23-tri-*tert*-butyl-4-((*S*)-2-(1-(dimethylamino)-furan-3(1H)-ylideneamino)-3-methylbutan-1-ol)- 25,26,27,28-tetrapropoxycalix[4]arene – (3.7)

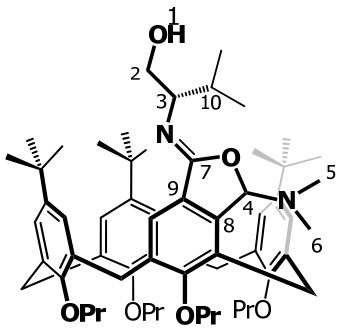

An oven dried Schlenk flask (10 ml) was placed under vacuum (0.5 mm Hg) and repeatedly flushed with nitrogen, after which the flask was charged with oxazoline calixarene **2.1** (166 mg, 0.19 mmol). Further drying was achieved by solvating the solid with the minimum volume of dry THF, followed by removal of the solvent under reduced pressure and heating the flask to 90 ºC under vacuum, this process was repeated three times. Freshly distilled dried Et_2O (1 ml), TMEDA (0.12 ml, 1.14 mmol, 6 eq) were introduced and the flask cooled to –40 ºC after which *s*BuLi (0.8 ml, 0.95 mmol, 5 eq) was slowly introduced. The flask was stirred at this temperature for 4.5 hours after which dry DMF (1.5 ml, 20 mmol, 105 eq) was introduced and the flask allowed to warm to RT overnight. Saturated NH_4Cl solution (5 ml) was added and the organic components extracted with EtOAc (50 ml). The organic layer was dried over $MgSO_4$ and the solvent removed under reduced pressure. The product was separated via silica gel column chromatography (40 mg, 0.042 mmol, 22 %); IR (film) /cm^{-1}: 3338 (OH stretch) 2961 (CH stretch), 1687(C=N stretch); ^{1}H NMR (600 MHz, BENZENE-d_6, 50 ºC) δ ppm 0.85 – 1.00 (m, 15 H, CH_2CH_3, CH(CH_3)$_2$), 1.10 (d, *J*=6.4 Hz, 3 H, CH(CH_3)$_2$), 1.20 (d, *J*=8.2 Hz, 27 H, C(CH_3)$_3$), 1.87 – 1.97 (m, 4 H, $CH_2CH_2CH_3$), 1.98 – 2.09 (m, 4 H, $CH_2CH_2CH_3$), 2.24 (br. s., 6 H, (atom 5, 6) N(CH_3)$_2$), 2.93 – 2.99 (m, 1 H, (atom 10) CH(CH_3)), 3.00 – 3.05 (m, 1 H, (atom 3) NCHCH$_2$), 3.19 – 3.28 (m, 3 H, ArCH_2Ar), 3.74 – 3.81 (m, 1 H, OCH_2CH$_2$), 3.83 – 4.01 (m, 8 H, OCH_2CH$_2$, ArCH_2Ar), 4.16 (br. s., 2 H, (atom 2) HOCH_2CH), 4.46 (d, *J*=13.0 Hz, 1 H, ArCH_2Ar), 4.56 (d, *J*=12.6 Hz, 1 H, ArCH_2Ar), 4.59 – 4.63 (m, 2 H, ArCH_2Ar), 5.48 (s, 1 H, (atom 4) NCHO), 5.69

(br. s., 1 H, (atom 1) *H*OCH$_2$), 6.87 – 6.90 (m, 2 H, Ar*H*), 6.92 (d, *J*=2.2 Hz, 1 H, Ar*H*), 6.98 – 7.01 (m, 3 H, Ar*H*), 7.61 (s, 1 H, Ar*H*); ^{13}C NMR (CHLOROFORM-*d*, 75.5MHz, 25°C): δ ppm 10.14 (CH$_2$*C*H$_3$), 10.28 (CH$_2$*C*H$_3$), 10.3 (CH$_2$*C*H$_3$), 10.39 (CH$_2$*C*H$_3$), 20.07 (CH(*C*H$_3$)$_2$), 21.48 (CH(*C*H$_3$)$_2$), 22.91 (CH$_2$*C*H$_2$CH$_3$), 23.09 (CH$_2$*C*H$_2$CH$_3$), 23.36 (CH$_2$*C*H$_2$CH$_3$), 26.43 (Ar*C*H$_2$Ar / CHCH(CH3)2), 26.49 (Ar*C*H$_2$Ar / CH*C*H(CH$_3$)$_2$), 31.05 (Ar*C*H$_2$Ar), 31.21 (Ar*C*H$_2$Ar), 31.3 (Ar*C*H$_2$Ar), 31.4 (C(*C*H$_3$)$_3$), 31.43 (C(*C*H$_3$)$_3$), 31.45 (C(*C*H$_3$)$_3$), 33.67 (*C*(CH$_3$)$_3$), 33.76 (*C*(CH$_3$)$_3$), 33.81 (*C*(CH$_3$)$_3$), 63.47 (atom 2), 65.73 (atom 3), 76.72 (O*C*H$_2$CH$_2$), 76.84 (O*C*H$_2$CH$_2$), 77.07 (O*C*H$_2$CH$_2$), 77.21 (O*C*H$_2$CH$_2$), 83.39 (atom 4), 122.62 (*C*$_{Ar}$H), 123.8 (*C*$_{Ar}$H), 124.44 (*C*$_{Ar}$H), 124.73 (*C*$_{Ar}$H), 125.23 (*C*$_{Ar}$H), 125.51 (*C*$_{Ar}$H), 125.91 (*C*$_{Ar}$H); 126.25 (atom 8 *C*$_{Ar}$), 132 (*C*$_{Ar}$CH$_2$), 132.1 (*C*$_{Ar}$CH$_2$), 132.28 (*C*$_{Ar}$CH$_2$), 133.64 (*C*$_{Ar}$CH$_2$), 134.06 (*C*$_{Ar}$CH$_2$), 134.12 (*C*$_{Ar}$CH$_2$), 134.23 (*C*$_{Ar}$CH$_2$), 137.26 (*C*$_{Ar}$CH$_2$), 139.98 (atom 9 *C*$_{Ar}$CON), 144.05 (*C*$_{Ar}$C(CH$_3$)$_3$), 144.51 (*C*$_{Ar}$C(CH$_3$)$_3$), 144.55 (*C*$_{Ar}$C(CH$_3$)$_3$), 153.66 (*C*$_{Ar}$OCH$_2$), 153.85 (*C*$_{Ar}$OCH$_2$), 153.88 (*C*$_{Ar}$OCH$_2$), 160.9 (*C*$_{Ar}$OCH$_2$), 170.05 (atom 7); MS (ESI+): m/z (%) = 967 (10) [M+Na]+; HRMS–ES+: m/z [M+H]+ calcd for $C_{61}H_{89}N_2O_6$: 945.6721; found: 945.6729.

(*cR*)-11,17,23-tri-*tert*-butyl-4-formyl-5-((*S*)-4-isopropyl-4,5-dihydrooxazol-2-yl)- 25,26,27,28-tetrapropoxycalix[4]arene – (3.8)

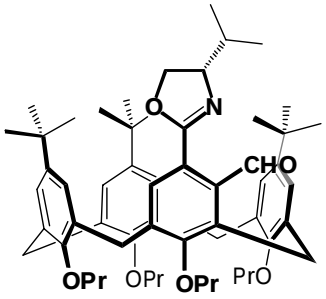

Formyl oxazoline **3.8** was synthesised in a procedure analogous to **3.8** from oxazoline calixarene **2.1** (50 mg, 0.057 mmol), TMEDA (0.684 mmol, 12 eq), *c*PentLi (0.344 mmol, 6 eq) and Et$_2$O (0.5 ml), with a reaction time of 30 hours at –78ºC. Freshly distilled DMF (0.1 ml, 18 eq) was added at –78 ºC, after which the reaction mixture was allowed to warm to RT, followed by stirring for 12 hours. Distilled water (5 ml) was then added and the mixture extracted into EtOAc (2 x 20 ml), the organic layers combined, dried over MgSO$_4$ and the solvent removed under reduced pressure affording a pale yellow solid (65 mg). MS (ESI+): m/z (%) = 918.61 (10) [M+H$_3$O]$^+$.

(*cR*)-11,17,23-tri-*tert*-butyl-4-methyl-5-((*S*)-4-isopropyl-4,5-dihydrooxazol-2-yl)- 25,26,27,28-tetrapropoxycalix[4]arene – (3.9)

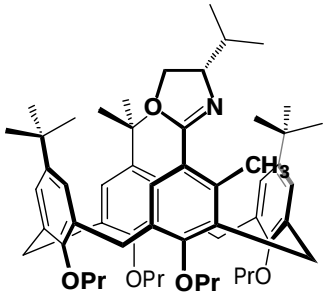

Methyl oxazoline **3.9** was synthesised according to the general procedure used to synthesise **3.7** from oxazoline calixarene **2.1** (95 mg, 0.11 mmol), *s*BuLi (0.33 ml, 0.33 mmol, 3 eq), TMEDA (0.1 ml, 0.66 mmol, 6eq) and diethyl ether (0.4 ml) with a reaction time of 3.75 hours at -45 ºC. Methyl iodide (0.1 ml, 1.6 mmol, 14 eq) was introduced at –45 ºC and the flask allowed to reach RT overnight with rapid stirring of the mixture. The same workup procedure employed for **3.7** was used, however it

was not possible to separate the methylated product **3.9** from the starting material **2.1**. R_f = 0.70 (EtOAc:PET, 10:90); MS (ESI+): m/z (%) = 886.64 (10) [M+H]+; HRMS–ES+: m/z [M+H]+ calcd for $C_{59}H_{84}NO_5$: 886.6349; found: 886.6367.

(*cR*)-11,17,23-tri-*tert*-butyl-4-fluoro-5-((*S*)-4-isopropyl-4,5-dihydrooxazol-2-yl)- 25,26,27,28-tetrapropoxycalix[4]arene – (3.10)

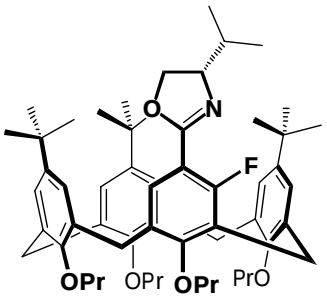

A hot oven dried Schlenk flask (10 ml) equipped with magnetic stirrer was cycled between high vacuum and argon according to standard Schlenk techniques. The flask was charged with *c*PentLi in pentane solution (0.26 ml, 0.34 mmol, 6 eq) and the pentane removed under reduced pressure affording a viscous white material. To a separate dry Schlenk flask **2.1** (50 mg, 0.057 mmol) and dry Et_2O (1 ml) were added. The Et_2O was then removed under reduced pressure with gentle heating after which the flask was placed under high vacuum and heated for 20 minutes. The solvation with Et_2O – evacuation process was repeated three times following which dried Et_2O (0.4 ml) and TMEDA (0.10 ml, 0.69 mmol, 12 eq) were added to the flask. The flask was cooled to 0 ºC, and its contents taken up in an oven dried gas tight syringe and slowly added to the Schlenk flask containing the lithium reagent at –78 ºC. The flask was sealed and the reaction stirred for 30 hours at –78 ºC while careful temperature control was maintained. *N*-fluorobenzenesulfonimide (215 mg, 0.68 mmol, 12 eq) was added to the stirred flask at –78 ºC under positive argon pressure, cooling was ceased and the flask was allowed to slowly warm to RT over approximately 2 hours. The flask was held at RT for 12 hours following which distilled water (2 ml) was added and the mixture stirred for 15 minutes. The contents of the vessel were transferred to a separating funnel along with a further portion of water (20 ml) and its organic contents extracted with EtOAc (2 × 60 ml), dried over $MgSO_4$, and the solvent removed under reduced pressure. The crude solution was suspended in DCM and filtered through sintered glass to remove residual *N*-fluorobenzenesulfonamide. ^{1}H and ^{19}F NMR was performed on the crude mixture to determine the diastereomeric ratio (27:1) and yield according to ^{1}H NMR (78 %). Further purification of the product was achieved by silica gel column chromatography (EtOAc:PET 2:98) affording a opaque gum (37 mg, 0.042 mmol, 73% yield). Mp 172–181°C (EtOH); $[\alpha]_D^{17.9}$ = –7.1° (*c* 0.011 g/ml, DCM); R_f = 0.42 (PET:EtOAc, 92:8); IR (film) cm^{-1}: 2961 (s, CH), 1652 (s, C=N), 1481 (s, C=C); ^{1}H NMR (300 MHz, CHLOROFORM-*d*) δ ppm 0.79 (s, 9 H, C(C*H*$_3$)$_3$), 0.85 (d, *J*=6.7 Hz, 3 H, CH(C*H*$_3$)$_2$), 0.89 – 0.99 (m, 9 H, CH(C*H*$_3$)$_2$, CH$_2$C*H*$_3$), 1.00 – 1.12 (m, 6 H, CH$_2$C*H*$_3$), 1.24 (s, 9 H, C(CH$_3$)$_3$), 1.27 (s, 9 H, C(CH$_3$)$_3$), 1.65 – 1.77 (m, 1 H, C*H*(CH$_3$)$_2$), 1.84 – 2.11 (m, 8 H, CH$_2$C*H*$_2$CH$_3$), 3.08 – 3.18(m, 3 H, ArC*H*$_2$Ar), 3.45 (dd, *J*=12.9, 1.6 Hz, 1 H, ArC*H*$_2$Ar), 3.66 –

4.06 (m, 10 H, OC*H*$_2$CH$_2$, OC*H*$_2$CHN, OCH$_2$C*H*N), 4.15 – 4.25 (m, 2 H, ArC*H*$_2$Ar, OC*H*$_2$CHN), 4.35 – 4.48 (m, 3 H, ArC*H*$_2$Ar), 6.34 (d, *J*=2.5 Hz, 1 H, Ar*H*), 6.40 (d, *J*=2.5 Hz, 1 H, Ar*H*), 6.98 – 7.03 (m, 3 H, Ar*H*), 7.09 – 7.13 (m, 1 H, Ar*H*), 7.15 (d, *J*=8.5 Hz, 1 H, Ar*H*); ^{13}C NMR (75 MHz, CHLOROFORM-*d*) δ ppm 9.92 (CH$_2$*C*H$_3$), 10.06 (CH$_2$*C*H$_3$), 10.47 (CH$_2$*C*H$_3$), 10.69 (CH$_2$*C*H$_3$), 18.31 (CH(*C*H$_3$)$_2$, 19.04 (CH(*C*H$_3$)$_2$), 22.93 (CH$_2$*C*H$_2$CH$_3$), 23.21 (CH$_2$*C*H$_2$CH$_3$), 23.24 (CH$_2$*C*H$_2$CH$_3$), 23.50 (CH$_2$*C*H$_2$CH$_3$), 26.36 (Ar*C*H$_2$Ar), 30.15 (Ar*C*H$_2$Ar), 30.99 (C(*C*H$_3$)$_3$), 31.20 (Ar*C*H$_2$Ar), 31.48 (C(*C*H$_3$)$_3$), 31.57 (C(*C*H$_3$)$_3$), 31.57 (Ar*C*H$_2$Ar) 33.01 (*C*(CH$_3$)$_3$), 33.44 (*C*(CH$_3$)$_3$), 33.95 (*C*H(CH$_3$)$_2$), 34.01 (*C*(CH$_3$)$_3$), 69.23 (CH$_2$*C*HN), 72.81 (O*C*H$_2$CHN), 76.46 (O*C*H$_2$CH$_2$), 76.84 (O*C*H$_2$CH$_2$), 76.93 (O*C*H$_2$CH$_2$), 77.20 (O*C*H$_2$CH$_2$), 110.18 (d, 11.8 Hz, CF*C*$_{Ar}$CH$_2$), 122.88 (d, 15.5 Hz, (CF*C*CON)), 124.64 (*C*$_{Ar}$H), 124.66 (*C*$_{Ar}$H), 125.21 (*C*$_{Ar}$H), 125.73 (*C*$_{Ar}$H), 125.94 (*C*$_{Ar}$H), 126.86 (d, 5.2 Hz, *C*$_{Ar}$H), 129.41 (*C*$_{Ar}$CH$_2$), 129.44 (*C*$_{Ar}$H), 132.11 (*C*$_{Ar}$CH$_2$), 132.44 (*C*$_{Ar}$CH$_2$), 132.88 (*C*$_{Ar}$CH$_2$), 133.98 (*C*$_{Ar}$CH$_2$), 134.83 (*C*$_{Ar}$CH$_2$), 135.41 (*C*$_{Ar}$CH$_2$), 144.07 (*C*C(CH$_3$)$_3$), 144.16 (*C*C(CH$_3$)$_3$), 144.71 (*C*C(CH$_3$)$_3$), 153.05 (*C*OCH$_2$), 154.40 (*C*OCH$_2$), 154.51 (*C*OCH$_2$), 158.41 (d, 257Hz, *C*F), 159.69 (d, 7.4 Hz, C*C*OCH$_2$), 159.95(d, 5.9 Hz, C*C*NO); ^{19}F NMR (400 MHz, CHLOROFORM-*d*) δ ppm -113.29 (C*F*), -114.25 (diastereomer-5a C*F*); MS (ES+): *m/z* (%) = 890.6 (100) [M+H]$^+$; HRMS–TOF MS ES+: *m/z* [M+H]$^+$ calcd for $C_{58}H_{81}FNO_5$: 890.6099; found: 890.6096.

11,17,23-tri-*tert*-butyl-5-(2,2-dimethyl-propan-1-one)- 25,26,27,28-tetrapropoxycalix[4]arene – (3.13) and 11,17,23-tri-*tert*-butyl-5-((4S)-2-tert-butyl-4-isopropyl-2-oxazolidine)-25,26,27,28-tetrapropoxycalix[4]arene – (3.12)

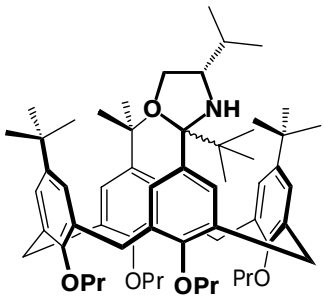

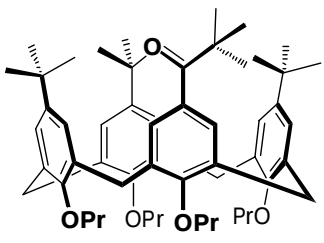

*t*BuLi addition products **3.13** and **3.12** were synthesised in a procedure analogous to **3.7** from oxazoline calixarene **2.1** (138.4 mg, 0.159 mmol), TMEDA (0.16 ml, 1 mmol, 6.3 eq), *t*BuLi (0.636 mmol, 4 eq) and Et$_2$O (0.7 ml), with a reaction time of 1.5 hours at –45 ºC. Freshly distilled DMF (1.5 ml, 19.5 mmol, 120 eq) was added at –45 ºC, after which the reaction mixture was allowed to warm to RT, followed by stirring for 12 hours. Distilled water (5 ml) was then added and the mixture extracted into EtOAc (2 x 20 ml), the organic layers combined, dried over MgSO$_4$ and the solvent removed under reduced pressure. Purification of the mixture was achieved using silica gel column chromatography (PET:EtOAc 99:1) affording a pale yellow solid (120 mg, ~ 0.129 mmol, 81 %). Further purification was achieved by crystallisation from an EtOH DCM mixture, however isolation of either one of these compounds (**3.13** or **3.12**) was not possible. ^{13}C NMR (75 MHz, CHLOROFORM-*d*) δ ppm 9.79, 9.96, 10.04, 10.47, 10.61, 10.77, 18.82, 19.63, 20.50, 21.21, 22.68, 22.74, 23.16, 23.19, 23.33, 23.46, 23.53, 26.23,

28.64, 29.70, 31.00, 31.06, 31.15, 31.24, 31.28, 31.41, 31.55, 31.61, 31.77, 32.89, 33.57, 33.97, 34.02, 37.40, 38.58, 43.57, 63.68, 66.45, 68.53, 69.85, 76.00, 76.70, 77.07, 77.21, 77.42, 102.95, 103.92, 124.18, 124.29, 124.42, 124.56, 124.72, 124.77, 125.31, 125.89, 127.92, 128.54, 129.05, 129.41, 130.38, 131.89, 132.08, 132.42, 132.46, 132.73, 133.78, 133.98, 134.25, 134.62, 134.71, 135.12, 135.36, 135.53, 136.70, 143.80, 143.93, 144.18, 144.37, 144.64, 152.73, 152.80, 152.91, 153.09, 154.31, 154.70, 154.80, 155.92, 156.25, 158.67, 205.06; MS (ES+): *m/z* (%) = 930.6 (100) $[M1+H]^+$, 888.6 (70). $[M2+H]^+$; HRMS–TOF MS ES+: *m/z* $[M+H]^+$ calcd for $C_{62}H_{92}NO_5$: 930.6976; found: 930.6959.

11,17,23-tri-*tert*-butyl-5-(2,2-dimethyl-propan-1-one)- 25,26,27,28-tetrapropoxycalix[4]arene – (3.13)

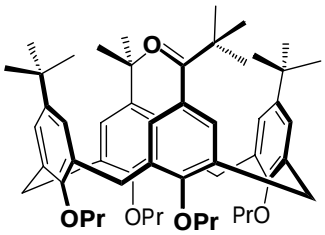

A mixture of **3.13** and **3.12** (46 mg), were suspended in an acetone (4 ml), water (1 ml) and conc. HCl (1 ml) mixture and stirred overnight at RT. Thereafter EtOAc (20 ml) was added, and layers separated, the organic phase dried over $MgSO_4$ and the solvent removed under reduced pressure. Purification of 3.13 was accomplished by crystallisation from DCM and MeCN afforded white crystals (30 mg). MP (EtOH/DCM) = 154 – 176°C; IR (ATR) cm^{-1}: 2962 (m, –C–H stretch), 1667 (s, C=O stretch), 1478 (s, C=C stretch), 1124 (m, C–O stretch), 1009 (m, C–O stretch), 799 (s, C–H oop bend);^{1}H NMR (400 MHz, CHLOROFORM-*d*) δ ppm 0.83 (s, 9 H, $C(CH_3)_3$), 0.97 (t, *J*=7.5 Hz, 6 H, CH_2CH_3), 1.02 – 1.09 (m, 6 H, CH_2CH_3), 1.19 (s, 9 H, $C(CH_3)_3$), 1.23 (s, 18 H, $C(CH_3)_3$), 1.91 – 2.12 (m, 8 H, $CH_2CH_2CH_3$), 3.13 (d, *J*=10.9 Hz, 2 H, $ArCH_2Ar$), 3.16 (d, *J*=10.7 Hz, 2 H, $ArCH_2Ar$), 3.76 (t, *J*=7.2 Hz, 2 H, OCH_2CH_2), 3.80 (t, *J*=7.4 Hz, 2 H, OCH_2CH_2), 3.86 – 4.00 (m, 4 H, OCH_2CH_2), 4.43 (d, *J*=8.0 Hz, 2 H, $ArCH_2Ar$), 4.46 (d, *J*=8.0 Hz, 2 H, $ArCH_2Ar$), 6.47 (s, 2 H, Ar*H*), 6.95 (d, *J*=2.5 Hz, 2 H, Ar*H*), 6.99 (d, *J*=2.5 Hz, 2 H, Ar*H*), 7.25 (s, 2 H, Ar*H*); ^{13}C NMR (101 MHz, CHLOROFORM-*d*) δ ppm 10.04, 10.46, 10.61, 23.16, 23.33, 23.46, 28.64, 31.15, 31.24, 31.61, 33.58, 33.96, 43.58, 77.07, 77.21, 124.73, 124.77, 125.89, 129.41, 130.38, 132.74, 133.79, 133.98, 135.11, 144.19, 144.64, 153.10, 154.31, 158.67, 205.08; MS (ES+): m/z (%) = 845.6 (100) $[M+H]^+$.

9.4 Chapter 4

11,17,23-tri-*tert*-butyl-5-((*R*)-4-isopropyl-4,5-dihydrooxazol-2-yl)- 25,26,27,28-tetrapropoxycalix[4]arene – (4.1)

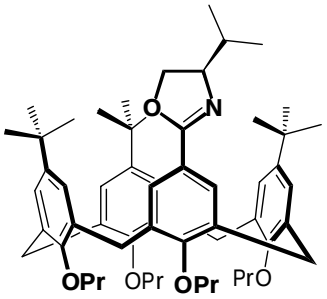

4.1 was synthesised using the general procedure used to synthesize oxazoline calixarene **2.1**. Carboxyl calixarene **2.2** (807 mg, 1 mmol), thionyl chloride (3 ml, 41 mmol, 41 eq), D-valinol (122 mg, 1.2 mmol, 1.2 eq) and triethylamine (0.5 ml, 3.6 mmol, 3.6 eq) in DCM (5 + 10 ml) and thionyl chloride (0.5 ml, 6.9 mmol, 6.9 eq) in DCM (10 ml) yielding a pale yellow solid (800 mg, 0.92 mmol, 92 % yield). Further purification was achieved by slow crystallisation from EtOH and DCM. Mp 179°C (EtOH); $[\alpha]_D^{18.0}$ = +18.0° (*c* 0.010, DCM); R_f = 0.70 (EtOAc:PET, 10:90); IR (film) cm^{-1}: 2961 (s, CH), 1651 (s, C=N), 1481 (s, C=C); ^{1}H NMR (400 MHz, CHLOROFORM-*d*) δ ppm 0.75 (s, 9 H, C(C*H*$_3$)$_3$), 0.83 (d, *J*=6.6 Hz, 3 H, CH(C*H*$_3$)$_2$), 0.92 – 1.00 (m, 9 H, CH(C*H*$_3$)$_2$, CH$_2$C*H*$_3$), 1.05 – 1.13 (m, 6 H, CH$_2$C*H*$_3$), 1.33 (s, 9 H, C(C*H*$_3$)$_3$), 1.33 (s, 9 H, C(C*H*$_3$)$_3$), 1.58 – 1.68 (m, 1 H, C*H*(CH$_3$)$_2$), 1.86 – 1.98 (m, 4 H, CH$_2$C*H*$_2$CH$_3$), 2.01 – 2.14 (m, 4 H, CH$_2$C*H*$_2$CH$_3$), 3.10 – 3.19 (m, 4 H, ArC*H*$_2$Ar), 3.67 – 3.75 (m, 4 H, OC*H*$_2$CH$_2$), 3.75 – 3.83 (m, 2 H, OCH$_2$C*H*N, OC*H*$_2$CHN), 3.91 – 4.03 (m, 4 H, OC*H*$_2$CH$_2$), 4.16 – 4.22 (m, 1 H, OC*H*$_2$CHN), 4.44 (d, *J*=12.9 Hz, 4 H, ArC*H*$_2$Ar), 6.30 (d, *J*=1.6 Hz, 2 H, Ar*H*), 7.04 (d, *J*=1.9 Hz, 1 H, Ar*H*), 7.06 – 7.10 (m, 3 H, Ar*H*), 7.12 (d, *J*=2.4 Hz, 2 H, Ar*H*); ^{13}C NMR (101 MHz, CHLOROFORM-*d*) δ ppm 9.91 (2 × CH$_2$*C*H$_3$), 10.63 (CH$_2$*C*H$_3$), 10.77 (CH$_2$*C*H$_3$), 18.56 (CH(*C*H$_3$)$_2$), 19.40 (CH(*C*H$_3$)$_2$), 23.06 (CH$_2$*C*H$_2$CH$_3$), 23.11 (CH$_2$*C*H$_2$CH$_3$), 23.35 (CH$_2$*C*H$_2$CH$_3$), 23.54 (CH$_2$*C*H$_2$CH$_3$), 30.77 (Ar*C*H$_2$Ar), 30.87 (Ar*C*H$_2$Ar), 30.93 (C(*C*H$_3$)$_3$), 31.08 (Ar*C*H$_2$Ar), 31.12 (Ar*C*H$_2$Ar), 31.64 (2 × C(*C*H$_3$)$_3$), 33.25 (2 × *C*(CH$_3$)$_3$), 33.33 (*C*(CH$_3$)$_3$), 34.05 (*C*H(CH$_3$)$_2$), 70.08 (O*C*H$_2$CHN), 72.85 (OCH$_2$*C*HN), 76.51 (O*C*H$_2$CH$_2$), 76.60 (O*C*H$_2$CH$_2$), 77.04 (O*C*H$_2$CH$_2$), 77.20 (O*C*H$_2$CH$_2$), 121.60 (*C*CNO), 124.31 (*C*$_{Ar}$H), 124.78 (*C*$_{Ar}$H), 125.40 (*C*$_{Ar}$H), 125.45 (*C*$_{Ar}$H), 125.79 (*C*$_{Ar}$H), 125.84 (*C*$_{Ar}$H), 127.62 (*C*$_{Ar}$CH$_2$), 127.97 (*C*$_{Ar}$CH$_2$), 132.13 (*C*$_{Ar}$CH), 132.30 (*C*$_{Ar}$CH), 133.52 (*C*$_{Ar}$CH$_2$), 133.64 (*C*$_{Ar}$CH$_2$), 134.71 (*C*$_{Ar}$CH$_2$), 134.84 (*C*$_{Ar}$CH$_2$), 135.59 (*C*$_{Ar}$CH$_2$), 135.68 (*C*$_{Ar}$CH$_2$), 143.85 (*C*C(CH$_3$)$_3$), 144.63 (*C*C(CH$_3$)$_3$), 144.70 (*C*C(CH$_3$)$_3$), 152.81 (*C*$_{Ar}$OPr), 154.69 (2 × C*C*OCH$_2$), 157.92 (*C*$_{Ar}$OPr), 163.15 (CC*N*O); MS (ES+): *m/z* (%) = 872.6 (100) $[M+H]^+$; HRMS–TOF MS ES+: *m/z* $[M+H]^+$ calcd for $C_{58}H_{82}NO_5$: 872.6193; found: 872.6172.

(*cS*)-11,17,23-tri-*tert*-butyl-4-fluoro-5-((*S*)-4-isopropyl-4,5-dihydrooxazol-2-yl)- 25,26,27,28-tetrapropoxycalix[4]arene – (4.2)

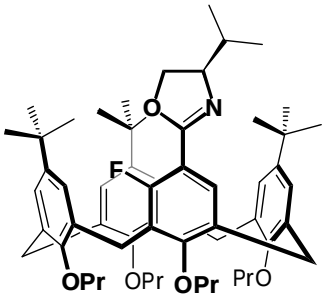

4.2 was prepared in a procedure analogous to that used for **3.10** from **4.1** (128 mg, 0.147 mmol), *c*PentLi (0.56 ml, 0.73 mmol, 5 eq), TMEDA (0.22 ml, 1.48 mmol, 10 eq), Et_2O (1 ml) and *N*-fluorobenzenesulfonimide (416 mg, 1.32 mmol, 9 eq) with a reaction time of 24 hours at –78 ºC. *dr*=1:30 (^{19}F NMR) (74% yield – ^{1}H NMR). Further purification of the product was achieved by silica gel column chromatography (EtOAc:PET 2:98) affording a opaque gum (82 mg, 0.92 mmol, 63% yield); $[\alpha]_D^{18.0}$ = +4.7° (*c* 0.013 g/ml, DCM); R_f = 0.42 (PET:EtOAc, 92:8); IR (film) cm^{-1}: 2961 (s, CH), 1645 (s, C=N), 1481 (s, C=C); ^{1}H NMR (400 MHz, CHLOROFORM-*d*) δ ppm 0.79 (s, 9 H, C(C*H*$_3$)$_3$), 0.85 (d, *J*=6.6 Hz, 3 H, CH(C*H*$_3$)$_2$), 0.91 – 0.99 (m, 9 H, CH$_2$C*H*$_3$, CH(C*H*$_3$)$_2$), 1.04 (t, *J*=7.5 Hz, 3 H, CH$_2$C*H*$_3$), 1.09 (t, *J*=7.4 Hz, 3 H, CH$_2$C*H*$_3$), 1.24 (s, 9 H, C(C*H*$_3$)$_3$), 1.27 (s, 9 H, C(C*H*$_3$)$_3$), 1.66 – 1.78 (m, 1 H, CHC*H*(CH$_3$)$_2$), 1.85 – 2.12 (m, 8 H, CH2C*H*$_2$CH$_3$), 3.09 – 3.18 (m, 3 H, ArC*H*$_2$Ar), 3.46 (dd, *J*=12.9, 1.4 Hz, 1 H, ArC*H*$_2$Ar), 3.67 – 4.05 (m, 10 H, OC*H*$_2$CH$_2$, OC*H*$_2$CHN, OCH$_2$C*H*N), 4.16 – 4.22 (m, 2 H, ArC*H*$_2$Ar, OC*H*$_2$CHN), 4.39 (d, *J*=12.7 Hz, 1 H, ArC*H*$_2$Ar), 4.44 (m, 2 H, ArC*H*$_2$Ar), 6.34 (d, *J*=2.4 Hz, 1 H, Ar*H*), 6.40 (d, *J*=2.4 Hz, 1 H, Ar*H*), 6.98 – 7.03 (m, 3 H, Ar*H*), 7.09 – 7.13 (m, 1 H, Ar*H*), 7.15 (d, *J*=8.4 Hz, 1 H, Ar*H*). ^{13}C NMR (101 MHz, CHLOROFORM-*d*) δ ppm 9.92 (CH$_2$*C*H$_3$), 10.06 (CH$_2$*C*H$_3$), 10.48 (CH$_2$*C*H$_3$), 10.69 (CH$_2$*C*H$_3$), 18.33 (CH(*C*H$_3$)$_2$), 19.05 (CH(*C*H$_3$)$_2$), 22.93 (CH$_2$*C*H$_2$CH$_3$), 23.22 (CH$_2$*C*H$_2$CH$_3$), 23.25 (CH$_2$*C*H$_2$CH$_3$), 23.51 (CH$_2$*C*H$_2$CH$_3$), 26.38 (Ar*C*H$_2$Ar), 30.15 (Ar*C*H$_2$Ar), 30.99 (C(*C*H$_3$)$_3$), 31.21 (Ar*C*H$_2$Ar), 31.48 (C(*C*H$_3$)$_3$), 31.57 (C(*C*H$_3$)$_3$), 31.64 (Ar*C*H$_2$Ar), 33.03 (*C*(CH$_3$)$_3$), 33.44 (*C*(CH$_3$)$_3$), 33.95 (*C*H(CH$_3$)$_2$), 34.02 (*C*(CH$_3$)$_3$), 69.24 (OCH$_2$*C*HN), 72.83 (O*C*H$_2$CHN), 76.46 (O*C*H$_2$CH$_2$), 76.84 (O*C*H$_2$CH$_2$), 76.93 (O*C*H$_2$CH$_2$), 77.48 (O*C*H$_2$CH$_2$), 110.18 (d, 11.8 Hz, (CF*C*$_{Ar}$CH$_2$)), 122.88 (d, 15.5 Hz, (CF*C*CNO)), 124.64 (*C*$_{Ar}$H), 124.66 (*C*$_{Ar}$H), 125.21 (*C*$_{Ar}$H), 125.73 (*C*$_{Ar}$H), 125.94 (*C*$_{Ar}$H), 126.86 (d, 5.2 Hz, *C*$_{Ar}$H), 129.41 (*C*$_{Ar}$H), 129.44 (*C*$_{Ar}$CH$_2$), 132.12 (*C*$_{Ar}$CH$_2$), 132.44 (*C*$_{Ar}$CH$_2$), 132.88 (*C*$_{Ar}$CH$_2$), 133.99 (*C*$_{Ar}$CH$_2$), 134.83 (*C*$_{Ar}$CH$_2$), 135.41 (*C*$_{Ar}$CH$_2$), 144.07 (*C*C(CH$_3$)$_3$), 144.15 (*C*C(CH$_3$)$_3$), 144.71 (*C*C(CH$_3$)$_3$), 153.05 (*C*$_{Ar}$OPr), 154.39 (*C*$_{Ar}$OPr), 154.52 (*C*$_{Ar}$OPr), 158.41 (d, 257Hz, *C*F), 159.69 (d, 7.4 Hz, C*C*OCH$_2$), 159.95 (d, 5.9 Hz, C*C*NO); ^{19}F NMR (400 MHz, CHLOROFORM-*d*) δ ppm −113.29 (C*F*), −114.25 (diastereomer-**4.3** C*F*); HRMS–TOF MS ES+: *m/z* $[M+H]^+$ calcd for $C_{58}H_{81}FNO_5$: 890.6099; found: 890.6096.

(*cR*)-11,17,23-tri-*tert*-butyl-5-((*S*)-4-isopropyl-4,5-dihydrooxazol-2-yl)-4-trimethylsilyl-25,26,27,28-tetrapropoxycalix[4]arene – (4.4)

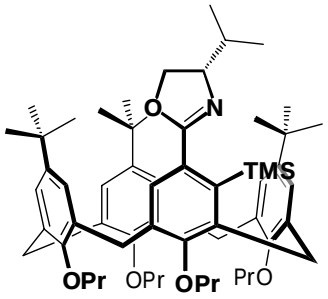

4.4 was prepared in a procedure analogous to that used for **3.10** from oxazoline **2.1** (59 mg, 0.068 mmol), *c*PentLi (0.17 ml, 0.22 mmol, 3.2 eq), TMEDA (0.060 ml, 0.41 mmol, 6 eq), Et_2O (0.45 ml) and freshly distilled trimethylsilyl chloride (0.1 ml, 0.79 mmol, 11.6 eq) with a reaction time of 14.5 hours at –78 ºC. Purification of the product was achieved by silica gel column chromatography (EtOAc:PET 1:99) affording a white solid (40 mg, 0.042 mmol, 62 % yield). Mp: 82–90°C (DCM); $[\alpha]_D^{18.5}$ = –26.8° (*c* 0.012 g/ml, DCM); R_f = 0.78 (PET:EtOAc, 92:8); IR (film) cm^{-1}: 2962 (s, CH), 1634 (s, C=N), 1480 (s, C=C), 1305 (m, C–Si); ^{1}H NMR (300 MHz, CHLOROFORM-*d*) δ ppm 0.09 (s, 9 H, Si(CH_3)$_3$), 0.84 (s, 9 H, C(CH_3)$_3$), 0.88 (d, *J*=6.7 Hz, 3 H, CH(CH_3)$_2$), 0.91 – 1.11 (m, 15 H, CH(CH_3)$_2$, CH_2CH_3), 1.18 (s, 9 H, C(CH_3)$_3$), 1.20 (s, 9 H, C(CH_3)$_3$), 1.54 – 1.68 (m, 1 H, CHCH(CH_3)$_2$), 1.90 – 2.11 (m, 8 H, $CH_2CH_2CH_3$), 3.04 – 3.17 (m, 3 H, ArCH_2Ar), 3.58 (d, *J*=12.6 Hz, 1 H, ArCH_2Ar), 3.73 – 4.02 (m, 10 H, OCH_2CH_2, OCH_2CHN, OCH_2CHN), 4.16 (d, *J*=12.6 Hz, 1 H), 4.26 – 4.50 (m, 4 H, ArCH_2Ar, OCH_2CHN), 6.45 (d, *J*=2.3 Hz, 1 H, Ar*H*), 6.50 (d, *J*=2.3 Hz, 1 H, Ar*H*), 6.86 (d, *J*=2.4 Hz, 1 H, Ar*H*), 6.90 (d, *J*=1.2 Hz, 2 H, Ar*H*), 7.00 (s, 1 H, Ar*H*), 7.24 (d, *J*=2.4 Hz, 1 H, ArH); ^{13}C NMR (75 MHz, CHLOROFORM-*d*)1.03 (Si(CH_3)$_3$), 10.10 (CH_2CH_3), 10.17 (CH_2CH_3), 10.43 (CH_2CH_3), 10.56 (CH_2CH_3), 18.95 (CH(CH_3)$_2$), 19.06 (CH(CH_3)$_2$), 23.10 ($CH_2CH_2CH_3$), 23.25 ($CH_2CH_2CH_3$), 23.30 ($CH_2CH_2CH_3$), 23.42 ($CH_2CH_2CH_3$), 25.90 (ArCH_2Ar), 29.70 (ArCH_2Ar), 30.06 (ArCH_2Ar), 31.18 (C(CH)$_3$), 31.24 (ArCH_2Ar), 31.40 (C(CH)$_3$), 31.52 (C(CH)$_3$), 31.76 (C(CH_3)$_3$), 33.51 (C(CH_3)$_3$), 33.67 (CH(CH_3)$_2$), 33.85 (C(CH_3)$_3$), 33.91 (C(CH_3)$_3$), 70.13 (OCH_2CHN), 71.71 (OCH_2CHN), 76.56 (OCH_2CH_2), 76.80 (OCH_2CH_2), 76.56 (OCH_2CH_2), 77.16 (OCH_2CH_2), 105.12 ($C_{Ar}CH_2$), 122.24 ($C_{Ar}CH_2$), 124.56 (C_{Ar}H), 124.90 (C_{Ar}H), 125.00 (C_{Ar}H), 125.05 (C_{Ar}H), 125.10 (C_{Ar}H), 125.21 (C_{Ar}H), 126.51 (C_{Ar}H), 127.74 ($C_{Ar}CH_2$), 132.70 (*C*CNO), 133.13 ($C_{Ar}CH_2$), 133.55 ($C_{Ar}CH_2$), 133.83 ($C_{Ar}CH_2$), 134.21 ($C_{Ar}CH_2$), 134.92 ($C_{Ar}CH_2$), 143.32 (CC(CH_3)$_3$), 143.83 (CC(CH_3)$_3$), 144.32 (CC(CH_3)$_3$), 153.39 (C_{Ar}OPr), 154.11 (C_{Ar}OPr), 154.35 (C_{Ar}OPr), 157.43 (C*C*Si), 160.21 (C_{Ar}OPr), 165.25 (C*C*NO); MS (ES+): *m/z* (%) = 888.6 (100) $[M–TMS+H_2O]^+$; HRMS–TOF MS ES+: *m/z* $[M\text{-}TMS+H_2O]^+$ calcd for $C_{58}H_{82}NO_6$: 888.6142; found: 888.6176.

(*cR*)-11,17,23-tri-*tert*-butyl-5-((*S*)-4-isopropyl-4,5-dihydrooxazol-2-yl)-4-diphenylphosphoryl- 25,26,27,28-tetrapropoxycalix[4]arene – (4.5)

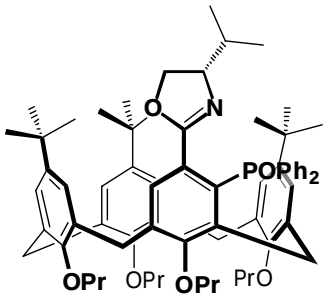

4.5 was prepared in a procedure analogous to that used for **3.10** from oxazoline **2.1** (118 mg, 0.138 mmol), *c*PentLi (0.53 ml, 0.69 mmol, 5 eq), TMEDA (0.25 ml, 1.66 mmol, 12 eq), Et_2O (1 ml) and freshly distilled diphenylphosphine chloride (0.25 ml, 1.38 mmol, 10 eq) with a reaction time of 24 hours at –78 ºC. Purification of the product was achieved by silica gel column chromatography (EtOH:DCM gradient elution 0 % to 3 %) affording a white solid (103 mg, 0.096 mmol, 70 % yield). Further purification was achieved by crystallisation from EtOH and DCM affording a co-crystal with DCM and EtOH. Mp 266–268°C (EtOH/DCM); $[\alpha]_D^{17.9}$ = –77.3° (*c* 0.011 g/ml, DCM); R_f = 0.39 (PET:EtOAc, 60:40); IR (film) cm^{-1}: 3054 (m, CH arom), 2961 (s, CH), 1661 (m, C=N), 1198 cm^{-1} (s, P=O); ^{1}H NMR (400 MHz, CHLOROFORM-*d*) δ ppm 0.69 (s, 9 H, C(C*H*$_3$)$_3$), 0.74 (d, *J*=6.6 Hz, 3 H, CH(C*H*$_3$)$_2$), 0.85 – 0.99 (m, 21 H, CH$_2$C*H*$_3$, CH(C*H*$_3$)$_2$, C(C*H*$_3$)$_3$), 1.06 (t, *J*=7.4 Hz, 3 H, CH$_2$C*H*$_3$), 1.34 (s, 9 H, C(C*H*$_3$)$_3$), 1.68 – 1.80 (m, 2 H, CH$_2$C*H*$_2$CH$_3$), 1.83 – 1.95 (m, 4 H, CH$_2$C*H*$_2$CH$_3$), 2.01 – 2.12 (m, 3 H, CH$_2$C*H*$_2$CH$_3$, C*H*(CH$_3$)$_2$), 3.06 (d, *J*=12.5 Hz, 1 H, ArCH$_2$Ar), 3.14 (d, *J*=12.3 Hz, 1 H, ArC*H*$_2$Ar), 3.19 – 3.31 (m, 2 H, OCH$_2$C*H*N, ArCH$_2$Ar), 3.34 – 3.47 (m, 2 H, OC*H*$_2$CHN, OC*H*$_2$CH$_2$), 3.49 – 3.68 (m, 4 H, OC*H*$_2$CHN, OC*H*$_2$CH$_2$), 3.90 – 4.15 (m, 5 H, ArC*H*$_2$Ar, OC*H*$_2$CH$_2$), 4.19 – 4.27 (m, 1 H, OC*H*$_2$CH$_2$), 4.36 (d, *J*=12.7 Hz, 1 H, ArC*H*$_2$Ar), 4.38 – 4.47 (m, 2 H, ArC*H*$_2$Ar), 6.20 – 6.24 (m, 2 H, Ar*H*), 6.45 (d, *J*=2.3 Hz, 1 H, Ar*H*), 6.57 (d, *J*=2.3 Hz, 1 H, Ar*H*), 7.10 (d, *J*=2.5 Hz, 1 H, Ar*H*), 7.12 (d, *J*=2.5 Hz, 1 H, Ar*H*), 7.31 – 7.37 (m, 2 H, POAr*H*), 7.38 – 7.46 (m, 3 H, POAr*H*, Ar*H*), 7.49 – 7.56 (m, 4 H, POAr*H*), 8.13 – 8.22 (m, 2 H, POAr*H*); ^{13}C NMR (101 MHz, CHLOROFORM-*d*) δ ppm 9.71 (CH$_2$*C*H$_3$), 9.88 (CH$_2$*C*H$_3$), 10.68 (CH$_2$*C*H$_3$), 10.73 (CH$_2$*C*H$_3$), 18.47 (CH(*C*H$_3$)$_2$), 18.67 (CH(*C*H$_3$)$_2$), 22.61 (CH$_2$*C*H$_2$CH$_3$), 23.13 (CH$_2$*C*H$_2$CH$_3$), 23.41 (CH$_2$*C*H$_2$CH$_3$), 23.50 (CH$_2$*C*H$_2$CH$_3$), 30.37 (d, *J*=5.1 Hz ,ArC*H*$_2$Ar), 30.73 (ArC*H*$_2$Ar), 30.87 (ArC*H*$_2$Ar), 31.12 (C(*C*H$_3$)$_3$), 31.24 (C(*C*H$_3$)$_3$), 31.32 (ArC*H*$_2$Ar), 31.75 (C(*C*H$_3$)$_3$), 32.41 (*C*H(CH$_3$)$_2$), 33.52 (*C*(CH$_3$)), 33.65 (*C*(CH$_3$)), 34.03 (*C*(CH$_3$)), 70.03 (O*C*H$_2$CHN), 72.39 (OCH$_2$*C*HN), 76.23 (O*C*H$_2$CH$_2$), 76.60 (O*C*H$_2$CH$_2$), 77.00(O*C*H$_2$CH$_2$), 77.59 (O*C*H$_2$CH$_2$), 123.35 (*C*$_{Ar}$H), 123.86 (*C*$_{Ar}$H), 125.04 (*C*$_{Ar}$H), 125.26 (*C*$_{Ar}$H), 125.38 (*C*$_{Ar}$H), 125.66 (*C*$_{Ar}$H), 127.46 (d, *J*= 8.8 Hz, NC*C*CP), 127.84 (*C*$_{Ar}$), 127.97 (*C*$_{Ar}$), 128.08 (*C*$_{Ar}$), 128.20 (*C*$_{Ar}$), 129.91 (*C*$_{Ar}$), 130.10 (*C*$_{Ar}$), 130.20 (*C*$_{Ar}$), 130.24 (*C*$_{Ar}$), 130.31 (*C*$_{Ar}$), 130.49 (*C*$_{Ar}$), 130.58 (*C*$_{Ar}$), 130.72 (*C*$_{Ar}$), 130.98 (*C*$_{Ar}$), 131.02 (*C*$_{Ar}$), 131.13 (*C*$_{Ar}$), 132.12 (*C*$_{Ar}$), 132.21 (*C*$_{Ar}$), 132.29 (*C*$_{Ar}$), 133.81 (*C*$_{Ar}$CH$_2$), 134.84 (*C*$_{Ar}$CH$_2$), 135.56 (*C*$_{Ar}$), 135.85 (*C*$_{Ar}$CH$_2$), 137.97 (*C*$_{Ar}$CH$_2$), 139.02 (*C*$_{Ar}$CH$_2$), 140.57 (d, *J*=2.2 Hz , *C*$_{Ar}$CH$_2$), 143.92 (*C*C(CH$_3$)$_3$), 144.15 (*C*C(CH$_3$)$_3$), 144.60 (*C*C(CH$_3$)$_3$), 146.22 (d, *J*=7.4 Hz, *C*$_{Ar}$CH$_2$), 152.83 (*C*$_{Ar}$OPr), 152.86

(C_{Ar}OPr), 154.74 (C_{Ar}OPr), 160.43 (d, *J*=12.5 Hz, C*C*OCH$_2$), 163.48(d, *J*=3.7 Hz, C*C*NO); ^{31}P NMR (400 MHz, CHLOROFORM-*d*) δ ppm 28.09 (C*P*O); MS (ES+): *m/z* (%) = 1072.6 (100) [M+H]$^+$; HRMS–TOF MS ES+: *m/z* [M+H]$^+$ calcd for $C_{70}H_{91}NO_6P$: 1072.6584; found: 1072.6488.

(*cR*)-11,17,23-tri-*tert*-butyl-4-ethoxycarbonyl-5-((*S*)-4-isopropyl-4,5-dihydrooxazol-2-yl)-25,26,27,28-tetrapropoxycalix[4]arene – (4.6)

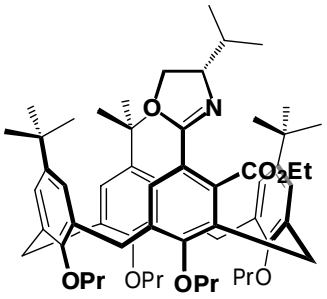

4.6 was prepared in a procedure analogous to that used for **3.10** from oxazoline **2.1** (200 mg, 0.23 mmol), *c*PentLi (0.55 ml, 0.71 mmol, 3.1 eq), TMEDA (0.21 ml , 1.38 mmol, 6 eq), Et$_2$O (2 ml) and freshly distilled ethyl chloroformate (0.21 ml, 2.22 mmol, 9.6 eq) with a reaction time of 18 hours at –78 ºC. Purification of the product was achieved by silica gel column chromatography (EtOAc:PET 2:98) affording a white solid (157 mg, 0.167 mmol, 73 % yield) Mp 76–130°C (DCM); $[\alpha]_D^{18.0}$ = –19.4° (*c* 0.012 g/ml, DCM); R_f = 0.43 (PET:EtOAc, 90:10); IR (film) cm^{-1}: 2961 (s, CH arom), 1733 (s, C=O), 1652 (w, C=N); ^{1}H NMR (400 MHz, CHLOROFORM-*d*) δ ppm 0.88 – 1.00 (m, 27 H, CH(C*H*$_3$)$_2$, CH$_2$C*H*$_3$, C(CH$_3$)$_3$) 1.01 – 1.08 (m, 9 H, CH(C*H*$_3$)$_2$, CH$_2$C*H*$_3$) 1.28 (s, 9 H, C(CH$_3$)$_3$) 1.35 (t, *J*=7.1 Hz, 3 H CH$_2$C*H*$_3$), 1.79 – 1.96 (m, 5 H, C*H*(CH$_3$)$_2$, CH$_2$C*H*$_2$CH$_3$) 2.00 – 2.13 (m, 4 H, CH$_2$C*H*$_2$CH$_3$) 3.12 – 3.25 (m, 3 H, ArC*H*$_2$Ar) 3.35 (d, *J*=13.7 Hz, 1 H, ArC*H*$_2$Ar) 3.62 – 3.77 (m, 4 H, OC*H*$_2$CH) 3.93 – 4.00 (m, 2 H, OC*H*$_2$CH) 4.02 – 4.12 (m, 4 H, OC*H*$_2$CHN, OCH$_2$C*H*N, OC*H*$_2$CH$_2$) 4.28 – 4.48 (m, 7 H, OC*H*$_2$CH$_1$N, ArC*H*$_2$Ar, OC*H*$_2$CH$_3$) 6.50 (d, *J*=2.2 Hz, 1 H, Ar*H*) 6.54 (d, *J*=2.4 Hz, 1 H, Ar*H*) 6.62 (d, *J*=2.2 Hz, 1 H, Ar*H*) 6.71 (d, *J*=2.4 Hz, 1 H, Ar*H*) 7.01 (d, *J*=2.0 Hz, 1 H, Ar*H*) 7.04 (d, *J*=2.0 Hz, 1 H, Ar*H*) 7.67 (s, 1 H, Ar*H*); ^{13}C NMR (101 MHz, CHLOROFORM-*d*) δ ppm 9.78 (CH$_2$*C*H$_3$), 10.06 (CH$_2$*C*H$_3$), 10.57 (CH$_2$*C*H$_3$), 10.63 (CH$_2$*C*H$_3$), 14.17 (OCH$_2$*C*H$_3$), 18.00 (CH(*C*H$_3$)$_2$), 19.06 (CH(*C*H$_3$)$_2$), 22.61 (CH$_2$*C*H$_2$CH$_3$), 23.27 (CH$_2$*C*H$_2$CH$_3$), 23.29 (CH$_2$*C*H$_2$CH$_3$), 23.49 (CH$_2$*C*H$_2$CH$_3$), 27.64 (Ar*C*H$_2$Ar), 31.05 (Ar*C*H$_2$Ar), 31.11 (Ar*C*H$_2$Ar), 31.13 (Ar*C*H$_2$Ar), 31.29 (C(*C*H$_3$)$_3$), 31.32 (C(*C*H$_3$)$_3$), 31.69 (C(*C*H$_3$)$_3$), 32.87 (*C*H(CH$_3$)$_2$), 33.69 (*C*(CH$_3$)$_3$), 33.72 (*C*(CH$_3$)$_3$), 33.96 (*C*(CH$_3$)$_3$), 61.25 (O*C*H$_2$CH$_3$), 69.92 (N*C*HCH$_2$), 72.80 (O*C*H$_2$CHN), 76.26 (O*C*H$_2$CH$_2$), 76.69 (O*C*H$_2$CH$_2$), 76.74 (O*C*H$_2$CH$_2$), 77.48 (O*C*H$_2$CH$_2$), 118.78 (*C*CCOO), 124.31 (C_{Ar}H), 124.85 (C_{Ar}H), 124.93 (C_{Ar}H), 124.99 (C_{Ar}H), 125.28 (C_{Ar}H), 125.29 (C_{Ar}H), 129.68 (C_{Ar}H), 131.09 (C_{Ar}CH$_2$), 131.22 (C_{Ar}CH$_2$), 132.09 (C_{Ar}CH$_2$), 132.50 (C_{Ar}CH$_2$), 133.58 (NC*C*C), 134.38 (C_{Ar}CH$_2$), 135.01 (C_{Ar}CH$_2$), 135.29 (C_{Ar}CH$_2$), 137.00 (C_{Ar}CH$_2$), 144.16 (*C*C(CH$_3$)$_3$), 144.29 (*C*C(CH$_3$)$_3$), 144.58 (*C*C(CH$_3$)$_3$), 153.11 (C_{Ar}OPr), 153.11 (C_{Ar}OPr) 154.50 (C_{Ar}OPr), 159.93 (C_{Ar}OPr), 162.40 (C*C*NO), 169.63 (C*C*OO); MS (ES+): *m/z* (%) = 944.6 (100) [M+H]$^+$; HRMS–TOF MS ES+: *m/z* [M+H]$^+$ calcd for $C_{61}H_{86}NO_7$: 944.6404; found: 944.6367.

(*cR*)-11,17,23-tri-*tert*-butyl-5-((*S*)-4-isopropyl-4,5-dihydrooxazol-2-yl)-4-methylthio-25,26,27,28-tetrapropoxycalix[4]arene – (4.7)

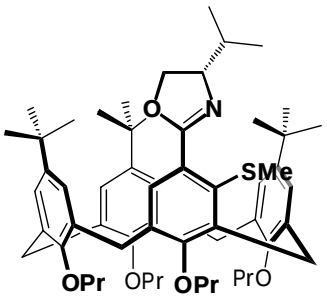

Thioether **4.7** was prepared in a procedure analogous to that used for **3.10** from oxazoline **2.1** (180 mg, 0.207 mmol), *c*PentLi (1.1 ml, 1.37 mmol, 6 eq), TMEDA (0.37 ml, 2.48 mmol, 12 eq), Et_2O (2 ml) and dimethyl disulfide (0.4 ml, 4.5 mmol, 20 eq) with a reaction time of 24 hours at –78ºC. Purification of the product was achieved by silica gel column chromatography (EtOAc:PET 2:98) affording a white solid (140 mg, 0.152 mmol, 73 % yield). Mp 78–80°C (DCM); $[\alpha]_D^{18.1}$ = –9.4° (*c* 0.012 g/ml, DCM); R_f = 0.42 (PET:EtOAc, 90:10); IR (film) cm^{-1}: 2961 (s, CH), 1651 (s, C=N), 1481 (s, C=C); ^{1}H NMR (400 MHz, CHLOROFORM-*d*) δ ppm 0.93 – 1.08 (m, 36 H, $CH(CH_3)_2$, CH_2CH_3, $C(CH_3)_3$), 1.13 (s, 9 H, $C(CH_3)_3$), 1.81 – 2.09 (m, 12 H, SCH_3, $CH_2CH_2CH_3$, $CH(CH_3)_2$), 3.15 (m, 3 H, $ArCH_2Ar$), 3.68 – 3.94 (m, 8 H, OCH_2CH_2, $ArCH_2Ar$, OCH_2CHN), 4.02 – 4.17 (m, 3 H, OCH_2CH_2, $OCHCH_2N$), 4.31 – 4.40 (m, 2 H, $ArCH_2Ar$, $OCHCH_2N$), 4.40 – 4.47 (m, 3 H, $ArCH_2Ar$), 6.67 (d, *J*=2.1 Hz, 2 H, Ar*H*), 6.75 (d, *J*=2.3 Hz, 2 H, Ar*H*), 6.81 – 6.88 (m, 2 H, Ar*H*), 7.19 (s, 1 H, Ar*H*); ^{13}C NMR (101 MHz, CHLOROFORM-*d*) δ ppm 10.12 (CH_2CH_3), 10.27 (CH_2CH_3), 10.35 (CH_2CH_3), 10.46 (CH_2CH_3), 18.50 ($CH(CH_3)_2$), 19.11 ($CH(CH_3)_2$), 21.31 (SCH_3), 22.88 ($CH_2CH_2CH_3$), 22.90 ($CH_2CH_2CH_3$), 23.32 ($CH_2CH_2CH_3$), 23.43 ($CH_2CH_2CH_3$), 28.68 ($ArCH_2Ar$), 30.54 ($ArCH_2Ar$), 31.17 ($ArCH_2Ar$), 31.37 ($C(CH_3)_3$), 31.43 ($C(CH_3)_3$), 31.47 ($ArCH_2Ar$), 31.50 ($C(CH_3)_3$), 32.95 ($CH(CH_3)_2$), 33.77 ($C(CH_3)_3$), 33.79 ($C(CH_3)_3$), 33.82 ($C(CH_3)_3$), 70.01 (OCH_2CHN), 72.94 (OCH_2CHN), 76.51 (OCH_2CH_2), 76.63 (OCH_2CH_2), 76.69 (OCH_2CH_2), 76.81 (OCH_2CH_2), 124.63 ($C_{Ar}H$), 124.68 ($C_{Ar}H$), 125.01 ($C_{Ar}H$), 125.14 ($C_{Ar}H$), 125.33 ($C_{Ar}H$), 125.82 ($C_{Ar}H$), 129.23 ($C_{Ar}CH_2$), 130.16 ($C_{Ar}H$), 132.01 ($C_{Ar}CH_2$), 132.02 (NC*C*CS), 133.06 ($C_{Ar}CH_2$), 133.08 ($C_{Ar}CH_2$), 133.46 ($C_{Ar}CH_2$), 134.12 ($C_{Ar}CH_2$), 134.50 ($C_{Ar}CH_2$), 135.85 ($C_{Ar}CH_2$), 140.77 ($CSCH_3$), 143.75 ($CC(CH_3)_3$), 144.38 ($CC(CH_3)_3$), 144.41 ($CC(CH_3)_3$), 153.56 ($C_{Ar}OPr$), 153.65 ($C_{Ar}OPr$), 154.06 ($C_{Ar}OPr$), 158.79 ($C_{Ar}OPr$), 164.92 (*C*CNO); MS (ES+): *m/z* (%) = 918.6 (100) $[M+H]^+$; HRMS–TOF MS ES+: *m/z* $[M+H]^+$ calcd for $C_{59}H_{84}NO_5S$: 918.6070; found: 918.6082.

(*cR*)-4-bromo-11,17,23-tri-*tert*-butyl-5-((*S*)-4-isopropyl-4,5-dihydrooxazol-2-yl)- 25,26,27,28-tetrapropoxycalix[4]arene – (4.8)

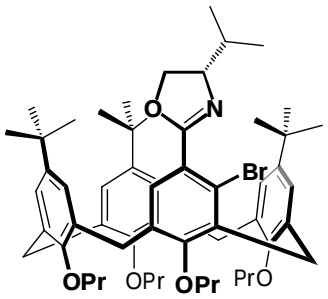

4.8 was prepared in a procedure analogous to that used for **3.10** from oxazoline **2.1** (238 mg, 0.275 mmol), *c*PentLi (1.1 ml, 1.38 mmol, 5 eq), TMEDA (0.49 ml, 3.3 mmol, 12 eq), Et_2O (2 ml) and freshly distilled dibromoethane (0.4 ml, 4.12 mmol, 15 eq) with a reaction time of 24 hours at –78 ºC. Purification of the product was achieved by silica gel column chromatography (EtOAc:PET 2:98) affording a white solid (188 mg, 0.198 mmol, 72% yield). Mp 90–130°C (DCM); $[\alpha]_D^{18}$ = –22.9° (*c* 0.012 g/ml, DCM); R_f = 0.42 (PET:EtOAc, 92:8); ^{1}H NMR (400 MHz, CHLOROFORM-*d*) δ ppm 0.94 – 1.08 (m, 36 H, CH(CH_3)$_2$, CH_2CH_3, C(CH_3)$_3$) 1.12 (s, 9 H, C(CH_3)$_3$), 1.84 – 2.11 (m, 9 H, $CH(CH_3)_2$, $CH_2CH_2CH_3$) 3.11 – 3.19 (m, 3 H, ArCH_2Ar) 3.68 – 3.98 (m, 9 H, OCH_2CH_2, ArCH_2Ar) 4.04 – 4.12 (m, 2 H, OCH_2CHN, OCH_2CHN) 4.30 – 4.47 (m, 5 H, ArCH_2Ar, CH_2CHN) 6.66 (d, *J*=2.2 Hz, 1 H, Ar*H*) 6.70 (d, *J*=2.4 Hz, 1 H, Ar*H*) 6.75 (d, *J*=2.4 Hz, 1 H, Ar*H*) 6.77 (d, *J*=1.9 Hz, 1 H, Ar*H*) 6.81 (d, *J*=1.9 Hz, 1 H, Ar*H*) 6.94 (d, *J*=2.2 Hz, 1 H, Ar*H*) 7.23 (s, 1 H, Ar*H*); ^{13}C NMR (101 MHz, CHLOROFORM-*d*) δ ppm 10.08 (CH_2CH_3), 10.25 (CH_2CH_3), 10.34 (CH_2CH_3), 10.45 (CH_2CH_3), 18.32 ($CH(CH_3)_2$), 18.97 ($CH(CH_3)_2$), 22.86 ($CH_2CH_2CH_3$), 22.99 ($CH_2CH_2CH_3$), 23.31 ($CH_2CH_2CH_3$), 23.40 ($CH_2CH_2CH_3$), 30.35 (ArCH_2Ar), 30.61 (ArCH_2Ar), 31.16 (ArCH_2Ar), 31.34 (C(CH_3)$_3$), 31.34 (C(CH_3)$_3$), 31.37 (ArCH_2Ar), 31.43 (C(CH_3)$_3$), 32.75 ($CH(CH_3)_2$), 33.72 (C(CH_3)$_3$), 33.78 (C(CH_3)$_3$), 33.81 (C(CH_3)$_3$), 69.85 (OCH_2CHN), 72.86 (OCH_2CHN), 76.69 (OCH_2CH_2), 76.71 (OCH_2CH_2), 76.83 (OCH_2CH_2), 77.32 (OCH_2CH_2), 121.36 (*C*Br), 124.63 (C_{Ar}H), 124.93 (C_{Ar}H), 125.09 ($C_{Ar}CH_2$), 125.15 (C_{Ar}H), 125.25 (C_{Ar}H), 125.33 (C_{Ar}H), 125.82 ($C_{Ar}CH_2$), 130.63 (C_{Ar}H), 131.01 (*C*CN), 131.80 (C_{Ar}H), 133.20 ($C_{Ar}CH_2$), 133.55 ($C_{Ar}CH_2$), 133.99 ($C_{Ar}CH_2$), 134.45 ($C_{Ar}CH_2$), 134.64 ($C_{Ar}CH_2$), 137.27 ($C_{Ar}CH_2$), 143.70 (*C*C(CH$_3$)$_3$), 144.44 (*C*C(CH$_3$)$_3$), 144.52 (*C*C(CH$_3$)$_3$), 153.44 (C_{Ar}OPr), 153.49 (C_{Ar}OPr), 154.01(C_{Ar}OPr), 159.17(C_{Ar}OPr), 164.04(*C*CNO); MS (ES+): *m/z* (%) = 950.65 (95) – matches expected isotope ratio for $[M+H]^+$.

(*cR*)-11,17,23-tri-*tert*-butyl-5-((*S*)-4-isopropyl-4,5-dihydrooxazol-2-yl)-4-trimethylsilyl-25,26,27,28-tetrapropoxycalix[4]arene trimethylsilyl salt – (4.9)

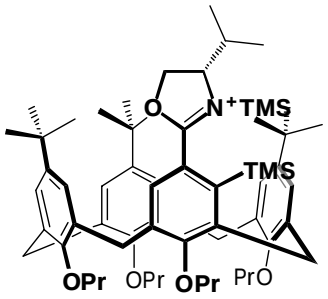

4.9 was prepared in a procedure analogous to that used for **3.10** from oxazoline **2.1** (100 mg, 0.115 mmol), *c*PentLi (0.78 ml, 0.69 mmol, 6 eq), TMEDA (0.21 ml, 1.38 mmol, 12 eq), Et_2O (1 ml) and freshly distilled trimethylsilyl chloride (0.2 ml, 1.58 mmol, 13.7 eq) with a reaction time of 30 hours at –78 ºC. After the addition of the trimethylsilyl chloride the reaction was left to stir for 18 hours at RT. Purification of the product was achieved by silica gel column chromatography (EtOAc:PET 1:99) affording a white solid (50 mg, 0.049 mmol, 43 % yield). Further purification of the product was achieved by crystallisation from MeCN and H_2O; Mp 94–98°C (MeCN); $[\alpha]_D^{18.5}$ = –27.4 (*c* 0.012 g/ml, DCM); R_f = 0.78 (PET:EtOAc, 92:8); IR (film) cm^{-1}: 2961 (s, CH), 2875 (m, CH), 1652 (s, C=N), 1481 (s, C=C); ^{1}H NMR (400 MHz, CHLOROFORM-*d*) δ ppm 0.08 (s, 9 H, NSi(CH_3)$_3$), 0.40 (s, 9 H, Si(CH_3)$_3$), 0.72 (s, 9 H, C(CH_3)$_3$), 0.89 (s, 9 H, C(CH_3)$_3$), 0.95 (m, 9 H, CH_2CH_3, CH(CH_3)$_2$), 1.05 (m, 6 H, CH_2CH_3, CH(CH_3)$_2$), 1.12 (t, *J*=7.3 Hz, 3 H, CH_2CH_3), 1.36 (s, 9 H, C(CH_3)$_3$), 1.89 (m, 5 H, $CH_2CH_2CH_3$, CH(CH_3)$_2$), 2.14 (m, 4 H, $CH_2CH_2CH_3$), 3.12 (m, 3 H, ArCH_2Ar), 3.55 (d, *J*=12.8 Hz, 1 H, ArCH_2Ar), 3.60 (t, *J*=7.3 Hz, 2 H, OCH_2CH_2), 3.68 (t, *J*=6.9 Hz, 2 H, OCH_2CH_2), 4.02 (m, 6 H, OCH_2CH_2, OCH_2CHN, OCH$_2$CHN), 4.33 (d, *J*=12.8 Hz, 1 H, ArCH_2Ar), 4.44 (m, 4 H, ArCH_2Ar, OCH_2CHN), 6.17 (d, *J*=2.3 Hz, 1 H, Ar*H*), 6.28 (d, *J*=2.3 Hz, 1 H, Ar*H*), 6.55 (m, 2 H, Ar*H*), 7.12 (d, *J*=2.6 Hz, 1 H, Ar*H*), 7.13 (d, *J*=2.6 Hz, 1 H, Ar*H*), 7.48 (s, 1 H, Ar*H*); ^{13}C NMR (101 MHz, CHLOROFORM-*d*) δ ppm 1.02 (NSi(CH_3)$_3$), 2.96 (ArSi(CH_3)$_3$), 9.85 (CH_2CH_3), 9.89 (CH_2CH_3), 10.65 (CH_2CH_3), 10.85 (CH_2CH_3), 18.94 (CH(CH_3)$_2$), 19.14 (CH(CH_3)$_2$), 22.81 ($CH_2CH_2CH_3$), 23.05 ($CH_2CH_2CH_3$), 23.51 ($CH_2CH_2CH_3$), 23.61 ($CH_2CH_2CH_3$), 30.16 (ArCH_2Ar), 31.10(ArCH_2Ar), 31.14 (ArCH_2Ar, C(CH_3)$_3$), 31.21 (ArCH_2Ar, C(CH_3)$_3$), 31.77 (C(CH_3)$_3$), 33.09 (C(CH_3)$_3$), 33.55 (CH(CH_3)$_2$), 33.65 (C(CH_3)$_3$), 34.06 (C(CH_3)$_3$), 70.62 (OCH_2CHN), 73.40 (OCH$_2$CHN), 76.48 (OCH_2CH_2), 76.58 (OCH_2CH_2), 77.22 (OCH_2CH_2), 77.59 (OCH_2CH_2), 123.61 (C_{Ar}H), 123.88 (C_{Ar}H), 124.88 (C_{Ar}H), 125.16 (C_{Ar}H), 125.32 (C_{Ar}H), 125.49 (C_{Ar}H), 129.67 ($C_{Ar}CH_2$), 129.98 (CCCNO), 130.98 (C_{Ar}H), 131.54 ($C_{Ar}CH_2$), 131.58 ($C_{Ar}CH_2$), 132.07 ($C_{Ar}CH_2$), 135.78 ($C_{Ar}CH_2$), 135.90 ($C_{Ar}CH_2$), 136.83 ($C_{Ar}CH_2$), 138.94 (CCSi), 143.86 (CC(CH$_3$)$_3$), 143.92 (CC(CH$_3$)$_3$), 144.59 (CC(CH$_3$)$_3$), 144.64 ($C_{Ar}CH_2$), 152.70 (CCOCH$_2$), 152.77 (CCOCH$_2$), 154.74 (CCOCH$_2$), 159.18 (CCOCH$_2$), 166.31 (CCNO) ; MS (ES+): *m/z* (%) = 944.6 (100) $[M\text{-}TMS+H]^+$; HRMS–TOF MS ES+: *m/z* $[M\text{-}TMS+H]^+$ calcd for $C_{61}H_{90}NO_5Si$: 944.6588; found: 944.6548.

(*cR*)-11,17,23-tri-*tert*-butyl-5-carboxy-4-fluoro-25,26,27,28-tetrapropoxycalix[4]arene – (4.10)

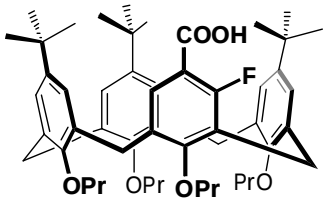

3.10 (65 mg, 0.073 mmol) was added to a 2.5 ml microwave reaction vessel along with glacial acetic acid (2 ml) and water (0.5 ml). The flask was heated to 170 ºC for 1 hour; thereafter the solvent was removed under reduced pressure affording an orange coloured oil. Water (1 ml), ethanol (1 ml) and sodium hydroxide (700 mg, 17.5 mmol) were added to the flask and it was heated to 140 ºC for 1 hour. The contents were transferred to a separating funnel and extracted from 1 M HCl (20 ml) with DCM (2 × 40 ml), the organic layers combined, dried over $MgSO_4$ and the solvent removed under reduced pressure. Product **4.10** was purified by silica gel chromatography (EtOAc:PET 8:92 to 12:88) affording a white solid (40 mg, 0.049 mmol, 67 % yield) further purification was achieved via re-crystallisation from MeCN and H_2O affording white crystals. Mp 196–200°C (MeCN/H_2O); $[\alpha]_D^{20.9}$ = –0.63° (*c* 0.016 g/ml, DCM); R_f = 0.38 (EtOAc:PET, 13:87); IR (film): 3444 (br, OH), 2962 (s, CH), 1694 (s, C=O), 1481 cm^{-1} (s, C=C); ^{1}H NMR (300 MHz, CHLOROFORM-*d*) δ ppm 0.73 (s, 9 H, C(C*H*$_3$)$_3$), 0.88 – 0.99 (m, 6 H, CH$_2$C*H*$_3$), 1.02 – 1.15 (m, 6 H, CH$_2$C*H*$_3$), 1.29 (s, 9 H, C(C*H*$_3$)$_3$), 1.32 (s, 9 H, C(C*H*$_3$)$_3$), 1.84 – 2.12 (m, 8 H, CH$_2$C*H*$_2$CH$_3$), 3.09 – 3.20 (m, 3 H, ArC*H*$_2$Ar), 3.38 – 3.47 (m, 1 H, ArC*H*$_2$Ar), 3.67 – 3.81 (m, 4 H, OC*H*$_2$CH$_2$), 3.82 – 4.12 (m, 4 H, OC*H*$_2$CH$_2$), 4.21 (d, *J*=13.2 Hz, 1 H, ArC*H*$_2$Ar), 4.37 – 4.50 (m, 3 H, ArC*H*$_2$Ar), 6.26 (d, *J*=2.4 Hz, 1 H, Ar*H*), 6.33 (d, *J*=2.4 Hz, 1 H, Ar*H*), 7.03 – 7.10 (m, 3 H, Ar*H*), 7.13 (dd, *J*=4.6, 2.4 Hz, 1 H, Ar*H*), 7.27 (d, *J*=8.7 Hz, 1 H, Ar*H*), 10.33 – 10.9 (br. s, 1 H, COO*H*); ^{13}C NMR (75 MHz, CHLOROFORM-*d*) δ ppm 9.84 (CH$_2$*C*H$_3$), 10.00 (CH$_2$*C*H$_3$), 10.50 (CH$_2$*C*H$_3$), 10.77 (CH$_2$*C*H$_3$), 22.84 (CH$_2$C*H*$_2$CH$_3$), 23.20 (CH$_2$C*H*$_2$CH$_3$), 23.31 (CH$_2$C*H*$_2$CH$_3$), 23.54 (CH$_2$C*H*$_2$CH$_3$), 26.73 (Ar*C*H$_2$Ar), 30.15 (Ar*C*H$_2$Ar), 30.92 (C(*C*H$_3$)$_3$), 31.27 (Ar*C*H$_2$Ar), 31.57 (Ar*C*H$_2$Ar, C(*C*H$_3$)$_3$), 31.63 (C(*C*H$_3$)$_3$), 33.34 (*C*(CH$_3$)$_3$), 34.00 (*C*(CH$_3$)$_3$), 34.08 (*C*(CH$_3$)$_3$), 76.30 (O*C*H$_2$CH$_2$), 76.81 (O*C*H$_2$CH$_2$), 77.20 (O*C*H$_2$CH$_2$), 77.66 (O*C*H$_2$CH$_2$), 111.30 (d, *J*=9.2 Hz, C*C*COO), 123.20 (d, *J*=15 Hz, *C*$_{Ar}$CH$_2$), 124.41 (*C*$_{Ar}$H), 124.68 (*C*$_{Ar}$H), 125.17 (*C*$_{Ar}$H), 126.09 (*C*$_{Ar}$H), 126.36 (*C*$_{Ar}$H), 126.79(d, *J*= 4.4 Hz , *C*$_{Ar}$H), 129.83(d, *J*=3.3 Hz , *C*$_{Ar}$CH$_2$), 131.61 (*C*$_{Ar}$H), 131.85 (*C*$_{Ar}$CH$_2$), 132.12 (*C*$_{Ar}$CH$_2$), 132.68 (*C*$_{Ar}$CH$_2$), 133.95 (*C*$_{Ar}$CH$_2$), 135.22 (*C*$_{Ar}$CH$_2$), 135.76 (*C*$_{Ar}$CH$_2$), 144.30 (*C*C(CH$_3$)$_3$), 144.39 (*C*C(CH$_3$)$_3$), 145.02 (*C*C(CH$_3$)$_3$), 152.92 (*C*$_{Ar}$OPr), 154.50 (*C*$_{Ar}$OPr), 154.59 (*C*$_{Ar}$OPr), 160.01 (d, *J*= 260 Hz, C*C*F), 161.47 (d, *J*=10.7 Hz, C*C*OCH$_2$), 167.94 (br. s, C*C*OOH); ^{19}F NMR (400 MHz, CHLOROFORM-*d*) δ ppm -112.42 (C*F*); MS (ES+): *m/z* (%) = 840.6 (100) [M+H_2O]$^+$; HRMS–TOF MS ES+: *m/z* [M+H_2O]$^+$ calcd for $C_{53}H_{73}FO_7$: 840.5340; found: 840.5352.

(*cS*)-11,17,23-tri-*tert*-butyl-5-carboxy-4-fluoro-25,26,27,28-tetrapropoxycalix[4]arene – (4.11)

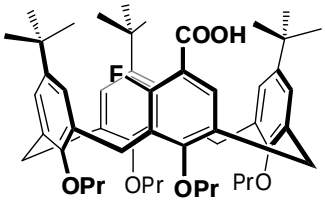

4.11 was prepared according to the general procedure used for **4.10** from **4.2** (50 mg, 0.056 mmol), acetic acid (1.6 ml) water (0.4 ml) with heating to 170 ºC for 1.25 hours, ethanol (1 ml), water (1 ml) and sodium hydroxide (200 mg, 5 mmol) with heating to 150 ºC for 2 hours. Product **4.11** was purified by silica gel chromatography (EtOAc:PET 8:92 to 12:88) affording a white solid (40 mg, 0.049 mmol, 88 % yield), further purification was achieved via re-crystallisation from MeCN and H_2O affording white crystals. Mp 233–250°C (MeCN/H_2O); $[\alpha]_D^{20.9}$ = +0.63° (*c* 0.02 g/ml, DCM); R_f = 0.38 (EtOAc:PET, 13:87); IR (film) cm^{-1}: 3444 (br, OH), 2961 (s, CH), 1694 (s, C=O), 1481 (s, C=C); ^{1}H NMR (400 MHz, CHLOROFORM-*d*) δ ppm 0.73 (s, 9 H, C(C*H*$_3$)$_3$), 0.90 – 0.98 (m, 6 H, CH$_2$C*H*$_3$), 1.06 (t, *J*=7.4 Hz, 3 H, CH$_2$C*H*$_3$), 1.10 (t, *J*=7.4 Hz, 3 H, CH$_2$C*H*$_3$), 1.29 (s, 9 H, C(C*H*$_3$)$_3$), 1.32 (s, 9 H, C(C*H*$_3$)$_3$), 1.87 – 2.11 (m, 8 H, CH$_2$C*H*$_2$CH$_2$), 3.11 – 3.18 (m, 3 H, ArC*H*$_2$Ar), 3.43 (d, *J*=12.5 Hz, 1 H, ArC*H*$_2$Ar), 3.69 – 3.81 (m, 4 H, OC*H*$_2$CH$_2$), 3.85 – 4.11 (m, 4 H, OC*H*$_2$CH$_2$), 4.22 (d, *J*=13.3 Hz, 1 H, ArC*H*$_2$Ar), 4.38 – 4.48 (m, 3 H, ArC*H*$_2$Ar), 6.27 (d, *J*=2.3 Hz, 1 H, Ar*H*), 6.33 (d, *J*=2.3 Hz, 1 H, Ar*H*), 7.04 – 7.10 (m, 3 H, Ar*H*), 7.11 – 7.15 (m, 1 H, Ar*H*), 7.27 (d, *J*=8.4 Hz, 1 H, Ar*H*), 10.75 – 11.28(br. s, COO*H*); ^{13}C NMR (101 MHz, CHLOROFORM-*d*) δ ppm 9.84 (CH$_2$*C*H$_3$), 10.00 (CH$_2$*C*H$_3$), 10.49 (CH$_2$*C*H$_3$), 10.77 (CH$_2$*C*H$_3$), 22.84 (CH$_2$C*H*$_2$CH$_3$), 23.20 (CH$_2$C*H*$_2$CH$_3$), 23.31 (CH$_2$C*H*$_2$CH$_3$), 23.54 (CH$_2$C*H*$_2$CH$_3$), 26.74 (Ar*C*H$_2$Ar), 30.14 (Ar*C*H$_2$Ar), 30.92 (C(*C*H$_3$)$_3$), 31.28 (Ar*C*H$_2$Ar), 31.57 (Ar*C*H$_2$Ar, C(*C*H$_3$)$_3$), 31.64 (C(*C*H$_3$)$_3$), 33.33 (*C*(CH$_3$)$_3$), 34.00 (*C*(CH$_3$)$_3$), 34.07 (*C*(CH$_3$)$_3$), 76.30 (O*C*H$_2$CH$_2$), 76.81 (O*C*H$_2$CH$_2$), 77.20 (O*C*H$_2$CH$_2$), 77.65 (O*C*H$_2$CH$_2$), 111.37 (d, *J*=10 Hz,C*C*COO), 123.20 (d, *J*=14.7 Hz, *C*$_{Ar}$CH$_2$), 124.42 (*C*$_{Ar}$H), 124.69 (*C*$_{Ar}$H), 125.18 (*C*$_{Ar}$H), 126.09 (*C*$_{Ar}$H), 126.36 (*C*$_{Ar}$H), 126.80 (d, *J*=4.4 Hz , *C*$_{Ar}$H), 129.83 (d, J= 2.2 Hz, *C*$_{Ar}$CH$_2$), 131.60 (*C*$_{Ar}$H), 131.86 (*C*$_{Ar}$CH$_2$), 132.12 (*C*$_{Ar}$CH$_2$), 132.68 (*C*$_{Ar}$CH$_2$), 133.96 (*C*$_{Ar}$CH$_2$), 135.21 (*C*$_{Ar}$CH$_2$), 135.76 (*C*$_{Ar}$CH$_2$), 144.30 (*C*C(CH$_3$)$_3$), 144.40 (*C*C(CH$_3$)$_3$), 145.02 (*C*C(CH$_3$)$_3$), 152.92 (*C*$_{Ar}$OPr), 154.50 (*C*$_{Ar}$OPr), 154.59 (*C*$_{Ar}$OPr), 160.12(d, *J*=270 Hz, C*C*F), 161.37 (d, *J*=10.3 Hz, C*C*OCH$_2$), 168.36(d, *J*=3.7 Hz ,C*C*OOH); ^{19}F NMR (400 MHz, CHLOROFORM-*d*) δ ppm -112.15 (C*F*); MS (ES+): *m/z* (%) = 840.6 (100) [M+H$_2$O]$^+$; HRMS–TOF MS ES+: *m/z* [M+H$_2$O]$^+$ calcd for $C_{53}H_{73}FO_7$: 840.5340; found: 840.5352.

(*cR*)-11,17,23-tri-*tert*-butyl-5-carboxy-4-diphenylphosphoryl-25,26,27,28-tetrapropoxycalix[4]arene – (4.13)

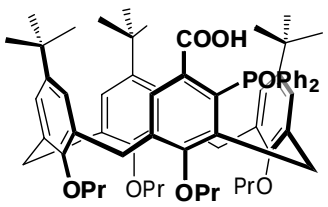

4.13 was prepared according to the procedure used for **4.10** from **4.5** (56 mg, 0.052 mmol), acetic acid (1.6 ml) water (0.4 ml) with heating to 170 ºC for 1.5 hours, ethanol (1 ml), water (1 ml) and sodium hydroxide (500 mg, 12.5 mmol) with heating to 150 ºC for 2 hours. The product **4.13** was purified by crystallisation from MeCN and DCM affording white crystals (52 mg, 0.052 mmol, 100 % yield). Mp 270–273°C (MeCN/DCM); $[\alpha]_D^{21.3}$ = +92.5° (*c* 0.024 g/ml , DCM); R_f = 0.15 (EtOH:DCM, 5:95); IR (film) cm^{-1}: 3056 (m, CH arom), 2961 (s, CH), 2875 (s, CH), 1705 (m, C=O), 1481 (m, C=C arom), 1200 cm^{-1} (s, P=O); ^{1}H NMR (400 MHz, CHLOROFORM-*d*) δ ppm 0.73 (s, 9 H, C(C*H*$_3$)$_3$), 0.87 – 1.00 (m, 18 H, C(C*H*$_3$)$_3$, CH$_2$C*H*$_3$), 1.07 (t, *J*=7.4 Hz, 3 H, CH$_2$C*H*$_3$), 1.35 (s, 9 H, C(C*H*$_3$)$_3$), 1.65 – 1.77 (m, 2 H, CH$_2$C*H*$_2$CH$_3$), 1.84 – 1.96 (m, 2 H, CH$_2$C*H*$_2$CH$_3$), 1.99 – 2.18 (m, 4 H, CH$_2$C*H*$_2$CH$_3$), 3.08 (d, *J*=12.5 Hz, 1 H, ArC*H*$_2$Ar), 3.16 (d, *J*=12.5 Hz, 1 H, ArC*H*$_2$Ar), 3.26 (d, *J*=12.9 Hz, 1 H, ArC*H*$_2$Ar), 3.31 – 3.40 (m, 1 H, OC*H*$_2$CH$_2$), 3.50 – 3.71 (m, 3 H, OC*H*$_2$CH$_2$), 3.75 (d, *J*=13.9 Hz, 1 H, ArC*H*$_2$Ar), 3.90 – 4.08 (m, 3 H, OC*H*$_2$CH$_2$, ArC*H*$_2$Ar), 4.13 – 4.27 (m, 2 H, OC*H*$_2$CH$_2$), 4.31 – 4.51 (m, 3 H, ArC*H*$_2$Ar), 5.10 – 5.80 (br. s, 1H, COO*H*), 6.16 (d, *J*=2.1 Hz, 1 H, Ar*H*), 6.28 (d, *J*=2.1 Hz, 1 H, Ar*H*), 6.45 (d, *J*=2.2 Hz, 1 H, Ar*H*), 6.60 (d, *J*=2.2 Hz, 1 H, Ar*H*), 7.11 (d, *J*=2.2 Hz, 1 H, Ar*H*), 7.14 (d, *J*=2.2 Hz, 1 H, Ar*H*), 7.30 – 7.38 (m, 2 H, Ar*H*), 7.38 – 7.51 (m, 4 H, Ar*H*), 7.62 (d, *J*=4.7 Hz, 1 H, Ar*H*), 7.64 – 7.73 (m, 2 H, Ar*H*), 7.84 – 7.94 (m, 2 H, Ar*H*) ^{13}C NMR (101 MHz, CHLOROFORM-*d*) δ ppm 9.70 (CH$_2$*C*H$_3$), 9.91 (CH$_2$*C*H$_3$), 10.69 (CH$_2$*C*H$_3$), 10.75 (CH$_2$*C*H$_3$), 22.47 (CH$_2$*C*H$_2$CH$_3$), 23.18 (CH$_2$*C*H$_2$CH$_3$), 23.37 (CH$_2$*C*H$_2$CH$_3$), 23.51 (CH$_2$*C*H$_2$CH$_3$), 29.67 (Ar*C*H$_2$Ar), 30.02 (Ar*C*H$_2$Ar), 30.07 (Ar*C*H$_2$Ar), 30.95 (Ar*C*H$_2$Ar), 31.21 (C(*C*H$_3$)$_3$), 31.24 (C(*C*H$_3$)$_3$), 31.75 (C(*C*H$_3$)$_3$), 33.54 (*C*(CH$_3$)$_3$), 33.68 (*C*(CH$_3$)$_3$), 34.04 (*C*(CH$_3$)$_3$), 76.08 (O*C*H$_2$CH$_2$), 76.69 (O*C*H$_2$CH$_2$), 77.00 (O*C*H$_2$CH$_2$), 77.61 (O*C*H$_2$CH$_2$), 123.44 (*C*$_{Ar}$H), 124.22 (*C*$_{Ar}$H), 124.77 (*C*$_{Ar}$H), 125.20 (*C*$_{Ar}$H), 125.35 (*C*$_{Ar}$H), 125.62 (*C*$_{Ar}$H), 128.14 (*C*$_{Ar}$), 128.22 (*C*$_{Ar}$), 128.26 (*C*$_{Ar}$), 128.34 (*C*$_{Ar}$), 129.55 (*C*$_{Ar}$), 129.74 (*C*$_{Ar}$), 130.55 (*C*$_{Ar}$), 130.67 (*C*$_{Ar}$), 131.04 (*C*$_{Ar}$), 131.16 (*C*$_{Ar}$), 131.27 (*C*$_{Ar}$), 131.42 (*C*$_{Ar}$), 131.44 (*C*$_{Ar}$), 131.51 (*C*$_{Ar}$), 131.61 (*C*$_{Ar}$), 132.05 (*C*$_{Ar}$), 132.15 (*C*$_{Ar}$), 132.28 (*C*$_{Ar}$), 132.34 (*C*$_{Ar}$), 133.22 (*C*$_{Ar}$), 134.26 (*C*$_{Ar}$), 134.86 (*C*$_{Ar}$), 135.49 (*C*$_{Ar}$), 135.73 (*C*$_{Ar}$), 135.90 (*C*$_{Ar}$), 140.63 (*C*$_{Ar}$), 140.66 (*C*$_{Ar}$), 144.01 (*C*C(CH$_3$)$_3$), 144.31 (*C*C(CH$_3$)$_3$), 144.71 (*C*C(CH$_3$)$_3$), 145.21 (d, *J*= 8.1 Hz ,*C*CPO), 152.88 (*C*$_{Ar}$OPr), 152.88 (*C*$_{Ar}$OPr), 154.71 (*C*$_{Ar}$OPr), 160.72 (d, *J*=12.6 Hz, C*C*OCH$_2$), 171.32(d, *J*=3.7 Hz C*C*OOH); ^{31}P NMR (400 MHz, CHLOROFORM-*d*) δ ppm 31.18 (C*P*O); MS (ES+): *m/z* (%) = 1005.6 (100) $[M+H]^+$; HRMS–TOF MS ES+: *m/z* $[M+H]^+$ calcd for $C_{65}H_{82}O_7P$: 1005.5798; found: 1005.5778.

(*cR*)-11,17,23-tri-*tert*-butyl-4,5-dicarboxy-25,26,27,28-tetrapropoxycalix[4]arene – (4.14)

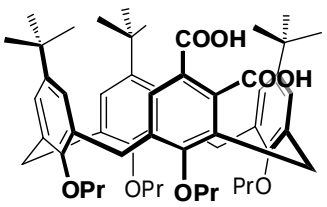

4.14 was prepared according to the procedure used for **4.10** from **4.6** (56 mg, 0.059 mmol), acetic acid (1.6 ml) water (0.4 ml) with heating to 170 ºC for 4 hours, ethanol (1 ml), water (1 ml) and sodium hydroxide (200 mg, 5 mmol) with heating to 150 ºC for 2 hours. Product **4.14** was purified by silica gel chromatography (EtOAc:PET 20:80 to EtOAc 100) affording a white solid (36 mg, 0.042 mmol, 72 % yield). Further purification was achieved via precipitation from MeCN and H_2O affording a white powder. Mp 202–208°C (DMSO); $[\alpha]_D^{20.9}$ = –39.1° (*c* 0.014 g/ml, DCM); R_f = 0.39 (EtOAc:PET:AcOH, 50:49:1); IR (film) cm^{-1}: 3060 (w, CH arom), 2960 (s, CH), 1713 (br, C=O); ^{1}H NMR (400 MHz, ACETIC ACID-*d*) δ ppm 1.01 – 1.11 (m, 30 H, C(CH_3)$_3$, CH_2CH_3), 1.13 (s, 9 H, C(CH_3)$_3$), 1.90 – 2.02 (m, 4 H, $CH_2CH_2CH_3$), 2.06 – 2.16 (m, 4 H, $CH_2CH_2CH_3$), 3.15 – 3.23 (m, 2 H, ArCH_2Ar), 3.29 (d, *J*=13.0 Hz, 1 H, ArCH_2Ar), 3.55 (d, *J*=13.5 Hz, 1 H, ArCH_2Ar), 3.74 – 3.88 (m, 3 H, OCH_2CH_2), 3.88 – 3.95 (m, 3 H, OCH_2CH_2), 4.01 – 4.13 (m, 2 H, OCH_2CH_2), 4.42 – 4.52 (m, 3 H, ArCH_2Ar), 4.55 (d, *J*=12.8 Hz, 1 H, ArCH_2Ar), 6.75 (d, *J*=2.4 Hz, 1 H, Ar*H*), 6.78 – 6.81 (m, 2 H, Ar*H*), 6.85 (d, *J*=2.4 Hz, 1 H, Ar*H*), 6.87 (d, *J*=2.4 Hz, 1 H, Ar*H*), 6.91 (d, *J*=2.6 Hz, 1 H, Ar*H*), 7.73 (s, 1 H, Ar*H*); ^{13}C NMR (101 MHz, ACETIC ACID-*d*) δ ppm 10.48 (CH_2CH_3), 10.80 (2 × CH_2CH_3), 10.98 (CH_2CH_3), 23.99 (2 × $CH_2CH_2CH_3$), 24.40 ($CH_2CH_2CH_3$), 24.44 ($CH_2CH_2CH_3$), 28.76 (ArCH_2Ar), 30.59 (ArCH_2Ar), 31.50 (ArCH_2Ar), 31.80 (C(CH_3)$_3$), 31.83 (C(CH_3)$_3$), 31.93 (C(CH_3)$_3$), 32.11 (ArCH_2Ar), 34.50 (*C*(CH_3)$_3$), 34.53 (*C*(CH_3)$_3$), 34.55 (*C*(CH_3)$_3$), 77.56 (OCH_2CH_2), 77.77 (OCH_2CH_2), 77.88 (OCH_2CH_2), 78.33 (OCH_2CH_2), 121.93 ($C_{Ar}CH_2$), 125.82 (C_{Ar}H), 126.11 (C_{Ar}H), 126.38 (C_{Ar}H), 126.59 (*C*COOH), 126.66 (C_{Ar}H), 126.93 (C_{Ar}H), 132.32 (C_{Ar}H), 132.53 (*C*COOH), 132.84 (C_{Ar}H), 134.54 ($C_{Ar}CH_2$), 134.95 ($C_{Ar}CH_2$), 135.02 ($C_{Ar}CH_2$), 135.05 ($C_{Ar}CH_2$), 135.41 ($C_{Ar}CH_2$), 135.57 ($C_{Ar}CH_2$), 137.77 ($C_{Ar}CH_2$), 145.29 (*C*(CH_3)$_3$), 145.67 (*C*(CH_3)$_3$), 145.70 (*C*(CH_3)$_3$), 154.76 (C_{Ar}OPr), 154.80 (C_{Ar}OPr), 155.05 (C_{Ar}OPr), 162.65 (C_{Ar}OPr), 171.52 (C*C*OOH), 175.29 (C*C*OOH); MS (ES-): *m/z* (%) = 847.6 (100) $[M-H]^-$; HRMS–TOF MS ES+: *m/z* $[M-H]^-$ calcd for $C_{54}H_{71}O_8$: 847.5149; found: 847.5125.

(*cR*)-11,17,23-tri-*tert*-butyl-5-dicarboxy-4-methylthio-25,26,27,28-tetrapropoxy-calix[4]arene – (4.15)

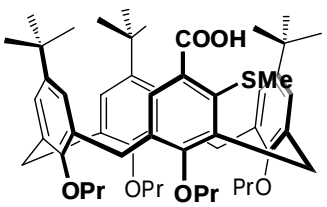

4.15 was prepared according to the procedure used for **4.10** from **4.7** (92 mg, 0.10 mmol), acetic acid (2.2 ml) water (0.5 ml) with heating to 170 ºC for 1 hour, ethanol (1 ml), water (1 ml) and sodium hydroxide (680 mg, 17 mmol) with heating to 140 ºC for 0.5 hours. The product **4.15** was purified by silica gel chromatography (EtOAc:PET 8:92 to 12:88) affording

a white solid (35 mg, 0.041 mmol, 41 % yield) further purification was achieved via precipitation from MeCN and H_2O affording a white powder. Mp 108–124°C; $[\alpha]_D^{18.6}$ = +31.8° (*c* 0.016 g/ml, DCM); R_f = 0.45 (EtOAc:PET, 15:85); IR (film) cm^{-1}: 2961 (s, CH), 2874 (s, CH), 1699 (s, C=O), 1481 (s, C=C); ^{1}H NMR (400 MHz, CHLOROFORM-*d*) δ ppm 0.92 – 0.98 (m, 12 H, CH_2CH_3, $C(CH_3)_3$), 0.98 – 1.08 (m, 9 H, CH_2CH_3), 1.14 (s, 9 H, $CH_3)_3$), 1.19 (s, 9 H, $CH_3)_3$), 1.82 – 2.06 (m, 12 H, SCH_3, $CH_2CH_2CH_3$), 3.13 – 3.26 (m, 3 H, $ArCH_2Ar$), 3.76 – 4.06 (m, 9 H, $ArCH_2Ar$, OCH_2CH_2), 4.41 – 4.54 (m, 4 H, $ArCH_2Ar$), 6.48 (s, 1 H, Ar*H*), 6.66 (d, *J*=1.8 Hz, 1 H, Ar*H*), 6.86 (d, *J*=2.1 Hz, 1 H, Ar*H*), 6.90 (s, 1 H, Ar*H*), 6.93 (d, *J*=2.1 Hz, 1 H, Ar*H*), 6.98 (br. s., 1 H, Ar*H*), 7.89 (s, 1 H, Ar*H*), 11.63 – 12.12 (br. s, 1H, COO*H*); ^{13}C NMR (101 MHz, CHLOROFORM-*d*) δ ppm 10.06 (CH_2CH_3), 10.28 (CH_2CH_3), 10.30 (CH_2CH_3), 10.54 (CH_2CH_3), 21.63 (SCH_3), 22.41 ($CH_2CH_2CH_3$), 23.16 ($CH_2CH_2CH_3$), 23.40 ($CH_2CH_2CH_3$), 23.45 ($CH_2CH_2CH_3$), 29.80 (br. s, $ArCH_2Ar$), 30.39 ($ArCH_2Ar$), 31.24 ($ArCH_2Ar$), 31.28 ($C(CH_3)_3$), 31.50 ($C(CH_3)_3$), 31.53 ($C(CH_3)_3$), 31.75 ($ArCH_2Ar$), 33.63 ($C(CH_3)_3$), 33.93 ($C(CH_3)_3$), 33.99 ($C(CH_3)_3$), 75.90 (OCH_2CH_2), 76.45(br. s, OCH_2CH_2) 76.69 (OCH_2CH_2), 77.19 (OCH_2CH_2), 123.90 ($C_{Ar}H$), 125.21 ($C_{Ar}H$), 125.50 ($C_{Ar}H$), 125.79 ($C_{Ar}H$), 125.93 ($C_{Ar}H$), 126.64 ($C_{Ar}H$), 126.79 (*C*COOH), 130.74 ($C_{Ar}CH_2$), 131.84 ($C_{Ar}H$), 132.21 ($C_{Ar}CH_2$), 133.23 ($C_{Ar}CH_2$), 133.45 ($C_{Ar}CH_2$), 134.49 ($C_{Ar}CH_2$), 134.54 ($C_{Ar}CH_2$), 134.62 ($C_{Ar}CH_2$), 136.54 ($C_{Ar}CH_2$), 140.44 (C*C*S), 143.87 ($CC(CH_3)_3$), 144.51 ($CC(CH_3)_3$), 145.07 ($CC(CH_3)_3$), 153.55 ($C_{Ar}OPr$), 154.05 ($C_{Ar}OPr$), 154.23 ($C_{Ar}OPr$), 160.82 ($C_{Ar}OPr$), 166.45 (C*C*OOH); MS (ES+): *m/z* (%) = 868.6 (100) $[M+H_2O]^+$; HRMS–TOF MS ES+: *m/z* $[M+H_2O]^+$ calcd for $C_{54}H_{76}O_7S$: 868.5312; found: 868.5327.

(*cR*)-4-bromo-11,17,23-tri-*tert*-butyl-5-carboxy-25,26,27,28-tetrapropoxycalix[4]arene – (4.16)

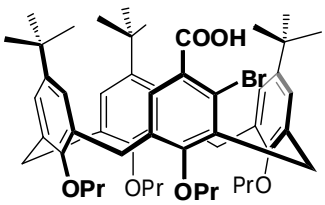

4.16 was prepared according to the procedure used for **4.10** from **4.8** (157 mg, 0.18 mmol), acetic acid (2 ml) water (0.4 ml) with heating to 170 ºC for 1 hours, ethanol (2 ml), water (2 ml) and sodium hydroxide (1200 mg, 30 mmol) with heating to 120 ºC for 1 hours. The product **4.16** was purified by silica gel chromatography (EtOAc:PET 5:95 to 15:85) affording a white solid (115 mg, 0.13 mmol, 72 % yield) further purification was achieved via re-crystallisation from EtOH and DCM affording white crystals. Mp 220–222°C (EtOH/DCM); $[\alpha]_D^{20.4}$ = –10.5° (*c* 0.02 g/ml, DCM); R_f = 0.30 (EtOAc:PET, 15:85); IR (film) cm^{-1}: 3564 (br, OH), 2961 (s, CH), 1699 (s, C=O), (s, C=C); 1H NMR (400 MHz, CHLOROFORM-*d*) δ ppm 0.97 – 1.11 (m, 39 H, $C(CH_3)_3$, CH_2CH_3), 1.86 – 1.98 (m, 4 H, $CH_2CH_2CH_3$), 1.98 – 2.12 (m, 4 H, $CH_2CH_2CH_3$), 3.14 – 3.22 (m, 3 H, $ArCH_2Ar$), 3.70 – 3.95 (m, 8 H, $ArCH_2Ar$, OCH_2CH_2), 3.95 –

4.04 (m, 1 H, OCH_2CH$_2$), 4.41 – 4.50 (m, 4 H, ArCH_2Ar), 6.69 – 6.79 (m, 4 H, Ar*H*), 6.81 (d, *J*=2.1 Hz, 1 H, Ar*H*), 7.01 (d, *J*=2.1 Hz, 1 H, Ar*H*), 7.62 (s, 1 H, Ar*H*); ^{13}C NMR (101 MHz, CHLOROFORM-*d*) δ ppm 10.11 (CH$_2$*C*H$_3$), 10.28 (CH$_2$*C*H$_3$), 10.33 (CH$_2$*C*H$_3$), 10.41 (CH$_2$*C*H$_3$), 22.89 (CH$_2$*C*H$_2$CH$_3$), 23.01 (CH$_2$*C*H$_2$CH$_3$), 23.35 (CH$_2$*C*H$_2$CH$_3$), 23.39 (CH$_2$*C*H$_2$CH$_3$), 30.37 (Ar*C*H$_2$Ar), 30.80 (Ar*C*H$_2$Ar), 31.23 (Ar*C*H$_2$Ar), 31.36 (C(*C*H$_3$)$_3$), 31.38 (2 × C(*C*H$_3$)$_3$, Ar*C*H$_2$Ar), 33.74 (*C*(CH$_3$)$_3$), 33.76 (*C*(CH$_3$)$_3$), 33.84 (*C*(CH$_3$)$_3$), 76.47 (OCH$_2$CH$_2$), 76.74 (OCH$_2$CH$_2$), 77.04 (OCH$_2$CH$_2$), 77.31 (OCH$_2$CH$_2$), 122.23 (*C*$_{Ar}$H), 124.71 (*C*$_{Ar}$H), 124.91 (*C*$_{Ar}$H), 125.03 (*C*$_{Ar}$H), 125.15 (*C*Br), 125.51 (*C*$_{Ar}$H), 125.59 (*C*$_{Ar}$H), 126.25 (*C*$_{Ar}$CH$_2$), 130.79 (*C*COOH), 131.70 (*C*$_{Ar}$CH$_2$), 132.39 (*C*$_{Ar}$H), 133.52 (*C*$_{Ar}$CH$_2$), 133.73 (*C*$_{Ar}$CH$_2$), 133.93 (*C*$_{Ar}$CH$_2$), 134.25 (*C*$_{Ar}$CH$_2$), 134.43 (*C*$_{Ar}$CH$_2$), 138.07 (*C*$_{Ar}$CH$_2$), 143.70 (*C*C(CH$_3$)$_3$), 144.65 (*C*C(CH$_3$)$_3$), 144.71 (*C*C(CH$_3$)$_3$), 153.54 (*C*$_{Ar}$OPr), 153.60 (*C*$_{Ar}$OPr), 153.87 (*C*$_{Ar}$OPr), 161.11 (*C*$_{Ar}$OPr), 171.36 (C*C*OOH); MS (ES+): *m/z* (%) = 900.5 (100) [M+H]$^+$; HRMS–TOF MS ES+: *m/z* [M+H$_2$O]$^+$ calcd for $C_{53}H_{73}BrO_7$: 900.4540; found: 900.4859.

9.5 Chapter 5

25,26,27,28-tetrahydroxylcalix[4]arene – (5.4)[9]

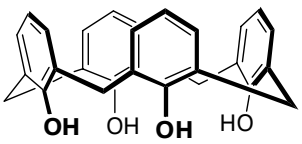

A round bottom flask (500 ml) was charged with calixarene **2.5** (20 g, 30.8 mmol), phenol (3.5 g, 37 mmol, 1.2 eq) and dry toluene (200 ml), placed under an inert atmosphere and rapidly stirred with a mechanical stirrer. $AlCl_3$ (20 g, 150 mmol, 4.9 eq) was added in one portion and the coloured mixture stirred for 2 hours at RT. The mixture was poured gently into crushed ice, following which a dilute HCl solution was added (1M, 250 ml), the organic phase separated and washed with H_2O (200 ml) and solvent removed under reduced pressure. Diethyl ether (50 ml) was and the resulting solid collected by filtration. The solid was dissolvent in hot MeOH and allowed to crystallise yielding an off white solid (11 g, 26 mmol, 84% yield). ^{1}H NMR (400 MHz, CHLOROFORM-d) δ ppm 3.58 (br. s., 4 H, ArCH_2Ar), 4.29 (br. s., 4 H, ArCH_2Ar), 6.76 (t, *J*=7.6 Hz, 4 H, Ar*H*), 7.08 (d, *J*=7.6 Hz, 8 H, Ar*H*), 10.23 (s, 4 H, ArO*H*).

25,26,27,28-tetrapropoxycalix[4]arene – (5.5)

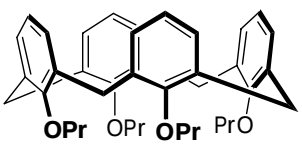

An oven dried round bottom flask (500 ml) was charged with sodium hydride (60% in mineral oil, 17.5 g, 435 mmol, 17 eq). NaH was suspended in Et_2O (3 x 10ml), and the solvent removed by syringe, while mainting the suspension under an inert atmosphere. Dry DMF (220 ml) debutylated calixarene **5.4** (11g, 25.9 mmol) and iodo propane (26 ml, 259 mmol, 10 eq) were added to the

flask and stirring was continued overnight at RT. 2M HCl (200 ml) was cautiously added to the mixture, the resulting precipitate was collected via filtration, washed with H_2O (3 × 50 ml), and dissolved in a $CHCl_3$ MeOH mixture. The white crystals were collected and used without further purification (11.7 g, 19 mmol, 74 % yield). ^{1}H NMR (300 MHz, CHLOROFORM-d) δ ppm 1.02 (t, *J*=7.4 Hz, 12 H, CH_2CH_3), 1.88 – 2.02 (m, 8 H, $CH_2CH_2CH_3$), 3.18 (d, *J*=13.4 Hz, 4 H, $ArCH_2Ar$), 3.84 – 3.92 (m, 8 H, OCH_2CH_2), 4.48 (d, *J*=13.4 Hz, 4 H, $ArCH_2Ar$), 6.55 – 6.66 (m, 12 H, ArH).

5-bromo-25,26,27,28-tetrapropoxycalix[4]arene – (5.3)

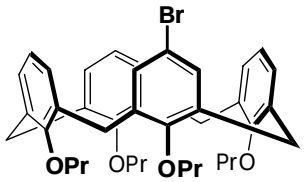

Tetrapropyl calixarene **5.5** (3 g, 5.1 mmol) was dissolved in freshly distilled methyl ethyl ketone (45 ml) to which freshly crystallised NBS (0.99 g, 5.6 mmol, 1.1 eq) was added. The reaction vessel was covered with aluminium foil and stirred at RT for 24 h. Sodium thiosulphate solution (10%, 50 ml) was added, the organic phase separated, dried over $MgSO_4$ and the solvent removed under reduced pressure. Further purification was achieved via silica gel column chromatography (DCM:PET 15:85) affording a white solid (2.6 g, 3.9 mmol, 76 % yield). ^{1}H NMR (400 MHz, CHLOROFORM-*d*) δ ppm 0.93 (t, *J*=7.5 Hz, 6 H, CH_2CH_3) 1.05 – 1.12 (m, 6 H, CH_2CH_3) 1.84 – 1.97 (m, 8 H, $CH_2CH_2CH_3$) 3.12 – 3.22 (m, 4 H, $ArCH_2Ar$) 3.71 – 3.87 (m, 4 H, OCH_2CH_2) 3.87 – 4.04 (m, 4 H, OCH_2CH_2) 4.45 (m, 4 H, $ArCH_2Ar$) 6.28 (d, *J*=7.6 Hz, 2 H, Ar*H*) 6.51 – 6.57 (m, 3 H, Ar*H*) 6.83 – 6.96 (m, 4 H Ar*H*) 7.00 (dd, *J*=7.3, 1.3 Hz, 2 H, Ar*H*).

5-carboxy-25,26,27,28-tetrapropoxycalix[4]arene – (5.2)

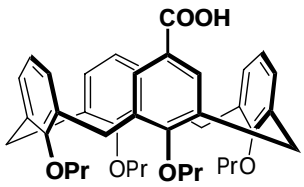

Bromo calixarene **5.3** (360 mg, 0.54 mmol) was added to an oven dried Schlenk flask and placed under a vacuum of less than 0.5 mmHg overnight. The crystals were dissolved in dry THF (5 ml), the solvent carefully removed under reduced pressure and the flask placed under a vacuum of less than 0.5 mmHg for 1 hour (this procedure was repeated twice). Dry THF (20 ml) and 60% NaH in mineral oil (100 mg) were added and the mixture stirred at RT for 1 hour. The flask was cooled (−78 ºC) and *n*BuLi (0.7 ml, 0.86 mmol, 1.6 eq) slowly added through a septum under a constant pressure of argon. The mixture was stirred for 1 hour at this temperature after which it was rapidly poured onto freshly condensed powdered CO_2 (350 ml). After warming to RT the mixture was dissolved in EtOAc (125 ml) and washed with successive portions of 1 M HCl (50 ml), H_2O (100 ml) and saturated $NaHCO_3$ (50 ml), the organic phase dried over $MgSO_4$ and the solvent removed under reduced pressure. Purification was performed by silica gel column chromatography (EtOAc:PET gradient elution 10:90 to 50:50) yielding a white solid (260 mg,

0.41 mmol, 76 %). Mp 276–278°C (MeOH); R_f = 0.64 (EtOAc:PET, 40:60); IR (ATR): 2960 (m, –C–H stretch), 2873 (m, –C–H stretch), 1676 (vs, C=O stretch), 1600 (w, C=C stretch), 1210 (s, C–O stretch), 967 (s, C–H oop bend), 758 cm^{-1} (vs, C–H oop bend); ^{1}H NMR (400 MHz, CHLOROFORM-*d*) δ ppm 0.96 – 1.08 (m, 12 H, CH_2CH_3), 1.86 – 1.99 (m, 8 H, $CH_2CH_2CH_3$), 3.17 (d, *J*=13.7 Hz, 2 H, $ArCH_2Ar$), 3.23 (d, *J*=13.7 Hz, 2 H, $ArCH_2Ar$), 3.80 – 3.90 (m, 6 H, OCH_2CH_2), 3.94 (t, *J*=7.32 Hz, 2 H, OCH_2CH_2), 4.43 – 4.52 (m, 4 H, $ArCH_2Ar$), 6.48 – 6.58 (m, 3 H, Ar*H*), 6.60 – 6.70 (m, 6 H, Ar*H*), 7.33 (s, 2 H, Ar*H*); ^{13}C NMR (101 MHz, CHLOROFORM-*d*) δ ppm 10.27, 10.31, 10.35, 23.21, 23.25, 23.32, 30.95, 76.60, 76.68, 76.74, 121.86, 122.16, 122.63, 128.11, 128.20, 128.56, 130.43, 134.45, 134.95, 135.36, 135.53, 156.43, 156.54, 161.63, 172.09; HRMS–TOF MS ES+: *m/z* $[M+Na]^+$ calcd for $C_{41}H_{48}NaO_6$: 659.3349; found: 659.3348.

5-((*S*)-4-isopropyl-4,5-dihydrooxazol-2-yl)- 25,26,27,28-tetrapropoxycalix[4]arene – (5.1)

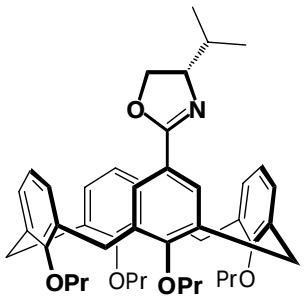

An oven dried flask (100 ml) was charged with carboxylic acid **5.2** (660 mg, 1.04 mmol), dry DCM (20 ml) and oxalyl chloride (0.45 ml, 5.1 mmol, 4.9 eq). The flask was stirred for 24 hours at RT under an atmosphere of argon, thereafter the solvent was removed under reduced pressure while maintaining inert conditions, affording a pale red foam, which was dried under a vacuum of less than 1 mmHg for 2 hours. The unpurified acid chloride product was dissolved in dry DCM (15 ml) and added at 30 ml per hour with a syringe pump to a mixture of L-Valinol (120 mg, 1.19 mmol, 1.14 eq) and Et_3N (0.35 ml, 2.55 mmol, 2.45 eq) in dry DCM (15 ml) under argon at 0 ºC. The mixture was warmed to RT and stirred for 24 hours, after which the solvent was removed under reduced pressure, and the amide product purified by silica gel column chromatography (EtOAc:PET, gradient elution, 20:80 to 50:50) yielding a white solid (700 mg, 0.97 mmol, 93% yield). The solid material was dissolved in dry DCM (20 ml) and added to a mixture of Et_3N (0.75 ml, 5.4 mmol, 5.5 eq) and mesyl chloride (0.2 ml, 2.6 mmol, 2.7 eq) and the mixture stirred for 24 hours at RT. DCM (40 ml) and saturated $NaHCO_3$ (20 ml) were added and the layers separated. The aqueous layer was extracted with a further portion of DCM (50 ml), the organic layers combined and washed with 2M NaOH (30 ml), dried over $MgSO_4$, and the solvent removed under reduced pressure affording a light yellow solid. Purification was accomplished by silica gel column chromatography (EtOAc:PET 6:94) yielding a white solid (647 mg, 0.91 mmol, 88 % yield from acid). Mp 115–120°C; $[\alpha]_D^{17}.6$ = –14.3 (*c* 0.27, DCM); R_f = 0.54 (EtOAc:PET, 10:90); IR (ATR) cm^{-1}: 2960 (w, –C–H stretch), 2873 (w, –C–H stretch), 1647 (w, C=N stretch), 1455 (s, C=C stretch), 1191 (s, C–O stretch), 1005 (s, C–O stretch), 966 (s, C–H oop bend), 756 (s, C–H oop bend); ^{1}H NMR (400 MHz, CHLOROFORM-*d*) δ ppm 0.92 – 0.98 (m, 9 H, CH_2CH_3, $CH(CH_3)_2$), 1.02 – 1.09 (m, 9 H,

CH_2CH_3, $CH(CH_3)_2$), 1.83 – 2.01 (m, 9 H, $CH_2CH_2CH_3$, $CH(CH_3)_2$), 3.16 (d, *J*=13.47 Hz, 2 H, $ArCH_2Ar$), 3.19 – 3.23 (m, 2 H, $ArCH_2Ar$), 3.73 – 3.80 (m, 4 H, OCH_2CH_2), 3.91 – 4.03 (m, 4 H, OCH_2CH_2), 4.04 – 4.15 (m, 2 H, OCH_2CHN), 4.32 – 4.41 (m, 1 H, OCH_2CHN), 4.45 (d, *J*=13.5 Hz, 4 H, $ArCH_2Ar$), 6.33 – 6.42 (m, 6 H, Ar*H*), 6.71 (t, *J*=7.4, Hz, 1 H, Ar*H*), 6.85 (d, *J*=7.4 Hz, 2 H, Ar*H*), 7.47 (d, *J*=2.2 Hz, 1 H, Ar*H*), 7.52 (d, *J*=2.2 Hz, 1 H, Ar*H*); ^{13}C NMR (101 MHz, CHLOROFORM-*d*) δ ppm 10.06, 10.56, 17.95, 19.14, 23.09, 23.12, 23.37, 30.87, 30.96, 32.81, 69.74, 72.47, 76.51, 76.60, 76.80, 76.83, 121.22, 121.78, 122.05, 127.83, 127.87, 128.47, 128.53, 128.59, 128.62, 133.52, 134.12, 136.12, 136.15, 136.24, 155.75, 157.28, 160.27, 163.62; HRMS–TOF MS ES+: *m/z* $[M+H]^+$ calcd for $C_{46}H_{58}NO_5$: 704.4315; found: 704.4333.

(*cR*)-5-((*S*)-4-isopropyl-4,5-dihydrooxazol-2-yl)-4-fluoro- 25,26,27,28-tetrapropoxycalix[4]arene – (5.6)

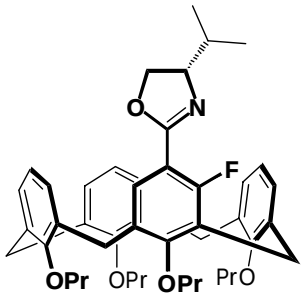

5.6 was synthesised in a procedure analogous to that used for **5.7** from oxazoline **5.1** (43 mg, 0.060 mmol), using TMEDA (0.090 ml, 0.604 mmol, 10 eq), *c*PentLi (0.37 ml, 0.30 mmol, 5 eq) and Et_2O (0.5 ml) with a 24 hour reaction at –78 ºC. The reaction was quenched with NFSI (160 mg, 0.513 mmol, 8.6 eq) at –78 ºC and left to warm to RT overnight. Yield by ^{1}H NMR 75 %; R_f = 0.54 (EtOAc:PET, 10:90); MS (ESI+): m/z (%) = 722.4 (100) [M+H]+; HRMS–ES+: m/z $[M+H]^+$ calcd for $C_{46}H_{57}FNO_6$: 722.4221; found: 722.4221.

(*cR*)-5-((*S*)-4-isopropyl-4,5-dihydrooxazol-2-yl)-4-methylthio- 25,26,27,28-tetrapropoxycalix[4]arene – (5.7)

Typical ortholithiation reaction procedure. An oven dried Schlenk flask was charged with pre-dried oxazoline **5.1** (170 mg, 0.24 mmol), TMEDA (0.36 ml, 2.34 mmol, 10 eq) and dry pentane (5 ml). The flask was cooled to −78 ºC and freshly titrated *c*PentLi (1.5 ml, 1.20 mmol, 5 eq) was slowly added, the flask sealed and stirred at −78 ºC for 5 hours, following which dimethyl disulphide (0.4 ml, 4.5 mmol, exs) was added and the flask was allowed to warm to RT overnight. H_2O (5ml) followed by EtOAc (10 ml) were added to the reaction vessel and stirring was continued for a further 5 minutes, thereafter additional EtOAc (50 ml) and H_2O (40 ml) were added and the layers separated. The aqueous layer was extracted with a further portion of EtOAc (50 ml), the organic layers combined, dried over $MgSO_4$, and the solvent removed under reduced pressure affording a light yellow semi-solid. Yield by ^{1}H NMR 93 %. Selectivity by ^{1}H 1:30. $[\alpha]_D^{22}.4$ = –11.5 (*c* 1.3, DCM); R_f = 0.54 (EtOAc:PET, 10:90); IR (film) cm^{-1}: 3061 (w, =C–H stretch), 2961 (s, –C–H

stretch), 2874 (s, –C–H stretch), 1661 (m, C=N stretch), 1587 (w, C=C stretch), 1456 (m, C=C stretch), 1196 (s, C–O stretch), 968 (m, C–H oop bend), 758 (m, C–H oop bend), 733 (m, C–H oop bend); ^{1}H NMR (400 MHz, CHLOROFORM-*d*) δ ppm 0.85 – 0.92 (m, 6 H, CH_2CH_3), 1.04 (d, *J*=6.82 Hz, 3 H, $CH(CH_3)_2$), 1.06 – 1.14 (m, 9 H, CH_2CH_3, $CH(CH_3)_2$), 1.81 – 2.02 (m, 9 H, $CH_2CH_2CH_3$, $CH(CH_3)_2$), 2.41 (s, 3 H, SCH_3), 3.11 – 3.20 (m, 3 H, $ArCH_2Ar$), 3.61 – 3.78 (m, 4 H, OCH_2CH_2), 3.97 – 4.06 (m, 4 H, OCH_2CH_2), 4.14 – 4.26 (m, 2 H, $ArCH_2Ar$, OCH_2CHN), 4.28 – 4.36 (m, 2 H, OCH_2CHN), 4.38 – 4.54 (m, 4 H, $ArCH_2Ar$), 5.97 (dd, *J*=7.7, 1.3 Hz, 1 H, Ar*H*), 6.05 (dd, *J*=7.6, 1.3 Hz, 1 H, Ar*H*), 6.09 – 6.19 (m, 3 H, Ar*H*), 6.23 (d, *J*=7.7 Hz, 1 H, Ar*H*), 6.92 (t, *J*=7.4 Hz, 1 H, Ar*H*), 7.11 (d, *J*=7.4 Hz, 2 H, Ar*H*), 7.34 (s, 1 H, Ar*H*); ^{13}C NMR (101 MHz, CHLOROFORM-*d*) δ ppm 9.82, 10.79, 18.48, 18.95, 21.30, 22.97, 23.49, 27.34, 30.70, 30.96, 31.00, 32.86, 70.47, 72.82, 76.46, 76.68, 76.91, 77.21, 121.75, 122.20, 122.25, 127.04, 127.25, 127.52, 127.63, 128.81, 128.92, 129.96, 132.03, 132.79, 133.05, 133.29, 133.47, 137.02, 137.17, 137.51, 142.25, 155.02, 155.08, 158.01, 160.22, 165.34; HRMS–TOF MS ES+: *m/z* $[M+H]^+$ calcd for $C_{47}H_{59}NO_5S$: 750.4114; found: 750.4161.

5-((*R*)-4-isopropyl-4,5-dihydrooxazol-2-yl)- 25,26,27,28-tetrapropoxycalix[4]arene – (5.9)

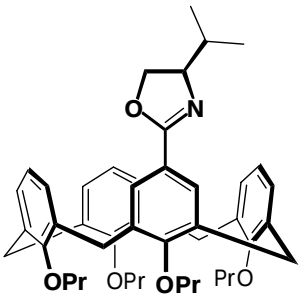

Carboxylic acid **5.2 (**122 mg, 0.19 mmol**)**, dry DCM (10 ml), and oxalyl chloride (0.1 ml, 2.1 mmol, 11 eq) were added to an oven dried flask under argon, and the mixture stirred at RT for 18 hours. The solvent was removed under reduced pressure (while maintaining inert conditions) and the flask placed under a vacuum of 1 mmHg for 1 hour. The light red solid was taken up in dry DCM (17 ml) and added at 35 ml/hour with a syringe pump to a stirred mixture of Et_3N (0.1 ml, 0.7 mmol, 3.8 eq), D-Valinol (27 mg, 0.27 mmol, 1.4 eq) in dry DCM (10 ml) at 0 ºC under argon. The mixture was allowed to warm to RT and stirred overnight. The solvent was removed under reduced pressure, and the amide product purified by silica gel column chromatography (EtOAc:PET gradient elution 10:90 to 50:50) yielding a white solid (100 mg, 0.14 mmol, 73 % yield). The amide was dissolved in dry DCM (10 ml) to which Et_3N (0.1 ml, 0.7 mmol, 5 eq) and mesyl chloride (0.05 ml, 0.64 mmol, 4.6 eq) were added under argon and the mixture stirred for 24 hours at RT. H_2O (20 ml) and additional DCM (20 ml) were added to the flask, the layers separated and the organic phase washed with saturated $NaHCO_3$ (30 ml), dried over $MgSO_4$ and the solvent removed under reduced pressure. Purification was accomplished by silica gel column chromatography (EtOAch:PET 6:94) affording a white solid (88 mg, 66 % yield from carboxylic acid **5.2**). Mp 110–120°C; $[\alpha]_D^{18}$ = 13.3 (*c* 0.29, DCM); R_f = 0.54 (EtOAc:PET, 10:90); IR (film): 2961 (s, –C–H stretch), 2875 (s, –C–H stretch), 1652 (s, C=N stretch), 1586 (w, C=C stretch), 1007 (w, C–O

stretch), 967 (w, C–H oop bend), 892 (s, C–H oop bend), 801 (s, C–H oop bend), 758 (s, C–H oop bend), 738 cm^{-1} (s, C–H oop bend); ^{1}H NMR (400 MHz, CHLOROFORM-*d*) δ ppm 0.92 – 0.98 (m, 9 H, CH_2CH_3, $CH(CH_3)_2$), 1.04 – 1.09 (m, 9 H, CH_2CH_3, $CH(CH_3)_2$), 1.84 – 2.02 (m, 9 H, $CH_2CH_2CH_3$, $CH(CH_3)_2$), 3.17 (d, *J*=13.5 Hz, 2 H, $ArCH_2Ar$), 3.19 – 3.26 (m, 2 H, $ArCH_2Ar$), 3.72 – 3.80 (m, 4 H, OCH_2CH_2), 3.92 – 4.03 (m, 4 H, OCH_2CH_2), 4.05 – 4.15 (m, 2 H, OCH_2CHN), 4.33 – 4.42 (m, 1 H, OCH_2CHN), 4.46 (d, *J*=13.5 Hz, 4 H, $ArCH_2Ar$), 6.34 – 6.42 (m, 6 H, Ar*H*), 6.72 (t, *J*=7.5 Hz, 1 H, Ar*H*), 6.86 (d, *J*=7.5 Hz, 2 H, Ar*H*), 7.48 (d, *J*=2.2 Hz, 1 H, Ar*H*), 7.53 (d, *J*=2.2 Hz, 1 H, Ar*H*); ^{13}C NMR (101 MHz, CHLOROFORM-*d*) δ ppm 10.05, 10.56, 17.95, 19.14, 23.09, 23.12, 23.37, 30.86, 30.96, 32.81, 69.73, 72.48, 76.51, 76.59, 76.80, 76.82, 121.23, 121.78, 122.05, 127.82, 127.86, 128.47, 128.53, 128.59, 128.62, 133.48, 134.11, 136.12, 136.15, 136.25, 155.74, 157.28, 160.27, 163.60; HRMS–TOF MS ES+: *m/z* $[M+H]^+$ calcd for $C_{46}H_{58}NO_5$: 704.4315; found: 704.432.

4-isopropyl-5-methylthio-5-((*R*)-4-Isopropyl-4,5-dihydrooxazol-2-yl)- cyclohexa-2,6-dienyl 25,26,27,28-tetrapropoxycalix[4]arene – (5.11)

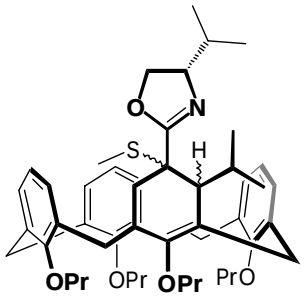

An oven dried Schlenk flask was charged with calixarene **5.1** (51 mg, 0.07 mmol) THF (1 ml), DMPU (0.09 ml, 0.72 mmol, 10 eq) and *i*PrLi (0.45 ml, 0.36 mmol, 5 eq) at –78 °C. After 5 hours, Me_2S_2 (0.1 ml, 1 mmol, 14 eq) was added and the flask allowed to warm to RT overnight. Purification was performed using silica gel column chromatography, yielding an off white solid (15 mg, 26% yield). ^{1}H NMR (400 MHz, CHLOROFORM-*d*) δ ppm 0.81 (t, *J*=7.6 Hz, 3 H, CH_2CH_3), 0.92 – 1.98 (m, 22 H, CH_2CH_3, $CH(CH_3)_2$), 1.78 – 1.96 (m, 9 H, $CH_2CH_2CH_3$), 1.98 – 2.14 (m, 1 H, $CH(CH_3)_2$), 2.16 – 2.27 (m, 1 H, $(CH_3)_2CH$), 2.32 (s, 3 H, SCH_3), 2.75 (d, *J*=14.1 Hz, 2 H, $ArCH_2Ar$), 3.00 – 3.19 (m, 2 H, $ArCH_2Ar$), 3.46 – 3.60 (m, 4 H, OCH_2CH_2), 3.62 (d, *J*=6.8 Hz, 1 H, $CH(CH_3)_2CHC$), 3.73 – 3.96 (m, 6 H, $ArCH_2Ar$, OCH_2CH_2), 4.04 (d, *J*=14.1 Hz, 1 H, $ArCH_2Ar$), 4.10 – 4.25 (m, 2 H, OCH_2CHN), 4.28 – 4.41 (m, 3 H, $ArCH_2Ar$, OCH_2CHN), 4.45 (d, *J*=13.7 Hz, 1 H, $(CH_3)_2CHCHC$), 5.78 (d, *J*=7.5 Hz, 1 H, Ar*H*), 6.07 (d, *J*=7.1 Hz, 1 H, Ar*H*), 6.11 (t, *J*=7.7 Hz, 1 H, Ar*H*), 6.33 (t, *J*=7.6 Hz, 1 H, Ar*H*), 6.41 (br. s., 1 H, SCC*H*C), 6.58 (d, *J*=7.5 Hz, 1 H, Ar*H*), 6.65 (d, *J*=7.3 Hz, 1 H, Ar*H*), 6.92 (t, *J*=7.4 Hz, 1 H, Ar*H*), 7.08 (dd, *J*=7.5, 1.6 Hz, 1 H, Ar*H*), 7.13 (dd, *J*=7.4, 1.6 Hz, 1 H, Ar*H*); ^{13}C NMR (101 MHz, CHLOROFORM-*d*) δ ppm 1.01, 9.59, 10.08, 10.16, 10.53, 10.79, 10.88, 12.97, 16.97, 18.32, 22.14, 22.26, 22.36, 22.61, 23.12, 23.18, 23.35, 23.43, 23.52, 23.54, 28.42, 29.69, 30.88, 30.96, 31.01, 31.44, 32.09, 32.10, 35.77, 36.20, 50.14, 50.15, 51.86, 69.00, 71.95, 75.53, 75.81, 75.94, 76.55, 121.53, 122.28, 122.72, 124.75,

125.39, 127.49, 127.62, 127.90, 128.15, 128.42, 128.50, 128.58, 128.79, 129.57, 133.20, 133.38, 134.02, 137.21, 138.16, 138.83, 150.24, 154.37, 155.35, 158.16.

(*cR*)-5-((*S*)-4-isopropyl-4,5-dihydrooxazol-2-yl)-4-diphenylphosphoryl- 25,26,27,28-tetrapropoxycalix[4]arene – (5.16)

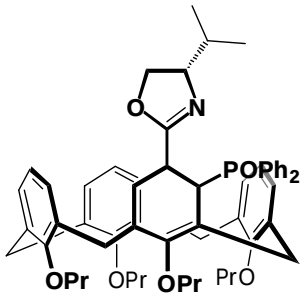

Phosphene oxide **5.16** was synthesised according to the general procedure from oxazoline **5.1** (120 mg, 0.17 mmol) using *c*PentLi (1.24 ml, 0.51 mmol, 3 eq) in dry Et_2O (1.5 ml) with TMEDA (0.15 ml, 1.01 mmol, 6 eq) and diphenyl phosphene chloride (0.14 ml, 0.77 mmol, 4.5 eq). The product was purified by silica gel column chromatography (EtOAc:PET 20:80) yielding a white solid (106 mg, 0.12 mmol, 69 % yield). Further purification can be achieved via crystallisation from PET. Mp >330°C (DCM); $[\alpha]_D^{22.4}$ = –54.5 (*c* 1.1, DCM); R_f = 0.26 (EtOAc:PET, 30:70); IR (ATR) cm^{-1}: 2960 (s, –C–H stretch), 1657 (s, C=N stretch), 1588 (w, C=C stretch), 1455 (s, C=C stretch), 1007 (s, C–O stretch), 967 (m, C–H oop bend), 758 (s, C–H oop bend), 701 (s, C–H oop bend); ^{1}H NMR (400 MHz, CHLOROFORM-*d*) δ ppm 0.72 (d, *J*=6.64 Hz, 3 H, $CH(CH_3)_2$), 0.82 – 0.99 (m, 12 H, $CH(CH_3)_2$, CH_2CH_3), 1.11 (t, *J*=7.42 Hz, 3 H, CH_2CH_3), 1.24 – 1.39 (m, 1 H, $CH(CH_3)_2$), 1.58 – 1.71 (m, 2 H, $CH_2CH_2CH_3$), 1.81 – 2.05 (m, 6 H, $CH_2CH_2CH_3$), 3.06 (d, *J*=13.67 Hz, 1 H, $ArCH_2Ar$), 3.14 (d, *J*=13.47 Hz, 1 H, $ArCH_2Ar$), 3.20 – 3.30 (m, 3 H, $ArCH_2Ar$, OCH_2CH_2), 3.34 (dt, *J*=9.37, 6.64 Hz, 1 H, OCH_2CH_2), 3.51 (dt, *J*=9.23, 6.52 Hz, 1 H, OCH_2CH_2), 3.60 – 3.70 (m, 2 H OCH_2CH_2), 3.77 – 4.05 (m, 6 H, OCH_2CH_2, OCH_2CHN, $ArCH_2Ar$), 4.15 (td, *J*=11.13, 5.27 Hz, 1 H, OCH_2CH_2), 4.35 (d, *J*=13.47 Hz, 1 H, $ArCH_2Ar$), 4.42 (d, *J*=13.08 Hz, 1 H, $ArCH_2Ar$), 4.47 (d, *J*=13.47 Hz, 1 H, $ArCH_2Ar$), 5.77 (d, *J*=6.64 Hz, 1 H, Ar*H*), 5.86 (d, *J*=7.42 Hz, 1 H, Ar*H*), 6.00 (t, *J*=7.52 Hz, 1 H, Ar*H*), 6.11 (t, *J*=7.91 Hz, 2 H, Ar*H*), 6.25 (t, *J*=7.62 Hz, 1 H, Ar*H*), 6.93 (t, *J*=7.42 Hz, 1 H, Ar*H*), 7.11 (ddd, *J*=11.38, 7.47, 1.46 Hz, 2 H, Ar*H*), 7.34 – 7.47 (m, 6 H, Ar*H*), 7.56 (d, *J*=4.69 Hz, 1 H, Ar*H*), 7.59 – 7.67 (m, 2 H, Ar*H*), 7.97 – 8.06 (m, 2 H, Ar*H*); ^{13}C NMR (101 MHz , CHLOROFORM-*d*) δ ppm 9.77, 9.79, 10.75, 10.81, 18.66, 19.96, 22.94, 23.34, 23.50, 30.49, 30.55, 30.78, 30.87, 31.02, 32.62, 70.47, 73.13, 76.41, 76.55, 76.57, 76.90, 77.20, 121.70, 122.15, 122.40, 126.75, 126.80, 126.83, 126.94, 127.03, 127.84, 128.00, 128.11, 128.23, 128.72, 129.01, 130.30, 130.44, 130.46, 130.60, 130.69, 130.89, 130.92, 131.35, 131.41, 131.52, 131.70, 131.80, 132.65, 132.71, 133.36, 133.93, 134.98, 137.13, 137.32, 137.36, 138.40, 141.14, 145.35, 145.43, 155.01, 158.19, 161.26, 161.38, 164.05, 164.09 HRMS–TOF MS ES+: *m/z* $[M+H]^+$ calcd for $C_{58}H_{67}NO_6P$: 904.4706; found: 904.4708.

9.6 Chapter 6

5-((*S*)-4-*tert*-butyl-4,5-dihydrooxazol-2-yl)- 25,26,27,28-tetrapropoxycalix[4]arene – (6.1)

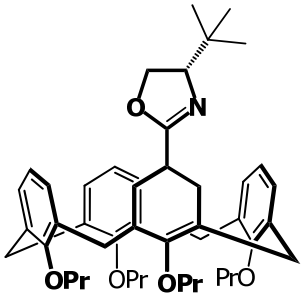

Calixarene acid **5.3** (230 mg, 0.36 mmol), oxalyl chloride (0.1 ml, 1.1 mmol, 3 eq) and DCM (2.5 ml) were added to an oven dried flask and stirred at RT for 3 hours. The solvent was removed under reduced pressure and the resulting solid was re-suspended in dry DCM (3 ml) and slowly added to a mixture of L-*tert*-leucinol (50 mg, 0.43 mmol, 1.2 eq), Et_3N (0.3 ml, 2.2 mmol, 6 eq) in DCM (3 ml) at 0°C and stirred overnight. Mesyl chloride (0.1 ml, 1.1 mmol, 3 eq) was slowly added and the flask stirred for a further 3 hours, following which H_2O (5 ml) and DCM (20 ml) were added, the layers separated and the aqueous layer washed with DCM (15 ml). The organic phases were combined, dried over $MgSO_4$ and the solvent removed under reduced pressure with purification via silica gel column chromatography affording a white glass (206 mg, 0.29 mmol, 80 % yield). Mp 144 – 146 °C (THF); $[\alpha]_D^{18.4}$ = –16.3 (c 2.2, DCM); Rf = 0.52 (EtOAc:PET, 10:90); IR (ATR) cm^{-1}: 2961 (m, –C–H stretch), 1653 (s, C=N stretch), 1557 (m, C=C stretch), 1455 (s, C=C stretch), 1193 (m, C–O stretch), 1006 (m, C–O stretch), 967 (m, C–H oop bend), 758 (s, C–H oop bend); ^{1}H NMR (300 MHz, CHLOROFORM-*d*) δ ppm 0.90 – 0.99 (m, 15 H, $C(CH_3)_3$, CH_2CH_3), 1.06 (t, *J*=7.4 Hz, 6 H, CH_2CH_3), 1.82 – 2.03 (m, 8 H, $CH_2CH_2CH_3$), 3.12 – 3.26 (m, 4 H, $ArCH_2Ar$), 3.76 (t, *J*=7.0 Hz, 4 H, OCH_2CH_2), 3.91 – 4.07 (m, 5 H, OCH_2CH_2, OCH_2CHN), 4.21 (dd, *J*=7.7, 8.6 Hz, 1 H, OCH_2CHN), 4.32 (dd, *J*=8.6, 10 Hz, 1 H, OCH_2CHN), 4.46 (d, *J*=13.4 Hz, 4 H, $ArCH_2Ar$), 6.31 – 6.43 (m, 6 H, Ar*H*), 6.72 (m, J=9.7, 1.2 Hz, 1 H, Ar*H*), 6.84 – 6.89 (m, 2 H, Ar*H*), 7.48 (d, J=2.2 Hz, 1 H, Ar*H*), 7.54 (d, J=2.1 Hz, 1 H, Ar*H*); ^{13}C NMR (75 MHz, CHLOROFORM-d) δ ppm 10.03, 10.57, 23.08, 23.10, 23.36, 25.92, 30.84, 30.87, 30.90, 30.95, 34.03, 68.47, 76.09, 76.50, 76.58, 76.78, 76.81, 121.26, 121.76, 122.04, 127.75, 127.84, 128.45, 128.55, 128.66, 133.45, 133.49, 134.05, 134.07, 136.12, 136.17, 136.20, 155.71, 157.30, 160.24, 163.53; HRMS–TOF MS ES+: m/z $[M+H]^+$ calcd for $C_{47}H_{60}NO_5$:718.4471; found: 718.4460.

(*cR*)-5-((*S*)-4-*tert*-butyl- 4,5-dihydrooxazol-2-yl)-4-methylthio- 25,26,27,28-tetrapropoxycalix[4]arene – (6.2)

Thioether **6.2** was synthesised according to the general procedure used to synthesise **5.7** from oxazoline **6.1** (20 mg, 0.03 mmol), *s*BuLi (0.15 ml, 0.14 mmol, 5 eq), TMEDA (0.04 ml, 0.28 mmol, 10 eq), pentane (0.5 ml) and Me_2S_2 (0.1 ml, 1 mmol, exs). Mp 94 – 139 °C (foam); R_f = 0.52 (EtOAc:PET, 10:90); $[\alpha]_D^{25.0}$ = –3.5 (c 1.0, DCM); IR (ATR): 2959 (s, –C–H stretch), 1652 (s, C=N stretch), 1456 (s, C=C stretch), 1195 (m, C–O stretch), 967 (m, C–H oop bend), 758 (s, C–H oop bend); ^{1}H NMR (400 MHz, CHLOROFORM-d) δ ppm 0.89 (m, 6 H, CH_2CH_3), 1.06 (s, 9 H, $C(CH_3)_3$), 1.10 (m, 6 H, CH_2CH_3), 1.81 – 2.02 (m, 8 H, $CH_2CH_2CH_3$), 2.42 (s, 3 H, SCH_3), 3.12 – 3.22 (m, 3 H, $ArCH_2Ar$), 3.62 – 3.78 (m, 5 H, $ArCH_2Ar$, OCH_2CH_2), 4.01 (m, 4 H, OCH_2CH_2), 4.13 (dd, J=10.2, 8.2 Hz, 1 H, OCH_2CHN), 4.29 – 4.35 (m, 2 H, OCH_2CHN), 4.39 – 4.50 (m, 4 H, $ArCH_2Ar$), 5.97 (dd, J=7.4, 1.4 Hz, 1 H, Ar*H*), 6.06 (dd, J=7.7, 1.4 Hz, 1 H, Ar*H*), 6.10 – 6.19 (m, 3 H, Ar*H*), 6.24 (t, J=7.6, 1 H, Ar*H*), 6.92 (t, J=7.6, 1 H, Ar*H*), 7.11 (d, J=7.4 Hz, 2 H, Ar*H*), 7.34 (s, 1 H, Ar*H*); ^{13}C NMR (75 MHz, CHLOROFORM-*d*) δ ppm 9.81, 10.79, 21.34, 22.98, 23.50, 26.12, 27.28, 30.73, 30.90, 30.98, 31.01, 34.03, 69.00, 76.47, 76.67, 76.70, 76.93, 77.20, 121.76, 122.21, 122.27, 127.06, 127.27, 127.56, 127.65, 128.83, 128.94, 129.07, 129.95, 132.03, 132.78, 133.05, 133.29, 133.44, 136.13, 137.04, 137.19, 137.57, 142.34, 155.03, 155.09, 158.03, 160.23, 165.38; HRMS–TOF MS ES+: m/z [M+H]+ calcd for $C_{48}H_{62}NO_5S$:764.4349; found: 764.4357.

(*cR*)-5-((*S*)-4-isopropyl-4,5-dihydrooxazol-2-yl)-4-bromo- 25,26,27,28-tetrapropoxycalix[4]arene – (6.6)

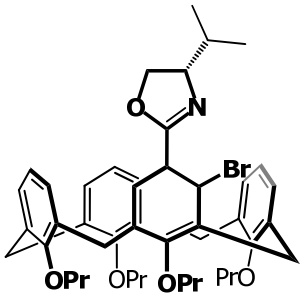

Bromo calixarene **6.6** was synthesised according to the general procedure used to synthesise **5.7** from oxazoline **5.1** (40 mg, 0.056 mmol), *s*BuLi (0.28 ml, 0.28 mmol, 5 eq), TMEDA (0.08 ml, 0.56 mmol, 10 eq), pentane (1 ml) and dibromoethane (0.5 ml, 0.56 mmol, 10 eq). Yield by ^{1}H NMR 80 %; $[\alpha]_D^{24.5}$ = –14.8 (*c* 1, DCM); R_f = 0.54 (EtOAc:PET, 10:90); IR (film): 2960 (m, –C–H stretch), 1651 (s, C=N stretch), 1585 (m, C=C stretch), 1450 (s, C=C stretch), 1194 (m, C–O stretch), 1005 (m, C–O stretch), 966 (m, C–H oop bend), 757 (s, C–H oop bend); ^{1}H NMR (500 MHz, CHLOROFORM-*d*) δ ppm 0.86 – 0.96 (m, 7 H, CH_2CH_3), 1.04 (d, J=6.6 Hz, 3 H, $CH(CH_3)_2$), 1.07 – 1.13 (m, 9 H, $CH(CH_3)_2$, CH_2CH_3), 1.82 – 2.02 (m, 9 H, $CH_2CH_2CH_3$, $CH(CH_3)2$), 3.15 (d, *J*=12.9 Hz, 1 H, $ArCH_2Ar$), 3.16 (d, *J*=13.6 Hz, 1 H, $ArCH_2Ar$), 3.18 (d, *J*=12.6 Hz, 1 H, $ArCH_2Ar$), 3.61 – 3.73 (m, 4 H, OCH_2CH_2), 3.97 – 4.05 (m, 4 H, OCH_2CH_2), 4.07 – 4.14 (m, 1 H, $ArCH_2Ar$), 4.16 – 4.25

(m, 2 H, OCH_2CHN), 4.35 – 4.46 (m, 4 H, $ArCH_2Ar$), 4.47 – 4.52 (m, 1 H, OCH_2CHN), 6.10 – 6.16 (m, 3 H, Ar*H*), 6.16 – 6.26 (m, 3 H, Ar*H*), 6.93 (t, J=1.0 Hz, 1 H, Ar*H*), 7.12 (d, J=7.6 Hz, 2 H, Ar*H*), 7.40 (s, 1 H, Ar*H*); ^{13}C NMR (75 MHz, CHLOROFORM-d) δ ppm 9.82, 10.79, 18.35, 18.90, 22.97, 23.47, 23.50, 29.61, 30.52, 30.93, 30.98, 32.75, 70.33, 72.84, 76.45, 76.84, 76.89, 77.20, 121.84, 121.93, 122.27, 124.78, 126.66, 127.48, 127.65, 127.72, 128.86, 128.92, 130.74, 131.76, 131.91, 133.10, 133.33, 135.92, 136.94, 137.10, 138.83, 154.98, 155.04, 157.90, 160.40, 164.21; MS (ES+): m/z (%) = 804 (100) $[M+H]^+$.

(*cR*)-4-bromo-carboxy-25,26,27,28-tetrapropoxycalix[4]arene – (6.7)

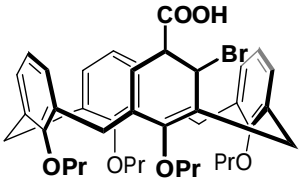

Bromo acid **6.7** was synthesised according to the general procedure used to synthesise acid **4.10** from **6.6** (19 mg, 0.024 mmol), acetic acid (1.5 ml) water (0.6 ml) with heating to 170 ºC for 2 hours, ethanol (2 ml), water (1.5 ml) and lithium hydroxide (200 mg, 8.3 mmol, exs) with heating to 150 ºC for 1 hour. Purification by silica gel chromatography yielded a white foam (13 mg, 0.018 mmol, 75 % yield); Mp 151 – 155 °C (foam); R_f = 0.67 (EtOAc:PET, 32:68); $[\alpha]_D^{24.5}$ = –11.2 (c 1.0, $CHCl_3$); IR (film) cm^{-1}: 2960 (s, –C–H stretch), 1696 (s, C=N stretch), 1454 (s, C=C stretch), 1206 (m, C–O stretch), 966 (m, C–H oop bend), 758 (s, C–H oop bend); ^{1}H NMR (300 MHz, CHLOROFORM-*d*) δ ppm 0.83 (m, 6 H, CH_2CH_3), 1.02 (t, *J*=7.3 Hz, 6 H, CH_2CH_3), 1.72 – 1.98 (m, 8 H, $CH_2CH_2CH_3$), 3.08 (d, *J*=13.4 Hz, 2 H, $ArCH_2Ar$), 3.15 (d, *J*=13.9 Hz, 1 H, $ArCH_2Ar$), 3.54 – 3.66 (m, 4 H, OCH_2CH_2), 3.87 – 4.16 (m, 5 H, OCH_2CH_2, $ArCH_2Ar$), 4.33 (d, *J*= 13.9 Hz, 1 H, $ArCH_2Ar$), 4.33 (d, *J*= 13.4 Hz, 3 H, $ArCH_2Ar$), 6.00 – 6.23 (m, 6 H, Ar*H*), 6.84 (t, *J*=7.4 Hz, 1 H, Ar*H*), 7.02 (d, *J*=7.5 Hz, 2 H, Ar*H*), 7.70 (s, 1 H, Ar*H*); ^{13}C NMR (75 MHz, CHLOROFORM-*d*) δ ppm 9.82, 9.83, 10.75, 10.78, 22.98, 23.12, 23.45, 23.50, 29.63, 30.66, 30.95, 31.01, 76.57, 76.85, 77.20, 77.42, 121.93, 122.31, 122.39, 122.62, 124.97, 126.62, 127.28, 127.83, 127.95, 128.86, 128.94, 131.56, 131.73, 132.30, 133.30, 133.60, 135.69, 136.85, 137.05, 139.69, 155.09, 155.15, 157.86, 162.32, 170.82; MS (ESI+): *m/z* (%) = 715.3 (100) $[M+H]^+$; HRMS–TOF MS ES–: *m/z* $[M–H]^-$ calcd for $C_{41}H_{46}O_6Br$: 713.2478; found: 713.2479.

(*cR*)-5-((*S*)-4-*tert*-butyl- 4,5-dihydrooxazol-2-yl)-4-bromo- 25,26,27,28-tetrapropoxycalix[4]arene – (6.4)

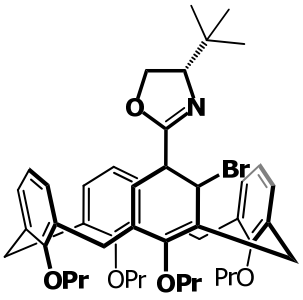

Bromo calixarene **6.4** was synthesised according to the general procedure used to synthesise **5.7** from oxazoline **6.1** (40 mg, 0.054 mmol), *s*BuLi (0.23 ml, 0.27 mmol, 5 eq), TMEDA (0.08 ml, 0.54 mmol, 10 eq), pentane (0.5 ml) and dibromoethane (0.1 ml, 2.4 mmol, exs). Yield by ^{1}H NMR 88 %; Mp 96 °C (foam); R_f = 0.52

(EtOAc:PET, 10:90); $[\alpha]_D^{24.5}$ = –19.6 (c 1.0, DCM); IR (ATR): 2959 (s, –C–H stretch), 1661 (s, C=N stretch), 1451 (s, C=C stretch), 1194 (m, C–O stretch), 966 (m, C–H oop bend), 759 (s, C–H oop bend); ^{1}H NMR (300 MHz, CHLOROFORM-*d*) δ ppm 0.89 (t, *J*=7.3 Hz, 6 H, CH_2CH_3), 1.06 (s, 9 H, $C(CH_3)_3$), 1.10 (t, *J*=7.4 Hz, 6 H, CH_2CH_3), 1.79 – 2.03 (m, 8 H, $CH_2CH_2CH_3$), 3.16 (d, *J*=13.2 Hz, 2 H, $ArCH_2Ar$), 3.18 (d, *J*=13.6 Hz, 1 H, $ArCH_2Ar$), 3.62 – 3.72 (m, 4 H, OCH_2CH_2), 3.94 – 4.17 (m, 6 H, OCH_2CH_2, $ArCH_2Ar$, OCH_2CHN), 4.27 – 4.49 (m, 6 H, $ArCH_2Ar$, OCH_2CHN), 6.09 – 6.28 (m, 6 H, Ar*H*), 6.93 (t, *J*=7.4 Hz, 1 H, Ar*H*), 7.12 (d, *J*=7.5 Hz, 2 H, Ar*H*), 7.39 (s, 1 H, Ar*H*); ^{13}C NMR (75 MHz, CHLOROFORM-d) δ ppm 9.80, 10.76, 10.79, 22.95, 23.47, 26.08, 29.62, 30.53, 30.95, 30.99, 34.09, 68.97, 76.44, 76.58, 76.85, 76.88, 77.20, 121.86, 121.96, 122.27, 124.91, 126.66, 127.51, 127.66, 127.75, 128.87, 128.93, 130.72, 131.76, 131.94, 133.11, 133.33, 135.90, 136.96, 137.11, 138.86, 155.00, 155.07, 157.92, 160.39, 164.20; MS (ESI+): *m/z* (%) = 896 (100) $[M+H]^+$; HRMS–TOF MS ESI+: *m/z* $[M+H]^+$ calcd for $C_{47}H_{59}NO_5Br$:796.3572; found: 796.3564.

(*cR*)-4-bromo-carboxy-25,26,27,28-tetrapropoxycalix[4]arene – (6.5)

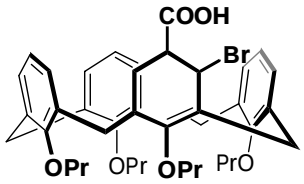

Bromo acid **6.5** was synthesised according to the general procedure used to synthesise acid **4.10** from **6.4** (22 mg, 0.028 mmol), acetic acid (1.5 ml) water (0.6 ml) with heating to 170 ºC for 2 hours, ethanol (2 ml), water (1.5 ml) and lithium hydroxide (200 mg, 8.3 mmol, exs) with heating to 150 ºC for 1 hour. Purification by silica gel chromatography yielded a white foam (11 mg, 0.015 mmol, 55 % yield); $[\alpha]_D^{24.5}$ = –10.8 (c 1.0, $CHCl_3$).

11,17,23-tri-*tert*-butyl-5-((*S*)-4-*tert*-butyl-4,5-dihydrooxazol-2-yl)- 25,26,27,28-tetrapropoxycalix[4]arene – (6.8)

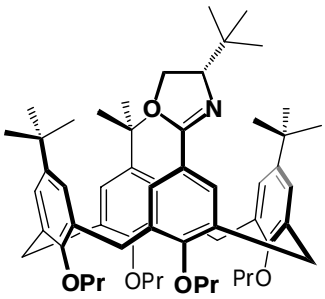

6.8 was synthesised using the procedure for the synthesis of oxazoline calixarene **2.1,** from carboxyl calixarene **2.2** (552 mg, 0.687 mmol), thionyl chloride (3 ml, 41 mmol, 60 eq), L-*tert*-luecinol (100 mg, 0.82 mmol, 1.2 eq) and triethylamine (0.34 ml, 2.5 mmol, 3.6 eq) in DCM (5 + 10 ml) and thionyl chloride (0.8 ml, 11.3 mmol, 16.4 eq) in DCM (10 ml) yielding a pale yellow solid after purification by column chromatography (PET:EtOAc 98:2) (571 mg, 0.64 mmol, 94 % yield). Further purification was achieved by slow crystallisation from EtOH and DCM. Mp 209–210°C (EtOH/DCM); R_f = 0.83 (EtOAc:PET, 10:90); $[\alpha]_D^{24.5}$ = –10.4 (c 2.2, DCM); IR (ATR) cm^{-1}: 2957 (m, –C–H stretch), 1654 (s, C=N stretch), 1480 (s, C=C stretch), 1201 (m, C–O stretch), 1008 (m, C–O stretch), 960 (m, C–H oop bend); ^{1}H NMR (400 MHz, CHLOROFORM-*d*) δ ppm

0.77 (s, 9 H, C(CH_3)$_3$), 0.85 (s, 9 H, C(CH_3)$_3$), 0.95 (t, *J*=7.4 Hz, 6 H, CH$_2$CH_3), 1.03 – 1.12 (m, 6 H, CH$_2$CH_3), 1.30 (s, 9 H, C(CH_3)$_3$), 1.30 (s, 9 H, C(CH_3)$_3$), 1.86 – 1.99 (m, 4 H, CH$_2$CH_2CH$_3$), 1.99 – 2.14 (m, 4 H, CH$_2$CH_2CH$_3$), 3.09 – 3.20 (m, 4 H, ArCH_2Ar), 3.68 – 3.75 (m, 4 H, OCH_2CH$_2$), 3.76 – 3.82 (m, 1 H,NC*H*CH$_2$), 3.89 – 4.01 (m, 5 H, OCH_2CH$_2$, OCH_2CH), 4.11 (dd, *J*=9.9, 8.5 Hz, 1 H, OCH_2CH), 4.40 – 4.46 (m, 4 H, ArCH_2Ar), 6.34 (d, *J*=2.5 Hz, 1 H, Ar*H*), 6.37 (d, *J*=2.5 Hz, 1 H, Ar*H*), 7.02 – 7.07 (m, 3 H, Ar*H*), 7.07 – 7.11 (m, 2 H, Ar*H*), 7.13 (d, *J*=2.0 Hz, 1 H, Ar*H*); ^{13}C NMR (101 MHz, CHLOROFORM-*d*) δ ppm 9.97 (2 x CH$_2$*C*H$_3$), 10.61 (CH$_2$*C*H$_3$), 10.72 (CH$_2$*C*H$_3$), 23.10 (CH$_2$*C*H$_2$CH$_3$), 23.15 (CH$_2$*C*H$_2$CH$_3$), 23.34 (CH$_2$*C*H$_2$CH$_3$), 23.52 (CH$_2$*C*H$_2$CH$_3$), 26.04 (C(*C*H$_3$)$_3$), 30.74 (Ar*C*H$_2$Ar), 30.84 (Ar*C*H$_2$Ar), 30.98 (C(*C*H$_3$)$_3$), 31.06 (Ar*C*H$_2$Ar), 31.09 (Ar*C*H$_2$Ar), 31.61 (2 x C(*C*H$_3$)$_3$), 33.39 (*C*(CH$_3$)$_3$), 33.62 (*C*(CH$_3$)$_3$), 34.04 (2 x *C*(CH$_3$)$_3$), 68.19 (OCH$_2$CHN), 76.08 (OCH$_2$CHN), 76.57 (O*C*H$_2$CH$_2$), 76.69 (O*C*H$_2$CH$_2$), 77.05 (O*C*H$_2$CH$_2$), 77.19 (O*C*H$_2$CH$_2$), 121.78 (*C*$_{Ar}$CNO), 124.28 (*C*$_{Ar}$H), 125.00 (*C*$_{Ar}$H), 125.39 (*C*$_{Ar}$H), 125.43 (*C*$_{Ar}$H), 125.69 (*C*$_{Ar}$H), 125.75 (*C*$_{Ar}$H), 127.67 (*C*$_{Ar}$H), 127.89 (*C*$_{Ar}$H), 132.25 (*C*$_{Ar}$CH$_2$), 132.49 (*C*$_{Ar}$CH$_2$), 133.66 (*C*$_{Ar}$CH$_2$), 133.73 (*C*$_{Ar}$CH$_2$), 134.54 (*C*$_{Ar}$CH$_2$), 134.70 (*C*$_{Ar}$CH$_2$), 135.39 (*C*$_{Ar}$CH$_2$), 135.50 (*C*$_{Ar}$CH$_2$), 143.95 (*C*$_{Ar}$C(CH$_3$)$_3$), 144.63 (*C*$_{Ar}$C(CH$_3$)$_3$), 144.66 (*C*$_{Ar}$C(CH$_3$)$_3$), 152.86 (*C*$_{Ar}$O), 154.56 (*C*$_{Ar}$O), 154.58 (*C*$_{Ar}$O), 157.92 (*C*$_{Ar}$O), 163.17 (C$_{Ar}$*C*NO); MS (ESI+): *m/z* (%) = 886.6 (100); [M+H]$^+$; HRMS–TOF MS ESI+: *m/z* [M+H]$^+$ calcd for C$_{59}$H$_{84}$NO$_5$: 886.6349; found: 886.6337.

(*cR*)-11,17,23-tri-*tert*-butyl-5-((*S*)-4-*tert*-butyl-4,5-dihydrooxazol-2-yl)-4-methylthio-25,26,27,28-tetrapropoxycalix[4]arene – (6.9)

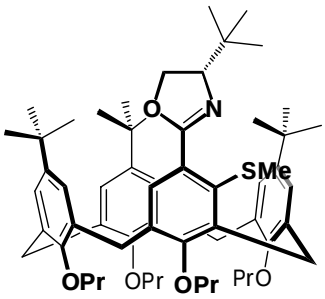

Thioether **6.9** was synthesised according to the general procedure used to synthesise **5.7** from oxazoline **6.8** (30 mg, 0.034 mmol), sBuLi (0.14 ml, 0.17 mmol, 5 eq), TMEDA (0.05 ml, 0.34 mmol, 10 eq), Et$_2$O (0.2 ml) and dimethyldisulfide (0.05 ml, 5 mmol, exs). Yield by HPLC 57 %; R$_f$ = 0.41 (EtOAc:PET, 10:90); $[\alpha]_D^{24.5}$ = –8.4 (c 1.0, DCM); IR (film) cm^{-1}: 2959 (s, –C–H stretch), 1661 (s, C=N stretch), 1463 (s, C=C stretch), 1199 (m, C–O stretch), 968 (m, C–H oop bend), 870 (s, C–H oop bend), 800 (s, C–H oop bend) 738 (s, C–H oop bend); ^{1}H NMR (500 MHz, CHLOROFORM-d) δ ppm 0.94 – 1.03 (m, 30 H, C(CH_3)$_3$, CH$_2$CH_3), 1.04 (s, 9 H, C(CH_3)$_3$), 1.13 (s, 9 H, C(CH_3)$_3$), 1.87 – 2.10 (m, 11 H, SCH_3, CH$_2$CH_2CH$_3$), 3.15 (d, J=12.6, 2 H, ArCH_2Ar), 3.16 (d, J=12.6, 1 H, ArCH_2Ar), 3.69 – 3.75 (m, 1 H, OCH_2CH$_2$), 3.76 – 3.94 (m, 7 H, OCH_2CH$_2$), 4.00 – 4.06 (m, 1 H, OCH$_2$CHN), 4.10 – 4.18 (m, 2 H, OCH$_2$CHN, ArCH_2Ar), 4.27 – 4.32 (m, 1 H, OCH$_2$CHN), 4.34 (d, J=12.9 Hz, 1 H, OCH$_2$CHN), 4.39 – 4.42 (d, *J*=12.6 Hz, 1 H, ArCH_2Ar), 4.44 (d, *J*=12.6 Hz, 2 H, ArCH_2Ar), 6.67 (br. s., 2 H, Ar*H*), 6.75 (s, 1 H, Ar*H*), 6.77 (br. s., 1 H, Ar*H*), 6.84 (br. s., 1 H,

Ar*H*), 6.86 (s, 1 H, Ar*H*), 7.16 (s, 1 H, Ar*H*); ^{13}C NMR (75 MHz, CHLOROFORM-*d*) δ ppm 10.11, 10.27, 10.35, 10.46, 21.47, 22.90, 23.31, 23.44, 26.13, 28.63, 28.65, 29.70, 30.53, 31.18, 31.37, 31.42, 31.52, 33.76, 33.78, 33.83, 33.90, 68.49, 76.58, 76.66, 76.81, 77.20, 124.63, 124.69, 125.00, 125.15, 125.31, 125.79, 125.83, 129.75, 130.01, 131.99, 132.93, 133.08, 133.44, 134.12, 134.51, 135.95, 140.77, 143.77, 144.38, 144.44, 153.55, 153.65, 154.06, 158.70, 165.02; MS (ESI+): *m/z* (%) = 932 (100) $[M+H]^+$; HRMS–TOF MS ESI+: *m/z* $[M+H]^+$ calcd for $C_{60}H_{86}NO_5S$: 932.6222; found: 932.6235.

(*cR*)-11,17,23-tri-*tert*-butyl-5-((*S*)-4-*tert*-butyl-4,5-dihydrooxazol-2-yl)-4-methylthio-25,26,27,28-tetrapropoxycalix[4]arene – (6.11)

Thio acid **4.15** (5 mg, 0.006 mmol) was added to an oven dried flask charged with DCM (3 ml) and oxalyl chloride (0.1 ml, 1.2 mmol, exs) and stirred for 4 hours at RT. The solvent was removed under reduced pressure, the mixture resuspended in DCM (2 ml) and added to a stirred mixture of Et_3N (0.3 ml, 2.2 mmol, exs), L-*tert*-leucinol (3 mg, 0.026 mmol, exs) in DCM (1 ml). Stirring was continued for 12 hours, thereafter mesyl chloride (0,1 ml, 1.2 mmol, exs) was added, followed by H_2O (5 ml) after a further 4 hours of stirring. Purification was accomplished via silica gel column chromatography yielding a white solid (4 mg, 0.004 mmol, 73% yield); MS (ES+): *m/z* (%) = 933 (100) $[M+H]^+$; HRMS–TOF MS ESI+: *m/z* $[M+H]^+$ calcd for $C_{60}H_{86}NO_5S$: 932.6222; found: 932.6204.

9.7 Chapter 7

ferrocenecarboxylic acid – (7.1)

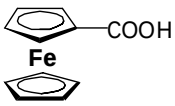

Ferrocene (2g, 10.8 mmol), *t*BuK (solution in *t*-butanol, 1.8 ml, 1.8 mmol, 0.1 eq) and dry THF (100 ml) were added to an oven dried round bottom flask (250 ml) under inert conditions. The mixture was cooled to –78 ºC for ten minutes following which, *t*BuLi (11.4 ml, 21.6 mmol, 2 eq) was slowly added and the mixture stirred for a further hour. Into the solution CO_2 (dried through a $CaCl_2$ column, exs) was bubbled with maintenance of the inert atmosphere, until the flask had warmed to RT. H_2O (50 ml) was added to the deep orange solution, the layers separated, and the organic phase extracted with 10 % NaOH solution (3 x 50 ml). The aqueous layers were combined, and conc HCl cautiously added until an acidic pH was obtained. The resulting precipitate was collected by filtration and thoroughly washed with H_2O (200 ml), and dried under vacuum yielding **7.1** as an orange solid

(2.16 g, 9.4 mmol, 87%). Mp 192 – 196 °C (decomposes) (H_2O); R_f = 0.17 (EtOAc:PET, 20:80); ^{1}H NMR (500 MHz, CHLOROFORM-*d*) δ ppm 4.27 (s, 5 H, Cp*H*), 4.48 (m, 2 H, Cp*H*), 4.87 (m, 2 H, Cp*H*), 11.03 (br. s., 1 H, COO*H*).

(*S*)-(4-isopropyl-4,5-dihydrooxazol-2-yl)-ferrocene – (7.2)

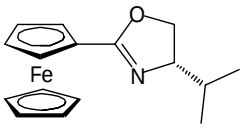

An oven dried flask was charged with carboxylic acid **7.1** (500 mg, 2.17 mmol) dry DCM (15 ml) and oxalyl chloride (0.56 ml, 6.52 mmol, 3 eq) and stirred for 4 hours at RT under an inert atmosphere. The solvent was removed under reduced pressure, affording a red solid. The solid was taken up in dry DCM (10 ml) and slowly added to a stirred mixture of L-valinol (324 mg, 2.82 mmol, 1.3 eq), Et_3N (0.9 ml, 6.51 mmol, 3 eq) in dry DCM (10 ml) at 0°C under an inert atmosphere. Stirring was continued for 4 hours, after which MsCl (0.33 ml, 4.34 mmol, 2 eq) and Et_3N (0.9 ml, 6.51 mmol, 3 eq) were added, with stirring continued for a further 3 hours. Aqueous $NaHCO_3$ (sat, 50 ml) and DCM (50 ml) were added to the flask, and the layers separated. The aqueous layer was extracted with further portions of DCM (2 x 50 ml), the organic layers combined, dried over $MgSO_4$ and the solvent removed under reduced pressure. Further purification was accomplished using silica gel column chromatography (PET:EtOAc 80:20) affording a deep red crystalline solid (653 mg, 2.11 mmol, 97 %). R_f = 0.48 (EtOAc:PET, 40:60); ^{1}H NMR (300 MHz, CHLOROFORM-*d*) δ ppm 0.94 (d, *J*=6.8 Hz, 3 H, CH(C*H*$_3$)$_2$), 1.01 (d, *J*=6.8 Hz, 3 H, CH(C*H*$_3$)$_2$), 1.77 – 1.95 (m, 1 H, C*H*(CH$_3$)$_2$), 3.94 – 4.12 (m, 2 H, OCH$_2$CHN), 4.19 (s, 5 H, Cp*H*), 4.25 – 4.35 (m, 3 H, OCH$_2$CHN, Cp*H*), 4.71 – 4.75 (m, 1 H, Cp*H*), 4.77 (m, 1 H, Cp*H*); MS (ES+): *m/z* (%) = 296.9 (100).

(*S*, $_p$*R*)-(4-isopropyl-4,5-dihydrooxazol-2-yl)- 2-methylthio- ferrocene – (7.3)

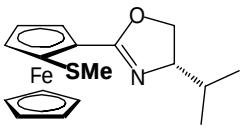

An oven dried round bottom flask was charged with oxazoline **7.2** (31 mg, 1 mmol), dry toluene (1 ml) and TMEDA (0.03 ml, 0.2 mmol, 2 eq) and cooled to –78 °C. *n*BuLi (0.08 ml, 0.15 mmol, 1.5 eq) was added and the red mixture stirred at –78°C for 2 hours, following which DMDS (0.1 ml, 1 mmol, exs) was added and the flask allowed to warm to RT. Et_2O (20 ml) and saturated $NaHCO_3$ (20 ml) were added, the organic phase separated, dried over $MgSO_4$ and the solvent removed under reduced pressure. R_f = 0.63 (EtOAc:PET, 40:60); ^{1}H NMR (300 MHz, CHLOROFORM-*d*) δ ppm 0.98 (d, *J*=6.8 Hz, 3 H, CH(C*H*$_3$)$_2$) 1.04 (d, *J*=6.8 Hz, 3 H, CH(C*H*$_3$)$_2$) 1.81 – 1.98 (m, 1 H, C*H*(CH$_3$)$_2$) 2.41 (s, 3 H, SC*H*$_3$) 4.00 – 4.17 (m, 2 H, OCH$_2$CHN) 4.17 – 4.21 (m, 5 H, Cp*H*) 4.27 – 4.35 (m, 2 H, OCH$_2$CHN, Cp*H*) 4.41 (m, 1 H, Cp*H*) 4.73 (m, 1 H, Cp*H*).

(*S*, $_p$*S*)-(4-isopropyl-4,5-dihydrooxazol-2-yl)-2-methylthio-ferrocene – (7.4)

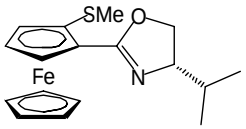

Thioether **7.4** was synthesised according to the general procedure used to synthesise **7.3** from, oxazoline **7.2** (28 mg, 1 mmol), dry toluene (1 ml) di-*t*Bu-diglyme (0.12 ml, 0.5 mmol, 5 eq) and *n*BuLi (0.18 ml, 0.2 mmol, 2 eq). $[\alpha]_D^{34}$ = 96.0 (*c* 0.9, DCM); R_f = 0.63 (EtOAc:PET, 40:60); IR (Film) cm^{-1}: 3097 (m, –C–H stretch), 2957 (m, –C–H stretch), 1652 (s, C=N stretch), 1106 (m, C–O stretch), 986 (m, C–H oop bend), 819 (m, C–H oop bend), ^{1}H NMR (300 MHz, CHLOROFORM-*d*) δ ppm 0.94 (d, *J*=6.8 Hz, 3 H, CH(C*H*$_3$)$_2$), 1.02 (d, *J*=6.8 Hz, 3 H, CH(C*H*$_3$)$_2$), 1.86 (dq, *J*=12.9, 6.6 Hz, 1 H, C*H*(CH$_3$)$_2$), 2.39 (s, 3 H, SC*H*$_3$), 4.01 – 4.15 (m, 2 H, OCH$_2$CHN), 4.22 (s, 5 H, Cp*H*), 4.27 – 4.37 (m, 2 H, OCH$_2$CHN, Cp*H*), 4.41 (dd, *J*=2.4, 1.7 Hz, 1 H, Cp*H*), 4.78 (dd, *J*=2.6, 1.5 Hz, 1 H, Cp*H*); ^{13}C NMR (75 MHz, CHLOROFORM-*d*) δ ppm 17.90, 18.66, 18.81, 32.53, 68.44, 69.35, 70.47, 70.91, 71.44, 71.65, 72.35, 85.71, 164.67; MS (EI+): *m/z* (%) = 342.9 (100); HRMS–TOF MS ESI+: *m/z* $[M]^+$ calcd for $C_{17}H_{21}NOSFe$: 343.0688; found: 343.0686.

(*S*)-(4-*tert*-butyl-4,5-dihydrooxazol-2-yl)-ferrocene – (7.7)

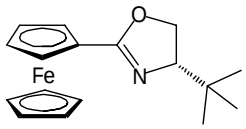

*t*Butyl oxazoline **7.7** was synthesised according to the general procedure used for oxazoline **7.2** from carboxylic acid **7.1** (262 mg, 1.14 mmol), oxalyl chloride (0.29 ml, 3.4 mmol, 3 eq), L-*t*-butyl-leucinol (133 mg, 1.14 mmol, 1 eq), Et_3N (0.3 ml, 3.4 mmol, 3 eq), MsCl (0.18 ml, 2.28 mmol, 2 eq) and Et_3N (0.3 ml, 3.4 mmol, 3 eq), yielding an ocre solid (346 mg, 1.11 mmol, 97%). Mp 142 – 143 °C (PET); R_f = 0.55 (EtOAc:PET, 20:80); ^{1}H NMR (300 MHz, CHLOROFORM-*d*) δ ppm 0.97 (s, 9 H, C(C*H*$_3$)$_3$), 3.90 (dd, *J*=10.1, 7.4 Hz, 1 H, OCH$_2$CHN), 4.12 – 4.28 (m, 7 H, OCH$_2$CHN, Cp*H*), 4.30 – 4.35 (m, 2 H, Cp*H*), 4.69 – 4.73 (m, 1 H, Cp*H*), 4.78 (m, 1 H, Cp*H*).

(*S*, $_p$*R*)-(4-*tert*-butyl-4,5-dihydrooxazol-2-yl)-2-methylthio-ferrocene – (7.8)

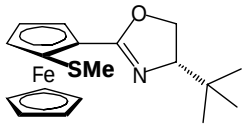

Thioether **7.8** was synthesised according to the general procedure used to synthesise **7.3** from, oxazoline **7.7** (30 mg, 1 mmol), dry toluene (0.5 ml) TMEDA (0.12 ml, 0.5 mmol, 5 eq) and *n*BuLi (0.18 ml, 0.2 mmol, 2 eq). R_f = 0.55 (EtOAc:PET, 20:80); IR (Film) cm^{-1}: 3097 (m, –C–H stretch), 2957 (m, –C–H stretch), 1661 (s, C=N stretch), 1143 (m, C–O stretch), 1106 (m, C–O stretch), 816 (m, C–H oop bend); ^{1}H NMR (300 MHz, CHLOROFORM-*d*) δ ppm 1.01 (s, 9 H, C(C*H*$_3$)$_3$), 2.42 (s, 3 H, SC*H*$_3$), 3.96 (dd, *J*=9.4, 7.5 Hz, 1 H, OCH$_2$CHN), 4.19 (s, 5 H, Cp*H*), 4.20 – 4.29 (m, 3 H, OCH$_2$CHN, Cp*H*), 4.41 (dd, *J*=2.6, 1.5 Hz, 1 H, Cp*H*), 4.69 (dd, *J*=2.6, 1.5 Hz, 1 H, Cp*H*); ^{13}C NMR (75 MHz,

CHLOROFORM-*d*) δ ppm 18.03, 25.86, 33.74, 67.98, 68.08, 70.06, 70.86, 71.58, 76.42, 87.16, 164.08.

(*S*)-(4-methyl-4,5-dihydrooxazol-2-yl)-ferrocene – (7.10)

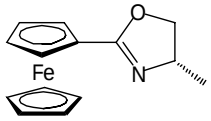

Methyl oxazoline **7.10** was synthesised according to the general procedure used for oxazoline **7.2** from carboxylic acid **7.1** (400 mg, 1.74 mmol), oxalyl chloride (0.45 ml, 5.2 mmol, 3 eq), (*S*)-2-amino-1-propanol (0.17 ml, 2.1 mmol, 1.2 eq), Et_3N (0.6 ml, 4.4 mmol, 2.5 eq), MsCl (0.34 ml, 4.4, 2.5 eq) and Et_3N (0.6 ml, 4.4 mmol, 2.5 eq), yielding an orange powder (448 mg, 1.7 mmol, 96%). Mp 79 – 80 °C (DCM); $[\alpha]_D^{34}$ = –25.4 (*c* 0.9, DCM); R_f = 0.1 (EtOAc:PET, 40:60); IR (Film) cm^{-1}: 3097 (m, –C–H stretch), 2960 (m, –C–H stretch), 1652 (s, C=N stretch), 1019 (m, C–O stretch), 821 (m, C–H oop bend); ^{1}H NMR (300 MHz, CHLOROFORM-*d*) δ ppm 1.32 (d, *J*=6.4 Hz, 3 H, CHC*H*$_3$) 3.87 (dd, *J*=7.8 Hz, 1 H, OC*H*$_2$CHN) 4.12 – 4.30 (m, 6 H, OCH$_2$C*H*N, Cp*H*) 4.32 – 4.37 (m, 2 H, Cp*H*) 4.42 (dd, *J*=9.2, 7.8 Hz, 1 H, OC*H*$_2$CHN) 4.72 – 4.78 (m, 2 H, Cp*H*); ^{13}C NMR (75 MHz, CHLOROFORM-*d*) δ ppm 21.60, 61.81, 68.93, 69.01, 69.64, 70.18, 70.25, 73.70, 165.89.

(*S*, $_p$*R*)-(4-methyl-4,5-dihydrooxazol-2-yl)-2-methylthio-ferrocene – (7.11)

Thioether **7.11** was synthesised according to the general procedure used to synthesise **7.3** from, oxazoline **7.10** (25 mg, 1 mmol), dry toluene (0.5 ml) TMEDA (0.12 ml, 0.5 mmol, 5 eq) and *n*BuLi (0.18 ml, 0.2 mmol, 2 eq). $[\alpha]_D^{34}$ = –203.5 (*c* 1.3, DCM); R_f = 0.16 (EtOAc:PET, 20:80); IR (Film): 3097 (m, –C–H stretch), 2961 (m, –C–H stretch), 1652 (s, C=N stretch), 1147 (m, C–O stretch), 1105 (m, C–O stretch), 818 (m, C–H oop bend); ^{1}H NMR (300 MHz, CHLOROFORM-*d*) δ ppm 1.35 (d, *J*=6.6 Hz, 3 H, CHC*H*$_3$), 2.40 (s, 3 H, SC*H*$_3$), 3.92 (dd, *J*=7.7, 7.2 Hz, 1 H, OC*H*$_2$CHN), 4.20 (s, 5 H, Cp*H*), 4.24 – 4.33 (m, 2 H, OCH$_2$C*H*N, Cp*H*), 4.39 – 4.48 (m, 2 H, OC*H*$_2$CHN, Cp*H*), 4.77 (dd, *J*=2.6, 1.5 Hz, 1 H, Cp*H*); ^{13}C NMR (75 MHz, CHLOROFORM-*d*) δ ppm 18.29, 21.72, 62.01, 68.49, 70.11, 70.37, 70.59, 71.06, 73.61, 87.16, 165.07.

(*S*, $_p$*S*)-(4-methyl-4,5-dihydrooxazol-2-yl)-2-methylthio-ferrocene – (7.12)

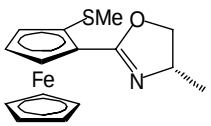

Thioether **7.12** was synthesised according to the general procedure used to synthesise **7.3** from, oxazoline **7.10** (25 mg, 1 mmol), dry toluene (0.5 ml) di-*t*Bu-diglyme (0.12 ml, 0.5 mmol, 5 eq) and *n*BuLi (0.18 ml, 0.2 mmol, 2 eq); $[\alpha]_D^{34}$ = 95.2 (*c* 1.2, DCM); R_f = 0.16 (EtOAc:PET, 20:80); IR (Film) cm^{-1}: 3080 (m, –C–H stretch), 2957 (m, –C–H stretch), 1652 (s, C=N stretch), 986 (m, C–H oop bend), 818 (m, C–H oop bend); ^{1}H NMR (300 MHz, CHLOROFORM-*d*) δ ppm 1.33 (d, *J*=6.4 Hz, 3 H, CHC*H*$_3$), 2.40

(s, 3 H, SC*H*$_3$), 3.90 (dd, *J*=7.5, 7.0 Hz, 1 H, OC*H*$_2$CHN), 4.21 (s, 5 H, Cp*H*), 4.27 – 4.39 (m, 2 H, OCH$_2$C*H*N, Cp*H*), 4.39 – 4.48 (m, 2 H, OC*H*$_2$CHN, Cp*H*), 4.77 (dd, *J*=2.7, 1.6 Hz, 1 H, Cp*H*); ^{13}C NMR (75 MHz, CHLOROFORM-*d*) δ ppm 18.40, 21.60, 62.09, 68.47, 70.44, 71.02, 71.06, 73.46, 86.20, 164.87.

(*S*)-(5-methyl-4,5-dihydrooxazol-2-yl)-ferrocene – (7.13)

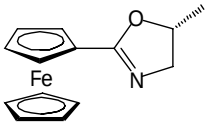

Methyl oxazoline **7.13** was synthesised according to the general procedure used for oxazoline **7.2** from carboxylic acid **7.1** (400 mg, 1.74 mmol), oxalyl chloride (0.45 ml, 5.2 mmol, 3 eq), (*R*)-1-amino-2-propanol (0.16 ml, 2.1 mmol, 1.2 eq), Et$_3$N (0.6 ml, 4.4 mmol, 2.5 eq), MsCl (0.34 ml, 4.4 mmol, 2.5 eq) and Et$_3$N (0.6 ml, 4.4 mmol, 2.5 eq), yielding an orange red powder (448 mg, 1.64 mmol, 94%). Mp 105 – 108 °C (PET); $[\alpha]_D^{34}$ = –24.4 (*c* 0.9, DCM); R_f = 0.17 (EtOAc:PET, 60:40); IR (Film): 3085 (m, –C–H stretch), 2946 (m, –C–H stretch), 1655 (s, C=N stretch), 1111, (m, C–O stretch), 922 (m, C–H oop bend), 831 (m, C–H oop bend); ^{1}H NMR (300 MHz, BENZENE-*d*$_6$) δ ppm 1.01 (d, *J*=6.2 Hz, 3 H, OCHC*H*$_3$), 3.27 (dd, *J*=13.8, 6.7 Hz, 1 H, OCHC*H*$_2$N), 3.76 (dd, *J*=13.8, 8.9 Hz, 1 H, OCHC*H*$_2$N), 3.97 – 4.04 (m, 2 H, Cp*H*), 4.08 (s, 5 H, Cp*H*), 4.20 – 4.35 (m, 1 H, OC*H*CH$_2$N), 4.91 (m, *J*=7.3 Hz, 1 H, Cp*H*); ^{13}C NMR (75 MHz, BENZENE-*d*$_6$) δ ppm 21.56, 62.60, 69.78, 69.86, 70.20, 70.61, 70.64, 72.52, 75.78, 165.68; MS (ES+): *m/z* (%) = 268.9 (100) HRMS–TOF MS ES+: *m/z* $[M]^+$ calcd for $C_{14}H_{15}NOFe$: 269.0498; found: 269.0485.

(*S*)-(5-methyl-4,5-dihydrooxazol-2-yl)-2-methylthio-ferrocene – (7.14)

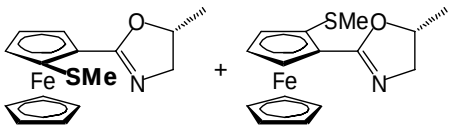

Thioether **7.14** was synthesised according to the general procedure used to synthesise **7.3** from, oxazoline **7.13** (25 mg, 1 mmol), dry toluene (0.5 ml) TMEDA (0.12 ml, 0.5 mmol, 5 eq) and *n*BuLi (0.18 ml, 0.2 mmol, 2 eq). $[\alpha]_D^{34}$ = 32.4 (*c* 0.9, DCM); R_f = 0.38 (EtOAc:PET, 75:25); IR (Film): 3085 (m, –C–H stretch), 2946 (m, –C–H stretch), 1652 (s, C=N stretch), 1142, (m, C–O stretch), 954 (m, C–H oop bend), 819 (m, C–H oop bend); ^{1}H NMR (300 MHz, BENZENE-*d*$_6$) δ ppm 1.01 (m, 3 H, OCHC*H*$_3$), 2.21 (s, 3 H, SC*H*$_3$), 3.30 (m, 1 H, NC*H*$_2$CHO), 3.78 (m, 1 H, NC*H*$_2$CHO), 3.91 – 3.98 (m, 1 H, Cp*H*), 4.03 – 4.38 (m, 8 H, NCH$_2$C*H*O, Cp*H*), 4.82 – 4.91 (m, 1 H, Cp*H*); ^{13}C NMR (75 MHz, BENZENE-*d*$_6$) δ ppm 18.89, 18.92, 21.44, 21.61, 62.81, 62.85, 68.76, 71.18, 71.28, 71.65, 71.67, 71.87, 72.00, 73.39, 75.39, 75.62, 87.41, 87.60, 164.76; *m/z* (%) = 314.9 (100) HRMS–TOF MS ES+: *m/z* $[M]^+$ calcd for $C_{15}H_{17}NOSFe$: 315.0375; found: 315.0361.

(4-*R*,5-*R*)-(4,5-diphenyl-4,5-dihydrooxazol-2-yl)-ferrocene – (7.15)

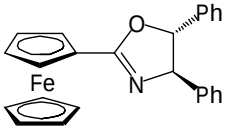

Diphenyl oxazoline **7.15** was synthesised according to the general procedure used for oxazoline **7.2** from carboxylic acid **7.1** (230 mg, 1 mmol), oxalyl chloride (0.3 ml, 3.5 mmol, 3.5 eq), (1*S*,2*R*)-2-amino-1,2-diphenylethanol (2.13 mg, 1 mmol, 1 eq), Et_3N (0.8 ml, 6 mmol, 6 eq), MsCl (0.23 ml, 3 mmol, 3 eq), yielding an orange glass (400 mg, 0.99 mmol, 99%). Mp 75 °C (PET); $[\alpha]_D^{34} = 119.7$ (*c* 1.3, DCM); $R_f = 0.59$ (EtOAc:PET, 40:60); IR (Film) cm^{-1}: 3085 (m, –C–H stretch), 2946 (m, –C–H stretch), 1652 (s, C=N stretch), 1110, (m, C–O stretch), 970 (m, C–H oop bend), 821 (m, C–H oop bend), 759 (m, C–H oop bend); ^{1}H NMR (300 MHz, CHLOROFORM-*d*) δ ppm 4.31 (s, 5 H, Cp*H*), 4.44 (m, 2 H, Cp*H*), 4.93 (m, 2 H, Cp*H*), 5.09 (d, *J*=7.3 Hz, 1 H, OCHCHN), 5.33 (d, *J*=7.5 Hz, 1 H, OCHCHN), 7.28 – 7.55 (m, 10 H, Ar*H*); ^{13}C NMR (75 MHz, CHLOROFORM-*d*) δ ppm 69.30, 69.33, 69.71, 69.97, 70.55, 78.89, 88.52, 125.69, 126.70, 127.67, 128.13, 128.38, 128.65, 128.81, 128.89, 140.67, 142.26, 166.85; *m/z* (%) = 407.0 (100) HRMS–TOF MS ES+: *m/z* $[M]^+$ calcd for $C_{25}H_{21}NOFe$: 407.0967; found: 407.0972.

(4-*R*,5-*R*,$_p$*S*)-(4,5-diphenyl-4,5-dihydrooxazol-2-yl)-2-methylthio-ferrocene – (7.16)

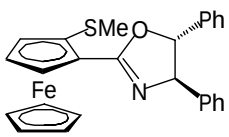

Thioether **7.16** was synthesised according to the general procedure used to synthesise **7.3** from oxazoline **7.10** (40 mg, 1 mmol), dry toluene (0.5 ml) TMEDA (0.12 ml, 0.5 mmol, 5 eq) and *n*BuLi (0.18 ml, 0.2 mmol, 2 eq). $[\alpha]_D^{34} = 235.2$ (*c* 1.1, DCM); $R_f = 0.42$ (EtOAc:PET, 20:80); IR (Film) cm^{-1}: 3085 (m, –C–H stretch), 2962 (m, –C–H stretch), 1652 (s, C=N stretch), 1260, (m, C–O stretch), 800 (m, C–H oop bend), 758 (m, C–H oop bend), 699 (m, C–H oop bend); ^{1}H NMR (500 MHz, CHLOROFORM-*d*) δ ppm 2.47 (s, 3 H, S*CH*$_3$), 4.29 (s, 5 H, Cp*H*), 4.38 (dd, *J*=2.5 Hz, 1 H, Cp*H*), 4.52 (dd, *J*=2.4, 1.4 Hz, 1 H, Cp*H*), 4.92 (dd, *J*=2.5, 1.6 Hz, 1 H, Cp*H*), 5.19 (d, *J*=6.9 Hz, 1 H, OCHCHN), 5.35 (d, *J*=6.6 Hz, 1 H OCHCHN), 7.29 – 7.49 (m, 10 H, Ar*H*); ^{13}C NMR (75 MHz, CHLOROFORM-*d*) δ ppm 18.20, 68.63, 70.16, 70.57, 71.15, 78.94, 87.70, 88.19, 125.59, 126.52, 127.52, 128.26, 128.79, 128.86, 141.00, 142.74, 166.03; *m/z* (%) = 453.0 (100) HRMS–TOF MS ES+: *m/z* $[M]^+$ calcd for $C_{26}H_{23}NOSFe$: 453.0844; found: 453.0830.

(4-*R*,5-*R*,$_p$*R*)-(4,5-diphenyl-4,5-dihydrooxazol-2-yl)-2-methylthio-ferrocene – (7.17)

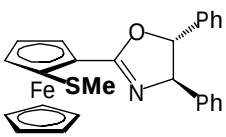

Thioether **7.17** was synthesised according to the general procedure used to synthesise **7.3** from, oxazoline **7.15** (40 mg, 1 mmol), dry toluene (0.5 ml) di-*t*Bu-diglyme (0.12 ml, 0.5 mmol, 5 eq) and *n*BuLi (0.18 ml, 0.2 mmol, 2 eq); $[\alpha]_D^{34} = -170.7$ (*c* 0.7, DCM); $R_f = 0.42$ (EtOAc:PET, 20:80); IR (Film): 3085 (m, –C–H stretch), 2962 (m, –C–H stretch), 1652 (s, C=N stretch), 1260, (m, C–O stretch), 802 (m, C–H oop bend),

758 (m, C–H oop bend), 699 (m, C–H oop bend); ^{1}H NMR (300 MHz, CHLOROFORM-*d*) δ ppm 2.41 (s, 3 H, SC*H*$_3$), 4.31 (s, 5 H, Cp*H*), 4.39 (t, *J*=2.5 Hz, 1 H, Cp*H*), 4.52 (dd, *J*=2.5, 1.6 Hz, 1 H, Cp*H*), 4.94 (dd, *J*=2.6, 1.5 Hz, 1 H, Cp*H*), 5.22 (d, *J*=7.2 Hz, 1 H, OCHCHN), 5.32 (d, *J*=7.2 Hz, 1 H, OCHCHN), 7.30 – 7.45 (m, 10H, Ar*H*); ^{13}C NMR (75 MHz, CHLOROFORM-*d*) δ ppm 18.70, 68.80, 70.56, 70.81, 71.15, 71.18, 71.73, 72.95, 78.89, 86.43, 88.14, 125.58, 125.73, 126.50, 126.58, 127.49, 128.32, 128.68, 128.78, 128.86, 140.85, 142.49, 165.97.

(4-*S*,5-*R*,)-(4,5-diphenyl-4,5-dihydrooxazol-2-yl)-ferrocene – (7.18)

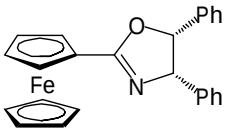

Diphenyl oxazoline **7.18** was synthesised according to the general procedure used for oxazoline **7.2** from carboxylic acid **7.1** (173 mg, 0.75 mmol), oxalyl chloride (0.26 ml, 3 mmol, 4 eq), (1*S*,2*S*)-2-amino-1,2-diphenylethanol (159 mg, 0.75 mmol, 1 eq), Et_3N (0.6 ml, 4.5 mmol, 6 eq) and MsCl (0.18 ml, 2.25 mmol, 3 eq), yielding an orange glass (70 mg, 0.18 mmol, 24%); $[\alpha]_D^{34}$ = –229.5 (*c* 0.7, DCM); R_f = 0.44 (EtOAc:PET, 35:65); IR (Film) cm^{-1}: 3029 (m, –C–H stretch), 2922 (m, –C–H stretch), 1652 (s, C=N stretch), 1112, (m, C–O stretch), 821 (m, C–H oop bend), 735 (m, C–H oop bend), 696 (m, C–H oop bend); ^{1}H NMR (300 MHz, CHLOROFORM-*d*) δ ppm 4.35 (s, 5 H, Cp*H*), 4.46 (m, 2 H, Cp*H*), 4.91 – 4.96 (m, 1 H, Cp*H*), 4.96 – 5.02 (m, 1 H, Cp*H*), 5.59 (d, *J*=10.0 Hz, 1 H, OCHCHN), 5.93 (d, *J*=10.0 Hz, 1 H, OCHCHN), 6.89 – 7.14 (m, 10 H, Ar*H*); ^{13}C NMR (75 MHz, CHLOROFORM-*d*) δ ppm 69.29, 69.70, 70.06, 70.56, 70.59, 74.22, 84.83, 126.31, 126.87, 127.33, 127.57, 127.65, 127.79, 136.68, 137.94, 167.70.

(4-*S*,5-*R*,$_p$*R*)-(4,5-diphenyl-4,5-dihydrooxazol-2-yl)-2-methylthio-ferrocene – (7.19)

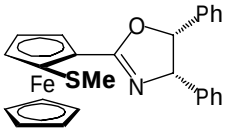

Thioether **7.19** was synthesised according to the general procedure used to synthesise **7.3** from oxazoline **7.18** (20 mg, 0.5 mmol), dry toluene (0.5 ml) TMEDA (0.6 ml, 0.25 mmol, 5 eq) and *n*BuLi (0.09 ml, 0.1 mmol, 2 eq). $[\alpha]_D^{34}$ = –279.0 (*c* 0.8, DCM); R_f = 0.32 (EtOAc:PET, 20:80); IR (Film) cm^{-1}: 3029 (m, –C–H stretch), 2962 (m, –C–H stretch), 1652 (s, C=N stretch), 1260 (m, C–O stretch), 800 (m, C–H oop bend), 697 (m, C–H oop bend); ^{1}H NMR (300 MHz, CHLOROFORM-*d*) δ ppm 2.48 (s, 3 H, SC*H*$_3$), 4.35 (s, 5 H, Cp*H*), 4.40 (dd, *J*=2.5 Hz, 1 H, Cp*H*), 4.55 (dd, *J*=2.4, 1.5 Hz, 1 H, Cp*H*), 5.63 (d, *J*=9.8 Hz, 1 H, OCHCHN), 5.93 (d, *J*=9.8 Hz, 1 H, OCHCHN), 6.97 – 7.14 (m, 10 H, ArH) ^{13}C NMR (75 MHz, CHLOROFORM-*d*) δ ppm 18.40, 68.73, 70.66, 70.82, 71.08, 74.34, 77.20, 85.03, 87.51, 126.59, 126.80, 127.40, 127.57, 127.69, 127.85, 136.66, 138.14, 166.78.

(4-*S*,5-*R*,$_p$*S*)-(4,5-diphenyl-4,5-dihydrooxazol-2-yl)-2-methylthio-ferrocene – (7.20)

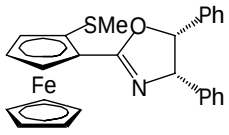

Thioether **7.20** was synthesised according to the general procedure used to synthesise **7.3** from oxazoline **7.18** (20 mg, 0.5 mmol), dry toluene (0.5 ml) di-*t*Bu-diglyme (0.6 ml, 0.25 mmol, 5 eq) and *n*BuLi (0.9 ml, 0.1 mmol, 2 eq); $[\alpha]_D^{30} = -123.0$ (*c* 0.1, DCM); $R_f = 0.32$ (EtOAc:PET, 20:80); IR (Film) cm^{-1}: 3029 (m, –C–H stretch), 2922 (m, –C–H stretch), 1652 (s, C=N stretch), 817 (m, C–H oop bend), 697 (m, C–H oop bend); ^{1}H NMR (400 MHz, CHLOROFORM-*d*) δ ppm 2.45 (s, 3 H, SC*H*$_3$), 4.33 (s, 5 H, Cp*H*), 4.41 (dd, *J*=2.6 Hz, 1 H, Cp*H*), 4.54 (dd, *J*=2.6, 1.6 Hz, 1 H, Cp*H*), 4.98 (dd, *J*=2.5, 1.5 Hz, 1 H, Cp*H*), 5.70 (d, *J*=10.1 Hz, 1 H, OCHCHN), 5.96 (d, *J*=10.1 Hz, 1 H, OCHCHN), 6.92 – 7.12 (m, 10 H, Ar*H*); ^{13}C NMR (126 MHz, CHLOROFORM-*d*) δ ppm 18.71, 68.77, 70.78, 71.07, 71.22, 71.77, 74.66, 75.25, 126.44, 126.85, 127.18, 127.54, 127.69, 127.95, 136.82, 138.05, 166.81.

9.8 Chiral Aminols

(*S*)-2-amino-3-methylbutan-1-ol (L-Valinol)[10]

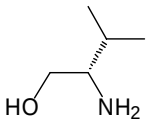

A slurry of L-Valine (5 g, 38.3 mmol) and $NaBH_4$ (3.46 g, 91.7 mmol, 2.4 eq) in dry THF (100 ml) was added to a two necked round-bottom flask (500 ml) equipped with a reflux condenser and addition funnel under an atmosphere of nitrogen. The flask was cooled to 0 ºC in an ice bath, and a solution of iodine (9.7 g, 38.2 mmol, 1.02 eq) in THF (25 ml) was slowly added with rapid stirring over the course of half an hour. The flask was heated to reflux for 19 hours under nitrogen after which it was cooled to RT and methanol was slowly added until the evolution of gas ceased. The flask was then stirred for a further 30 minutes at RT. The contents of the flask were then transferred to a single necked round-bottom flask and the solvent removed under reduced pressure affording a white viscous material, which was taken up in 20 % aqueous KOH solution (50 ml) and stirred overnight. The mixture was extracted with DCM (3 x 100 ml), the organic layers combined, dried over $MgSO_4$ and the solvent removed under reduced pressure. Purification of the product was achieved by low pressure distillation (78 ºC, 2 mm Hg) affording a clear oil which solidified on standing (2.9 g, 28.2 mmol, 73 %). Mp 18 °C; 1H NMR (300 MHz, CHLOROFORM-*d*) δ ppm 0.91 (d, *J*=4.1 Hz, 3 H, CH(C*H*$_3$)$_2$), 0.93 (d, *J*=4.1 Hz, 3 H, CH(C*H*$_3$)$_2$), 1.48 – 1.65 (m, 1 H, C*H*(CH$_3$)$_2$), 1.82 (br. s, 3 H, CH$_2$O*H*, CHN*H*$_2$), 2.51 – 2.60 (m, 1 H, CH$_2$C*H*N), 3.28 (dd, *J*=10.5, 8.8 Hz, 1 H, OC*H*$_2$CH), 3.64 (dd, *J*=10.5, 4.0 Hz, 1 H, OC*H*$_2$CH).

(*R*)-2-amino-3-methylbutan-1-ol (D-Valinol)[10]

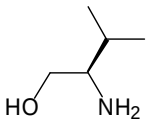

D-Valinol was synthesised according to the same procedure used for **L-Valinol** from D-Valine (5g, 42.7 mmol), $NaHBH_4$ (4.2 g, 111 mmol, 2.6 eq) and iodine (11.9 g, 47 mmol, 1.1 eq) which after purification by distillation (58 ºC / 1.5 mm Hg) yielded an opaque liquid that solidified on standing (2.26 g, 22 mmol, 52 % yield) ^{1}H NMR (400 MHz, CHLOROFORM-*d*) δ ppm 0.92 (m, 6 H, CH(C*H*$_3$)$_2$), 1.50 – 1.63 (m, 1 H C*H*(CH$_3$)$_2$), 1.63 – 1.92 (br. s, 3 H, O*H*, N*H*$_2$), 2.52 – 2.58 (m, 1 H, CH$_2$C*H*N), 3.28 (dd, *J*=10.4, 8.9 Hz, 1 H, OC*H*$_2$CH), 3.64 (dd, *J*=10.4, 4.0 Hz, 1 H, OC*H*$_2$CH).

(*S*)-2-amino-2-phenylethanol (L-Phenylglycinol)[10]

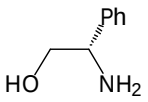

L-Phenylglycinol was synthesised according to the same procedure used for **L-Valinol** from L-phenylglycine (5g, 33.1 mmol), $NaHBH_4$ (3 g, 79.4 mmol, 2.4 eq) and iodine (8.80 g, 33.1 mmol, 1.05 eq) which after purification by distillation (100 ºC / 0.5 mm Hg) yielded an opaque liquid that solidified on standing (3.68 g, 27 mmol, 82 % yield). Further purification was achieved by crystallisation from a solution of hot toluene, yielding a white crystalline product. ^{1}H NMR (400 MHz, CHLOROFORM-*d*) δ ppm 2.05 (d, *J*=0.9 Hz, 3 H, O*H*, CHN*H*$_2$), 3.49 (dd, *J*=10.9, 8.3 Hz, 1 H, NH$_2$C*H*CH$_2$), 3.67 (dd, *J*=10.9, 4.4 Hz, 1 H, HOC*H*$_2$CH), 3.98 (dd, *J*=8.3, 4.4 Hz, 1 H, HOC*H*$_2$CH), 7.18 – 7.32 (m, 5 H, Ar*H*); ^{13}C NMR (101 MHz, CHLOROFORM-*d*) δ ppm 57.32 (H$_2$N*C*HCH$_2$), 67.99 (CH*C*H$_2$OH), 126.42 (*C*$_{Ar}$H), 127.47 (*C*$_{Ar}$H), 128.60 (*C*$_{Ar}$H), 142.68 (CH*C*$_{Ar}$).

(*S*)-2-amino-3,3-dimethylbutan-1-ol (L-*tert*-Leucinol)[10]

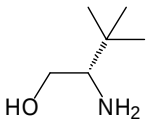

L-*tert*-Leucinol was synthesised according to the same procedure used for **L-Valinol** from L-*tert*-Leucine (3.3g, 25 mmol), $NaHBH_4$ (2.3 g, 60 mmol, 2.4 eq) and iodine (6.3 g, 25 mmol, 1 eq) which after purification by distillation (50 ºC / 0.1 mm Hg) yielded an opaque liquid that solidified on standing (1.94 g, 17 mmol, 66 % yield). ^{1}H NMR (400 MHz, CHLOROFORM-*d*) δ ppm 0.88 (s, 9 H, C(C*H*$_3$)$_3$), 2.00 (br. s., 3 H, O*H*, N*H*$_2$), 2.50 (dd, *J*=9.9, 3.8 Hz, 1 H, NH$_2$C*H*CH$_2$), 3.20 (m, 1 H, CHC*H*$_2$O), 3.70 (dd, *J*=10.2, 3.8 Hz, 1 H, CHC*H*$_2$O); ^{13}C NMR (101 MHz, CHLOROFORM-*d*) δ ppm 26.22 (C(*C*H$_3$)$_3$), 33.19 (*C*(CH$_3$)$_3$), 61.72 (CH$_2$CH), 62.34 (CH$_2$CH).

9.9 Model Compounds

1-iodo-4-propoxybenzene – (3.1)

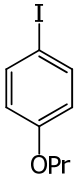

A mixture of iodo phenol (2.6 g, 12 mmol), DMF (70 ml), and potassium carbonate (3.32 g, 24.3 mmol, 2.1 eq) were brought to reflux under an atmosphere of nitrogen. After half an hour of reflux, propyl iodide (4.5 ml, 46 mmol, 3.8 eq) was added to the solution and reflux was continued for approximately 17 hours, after which the solution was cooled to RT and ethyl acetate (200 ml) was added. The ethyl acetate layer was washed with a 1 M HCl solution (100 ml), followed by washing with a further portion of H_2O (70 ml), dried over $MgSO_4$ and the solvent removed under reduced pressure. Purification was accomplished by silica gel chromatography (1:99 EtOAc:PET) to yield a clear oil (2.81 g, 10.7 mmol, 89% yield). R_f = 0.8 (EtOAc:PET, 20:80); ^{1}H NMR (CHLOROFORM-*d*, 300MHz): δ ppm 1.04 (t, *J*=7.41 Hz, 3H, CH_2CH_3), 1.81 (m, 2H, $CH_2CH_2CH_3$), 3.89 (t, *J*=6.60 Hz, 2H, OCH_2CH_2), 6.69 (d, *J*=8.73 Hz, 2H, Ar*H*), 7.55 (d, *J*=8.73 Hz, 2H, Ar*H*).

4-propoxybenzoic acid – (3.2)

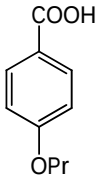

An oven dried Schlenk flask (30 ml) was evacuated and flushed with nitrogen. To this iodo propyl phenol (1.9 g, 7.3 mmol) was added along with *s*BuMg·$LiCl_2$ (25 ml, ~ 15 mmol) at RT and the flask stirred for 2 hours. The mixture was then poured rapidly and with constant stirring into freshly prepared solid carbon dioxide (~200 ml). After the solid contents of the flask had either evaporated or sublimed, 1M HCl (50 ml) was added to the beaker along with EtOAc (150 ml). The layers were separated and the organic layers washed with H_2O (3 x 60 ml), dried over $MgSO_4$, and the solvent removed under reduced pressure and the solid product triturated with PET (20 ml) with subsequent filtration of the mixture. The solid material was recystallised from EtOAc and PET to yield carboxyl acid **3.2** (0.922 g, 5.11 mmol, 70%) as opaque white thin plate crystals. Mp 135°C (PET); R_f= 0.17 (EtOAc:PET, 20:80); ^{1}H NMR (CHLOROFORM-*d*, 300MHz): δ ppm 1.07 (t, *J*=7.41 Hz, 3H, CH_2CH_3), 1.85 (m, 2H, $CH_2CH_2CH_3$), 4.00 (t, *J*=6.53 Hz, 2H, OCH_2CH_2), 6.95 (d, *J*=9.03 Hz, 2H, Ar*H*), 8.07 (d, *J*=9.03 Hz, 2H, Ar*H*).

4,5-dihydro-2-(4-propoxyphenyl)oxazole – (3.3)

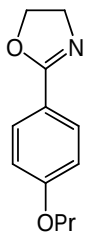

Carboxyl acid **3.2** (344 mg, 1.9 mmol) and $SOCl_2$ (4 ml, 55 mmol, 29 eq) was stirred at RT for 16 hours in a round-bottomed flask (25 ml). The solvent was removed under reduced pressure and the solids taken up in dry DCM (10 ml) and slowly added at RT to ethanol amine (0.26 ml, 4.4 mmol, 2.3 eq) in dry DCM (5 ml) and the mixture stirred for

a further 2 hours under a positive nitrogen pressure at RT. Saturated $NaHCO_3$ solution (30 ml) was added, the organic and aqueous layers separated, and the aqueous layer extracted with DCM (2 x 40 ml). The organic layers were combined, and the solvent removed under reduced pressure to yield a white fluffy solid. Purification or characterization was not performed and the solid was taken up in dry DCM (10 ml). To this $SOCl_2$ (4 ml, 55 mmol, 29 eq) was added and the flask stirred under nitrogen for 2 hours. The solvent was then removed under reduced pressure and the solids taken up in ethyl acetate (50 ml). The organic layer was washed with saturated $NaHCO_3$ solution (20 ml), followed by washing with brine (20 ml). The organic layer was dried over $MgSO_4$, and the solvent removed under reduced pressure. Purification was performed by gradient elution column chromatography in a mixture of EtOAc and PET to yield a pale yellow oil which crystallized upon standing to yield ethyl oxazoline propyl phenol (343 mg, 1.7 mol, 88% reaction yield). Mp 62°C (PET); R_f = 0.70 (EtOAc, 100); ^{1}H NMR (CHLOROFORM-d, 300MHz, 25°C): δ ppm 1.05 (t, *J*=7.42 Hz, 3H, CH_2CH_3), 1.83 (m, 2H, $CH_2CH_2CH_3$), 3.96 (t, *J*=6.64 Hz, 2H, OCH_2CH_2), 4.04 (t, *J*=9.33 Hz, 2H, CH_2CH_2N), 4.41 (t, *J*=9.33 Hz, 2H, CH_2CH_2N), 6.91 (d, *J*=8.98 Hz, 2H, Ar*H*), 7.88 (d, *J*=8.98 Hz, 2H, Ar*H*); ^{13}C NMR (CHLOROFORM-*d*, 75 MHz): δ ppm 10.47 ($CH_2CH_2CH_3$), 22.49 ($CH_2CH_2CH_3$), 54.83 (NCH_2CH_2O), 67.46 (NCH_2CH_2O), 69.55 (OCH_2), 114.16 ($C_{Ar}CNO$), 119.39 ($C_{Ar}CNO$), 120.00 ($C_{Ar}H$), 129.80 ($C_{Ar}H$), 161.60 ($C_{AR}O$), 164.47 ($C_{Ar}CNO$); MS (ESI+): *m/z* (%) = 206 (100) $[M+H]^+$.

4,5-dihydro-2-(2-methyl-4-propoxyphenyl)oxazole – (3.4)

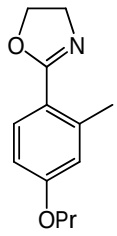

An oven dried Schlenk flask (25 ml) was repeatedly cycled through alternative flushing with nitrogen followed by high vacuum. The flask was equipped with a septum and charged with oxazoline **3.3** (98 mg, 0.47 mmol). Further drying of the material was performed by solvating the solid in the minimum volume of dry THF, followed by removal of the solvent under reduced pressure and heating under high vacuum. This process was repeated three times. Thereafter dry THF (4 ml) was introduced and the flask cooled to –78 ºC. *s*BuLi (0.45 ml, 0.54 mmol, 1.14 eq) was slowly introduced under a positive pressure of nitrogen and the flask stirred at this temperature for 35 minutes after which iodomethane (0.2 ml, 3.2 mmol, 6.8 eq) was introduced and the flask allowed to warm to RT over 0.5 hours after which saturated NH_4Cl solution (5 ml) was introduced. The organic components were extracted with DCM (50 ml), dried over $MgSO_4$ and the solvent removed under reduced pressure affording an oil. The yield was determined by ^{1}H NMR (89%). ^{1}H NMR (CHLOROFORM-*d*, 400MHz): δ ppm 1.03 (t, *J*=7.4 Hz, 3 H, CH_2CH_3), 1.77 – 1.85 (m, 2 H, $CH_2CH_2CH_3$), 2.57 (s, 3H, $C_{Ar}CH_3$), 3.93 (t, *J*=6.5 Hz, 2H, OCH_2CH_2), 4.06 (t, *J*=9.7 Hz, 2H, OCH_2CH_2N), 4.34 (t, 2 H, *J*=9.7 Hz, 2H, OCH_2CH_2N), 6.70 – 6.77 (m, 3H, Ar*H*), 7.76 (d, J=8.59

Hz, 1 H, Ar*H*); ^{13}C NMR (101 MHz, CHLOROFORM-*d*) δ ppm 10.48 (CH_2CH_3), 22.24 ($C_{Ar}CH_3$), 22.52 ($CH_2CH_2CH_3$), 55.28 (NCH_2CH_2O), 66.49 (NCH_2CH_2O), 69.40 (OCH_2CH_2), 111.25 ($C_{Ar}H$), 117.15 ($C_{Ar}H$), 131.59 ($C_{Ar}H$), 140.91 ($C_{Ar}CH_3$), 160.63 ($C_{Ar}O$), 164.83 ($C_{Ar}CNO$) MS (ES+): *m/z* (%) = 220 (100) $[M+H]^+$.

2-(4,5-dihydrooxazol-2-yl)-5-propoxybenzaldehyde – (3.6)

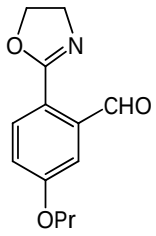

3.6 was prepared using a procedure analogous to that used to synthesise **3.4** from oxazoline **3.3** (116 mg, 0.56 mmol), THF (4 ml), *s*BuLi (0.94 ml, 0.9 mmol, 1.6 eq) and freshly purified DMF (0.35 ml, 4.5 mmol, 8 eq) with a 50 minute reaction at – 78 ºC. As it proved impossible to purify the product via conventional column chromatography due to decomposition of the material ^{1}H NMR was used to determine the yield. (~ 70%); ^{1}H NMR (CHLOROFORM-*d*, 300MHz): δ ppm 1.05 (t, J=7.41 Hz, 3H, CH_2CH_3), 1.77 – 1.90 (m, 2H, $CH_2CH_2CH_3$), 4.01 (t, J=6.53 Hz, 2H, OCH_2CH_2), 4.05 – 4.13 (m, 2H, OCH_2CH_2N), 4.41 – 4.48 (m, 2H, OCH_2CH_2N), 7.11 (dd, *J*=8.6, 2.8 Hz, 1H, Ar*H*), 7.43 (d, J=2.8 Hz, 1H, Ar*H*), 7.85 (d, J=8.6 Hz, 1 H, Ar*H*), 10.75 (s, 1H, $C_{Ar}CHO$).

2-methyl-1-(4-propoxyphenyl)butan-1-one – (3.5)

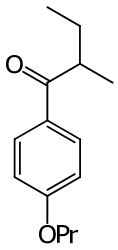

^{1}H NMR (CHLOROFORM-*d*, 300 MHz,) δ ppm 0.91 (t, *J*=7.4 Hz, 3 H, CH_2CH_3), 1.06 (t, *J*=7.5 Hz, 3 H, $CHCH_2CH_3$), 1.18 (d, *J*=6.7 Hz, 3 H, CH_2CHCH_3), 1.40 – 1.57 (m, 1 H, CH_3CH_2CH), 1.73 – 1.93 (m, 3 H, $CH_2CH_2CH_3$, CH_3CH_2CH), 3.28 – 3.44 (m, 1 H, CH_3CHCH_2), 3.99 (t, *J*=6.6 Hz, 2 H, OCH_2CH_2), 6.93 (m, 2 H, Ar*H*), 7.94 (m, 2 H, Ar*H*); ^{13}C NMR (75 MHz, CHLOROFORM-*d*) δ ppm 10.45 (CH_2CH_3), 11.83 (CH_2CH_3), 16.97 ($CHCH_3$), 22.44 ($CH_2CH_2CH_3$), 26.84 (CH_3CH_2CH), 41.67 (CH_3CHCH_2), 69.67 (OCH_2CH_2), 114.16 ($C_{Ar}H$), 129.56 ($C_{Ar}C=O$), 130.45 ($C_{Ar}H$), 162.89 ($C_{Ar}O$), 203.02 ($C_{Ar}C=O$); MS (ES+): *m/z* (%) = 221 (100) $[M+H]^+$.

9.10 Grignard and lithium reagents.

isopropyl magnesium lithium dichloride – (*i*PrMg·LiCl$_2$)[11]

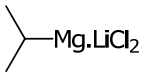

***i*PrMg·LiCl$_2$** – A Schlenk flask was dried according to standard Schlenk techniques. Oven dried Mg (4.0 g, 164 mmol, 1.64 eq), dry THF (100 ml), *i*PrCl (9.2 ml, 100 mmol) and LiCl (4.66 g, 110 mmol, 1.1 eq) were added to the flask under a positive pressure of nitrogen, thereafter it was stirred for 24 hours at RT yielding a grey black solution (0.88 mmol/ml, 88 % yield, by titration with *t*BuOH and 2,2`-bipyridine). The solution was stored at 0 ºC.

sec-butyl magnesium lithium dichloride – (_s_BuMg·LiCl$_2$)

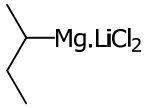

_s_BuMg·LiCl$_2$ was synthesised according to the same procedures used to synthesise **_i_PrMg·LiCl$_2$** from powdered magnesium (2.5 g, 103 mmol, 1.7 eq), *sec*-chlorobutane (5.3 ml, 50 mmol), lithium chloride (2.54 g, 60 mmol, 1.2 eq) in THF (50 ml) yielding a 0.9 M solution (90 % yield).

sec-butyl lithium – (_s_BuLi)[12]

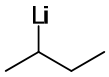

_s_BuLi – An oven dried two necked 100 ml round-bottom flask fitted with a reflux condenser was placed under high vacuum and repeatedly flushed with nitrogen followed by low pressure evacuation. Once the flask had cooled to RT high sodium content Li pellets (1.24 g, 180 mmol, 3 eq) and dry pentane (20 ml) were added. The mixture was brought to reflux with gentle heating after which 2 ml of a *s*BuCl (6.5 ml, 60 mmol) in pentane (20 ml) solution was added via syringe. The solution was maintained at reflux with gentle heating while the *s*BuCl solution was added at 8.5 ml/hour via syringe pump over approximately 3.5 hours. Upon completion of the addition process the dark purple solution was held at reflux for a further hour. The flask was then cooled to RT and the solution filtered under inert conditions into a dried Schlenk flask, yielding a light yellow solution (1.06 mmol/ml, 62 % yield).

tert-butyl lithium – (_t_BuLi)[13]

_t_BuLi – An oven dried two necked 100 ml round-bottom flask fitted with a reflux condenser was placed under high vacuum and repeatedly flushed with nitrogen followed by evacuation. Once the flask had cooled to RT 2% sodium content Li powder (6 g, 869 mmol, 15 eq), dry pentane (12 ml) and *n*BuLi (0.25 ml, 0.25 mmol, in hexanes) were added under a positive pressure of nitrogen. The mixture was brought to reflux with gentle heating and 2 ml of a *t*BuCl (6.6 ml, 60 mmol), THF (0.05 ml) and nBuLi (0.25 ml, 0.25 mmol) solution in pentane (13 ml) was added via syringe. The intensity of reflux was observed to increase immediately after the addition and the heat source was removed. The *t*BuCl solution was added at a rate of 13 ml/hour maintaining a gentle reflux in the flask. Upon completion of the addition process the dark purple solution was stirred at RT for a further 30 minutes before it was filtered inertly, yielding a pale yellow solution (2.3 mmol/ml, 77 % yield).

isopropyl lithium – (_i_PrLi)

_i_PrLi was synthesised using the same method employed for the synthesis of **_s_BuLi** from high sodium content Li (1.24g, 60 mmol, 3 eq) pellets and *i*PrCl (5.5 ml, 60 mmol) using the same volumes of pentane and an addition rate of 7 ml/hour over 4 hours and yielding a light

yellow solution (1.24 mmol/ml, 65% yield). The solution was stored at 0 ºC and stirred before use.

cyclohexyl lithium – (*c*HexLi)

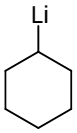

***c*HexLi** was prepared according to the same methodology used for the synthesis of ***s*BuLi** from fine Li sand (1.4 g, 210 mmol) in dry pentane (15 ml) and cyclohexyl bromide (4.9 ml, 40 mmol) in dry pentane (10 ml) with an addition rate of 4 ml/hour. After filtration a yellow solution was obtained (0.11 mmol/ml, 5 % yield). The solution was stored at 0 ºC and stirred before use.

cyclopentyl lithium – (*c*PentLi)

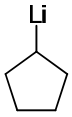

***c*PentLi** was prepared in a procedure analogous to that used to prepare ***s*BuLi** from high content fine Li sand (1.5g, 217 mmol, 6 eq) in pentane (15 ml) and cyclopentyl bromide (3.8 ml, 36 mmol) in pentane (10 ml) with an addition rate of 4 ml/hour. After filtration a yellow solution was obtained (0.79 mmol/ml, 55 % yield). The solution was stored at 0 ºC and stirred before use.

methyl lithium – (MeLi)[14]

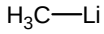

To a solution of lithium sand (2.5 g, 360 mmol, 7 eq) in freshly distilled diethyl ether (40 ml), methyl iodide (3.7 ml, 60 mmol) was added at 7.5 ml/hour at RT. The solution was left to stand overnight, after which the excess lithium was removed by filtration. A yield (70 %) was calculated by titration of 2,5 dimethoxybenzyl alcohol,[15] with 2,2'-biphyridine in THF.

9.11 Ligands

***N*,*N*-dimethylbutylamine – (DMBA)[16]**

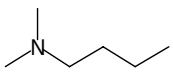

Butyl amine (14.6 g, 0.2 mol) was added to a water cooled solution of formic acid (51.2 g, 1 mol, 5 eq) in a 500 ml round bottom flask. Formaldehyde (37% solution, 45 ml, 0.6 mmol, 3 eq) was added and the flask was heated to approximately 90°C following which the rapid evolution of carbon dioxide occurred. After the evolution of gas has ceased the flask was heated to reflux overnight. HCl solution (4N, 100 ml) was added and the solvent removed under reduced pressure. The yellow oily residue was dissolved in H_2O (60 ml) following which aqueous NaOH solution (18N, 50 ml) was cautiously added. The aqueous solution was extracted with DCM (3 x 60 ml), the organic layers combined and dried over $MgSO_4$. Purification of the product *N*,*N*-dimethylbutylamine was accomplished by distillation

(90 – 95°C) lit 93.3°C affording a colourless liquid (3 g, 29 mmol, 14 % yield). Further purification was accomplished by distillation from sodium sand.

di-tosyl-ethylene glycol

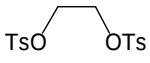

A round bottom flask (500 ml) was charged with ethylene glycol (4.5 ml, 80 mmol), tosyl chloride (34 g, 177 mmol, 2.2 eq), DMAP (cat), Et_3N (25 ml, 177 mmol, 2.2 eq) and DCM (150 ml) and stirred for 36 hours. The resulting crystalline precipitate was collect via filtration and washed with MeOH (100 ml) and dried under vacuum affording white crystalline material (20.5 g, 55 mmol, 68 % yield). ^{1}H NMR (400 MHz, CHLOROFORM-*d*) δ ppm 2.47 (s, 6 H, ArC*H*$_3$), 4.19 (s, 4 H, OCH_2CH_2O), 7.33 – 7.37 (m, 4 H, Ar*H*), 7.72 – 7.77 (m, 4 H, Ar*H*).

di-isopropyl-glyme

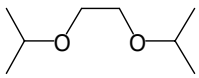

Di-tosylethylene glycol (20 g, 55 mmol) and tosic acid (600 mg, 3.5 mmol) were refluxed in *i*PrOH (170 ml) for 7 days. Unreacted di-tosylethylene glycol was removed by filtration, following which the solvent was removed under reduced pressure. The remaining material was suspended in 50 ml aqueous NaOH (2 M) and extracted with DCM (3 x 100 ml). The organic phases were combined, dried over $MgSO_4$, the solvent removed under reduced pressure, with purification of the di-isopropyl ethylene glycol by reduced pressure distillation (50°C at 20 mmHg), affording a colourless liquid (1 g, 6.8 mmol, 12% yield). ^{1}H NMR (300 MHz, CHLOROFORM-*d*) δ ppm 1.18 (d, *J*=6.2 Hz, 12 H, $CH(CH_3)_2$), 3.53 – 3.76 (m, 6 H, $CH(CH_3)_2$, OCH_2CH_2O).

di–tosyl diethylene glycol – (5.14)

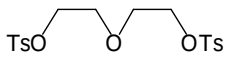

A round bottom flask (500 ml), cooled to 0°C in an ice bath, was charged with dry DCM (150 ml), diethylene glycol (9 ml, 93.3 mmol), tosyl chloride (39 g, 205 mmol, 2.2 eq), Et_3N (39 ml, 280 mmol, 3 eq) and DMAP (cat). The mixture was allowed to warm to RT and stirred overnight. The contents of the flask were transferred to a separating funnel along with additional DCM (100 ml) and were washed with H_2O (100 ml) and 1M HCl (100 ml), the organic phase dried over $MgSO_4$ and the solvent removed under reduced pressure. The resulting pale yellow solid was dissolved in hot toluene (100 ml), and PET (20 ml) slowly added. After cooling the crystalline material was collected by filtration, and placed under high vacuum returning a white crystalline material of high purity (37.5 g, 85 mmol, 90 % yield). ^{1}H NMR (400 MHz, CHLOROFORM-*d*) δ ppm 2.44 (s, 6 H), 3.57 – 3.62 (m, 4 H), 4.06 – 4.10 (m, 4 H), 7.31 – 7.36 (m, 4 H), 7.75 – 7.79 (m, 4 H).

di–mesyl–diethylene glycol[17]

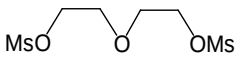

A round bottom flask (1000 ml) was charged with diethylene glycol (16 ml, 169 mmol), Et_3N (75 ml, 540 mmol, 3.2 eq), and DCM (500 ml). The flask was cooled to 0°C in an ice bath and a solution of mesyl chloride (33 ml, 423 mmol, 2.5 eq) in DCM (90 ml) was added dropwise to the rapidly stirred solution. The flask was allowed to warm to RT and stirred overnight, after which its contents were transferred to a separating funnel and washed with 1 M HCl (100 ml), H_2O (3 x 100 ml) $NaHCO_3$ (100 ml) and the organic phase dried over $MgSO_4$. The solvent was removed under reduced pressure affording a solid which was recrystallised from hot toluene (100 ml) and PET (10 ml) affording white crystalline material of high purity (37.8 g, 144 mmol, 85% yield). ^{1}H NMR (300 MHz, CHLOROFORM-*d*) δ ppm 3.07 (s, 6 H, SO_2CH_3), 3.76 – 3.83 (m, 4 H, OCH_2CH_2O), 4.34 – 4.41 (m, 4 H, OCH_2CH_2O).

di–isopropyl diethylene glycol – (5.12)

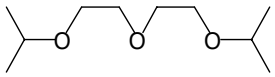

An oven dried round bottom flask (500 ml) was charged with *i*PrOH (50 ml, exs), THF (40 ml) and Na (5 g, 208 mmol, 5.7 eq). The mixture was heated to reflux until no sign of metallic Na remained (5 hours). Di-tosyl-diglyme **5.14** (15 g, 36.5 mmol) was added and the mixture heated at reflux for 18 hours. H_2O (100 ml) and ether (200 ml) were cautiously added, the layers separated and the organic phase washed with $NaHCO_3$ (sat, 100 ml), dried over $MgSO_4$ and the solvent removed under reduced pressure. Further purification was accomplished by distillation (90°C at 13 mmHg) afforded a colourless liquid (5 g, 26 mmol, 71 % yield). ^{1}H NMR (300 MHz, CHLOROFORM-*d*) δ ppm 1.17 (d, *J*=6.2 Hz, 12 H, $OCH(CH_3)_2$), 3.54 – 3.68 (m, 10 H, $OCH(CH_3)_2$, OCH_2CH_2O); ^{13}C NMR (75 MHz, CHLOROFORM-*d*) δ ppm 22.00, 67.33, 70.86, 71.79.

di–*tert*–butyl diethylene glycol – (5.13)

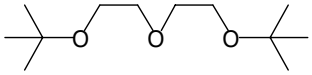

An oven dried round bottom flask (500 ml) was placed under an inert atmosphere and charged with *t*BuOH (60 ml, exs), dry THF (40 ml) and Na (5 g, 208 mmol, 5.8 eq). The flask was stirred at RT for 18 hours after which di-tosyl-diglyme **5.14** (15 g, 36 mmol) was added and the flask was brough to reflux for 18 hours, followed by stirring at RT for a further 18 hours. PET (100 ml) was added, the precipitate removed by filtration. After washing the precipitate with ether (200 ml), the organic phases were combined, washed with $NaHCO_3$ solution (sat, 2 x 70 ml), dried over $MgSO_4$ and the solvent removed under reduced pressure. Further purification was accomplished by distillation under reduced pressure (105°C at 13 mmHg) affording a clear liquid (2.2 g, 10 mmol, 28 % yield). ^{1}H NMR (300 MHz, CHLOROFORM-*d*) δ ppm 1.17 – 1.21 (m, 18 H, $C(CH_3)_3$), 3.47 – 3.53 (m, 4 H,

OCH_2CH_2O), 3.57 – 3.63 (m, 4 H, OCH_2CH_2O); ^{13}C NMR (75 MHz, CHLOROFORM-*d*) δ ppm 27.45, 61.10, 71.15, 72.90.

di–phenyl diethylene glycol – (7.5)

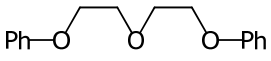

An oven dried round bottom flask (500 ml) was placed under an inert atmosphere, phenol (15 g, 160 mmol, 3.7 eq), dry DMF (80 ml) and NaH (60% in mineral oil, 6.4 g, 160 mmol, 3.7 eq) were cautiously added and the flask stirred at RT for 1 hour. Di-tosyl-diglyme **5.14** (17.9 g, 43 mmol) was added and the flask stirred at RT for 48 hours. Ether (250 ml) was added, the contents transferred to a separating funnel and the organic phase washed with $NaHCO_3$ solution (sat, 2 x 100 ml), H_2O (2 x 100 ml) followed by drying over $MgSO_4$ and the solvent removed under reduced pressure. Purification was accomplished by silica gel column chromatography yielding a white solid (9 g, 36 mmol, 84% yield). Further purification was achieved via crystallisation from a hot solution of PET. ^1H NMR (300 MHz, CHLOROFORM-*d*) δ ppm 3.92 – 3.99 (m, 4 H, OCH_2CH_2O), 4.13 – 4.21 (m, 4 H, OCH_2CH_2O), 6.90 – 6.98 (m, 5 H, Ar*H*), 7.24 – 7.33 (m, 5 H, Ar*H*).

di-triethyl diethylene glycol – (7.6)

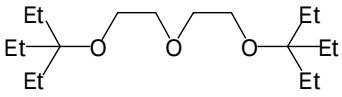

An oven dried round bottom flask (500 ml) was charged with ether (150 ml), *t*EtOH (12.4 g, 88 mmol, 2.3 eq) and NaH (60% in mineral oils, 3.5 g, 88 mmol, 2.3 eq). The flask was brought to reflux for 1.5 hours after which a solution of di-mesyl-diglyme (10 g, 38 mmol) in THF (50 ml) was added and reflux was continued for 18 hours. After cooling, H_2O (100 ml) was cautiously added, the layers separated, the organic phase washed with H_2O (2 x 100 ml), dried over $MgSO_4$ and the solvent removed under reduced pressure. Further purification was accomplished by silica gel column chromatography yielding a clear liquid (340 mg, 1.2 mmol, 3% yield). ^1H NMR (300 MHz, CHLOROFORM-*d*) δ ppm 0.74 – 0.83 (t, *J*=7.5 Hz, 18 H, $C(CH_2CH_3)_3$), 1.44 (d, *J*=7.5 Hz, 12 H, $C(CH_2CH_3)_3$), 3.39 (t, *J*=5.6 Hz, 4 H, OCH_2CH_2O), 3.61 (t, *J*=5.7 Hz, 4 H, OCH_2CH_2O); ^{13}C NMR (75 MHz, CHLOROFORM-*d*) δ ppm 7.46, 26.07, 59.64, 71.10, 78.91.

trimethoxy glycerol

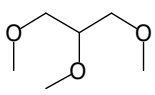

An oven dried flask was placed under an inert atmosphere and charged with Na (5.6 g, 240 mmol) and MeOH (85 ml). It was heated to reflux and epichlorohydrin (20 ml, 244 mmol) was cautiously added. Reflux was continued for 1 hour, following which H_2O (10 ml) was cautiously added, the solvent was removed under reduced pressure and dimethoxy glycerol purified by reduced pressure distillation (45 °C at 3 mmHg) yielding a clear liquid.[18]

Dimethoxy glycerol (5g, 42 mmol), THF (30 ml) and NaH (60% in mineral oil, 320 mg, 83 mmol) were cautiously added to an oven dried round bottom flask. The flask was heated to reflux for 1 hour, following which it was cooled to RT and MeI (0.52 ml, 83 ml, 83 mmol) was added and the flask stirred at RT overnight. Purification by distillation yielded a clear liquid (4 g, 30 mmol, 71% yield). ^{1}H NMR (300 MHz, CHLOROFORM-*d*) δ ppm 3.47 – 3.38 (m, 14 H).

9.12 References

(1) Williams, D. B. G.; Lawton, M. *J. Org. Chem.*, **2010**, *75*, 8351.

(2) Perrin, D. D.; Armarego, W. L. F. *Purification of Laboratory Chemicals. 3rd Ed*, 1988.

(3) Marat, K.; SpinWorks 3.1.7 ed.; University of Manitoba: 2010.

(4) Gutsche, C. D.; Iqbal, M. *Org. Synth.* **1990**, *68*, 234.

(5) Iwamoto, K.; Araki, K.; Shinkai, S. *J. Org. Chem.* **1991**, *56*, 4955.

(6) Verboom, W.; Durie, A.; Egberink, R. J. M.; Asfari, Z.; Reinhoudt, D. N. *J. Org. Chem.* **1992**, *57*, 1313.

(7) Bitter, I.; Gruen, A.; Toth, G.; Szollosy, A.; Horvath, G.; Agai, B.; Toke, L. *Tetrahedron* **1996**, *52*, 639.

(8) Krasnokutskaya, E. A.; Semenischeva, N. I.; Filimonov, V. D.; Knochel, P. *Synthesis-Stuttgart* **2007**, 81.

(9) Gutsche, C. D.; Lin, L.-G. *Tetrahedron* **1986**, *42*, 1633.

(10) McKennon, M. J.; Meyers, A. I.; Drauz, K.; Schwarm, M. *J. Org. Chem.* **1993**, *58*, 3568.

(11) Krasovskiy, A.; Straub, B. F.; Knochel, P. *Angew. Chem. Int. Ed.* **2006**, *45*, 159.

(12) Bryce-Smith, D.; Turner, E. E. *J. Chem. Soc.* **1953**, 861.

(13) Kamienski, C. W.; Esmay, D. L. *J. Org. Chem.* **1960**, *25*, 1807.

(14) Lusch, M. J.; Phillips, W. V.; Sieloff, R. F.; Nomura, G. S.; House, H. O. *Org. Synth.* **1984**, *62*, 101.

(15) Winkle, M. R.; Lansinger, J. M.; Ronald, R. C. *J. Chem. Soc., Chem. Commun.* **1980**, 87.

(16) Icke, R. N.; Wisegarver, B. B.; Alles, G. A. *Org. Synth.* **1945**, *25*, 89.

(17) Ingham, A. M.; Xu, C.; Whitcombe, T. W.; Xu, C. T.; Bridson, J. N.; McAuley, A. *Can. J. Chem.* **2002**, *80*, 155.

(18) Garcia, J. I.; Garcia-Marin, H.; Mayoral, J. A.; Perez, P. *Green. Chem.* **2010**, *12*, 426.

APPENDIX I

Structural Analysis of Calixarenes using ^{1}H NMR Spectroscopy

A1.1 Interpretation of ^{1}H NMR spectra

The NMR spectra of calix[4]arene have been very well studied in the chemical literature.[1-3] This appendix seeks to provide a brief summary of the structural information that can be gained from the interpretation of the spectra in order for the reader to gain an understanding of the structural information that can be gained from the ^{1}H NMR spectra of the calixarene. This will be presented by following the impact of functionalisation on the conformation in the ^{1}H NMR spectra of various calixarenes from Chapter 2.

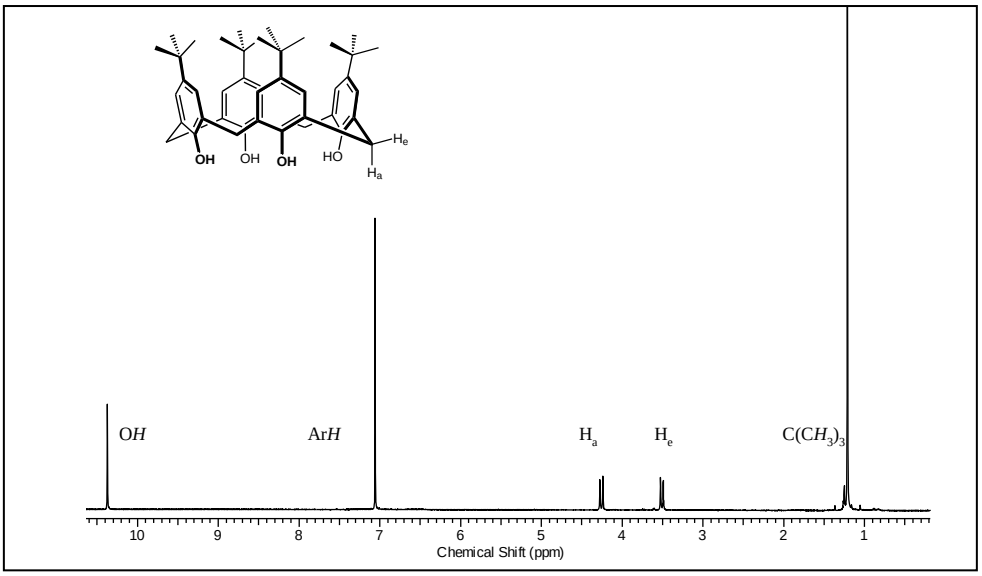

Figure A1. 1: ^{1}H spectrum of *t*-butyl calix[4]arene with solvent signals removed for clarity

A room temperature spectrum of calixarene **2.5** displays poorly defined signals for the methylene bridges. On cooling the sample to 0 ºC two well defined signals appear (Figure A1. 1). Using NOE experiments Ungaro *et al.* identified the upfield signals as belonging to the equatorial protons on the methylene bridge,[4] with the downfield signals being attributed to the axial protons. The temperature dependence of these signals has been attributed to the inversion of the molecule in solution.[1,3,5-7] Inspection of the methylene bridging signals also allows the conformation (cone, pinch cone, partial cone etc) of the calixarene to be deduced as changes in conformation manifest themselves in the ^{1}H signals of the bridging protons.[8]

The ^1H NMR spectrum of tripropoxy calixarene **2.6** reveals the loss in symmetry in the molecule (C_4 to C_V) due to the tri-alkylation of the phenolic positions (Figure A1.3). The alkylation also affects the conformation of the molecule as the strong hydrogen-bonded ring formed in the phenolic system no longer dictates that the molecule sits in the cone conformation, with the molecule now adopting the more energetically favourable pinched cone or boat conformation.[6] This change in conformation is visible in the appearance of two doublets in the ^1H NMR spectrum of **2.6** for both the equatorial and axial methylene protons as seen in Figure A1.2.[4,6] The precise shifts of the methylene bridges are obviously a combined feature of the electronic effect of the functional groups on the aryl rings as well as the conformation of the molecule. An increase in the separation of the axial and equatorial signals can be associated with the pinch cone conformation that this molecule has adopted compared to the true cone of calixarene **2.5**.

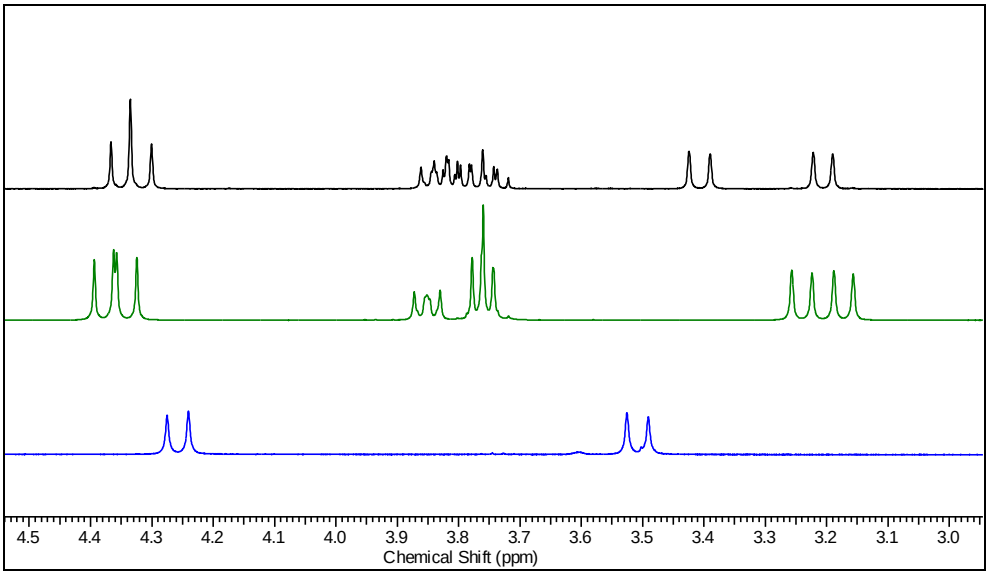

Figure A1.2: ^1H NMR spectrum of methylene bridging protons. Colours Blue = *t*-butyl calix[4]arene **2.5** (bottom) (0 ºC), Green = triprotected calixarene **2.6** (middle), Black = nitrated calixarene **2.7** (top).

The signals associated with the *t*-butyl groups provide a clear indication as to the loss of symmetry in the molecule with three separate signals being visible (Figure A1.3). The number of visible signals is a consequence of the symmetry associated with the molecule. The non-propylated and its distil counter-part appear as two distinct signals, with the symmetrical nature of the two proximal rings results in them appearing as a single signal. Scrutiny of the aromatic region of the ^1H NMR spectrum also supports this information, with the appearance of two slightly coalescing systems of doublets. The doublets arise from the two rings adjacent to the non-alkylated phenolic ring having non-equivalent sides, therefore causing ^4J coupling between the two sets of protons.

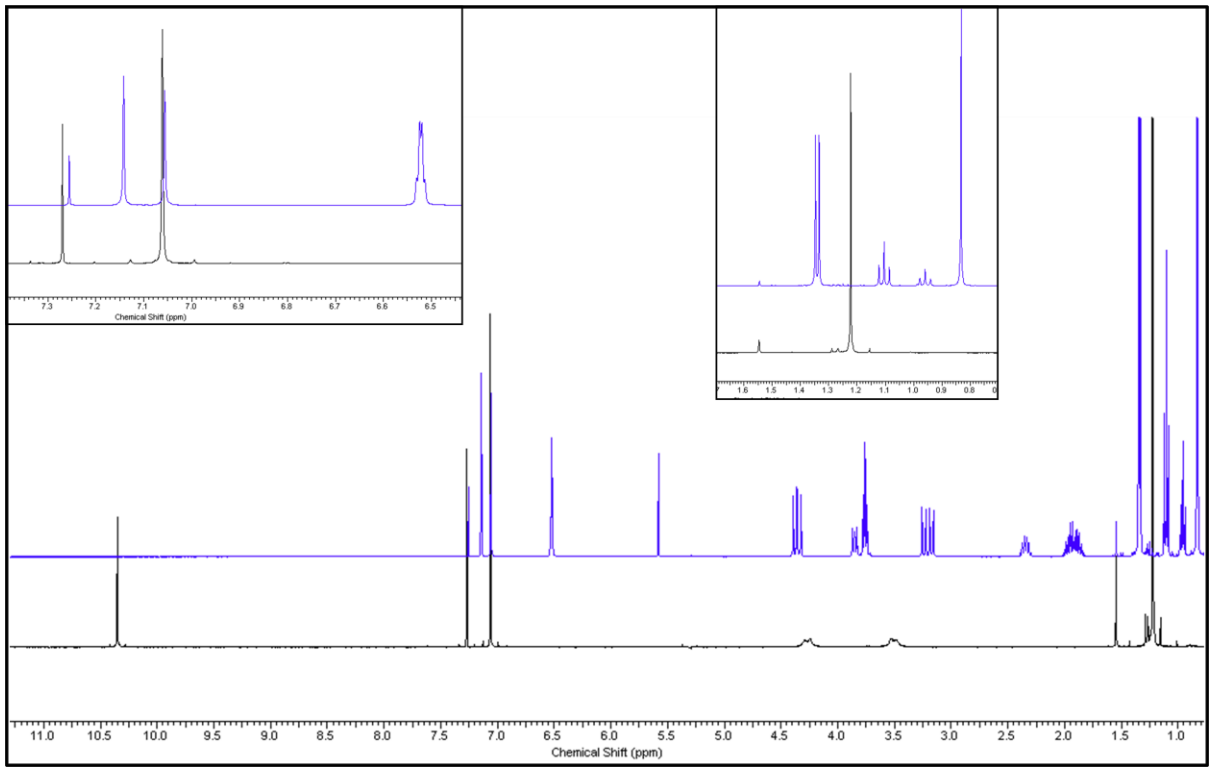

Figure A1.3: ^{1}H NMR spectrum of triprotected calixarene 2.6 (blue) and calix[4]arene 2.5 (black).

Perhaps more importantly due to the calixarenes cyclic structure notable anisotropic effects are in operation. Briefly rationalising the appearance of shielding effect in specific areas of the molecule allows for the conformation of the molecule to be determined. The downfield nature of the *t*-butyl signals associated with the non-propylated ring and its distal counterpart indicate that they fail to experience anisotropic shielding. Conversely the upfield nature of the two symmetry related rings indicates that they experience shielding inducing the upfield shift. The upright nature of these rings brings them within the electronic influence of the two outward lying rings inducing shielding. A similar situation in the aromatic region is observed with the appearance of two distinctly different signals indicative a shielded and non-shielded environment associated with the pinch cone.

The ^{1}H NMR spectrum of **2.7** further illustrates how the ^{1}H NMR spectrum imparts such definitive structural information (Figure A1.4). The molecule evidently sits in the pinch cone or boat conformation as visible by the splitting of the methylene bridges into the two sets of doublets. Similarly to **2.6** the molecule sits with the functionalised rings and its opposite counterpart lying outwards, presumably due to the smaller steric bulk of the phenolic group on the nitro-group functionalised ring Figure A1.4.

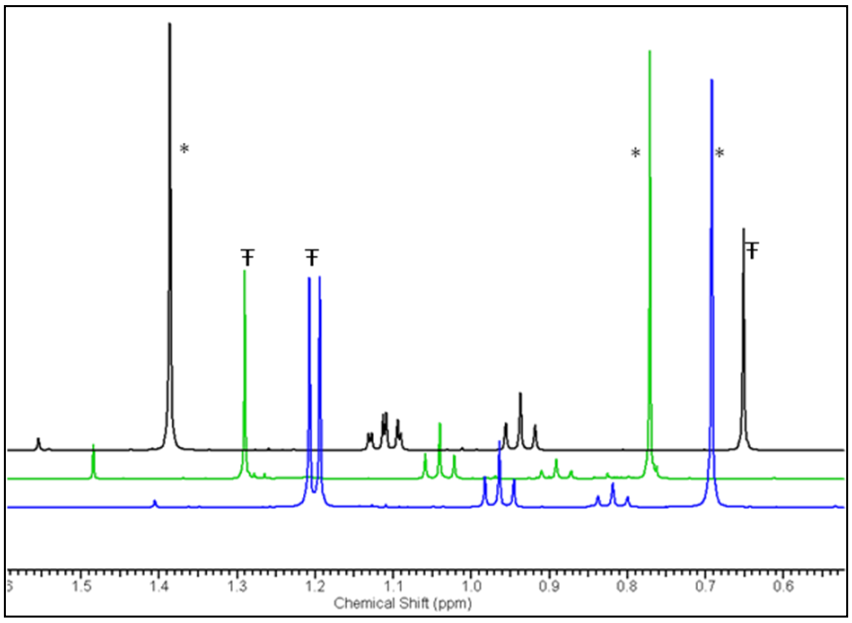

Figure A1.4: ^{1}H NMR spectra of *t*-butyl groups. Notes: An offset of 0.07 ppm has been used. Key: * marks the symmetry related t-butyl groups, Ŧ marks the non-symmetry related groups. Triprotected calixarene **2.6** bottom (Blue), nitro calixarene **2.7** (Green), tetraprotected calixarene **2.8** (Black)

Interpretation of the ^{1}H NMR spectrum of calixarene **2.8** indicated that a change in conformation of the molecule had occurred. This was indicated by a change in the shifts of the *t*-butyl groups as shown in Figure A1.5. Both triprotected calixarenes (**2.6** and **2.7**) had the functionalised ring lying outwards, whereas the shifts of **2.8** indicating a reversal in conformation having occurred, with the two rings proximal to the functionalised ring lying outwards. This can be rationalised by considering the increase in bulk of the newly alkylated phenolic position and the relatively small steric bulk of the nitro group. This change in conformation is also mirrored by the signals in the aromatic region, with the considerable upfield shifts of the two singlets assigned to the nitro-functionalised ring and its opposite counterpart and the downfield shifts of the two doublets as shown in Figure A1.5. This dramatic shift in both signals can be attributed to the anisotropic shielding effect of the ring system.

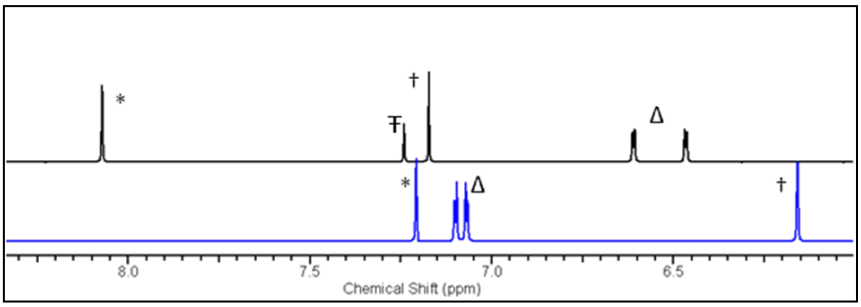

Figure A1.5: 1H NMR shifts of aromatic region of triprotected calixarene 3 and tetraprotected calixarene 4. Notes: The solvent signals have been removed for clarity. Key: Calixarene 4 bottom (blue), calixarene 3 top, green) * ArH ortho to NO2, † ArH ortho to t-butyl (opposite functionalised ring),Δ ArH, Ŧ phenolic OH.

Using the aforementioned characteristic feature of the 1H NMR spectra of the functionalized calixarenes, it is possible to ascertain what conformation the molecule exists in.

A1.2 References

(1) Kammerer, H.; Happel, G.; Caesar, F. *Makromol. Chem.* **1972**, *162*, 179.

(2) Gueniffe.H; Kammerer, H.; Klesper, E. *Makromol. Chem.* **1972**, *162*, 199.

(3) Gutsche, D. C. *Calixarenes: an introduction* 2ed.; RSC Publishing: Cambridge, 2008.

(4) Arduini, A.; Pochini, A.; Reverberi, S.; Ungaro, R. *J. Chem. Soc., Chem. Commun.* **1984**, 981.

(5) Simaan, S.; Biali, S. E. *J. Phys. Org. Chem.* **2004**, *17*, 752.

(6) Dahan, E.; Biali, S. E. *J. Org. Chem.* **1991**, *56*, 7269.

(7) Grootenhuis, P. D. J.; Kollman, P. A.; Groenen, L. C.; Reinhoudt, D. N.; Van Hummel, G. J.; Ugozzoli, F.; Andreetti, G. D. *J. Am. Chem. Soc.* **1990**, *112*, 4165.

(8) Gutsche, C. D.; Bauer, L. J. *J. Am. Chem. Soc.* **1985**, *107*, 6052.

APPENDIX II

Selected Computation Data

A2.1 DFT optimisations of calixarene conformations (rb3lyp/6-31+g(d,p))

Isopropyl Oxazoline **5.1** inward conformation				Isopropyl Oxazoline **5.1** outward conformation			
Atom	X	Y	Z	Atom	X	Y	Z
C	-2.325195	1.44051	-0.74851	C	2.153492	1.59287	0.803144
C	-2.916086	1.082939	0.469006	C	2.941112	0.768337	-0.00633
C	-4.25932	0.484848	0.481432	C	4.193682	0.183352	0.494707
N	-4.994707	0.243435	-0.53784	N	5.020214	-0.53028	-0.17309
C	0.095083	0.521063	3.505792	C	0.570629	-0.96347	-3.16381
C	-0.691887	0.005532	4.543859	C	1.493299	-1.8622	-3.71483
C	1.037747	-0.33184	2.904567	C	-0.545713	-1.49168	-2.4913
C	-0.568664	-1.32745	4.941809	C	1.326843	-3.24073	-3.56634
C	-0.131872	1.921028	2.952523	C	0.816337	0.53904	-3.17653
C	1.110023	-1.70041	3.218271	C	-0.680452	-2.86842	-2.24038
C	-0.934329	1.866729	1.650804	C	1.330503	1.016744	-1.81667
C	0.306576	-2.17769	4.262644	C	0.262406	-3.73502	-2.80964
C	-0.411855	2.323531	0.422577	C	0.615192	1.940431	-1.02034
C	1.945604	-2.63905	2.360234	C	-1.7454	-3.37026	-1.27616
C	3.102507	0.708862	2.491656	C	-2.543769	-0.36018	-2.98425
C	-2.19797	1.269747	1.654887	C	2.50146	0.463164	-1.30024
C	-1.069666	2.046905	-0.79579	C	0.980038	2.179736	0.319287
C	1.233738	-2.95222	1.043322	C	-1.334208	-3.10775	0.173492
C	-0.051584	-3.5078	1.063238	C	-0.111716	-3.59968	0.647923
C	1.802906	-2.63697	-0.20632	C	-2.116326	-2.32068	1.041832
C	1.06762	-2.76543	-1.40119	C	-1.643469	-1.93979	2.312938
C	-0.215385	-3.32202	-1.33322	C	-0.414445	-2.45318	2.744632

C	1.598955	-2.25488	-2.74008	C	-2.390675	-0.9365	3.19091
C	0.713727	-1.142	-3.28945	C	-1.545987	0.309413	3.429467
C	-0.221934	-1.40275	-4.29901	C	-0.864652	0.493851	4.63964
C	-1.163056	-0.44204	-4.67465	C	0.061647	1.52737	4.794271
C	0.715335	0.140393	-2.70367	C	-1.314228	1.23507	2.391593
C	-0.28984	1.083395	-2.98865	C	-0.30631	2.212908	2.485971
C	-1.213551	0.777336	-3.99771	C	0.359987	2.355501	3.71111
C	-0.764593	-3.71837	-0.11549	C	0.337368	-3.29961	1.932458
C	-0.428093	2.345598	-2.15101	C	0.112209	3.01357	1.262253
C	4.09041	-3.20797	-0.37678	C	-4.427325	-2.80676	0.932064
C	2.991357	0.712429	-2.27186	C	-3.397431	1.57013	1.27891
C	0.735521	4.377351	0.849221	C	-0.216332	3.646024	-2.4747
H	0.363928	-3.22771	4.540047	H	0.164303	-4.80625	-2.64965
H	-0.670977	2.514397	3.700752	H	1.55144	0.770587	-3.95649
H	0.821274	2.415514	2.764637	H	-0.101587	1.07384	-3.42125
H	-1.412929	0.653034	5.037023	H	2.355089	-1.47686	-4.25436
H	-0.507382	-3.75358	2.018152	H	0.507133	-4.20302	-0.01005
H	-0.797145	-3.42343	-2.24525	H	-0.034311	-2.16483	3.720819
H	-1.981971	1.504097	-4.24973	H	1.122022	3.12462	3.81252
H	3.173445	0.097709	-3.16327	H	-3.804902	1.382158	2.280932
H	3.674282	0.381271	-1.48598	H	-3.935953	0.937919	0.569194
H	4.001975	-3.89642	0.477181	H	-4.224589	-3.7752	0.45045
H	0.543431	2.806664	-1.98213	H	-0.760292	3.364328	0.713603
H	-1.048362	3.064877	-2.69932	H	0.673544	3.895142	1.595011
H	2.916701	-2.19529	2.136947	H	-2.700744	-2.8787	-1.46515
H	2.121422	-3.5665	2.918642	H	-1.886584	-4.44641	-1.43437
H	1.613023	-3.07603	-3.46656	H	-2.615274	-1.39344	4.16204
H	2.62813	-1.92173	-2.6068	H	-3.342613	-0.69437	2.718276
H	1.768196	4.627835	1.116373	H	-1.140566	3.765397	-3.05103
H	2.865068	1.503922	3.214976	H	-2.09581	0.081943	-3.88736

O	3.109123	-2.16542	-0.26034	O	-3.368974	-1.88486	0.62621
O	1.669427	0.4567	-1.76186	O	-2.026514	1.133118	1.217327
O	0.789252	3.0107	0.397753	O	-0.493447	2.583614	-1.54245
O	1.884894	0.178848	1.941326	O	-1.514113	-0.62862	-2.01778
H	-0.223273	-2.37778	-4.78089	H	-1.048797	-0.19443	5.461349
C	-6.720236	-1.56351	-0.80135	C	7.502033	-0.72641	0.16184
C	-6.832712	-1.29974	-2.30891	C	7.669603	-1.46082	-1.17514
H	-7.60155	-0.54397	-2.51583	H	7.571586	-2.5456	-1.03854
H	-7.114969	-2.2153	-2.84113	H	8.66073	-1.26741	-1.60099
H	-5.885725	-0.93633	-2.71458	H	6.910912	-1.14326	-1.89424
H	-2.621443	0.918309	2.589106	H	3.077069	-0.24267	-1.88959
H	3.902486	-3.79141	-1.29092	H	-4.462891	-2.98022	2.018347
H	3.632374	-0.0839	3.04204	H	-3.019652	-1.30581	-3.28679
H	0.124276	4.446556	1.759262	H	0.577559	3.337008	-3.16804
O	-4.76882	0.176604	1.71961	O	4.486512	0.428146	1.81384
C	-6.012842	-0.51915	1.470201	C	5.805284	-0.12462	2.034538
H	-5.863037	-1.57695	1.720093	H	6.503346	0.711653	2.166078
H	-6.775519	-0.09643	2.127383	H	5.77501	-0.71738	2.951093
C	-6.271047	-0.29911	-0.04391	C	6.093079	-0.94219	0.747146
H	-7.043702	0.472019	-0.19578	H	5.973325	-2.02061	0.939351
H	-2.861354	1.228306	-1.66734	H	2.456906	1.771624	1.828634
C	0.211341	5.348637	-0.208	C	0.161443	4.964345	-1.80037
H	-0.803342	5.052801	-0.49948	H	1.062041	4.814914	-1.19313
H	0.837302	5.270977	-1.10485	H	-0.642563	5.256444	-1.11449
C	0.204752	6.793962	0.305558	C	0.406357	6.076105	-2.82849
H	1.211599	7.123614	0.588555	H	-0.485397	6.261109	-3.43922
H	-0.44045	6.902471	1.185249	H	1.227363	5.818238	-3.50764
H	-0.164616	7.481432	-0.46185	H	0.669424	7.016627	-2.3343
C	3.22348	2.1849	-2.60683	C	-3.562669	3.046898	0.924548
H	2.517444	2.494685	-3.38717	H	-3.002445	3.656945	1.643908

H	3.004768	2.785461	-1.71674	H	-3.118396	3.221927	-0.06174
C	4.660214	2.438536	-3.08052	C	-5.037228	3.469739	0.927069
H	5.390159	2.154116	-2.31319	H	-5.62116	2.886995	0.204648
H	4.818262	3.497117	-3.31098	H	-5.144528	4.526831	0.662934
H	4.891002	1.865508	-3.98656	H	-5.493957	3.328392	1.913936
C	3.961774	1.249781	1.361651	C	-3.561745	0.585794	-2.37071
H	4.188987	0.42432	0.67946	H	-3.995842	0.097437	-1.49221
H	3.367852	1.976678	0.797276	H	-3.030324	1.474343	-2.01358
C	5.256236	1.888371	1.87891	C	-4.661481	0.972889	-3.36652
H	5.050088	2.734913	2.544858	H	-4.248662	1.486573	-4.24307
H	5.866813	2.262522	1.050614	H	-5.390255	1.646236	-2.90345
H	5.865948	1.168768	2.43872	H	-5.208577	0.09322	-3.72672
C	5.475818	-2.57808	-0.41675	C	-5.745314	-2.22723	0.437429
H	5.621377	-1.98671	0.495308	H	-5.665606	-2.03603	-0.63955
H	5.520781	-1.87632	-1.2584	H	-5.907796	-1.25539	0.919208
C	6.584924	-3.62881	-0.54678	C	-6.92919	-3.15945	0.72121
H	7.571612	-3.15562	-0.5698	H	-7.866186	-2.72219	0.362217
H	6.476232	-4.21365	-1.46752	H	-7.041658	-3.3483	1.795186
H	6.573015	-4.32979	0.295933	H	-6.804048	-4.12857	0.224425
C	-8.047276	-2.09546	-0.23596	C	8.582461	-1.16019	1.166062
H	-8.84701	-1.35302	-0.35439	H	8.497423	-2.23096	1.391768
H	-8.357756	-3.00235	-0.76582	H	9.583595	-0.98793	0.756445
H	-7.977494	-2.34534	0.828921	H	8.516855	-0.6122	2.113036
H	-1.875843	-0.65662	-5.46549	H	0.573999	1.663453	5.742239
H	-1.758767	-4.15448	-0.0814	H	1.286392	-3.69357	2.284339
H	-1.174553	-1.70959	5.75829	H	2.043102	-3.92565	-4.01076
H	-5.942083	-2.32509	-0.64251	H	7.610177	0.353181	-0.02207
Energy: -1391958.396 kcal.mol^{-1}				Energy: -1391958.423kcal.mol^{-1}			

Isopropyl oxazoline **2.1** inward conformation				Isopropyl oxazoline **2.1** outward conformation			
Atom	X	Y	Z	C	-0.986411	1.886051	1.802755
C	1.70601	-0.75804	2.161109	C	-2.14668	1.12349	1.634914
C	2.090166	0.587782	2.121188	C	-3.386188	1.725434	1.121762
C	3.493388	0.939593	1.857767	N	-4.520891	1.144636	1.002368
N	4.463897	0.122409	1.688171	C	-1.115353	-3.05959	1.285215
C	-1.381406	3.089482	1.374969	C	-2.355678	-3.57261	0.895166
C	-0.749571	4.316068	1.150366	C	-0.056196	-3.10587	0.362344
C	-2.068911	2.489511	0.305465	C	-2.584236	-4.09929	-0.38769
C	-0.754676	4.948308	-0.10488	C	-0.931119	-2.36248	2.626938
C	-1.24733	2.360439	2.705268	C	-0.263936	-3.52577	-0.95831
C	-2.015213	3.031828	-0.98555	C	-0.966533	-0.842	2.458969
C	-0.202346	1.246675	2.621517	C	-1.525397	-4.03521	-1.3032
C	-1.372917	4.267306	-1.16174	C	0.151686	-0.0226	2.73836
C	-0.534766	-0.11603	2.774904	C	0.819485	-3.32424	-2.00893
C	-2.53856	2.239397	-2.17599	C	2.001647	-3.73217	1.308669
C	-4.128528	1.542056	0.922157	C	-2.111432	-0.24414	1.933941
C	1.120043	1.577402	2.313431	C	0.177126	1.329921	2.343234
C	0.39683	-1.13142	2.465732	C	0.8712	-1.86866	-2.47585
C	-1.553608	1.141212	-2.57963	C	-0.274028	-1.28187	-3.03337
C	-0.24726	1.492186	-2.94984	C	2.016854	-1.07427	-2.30826
C	-1.894577	-0.22008	-2.53427	C	1.976487	0.306828	-2.57926
C	-0.91345	-1.21043	-2.73431	C	0.810508	0.842302	-3.13191
C	0.37395	-0.80762	-3.09731	C	3.137687	1.235553	-2.22479
C	-1.201761	-2.69448	-2.50899	C	2.72597	2.248682	-1.16216
C	-0.380008	-3.24932	-1.35026	C	2.403111	3.56156	-1.51801
C	0.778169	-3.99371	-1.59361	C	1.849289	4.479814	-0.60961
C	1.660286	-4.37997	-0.56985	C	2.53368	1.857015	0.177922
C	-0.693344	-2.92255	-0.01543	C	1.880756	2.702546	1.087078
C	0.213501	-3.19017	1.021055	C	1.566483	4.008345	0.678097

C	1.367137	-3.93251	0.723815	C	-0.325616	0.065751	-3.40276
C	0.732611	0.540019	-3.24623	C	1.439952	2.184217	2.448233
C	0.001427	-2.6069	2.411201	C	4.032701	-2.15224	-2.90399
C	-4.011994	-0.7256	-3.45132	C	4.324117	0.397152	0.766958
C	-3.062089	-3.0514	0.223268	C	1.117024	-0.80522	4.779434
C	-2.0786	-0.28094	4.591605	H	-1.665606	-4.38311	-2.32124
H	-1.362591	4.691126	-2.16049	H	-1.731169	-2.68113	3.305572
H	-0.957339	3.083401	3.477017	H	0.017873	-2.6535	3.07726
H	-2.205814	1.933057	2.999876	H	-3.166052	-3.55172	1.61932
H	-0.23576	4.784745	1.986011	H	-1.149145	-1.90914	-3.15733
H	-0.0033	2.547712	-2.98394	H	0.793005	1.90893	-3.33744
H	1.121129	-1.58134	-3.24929	H	1.089941	4.659977	1.402819
H	2.04378	-4.15655	1.541481	H	4.882386	0.994362	0.033641
H	-2.974258	-3.81135	-0.5646	H	4.497687	-0.65893	0.547532
H	-3.85727	-2.35837	-0.06102	H	3.479972	-2.9034	-3.48822
H	-4.028918	0.231523	-3.99436	H	2.227016	1.586043	2.903721
H	-1.040735	-2.70067	2.71087	H	1.247609	3.040633	3.105931
H	0.608351	-3.1741	3.127061	H	1.797015	-3.59746	-1.60915
H	-3.499683	1.780501	-1.94003	H	0.612565	-3.98171	-2.86217
H	-2.694646	2.92639	-3.01669	H	3.457982	1.782377	-3.11966
H	-0.947417	-3.25786	-3.41462	H	3.982322	0.630521	-1.89426
H	-2.270545	-2.82332	-2.33708	H	1.894562	-1.53879	5.019986
H	-3.170315	-0.21718	4.661679	H	1.496997	-4.15458	2.191478
H	-4.148007	2.13509	1.849681	O	3.197093	-1.64862	-1.85028
O	-3.206157	-0.59659	-2.26997	O	2.9104	0.596213	0.586511
O	-1.864661	-2.25547	0.27279	O	1.259855	-0.56211	3.367075
O	-1.804815	-0.47285	3.190864	O	1.19887	-2.68013	0.750589
O	-2.767294	1.318087	0.521478	H	2.579402	3.865269	-2.54701
H	0.999036	-4.26463	-2.62328	C	-6.796638	2.192505	1.170123
C	6.554116	0.45742	0.336813	C	-7.4706	0.816283	1.252326

C	6.940469	-1.02142	0.47367	H	-7.720664	0.444987	0.250101
H	7.564351	-1.17994	1.362903	H	-8.401829	0.875217	1.827205
H	7.514255	-1.35402	-0.39876	H	-6.811499	0.085342	1.726403
H	6.052596	-1.65063	0.569289	H	-2.99034	-0.8436	1.722185
H	1.399256	2.61952	2.204804	H	4.298001	-1.33284	-3.58948
H	-3.567336	-1.47644	-4.12236	H	2.105571	-4.54553	0.573852
H	-4.647752	2.130533	0.14985	H	0.141355	-1.26753	4.982398
H	-1.661536	0.678615	4.926162	O	-3.302065	3.040619	0.735024
O	3.78028	2.282907	1.815474	C	-4.652387	3.443674	0.406239
C	5.167751	2.375991	1.413398	H	-4.991453	4.144678	1.179046
H	5.195295	2.754266	0.383963	H	-4.628354	3.953603	-0.55902
H	5.665001	3.08912	2.07403	C	-5.456784	2.115914	0.412397
C	5.691137	0.92018	1.525893	H	-5.674328	1.79085	-0.61761
H	6.292913	0.797465	2.441066	H	-0.990751	2.928292	1.503722
H	2.451247	-1.51615	1.945317	C	-1.563642	0.710439	-4.0554
C	2.159741	0.91353	-3.69088	C	-1.177213	1.265041	-5.44853
C	2.437253	0.308456	-5.08868	H	-2.046419	1.729148	-5.93004
H	3.452308	0.559638	-5.41957	H	-0.81347	0.463715	-6.10127
H	1.730945	0.697502	-5.83046	H	-0.389911	2.022188	-5.37939
H	2.348213	-0.78228	-5.08213	C	-2.079316	1.87022	-3.16974
C	3.1849	0.349483	-2.67787	H	-2.956755	2.338691	-3.6324
H	4.204716	0.615522	-2.98171	H	-1.321705	2.647008	-3.03065
H	3.132198	-0.74093	-2.60801	H	-2.366919	1.506507	-2.17814
H	3.007681	0.753195	-1.67586	C	-2.717649	-0.29355	-4.24438
C	2.366182	2.438258	-3.78141	H	-3.567997	0.210004	-4.71717
H	3.388933	2.650466	-4.11204	H	-3.06405	-0.69998	-3.28835
H	2.223323	2.926759	-2.81172	H	-2.428985	-1.1303	-4.89001
H	1.683717	2.900524	-4.5031	C	1.553168	5.924245	-1.05853
C	2.899214	-5.23505	-0.90028	C	2.868916	6.60174	-1.51381
C	2.445134	-6.57769	-1.5239	H	3.33449	6.066228	-2.3471

H	1.871793	-6.42447	-2.44344	H	3.594007	6.637077	-0.69338
H	1.813379	-7.13812	-0.82608	H	2.675165	7.62972	-1.8427
H	3.314781	-7.19836	-1.77071	C	0.552072	5.9121	-2.23968
C	3.800568	-4.48345	-1.91026	H	0.944165	5.360883	-3.10005
H	3.275186	-4.27503	-2.84748	H	0.339782	6.936033	-2.5699
H	4.685615	-5.08389	-2.15243	H	-0.39389	5.445381	-1.94478
H	4.139186	-3.52825	-1.49523	C	0.944236	6.777139	0.071879
C	3.744874	-5.55099	0.349198	H	1.614925	6.848206	0.935036
H	3.171175	-6.10643	1.099119	H	-0.015751	6.376008	0.414042
H	4.135566	-4.64213	0.818885	H	0.765162	7.794813	-0.29181
H	4.602848	-6.16973	0.064926	C	-3.962953	-4.69167	-0.74009
C	-0.073091	6.320163	-0.276	C	-4.026964	-5.20851	-2.19078
C	-0.200365	6.865655	-1.71216	H	-3.291915	-5.99934	-2.37601
H	-1.247143	6.996338	-2.0075	H	-3.859658	-4.40637	-2.91762
H	0.283723	6.209871	-2.44376	H	-5.01967	-5.62783	-2.38721
H	0.286155	7.844876	-1.77671	C	-5.056921	-3.60976	-0.56811
C	1.433533	6.198351	0.059042	H	-4.868581	-2.75444	-1.2255
H	1.924998	5.482078	-0.60808	H	-5.103082	-3.23417	0.458326
H	1.597016	5.860585	1.086902	H	-6.042005	-4.02219	-0.81708
H	1.930106	7.169299	-0.0563	C	-4.2683	-5.87976	0.20507
C	-0.727833	7.34463	0.682857	H	-3.513707	-6.66705	0.099974
H	-1.795505	7.456517	0.464593	H	-5.24816	-6.31218	-0.03008
H	-0.252513	8.326811	0.57442	H	-4.283521	-5.56977	1.254544
H	-0.631089	7.041009	1.729713	C	1.289915	0.449497	5.634744
C	-1.557405	-1.41505	5.473628	H	0.533329	1.189473	5.348246
H	-0.469205	-1.48976	5.362387	H	2.269179	0.894115	5.42104
H	-1.980634	-2.36273	5.120074	C	1.170246	0.135896	7.131417
C	-1.916376	-1.19626	6.948725	H	1.927513	-0.59008	7.450807
H	-3.001918	-1.13722	7.092412	H	0.185982	-0.28075	7.375374
H	-1.478881	-0.26764	7.333731	H	1.304696	1.039968	7.73362

H	-1.545073	-2.01808	7.569016	C	4.800354	0.740228	2.177755
C	-3.387232	-3.72966	1.553751	H	4.593136	1.797568	2.383937
H	-2.561618	-4.39579	1.832776	H	4.219552	0.150963	2.896315
H	-3.459455	-2.96102	2.331433	C	6.299554	0.466104	2.352592
C	-4.69228	-4.53221	1.47586	H	6.53766	-0.58885	2.171434
H	-5.542309	-3.89022	1.21558	H	6.629257	0.709502	3.367915
H	-4.919889	-5.00932	2.434674	H	6.900024	1.065674	1.657956
H	-4.630509	-5.32375	0.719466	C	3.361652	-3.16798	1.684311
C	-4.811974	0.200486	1.12891	H	3.824595	-2.76636	0.777089
H	-4.788725	-0.34443	0.17975	H	3.206918	-2.32361	2.364649
H	-4.219288	-0.37908	1.844726	C	4.267029	-4.226	2.325737
C	-6.255423	0.361427	1.620067	H	3.827906	-4.62811	3.246787
H	-6.297187	0.888509	2.580955	H	5.243342	-3.80287	2.58409
H	-6.73423	-0.61357	1.758209	H	4.442758	-5.07041	1.648259
H	-6.864205	0.929165	0.905931	C	5.285036	-2.76502	-2.29198
C	-5.420081	-1.13696	-3.04389	H	4.986942	-3.55951	-1.59725
H	-5.824678	-0.38138	-2.3596	H	5.798281	-2.00092	-1.6957
H	-5.363801	-2.07553	-2.47921	C	6.233849	-3.32585	-3.35811
C	-6.348388	-1.30409	-4.25254	H	7.125591	-3.76305	-2.89795
H	-7.35387	-1.59895	-3.93602	H	6.567367	-2.5428	-4.04898
H	-5.977842	-2.07442	-4.93889	H	5.749468	-4.10935	-3.95244
H	-6.440178	-0.37027	-4.81951	C	-7.733422	3.224075	0.520416
C	7.805216	1.339546	0.19167	H	-7.975454	2.935719	-0.5106
H	8.435729	1.273833	1.087773	H	-8.676269	3.293543	1.073503
H	8.410778	1.015541	-0.66166	H	-7.294911	4.228106	0.492854
H	7.55625	2.395257	0.034142	H	-6.566669	2.525161	2.19357
H	5.939884	0.570349	-0.56857	C	-0.986411	1.886051	1.802755
Energy: -1688019.129. kcal.mol^{-1}				Energy: -1688019.432 kcal.mol^{-1}			

t-Butyl oxazoline **6.1** inward conformation				*t*-Butyl oxazoline **6.1** outward conformation			
Atom	X	Y	Z	Atom	X	Y	Z
C	-2.135898	1.556894	-0.79096	C	2.010975	1.563577	0.814217
C	-2.736361	1.300374	0.447278	C	2.79248	0.721375	0.017196
C	-4.107144	0.770077	0.497924	C	4.034457	0.125008	0.531683
N	-4.865697	0.529369	-0.50378	N	4.832558	-0.64133	-0.11097
C	0.271538	0.773219	3.496996	C	0.421076	-1.00185	-3.1482
C	-0.518529	0.357635	4.576657	C	1.334494	-1.91616	-3.68893
C	1.16225	-0.15736	2.932537	C	-0.706904	-1.51086	-2.48045
C	-0.448632	-0.95347	5.052572	C	1.147464	-3.29145	-3.53514
C	0.10111	2.148205	2.866419	C	0.687739	0.496974	-3.16704
C	1.178744	-1.50631	3.328343	C	-0.862782	-2.88432	-2.22389
C	-0.713186	2.057011	1.574574	C	1.197152	0.976027	-1.80589
C	0.374267	-1.8825	4.412467	C	0.071216	-3.76693	-2.7831
C	-0.178199	2.418265	0.320249	C	0.488247	1.914763	-1.02154
C	1.954342	-2.53352	2.516864	C	-1.940199	-3.36613	-1.26336
C	3.262007	0.761133	2.419236	C	-2.685745	-0.35351	-2.99089
C	-2.003021	1.52095	1.617991	C	2.356802	0.410594	-1.27674
C	-0.8542	2.100759	-0.8778	C	0.847458	2.160165	0.318484
C	1.211451	-2.88317	1.226696	C	-1.533661	-3.1005	0.187059
C	-0.102559	-3.36328	1.290188	C	-0.319997	-3.60491	0.67096
C	1.784531	-2.67716	-0.04378	C	-2.310423	-2.29858	1.046571
C	1.030818	-2.83712	-1.22336	C	-1.839469	-1.91593	2.317876
C	-0.279594	-3.31761	-1.11178	C	-0.619054	-2.44176	2.759
C	1.572418	-2.43774	-2.59577	C	-2.579068	-0.89872	3.186258
C	0.740832	-1.31239	-3.20106	C	-1.720695	0.338248	3.422562
C	-0.224088	-1.58191	-4.18037	C	-1.043863	0.521031	4.635494
C	-1.12091	-0.59658	-4.59857	C	-0.106173	1.544293	4.789789
C	0.819226	0.000511	-2.69288	C	-1.472058	1.255308	2.380943
C	-0.142688	0.975606	-3.0162	C	-0.452974	2.221505	2.4757

C	-1.097997	0.660397	-3.99267	C	0.208004	2.362903	3.703907
C	-0.837884	-3.60685	0.131714	C	0.126232	-3.3025	1.955933
C	-0.204089	2.287574	-2.24907	C	-0.01708	3.01003	1.250078
C	4.034166	-3.38328	-0.20765	C	-4.626737	-2.75693	0.926584
C	3.129279	0.474451	-2.34357	C	-3.545225	1.61005	1.256216
C	1.063696	4.439827	0.616826	C	-0.312826	3.622285	-2.49095
H	0.388982	-2.91569	4.75162	H	-0.04307	-4.83587	-2.61864
H	-0.404595	2.80604	3.583347	H	1.432559	0.713773	-3.94202
H	1.073425	2.588821	2.645132	H	-0.220481	1.043139	-3.42269
H	-1.199904	1.066044	5.041836	H	2.205021	-1.54551	-4.22471
H	-0.561215	-3.52377	2.261775	H	0.294703	-4.22	0.020021
H	-0.875567	-3.44308	-2.01159	H	-0.240386	-2.15218	3.735399
H	-1.83264	1.410318	-4.27573	H	0.978632	3.12337	3.805536
H	3.260251	-0.21103	-3.19114	H	-3.959408	1.43329	2.257549
H	3.814092	0.167136	-1.5497	H	-4.088548	0.980251	0.548016
H	3.925045	-4.01647	0.685833	H	-4.432741	-3.73087	0.452537
H	0.794019	2.697922	-2.10676	H	-0.881788	3.367376	0.693393
H	-0.783683	3.011442	-2.83463	H	0.552106	3.887076	1.581421
H	2.944951	-2.15562	2.260334	H	-2.887695	-2.86276	-1.46065
H	2.088575	-3.43605	3.125471	H	-2.095008	-4.44117	-1.41623
H	1.531007	-3.30028	-3.27149	H	-2.814182	-1.34751	4.158696
H	2.620258	-2.15512	-2.49456	H	-3.525649	-0.64793	2.707351
H	2.10822	4.658983	0.864763	H	-1.230727	3.748122	-3.07599
H	3.074237	1.61078	3.093501	H	-2.226718	0.080854	-3.89221
O	3.113961	-2.28269	-0.13464	O	-3.555401	-1.84985	0.621678
O	1.808916	0.322259	-1.78988	O	-2.179542	1.155596	1.203563
O	1.052996	3.046574	0.251781	O	-0.608962	2.567498	-1.55592
O	2.011125	0.253945	1.924261	O	-1.66574	-0.63191	-2.01701
H	-0.284525	-2.58212	-4.60326	H	-1.240838	-0.16056	5.459817
C	-6.638645	-1.25552	-0.6906	C	7.331077	-0.85887	0.176026

C	-6.866138	-0.93967	-2.18237	C	7.439549	-1.80985	-1.03275
H	-7.616707	-0.14978	-2.30874	H	7.297529	-2.85373	-0.72756
H	-7.224696	-1.82987	-2.71236	H	8.429305	-1.72852	-1.49708
H	-5.939732	-0.60256	-2.65476	H	6.681733	-1.57274	-1.78424
H	-2.436277	1.244656	2.572802	H	2.926731	-0.3079	-1.85631
H	3.796083	-4.00592	-1.08338	H	-4.671367	-2.92291	2.013711
H	3.765855	-0.01853	3.011075	H	-3.17115	-1.2941	-3.29404
H	0.461256	4.592838	1.522585	H	0.48386	3.301768	-3.17589
O	-4.611341	0.52669	1.751061	O	4.352214	0.427947	1.83181
C	-5.922109	-0.0545	1.551082	C	5.63449	-0.19272	2.087781
H	-5.893061	-1.08148	1.927753	H	6.362083	0.605523	2.26489
H	-6.640255	0.520905	2.139969	H	5.541971	-0.79796	2.992482
C	-6.153017	0.044299	0.016041	C	5.917067	-1.02592	0.805267
H	-6.910019	0.814012	-0.19643	H	5.800494	-2.09739	1.026974
H	-2.686601	1.315124	-1.69368	H	2.310434	1.747522	1.839922
C	0.57885	5.366535	-0.49767	C	0.072298	4.940157	-1.81991
H	-0.45298	5.10662	-0.76205	H	0.966972	4.785257	-1.20532
H	1.190689	5.197973	-1.39178	H	-0.734055	5.2427	-1.14133
C	0.652929	6.840524	-0.07976	C	0.335037	6.045007	-2.85102
H	1.678512	7.134142	0.174139	H	-0.55062	6.236016	-3.46875
H	0.023341	7.040114	0.795264	H	1.158214	5.77642	-3.52338
H	0.312132	7.495148	-0.88804	H	0.603756	6.985057	-2.35898
C	3.426411	1.90494	-2.79114	C	-3.689999	3.086538	0.892177
H	2.711389	2.196733	-3.57023	H	-3.125003	3.693643	1.610266
H	3.271412	2.579167	-1.94128	H	-3.239267	3.249754	-0.09321
C	4.857319	2.043794	-3.3265	C	-5.15891	3.528465	0.885568
H	5.597767	1.775608	-2.5634	H	-5.747175	2.949063	0.163976
H	5.063114	3.072409	-3.63989	H	-5.2513	4.585268	0.614724
H	5.024758	1.394348	-4.19402	H	-5.621787	3.398923	1.871207
C	4.124861	1.188507	1.243859	C	-3.695992	0.606211	-2.38604

H	4.300518	0.311662	0.612529	H	-4.139471	0.125973	-1.50775
H	3.556421	1.906846	0.643555	H	-3.156381	1.490134	-2.02975
C	5.456465	1.795089	1.701918	C	-4.786647	1.001708	-3.38848
H	5.300628	2.688276	2.318946	H	-4.364186	1.507715	-4.26492
H	6.06891	2.090674	0.843778	H	-5.510164	1.684666	-2.93127
H	6.042356	1.08241	2.295018	H	-5.341678	0.126791	-3.74813
C	5.450677	-2.83463	-0.30765	C	-5.934349	-2.16462	0.419719
H	5.650718	-2.20895	0.570544	H	-5.845677	-1.982	-0.65806
H	5.512933	-2.17762	-1.18368	H	-6.087547	-1.18745	0.893712
C	6.4972	-3.95042	-0.41077	C	-7.131477	-3.08	0.702665
H	7.507342	-3.53444	-0.47853	H	-8.060692	-2.6338	0.334563
H	6.333757	-4.57079	-1.29957	H	-7.253026	-3.25961	1.777241
H	6.468481	-4.60958	0.464731	H	-7.015288	-4.05421	0.213689
C	-7.974651	-1.6969	-0.05936	C	8.392565	-1.2525	1.223211
H	-8.726477	-0.90062	-0.12338	H	8.23088	-2.27426	1.588367
H	-8.374117	-2.57261	-0.58325	H	9.395802	-1.21252	0.784165
H	-7.862539	-1.97181	0.996027	H	8.388948	-0.58002	2.089126
H	-1.856732	-0.81889	-5.36586	H	0.402447	1.679501	5.739894
H	-1.853932	-3.98464	0.199124	H	1.06834	-3.70634	2.315131
H	-1.056113	-1.25732	5.900185	H	1.856773	-3.98864	-3.97158
C	-5.597288	-2.38368	-0.56704	C	7.568046	0.587038	-0.29876
H	-4.641725	-2.08007	-1.00496	H	6.818821	0.879287	-1.04073
H	-5.417175	-2.66941	0.475664	H	7.528288	1.307932	0.525936
H	-5.946893	-3.27895	-1.0938	H	8.558495	0.674917	-0.75964
Energy: -1416629.513 kcal.mol^{-1}				Energy -1416629.541 kcal.mol^{-1}			

t-Butyl oxazoline **6.8** inward conformation				*t*-Butyl oxazoline **6.8** outward conformation			
Atoms	X	Y	Z	Atoms	X	Y	Z
C	1.773913	-0.79756	2.081928	C	-1.144527	1.82016	1.663245

C	2.198309	0.536333	2.040868	C	-2.209809	0.938618	1.453065
C	3.614035	0.84657	1.790294	C	-3.475533	1.40147	0.864582
N	4.571133	0.002808	1.68969	N	-4.513807	0.688158	0.638774
C	-1.279718	3.116863	1.398942	C	-0.750946	-3.13767	1.290364
C	-0.627395	4.318491	1.107329	C	-1.910943	-3.79153	0.865087
C	-2.078964	2.534192	0.399948	C	0.352585	-3.10673	0.420497
C	-0.721113	4.942187	-0.14861	C	-2.019037	-4.38442	-0.40477
C	-1.068213	2.404609	2.728623	C	-0.703767	-2.38087	2.61084
C	-2.121598	3.066565	-0.896	C	0.254065	-3.58729	-0.89189
C	-0.061318	1.260857	2.599319	C	-0.882491	-0.87767	2.38833
C	-1.453797	4.276613	-1.14017	C	-0.929846	-4.23706	-1.27381
C	-0.427728	-0.092	2.763675	C	0.129928	0.057988	2.703242
C	-2.781781	2.289682	-2.02731	C	1.361422	-3.30753	-1.89885
C	-4.114778	1.668162	1.192529	C	2.406896	-3.50132	1.488128
C	1.261092	1.553544	2.254129	C	-2.050252	-0.41282	1.784697
C	0.462372	-1.133	2.419032	C	0.040654	1.396297	2.271814
C	-1.873408	1.162184	-2.51881	C	1.289247	-1.86794	-2.41086
C	-0.602053	1.474607	-3.02088	C	0.119636	-1.41943	-3.04095
C	-2.243456	-0.18878	-2.42562	C	2.33691	-0.95404	-2.21483
C	-1.312158	-1.20667	-2.70819	C	2.168007	0.407532	-2.532
C	-0.05755	-0.84198	-3.20238	C	0.981826	0.803525	-3.15496
C	-1.612869	-2.6789	-2.42789	C	3.21032	1.460549	-2.15523
C	-0.697824	-3.23395	-1.34119	C	2.650211	2.456474	-1.14568
C	0.421359	-3.99973	-1.68108	C	2.224021	3.722667	-1.55762
C	1.388543	-4.39035	-0.73945	C	1.543506	4.608994	-0.70529
C	-0.882346	-2.89099	0.01379	C	2.430458	2.085065	0.196019
C	0.108509	-3.1702	0.967064	C	1.660806	2.891226	1.048007
C	1.220496	-3.9308	0.572028	C	1.245524	4.149047	0.583107
C	0.317971	0.494275	-3.40414	C	-0.052885	-0.09494	-3.45421
C	0.021906	-2.59561	2.374754	C	1.207573	2.373645	2.405842

C	-4.448572	-0.64335	-3.1342	C	4.474121	-1.84645	-2.6778
C	-3.226273	-2.96333	0.457432	C	4.317757	0.810342	0.906916
C	-1.887383	-0.2149	4.65042	C	1.058605	-0.57422	4.812649
H	-1.518549	4.694686	-2.13929	H	-0.984404	-4.63116	-2.28316
H	-0.704642	3.132514	3.463602	H	-1.499119	-2.75742	3.265009
H	-2.015511	2.01203	3.097667	H	0.24734	-2.55782	3.113272
H	-0.029683	4.776	1.891619	H	-2.75309	-3.8314	1.551248
H	-0.335185	2.522744	-3.09006	H	-0.677894	-2.13894	-3.18519
H	0.650363	-1.63721	-3.41822	H	0.864083	1.856683	-3.3942
H	1.962904	-4.1641	1.327832	H	0.677001	4.772766	1.264783
H	-3.220396	-3.73487	-0.32387	H	4.852561	1.445368	0.18819
H	-4.023904	-2.25308	0.227248	H	4.595935	-0.22829	0.714557
H	-4.483874	0.307284	-3.68763	H	4.024192	-2.67015	-3.25237
H	-0.996882	-2.66488	2.751218	H	2.02594	1.869807	2.917017
H	0.665439	-3.1884	3.035607	H	0.9017	3.226746	3.023517
H	-3.728876	1.860328	-1.69769	H	2.340699	-3.46908	-1.44614
H	-2.997139	2.980202	-2.85181	H	1.261517	-4.00678	-2.73795
H	-1.459207	-3.265	-3.34169	H	3.516332	2.011951	-3.05227
H	-2.663168	-2.77681	-2.15352	H	4.095032	0.954678	-1.76832
H	-2.970489	-0.09974	4.771249	H	1.884643	-1.22953	5.110714
H	-4.040603	2.270239	2.111609	H	1.900521	-3.93618	2.363996
O	-3.53343	-0.52731	-2.03362	O	3.545673	-1.38855	-1.68259
O	-2.009153	-2.19885	0.401658	O	2.901273	0.877015	0.661737
O	-1.686882	-0.41203	3.237982	O	1.251199	-0.35089	3.403094
O	-2.798341	1.391646	0.689173	O	1.539835	-2.54861	0.852648
H	0.541397	-4.28563	-2.72314	H	2.420886	4.012507	-2.58692
C	6.769919	0.206603	0.454303	C	-6.922216	1.432225	0.727613
C	7.192918	-1.21881	0.861848	C	-7.425225	-0.01345	0.544584
H	7.713853	-1.21611	1.827072	H	-7.523682	-0.2645	-0.51848
H	7.872806	-1.64582	0.115453	H	-8.409466	-0.13979	1.010567

H	6.320773	-1.87184	0.95247	H	-6.731696	-0.7277	0.996063
C	6.074015	0.151726	-0.91785	C	-6.828318	1.748182	2.232318
H	6.750466	-0.27668	-1.66624	H	-7.80922	1.62794	2.706114
H	5.781364	1.145104	-1.27561	H	-6.500765	2.776979	2.421811
H	5.1745	-0.46904	-0.87413	H	-6.124468	1.072624	2.727777
H	1.569506	2.587762	2.147577	H	-2.849403	-1.10471	1.540556
H	-4.091687	-1.41655	-3.83173	H	4.689579	-1.03108	-3.38521
H	-4.672453	2.267794	0.456495	H	2.618633	-4.32781	0.79218
H	-1.410056	0.721595	4.969056	H	0.118562	-1.11722	4.980459
O	3.931702	2.180007	1.699784	O	-3.535404	2.733107	0.537925
C	5.341219	2.231453	1.370394	C	-4.881512	2.971451	0.061376
H	5.431941	2.597786	0.342541	H	-5.362707	3.667071	0.755547
H	5.820662	2.941558	2.047315	H	-4.813566	3.439936	-0.92318
C	5.822112	0.766586	1.552317	C	-5.533365	1.559286	0.034561
H	6.365772	0.675575	2.505581	H	-5.674522	1.236792	-1.00766
H	2.491379	-1.57806	1.851657	H	-1.239413	2.851203	1.341405
C	1.703075	0.828159	-3.99006	C	-1.320716	0.399426	-4.17735
C	1.840831	0.181828	-5.39034	C	-0.928701	1.009651	-5.54519
H	2.82487	0.406646	-5.81877	H	-1.820043	1.372506	-6.07106
H	1.075318	0.563791	-6.07482	H	-0.43886	0.263176	-6.18028
H	1.736892	-0.90667	-5.34632	H	-0.242066	1.853971	-5.43086
C	2.807777	0.271638	-3.06062	C	-2.022052	1.47966	-3.31845
H	3.799698	0.502179	-3.46713	H	-2.92044	1.846075	-3.83037
H	2.736987	-0.81442	-2.94979	H	-1.369472	2.337619	-3.13153
H	2.736339	0.712347	-2.06095	H	-2.3218	1.071937	-2.34762
C	1.925237	2.345857	-4.14113	C	-2.330417	-0.73641	-4.43439
H	2.915167	2.531092	-4.57234	H	-3.203625	-0.3376	-4.9622
H	1.884325	2.860869	-3.17551	H	-2.685475	-1.18498	-3.50077
H	1.183835	2.802478	-4.80611	H	-1.90168	-1.52963	-5.05677
C	2.578937	-5.26674	-1.17594	C	1.13274	6.004963	-1.21358

C	2.049665	-6.61134	-1.73253	C	2.39594	6.788084	-1.64748
H	1.39102	-6.46276	-2.59396	H	2.936601	6.275508	-2.44912
H	1.482984	-7.15415	-0.96808	H	3.085694	6.912707	-0.80561
H	2.883431	-7.2467	-2.0545	H	2.120726	7.784395	-2.01387
C	3.386871	-4.54194	-2.28002	C	0.181491	5.861069	-2.42691
H	2.77724	-4.34289	-3.1669	H	0.657218	5.32706	-3.25531
H	4.238929	-5.15631	-2.5947	H	-0.117843	6.849208	-2.79641
H	3.773416	-3.58426	-1.91551	H	-0.724606	5.311775	-2.14958
C	3.539183	-5.57755	-0.01093	C	0.406373	6.832478	-0.135
H	3.037133	-6.1197	0.79779	H	1.036002	6.994765	0.746555
H	3.982029	-4.66782	0.408074	H	-0.523467	6.353666	0.189904
H	4.359713	-6.2076	-0.37099	H	0.145647	7.815974	-0.54084
C	-0.016239	6.291617	-0.38991	C	-3.303674	-5.14224	-0.79401
C	-0.240797	6.825318	-1.81848	C	-3.240019	-5.71043	-2.22568
H	-1.303403	6.983801	-2.03234	H	-2.411353	-6.41613	-2.34908
H	0.165061	6.147312	-2.57697	H	-3.131801	-4.91869	-2.97486
H	0.266863	7.78901	-1.93429	H	-4.16802	-6.2483	-2.44761
C	1.508133	6.131305	-0.17162	C	-4.522164	-4.1914	-0.70983
H	1.927476	5.396888	-0.86761	H	-4.40264	-3.34034	-1.38838
H	1.741434	5.7974	0.843846	H	-4.660843	-3.79289	0.299379
H	2.019503	7.087552	-0.33461	H	-5.439777	-4.7239	-0.98704
C	-0.565179	7.343949	0.604678	C	-3.512942	-6.32684	0.181428
H	-1.64297	7.48506	0.468494	H	-2.668766	-7.02383	0.137163
H	-0.071696	8.310594	0.44839	H	-4.424741	-6.87868	-0.07699
H	-0.39598	7.047022	1.644241	H	-3.610621	-5.98674	1.217058
C	-1.381697	-1.37763	5.503766	C	1.076575	0.710147	5.640833
H	-0.304893	-1.50506	5.341439	H	0.271033	1.371629	5.300601
H	-1.867227	-2.3016	5.168035	H	2.020918	1.237087	5.459762
C	-1.660099	-1.14871	6.994696	C	0.914613	0.421073	7.138486
H	-2.73329	-1.03469	7.189152	H	1.718606	-0.22461	7.511558

H	-1.157803	-0.24584	7.361357	H	-0.038187	-0.07872	7.348777
H	-1.303176	-1.99179	7.594551	H	0.937406	1.347286	7.721284
C	-3.46226	-3.6171	1.818562	C	4.695192	1.216513	2.330863
H	-2.638918	-4.30812	2.037431	H	4.389383	2.255511	2.504665
H	-3.444879	-2.8388	2.589743	H	4.132154	0.591964	3.033485
C	-4.79521	-4.37543	1.857893	C	6.202032	1.073201	2.579767
H	-5.6418	-3.70691	1.660892	H	6.535323	0.039778	2.426411
H	-4.958636	-4.8359	2.837708	H	6.461684	1.355882	3.605159
H	-4.822988	-5.17541	1.108349	H	6.782567	1.712533	1.903886
C	-4.825564	0.353414	1.467147	C	3.691065	-2.80229	1.902303
H	-4.890134	-0.20231	0.526202	H	4.169733	-2.40593	1.000965
H	-4.200914	-0.23874	2.144342	H	3.427059	-1.94283	2.527869
C	-6.223073	0.567466	2.060314	C	4.645223	-3.74359	2.646551
H	-6.178108	1.100696	3.01764	H	4.191002	-4.13379	3.565338
H	-6.723807	-0.38957	2.240216	H	5.566772	-3.22442	2.929771
H	-6.862042	1.151978	1.387252	H	4.928724	-4.60366	2.027759
C	-5.826945	-1.0019	-2.59609	C	5.750366	-2.30871	-1.98818
H	-6.145287	-0.22346	-1.89222	H	5.498941	-3.10326	-1.27529
H	-5.751254	-1.93376	-2.02276	H	6.157469	-1.4758	-1.40214
C	-6.862374	-1.15566	-3.71647	C	6.798668	-2.81033	-2.98854
H	-7.845517	-1.41124	-3.30881	H	7.708126	-3.1348	-2.47309
H	-6.577864	-1.94865	-4.41782	H	7.08226	-2.02467	-3.69849
H	-6.972365	-0.22804	-4.29019	H	6.424048	-3.66238	-3.56768
C	8.022566	1.103081	0.37397	C	-7.910946	2.399185	0.044997
H	8.529648	1.166918	1.34465	H	-7.986534	2.195998	-1.03033
H	8.738898	0.695156	-0.34805	H	-8.912944	2.287703	0.474588
H	7.779429	2.122539	0.051829	H	-7.617532	3.448019	0.170883
Energy: -1712689.726 kcal.mol^{-1}				Energy: -1712690.55 kcal.mol^{-1}			

A2.2 Rotation of oxazoline (DFT rb3lyp/6-31)

Rotation of isopropyl oxazoline **5.1**					
No	1	2	3	4	5
Dihedral Angle	3.157560000E+00	8.157480000E+00	1.315749000E+01	1.815747000E+01	2.315773000E+01
E /HF	-1.935899300E+03	-1.935899240E+03	-1.935899058E+03	-1.935898746E+03	-1.935898331E+03
E /kcal/mol	-1.214781002E+06	-1.214780964E+06	-1.214780850E+06	-1.214780654E+06	-1.214780394E+06
No	6	7	8	9	10
Dihedral Angle	2.815748000E+01	3.315724000E+01	3.815736000E+01	4.315738000E+01	4.815730000E+01
E /HF	-1.935897783E+03	-1.935897122E+03	-1.935896330E+03	-1.935895472E+03	-1.935894553E+03
E /kcal/mol	-1.214780050E+06	-1.214779635E+06	-1.214779138E+06	-1.214778600E+06	-1.214778023E+06
No	11	12	13	14	15
Dihedral Angle	5.315723000E+01	5.815721000E+01	6.315731000E+01	6.815729000E+01	7.315753000E+01
E /HF	-1.935893575E+03	-1.935892556E+03	-1.935891547E+03	-1.935890612E+03	-1.935889815E+03
E /kcal/mol	-1.214777409E+06	-1.214776770E+06	-1.214776137E+06	-1.214775550E+06	-1.214775050E+06
No	16	17	18	19	20
Dihedral Angle	7.815736000E+01	8.315746000E+01	8.815747000E+01	9.315744000E+01	9.815773000E+01
E /HF	-1.935889292E+03	-1.935888985E+03	-1.935889075E+03	-1.935889350E+03	-1.935889853E+03
E /kcal/mol	-1.214774722E+06	-1.214774529E+06	-1.214774586E+06	-1.214774758E+06	-1.214775074E+06
No	21	22	23	24	25
Dihedral Angle	1.031578100E+02	1.081578400E+02	1.131577600E+02	1.181576900E+02	1.231575700E+02
E /HF	-1.935890513E+03	-1.935891299E+03	-1.935892149E+03	-1.935893042E+03	-1.935893975E+03
E /kcal/mol	-1.214775488E+06	-1.214775981E+06	-1.214776514E+06	-1.214777075E+06	-1.214777660E+06
No	26	27	28	29	30
Dihedral Angle	1.281576300E+02	1.331576400E+02	1.381574900E+02	1.431575600E+02	1.481575300E+02
E /HF	-1.935894899E+03	-1.935895764E+03	-1.935896519E+03	-1.935897148E+03	-1.935897702E+03
E /kcal/mol	-1.214778240E+06	-1.214778783E+06	-1.214779256E+06	-1.214779651E+06	-1.214779999E+06
No	31	32	33	34	35
Dihedral Angle	1.531575900E+02	1.581574400E+02	1.631576800E+02	1.681575900E+02	1.731576700E+02
E /HF	-1.935898241E+03	-1.935898658E+03	-1.935898978E+03	-1.935899192E+03	-1.935899296E+03
E /kcal/mol	-1.214780337E+06	-1.214780599E+06	-1.214780800E+06	-1.214780934E+06	-1.214780999E+06

No	36	37	38	39	40
Dihedral Angle	1.781574600E+02	-1.768425300E+02	-1.718426500E+02	-1.668424600E+02	-1.618423800E+02
E /HF	-1.935899293E+03	-1.935899178E+03	-1.935898952E+03	-1.935898622E+03	-1.935898211E+03
E /kcal/mol	-1.214780997E+06	-1.214780925E+06	-1.214780783E+06	-1.214780576E+06	-1.214780318E+06
No	41	42	43	44	45
Dihedral Angle	-1.568425800E+02	-1.518425700E+02	-1.468425600E+02	-1.418424600E+02	-1.368425600E+02
E /HF	-1.935897709E+03	-1.935897146E+03	-1.935896533E+03	-1.935895851E+03	-1.935895134E+03
E /kcal/mol	-1.214780003E+06	-1.214779650E+06	-1.214779265E+06	-1.214778838E+06	-1.214778388E+06
No	46	47	48	49	50
Dihedral Angle	-1.318426200E+02	-1.268426500E+02	-1.218426100E+02	-1.168422000E+02	-1.118424300E+02
E /HF	-1.935894408E+03	-1.935893684E+03	-1.935892984E+03	-1.935892345E+03	-1.935891803E+03
E /kcal/mol	-1.214777932E+06	-1.214777477E+06	-1.214777038E+06	-1.214776638E+06	-1.214776297E+06
No	51	52	53	54	55
Dihedral Angle	-1.068425800E+02	-1.018425000E+02	-9.684244000E+01	-9.184260000E+01	-8.684265000E+01
E /HF	-1.935891398E+03	-1.935891113E+03	-1.935890951E+03	-1.935890945E+03	-1.935891085E+03
E /kcal/mol	-1.214776043E+06	-1.214775864E+06	-1.214775763E+06	-1.214775759E+06	-1.214775847E+06
No	56	57	58	59	60
Dihedral Angle	-8.184242000E+01	-7.684272000E+01	-7.184245000E+01	-6.684243000E+01	-6.184246000E+01
E /HF	-1.935891342E+03	-1.935891688E+03	-1.935892124E+03	-1.935892637E+03	-1.935893242E+03
E /kcal/mol	-1.214776008E+06	-1.214776225E+06	-1.214776499E+06	-1.214776821E+06	-1.214777200E+06
No	61	62	63	64	65
Dihedral Angle	-5.684244000E+01	-5.184283000E+01	-4.684243000E+01	-4.184244000E+01	-3.684250000E+01
E /HF	-1.935893881E+03	-1.935894502E+03	-1.935895158E+03	-1.935895815E+03	-1.935896437E+03
E /kcal/mol	-1.214777601E+06	-1.214777991E+06	-1.214778403E+06	-1.214778815E+06	-1.214779205E+06
No	66	67	68	69	70
Dihedral Angle	-3.184252000E+01	-2.684251000E+01	-2.184222000E+01	-1.684243000E+01	-1.184237000E+01
E /HF	-1.935897068E+03	-1.935897636E+03	-1.935898117E+03	-1.935898506E+03	-1.935898856E+03
E /kcal/mol	-1.214779601E+06	-1.214779957E+06	-1.214780259E+06	-1.214780503E+06	-1.214780723E+06
No	71	72	73	74	75
Dihedral Angle	-6.842240000E+00	-1.842390000E+00	3.157530000E+00	8.157590000E+00	1.315743000E+01
E /HF	-1.935899150E+03	-1.935899294E+03	-1.935899301E+03	-1.935899237E+03	-1.935899060E+03

E /kcal/mol	-1.214780908E+06	-1.214780998E+06	-1.214781002E+06	-1.214780962E+06	-1.214780851E+06

Rotation of Methyl ferrocenyloxazoline					
No	1	2	3	4	5
Dihedral Angle	1.16208000E+01	1.66207900E+01	2.16207300E+01	2.66207200E+01	3.16207300E+01
E /HF	-2.21749476E+03	-2.21749431E+03	-2.21749371E+03	-2.21749298E+03	-2.21749217E+03
E /kcal/mol	-1.39148276E+06	-1.39148248E+06	-1.39148211E+06	-1.39148165E+06	-1.39148114E+06
No	6	7	8	9	10
Dihedral Angle	3.66207200E+01	4.16207700E+01	4.66207100E+01	5.16207300E+01	5.66207200E+01
E /HF	-2.21749124E+03	-2.21749019E+03	-2.21748910E+03	-2.21748798E+03	-2.21748686E+03
E /kcal/mol	-1.39148055E+06	-1.39147990E+06	-1.39147921E+06	-1.39147851E+06	-1.39147781E+06
No	11	12	13	14	15
Dihedral Angle	6.16207700E+01	6.66207800E+01	7.16207500E+01	7.66207400E+01	8.16207900E+01
E /HF	-2.21748578E+03	-2.21748478E+03	-2.21748384E+03	-2.21748307E+03	-2.21748250E+03
E /kcal/mol	-1.39147713E+06	-1.39147650E+06	-1.39147591E+06	-1.39147543E+06	-1.39147507E+06
No	16	17	18	19	20
Dihedral Angle	8.66208400E+01	9.16208900E+01	9.66209600E+01	1.01621000E+02	1.06620950E+02
E /HF	-2.21748217E+03	-2.21748215E+03	-2.21748245E+03	-2.21748303E+03	-2.21748380E+03
E /kcal/mol	-1.39147486E+06	-1.39147485E+06	-1.39147504E+06	-1.39147540E+06	-1.39147589E+06
No	21	22	23	24	25
Dihedral Angle	1.11621000E+02	1.16620950E+02	1.21620960E+02	1.26620960E+02	1.31620990E+02
E /HF	-2.21748470E+03	-2.21748569E+03	-2.21748679E+03	-2.21748796E+03	-2.21748907E+03
E /kcal/mol	-1.39147645E+06	-1.39147707E+06	-1.39147776E+06	-1.39147849E+06	-1.39147919E+06
No	26	27	28	29	30
Dihedral Angle	1.36620950E+02	1.41620960E+02	1.46620920E+02	1.51620920E+02	1.56620980E+02
E /HF	-2.21749010E+03	-2.21749113E+03	-2.21749207E+03	-2.21749287E+03	-2.21749361E+03
E /kcal/mol	-1.39147984E+06	-1.39148049E+06	-1.39148108E+06	-1.39148158E+06	-1.39148204E+06
No	31	32	33	34	35
Dihedral Angle	1.61620880E+02	1.66620920E+02	1.71620830E+02	1.76620900E+02	-1.78379140E+02
E /HF	-2.21749424E+03	-2.21749468E+03	-2.21749494E+03	-2.21749514E+03	-2.21749520E+03

E /kcal/mol	-1.39148244E+06	-1.39148271E+06	-1.39148288E+06	-1.39148300E+06	-1.39148304E+06
No	36	37	38	39	40
Dihedral Angle	-1.73379180E+02	-1.68379190E+02	-1.63379210E+02	-1.58379240E+02	-1.53379220E+02
E /HF	-2.21749507E+03	-2.21749481E+03	-2.21749445E+03	-2.21749392E+03	-2.21749329E+03
E /kcal/mol	-1.39148296E+06	-1.39148280E+06	-1.39148257E+06	-1.39148223E+06	-1.39148184E+06
No	41	42	43	44	45
Dihedral Angle	-1.48379210E+02	-1.43379250E+02	-1.38379210E+02	-1.33379210E+02	-1.28379210E+02
E /HF	-2.21749255E+03	-2.21749166E+03	-2.21749064E+03	-2.21748955E+03	-2.21748842E+03
E /kcal/mol	-1.39148137E+06	-1.39148082E+06	-1.39148018E+06	-1.39147949E+06	-1.39147879E+06
No	46	47	48	49	50
Dihedral Angle	-1.23379220E+02	-1.18379220E+02	-1.13379220E+02	-1.08379220E+02	-1.03379260E+02
E /HF	-2.21748724E+03	-2.21748604E+03	-2.21748492E+03	-2.21748390E+03	-2.21748309E+03
E /kcal/mol	-1.39147804E+06	-1.39147729E+06	-1.39147659E+06	-1.39147595E+06	-1.39147544E+06
No	51	52	53	54	55
Dihedral Angle	-9.83792100E+01	-9.33791800E+01	-8.83790900E+01	-8.33790700E+01	-7.83790700E+01
E /HF	-2.21748246E+03	-2.21748219E+03	-2.21748220E+03	-2.21748250E+03	-2.21748302E+03
E /kcal/mol	-1.39147504E+06	-1.39147488E+06	-1.39147488E+06	-1.39147507E+06	-1.39147539E+06
No	56	57	58	59	60
Dihedral Angle	-7.33789500E+01	-6.83789500E+01	-6.33789700E+01	-5.83790100E+01	-5.33789900E+01
E /HF	-2.21748380E+03	-2.21748470E+03	-2.21748573E+03	-2.21748687E+03	-2.21748802E+03
E /kcal/mol	-1.39147588E+06	-1.39147645E+06	-1.39147709E+06	-1.39147781E+06	-1.39147854E+06
No	61	62	63	64	65
Dihedral Angle	-4.83789800E+01	-4.33789600E+01	-3.83789500E+01	-3.33789900E+01	-2.83790400E+01
E /HF	-2.21748920E+03	-2.21749028E+03	-2.21749127E+03	-2.21749220E+03	-2.21749302E+03
E /kcal/mol	-1.39147927E+06	-1.39147995E+06	-1.39148057E+06	-1.39148116E+06	-1.39148167E+06
No	66	67	68	69	70
Dihedral Angle	-2.33791300E+01	-1.83789800E+01	-1.33790800E+01	-8.37910000E+00	-3.37912000E+00
E /HF	-2.21749373E+03	-2.21749430E+03	-2.21749476E+03	-2.21749506E+03	-2.21749521E+03
E /kcal/mol	-1.39148211E+06	-1.39148247E+06	-1.39148276E+06	-1.39148295E+06	-1.39148304E+06
No	71	72	73	74	75
Dihedral Angle	1.62086000E+00	6.62082000E+00	1.16208000E+01	1.66207100E+01	2.16207700E+01

E /HF	-2.21749520E+03	-2.21749506E+03	-2.21749476E+03	-2.21749431E+03	-2.21749371E+03
E /kcal/mol	-1.39148304E+06	-1.39148295E+06	-1.39148276E+06	-1.39148248E+06	-1.39148211E+06